String theory : Supersymmetry breaking, moduli stabilitzation and cosmological considerations

Thibaut Coudarchet

INSTITUT POLYTECHNIQUE DE PARIS

NNT : 2021IPPAX071

Thèse de doctorat

CPHT Centre de Physique Théorique

ÉCOLE POLYTECHNIQUE

IP PARIS

String theory: Supersymmetry breaking, moduli stabilization and cosmological considerations

Thèse de doctorat de l'Institut Polytechnique de Paris
préparée à l'École Polytechnique

École doctorale n°626, École doctorale de l'Institut Polytechnique de Paris (EDIPP)
Spécialité de doctorat : Physique

Thèse présentée et soutenue à Palaiseau, le 30 septembre 2021, par

Thibaut Coudarchet

Composition du jury :

Ignatios Antoniadis Directeur de recherche, LPTHE, Sorbonne Université	Président
Mariana Graña Chercheuse CEA, IPhT, CEA/Saclay	Rapporteuse
Dan Israël Maître de conférences, LPTHE, Sorbonne Université	Rapporteur
Augusto Sagnotti Professeur, École Normale Supérieure de Pise	Examinateur
Nicolaos Toumbas Professeur associé, Département de physique, Université de Chypre	Examinateur
Jan Troost Directeur de recherche, LPENS, École Normale Supérieure	Examinateur
Hervé Partouche Directeur de recherche, CPHT, École Polytechnique	Directeur de thèse

Acknowledgements/Remerciements

I first want to thank the members of my jury for accepting to be part of it and evaluate my work. I thank the examiners Ignatios Antoniadis, Augusto Sagnotti, Jan Troost and Nicolaos Tumbas as well as the referees Mariana Graña and Dan Israël for their careful reading of my manuscript.

Je remercie tous les membres permanents du groupe corde du laboratoire CPHT et son directeur Jean-René, pour leur accueil, leur disponibilité et leur joie de vivre. Malika, Fadila et Florence sont d'incroyables secrétaires sans qui le labo ne serait pas le même. Je remercie Marios pour la fraîcheur qu'il apporte au groupe et son analyse précise et méthodique des meilleures horaires pour aller manger à la cantine. Je remercie Guillaume, à qui j'ai demandé avec qui il faisait sa thèse la première fois que je l'ai vu... Pour sa gentillesse, son ouverture d'esprit et ses riches connaissances en physique. Je remercie grandement Emilian avec qui nous avons beaucoup échangé et collaboré. Pour sa grande sympathie et la qualité de ses explications, des heures durant, une craie à la main, sans fatiguer. Également pour son soutien pour les candidatures de post-doctorat à travers sa lettre de recommandation. Je remercie aussi les autres membres du groupe, Blaise, Andrea, Balt, Eric et Kenta. Même si nous n'avons pas beaucoup échangé durant ma thèse, je sais que leur porte était toujours ouverte si besoin.

Je remercie Lucien pour la collaboration que nous avons faite ensemble. Voilà encore quelqu'un d'extrêmement sympathique et jovial avec qui c'est un plaisir de discuter.

I thank Steve for our long collaboration and his hospitality in Durham University. I am very grateful for his support of my post-doctoral applications.

Je remercie également les doctorants et post-doctorants du CPHT pour l'agréable et stimulante atmosphère de travail qu'ils ont créée. Je remercie Sabine pour les diverses discussions lors de nos pauses café (et thé !). Je remercie Alexandre avec qui nous avons bien rigolé lors de discussions plus perchées les unes que les autres. Je remercie la "team Marios", Charles et Luca, pour leur constante bonne humeur, leur humour et leur capacité à discuter de tous les sujets. Je suis vraiment ravi de les avoir rencontrés. Je remercie Balthazar, mon co-thésard, avec qui je n'ai pas travaillé mais bien discuté, de sujets très variés, aussi sérieux que les enjeux climatiques et aussi légers que le cinéma. C'était un réel plaisir de partager son bureau. Je remercie mon autre co-bureau, Quentin, que j'ai harcelé de questions, plus ou moins en lien avec la physique, auxquelles il a toujours pris le temps de répondre (quitte à reporter la réponse au trajet de retour en RER). J'ai découvert un ami drôle, intéressant, aux questionnements profonds et à l'esprit critique affûté.

Je remercie chaleureusement Grégoire et Osmin, deux collègues et amis du LPTHE que j'ai rencontrés lors de l'école "LACES" à Florence et que j'apprécie beaucoup.

Je remercie Daniel Bernard pour m'avoir offert l'expérience assez unique de voir mon travail de thèse représenté dans des œuvres de peinture dans le cadre d'une exposition arts-sciences présentée à l'École Polytechnique (voir Fig. 1).

Je remercie aussi mes amis de longue date. Les gens rencontrés lors des années lyonnaises qui pour beaucoup se sont retrouvés en région parisienne aussi, Sousou, Clémence, Trotro, Marie, Lulu, Guillaume, Guigui, Céline, Baptiste, Dédé, Michou, Péné, Alex. Un de mes compagnons de théorie, Percy, bon public pour mes blagues pas drôles et d'une sympathie sans égale. Mon autre compagnon de théorie, rencontré déjà à l'époque de la prépa, Lilian, moins bon public pour mes blagues pas drôles mais tout aussi sympathique, avec qui j'ai partagé le même parcours et la même passion pour la physique des hautes énergies depuis 10 ans.

Il y a aussi les amis de très longue date, du lycée, du collège et même d'avant cela, avec qui les retrouvailles sont toujours un plaisir et avec un sentiment de s'être quittés la veille. Mathieu, Adrien, Walid, Elodie, Marie, CK, Laurie et Thomas (26 ans d'amitié !).

Je remercie également ma famille et belle-famille pour leur soutien durant ces trois années de thèse et les deux années, pas faciles, qui ont précédé. Je les remercie aussi pour leur accueil lors des divers confinements durant lesquels je me suis exilé de la capitale pour retrouver la campagne auvergnate.

Je remercie énormément Hervé, pour sa dévotion sans faille envers ses étudiants, toujours disponible pour discuter, expliquer et réfléchir sans cesse à comment faire au mieux pour nous. Je réalise la chance que c'est d'avoir un excellent directeur de thèse qui prend ce statut au sérieux.

Enfin, je remercie Léa, mon binôme de vie depuis 11 ans, qui me supporte, m'enthousiasme et me fait rire au quotidien. Elle m'a dit un jour que j'étais son étoile, qu'elle espérait ne jamais voir cesser de briller, qu'elle sache alors que mon cœur ne brûle que pour elle.

(a) *Extensions*, 2020, acrylique et encre sur lavis.

(b) *Cordes cosmiques*, 2020, acrylique et encre sur lavis.

Figure 1: Œuvres inspirées de mes travaux de thèse, realisées par Daniel Bernard pour une exposition arts-sciences intitulée *Entre les vagues et le vent* présentée à l'École Polytechnique début 2021. Commentaires de l'artiste : "Les recherches de Thibaut Coudarchet étant extrêmement théoriques, je me suis intéressé à l'aspect purement esthétique de ce que pouvait évoquer le terme "théorie des cordes" à un non-initié. Dans un tableau, les doigts forment des cordes et enserrent une sphère lumineuse, une représentation artistique de la constante cosmologique, un paramètre qui intervient dans certaines équations décrivant l'évolution de l'univers. Une idée semblable est évoquée dans le second, la théorie des cordes expliquant entre autres l'univers, les planètes, les étoiles. Une femme apparaît comme le reflet de l'autre, il s'agit d'une interprétation du terme supersymétrie..."

Synthèse en français

Le défi majeur de la physique fondamentale moderne est de construire une théorie quantique cohérente de l'interaction gravitationnelle. Plus largement, le besoin de nouvelle physique au-delà du modèle standard de la physique des particules et de la relativité générale est motivé par différents facteurs : premièrement, le modèle standard de la physique des particules qui décrit toutes les autres interactions dans un cadre à la fois quantique et relativiste ne rend pas compte de certaines observations. Tout d'abord, les neutrinos oscillent, ce qui est incompatible avec leur masse nulle dans le modèle standard. Certaines observables, mesurées expérimentalement avec une grande précision, ne s'accordent pas avec la valeur théorique attendue. C'est le cas du moment magnétique anomal du muon ou encore de taux de désintégration de certains mésons. Nous pouvons aussi citer des mesures du moment magnétique du neutron qui contraignent un paramètre du lagrangien de la chromodynamique quantique à être extrêmement petit, ce qui ne semble pas naturel. En plus de ces tensions entre théorie et expérience, l'observation à l'échelle cosmologique des effets induits par la matière noire et l'énergie noire, qui représentent 95% du contenu énergétique de l'univers, ne trouvent pas d'explications au sein du modèle standard. Enfin, des raisons purement théoriques justifient le désir de posséder une théorie quantique de la gravitation. Nous connaissons des systèmes physiques comme les trous noirs ou encore notre univers à ses débuts dans lesquels les effets associés à la gravitation ou à la mécanique quantique ne peuvent pas être négligés et où une unification des deux théories semble inévitable.

Dans cette quête, la théorie des cordes est une candidate possible, qui offre un cadre cohérent de gravitation quantique en unifiant également toutes les autres interactions de jauge et la matière. Cela est fait simplement en modifiant la nature des degrés de liberté des particules fondamentales pour les décrire comme des cordes étendues plutôt que comme des objets ponctuels. Ce simple postulat de départ produit des théories cohérentes qui possèdent la relativité générale comme limite à basse énergie tout en possédant des symétries de jauge suffisamment élaborées pour contenir le modèle standard de la physique des particules.

La théorie est construite grâce à un élément essentiel qu'est la supersymétrie, reliant les champs bosoniques et fermioniques. Cet ingrédient est cependant problématique car le monde dans lequel nous vivons n'est manifestement pas supersymétrique et si la supersymétrie doit être présente au niveau fondamental alors elle doit être brisée d'une certaine manière à notre échelle. Ces mécanismes de brisure et l'étude de leurs conséquences sont au cœur de cette thèse.

Après un premier chapitre qui rappelle brièvement quelques ingrédients clés de la théorie des cordes et de sa construction, le deuxième chapitre présente un nouveau mécanisme de brisure de supersymétrie dans des modèles de cordes ouvertes. Ce mécanisme partage des similarités avec un mécanisme existant appelé "brane supersymmetry breaking" avec notamment une brisure possible à l'échelle de la corde et une réalisation non-linéaire de la supersymétrie. Cependant, contrairement

à ce mécanisme, notre construction évite les tadpoles de Neveu–Schwarz–Neveu–Schwarz (NS-NS) habituels et un regard attentif porté sur le secteur fermé y révèle une brisure spontanée de supersymétrie à la Scherk–Schwarz.

Dans le troisième chapitre, nous étudions les propriétés du potentiel généré à une boucle par un mécanisme de Scherk–Schwarz dans des modèles de type I avec une brisure de supersymétrie $\mathcal{N} = 2 \to \mathcal{N} = 0$. L'objectif est de déterminer les masses à une boucle acquises par la grande variété de modules présents au niveau des arbres. Leur diversité implique l'utilisation de différentes méthodes pour calculer ces masses à une boucle et conclure quant à leur stabilité ou non. Cela passe par exemple par le calcul de l'expansion de Taylor du potentiel effectif, par l'évaluation de fonctions de corrélation à deux points à une boucle ou encore par l'utilisation d'arguments de dualité entre la théorie des cordes de type I et les cordes hétérotiques.

Le quatrième chapitre explore les conséquences cosmologiques induites par le potentiel à une boucle dans les théories de cordes hétérotiques avec brisure spontanée de supersymétrie. L'objectif est d'étudier l'influence du potentiel à une boucle sur des modèles appelés "sans échelle" dans lesquels la supersymétrie est spontanément brisée et où l'échelle de brisure est une direction plate du potentiel au niveau des arbres. Il est naturel de penser que les effets quantiques *via* la présence du potentiel à une boucle vont drastiquement perturber la dynamique cosmologique. Cependant, nous montrons que sous certaines conditions, la cosmologie n'est asymptotiquement pas modifiée par la présence du potentiel à une boucle dont les effets sont complètement dominés. Dans un autre projet, avec implémentation de la température au sein du modèle, nous élaborons un mécanisme pour générer une densité relique de matière noire lors de l'évolution cosmologique de l'univers. Dans des modèles spécifiques, un attracteur cosmologique impose la condensation d'un module qui a pour effet de générer une masse soudaine à certains états interprétés comme des candidats de matière noire. Le moment où cette transition de phase se produit modifie grandement le scénario standard de gel (freeze-out) invoqué pour expliquer la création d'une densité relique de matière noire.

Contents

Introduction

After more than a century of immense advances in fundamental physics, from the elaboration of the theories of relativity and quantum mechanics to the successes of quantum field theory and particle physics with the advent of the standard model, modern theoretical physics faces new challenges and feels the need to move even further. This need originates from three different sources: Experimental tensions between predictions of the standard model of particle physics and observations, unexplained cosmological features and eventually theoretical reasons for the desire to possess a quantum theory of gravity.

One important discrepancy between the standard model and experimental results concerns the observation of neutrinos oscillation [1–3] which implies that they have a non-zero mass, not explained by the standard model. Some specific experimentally measured quantities also do not match their theoretical expectations with a quite high number of standard deviations. It is the case for the anomalous magnetic dipole moment of the muon (for a very recent result, see [4]) or decay rates of B-mesons [5, 6]. Besides that, constraints on the neutron magnetic dipole moment [7, 8] lead to the so-called strong Charge-Parity (CP) problem (see [9] for recent lecture notes) implying a parameter of the quantum chromodynamics Lagrangian to be extremely small, which seems unnatural. As for cosmological observations, the explanation for the presence and nature of dark matter [10–12] and dark energy [13, 14], which represent roughly 95% of the energy content of the universe [15] cannot be found inside the standard model.

As for the theoretical considerations, they are themselves diverse. Inspired by the famous unifications formalized in fundamental physics and the success of the quantization of the other interactions, one would naively expect the need to marry general relativity with quantum mechanics. Besides that, we know physical systems such as black holes or the singular past of our universe where the effects associated with these two theories become comparable, near the Planck scale, so that a unification seems unavoidable.

String theory is not only a consistent quantum gravity framework but also a unifying theory describing all gauge interactions and matter. Only by revisiting the nature of the fundamental degrees of freedom of particles, promoting them from points to strings, the quantized theory naturally contains a massless spin two state identified with the graviton and reproduces the general theory of relativity at low energies. Besides that, several ingredients can generate non-abelian gauge groups with far enough room to incorporate the standard model of particle physics while the first string revolution uncovered fully consistent, anomaly-free theories. All this, even nowadays after few decades of existence without any experimental confirmation that the theory provides a correct description of fundamental particles, makes string theory a promising candidate for a correct quantum theory of gravity.

The theory comes with a natural ingredient which is supersymmetry. It is a symmetry between

bosonic and fermionic fields and it proves to be a powerful tool to guarantee stability in vacua construction. However, we are obviously not living in an exactly supersymmetric universe and supersymmetry must thus be broken in some way at our scales. Handling this breaking is a difficult task that comes with a wide variety of problems, both at the field-theory and string levels. In this thesis, we will be interested in breaking mechanisms realized directly at the perturbative string level.

In the literature, a lot of different supersymmetry-breaking mechanisms have been explored, all carrying interesting features as well as caveats. An important one for the works conducted in this thesis is the Scherk–Schwarz breaking or coordinate-dependent compactification, which can be implemented in field theory [16, 17] or directly at the perturbative string level [18–22]. The scale of the spontaneous breaking induced by the mechanism is determined by the volume of the internal space used to perform the breaking. Moreover, tree-level tachyonic instabilities yielding Hagedorn-like phase transitions [23–32] are typically present for some range of this volume [33, 34]. Also, the one-loop potential typically drives a runaway for the moduli associated with the breaking scale which makes the task to find a true vacuum difficult. These difficulties have been addressed in various works and as we will see soon, some studies are precisely the purpose and content of this thesis. Tachyon-free models have been built [35, 36] and the running-away modulus can be stabilized at the price of having a negative potential [37]. The effect of the runaway on the cosmology of the models has been studied at finite temperature [38–42] or not [43, 44]. In models showing a Bose/Fermi degeneracy at the massless levels, the one-loop potential is exponentially small when the supersymmetry scale is low [45–51] but not vanishing [52–55] and the moduli stability in this context can be studied [56–61]. Another important mechanism called brane supersymmetry breaking has been extensively explored [62–67]. In these models, supersymmetry is non-linearly realized [68, 69] and the supersymmetry-breaking scale is the string scale in the open sector while the closed-string sector is insensitive to it. However, all these constructions suffer from uncancelled Neveu–Schwarz–Neveu–Schwarz (NS-NS) tadpoles due to the presence of anti-D-branes. Attempts to deal with these tadpoles have been pursued [70–73] but with limited applications. One can also make use of internal magnetic fields to break supersymmetry [74–76] but this option will not be evoked further in this thesis.

After an overview of the construction and key features of string theory presented in Chapter 1, the works presented in this manuscript are organized as a triptych. The first part of it in Chapter 2 concerns the very elaboration of supersymmetry-breaking mechanisms at the string-theory level. The proposed mechanism takes place in orientifold models and shows similarities with brane supersymmetry breaking. Crucially though, it avoids the usual NS-NS tadpoles and comes with a breaking scale that can either be the string scale or a compactification scale. A close look at the geometric interpretation of the mechanism as well as effective field-theory considerations will however reveal a soft breaking in the closed sector, *à la* Scherk–Schwarz. The chapter is based on the work [77], published during the thesis.

The second part of the triptych developed in Chapter 3 is about the moduli dependence of the one-loop potential typically generated by supersymmetry-breaking mechanisms. Such potentials can be independent on some scalars in which case these states remain moduli at one loop. However, they can also induce a one-loop mass squared that can be positive or negative. In the former case, the tree-level moduli are actually stabilized at one loop and in the latter case, a tachyonic instability is created and the vacuum around which perturbation theory is performed is not valid anymore.

We will perform such a stability analysis in the context of the type I string theory showing an $\mathcal{N} = 2 \to \mathcal{N} = 0$ spontaneous breaking of supersymmetry. The presence of a rich variety of moduli in the model will require the use of various techniques to establish their one-loop stability, ranging from Taylor expansion of the effective potential to the evaluation of genus-1 two-point correlation functions through arguments arising from the duality between the heterotic and type I string. The chapter is based on the works [59–61].

Eventually, the last part of the triptych presented in Chapter 4 treats the cosmological dynamics induced at one loop by supersymmetry breaking. Indeed, after implementation of a breaking at the string level and study of the one-loop potential, one generally does not have a true vacuum and the full cosmological dynamics should be taken into account. More precisely, no-scale models [78–81] are defined as classical models with spontaneously broken supersymmetry and a breaking scale that is a flat direction of the tree-level potential (hence the name "no-scale"). Such models are expected to be drastically disturbed by quantum effects and the generation of a one-loop potential. In specific cases, referred to as "super no-scale models", the potential is exponentially suppressed at one loop and the no-scale structure is preserved [45–47, 56, 57, 82–87]. In generic cases however, the time-dependence of the one-loop potential should be taken seriously and its backreaction on the cosmological equations of motion of the no-scale models carefully studied. We will study this backreaction and show that under certain conditions, a no-scale cosmological behaviour can effectively be reached asymptotically. The two first sections of the chapter are based on the works [43, 44]. In a third section based on the works [88, 89], we put forward a new mechanism to generate a dark-matter relic density in the cosmological story of the universe. This is done in a heterotic string context with spontaneously broken supersymmetry and with implementation of finite temperature. In specific setups, a cosmological attractor enforces the condensation of a modulus as the universe evolves, that gives a sudden mass to some states playing the role of dark-matter candidates. The moment when this phase transition occurs affects the standard scenario invoked for generating a relic density.

The appendix A gives some notations used in this document about characters and Jacobi theta functions while appendices B and C provide additional details about what is presented respectively in Chapters 3 and 4.

The publications produced during the thesis upon which this manuscript rests are attached at the very end of the manuscript.

1 Key ingredients of string theory

The goal of this chapter is to introduce string theory and related concepts that are explored in this thesis. After a brief overview about the construction of string theory and the various superstring theories, we discuss the main ingredient of this thesis that is supersymmetry breaking and more particularly the breaking by coordinate-dependent compactification. Eventually, we talk about cosmology and how string theory could help in this vast domain.

1.1 Foundations of string theory

This section recalls the definition of the relativistic superstring, its equations of motion, boundary conditions and constraints. The quantification procedure in light-cone gauge is then briefly reviewed. This section is strongly inspired by the most famous textbooks and lectures which introduce string theory and constitute permanent companions for the young string theorist [90–96].

1.1.1 The classical action of the relativistic string

The basic idea of string theory is to revisit what the degrees of freedom of fundamental particles are. The replacement of a pointlike description by a string-like one allows for internal vibrating modes associated to a new energy scale: The string scale. Formally, the relativistic particle of mass m is promoted to a relativistic string by generalizing its dynamics as a variational principle. As the particle action $S_{\text{pointlike}}$ is proportional to the invariant length of its trajectory $X^\mu(\tau)$ in spacetime parametrized by τ (called the *worldline*), the string one is proportional to the area spanned by the string while it propagates, called the *worldsheet*. The worldsheet is parametrized by an additional spacelike coordinate which we label by σ. The action thus becomes the following Nambu–Goto action [97, 98] S_{NG},

$$S_{\text{pointlike}} = -m \int \mathrm{d}\tau \sqrt{-g_{\mu\nu} \frac{\mathrm{d}X^\mu}{\mathrm{d}\tau} \frac{\mathrm{d}X^\nu}{\mathrm{d}\tau}} \quad \longrightarrow \quad S_{\text{NG}} = -T \int \mathrm{d}^2\sigma \sqrt{-h} \ , \tag{1.1.1}$$

where T denotes the *tension* of the string, $\mathrm{d}^2\sigma = \mathrm{d}\tau\mathrm{d}\sigma$ is the area element and h is the determinant of the induced metric on the worldsheet which is embedded in spacetime with coordinates $X^\mu(\tau, \sigma)$, $\mu \in \{0, \dots, d-1\}$. This metric is thus defined as the pullback of the spacetime metric $g_{\mu\nu}$ on the worldsheet submanifold,

$$h = \det(h_{\alpha\beta}) \qquad \text{and} \qquad h_{\alpha\beta} = g_{\mu\nu} \partial_\alpha X^\mu \partial_\beta X^\nu \ . \tag{1.1.2}$$

In units where $\hbar = c = 1$, the string tension T has the dimension of a mass squared and it can be expressed as the inverse of the *Regge slope* α' as $T = \frac{1}{2\pi\alpha'}$.

In the Nambu–Goto formalism, one directly finds and solves the equations of motion in terms of the embedding coordinates $X^\mu(\tau,\sigma)$. However, this formalism is not convenient for quantizing the theory and an equivalent one can be defined. It follows the same logic as for the relativistic particle where an auxiliary field can be introduced to define a new action. In this formalism, both the equations of motion for the auxiliary field and for the embedding coordinates must be worked out. If a particular expression for the auxiliary field is chosen *i.e.* for a particular gauge, the dynamics is given by the equations of motion of the embedding coordinates with the additional constraints imposed by the validity of the equations of motion of the auxiliary field at the particular gauge value. The string action $S_{\rm P}$ in this formalism is called *Polyakov action* or *sigma-model action* [99–101] and reads

$$S_{\rm P} = -\frac{T}{2}\int \mathrm{d}^2\sigma\sqrt{-h}h^{\alpha\beta}g_{\mu\nu}\partial_\alpha X^\mu\partial_\beta X^\nu \ , \tag{1.1.3}$$

where now the Minkowskian two-dimensional worldsheet metric $h_{\alpha\beta}$ plays the role of the auxiliary field and is thus no more defined as the pullback of the spacetime metric which however appears explicitly in the action. If one injects the equations of motion of the auxiliary metric into the Polyakov action, one recovers the Nambu–Goto description which shows that the two formalisms are equivalent.

The two local symmetries of the Polyakov action (1.1.3) that are reparametrization of the worldsheet coordinates τ and σ and Weyl transformations (rescaling of the worldsheet metric) can be used to completely gauge-fix $h_{\alpha\beta}$. If no topological obstruction prevents from it, it is convenient to fix the metric to the flat Minkowski one: $h_{\alpha\beta} = \eta_{\alpha\beta}$. Note that this gauge is called the *conformal gauge*. Worldsheet indices are thus raised and lowered with this flat metric and the action becomes

$$S = -\frac{T}{2}\int \mathrm{d}^2\sigma\partial^\alpha X^\mu\partial_\alpha X_\mu \ . \tag{1.1.4}$$

The constraints imposed by the equations of motions of the auxiliary metric after gauge fixing should not be forgotten. The variation of the action with respect to the metric defines the worldsheet energy-momentum tensor $T_{\alpha\beta}$ and the equations of motion impose it to vanish,

$$T_{\alpha\beta} \equiv -\frac{2}{T\sqrt{-h}}\frac{\delta S_{\rm P}}{\delta h^{\alpha\beta}} = 0 \ . \tag{1.1.5}$$

In the flat gauge, this constraint reads

$$\partial_\alpha X^\mu\partial_\beta X_\mu - \frac{1}{2}\eta_{\alpha\beta}\partial^\gamma X^\mu\partial_\gamma X_\mu = 0 \ . \tag{1.1.6}$$

The bosonic string discussed so far yields, after quantization, a theory without fermions and which in addition contains a tachyon. To remedy these issues, one can build the fermionic superstring in what is called the Ramond–Neveu–Schwarz (RNS) formalism [102, 103] by adding fermionic Majorana fields on the worldsheet $\psi^\mu(\tau,\sigma) \equiv \begin{pmatrix}\psi^\mu_- \\ \psi^\mu_+\end{pmatrix}$ which are vectors from the spacetime point of view. The superstring action in (super)conformal gauge is given by

$$S = -\frac{T}{2}\int \mathrm{d}^2\sigma\left(\partial^\alpha X^\mu\partial_\alpha X_\mu + \alpha'\overline{\psi}^\mu\gamma^\alpha\partial_\alpha\psi_\mu\right) \ , \tag{1.1.7}$$

where the matrices γ^α, $\alpha = 0, 1$, are two-dimensional Dirac matrices that satisfy the Clifford algebra $\{\gamma^\alpha,\gamma^\beta\} = 2\eta^{\alpha\beta}$ and the Dirac conjugate $\overline{\psi}^\mu$ is defined as $\overline{\psi}^\mu = i\gamma^0\psi^{\mu\dagger}$. Varying the action with

respect to the bosonic and fermionic fields, one finds the equations of motion, which are simply the usual two-dimensional wave equation and Dirac equation:

$$\partial_\alpha \partial^\alpha X^\mu = 0 \qquad \text{and} \qquad \gamma^\alpha \partial_\alpha \psi_\mu = 0 \ . \tag{1.1.8}$$

Like for the bosonic string, one should not forget the constraints coming from the vanishing of the energy-momentum tensor which read

$$\partial_\alpha X^\mu \partial_\beta X_\mu - \frac{1}{2}\eta_{\alpha\beta}\partial^\gamma X^\mu \partial_\gamma X_\mu + \frac{\alpha'}{2}\bar{\psi}^\mu \gamma_\alpha \partial_\beta \psi_\mu + \frac{\alpha'}{2}\bar{\psi}^\mu \gamma_\beta \partial_\alpha \psi_\mu = 0 \ . \tag{1.1.9}$$

Actually, other constraints need to be imposed. Note that the superstring action (1.1.7) is invariant under global supersymmetry transformations to which a supercurrent is associated. In this setup, nothing requires the vanishing of this supercurrent but in a more fundamental construction of the superstring action which possesses local supersymmetry [104–106], this cancellation arises as the equations of motion of a gravitino gauge field. Eventually, the additional constraints are

$$\gamma^\beta \gamma_\alpha \psi^\mu \partial_\beta X_\mu = 0 \ . \tag{1.1.10}$$

1.1.2 Boundary conditions and mode expansion

The equations of motion (1.1.8) and the constraints (1.1.9) and (1.1.10) need to be supplemented by appropriate boundary conditions for the system to be fully defined. For the embedding bosonic coordinates, one can talk about *closed strings* or *open strings* and we fix the range of the σ parameter to be $[0, \pi]$ for both kinds of strings. The closed strings satisfy a periodicity condition under translation of the spacelike coordinate σ while for each end at $\sigma = \sigma_{\rm e} \equiv 0, \pi$, the open strings can verify either Neumann or Dirichlet boundary conditions. The possible bosonic boundary conditions are then

$$\underline{\text{Closed strings:}}\ X(\tau, \sigma + \pi) = X(\tau, \sigma) \ , \ \underline{\text{Open strings:}}\ \begin{cases} \text{Neumann: } \partial_\sigma X^\mu(\tau,\sigma)|_{\sigma=\sigma_{\rm e}} = 0 \\ \text{Dirichlet: } \ X(\tau, \sigma_{\rm e}) = \text{cst} \end{cases} . \tag{1.1.11}$$

The Dirichlet conditions which break Lorentz invariance will be discussed later when open-string theories and D-branes are introduced.

From the fermionic fields point of view, several Lorentz-preserving conditions exist for which the boundary terms arising when varying the superstring action vanish. These conditions are expressed in terms of the Majorana components ψ_-^μ and ψ_+^μ which describe respectively left-moving and right-moving waves. For closed strings, ψ_-^μ and ψ_+^μ can independently satisfy periodicity (*Ramond boundary condition*) or antiperiodicity (*Neveu–Schwarz boundary condition*) under the translation $\sigma \to \sigma + \pi$. This naturally gives rise to four sectors: Ramond–Ramond (R-R), Ramond–Neveu–Schwarz (R-NS), Neveu–Schwarz–Ramond (NS-R) and Neveu–Schwarz–Neveu–Schwarz (NS-NS). For open strings, fixing without loss of generality $\psi_-^\mu(\tau,\sigma)|_{\sigma=0} = \psi_+^\mu(\tau,\sigma)|_{\sigma=0}$, two inequivalent choices arise if we choose the same condition at the other end $\sigma = \pi$ (*Ramond boundary condition*) or its opposite (*Neveu–Schwarz boundary condition*). The possible boundary conditions are thus

$$\underline{\text{Closed strings:}}\ \begin{cases} \text{R-R:} & \psi_-^\mu(\tau,\sigma+\pi) = \psi_-^\mu(\tau,\sigma) \\ & \psi_+^\mu(\tau,\sigma+\pi) = \psi_+^\mu(\tau,\sigma) \\ \text{NS-R:} & \psi_-^\mu(\tau,\sigma+\pi) = -\psi_-^\mu(\tau,\sigma) \\ & \psi_+^\mu(\tau,\sigma+\pi) = \psi_+^\mu(\tau,\sigma) \end{cases} \quad \begin{cases} \text{R-NS:} & \psi_-^\mu(\tau,\sigma+\pi) = \psi_-^\mu(\tau,\sigma) \\ & \psi_+^\mu(\tau,\sigma+\pi) = -\psi_+^\mu(\tau,\sigma) \\ \text{NS-NS:} & \psi_-^\mu(\tau,\sigma+\pi) = -\psi_-^\mu(\tau,\sigma) \\ & \psi_+^\mu(\tau,\sigma+\pi) = -\psi_+^\mu(\tau,\sigma) \end{cases}$$

$$\underline{\text{Open strings:}} \quad \begin{cases} \text{Ramond (R):} & \psi_-^\mu(\tau,\sigma)\big|_{\sigma=\pi} = \psi_+^\mu(\tau,\sigma)\big|_{\sigma=\pi} \\ \text{Neveu–Schwarz (NS):} & \psi_-^\mu(\tau,\sigma)\big|_{\sigma=\pi} = -\,\psi_+^\mu(\tau,\sigma)\big|_{\sigma=\pi} \end{cases} . \tag{1.1.12}$$

Defining the *light-cone coordinates* $\sigma^\pm \equiv \tau \pm \sigma$ whose associated derivative read $\partial_\pm = \frac{1}{2}(\partial_\tau \pm \partial_\sigma)$, the equations of motion (1.1.8) become

$$\partial_+\partial_- X^\mu = 0 \qquad \text{and} \qquad \begin{cases} \partial_+\psi_- = 0 \\ \partial_- + = 0 \end{cases} . \tag{1.1.13}$$

Together with the various boundary conditions, they give rise to different mode expansions of the bosonic and fermionic fields. Let us start with the bosonic ones. The equations of motion imply that the most general form for $X^\mu(\tau,\sigma)$ is a sum of *right-moving* and *left-moving* waves that depend only on σ^- and σ^+ respectively,

$$X^\mu(\tau,\sigma) = X_{\rm R}^\mu(\tau-\sigma) + X_{\rm L}^\mu(\tau+\sigma) . \tag{1.1.14}$$

Expanding this solution in Fourier modes yields the following mode expansions for the closed string and the open string (assuming Neumann boundary conditions in all directions)

$$\underline{\text{Closed strings:}} \quad \begin{cases} X_{\rm R}^\mu(\tau-\sigma) = \frac{1}{2}x^\mu + \alpha' p^\mu(\tau-\sigma) + i\sqrt{\frac{\alpha'}{2}}\sum_{n\neq 0}\frac{\alpha_n^\mu}{n}e^{-2in(\tau-\sigma)} \\ X_{\rm L}^\mu(\tau+\sigma) = \frac{1}{2}x^\mu + \alpha' p^\mu(\tau+\sigma) + i\sqrt{\frac{\alpha'}{2}}\sum_{n\neq 0}\frac{\tilde\alpha_n^\mu}{n}e^{-2in(\tau+\sigma)} \end{cases} , \tag{1.1.15}$$

$$\underline{\text{Open strings:}} \quad X^\mu(\tau,\sigma) = x^\mu + 2\alpha' p^\mu \tau + i\sqrt{2\alpha'}\sum_{n\neq 0}\frac{\alpha_n^\mu}{n}e^{-in\tau}\cos(n\sigma) .$$

In these expressions, x^μ and p^μ which appear as integration constants are the position and momentum of the string center of mass. For the closed string, there are two sets of Fourier coefficients, α_n^μ and $\tilde\alpha_n^\mu$ and only one for the open string. A reality condition on the coordinate X^μ implies that $\alpha_{-n}^\mu = (\alpha_n^\mu)^*$ and $\tilde\alpha_{-n}^\mu = (\tilde\alpha_n^\mu)^*$. It is convenient to define coefficients for $n=0$ as follows: $\alpha_0^\mu = \tilde\alpha_0^\mu \equiv \sqrt{\frac{\alpha'}{2}}p^\mu$ for the closed string and $\alpha_0^\mu \equiv \sqrt{2\alpha'}p^\mu$ for the open string.

Let us turn to the fermionic fields. For closed strings, ψ_-^μ and ψ_+^μ can be independently periodic or antiperiodic. For periodic boundary conditions (R), we denote the Fourier coefficients by d_n^μ while we write b_r^μ for antiperiodic fields (NS). We add tildes on these coefficients for the right-movers ψ_+^μ. The idea is that the "d coefficients" will come with integer indices n while the "b coefficients" will come with half-integer indices. For open strings, the coefficients d_n^μ appear both in ψ_-^μ and ψ_+^μ for Ramond boundary conditions while they are replaced by b_r^μ for Neveu–Schwarz conditions.

$$\underline{\text{Closed strings:}} \quad \begin{cases} & \text{(R)} & \text{(NS)} \\ \text{Right-movers: } \psi_-^\mu(\tau,\sigma) = \displaystyle\sum_{n\in\mathbb{Z}} d_n^\mu e^{-2in(\tau-\sigma)} & \psi_-^\mu(\tau,\sigma) = \displaystyle\sum_{r\in\mathbb{Z}+\frac{1}{2}} b_r^\mu e^{-2ir(\tau-\sigma)} \\ \text{Left-movers: } \psi_+^\mu(\tau,\sigma) = \displaystyle\sum_{n\in\mathbb{Z}} \tilde{d}_n^\mu e^{-2in(\tau+\sigma)} & \psi_+^\mu(\tau,\sigma) = \displaystyle\sum_{r\in\mathbb{Z}+\frac{1}{2}} \tilde{b}_r^\mu e^{-2ir(\tau+\sigma)} \end{cases}$$

$$\underline{\text{Open strings:}} \quad \begin{cases} \text{R:} \quad \psi_-^\mu(\tau,\sigma) = \frac{1}{\sqrt{2}} \displaystyle\sum_{n\in\mathbb{Z}} d_n^\mu e^{-in(\tau-\sigma)} & \text{and} \quad \psi_+^\mu(\tau,\sigma) = \frac{1}{\sqrt{2}} \displaystyle\sum_{n\in\mathbb{Z}} d_n^\mu e^{-in(\tau+\sigma)} \\ \text{NS:} \ \psi_-^\mu(\tau,\sigma) = \frac{1}{\sqrt{2}} \displaystyle\sum_{r\in\mathbb{Z}+\frac{1}{2}} b_r^\mu e^{-ir(\tau-\sigma)} & \text{and} \quad \psi_+^\mu(\tau,\sigma) = \frac{1}{\sqrt{2}} \displaystyle\sum_{r\in\mathbb{Z}+\frac{1}{2}} b_r^\mu e^{-inr(\tau+\sigma)} \cdot \end{cases} \tag{1.1.16}$$

The Majorana conditions on the fermionic fields implies $d_{-n}^\mu = (d_n^\mu)^*$, $b_{-r}^\mu = (b_r^\mu)^*$ and similar relations for coefficients with tildes.

Inserting these mode expansions into the energy-momentum tensor and supercurrent, one obtains the Fourier expansion of these currents whose vanishing must be ensured by the vanishing of each individual Fourier coefficient. The energy-momentum coefficients are denoted L_n and are further split into a bosonic and a fermionic contribution corresponding to the first and last two terms in (1.1.9) respectively. We thus write $L_n \equiv L_n^{(\mathrm{b})} + L_n^{(\mathrm{f})}$. The bosonic part is given by (for closed strings, all the following formulas are to be duplicated upon replacement of the coefficients by their tilde version)

$$L_n^{(\mathrm{b})} = \frac{1}{2} \sum_{m\in\mathbb{Z}} \alpha_{-m} \cdot \alpha_{n+m} \quad \text{for} \quad n \in \mathbb{Z} \ , \tag{1.1.17}$$

where the scalar product stands for a contraction of the Lorentz indices with the flat spacetime metric $\eta_{\mu\nu}$. The expressions of the fermionic part along with the supercurrent coefficients depend on the sector (Ramond or Neveu–Schwarz) under consideration. For Ramond fields, the supercurrent coefficients are denoted by F_n and they are written G_r for Neveu–Schwarz expansions. They are

$$\begin{aligned} &\underline{\text{R sector:}} \quad L_n^{(\mathrm{f})} = \frac{1}{2} \sum_{m\in\mathbb{Z}} \left(m + \frac{n}{2}\right) d_{-m} \cdot d_{n+m}, \ n \in \mathbb{Z} \quad \text{and} \quad F_n = \sum_{m\in\mathbb{Z}} \alpha_{-m} \cdot d_{n+m}, \ n \in \mathbb{Z} \\ &\underline{\text{NS sector:}} \quad L_n^{(\mathrm{f})} = \frac{1}{2} \sum_{r\in\mathbb{Z}+\frac{1}{2}} \left(r + \frac{n}{2}\right) b_{-r} \cdot b_{n+r}, \ n \in \mathbb{Z} \quad \text{and} \quad G_r = \sum_{m\in\mathbb{Z}} \alpha_{-m} \cdot b_{r+m}, \ r \in \mathbb{Z} + \frac{1}{2} \end{aligned} \tag{1.1.18}$$

The zero mode L_0 and its counterpart $\tilde{L}_0$ for closed strings are important since they involve $p_\mu p^\mu$ in the $m = 0$ term of the sum. This means that their vanishing gives a formula for the mass of the strings. We will write these formulas in the next subsection after quantization of the theory.

1.1.3 Quantization and spectrum

A first challenge for the construction of string theory is to consistently quantify the relativistic theory described so far. Here we will only review the fastest method to get to the spectrum which is called *light-cone quantization*. It consists in fixing all the remaining gauge degrees of freedom available to obtain the physical solutions before quantizing these solutions.

The starting point is to realize that when going to flat gauge by making use of the reparametrization and Weyl invariance of the Polyakov action, there is still some remaining gauge invariance. This means that there is an unphysical redundancy in the field solutions that we wrote. The remaining freedom lies in the particular globally well-defined reparametrizations of the worldsheet coordinates that only induce a rescaling of the flat worldsheet metric. These *conformal* transformations are symmetries since the induced rescaling can be undone by a Weyl transformation. More specifically, any change of coordinates which just redefines σ^+ as a function of itself and independently σ^- as a function of itself also, only produces a rescaling of the flat metric.

We define the spacetime *light-cone coordinates* X^+ and X^- and the *light-cone fermions* ψ^+ and ψ^- as[1]

$$X^\pm \equiv \frac{X^0 \pm X^{d-1}}{\sqrt{2}} \quad \text{and} \quad \psi^\pm \equiv \frac{\psi^0 \pm \psi^{d-1}}{\sqrt{2}} \ . \tag{1.1.19}$$

We can make full use of the residual gauge freedom to fix the values of X^+ and ψ^+ to

$$X^+ = x^+ + \alpha' p^+ \tau \quad \text{and} \quad \psi^+ = 0 \ , \tag{1.1.20}$$

where x^+ and p^+ are integration constants. The constraints then completely determine the expressions of X^- and ψ^- in terms of the other fields. The only remaining sets of non-trivial Fourier coefficients are thus those associated with the *transverse* directions X^i, $i \in \{1, \dots, d-2\}$.

It is then possible to quantize the theory using the standard canonical way. In the classical theory, for transverse directions, the momenta P^i associated to the bosonic fields X^i and Π^i associated to the fermionic ones ψ^i can be defined in the usual way from the superstring action (1.1.7),

$$P^i(\tau,\sigma) \equiv \frac{\delta S}{\delta(\partial_\tau X_i)} = T\partial_\tau X^i \ , \quad \Pi^i_+ \equiv \frac{\delta S}{\delta(\partial_\tau \psi_{+,i})} = -\frac{i}{4\pi}\psi^i_+ \ , \quad \Pi^i_- = -\frac{i}{4\pi}\psi^i_- \ . \tag{1.1.21}$$

They obey canonical commutation and anticommutation rules in terms of the Poisson brackets which are promoted to true commutators and anticommutators on the fields that are themselves promoted to operators. The only non-trivial relations are

$$\left[P^i(\tau,\sigma), P^j(\tau,\sigma)\right] = i\delta^{ij}\delta(\sigma-\sigma') \quad \text{and} \quad \left\{\psi^i_\pm(\tau,\sigma), \psi^j_\pm(\tau,\sigma')\right\} = \pi\delta^{ij}\delta(\sigma-\sigma') \ . \tag{1.1.22}$$

Inserting the mode expansions of the fields, these commutation and anticummutation relations translates into rules for the various Fourier coefficients that are promoted to operators called *oscillators*. The non-trivial rules are (for closed strings, the same relations hold for tilde operators)

$$\left[\alpha^i_n, \alpha^j_m\right] = n\delta_{n+m,0}\delta^{ij} \ , \left\{b^i_r, b^j_s\right\} = \delta_{r+s,0}\delta^{ij} \ , \left\{d^i_n, d^j_m\right\} = \delta_{n+m,0}\delta^{ij} \ . \tag{1.1.23}$$

The rescaling $\alpha^i_n \to \frac{\alpha^i_n}{\sqrt{n}}$ together with the definitions $\alpha^{i\dagger}_n \equiv \frac{\alpha^i_{-n}}{\sqrt{n}}$ for $n>0$, $\tilde{\alpha}^{i\dagger}_n \equiv \frac{\tilde{\alpha}^i_{-n}}{\sqrt{n}}$ for $n>0$, $b^{i\dagger}_r \equiv b^i_{-r}$ for $r>0$ and $d^{i\dagger}_n \equiv d^i_{-n}$ for $n>0$ yield usual algebras of raising and lowering operators. We can thus build the spectrum starting from a vacuum state annihilated by all the lowering operators and act on it with raising operators. The vacua $|0\rangle_{\rm R}$ and $|0\rangle_{\rm NS}$ in the R and NS sectors are such that

$$\begin{aligned} &\alpha^i_n |0\rangle_{\rm R} = d^i_n |0\rangle_{\rm R} = 0 \qquad \text{for} \quad n>0 \ , \\ &\alpha^i_n |0\rangle_{\rm NS} = b^i_r |0\rangle_{\rm NS} = 0 \qquad \text{for} \quad n,r>0 \ , \end{aligned} \tag{1.1.24}$$

[1] When the plus or minus index is subscripted, as it was the case so far, this indicates the components of the worldsheet spinors while when it is superscripted it denotes the light-cone definition of the fields.

and the raising operators are the negative modes. For closed strings, the same relations must hold for tilde operators. The vacua carry a momentum which is an eigenvalue of the operator p^μ and up to this momentum, the NS vacuum is unique and describes a zero-spin state. The raising operators being Lorentz vectors, all states built from the NS vacuum are spacetime bosons. There is a subtlety concerning the R vacuum since it turns out that the action of the operator d_0^i does not change the mass of the state. The explanation for this is that the R vacuum is actually a spacetime fermion carrying irreducible spinor quantum numbers in $d-2$ dimensions. Because the raising operators are Lorentz vectors, the states arising in the R sector are consequently spacetime fermions. Note that for open strings, extra quantum numbers called *Chan-Paton factors* [107] that are carried by the ends of the string can consistently be added. We will come back to this later when we study more deeply the open-string theories.

To finalize the quantization procedure, the constraints must be imposed. Recall that they were given classically by the vanishing of the Fourier coefficients of the energy-momentum tensor and supercurrent. The coefficients are now operators which verify commutation rules of a *super-Virasoro algebra*. They are defined to be normal ordered, with the raising operators on the left and the lowering ones on the right. This produces an ambiguity for the zero mode L_0 which is tackled by adding extra constants $a_{\rm R}$ and $a_{\rm NS}$ in the corresponding sectors (the same formulas with tildes define $\tilde{L}_0$),

$$\begin{aligned} &\underline{\text{R sector}}: \qquad L_0 \equiv \frac{\alpha_0^2}{2} + \sum_{n=1}^{+\infty} \alpha_{-n}\cdot\alpha_n + \sum_{n=0}^{+\infty} n d_{-n}\cdot d_n - a_{\rm R}\ , \\ &\underline{\text{NS sector}}: \qquad L_0 \equiv \frac{\alpha_0^2}{2} + \sum_{n=1}^{+\infty} \alpha_{-n}\cdot\alpha_n + \sum_{r=\frac{1}{2}}^{+\infty} r b_{-r}\cdot b_r - a_{\rm NS}\ . \end{aligned} \tag{1.1.25}$$

The constraints then amount to impose the physical states to be annihilated by the positive modes L_n and F_n, $n\geq 0$ in the R sector and L_n, $n\geq 0$ and G_r, $r>0$ in the NS sector. As mentioned earlier, the L_0 constraint gives a formula for the mass squared M^2 of the states since it involves $p_\mu p^\mu = -M^2$. Thanks to the light-cone gauge, everything can be expressed in terms of the transverse oscillators and the result is (there is a factor 4 between open and closed strings due to the definition of α_0 which is different)

$$\begin{aligned} &\underline{\text{R sector}}: \qquad \frac{\alpha'}{4}M^2_{\rm closed} = \alpha' M^2_{\rm open} = \sum_{n=1}^{+\infty} \alpha^i_{-n}\alpha^i_n + \sum_{n=0}^{+\infty} n d^i_{-n} d^i_n - a_{\rm R}\ , \\ &\underline{\text{NS sector}}: \qquad \frac{\alpha'}{4}M^2_{\rm closed} = \alpha' M^2_{\rm open} = \sum_{n=1}^{+\infty} \alpha^i_{-n}\alpha^i_n + \sum_{r=\frac{1}{2}}^{+\infty} r b^i_{-r} b^i_r - a_{\rm NS}\ . \end{aligned} \tag{1.1.26}$$

For closed strings, the same formulas hold for the sets of tilde oscillators. This means that the right-hand sides are equal to the same expressions with tildes. This is called the *level-matching condition* since it ensures that the number of excitations are the same for left- and right-movers. The values of $a_{\rm R}$, $a_{\rm NS}$ and the number of spacetime dimensions d are constrained by the requirement to obtain in the end a Lorentz invariant theory, which was not guaranteed by the light-cone gauge since it hides this symmetry. Several arguments can be invoked to find these values and they all yield the same result: $a_{\rm R}=0$, $a_{\rm NS}=\frac{1}{2}$ and $d=10$. Note that in the case of the bosonic string, the constraint on the number of dimensions is $d=26$.

In the R sector, because $a_{\rm R} = 0$, the ground state (which is a spacetime fermion) is massless. The physical excited states are massive and are built by acting with the transverse oscillators α^i_{-n} and d^i_{-n}. In the NS sector, the ground state is a scalar and has a negative mass squared because of $a_{\rm NS} = \frac{1}{2}$. Contrary to the bosonic string theory, we will see that there is a consistent way to project out this tachyon. The first excited state is a massless vector obtained with the action of $b^i_{-1/2}$ on the ground state.

For the closed string, remember that there are four sectors depending on the choice R or NS both for left- and right-moving oscillators. The states are thus tensor products of the two sides which then decompose into SO(8) representations (we will give the precise decomposition in the next section because some work remains to be done to obtain fully consistent theories). The ground states in the NS-NS, NS-R and R-NS are tachyons while the ground state in the R-R sector is massless. The first excited state in the NS-NS sector obtained with the action of $b^i_{-1/2}$ and $\tilde{b}^i_{-1/2}$ is massless and contains among other things (see next section) the graviton. The first excited states in the R-NS and NS-R sectors obtained with the action of $b^i_{-1/2}$ or $\tilde{b}^i_{-1/2}$ in the NS side, are massless and contain a gravitino.

1.2 The different superstring theories

Now that we have laid the basics of superstring theory and found its spectrum, we can go further and discover the five types of string theories. For each one of them, we will discuss the one-loop vacuum amplitudes, objects that are highly important in this thesis.

1.2.1 The one-loop torus amplitude

The *one-loop vacuum amplitudes* are very important objects in string theory and lie at the core of this thesis. They are the analogue of their field theory counterparts which are given by Feynman diagrams simply describing a loop of particles. Of course, the very values of the one-loop vacuum amplitudes are important since they induce a quantum potential and possibly a cosmological constant. But besides from their numerical values, it turns out that the structure of the partition functions contains a lot of information about the spectrum of the theory.

In field theory, the one-loop vacuum amplitude captures the contributions of the whole spectrum to the loop. Each contribution comes as an integral over a Schwinger parameter t weighted by an exponential depending on the squared mass M^2 of the state under consideration. In a theory with bosonic and fermionic degrees of freedom, the sum over the spectrum is a supertrace and an ultraviolet cutoff ϵ should be introduce to account for the divergence at low Schwinger parameter. Denoting V the spacetime volume, the one-loop vacuum energy schematically takes the following form

$$\mathcal{V}_{1-\text{loop}} \propto \int_\epsilon^{+\infty} \frac{\mathrm{d}t}{t^{1+\frac{D}{2}}} \mathrm{Str}\left(e^{-tM^2}\right) \ . \tag{1.2.1}$$

In a closed-string theory, the loops undergone by the states are not circles anymore but tori representing the closed-strings going back to themselves. The diffeomorphism and Weyl invariance of the theory can be used to map any torus metric to a flat one but it turns out that several conformally inequivalent flat metrics exist. It is then natural to sum over all these inequivalent metrics to obtain the vacuum energy. More specifically, a flat torus can be defined as an identification on the complex plane which depends on a complex parameter $\tau \equiv \tau_1 + i\tau_2$ called the *Teichmüller parameter* or

modulus of the torus[2],

$$\text{Torus: } \{z \in \mathbb{C} \text{ with the identifications } z \equiv z+1,\ z \equiv z+\tau\}\ . \tag{1.2.2}$$

The important thing is to determine the *moduli space i.e.* which Teichmüller parameters give conformally inequivalent tori to sum only on them. Given a modulus τ, two *modular transformations* T and S generate the same torus:

$$T:\ \tau \to \tau+1 \qquad \text{and} \qquad S:\ \tau \to -\frac{1}{\tau}\ . \tag{1.2.3}$$

The group generated by these transformations is $\mathrm{PSL}(2,\mathbb{Z})$ so that the moduli space is given by the complex plane modded by this group. This defines the *fundamental domain* $\mathcal{F}$ over which we will integrate and it reads

$$\mathcal{F}:\ \left\{\tau \in \mathbb{C} \text{ such that } |\tau| \geq 1 \text{ and } \mathrm{Re}\,\tau \in \left[-\frac{1}{2},\frac{1}{2}\right]\right\}\ . \tag{1.2.4}$$

The fact that the region near $\tau = 0$ is not present in the fundamental domain implies that no ultraviolet divergence can arise unlike in field theory. In the end, thanks to the mass formulas (1.1.26), the vacuum energy involves four contributions coming from the four sectors. For example, in the NS-NS sector, the contribution $\mathcal{T}_{\text{NS-NS}}$ is given by

$$\mathcal{T}_{\text{NS-NS}} \equiv \int_{\mathcal{F}} \frac{\mathrm{d}^2\tau}{\tau_2^{1+\frac{d}{2}}} \mathrm{Str}_{\text{NS-NS}}\, q^{\sum_{n=1}^{+\infty}\alpha^i_{-n}\alpha^i_n + \sum_{r=\frac{1}{2}}^{+\infty} r b^i_{-r} b^i_r - \frac{1}{2}} \bar{q}^{\sum_{n=1}^{+\infty}\tilde{\alpha}^i_{-n}\tilde{\alpha}^i_n + \sum_{r=\frac{1}{2}}^{+\infty} r \tilde{b}^i_{-r} \tilde{b}^i_r - \frac{1}{2}}\ , \tag{1.2.5}$$

where we defined $q = e^{2i\pi\tau}$ and $\mathrm{d}^2\tau = \mathrm{d}\tau_1\mathrm{d}\tau_2$. The integral over τ_1 implements the level-matching condition and the integral over τ_2 is the analogue of the integral over the Schwinger parameter t in field theory but without any ultraviolet divergence. Note that compared to t, τ_2 is scaled with a factor $(\alpha'\pi)^{-1}$.

To write things in a more compact way, we redefine L_0 and $\tilde{L}_0$ to be those of the Conformal Field Theory (CFT) language. They only count the transverse oscillators acting on the ground state and the R vacuum has conformal weight 1/2. Central charges must be taken into account in the trace so that the full torus partition function $\mathcal{T}$ is expressed like

$$\mathcal{T} \equiv \int_{\mathcal{F}} \frac{\mathrm{d}^2\tau}{\tau_2^{1+\frac{d}{2}}} \mathrm{Str}\left(q^{L_0-\frac{1}{2}} \bar{q}^{\tilde{L}_0-\frac{1}{2}}\right)\ , \tag{1.2.6}$$

where it is understood that the trace runs over the four sectors.

1.2.2 Type IIA and IIB

As we said in the previous section, the superstring spectrum contains an undesired tachyon in the NS sector. More generally, it can be shown that the spectrum as a whole is not consistent with modular invariance of the one-loop torus amplitude. Moreover, the spectrum has another problem: It is not spacetime supersymmetric as it should be since it contains a massless gravitino, the gauge field of local supersymmetry. To solve these problems and obtain consistent spectra, without tachyons and supersymmetric in the ten-dimensional spacetime, we need to apply the Gliozzi–Scherk–Olive

[2]Note that the notation is the same but it has nothing to do with the timelike worldsheet coordinate τ.

(GSO) projection [108, 109]. In the NS sector, it consists in keeping only states for which the number of b-oscillators is odd. This obviously projects out the tachyon while keeping the massless state. Some massive states disappear from the spectrum if they correspond to the action of an even number of b-oscillators. In the R sector, the projection counts the number of d-oscillators and is coupled to the chirality operator in ten dimensions. At the massless level, this amounts to choose (equivalently) the fermionic ground state to have a definite positive or negative Weyl chirality in ten dimensions. It can be shown that such a projection yields a spectrum that contains an equal number of bosonic and fermionic on-shell degrees of freedom at all mass levels. Moreover, in the Green–Schwarz formalism where spacetime supersymmetry is manifest, it is shown that after the GSO projection, supersymmetry is indeed preserved [104–106].

Two consistent closed-string theories can be obtained from the projection. If the same Weyl chirality of the ground state is chosen both for left and right oscillators, this gives the *type IIB theory*. On the contrary, if opposite chiralities are chosen, this defines the *type IIA theory*. After the GSO projection, the massless NS-NS sectors of the two theories are identical and contain, in terms of SO(8) representations, the dilaton scalar, an antisymmetric two-form gauge field and the spin two graviton which is symmetric and traceless. The NS-R and R-NS sectors each contain a spin 3/2 Majorana-Weyl gravitino and the spin 1/2 Majorana-Weyl dilatino. In this sector, the difference between the two theories lies in the chirality of the gravitinos: They are the same in type IIB and are opposite in type IIA. In the R-R sector, one finds a one-form and a three-from gauge fields in type IIA and a scalar, a two-form and a self-dual four-form gauge fields in type IIB.

From the spectrum in each sector, one can compute explicitly the supertraces in the partition function (1.2.6) for the type IIA and IIB theories. The conventions used in this thesis for the SO(8) characters, the Dedekind function and the Jacobi theta functions can be found in Appendix A. The torus partition functions are

$$\text{Type IIA: } \mathcal{T} = \int_{\mathcal{F}} \frac{\mathrm{d}^2\tau}{\tau_2^6} \left(\frac{V_8 - C_8}{\eta^8}\right)\left(\frac{\bar{V}_8 - \bar{S}_8}{\bar{\eta}^8}\right) \ , \quad \text{Type IIB: } \mathcal{T} = \int_{\mathcal{F}} \frac{\mathrm{d}^2\tau}{\tau_2^6} \left|\frac{V_8 - S_8}{\eta^8}\right|^2 \ , \tag{1.2.7}$$

in which the left-right symmetry of type IIB and the asymmetry of type IIA are explicit. The expansions of the characters V_8 and S_8 with respect to q tell us the number of bosonic and fermionic degrees of freedom at each mass level (they are of course equal thanks to supersymmetry). In particular, at the massless level we have

$$\frac{V_8}{\eta^8} = \frac{S_8}{\eta^8} = \frac{C_8}{\eta^8} = 8 + \mathcal{O}(q) \ , \tag{1.2.8}$$

from which we count $8^2 + 8^2 = 128$ bosonic and fermionic degrees of freedom. This matches the particle content of the theories displayed earlier. Indeed, on-shell, the NS-NS sector yields $\frac{8\times 9}{2} - 1 = 35$ (graviton traceless) $+\frac{8\times 7}{2} = 28$ (two-form) $+1$ (dilaton) $= 64$ degrees of freedom. The R-R sector gives $\frac{8\times 7\times 6}{6} = 56$ (three-form) $+8$ (one-form) $= 64$ for type IIA and $\frac{8\times 7\times 6\times 5}{24}/2 = 35$ (self-dual four-form) $+\frac{8\times 7}{2} = 28$ (two-form) $+1$ (scalar) $= 64$ for type IIB. This gives the 128 bosonic degrees of freedom for the two theories. The NS-R and R-NS sectors give together 2×56 (two Majorana-Weyl spin 3/2) $+2 \times 8$ (two Majorana-Weyl spin 1/2) $= 128$ fermionic degrees of freedom.

1.2.3 Non-abelian gauge groups

In the ten-dimensional type IIA and IIB superstring theories, there is no non-abelian gauge symmetries. Generating non-abelian gauge groups is crucial since we ideally want to recover the standard model at low energies which involves the gauge group $\mathrm{SU}(3)\times\mathrm{SU}(2)\times\mathrm{U}(1)$. Let us mention various strategies to generate non-abelian gauge groups in string theory.

- Toroidal compactification of the bosonic string theory generically leads to abelian U(1) gauge factors coming from the dimensional reduction of the background spacetime metric and antisymmetric tensor. However, a pure stringy effect called *symmetry enhancement* can occur. It has the effect of producing additional gauge bosons for particular values of the background fields. This means that at particular points in the moduli space of the compactification, an abelian U(1) factor is enhanced to a non-abelian group. The simplest example arises in compactification on a single circle where a $\mathrm{U}(1)\times\mathrm{U}(1)$ becomes $\mathrm{SU}(2)\times\mathrm{SU}(2)$ if the radius is the *self-dual radius* $\sqrt{\alpha'}$. One can understand why this is a pure stringy effect because the additional massless states have non-trivial winding numbers which are themselves characteristic to strings. At first sight, this seems to be an efficient way for generating non-abelian groups but it turns out that such symmetry enhancements are impossible in the superstring formalism where the supergravity multiplets cannot be enlarged. The idea to combine both the bosonic and fermionic frameworks to benefit from both the symmetry enhancement mechanism as well as the superstring features leads to the *heterotic string theories* [110–112] whose description is given in the next subsection. The heterotic string is the framework inside which cosmological considerations and moduli dynamics have been worked out during this thesis (see Chapter 4).

- Actually, away from the enhancement points, the generic U(1) factors that arise in toroidal compactifications reflect the symmetries of the internal space itself (in this case a torus) which are abelian. Other compact spaces like spheres for example produce non-abelian gauge symmetries at generic points of the moduli space.

- Another possibility for producing non-abelian symmetries is to introduce *Chan-Paton factors* [107] for open strings. These are non-dynamical degrees of freedom carried by the ends of the strings which are attached to *D-branes*. The rich variety of open-string theories constitutes the playground for some of the works done in the thesis that are presented in Chapters 2 and 3. The construction and features of open-string theories are described just after the heterotic string.

1.2.4 The heterotic string theories

The heterotic string [110–112] is a peculiar closed-string theory which uses at the same time the 26-dimensional bosonic framework for the left-movers and the 10-dimensional fermionic description for the right-movers. In its *bosonic construction* (there is also an equivalent *fermionic construction*), in addition to the 10 usual left-moving coordinates $X^\mu_{\mathrm{L}}(\tau+\sigma)$, $\mu\in\{0,\dots,10\}$, we introduce 16 compact coordinates $X^I_{\mathrm{L}}(\tau+\sigma)$, $I\in\{10,\dots,25\}$ which describe a 16-dimensional torus T^{16}. As evoked in the previous subsection, a non-abelian gauge structure can come from the compact space for left-movers thanks to enhancements. Crucially, the constraint of modular invariance of the ten-dimensional theory drastically reduces the consistent possibilities for the allowed lattice of momenta along the torus T^{16} (the lattice must be even and self-dual). As a result, in ten dimensions, the generic

$\mathrm{U}(1)^{16}$ gauge structure associated to the torus T^{16} is automatically enhanced to either $\mathrm{Spin}(32)/\mathbb{Z}_2$ or $\mathrm{E}_8 \times \mathrm{E}_8$. This means that the moduli space is only composed of two points corresponding to the two theories. The one-loop partition function is given by

$$\text{Heterotic: } \mathcal{T} = \int_{\mathcal{F}} \frac{\mathrm{d}^2\tau}{\tau_2^6} \left(\frac{V_8 - C_8}{\eta^8} \right) \frac{\bar{\Gamma}_{16}}{\bar{\eta}^{16}} \ , \tag{1.2.9}$$

where $\bar{\Gamma}_{16}$ is the lattice corresponding to either the $\mathrm{Spin}(32)/\mathbb{Z}_2$ or $\mathrm{E}_8 \times \mathrm{E}_8$ theory. In terms of Jacobi theta functions, we have

$$\bar{\Gamma}_{\mathrm{Spin}(32)/\mathbb{Z}_2} = \frac{1}{2} \sum_{a,b=0,1} \bar{\vartheta}[\,{}^{a}_{b}\,]^{16} \quad \text{and} \quad \bar{\Gamma}_{\mathrm{E}_8 \times \mathrm{E}_8} = \left(\frac{1}{2} \sum_{a,b=0,1} \bar{\vartheta}[\,{}^{a}_{b}\,]^{8} \right)^2 \ . \tag{1.2.10}$$

When the theory is further compactified for both left- and right-movers on a n-dimensional torus T^n, $n > 0$, the lattice of momenta includes the original 16 left-moving dimensions plus n additional left- and right-moving dimensions. Modular invariance again constrains this so called *Narain lattice* [113, 114] to be even and self-dual and the moduli space is now much richer than in ten dimensions. It is parametrized by the background internal values of the spacetime metric and antisymmetric tensor as well as by the scalars arising from the dimensional reduction of the gauge fields associated to the $\mathrm{Spin}(32)/\mathbb{Z}_2$ or $\mathrm{E}_8 \times \mathrm{E}_8$ groups. The moduli space is described by the following $n(16+n)$-dimensional manifold $\mathcal{M}_{16+n,n}$

$$\mathcal{M}_{16+n,n} = \frac{\mathrm{O}(16+n, n; \mathbb{R})}{\mathrm{O}(16+n; \mathbb{R}) \times \mathrm{O}(n; \mathbb{R})} \ , \tag{1.2.11}$$

up to a quotient by the T-duality group $\mathrm{O}(16+n, n; \mathbb{Z})$.

In the fermionic construction of the heterotic string, there are 10 bosonic left- and right-movers, 10 fermionic right-movers and instead of adding 16 left-moving bosons like in the bosonic construction, 32 left-moving fermions are added. These additional fermions are however not like the other ones since they are assumed to be singlets under Lorentz spacetime transformations. In this construction, which is equivalent to the bosonic one, it is less mysterious that the theory is ten dimensional since only 10 bosonic fields are present, both left- and right-moving.

1.2.5 Type I string theory

In this subsection, we discuss quite deeply the type I superstring theory to prepare the groundwork of the results presented in Chapter 2 and 3. Reviews about open-string theories can be found in [115, 116].

Chan-Paton factors and orientifold

All the theories presented so far only contain closed strings and as we saw, open strings can be used to generate a non-abelian gauge structure thanks to Chan-Paton factors [107]. Let us start by defining precisely what they are. The idea is to associate a number N of non-dynamical degrees of freedom to each of the strings ends. An open-string state is then characterized by its number of transverse oscillators, its momentum k and two integers $i, j \in \{1, \dots, N\}$ labelling each end of the string. The number of states is thus multiplied by N^2 and the spectrum is N^2 times larger. Without

writing the oscillators, a state has the following form: $|k, ij\rangle$. A generic state $|k, \lambda\rangle$ is then given by a linear combination of these states with coefficients λ_{ij} which are the so-called Chan-Paton factors,

$$|k, \lambda\rangle = \sum_{i,j=1}^{N} |k, ij\rangle \, \lambda_{ij} \ . \tag{1.2.12}$$

The generic string states are thus $N \times N$ matrices and in all amplitudes, the Chan-Paton factors appear as products in traces which are invariant under a global $\mathrm{U}(N)$ transformation. From the spacetime point of view, it can be shown that the global $\mathrm{U}(N)$ becomes local and yield a $\mathrm{U}(N)$ gauge symmetry [117]. Geometrically, the Chan-Paton factors are interpreted in terms of coincident *D-branes*, extended objects where the ends of the strings can attach with Dirichlet boundary conditions [118].

One way to build a consistent theory incorporating open strings is to start with the type IIB theory and use its symmetry under the worldsheet reversal by gauging it. This parity operation Ω is called *orientifold projection* and its action on the spacelike worldsheet coordinate σ is

$$\underline{\text{Closed strings:}}\ \Omega : \sigma \to -\sigma \ , \qquad \underline{\text{Open strings:}}\ \Omega : \sigma \to \pi - \sigma \ . \tag{1.2.13}$$

This translates into a non-trivial action on the open-string oscillators. For Neumann boundary conditions, the action is

$$\underline{\text{Open strings:}}\ \Omega : \alpha_n^\mu \to (-1)^n \alpha_n^\mu \ , \qquad d_n^\mu \to (-1)^n d_n^\mu \ , \qquad b_r^\mu \to i^{2r} b_r^\mu \ . \tag{1.2.14}$$

Gauging this transformation means that we project the theory onto states that survive the projection $\frac{1+\Omega}{2}$. As a result, the strings are unoriented and the states are left-right symmetric. This defines the *type I superstring theory*.

The projection also affects the behaviour of the Chan-Paton factors. The action of Ω on states $|k, ij\rangle_{\mathrm{NS}}$ and $|k, ij\rangle_{\mathrm{R}}$ in the NS and R sectors reverses i and j and acts with a unitary matrix γ_Ω up to phases ϵ_{NS} and ϵ_{R}:

$$|k, ij\rangle_{\mathrm{NS}} \to \sum_{i',j'=1}^{N} \epsilon_{\mathrm{NS}} \, (\gamma_\Omega)_{ii'} \, |k, j'i'\rangle_{\mathrm{NS}} \left(\gamma_\Omega^{-1}\right)_{j'j} \ , \quad |k, ij\rangle_{\mathrm{R}} \to \sum_{i',j'=1}^{N} \epsilon_{\mathrm{R}} \, (\gamma_\Omega)_{ii'} \, |k, j'i'\rangle_{\mathrm{R}} \left(\gamma_\Omega^{-1}\right)_{j'j} \ . \tag{1.2.15}$$

The phases and the γ_Ω matrix are constrained by consistency conditions of the action of Ω on the spectrum. One must take $\epsilon_{\mathrm{NS}} = -i$ and $\epsilon_{\mathrm{R}} = -1$ and two choices are possible for the matrix γ_Ω, yielding different gauge groups. The matrix can be the $N \times N$ identity matrix I_N and the associated gauge group is $\mathrm{SO}(N)$, or it can be the matrix iJ_N where J_N is defined as

$$J_N = \begin{pmatrix} 0 & I_{\frac{N}{2}} \\ -I_{\frac{N}{2}} & 0 \end{pmatrix} , \tag{1.2.16}$$

which gives a $\mathrm{USp}(N)$ gauge group. We will see later that anomaly cancellation provides additional constraints on the number N and forbids the $\mathrm{USp}(N)$ type I theory.

One-loop amplitudes

In open-string theories, additional one-loop diagrams exist besides the torus one. The one-loop amplitude of an oriented open string has the topology of an annulus (or cylinder). In type I string

which is an unoriented theory, two more unoriented surfaces appear: The Klein bottle for closed strings and the Möbius strip for open strings.

The orientifold projection [119] is realized by inserting $\frac{1+\Omega}{2}$ inside the traces in the definition of the one-loop amplitudes. In the closed-string sector, the term with 1 gives half of the previously defined torus amplitude $\mathcal{T}$ in (1.2.6) and the insertion of Ω defines the Klein bottle amplitude $\mathcal{K}$,

$$\mathcal{K} \equiv \int_0^{+\infty} \frac{\mathrm{d}\tau_2}{\tau_2^{1+\frac{D}{2}}} \mathrm{Str}\left(\frac{\Omega}{2} q^{L_0-\frac{1}{2}} \bar{q}^{\tilde{L}_0-\frac{1}{2}}\right) . \tag{1.2.17}$$

Because the orientifold projection is on the type IIB string theory, the torus partition function is simply given by half of the IIB one expressed in (1.2.7). In the Klein bottle, only the invariant states under Ω contribute. In particular, the NS-R and R-NS sectors do not contribute and thus fermions do not run in the Klein bottle. The characters are taken at the parameter of its doubly covering torus which is $\tau = 2i\tau_2$. We do not write the argument but it is understood to be the correct one for each amplitude (we will mention the correct argument when we meet the various surfaces for the first time). Integrating over the different Klein bottles amounts to integrate over all positive τ_2. We obtain

$$\mathcal{K} = \int_0^{+\infty} \frac{\mathrm{d}\tau_2}{\tau_2^6} \frac{V_8 - S_8}{\eta^8} . \tag{1.2.18}$$

We can count the number of closed-string states in $\frac{1}{2}\mathcal{T} + \mathcal{K}$ using (1.2.8) where $\mathcal{T}$ is the type IIB torus in (1.2.7). We find 64 bosonic and fermionic degrees of freedom. This is consistent with the action of the orientifold which projects out the left-right asymmetric part of the type IIB spectrum. What remains in the NS-NS sector is the graviton and the dilaton ($35 + 1 = 36$ degrees of freedom) while in the R-R sector, only the two form survives (28 degrees of freedom). This yields the 64 bosons. In the NS-R and R-NS sectors which are swapped under Ω, only one linear combination of the two gravitinos and one combination of the two dilatinos remain. This gives 64 fermions matching the number of bosons.

The open-string sector can be seen as the *twisted sector* associated with the orientifold projection. As we will see soon, its existence is required to obtain a consistent anomaly-free theory. The oriented one-loop annulus topology $\mathcal{A}$ and the unoriented Möbius strip surface $\mathcal{M}$ are defined as

$$\mathcal{A} \equiv \int_0^{+\infty} \frac{\mathrm{d}\tau_2}{\tau_2^{1+\frac{D}{2}}} \mathrm{Str}\left(\frac{1}{2} q^{\frac{1}{2}(L_0-1)}\right) , \qquad \mathcal{M} \equiv \int_0^{+\infty} \frac{\mathrm{d}\tau_2}{\tau_2^{1+\frac{D}{2}}} \mathrm{Str}\left(\frac{\Omega}{2} q^{\frac{1}{2}(L_0-1)}\right) . \tag{1.2.19}$$

In the annulus, the sum over the Chan-Paton indices of the strings produces a multiplicity N^2 (we do not consider Wilson lines for now). In the Möbius strip, the action of Ω (1.2.15) on the Chan-Paton indices produces a factor $\epsilon_{\mathrm{NS/R}} \mathrm{tr}\left(\gamma_\Omega^{\mathrm{T}} \gamma_\Omega^{-1}\right)$. In the NS sector, the product of $\epsilon_{\mathrm{NS}} = -i$ by the $\pm i$ factor induced by the action of Ω on the oscillators produces alternate signs in the characters, starting with a minus that we factorize. One obtains the same structure in the R sector and the trace $\mathrm{tr}\left(\gamma_\Omega^{\mathrm{T}} \gamma_\Omega^{-1}\right)$ together with the factorized minus sign gives an overall factor ϵN where $\epsilon = -1$ if $\gamma_\Omega = I_N$ or $\epsilon = 1$ if $\gamma_\Omega = iJ_N$. The amplitudes are then

$$\mathcal{A} = \frac{N^2}{2} \int_0^{+\infty} \frac{\mathrm{d}\tau_2}{\tau_2^6} \frac{V_8 - S_8}{\eta^8} , \qquad \mathcal{M} = \frac{\epsilon N}{2} \int_0^{+\infty} \frac{\mathrm{d}\tau_2}{\tau_2^6} \frac{\hat{V}_8 - \hat{S}_8}{\hat{\eta}^8} . \tag{1.2.20}$$

In the annulus, the characters are taken at argument $i\frac{\tau_2}{2}$ and the hatted characters in the Möbius, defined in Appendix A, are taken at argument $\frac{1}{2} + i\frac{\tau_2}{2}$. In this case, the fact that the covering torus is tilted induces the alternate signs in the characters.

We can recover the open-string gauge groups associated with the value of ϵ (coming from the choice of orientifold action on the Chan-Paton indices) by writing the zero modes of $\mathcal{A}+\mathcal{M}$. This gives the following "field-theory" spectrum

$$\mathcal{A}+\mathcal{M}|_{\rm FT} = \int_0^{+\infty} \frac{\mathrm{d}\tau_2}{\tau_2^6} \frac{N(N+\epsilon)}{2} \left.\frac{V_8-S_8}{\eta^8}\right|_0 , \tag{1.2.21}$$

where the index 0 stands for the constant mode of the characters (hatted or not). With $\epsilon=-1$, we recognize the dimension $\frac{N(N-1)}{2}$ of the adjoint representation of SO(N) while if $\epsilon=+1$, we recognize the dimension $\frac{N(N+1)}{2}$ of the adjoint representation of USp(N). We will be able to conclude on the allowed group and value of N in the next paragraph.

Tree-level channel and tadpoles

The *tree-level channel amplitudes* are defined by performing a S-transformation (1.2.3) on the one-loop amplitudes. More precisely, for the Möbius strip, in order to keep a $\frac{1}{2}$ real part of the parameter and inverse the imaginary part ($\frac{1}{2}+i\frac{\tau_2}{2} \to \frac{1}{2}+\frac{i}{2\tau_2}$), the transformation to be performed is the combination TST^2S. The behaviours of the characters under these transformations are displayed in Appendix A. In the tree-level amplitudes, the integration parameter is written l and its precise definition from τ_2 depends on the surface,

$$\text{Klein bottle and Möbius strip: } l \equiv \frac{1}{2\tau_2} , \quad \text{Annulus: } l \equiv \frac{2}{\tau_2} . \tag{1.2.22}$$

The tree-level amplitudes denoted with tildes are then

$$\tilde{\mathcal{K}} = \frac{2^5}{2}\int_0^{+\infty} \mathrm{d}l \frac{V_8-S_8}{\eta^8} , \qquad \tilde{\mathcal{A}} = \frac{2^{-5}N^2}{2}\int_0^{+\infty} \mathrm{d}l \frac{V_8-S_8}{\eta^8} , \quad \tilde{\mathcal{M}} = \frac{\epsilon N}{2}\int_0^{+\infty} \mathrm{d}l \frac{\hat{V}_8-\hat{S}_8}{\eta^8} , \tag{1.2.23}$$

where the characters are all taken at argument il in the Klein bottle and Annulus and $\frac{1}{2}+il$ in the Möbius strip. The ultraviolet divergences near $\tau_2=0$ in $\mathcal{K}$, $\mathcal{A}$ and $\mathcal{M}$ are mapped to infrared divergences near $l=+\infty$. These divergences only occur for the constant modes of the characters since no exponentially suppressed contribution is there to soften the behaviour at infinity.

The cancellation of the divergences (with the specific definitions (1.2.22) for l) is required for the theory to be consistent. This is because it can be tracked back to anomalies whose vanishing is mandatory [120–124]. Such a cancellation is also called *R-R tadpole cancellation* since it can be linked to tadpole diagrams for the R-R closed-string fields (more on this in the next paragraph). From (1.2.23), the contributions from the zero modes are

$$\tilde{\mathcal{K}}+\tilde{\mathcal{A}}+\tilde{\mathcal{M}}|_0 = \frac{(N+\epsilon 2^5)^2}{2^6}\int_0^{+\infty} \mathrm{d}l \left.\frac{V_8-S_8}{\eta^8}\right|_0 . \tag{1.2.24}$$

The only possibility for this to vanish is to choose $\epsilon=-1$ and $N=32$. As a consequence, the only consistent type I ten-dimensional theory has an SO(32) gauge group.

Geometrical interpretations

A very nice and important feature of unoriented string theories is the possible geometrical interpretation of lots of things, in terms of orientifold planes and D-branes. Geometrical considerations will be very helpful for the work presented in Chapter 2.

The *orientifold planes* are defined as the fixed points of the orientifold projection Ω. In the type I theory, Ω is just the worldsheet parity so that the whole spacetime is a fixed point. This is interpreted by the presence of a spacetime-filling orientifold plane: An O9-plane. Typically, if some dimensions are compactified, the theory obtained after a T-duality on the internal directions corresponds to an orientifold projection Ω' which is the original Ω times parities along the compact dimensions. Let us understand this basic fact with the following diagram:

$$\begin{array}{ccc} \text{Type IIB, compactified} & \xleftrightarrow{\text{T-duality}} & \text{T-dual, type IIA} \\ \Big\downarrow \; \Omega\,|\vec{m},\vec{n}\rangle = |\vec{m},-\vec{n}\rangle & & \Big\downarrow \; \Omega'\,|\vec{m},\vec{n}\rangle = ? \\ \text{Type I: } |\vec{m},\vec{0}\rangle & \xleftrightarrow{\text{T-duality}} & \text{Type I}'\text{: } |\vec{0},\vec{n}\rangle \end{array}$$

Starting from the upper-left corner with the type IIB theory compactified on say n dimensions, the usual orientifold projection acts on lattice states with momentum and windings numbers $\vec{m}$ and $\vec{n}$ by changing the sign of the winding numbers. In the obtained type I theory in the bottom-left corner, lattice states have thus trivial windings. A T-duality along the compact directions on this type I theory gives the type I$'$ in the bottom-right corner where momentum and winding numbers are exchanged, so that the surviving states have now trivial momenta. Going back to the type IIB, the T-duality applied here gives type IIA in the upper-right corner. Because the T-duality and the orientifold projection should commute, the question is: What projection Ω' on type IIA should we take to obtain the type I$'$ found earlier with trivial momenta? The combination of Ω with the parity reversal operation Π_n along the n compact directions does the trick. Indeed, we have $\Omega\Pi_n\,|\vec{m},\vec{n}\rangle = \Omega\,|-\vec{m},-\vec{n}\rangle = |-\vec{m},\vec{n}\rangle$. The fixed points of Ω' are no more everywhere in spacetime but are localized at specific coordinates in the compact directions while filling the extended ones. More precisely, the original O9-plane becomes 2^n O$(9-n)$-planes in the T-dual picture. Note that unlike D-branes, the orientifold planes are non-dynamical objects.

The tree-level amplitudes can be interpreted as describing closed-string states propagation between O-planes and D-branes. More specifically, the Klein bottle tree-level amplitude describes the propagation of closed strings between two O-planes, the annulus represents the propagation of closed strings between two D-branes and the Möbius strip describes the closed-sates propagation between an O-plane on one side and a D-brane on the other. Remarkably, the amplitudes are completely determined by the geometry of the theory *i.e.* where the O-planes and D-branes are and what are their precise types. Let us understand how this precisely works.

We assume the following typical setup mentioned above: n dimensions are compactified on circles of radii R_i, $i \in \{1,\dots n\}$ and O$(9-n)$-planes as well as D$(9-n)$-branes, orthogonal to the n compact directions, sit at some positions in the internal space. We consider the propagation of a closed-string state labelled by an index a and Kaluza-Klein momentum numbers $\vec{m}$ along the circles between two objects A and B referring independently to an O-plane or to a D-brane. The whole tree-level amplitude $\tilde{\Sigma} \equiv \tilde{\mathcal{K}} + \tilde{\mathcal{A}} + \tilde{\mathcal{M}}$ is formally given by

$$\tilde{\Sigma} = \sum_{a,\vec{m}} \sum_{A,B} (-1)^{F_{\rm L}} C_{aA} C_{aB} G_{a,\vec{m}}(\vec{x}_A, \vec{x}_B) \ . \tag{1.2.25}$$

The sum is over all closed-string NS-NS and R-R states and all objects A and B. $F_{\rm L}$ denotes the left fermion number so that the overall sign depends on the sector in which the state a is: $+1$ for

NS-NS states and -1 for R-R states. The closed-string states have different Lorentz structures but their propagators and their couplings to A and B can be written as a universal scalar propagator $G_{a,\vec{m}}(\vec{x}_A, \vec{x}_B)$ with effective couplings C_{aA} and C_{aB}. For NS-NS states, the coupling C_{aA} is given by the tension T_A of object A while it is given by its charge q_A for R-R states. When A and B refer to O-planes, the contribution is $\tilde{\mathcal{K}}$. When they refer to D-branes, this gives $\tilde{\mathcal{A}}$ and when they refer to an O-plane on one side and a D-brane on the other, it gives $\tilde{\mathcal{M}}$. The scalar propagator for state a of mass squared M_a^2 and internal momentum $p_{||}$ is given by

$$G_{a,\vec{m}}(\vec{x}_A, \vec{x}_B) = \frac{e^{i\vec{m}\cdot(\vec{x}_A-\vec{x}_B)}}{p_{||}^2 + M_a^2 + \sum_{i=1}^n \frac{m_i^2}{R_i^2}} = \frac{\pi\alpha'}{2} e^{i\vec{m}\cdot(\vec{x}_A-\vec{x}_B)} \int_0^{+\infty} \mathrm{d}l e^{-\pi\frac{l}{2}\alpha'\left(M_a^2+\sum_{i=1}^n \frac{m_i^2}{R_i^2}\right)} , \qquad (1.2.26)$$

where the coordinate components x_A^i, x_B^i are normalized by the radius R_i so that $x_A^i, x_B^i \in [-\pi, \pi]$. Note that the expression of the scalar propagator is a bit schematic since the Möbius contribution should alternate signs between the mass levels. The total tree-level contribution is then

$$\tilde{\Sigma} \propto \sum_{a,\vec{m}} (-1)^{F_\mathrm{L}} \Bigg(\underbrace{\sum_{\substack{A\in \text{O-planes}\\ B\in \text{O-planes}}}}_{\tilde{\mathcal{K}}} + \underbrace{\sum_{\substack{A\in \text{D-branes}\\ B\in \text{D-branes}}}}_{\tilde{\mathcal{A}}} + 2\underbrace{\sum_{\substack{A\in \text{O-planes}\\ B\in \text{D-branes}}}}_{\tilde{\mathcal{M}}} \Bigg) C_{aA}C_{aB} e^{i\vec{m}\cdot(\vec{x}_A-\vec{x}_B)} \int_0^{+\infty} \mathrm{d}l e^{-\pi\frac{l}{2}\alpha'\left(M_a^2+\sum_{i=1}^n \frac{m_i^2}{R_i^2}\right)} . \qquad (1.2.27)$$

We see that the sole knowledge of the O-planes/D-branes positions as well as their tensions and charges completely determines the tree-level amplitudes $\tilde{\mathcal{K}}$, $\tilde{\mathcal{A}}$ and $\tilde{\mathcal{M}}$ by telling us what is the projector on the momentum numbers. When $M_a^2 = 0$ and $\vec{m} = \vec{0}$, the integral diverges and $\tilde{\Sigma}$ factorizes as a perfect square:

$$\begin{aligned} \tilde{\Sigma}|_0 &\propto \sum_{a|M_a^2=0} (-1)^{F_\mathrm{L}} \left(\sum_{A\in \text{O-planes}} C_{aA} + \sum_{A\in \text{D-branes}} C_{aA} \right)^2 \int_0^{+\infty} \mathrm{d}l \qquad (1.2.28) \\ &\propto \left[\sum_{\substack{a|M_a^2=0\\ a\in \text{NS-NS}}} \left(\sum_{A\in \text{O-planes}} T_A + \sum_{A\in \text{D-branes}} T_A \right)^2 - \sum_{\substack{a|M_a^2=0\\ a\in \text{R-R}}} \left(\sum_{A\in \text{O-planes}} q_A + \sum_{A\in \text{D-branes}} q_A \right)^2 \right] \int_0^{+\infty} \mathrm{d}l . \end{aligned}$$

Diagrammatically, this formula is the square of massless tadpoles in front of O-planes (crosscaps) and D-branes (boundaries). Even though the expression automatically gives zero in supersymmetric cases where the objects all have their tensions equal to their charges, the NS-NS and R-R tadpoles should vanish independently. The cancellation is ensured if the global tension and charge of the O-planes and D-branes vanish independently. Note that actually, consistency of the theory only requires the cancellation of the R-R tadpole. The NS-NS divergence is a usual tadpole signalling a perturbation expansion around a point which is not a vacuum but does not make the theory inconsistent by introducing anomalies. In a supersymmetric theory, cancellation of the one implies vanishing of the other but not necessarily in non-supersymmetric setups.

In this thesis, we will encounter all four types of orientifold and antiorientifold planes: O$_-$ and O$_+$-planes as well as $\overline{\text{O}}_-$ and $\overline{\text{O}}_+$-planes. They differ by the signs of their tensions and charges, which are equal in absolute value. In this work, we use the conventions displayed in Table. 1.1,

Moreover, regular D-branes have positive tension and positive charge and the absolute value of an O-plane tension extended in p dimensions is related to the tension of a Dp-brane through the

Orientifold plane type	Tension T	Charge q
O$_-$-plane	< 0	< 0
O$_+$-plane	> 0	> 0
$\overline{\text{O}}_-$-plane	< 0	> 0
$\overline{\text{O}}_+$-plane	> 0	< 0

Table 1.1: Conventions for the signs of tensions and charges of the various orientifold planes.

expression

$$|T_{\text{O}p}| = 2^{p-4} T_{\text{D}p} \ . \tag{1.2.29}$$

One can then recover the consistency conditions of type I theory with a purely geometrical interpretation. The action of Ω on the Chan-Paton indices with $\gamma_\Omega = I_N$ produces a spacetime-filling O9$_-$-plane while the choice $\gamma_\Omega = iJ_N$ produces a spacetime-filling O9$_+$-plane. Since the O9$_+$-plane has positive tension and charge, the addition of regular D-branes cannot compensate the tadpole and thus USp(N) is not allowed. The O9$_-$-plane has negative tension and charge whose absolute value is equal to 32 times the tension and charge of a D9-brane as can be seen from (1.2.29). Thus, the addition of $N = 32$ D9-branes cancels the tadpole, which leaves the SO(32) type I theory as the only consistent choice.

1.3 Supersymmetry breaking in string theory

Consistency of string theory requires the ingredient of supersymmetry. However, a strictly supersymmetric universe does not look like ours since for all light particles we know, their superpartners should exist with the same masses. This is of course not what we observe. If supersymmetry is to be kept as a fundamental feature carried by the underlying theory describing elementary particles and their interactions, it must be broken in some way to allow superpartners to have different masses. In this thesis, we are interested in supersymmetry-breaking mechanisms that can be implemented at the string theory level and not directly in the effective field theory. To begin this section, we present in detail the *Scherk–Schwarz mechanism* or *coordinate-dependent compactification* which is extensively used in the works presented in this thesis to implement the supersymmetry breaking. We will then mention another mechanism and its features called *brane supersymmetry breaking*. This will motivate the work presented in Chapter 2.

1.3.1 Scherk–Schwarz mechanism

The mechanism makes use of compactified dimensions to generate a spontaneous breaking of supersymmetry. It is not stringy in nature and can be implemented at the field-theory level [16, 17]. We will start by understanding the key idea of the mechanism and then move onto its implementation at the string-theory level [18–22] described right after.

The mechanism

Extra compact dimensions are required for the mechanism to take place. Let us assume a very general setup where the geometrical background consists in the four extended spacetime dimensions $\mathbb{R}^{1,3}$ times some compact manifold $\mathcal{C}$. We denote by x a point in the Minkowski spacetime and by

y a point in the compact manifold. This compact manifold is expressed as a quotient of some non-compact space $\mathcal{M}$ by a discrete group $\mathcal{G}$ which is freely-acting on $\mathcal{M}$ with operators $\tau_g : \mathcal{M} \to \mathcal{M}$, $g \in \mathcal{G}$ forming a representation of the group. The points y and $\tau_g(y)$ are identified in the compact manifold and a trivial boundary condition for some field $\phi(x, y)$ is simply $\phi(x, y) = \phi(x, \tau_g(y))$. This boundary condition can actually be twisted using some element T of a global symmetry group of the theory and becomes $\phi(x, y) = T(\phi(x, \tau_g(y)))$.

As an example, we take the compact manifold $\mathcal{C}$ to be a circle of radius R obtained from the real line $\mathbb{R}$ modded by $\mathcal{G} = \mathbb{Z}$ with operators τ_n, $n \in \mathbb{Z}$ such that $\tau_n(y) = y + 2\pi n R$. Using an U(1) global symmetry, we write $T = e^{i\pi Q}$ for some charge Q and the boundary condition becomes

$$\phi(x, y + 2\pi R) = e^{i\pi Q}\phi(x, y) \ . \tag{1.3.1}$$

Solving this equation by expanding the field in Fourier modes along the circle, we find

$$\phi(x, y) = e^{\frac{iQy}{2R}} \sum_{m\in\mathbb{Z}} \phi_m(x) e^{\frac{imy}{R}} = \sum_{m\in\mathbb{Z}} \phi_m(x) e^{\frac{i\left(m+\frac{Q}{2}\right)y}{R}} \ , \tag{1.3.2}$$

from which we see that the usual Kaluza-Klein mass $\frac{m}{R}$ of $\phi_m(x)$ receives a correction from Q,

$$M_{\phi_m(x)} = \frac{\left|m + \frac{Q}{2}\right|}{R} \ . \tag{1.3.3}$$

The mechanism thus provides a mass shift for states associated to a non-trivial charge Q. To introduce supersymmetry breaking, the simplest choice of Q is F, the fermion number of the field. Then, bosons keep the usual Kaluza-Klein mass since $Q = F = 0$ and fermions acquire a mass shift $\frac{1}{2R}$ since $Q = F = 1$. From the lower dimensional point of view, the breaking is spontaneous and the mass shift defines the supersymmetry-breaking scale. We see that in the typical case where a circle of radius R is used, the scale behaves like $\frac{1}{R}$ so that supersymmetry is recovered in the decompactification limit.

Implementation in string theory

The simplest way to implement such a shift in momenta in string theory is to couple a freely-acting orbifold on an internal circle to a the non-supersymmetric operator $(-1)^F$ where F is the spacetime fermion number. Let us build the corresponding one-loop amplitudes for the type IIB theory and its type I open descendants.

To implement the mechanism, as in field theory, we need at least one compact direction. We thus compactify the X^9 direction on a circle of radius R_9. Along a compact direction, in addition to the Kaluza-Klein momentum number m_9, a closed-string possesses a winding number n_9 corresponding to the number of times the string wraps the internal direction before closing itself. These winding numbers are specific to closed string and they have no equivalent for pointlike particles or open strings. The block $\sum_{m_9,n_9} \Lambda_{m_9,n_9}$ of the partition function describing the closed string along the circle then involves momentum and winding numbers through the following expression

$$\Lambda_{m_9,n_9} = q^{\frac{\alpha'}{4}\left(\frac{m_9}{R_9}+\frac{n_9 R_9}{\alpha'}\right)^2} \bar{q}^{\frac{\alpha'}{4}\left(\frac{m_9}{R_9}-\frac{n_9 R_9}{\alpha'}\right)^2} \ . \tag{1.3.4}$$

This Hamiltonian form reveals how the winding number affects the mass of the closed string from the nine-dimensional point of view:

$$M^2_{\text{closed}} \equiv \text{oscillators} \ + \frac{m_9^2}{R_9^2} + \frac{n_9^2 R_9^2}{\alpha'^2} \ , \tag{1.3.5}$$

while the mass of the open string only has the momentum term. Before any orbifold, the torus partition function of type IIB compactified on a circle $S^1(R_9)$ is (for lighter expressions throughout this thesis, we choose sometimes not to write the sums over momenta and winding numbers)

$$\mathcal{T} = \int_{\mathcal{F}} \frac{\mathrm{d}^2\tau}{\tau_2^{\frac{11}{2}}} \left| \frac{V_8 - S_8}{\eta^8} \right|^2 \Lambda_{m_9,n_9} \ , \tag{1.3.6}$$

where the τ_2 power is lowered by one half due to the lack of one extended direction compared to the ten-dimensional case.

The orbifold is implemented by inserting $\frac{1+g'}{2}$ inside the traces in the definitions of the amplitudes where $g' = (-1)^F \delta_{p_9}$ and δ_{p_9} is the following freely-acting generator (called *momentum shift*),

$$g' = (-1)^F \delta_{p_9} \qquad \text{and} \qquad \delta_{p_9} : X^9 \to X^9 + \pi R_9 \ . \tag{1.3.7}$$

The insertion of g' in the trace changes the sign of the spinorial character S_8 and produces a sign $(-1)^{m_9}$ in the circle lattice. However, this cannot be the end of the story since the obtained partition function would not be modular invariant. This is because the presence of g' allows for additional boundary conditions. All states satisfying such new conditions constitute the *twisted sector* and one must not forget to trace over this sector in order to obtain the full one-loop amplitude. The result is

$$\begin{aligned} \mathcal{T} = \frac{1}{2} \int_{\mathcal{F}} \frac{\mathrm{d}^2\tau}{\tau_2^{\frac{11}{2}}} \Bigg\{ & \left(\left| \frac{V_8 - S_8}{\eta^8} \right|^2 + (-1)^{m_9} \left| \frac{V_8 + S_8}{\eta^8} \right|^2 \right) \Lambda_{m_9,n_9} \\ & + \left(\left| \frac{O_8 - C_8}{\eta^8} \right|^2 + (-1)^{m_9} \left| \frac{O_8 + C_8}{\eta^8} \right|^2 \right) \Lambda_{m_9,n_9+\frac{1}{2}} \Bigg\} \ . \end{aligned} \tag{1.3.8}$$

Rescaling $R_9 \to 2R_9$ and splitting spacetime bosons and fermions gives

$$\begin{aligned} \mathcal{T} = \int_{\mathcal{F}} \frac{\mathrm{d}^2\tau}{\tau_2^{\frac{11}{2}}} \Bigg\{ & \left(|V_8|^2 + |S_8|^2 \right) \Lambda_{m_9,2n_9} - \left(V_8 \bar{S}_8 + S_8 \bar{V}_8 \right) \Lambda_{m_9+\frac{1}{2},2n_9} \\ & + \left(|O_8|^2 + |C_8|^2 \right) \Lambda_{m_9,2n_9+1} - \left(O_8 \bar{C}_8 + C_8 \bar{O}_8 \right) \Lambda_{m_9+\frac{1}{2},2n_9+1} \Bigg\} \frac{1}{|\eta^8|^2} \ . \end{aligned} \tag{1.3.9}$$

We see that the fermions have a half-shifted momentum compared to bosons which implies a mass gap between them. At the massless level ($m_9 = n_9 = 0$), only bosons remain in the first term of the first line. Note that the character $|O_8|^2$ starts with a negative power of q, meaning that if the radius R_9 is not large enough ($R_9 < \sqrt{2\alpha'}$), a tachyon is present. This is a characteristic feature of the Scherk–Schwarz mechanism in string theory and it signals Hagedorn-like phase transitions [23–34] .

In the type I string amplitudes, only momentum numbers are present through lattices $P_{m_9} \equiv \Lambda_{m_9,0}$. Their expressions (without Wilson lines) are

$$\begin{aligned} \mathcal{K} &= \frac{1}{2} \int_0^{+\infty} \frac{\mathrm{d}\tau_2}{\tau_2^{\frac{11}{2}}} \frac{V_8 - S_8}{\eta^8} P_{m_9} \ , & \mathcal{A} &= \frac{N^2}{2} \int_0^{+\infty} \frac{\mathrm{d}\tau_2}{\tau_2^{\frac{11}{2}}} \frac{V_8 P_{m_9} - S_8 P_{m_9+\frac{1}{2}}}{\eta^9} \ , \\ \mathcal{M} &= -\frac{N}{2} \int_0^{+\infty} \frac{\mathrm{d}\tau_2}{\tau_2^{\frac{11}{2}}} \frac{V_8 P_{m_9} - S_8 P_{m_9+\frac{1}{2}}}{\eta^9} \ , \end{aligned} \tag{1.3.10}$$

where $N = 32$. We observe that the Klein bottle is insensitive to the mechanism and stays supersymmetric unlike the annulus and Möbius strip.

One-loop potential

We give here the generic form of the one-loop potential generated by the Scherk–Schwarz mechanism as it will be important in Chapters 3 and 4. When the Scherk–Schwarz radius is sufficiently large and if there is no mass scale in the model below the breaking scale $M \propto 1/R_9$, the dominant contributions arise from the Kaluza-Klein modes along the Scherk–Schwarz direction. The states associated with any other mass scale generically written $cM_{\rm s}$, with $M_{\rm s} \equiv 1/\sqrt{\alpha'}$ and where c is some $\mathcal{O}(1)$ moduli-dependent constant, yield exponentially suppressed contributions. The one-loop potential then takes the following generic form at an extremal point[3] in d dimensions [45–51, 56–61]:

$$\mathcal{V}_{\text{1-loop}} = \xi_d (n_{\rm F} - n_{\rm B}) M^d + \mathcal{O}\left((M_{\rm s} M)^{\frac{d}{2}} e^{-2\pi c \frac{M_{\rm s}}{M}} \right) , \tag{1.3.11}$$

where ξ_d is a positive constant which depends on the dimension d, and $n_{\rm F}$ and $n_{\rm B}$ counts the numbers of massless fermionic and bosonic degrees of freedom. We see that the sign of the potential is determined by the number of light bosons relatively to light fermions. Note that the Scherk–Scwharz radius does not need to be huge for the dominated contributions to be small. If $cM_{\rm s}$ is roughly a tenth of the the Planck scale, a radius of only $10^2\sqrt{\alpha'}$ makes the exponential terms highly negligible compared to the dominant $\mathcal{O}(M^d)$ term. Also, a big radius ensures to be far away from the Hagedorn value.

One disadvantage of the Scherk–Schwarz mechanism is that it only shifts the masses of the fermions. At the massless level, one thus ends up with a theory without fermions and a generic negative potential. One way to complexify the mechanism to leave both massless fermions and massless bosons is to combine it with non-trivial Wilson lines in type I string (or non-trivial D-brane positions in the T-dual picture). Such a setup is the framework of Chapter 3. Another way to achieve that is to turn on discrete deformations in the internal lattice of the heterotic string. This is used in the works presented in Chapter 4. In this latter case, it is useful to implement the Scherk–Schwarz supersymmetry breaking following another strategy without mentioning orbifolds and starting directly with modular-invariant deformed partition functions. This way of performing the Scherk–Schwarz mechanism is easier to manipulate when one wants to introduce more complex breaking patterns from which the simple realization presented before is just a particular case.

Also note that in the little example in type I presented here, the Scherk–Schwarz direction is parallel to the spacetime-filling D9-branes. In the setups where D-branes are not filling the whole spacetime and where the mechanism is implemented in a direction orthogonal to the branes, the open spectrum is not "Scherk–Schwarz-like" since it remains supersymmetric at tree level. Such breaking is called *M-theory breaking* or *brane supersymmetry* [86, 87, 125–127] in the literature.

1.3.2 Brane supersymmetry breaking

In a standard Scherk–Schwarz mechanism, the supersymmetry-breaking scale, defined as the mass shift between bosons and fermions, depends on the size of the internal space along which the mechanism is performed. In the case of a circle, the scale is the inverse of the radius and supersymmetry is restored in the decompactification limit. In *brane supersymmetry breaking* setups [62–67], the breaking scale is the string scale. In the simplest models in ten dimensions, the R-R tadpole condition imposes to add anti-D-branes to compensate the charge of an O9$_+$-plane. The annulus amplitude is the supersymmetric one and only the Möbius strip displays supersymmetry breaking. Moreover,

[3] With respect to all other moduli but the breaking scale.

typically, the presence of a massless singlet fermions signals a non-linear realization of supersymmetry [68, 69]. In such a setup however, the global tension is not zero and the model suffers from NS-NS tadpoles.

This motivates the work exposed in Chapter 2 where we explore a novel realization of brane supersymmetry breaking with only regular branes and without NS-NS tadpoles while avoiding brane instabilities.

1.4 Cosmology and string theory

Because string theory provides a framework for quantum gravity, it seems natural to study cosmology in a string context in order to derive the features of the standard model for cosmology and try to overcome its pitfalls. In this section, we very briefly describe the standard model of cosmology and review the state of the art concerning the universe, its past evolution and characteristics. We then evoke how string-theory ingredients affect cosmology and how they could help solving issues of the standard cosmology. This section will not be exhaustive at all since string cosmology is a vast domain that is only slightly touched in this thesis. The idea is to introduce the concepts that will motivate and be useful for the works presented in Chapter 4.

1.4.1 Basics of cosmology

Classically, the ansatz for a d-dimensional spacetime metric to describe an homogeneous and isotropic universe is the *Friedmann-Lemaître-Robertson-Walker (FLRW) metric*. It takes the following form in spherical coordinates,

$$\mathrm{d}s^2 = -\mathrm{d}t^2 + a(t)^2 \left(\frac{\mathrm{d}r^2}{1-kr^2} + r^2 \mathrm{d}\Omega_{d-2}^2 \right) \ , \tag{1.4.1}$$

where $\mathrm{d}\Omega_{d-2}^2$ is the metric of the unit $(d-2)$-sphere, $k \in \{-1, 0, 1\}$ characterizes the space curvature and $a(t)$ is the *scale factor*, which describes the size of the universe. In such a framework, the dynamics is entirely given by that of the scale factor and it is obtained by solving the Einstein equations. The solutions depend on the precise nature of the universe content, whose energy-momentum tensor is characterized by a density ρ and a pressure p. With a cosmological constant Λ and defining the Hubble factor $H(t) \equiv \dot{a}(t)/a(t)$, the Einstein equations with the FLRW metric read in Planck units

$$\frac{(d-1)(d-2)}{2} H^2 = \rho - \frac{k}{a^2} + \Lambda \quad \text{and} \quad (d-2)\dot{H} + \frac{(d-1)(d-2)}{2} H^2 = -p + \Lambda \ . \tag{1.4.2}$$

If the total density is positive, the cosmologies derived from these equations describe an expanding universe ($\dot{a}(t) > 0$) which, by time reversal, starts from a singularity where $a = 0$: The *Big Bang*.

The paradigm of an expanding universe starting from a small size explains lots of observations: The expansion can be measured, the relative abundance of elements can be computed and the presence of the observed Cosmological Microwave Background (CMB) is a natural consequence. Postulating in addition a phase of extremely rapid growth in the early universe called *inflation* [128] then explains how seemingly causally disconnected parts of the CMB were connected before and why we observe an homogeneous and almost flat space. Formally, the simplest realization of inflation is described with the dynamics of a single scalar field called inflaton. A popular setup is called

"slow-roll inflation" where the scalar starts on an almost flat plateau producing inflation before stabilizing in a well. While the scalar goes to its minimum (either with damped oscillations or not), it transfers its energy to produce the particles we see now. This phase is called *reheating* and is assumed to be followed by *baryogenesis*, the phase where matter slightly dominates antimatter.

The paradigm must be supplemented by additional ingredients: Most importantly dark matter and dark energy. Dark matter is required to explain the behaviours of galaxy clusters [10–12] and dark energy to explain the acceleration of the expansion of the universe observed nowadays [13, 14]. Dark matter and dark energy constitute roughly 95% of the energy content of the universe [15]. After baryogenesis, the universe entered a radiation-dominated era, followed by a matter-dominated one to eventually reach a dark-energy-dominated epoch in which we are living now.

The Big Bang paradigm together with inflation and the incorporation of dark matter and dark energy define the *standard model of cosmology*.

1.4.2 Dark-matter relic density

Dark matter is responsible for about 27% of the energy content of the universe [15]. It is commonly assumed to be composed of weakly interacting and yet undiscovered particles which are non-relativistic (this defines *cold* dark matter). Cosmology needs to face the challenge to generate such a relic density, decoupled from the standard model particles. The usual scenario invoked to produce such a relic density is called *thermal freeze-out* and we explain how it goes in this subsection.

An initial density of dark matter particles is assumed in the early stage of the universe where the temperature is high. Relativistic dark-matter particles and standard-model particles are in equilibrium through annihilation processes with cross-section $\sigma_{\mathrm{DM}\leftrightarrow\mathrm{SM}}$. This equilibrium is perturbed by the expansion rate of the universe which tends to reduce the interactions. Formally, the dynamics of the dark-matter density n_{DM} as a function of time t, is described by the Boltzmann equation

$$\frac{\mathrm{d}n_{\mathrm{DM}}}{\mathrm{d}t} + (d-1)Hn_{\mathrm{DM}} = -\langle\sigma_{\mathrm{DM}\leftrightarrow\mathrm{SM}}v\rangle\left[n_{\mathrm{DM}}^2 - n_{\mathrm{DM,eq}}^2\right] \ , \tag{1.4.3}$$

where $n_{\mathrm{DM,eq}}$ is the equilibrium density, v is the dark-matter velocity and the brackets stand for the mean over velocity distribution so that $\langle\sigma_{\mathrm{DM}\leftrightarrow\mathrm{SM}}v\rangle$ characterizes the efficiency of the particles creation or annihilation to reach the equilibrium. On the left-hand side, the term $(d-1)Hn_{\mathrm{DM}}$ describes the universe expansion. It is useful to describe things as functions of the temperature T rather than time t. Then, instead of showing the typical evolution of the dark-matter density $n_{\mathrm{DM}}(T)$, we define the *dark-matter yield* $Y_{\mathrm{DM}}(T)$ like

$$Y_{\mathrm{DM}}(T) = \frac{n_{\mathrm{DM}}(T)}{s(T)} \ , \tag{1.4.4}$$

where $s(T)$ is the entropy density of the thermal bath which goes like T^{d-1} in d dimensions. The behaviour of the dark-matter yield depends on the ratio $x = m_{\mathrm{DM}}/T$ which increases as the universe evolves and its temperature drops. The typical evolution of the yield in the standard freeze-out scenario is plotted in Fig. 1.1 (blue line).

- As said before, when the temperature is far greater than the dark-matter mass, an equilibrium is maintained between dark matter and standard-model particles. The dark-matter density goes like T^{d-1} so that the yield is constant at this stage.

- As the temperature begins to drop, the density decreases and follows the Boltzmann equilibrium (black dashed line in figure 1.1).
- This depletion of dark matter can no more occur when the expansion of the universe makes interactions between particles unlikely, which formally happens when $(d-1)H \lesssim n_{\rm DM}\langle\sigma_{\rm DM\leftrightarrow SM}v\rangle$. In four dimensions, the points $(x, Y_{\rm DM})$ where $(d-1)H = n_{\rm DM}\langle\sigma_{\rm DM\leftrightarrow SM}v\rangle$ form a straight line (the red dashed line in Fig. 1.1 which does not appear straight because of a log scale along the x-axis). When the yield crosses this line, particles depletion stops and dilution keeps going so that the yield remains constant at some relic value.

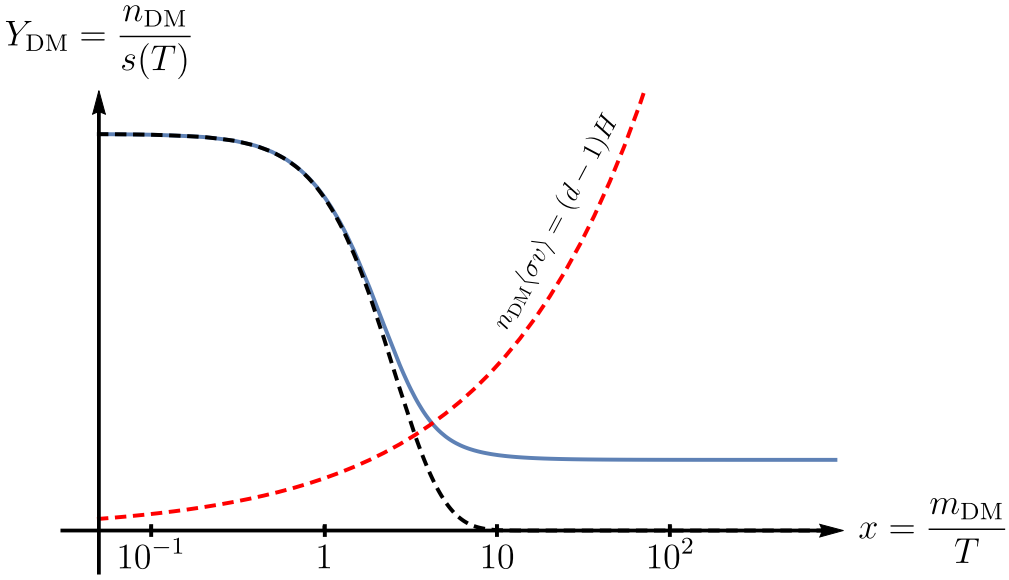

Figure 1.1: Evolution of the dark-matter yield $Y_{\rm DM} = n_{\rm DM}/s$ as a function of $x = m_{\rm DM}/T$ in the standard thermal freeze-out scenario, in 4 dimensions (blue solid line). The black-dashed line represents the value that the yield would follow if thermal equilibrium could be maintained all along the history of the universe. Freeze-out takes place when interactions with the standard-model particles are too weak, as compared to the expansion rate of the universe (after crossing of the red dashed line).

When the decoupling occurs near $x = 1$, the dark matter is cold *i.e.* non-relativistic. This is in agreement with preservation of the large-scale structures in the universe and cosmological measurements [129]. If the decoupling happened earlier when $x \ll 1$, the dark matter would be relativistic at the freeze-out and we would talk about a hot dark matter relic density.

1.4.3 String theory ingredients

The past singularity at the core of the standard model of cosmology and the breakdown of general relativity there, is the obvious reason why a UV-complete theory such as string theory may provide crucial ingredients to better understand cosmology and its beginning. A lot of efforts have been put in trying to describe the inflation era in a string-theory framework (see *e.g.* [130, 131] for reviews). Moduli arising in string theory provide good candidates for inflatons but they are numerous and massless so that it is hard to obtain a fully consistent model reproducing a slow-roll scenario for example. Also, string theory comes with a wide variety of new particles, some of which could be dark-matter candidates and illuminate this (dark) side of cosmology.

In this thesis, we tackle cosmological considerations in string theory of another kind. In Chapter 4, we study the quantum stability of flat Minkowski spacetime in a heterotic string framework. The idea is the following: If one assumes a classically flat expanding universe, quantum corrections should backreact on the system and potentially break down the flat expanding dynamics. In heterotic string models with Scherk–Schwarz breaking of supersymmetry, the one-loop potential can be computed and its influence on the cosmology of the classical background studied. The analysis is performed in a toy model and in a more generic one where the moduli dynamics is further discussed.

We also propose a new scenario for generating a cold dark-matter relic density again in a heterotic string-theory framework. It exploits the fact that throughout the cosmological evolution of the universe in some models, as the temperature drops, a modulus can become tachyonic, acquire a vacuum expectation value and suddenly give a mass to some dark-matter particle. Depending on when the transition occurs, this perturbs the standard thermal freeze-out scenario.

2 A supersymmetry-breaking mechanism in orientifold models

This chapter delves into the first component of the triptych underlying this thesis: The very construction of supersymmetry-breaking mechanisms. We describe a mechanism to break supersymmetry in orientifold models, without introducing tadpoles, anti-branes and brane instabilities. The mechanism shares common features with brane supersymmetry breaking but it does not introduce NS-NS tadpoles.

As mentioned in Chapter 1 and in the introduction, the mechanism of brane supersymmetry breaking has been extensively explored [62–67]. In these models, supersymmetry is non-linearly realized [68, 69] and the supersymmetry-breaking scale is the string scale in the open sector while the closed-string sector is insensitive to it. All these constructions suffer from uncancelled NS-NS tadpoles due to the presence of anti-D-branes. Attempts to deal with these tadpoles have been pursued [70–73] but with limited applications.

The goal of the work presented in this chapter is to build brane-supersymmetry-breaking-like vacua without introducing NS-NS tadpoles [77]. Starting with a supersymmetric orientifold model containing O_- and O_+-planes, the mechanism amounts to consistently replace O_- - O_+ pairs into their counterparts which preserve the other half of the supersymmetries *i.e.* $\overline{O}_-$ - $\overline{O}_+$ pairs. Both kind of pairs having zero net tension and charge, neither R-R nor NS-NS tadpoles are generated. As we will see, in such models the supersymmetry-breaking pattern in the open sector depends on the location of the D-branes and on the value of some internal radius. In the closed-string sector, arguments coming from the detailed study of the orientifold projection giving rise to the supersymmetry-breaking geometry suggest a soft-breaking *à la* Scherk–Schwarz. Field-theory considerations also tend to lead to the same conclusion.

Such constructions were already anticipated in the pioneering paper [132]. This was done using the tools of the so-called "Tor-Vergata school" [115, 116, 133–139] and we provide here the appropriate geometric interpretation of the models. Also, we give arguments in favour of the inconsistency of the supersymmetric torus shown in [132] and we give configurations without tachyonic brane instabilities.

In this chapter, we first define the basic supersymmetric model upon which our mechanism will be applied. It is the rank 8 orientifold projection of type IIB in eight dimensions. We then implement our mechanism which breaks supersymmetry and we explore its features. After that, the closed-string sector is discussed and the correct torus partition function is built and motivated. Eventually, we investigate consistency constraints coming from the addition of probe branes and we end the chapter with some outlooks for future works.

2.1 The rank 8 supersymmetric orientifold of type IIB

2.1.1 The torus amplitude

We start with the construction of a known alternative orientifold projection of type IIB which features a gauge group of rank 8 which is half of the rank of the SO(32) type I string. Spacetime is compactified on two circles of radii R_8 and R_9 and the orientifold projection is performed. If nothing new is introduced, this would simply yield the usual type I theory in eight dimensions in which the internal antisymmetric tensor B_{ij}, $i,j \in \{8,9\}$ is projected out. The key idea [140, 141] is that it is possible to keep a discrete background for B_{ij} that survives the orientifold projection. The metric G_{ij} of the internal squared T^2 and its antisymmetric tensor are then[1]

$$G = \frac{1}{\alpha'}\begin{pmatrix} R_8^2 & 0 \\ 0 & R_9^2 \end{pmatrix} \qquad \text{and} \qquad B = \begin{pmatrix} 0 & \frac{1}{2} \\ -\frac{1}{2} & 0 \end{pmatrix} . \tag{2.1.1}$$

Using the definition of the circle lattice (1.3.4) along direction X^9, straightforwardly generalized for an arbitrary direction, the torus partition function becomes (remember that we omit the sums over momentum and winding numbers for lighter expressions)

$$\begin{aligned}\mathcal{T} = \int \frac{\mathrm{d}^2\tau}{\tau_2^5} \big[&\Lambda_{m_9,2n_9}\Lambda_{m_8,2n_8} + \Lambda_{m_9+1/2,2n_9}\Lambda_{m_8,2n_8+1} \\ &+ \Lambda_{m_9,2n_9+1}\Lambda_{m_8+1/2,2n_8} + \Lambda_{m_9+1/2,2n_9+1}\Lambda_{m_8+1/2,2n_8+1}\big] \left|\frac{V_8 - S_8}{\eta^8}\right|^2 .\end{aligned} \tag{2.1.2}$$

A feature of this partition function is that it is invariant under a T-duality transformation $(R_8, R_9) \to \left(\frac{\alpha'}{2R_8}, \frac{\alpha'}{2R_9}\right)$.

The same model can be built following another strategy [142] by applying a specific freely-acting orbifold on the usual eight-dimensional IIB theory without antisymmetric tensor. The generator is $g = \delta_{w_8}\delta_{p_9}$ where δ_{p_9} is the momentum shift already encountered in (1.3.7) whose action is repeated below and δ_{w_8} is a *winding shift* which acts asymmetrically on the left and right coordinates:

$$\delta_{w_8} : \begin{cases} X_{\mathrm{L}}^8 \to X_{\mathrm{L}}^8 + \frac{\alpha'\pi}{2R_8} \\ X_{\mathrm{R}}^8 \to X_{\mathrm{L}}^8 - \frac{\alpha'\pi}{2R_8} \end{cases} , \qquad \delta_{p_9} : X^9 \to X^9 + \pi R_9 . \tag{2.1.3}$$

The momentum shift produces a sign $(-1)^{m_9}$ when inserted in the trace and the winding shift produces a sign $(-1)^{n_8}$. As usual with orbifold constructions, there is a twisted sector required for modular invariance. The obtained torus amplitude is then

$$\mathcal{T} = \frac{1}{2}\int \frac{\mathrm{d}^2\tau}{\tau_2^5}\left[1 + (-1)^{n_8+m_9}\right]\left(\Lambda_{m_8,n_8}\Lambda_{m_9,n_9} + \Lambda_{m_8+\frac{1}{2},n_8}\Lambda_{m_9,n_9+\frac{1}{2}}\right)\left|\frac{V_8 - S_8}{\eta^8}\right|^2 , \tag{2.1.4}$$

which is the same as (2.1.2) up to a rescaling $R_9 \to 2R_9$.

2.1.2 The open-string amplitudes

To easily determine the open-string partition functions, we will fully make use of the geometrical interpretation of the tree-level amplitudes. In the T-dual type I′ theory along the internal circles,

[1] We define the tensors G and B to be dimensionless in this thesis. This contrasts with [77].

the orientifold projection becomes $\Omega' = \Omega\Pi_8\Pi_9(-1)^{F_L}$, where Π_i is the parity operation $X^i \to -X^i$ and F_L is the left fermion number. The presence of the parities is explained in Chapter 1 and the naively unexpected $(-1)^{F_L}$ factor is necessary for consistency. The original spacetime filling O9$_-$-plane becomes four O7$_-$-planes whose locations in the internal space are the fixed points of Ω'. It has actually only one fixed point which is the origin but it needs to be combined with the periodicity conditions $\delta_{2p_i} : X^i \to X^i + 2\pi R_i$ for $i \in \{8, 9\}$. The fixed points of Ω', $\Omega'\delta_{2p_8}$, $\Omega'\delta_{2p_9}$ and $\Omega'\delta_{2p_8}\delta_{2p_9}$ are thus respectively the origin and the points of coordinates $(\pi R_8, 0)$, $(0, \pi R_9)$ and $(\pi R_8, \pi R_9)$. The geometry is depicted in Fig. 2.1a. The four O7$_-$-planes have global tension and charge equal to -32 in units of a D7-brane tension requiring the addition of 32 objects and gauge group SO(32). Because the projection Ω' gives rise to pairs of branes, we refer to 32 "half-D7-branes" or alternatively to 16 regular D7-branes whose tensions are twice the ones involved in (1.2.29).

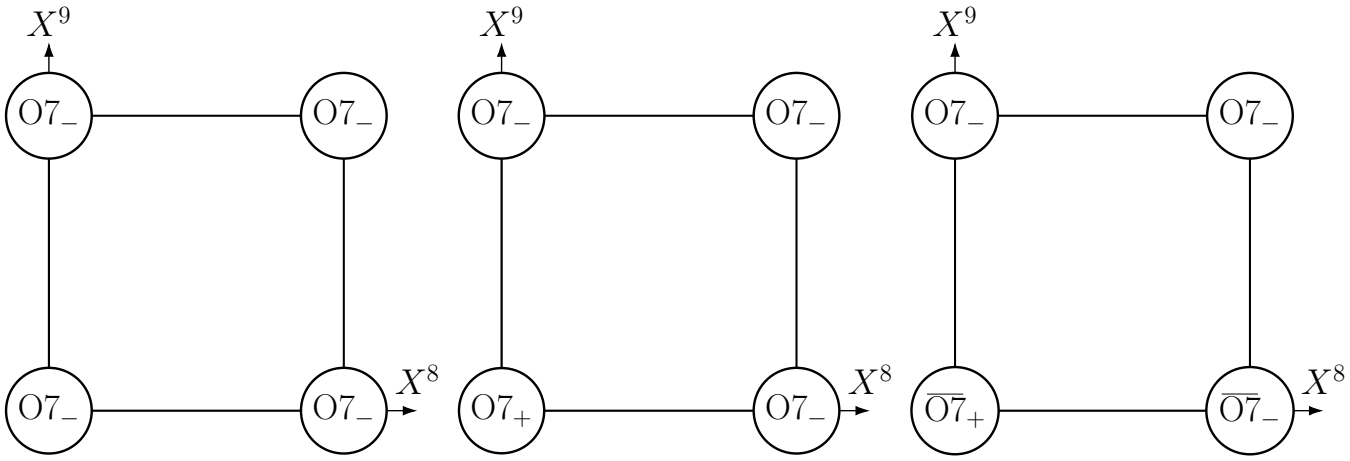

(a) Geometry of the standard SO(32) superstring. There is an O7$_-$-plane at each of the four fixed points.

(b) Geometry of the supersymmetric USp(16) model. There is 1 O7$_+$-plane at $(0,0)$ and 3 O7$_-$-planes at $(\pi R_8, 0)$, $(0, \pi R_9)$ and $(\pi R_8, \pi R_9)$.

(c) Geometry of the non-supersymmetric USp(16) model. There is 1 $\overline{\text{O7}}_+$-plane at $(0,0)$, 1 $\overline{\text{O7}}_-$-plane at $(\pi R_8, 0)$ and 2 O7$_-$-planes at $(0, \pi R_9)$ and $(\pi R_8, \pi R_9)$.

Figure 2.1: Eight-dimensional T-dual geometries: The standard SO(32) superstring theory, the USp(16) supersymmetric theory and its non-supersymmetric version.

The geometry is different for the model with discrete B_{ij} where it has been shown [143] that the orientifold plane at the origin becomes an O7$_+$-plane (see Fig. 2.1b). This change has dramatic consequences since now the global tension and charge of the O7-planes is -16, requiring the addition of only $N = 16$ half-D7-branes (8 D7-branes) to cancel the tadpoles. The rank of the gauge group is thus divided by two compared to the usual type I theory. As explained in Chapter 1, the positions of the O7-planes and their kinds completely determine the Klein-bottle tree-level amplitude. The phases $e^{i\vec{m}\cdot(\vec{x}_A - \vec{x}_B)}$ in (1.2.27) take values 1, $(-1)^{m_8}$, $(-1)^{m_9}$ and $(-1)^{m_8+m_9}$. Weighted by the correct product of tension and charge, this gives rise to a projector on the momentum numbers. In the SO(32) theory, the 16 terms corresponding to the 4×4 O-plane pairings yield a projection onto even momentum numbers. On the contrary, in the rank 8 case, no projection remains when summing the 16 contributions because of the presence of the O7$_+$-plane. The respective projectors $\Pi^{(16)}_{\tilde{K}}$ and $\Pi^{(8)}_{\tilde{K}}$ are

$$\Pi^{(16)}_{\tilde{K}} = 4\,[1 + (-1)^{m_8}]\,[1 + (-1)^{m_9}] \quad \text{and} \quad \Pi^{(8)}_{\tilde{K}} = 4\ . \tag{2.1.5}$$

For the tree-level annulus amplitude, it is trivial with no projection if we restrict to the case of a single stack of N half-D7-branes. The Möbius tree-level amplitude depends on where the stack is placed since it will produce different phases. Let us assume the branes to sit on top of the O7$_+$-plane at the origin. The four possible pairings D7-branes/O7-planes (with multiplicity N) weighted by the correct tensions and charges give the following projector:

$$\Pi = \frac{1-(-1)^{m_8}-(-1)^{m_9}-(-1)^{m_8+m_9}}{2} \ . \tag{2.1.6}$$

Then, the tree-level amplitudes of the rank 8 theory read

$$\tilde{\mathcal{K}} = \frac{2^5\alpha'}{8R_9R_8}\int_0^\infty \mathrm{d}l\, P_{m_9}P_{m_8}\frac{V_8-S_8}{\eta^8} \ , \qquad \tilde{\mathcal{A}} = \frac{2^{-5}N^2\alpha'}{2R_9R_8}\int_0^\infty \mathrm{d}l\, P_{m_9}P_{m_8}\frac{V_8-S_8}{\eta^8} \ ,$$
$$\tilde{\mathcal{M}} = \frac{N\alpha'}{2R_9R_8}\int_0^\infty \mathrm{d}l\, \big[P_{2m_9+1}-(-1)^{m_8}P_{2m_9}\big]P_{m_8}\frac{\hat{V}_8-\hat{S}_8}{\hat{\eta}^8} \ . \tag{2.1.7}$$

The lattices P_{m_i} in the amplitudes, which depend on l and the coming lattices W_{n_i} in the loop amplitudes which depend on τ_2 are defined as

$$P_{m_i} \equiv e^{-\pi\frac{l}{2}m_i^2\frac{\alpha'}{R_i^2}} \quad \text{and} \quad W_{n_i} \equiv e^{-\pi\tau_2 n_i^2\frac{R_i^2}{\alpha'}} \ . \tag{2.1.8}$$

Back to the loop channel, we obtain

$$\mathcal{K} = \frac{1}{2}\int_0^\infty \frac{\mathrm{d}\tau_2}{\tau_2^5}\, W_{2n_9}W_{2n_8}\frac{V_8-S_8}{\eta^8} \ , \qquad \mathcal{A} = \frac{N^2}{2}\int_0^\infty \frac{\mathrm{d}\tau_2}{\tau_2^5}\, W_{n_9}W_{n_8}\frac{V_8-S_8}{\eta^8} \ ,$$
$$\mathcal{M} = \frac{N}{2}\int_0^\infty \frac{\mathrm{d}\tau_2}{\tau_2^5}\, W_{n_9}\big[(-1)^{n_9}W_{2n_8}-W_{2n_8+1}\big]\frac{\hat{V}_8-\hat{S}_8}{\hat{\eta}^8} \ , \tag{2.1.9}$$

from which the field-theory spectrum can be read

$$(\mathcal{A}+\mathcal{M})|_{\mathrm{FT}} = \int_0^\infty \frac{\mathrm{d}\tau_2}{\tau_2^5}\left[\frac{N(N+1)}{2}W_{2n_9}W_{2n_8}+\frac{N(N-1)}{2}\big(W_{2n_9+1}W_{2n_8}+W_{n_9}W_{2n_8+1}\big)\right]\frac{V_8-S_8}{\eta^8}\bigg|_0 \ . \tag{2.1.10}$$

In this case, we read the dimension of the adjoint of an unitary symplectic group at the massless level and thus the open-string sector carries a USp(16) gauge group. We can show that when the branes are put on top of one of the three O7$_-$-planes, the detailed structure of the low-lying spectrum changes but the gauge group is always SO(16).

2.2 The supersymmetry-breaking mechanism

We are now ready to implement our supersymmetry-breaking mechanism, starting from the eight-dimensional rank 8 orientifold model described in the previous section. We first build the orientifold amplitudes ($\mathcal{K}$, $\mathcal{A}$ and $\mathcal{M}$) from the geometrical interpretation of the mechanism and then we uncover the corresponding altered orientifold projection. After that, we discuss how the torus partition function is affected and we end the section with a discussion on the different possible breaking patterns in this eight-dimensional setup[2].

[2]The followed logic for the description of the breaking mechanism, starting by the orientifold amplitudes and then turning to the torus partition function, matches the way we have built and uncovered the model and is chosen here for pedagogical purposes. Note that in the end, the model turns out to be an open descendant of a Scherk–Scwharz compacitfication and could have been described this way.

2.2.1 Orientifold amplitudes

Geometrically, we want to replace a pair of O7$_-$ and O7$_+$-planes which has net tension and charge zero by its counterpart with an $\overline{\text{O7}}_-$ and a $\overline{\text{O7}}_+$-plane which also has zero net tension and charge. This replacement does not change the tadpole cancellation condition and consequently does not introduce anomalies or even NS-NS tadpoles. As it will be seen explicitly in the amplitudes, the simultaneous presence of anti-orientifold planes with regular D7-branes breaks supersymmetry.

We thus consider the model with geometry depicted on Fig. 2.1c where, compared to the rank 8 supersymmetric geometry, the pair O7$_+$ - O7$_-$ at the bottom is replaced by a pair $\overline{\text{O7}}_+$ - $\overline{\text{O7}}_-$. This changes the computation of the tree-level Klein-bottle amplitude but it turns out that the result is the same as in the supersymmetric case *i.e.* without any projection on the momentum numbers. The tree-level annulus amplitude is also not affected by the supersymmetry breaking since it only feels the D7-branes which are untouched. Among the orientifold amplitudes, only the Möbius strip is sensitive to the breaking mechanism. Again, the precise expression of the tree-level Möbius depends on where the D7-branes are. When put at the origin on the $\overline{\text{O7}}_+$-plane, the projector now depends on the nature (NS-NS or R-R) of the closed-string state propagating between the O7-planes and the D7-branes. We thus have two projectors $\Pi_{\text{NS-NS}}$ and $\Pi_{\text{R-R}}$,

$$\begin{aligned}\Pi_{\text{NS-NS}} &= \frac{+1-(-1)^{m_9}-(-1)^{m_8}-(-1)^{m_9+m_8}}{2}\\ \Pi_{\text{R-R}} = (-1)^{m_8}\Pi_{\text{NS-NS}} &= \frac{-1-(-1)^{m_9}+(-1)^{m_8}-(-1)^{m_9+m_8}}{2}\ ,\end{aligned} \tag{2.2.1}$$

where $\Pi_{\text{NS-NS}}$ is the same as in the supersymmetric case in (2.1.6). The geometry is neatly encoded in these projectors: A change of sign among the four terms between the two projectors signals that the O7-plane at the corresponding fixed point has been promoted to an $\overline{\text{O7}}$-plane. The sign changes for the terms 1 and $(-1)^{m_8}$, consistently with the locations of the anti-orientifold planes in our geometry at the origin and at coordinates $(\pi R_8, 0)$. Altogether, the tree-level amplitudes are

$$\begin{aligned}\tilde{\mathcal{K}} &= \frac{2^5\alpha'}{8R_9R_8}\int_0^\infty \mathrm{d}l\, P_{m_9}P_{m_8}\frac{V_8-S_8}{\eta^8}\ , &\qquad \tilde{\mathcal{A}} &= \frac{2^{-5}N^2\alpha'}{2R_9R_8}\int_0^\infty \mathrm{d}l\, P_{m_9}P_{m_8}\frac{V_8-S_8}{\eta^8}\ ,\\ \tilde{\mathcal{M}} &= \frac{N\alpha'}{2R_9R_8}\int_0^\infty \mathrm{d}l\,\big[P_{2m_9+1}-(-1)^{m_8}P_{2m_9}\big]P_{m_8}\frac{\hat{V}_8-(-1)^{m_8}\hat{S}_8}{\hat{\eta}^8}\ ,\end{aligned} \tag{2.2.2}$$

where supersymmetry breaking is indeed visible in the Möbius strip. By modular transformation, the loop-channel amplitudes are

$$\begin{aligned}\mathcal{K} &= \frac{1}{2}\int_0^\infty \frac{\mathrm{d}\tau_2}{\tau_2^5}\,W_{2n_9}W_{2n_8}\frac{V_8-S_8}{\eta^8}\ , &\qquad \mathcal{A} &= \frac{N^2}{2}\int_0^\infty \frac{\mathrm{d}\tau_2}{\tau_2^5}\,W_{n_9}W_{n_8}\frac{V_8-S_8}{\eta^8}\ ,\\ \mathcal{M} &= \frac{N}{2}\int_0^\infty \frac{\mathrm{d}\tau_2}{\tau_2^5}\,W_{n_9}\big[(-1)^{n_9}W_{2n_8}-W_{2n_8+1}\big]\frac{\hat{V}_8+(-1)^{n_9}\hat{S}_8}{\hat{\eta}^8}\ .\end{aligned} \tag{2.2.3}$$

The changing compared to the supersymmetric case can be interpreted as a modification of the orientifold projection performed on the type IIB theory. Remembering that a winding shift δ_{w_9} along direction X^9 acts with $(-1)^{n_9}$ on the lattice states, we deduce an orientifold projection Ω'' which is

$$\Omega'' \equiv \Omega'(-\delta_{w_9})^F = \Omega\Pi_8\Pi_9(-1)^{F_{\text{L}}}(-\delta_{w_9})^F\ . \tag{2.2.4}$$

In this expression, F is the spacetime fermion number and ensures that the winding shift is only present in the projection for fermions. As evoked in Chapter 1, no fermions run in the Klein bottle so it is natural that Ω'' does not perturb it. A look at the field-theory spectrum gives[3]

$$(\mathcal{A}+\mathcal{M})|_{\rm FT} = \int_0^\infty \frac{\mathrm{d}\tau_2}{\tau_2^5}\left[\frac{N(N+1)}{2}\,\frac{V_8}{\eta^8}\bigg|_0 - \frac{N(N-1)}{2}\,\frac{S_8}{\eta^8}\bigg|_0\right] . \tag{2.2.5}$$

It is not supersymmetric with breaking at the string scale. The gauge group is still USp(16) but the fermions live in the antisymmetric representation. As it is typically the case in brane supersymmetry breaking scenarios, this antisymmetric representation contains a goldstino singlet which indicates a nonlinear realization of supersymmetry.

If the D7-branes rather sit at another fixed point, the gauge group is SO(16). When the branes are on the $\overline{\rm O7}_-$-plane, we still interpret a nonlinear supersymmetry while when they are on either of the two O7$_-$-planes, the spectrum is supersymmetric at the massless level and the breaking only occurs at the massive levels.

2.2.2 Brane stability

We described the field-theory interpretations depending on where the D7-branes are without mentioning their stability. Actually, they have no net interactions with orientifold planes but are attracted by the $\overline{\rm O7}_+$-plane and repelled by the $\overline{\rm O7}_-$-planes. We thus anticipate that the only stable configuration is when the branes are at the origin on the $\overline{\rm O7}_+$-plane. The instability of branes sitting elsewhere could naively be circumvented by placing only rigid half-branes there and put the rest at the origin. However, for consistency, single half-branes can only be put on O$_-$ or on $\overline{\rm O}_-$-planes and we can show that in eight dimensions, constraints coming from probe D5-branes forbid such configurations (see Sect. 2.3).

These energetic considerations can be recovered numerically by plotting the one-loop potential for arbitrary brane positions or equivalently, the vector field defined as minus the derivative of the potential with respect to the positions along X^8 and X^9. To plot such a vector field, we need the expression of the Möbius amplitude for arbitrary half-brane positions $2\pi a^i_\alpha$, $\alpha \in \{1,\dots,16\}$ along X^i, $i\in\{8,9\}$,

$$\begin{aligned}
\mathcal{M} &= \frac{1}{2}\sum_\alpha \int \frac{\mathrm{d}\tau_2}{\tau_2^5}\Bigg\{ \left[(-1)^{n_9} W_{2n_8+2a_\alpha^2} - W_{2n_8+1+2a_\alpha^2}\right]\frac{\hat V_8}{\hat\eta^8} \\
&\qquad - \left[(-1)^{n_9} W_{2n_8+1+2a_\alpha^2} - W_{2n_8+2a_\alpha^2}\right]\frac{\hat S_8}{\hat\eta^8}\Bigg\} W_{n_9+2a_\alpha^1} \ , \\
\tilde{\mathcal{M}} &= \frac{\alpha'}{2R_9R_8}\sum_\alpha \int \mathrm{d}l\, e^{4i\pi m_9 a_\alpha^1} e^{2i\pi m_8 a_\alpha^2} P_{m_8}\Bigg\{ \left[e^{2i\pi a_\alpha^1} P_{2m_9+1} - (-1)^{m_8} P_{2m_9}\right]\frac{\hat V_8}{\hat\eta^8} \\
&\qquad - \left[e^{2i\pi a_\alpha^1}(-1)^{m_8} P_{2m_9+1} - P_{2m_9}\right]\frac{\hat S_8}{\hat\eta^8}\Bigg\} .
\end{aligned} \tag{2.2.6}$$

From these expressions, the dependence of the one-loop potential on the positions a^i_α can be found in various regimes for the radii. Labelling the dynamical branes (at most 8) with an index r, the

[3]Here we assume the radii to not introduce scales lower than the string scale. The other possibilities will be discussed in Sect. 2.2.4 once the closed sector is better understood.

typical vector field $\left(-\frac{\partial\mathcal{V}}{\partial a_r^8}, -\frac{\partial\mathcal{V}}{\partial a_r^9}\right)$ for brane r at an arbitrary position is plotted in Fig. 2.2. We see that all positions but the origin yield unstable configurations.

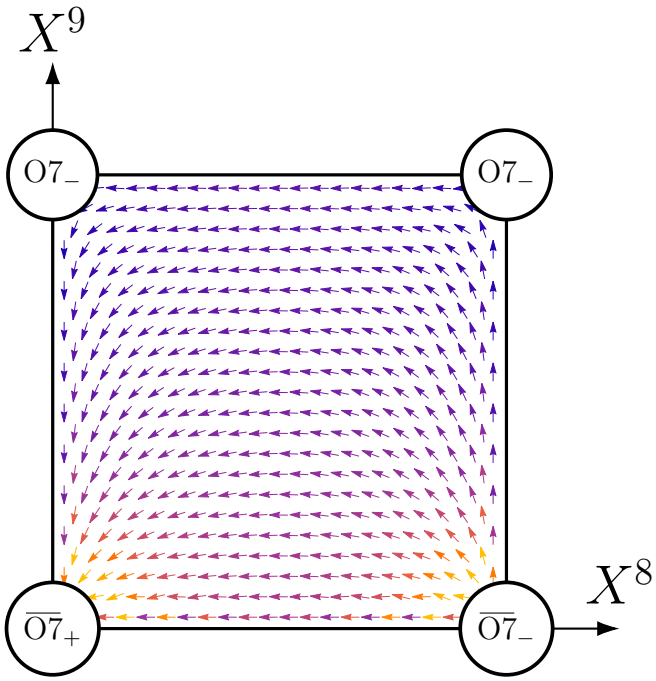

Figure 2.2: Example of vector field $\left(-\frac{\partial\mathcal{V}}{\partial a_r^8}, -\frac{\partial\mathcal{V}}{\partial a_r^9}\right)$ obtained numerically. The lighter the color, the longer the vector norm. We observe an attraction towards the origin, as expected.

2.2.3 The closed sector

We need now to discuss what happens in the torus partition function. Naively, one could think the supersymmetric torus (2.1.2) remains valid for the non-supersymmetric model. If this was the case, one would have completely supersymmetric closed-string one-loop amplitudes. This would not be equivalent to a supersymmetric closed-string sector since transmission of the breaking from the open sector should happen. Ignoring this transmission, we will argue in this subsection that the supersymmetric torus is not consistent and should actually reveal a soft breaking of supersymmetry *à la* Scherk–Schwarz.

Before arguing on the consistency or not of the closed sector with the breaking mechanism, let us construct a softly broken version of the supersymmetric torus (2.1.2). To this end, the construction of the model *via* the freely-acting orbifold $g = \delta_{w_8}\delta_{p_9}$ is useful since it is easy to build a Scherk–Schwarz deformation from it: One simply couples g with the usual non-supersymmetric generator $(-1)^F$. Gauging the type IIB theory with $g' = (-1)^F\delta_{w_8}\delta_{p_9}$ we obtain as usual four contributions in the torus: With or without the g' insertion and the twisted sector. The partition function is

$$\begin{aligned}\mathcal{T} = \frac{1}{2}\int\frac{\mathrm{d}^2\tau}{\tau_2^5}\Big\{&\Lambda_{m_8,n_8}\Lambda_{m_9,n_9}\left|V_8-S_8\right|^2 + (-1)^{n_8+m_9}\Lambda_{m_8,n_8}\Lambda_{m_9,n_9}\left|V_8+S_8\right|^2\\ &+\Lambda_{m_8+\frac{1}{2},n_8}\Lambda_{m_9,n_9+\frac{1}{2}}\left|O_8-C_8\right|^2 + (-1)^{n_8+m_9}\Lambda_{m_8+\frac{1}{2},n_8}\Lambda_{m_9,n_9+\frac{1}{2}}\left|O_8+C_8\right|^2\Big\}\frac{1}{|\eta^8|^2}\ .\end{aligned} \tag{2.2.7}$$

We then perform the rescaling of the radius $R_9 \to 2R_9$ and we obtain

$$\begin{aligned}\mathcal{T} = \int \frac{\mathrm{d}^2\tau}{\tau_2^5}\Big\{ & \left(\Lambda_{m_8,2n_8}\Lambda_{m_9,2n_9} + \Lambda_{m_8,2n_8+1}\Lambda_{m_9+\frac{1}{2},2n_9}\right)\left(|V_8|^2 + |S_8|^2\right) \\ & - \left(\Lambda_{m_8,2n_8+1}\Lambda_{m_9,2n_9} + \Lambda_{m_8,2n_8}\Lambda_{m_9+\frac{1}{2},2n_9}\right)\left(V_8\overline{S}_8 + \overline{V}_8 S_8\right) \\ & + \left(\Lambda_{m_8+\frac{1}{2},2n_8}\Lambda_{m_9,2n_9+1} + \Lambda_{m_8+\frac{1}{2},2n_8+1}\Lambda_{m_9+\frac{1}{2},2n_9+1}\right)\left(|O_8|^2 + |C_8|^2\right) \\ & - \left(\Lambda_{m_8+\frac{1}{2},2n_8+1}\Lambda_{m_9,2n_9+1} + \Lambda_{m_8+\frac{1}{2},2n_8}\Lambda_{m_9+\frac{1}{2},2n_9+1}\right)\left(O_8\overline{C}_8 + \overline{O}_8 C_8\right)\Big\}\frac{1}{|\eta^8|^2}\ .\end{aligned} \tag{2.2.8}$$

From the second line of this expression, we read the two masses M_1 and M_2 acquired by the gravitinos:

$$M_1 = \frac{R_8}{\alpha'} \quad \text{and} \quad M_2 = \frac{1}{2R_9}\ , \tag{2.2.9}$$

which go to zero in the two supersymmetric limits $R_8 \to 0$ and/or $R_9 \to +\infty$. In M_2, we recognize the usual Scherk–Schwarz mass proportional to the inverse of the radius R_9. In M_1, the mass is proportional to the radius because along direction X^8, g' acts with a winding shift instead of a momentum shift. As it is the case with the standard mechanism described in Chapter 1, there is a tachyon due to the twisted $|O_8|^2$ character if the radii satisfy

$$\frac{\alpha'^2}{4R_8^2} + R_9^2 < 2\alpha'\ . \tag{2.2.10}$$

We can now understand why the supersymmetric torus seems inconsistent with the broken open sector and why the softly broken version seems much more plausible. We saw that the orientifold planes are the fixed points of the orientifold projection, modulo the periodicity identifications. With the supersymmetric torus, the identifications are simply the classical ones for circles, $\delta_{2p_8} : X^8 \to X^8 + 2\pi R_8$ and $\delta_{2p_9} : X^9 \to X^9 + 2\pi R_9$. As for the orientifold projection of the broken model Ω'', it contains the non-supersymmetric generator $(-\delta_{w_9})^F$. Because the presence of a non-supersymmetric generator should produce an anti-orientifold plane, the four fixed points of Ω'', $\Omega''\delta_{2p_8}$, $\Omega''\delta_{2p_9}$ and $\Omega''\delta_{2p_8}\delta_{2p_9}$ should be anti-orientifold planes and preserve the same supersymmetries, which is inconsistent with the geometry of the model displayed in Fig. 2.1c.

On the contrary, in the softly broken torus, the periodicity along X^9 is replaced by the action of g' in which the rescaling of the radius $R_9 \to 2R_9$ has been performed. The periodicity condition thus becomes $\delta'_{2p_9} \equiv (-1)^F \delta_{w_8}\delta_{2p_9}$. The four fixed points are then:

- Fixed point of $\Omega'' = \Omega\Pi_8\Pi_9(-1)^{F_{\mathrm{L}}}(-\delta_{w_9})^F$: The projection contains a non-supersymmetric generator and the two parities. The fixed point is thus at the origin and is an anti-orientifold plane.
- Fixed point of $\Omega''\delta_{2p_8} = \Omega\Pi_8\delta_{2p_8}\Pi_9(-1)^{F_{\mathrm{L}}}(-\delta_{w_9})^F$: The parity along X^8 combined with the periodicity fixes the point $(\pi R_8, 0)$ and we still have an anti-orientifold plane.
- Fixed point of $\Omega''\delta'_{2p_9} = \Omega\Pi_8\delta_{w_8}\Pi_9\delta_{2p_9}(-1)^{F_{\mathrm{L}}}(-\delta_{w_9})^F(-1)^F$: The two non-supersymmetric factors cancel each other to yield an orientifold plane. Due to the combination of the parity along X^9 with the periodicity δ_{2p_9}, it is located at $(0, \pi R_9)$.

- Fixed point of $\Omega''\delta_{2p_8}\delta'_{2p_9} = \Omega\Pi_8\delta_{2p_8}\delta_{w_8}\Pi_9\delta_{2p_9}(-1)^{F_{\rm L}}(-\delta_{w_9})^F(-1)^F$: This is again an orientifold plane and it is located at $(\pi R_8, \pi R_9)$ due to the presence of the two periodicities together with the two parities.

All this gives a geometrical interpretation consistent with the model depicted in Fig. 2.1c. If one performs the same analysis with the supersymmetric torus and hence with the standard periodicity δ_{2p_9}, one would not understand why both kinds of orientifold planes appear in the model.

We expect that the fundamental reason why the supersymmetric torus is not compatible with the projection Ω'' is simply because it is not a symmetry of the supersymmetric spectrum and it is therefore not allowed to gauge it. However, the detailed demonstration of this fact has not been carried out. Also note that the presence of massless gravitinos along with broken supersymmetry would also be difficult to explain from a supergravity point of view.

2.2.4 Breaking scales and gravitino mass

As a consequence of the soft breaking in the closed sector, our eight-dimensional model contains two breaking scales. The one from the closed sector is the usual momentum scale or winding scale and in the open-string sector, it can be the string scale or the winding scale depending on which one is smaller. Let us begin by a deeper study of the supersymmetry-breaking pattern in the stable configuration where the branes are put at the origin on top of the $\overline{\rm O7}_+$-plane.

The full field-theory spectrum (2.2.5) without omitting the winding modes is

$$\begin{aligned}(\mathcal{A}+\mathcal{M})|_{\rm FT} = \int_0^\infty \frac{{\rm d}\tau_2}{\tau_2^5}\Bigg\{ &\frac{N(N+1)}{2}\,W_{2n_9}\left(W_{2n_8}\frac{V_8}{\eta^8} - W_{2n_8+1}\frac{S_8}{\eta^8}\right)\Bigg|_0 \\ &+\frac{N(N-1)}{2}\left[W_{2n_9}\left(W_{2n_8+1}\frac{V_8}{\eta^8} - W_{2n_8}\frac{S_8}{\eta^8}\right) + W_{2n_9+1}W_{n_8}\frac{V_8-S_8}{\eta^8}\right]\Bigg|_0\Bigg\}\,.\end{aligned} \tag{2.2.11}$$

At the zero-winding level, we recover (2.2.5). As already said, the open-string gauge group is USp(16) and we see in (2.2.11) that the breaking scale depends on the value of R_8. If it is large, the breaking scale is the string scale and we interpret a nonlinear realization of supersymmetry. As R_8 goes to zero, the even-windings and odd-windings lattices become equal and the spectrum (2.2.11) becomes supersymmetric. In this case, we can interpret a spontaneous breaking in the open sector with a familiar winding Scherk–Schwarz scale proportional to R_8. From another point of view, the breaking shares common features with brane supersymmetry breaking since only the Möbius is affected[4] by exchanging symmetric and antisymmetric representations for fermions compared to bosons.

In the other closed-string supersymmetric limit $R_9 \to +\infty$, supersymmetry is not recovered in the open sector and this regime looks like a true brane supersymmetry breaking mechanism with untouched closed sector. However, it is highly likely that the two limits $R_8 \to 0$ and $R_9 \to +\infty$ are not consistent from a field-theory point of view. In the former limit, the spectrum cannot be interpreted from a nine-dimensional perspective. Indeed, in this limit, the first and second terms in (2.2.11) combine together with an overall multiplicity N^2. Such a multiplicity cannot be interpreted in terms of representations of the USp(N) gauge group. In the latter limit, there are local tensions and charges that generate a strong backreaction *i.e.* local tadpoles remain uncancelled because of the collapse of a Kaluza–Klein tower of states. From a more general point of view, the fact that

[4] In Chapter 1 in (1.3.10), we saw that in a standard Scherk–Schwarz mechanism, both the annulus and Möbius are affected.

the effective theory breaks down in some limits is just the consequence of the existence of moduli branches that only exist in lower dimensions and which are not connected to moduli spaces in higher dimensions.

If the D7-branes are put on the upper-right O7$_-$-plane, the field-theory spectrum is

$$(\mathcal{A}+\mathcal{M})|_{\mathrm{FT}} = \int_0^\infty \frac{\mathrm{d}\tau_2}{\tau_2^5}\left\{\frac{N(N-1)}{2}\left[W_{2n_9}W_{n_8}\frac{V_8-S_8}{\eta^8}+W_{2n_9+1}\left(W_{2n_8}\frac{V_8}{\eta^8}-W_{2n_8+1}\frac{S_8}{\eta^8}\right)\right]\right|_0 + \frac{N(N+1)}{2}W_{2n_9+1}\left(W_{2n_8+1}\frac{V_8}{\eta^8}-W_{2n_8}\frac{S_8}{\eta^8}\right)\Bigg|_0\Bigg\}\ . \tag{2.2.12}$$

In this case the gauge group is SO(16). The $R_8 \to 0$ limit gives again a supersymmetric spectrum with a spontaneous breaking interpretation. When $R_9 \to +\infty$, the non-zero winding states along X^9 become supermassive and decouple. But again, these limits are certainly not consistent at the field-theory level.

2.3 Probe branes

In this section, we explore consistency conditions coming from the insertion of probe branes in the model. The probe branes carrying an SU(2) gauge group are subject to the Witten four-dimensional SU(2) anomalies, related to consistency constraints coming from K-theory [144–147]. The term *probe branes* refer to D-branes that are not subject to consistency constraint from the tadpole cancellation condition unlike the *background branes*. The background branes are D9-branes in type I string and the probe branes can be D7, D5, D3 or D1-branes. Because we are interested in four-dimensional probe gauge theories for constraints to arise, we will ignore the D1-branes that lead to two-dimensional theories.

In type I, the D7 and D3-branes carry unitary gauge groups U(M) for some M while the D5-branes support USp(M) gauge groups for $B_{ij}=0$ [148,149]. In the case $B_{ij}\neq 0$, SO(M) groups are also possible but we are only interested in SU(2) anomalies with SU(2) $\subset$ U(2), USp(2). The Witten anomaly arises from strings stretched between the background D9-branes and the probe branes which transform in the fundamental representation of the SU(2) probe-brane gauge group: The number of SU(2) doublets should be even to avoid anomalies. Such states only arise in the cylinder amplitude and thus our supersymmetry-breaking mechanism does not change the discussion. After T-duality, one obtains a geometry with O$_+$, O$_-$, $\overline{\mathrm{O}}_+$ and $\overline{\mathrm{O}}_-$-planes but we focus on supersymmetric geometries without anti-orientifold planes due to the argument above and we assume the background branes to sit on O$_-$-planes for constraints to arise.

In eight dimensions, the strongest constraint comes from the addition of two probe D5-branes before T-duality. The D9-D5 states contain six-dimensional Majorana-Weyl fermions in the $(M,2)$ representation of SO$(M)_9 \times$ USp$(2)_5$. When the D5-branes (extended along the four spacetime dimensions) wrap the compactified T^2, the states becomes D7-D3 strings after T-duality and the probe gauge theory is indeed four-dimensional. The following tables show what the branes become under T-duality. The dimensions labels are written in the first line and for each kind of brane, a cross means that it wraps the corresponding direction while a dot means it does not.

8d	0	1	2	3	4	5	6	7	8	9
D9	x	x	x	x	x	x	x	x	x	x
D5	x	x	x	x	·	·	·	·	x	x

T-duality $\longrightarrow$

8d	0	1	2	3	4	5	6	7	8	9
D7	x	x	x	x	x	x	x	x	·	·
D3	x	x	x	x	·	·	·	·	·	·

In this case, if we place M D7-branes and probe D3-branes on an O7$_-$-plane, because the D3-branes are points inside the T^2, the number of SU(2) doublets is equal to M. We thus learn that M should be even. We conclude that in eight dimensions, configurations with rigid half-D7-branes are forbidden for consistency.

If before T-duality the probe D5-branes wrap the T^2 differently, this will not produce a four-dimensional probe gauge theory after T-duality and thus there is no constraint. A similar argument holds for probe D7-branes. As for the probe D3-branes, they indeed yield a four-dimensional probe gauge theory after T-duality but the obtained probe D5-branes wrap the whole T^2 so that no constraint arises since they see all the background branes (see table below).

8d	0	1	2	3	4	5	6	7	8	9
D9	x	x	x	x	x	x	x	x	x	x
D3	x	x	x	x	·	·	·	·	·	·

T-duality $\longrightarrow$

8d	0	1	2	3	4	5	6	7	8	9
D7	x	x	x	x	x	x	x	x	·	·
D5	x	x	x	x	·	·	·	·	x	x

2.4 Conclusions and outlook

In this first part of the thesis, we explored a new mechanism to break supersymmetry at the string level in orientifold models. By consistently replacing pairs of orentifold planes that have zero net tension and charge by their anti-orientifold counterparts, the breaking affects only the Möbius amplitude in the open sector and does not introduce NS-NS tadpoles. We saw that the breaking scale can either be the string scale or a compactification scale depending on the location in moduli space.

We gave strong arguments to discard the supersymmetric torus amplitude as the correct closed sector for our model with broken supersymmetry. We suggested instead a soft breaking in the torus, which seems in agreement with the geometry. However, it would be interesting to study further the field-theory limits to completely settle the question. If it is consistent to keep the supersymetric torus with the supersymmetric open sector, this would provide new perfect models of brane supersymetry breaking type, without tadpoles. Such orientifold vacua would be at odds with the gravitino mass conjecture [150, 151] whereas our models are in agreement with it since the supersymmetric limits exhibited in our models are argued not to be consistent from a field-theory point of view.

Note that all brane supersymmetry breaking models which feature a supersymmetric closed-string sector suffer from NS-NS tadpoles that may induce a breakdown of the effective field theory around the true vacuum so that in the end, the models would be in agreement with the gravitino mass conjecture. Also, even when we talk of a supersymmetric closed-string sector, it is understood to be at tree-level since because the open-string sector is broken, it should transmit the breaking to the closed sector *via* quantum corrections. It is unclear to us if the conjecture should hold for the tree-level spectrum or for the quantum theory. A last remark is that in our models, the gravitino mass can be much lower than the typical scale of the quantum potential. This could be useful in inflationary models of the type studied in [152–157].

As a complexification of the models described here, it would be very interesting to consider non-freely-acting orbifold compactifications in order to produce a more realistic chiral spectrum in four dimensions. The combination of our supersymmetry-breaking mechanism with orbifolds may yield interesting new breaking patterns.

3 | Open-string moduli stabilization

This chapter tackles the second part of our guiding tryptich: The generic study of moduli stabilization in models with perturbative spontaneous breaking of supersymmetry. We do this in the context of open-string models to develop an intuitive geometric reasoning in terms of D-brane positions. Supersymmetry is broken with a Scherk–Schwarz mechanism performed along a circle and we focus on the regime where the radius of the circle is moderately large without any mass scale below the breaking scale so that the approximation (1.3.11) for the one-loop potential holds, up to exponentially suppressed terms.

Generically, the Scherk–Schwarz mechanism yields an excess of massless bosons so that the one-loop potential is negative. However, the addition of open-string Wilson lines can help uplifting the potential and maybe reach a vanishing potential up to the exponentially suppressed terms. Such uplifting is expected to be hard to achieve while maintaining a non-tachyonic configuration, as can be understood from the schematic Taylor expansion of the one-loop potential with respect to the Wilson lines generically denoted ϕ^I here, around an extremal point with respect to them [44, 56–59]:

$$\mathcal{V}_{\text{1-loop}} \approx \xi_d(n_{\text{F}} - n_{\text{B}})M^d + \xi_{d-2}(T_{\mathcal{R}_{\text{B}}} - T_{\mathcal{R}_{\text{F}}})(\phi^I)^2 M^d + \cdots \ . \tag{3.0.1}$$

In this schematic expression (the precise formula in an $\mathcal{N} = 4 \to \mathcal{N} = 0$ context is given in (3.1.28)), we have already defined the positive constant ξ_d and the numbers of massless fermionic and bosonic degrees of freedom n_{F} and n_{B}. ξ_{d-2} is another positive constant and $T_{\mathcal{R}_{\text{B}}}$ and $T_{\mathcal{R}_{\text{F}}}$ are the Dynkin indices of the representations in which the massless bosons and fermions live. We see that on the one hand, increasing the number of massless fermions tends to increase the value of the potential but on the other hand, it tends to degrade the stability of the moduli and to generate tachyonic instabilities.

Let us briefly review the results of [58], where the stability analysis is done in an $\mathcal{N} = 4 \to \mathcal{N} = 0$ open-string model. The authors try to increase the value of the potential by increasing the number of massless fermions compared to bosons while keeping a non-tachyonic configuration. This is done thanks to the interplay between the Sherk–Schwarz mechanism and the open-string Wilson lines to give the mass shift to some bosons instead of only to fermions. The stability is ensured by the use of rigid/frozen half-branes that are stuck at a fixed point and, if single, produce a "gauge factor" SO(1). Upon compactification to lower dimensions, they can produce enough such factors to uplift the potential to zero (up to the exponentially small contributions) or to slightly positive values. In the obtained configurations, all moduli are non-tachyonic. Of course, these conclusions may not hold once the cosmology of the system is studied but as an approximate general rule in Scherk–Schwarz setups, the mere implementation of finite temperature makes the naive expectations correct.

We will start this chapter by explaining the results of [59] where the stability analysis is done in a more complex setup with a non-freely acting orbifold producing $\mathcal{N} = 2 \to \mathcal{N} = 0$ models. As

we will see, the stability study will lead us to the need to evaluate one-loop masses of states in the Neumann–Dirichlet sector of the theory. To evaluate the masses of such states, we compute their one-loop correlation functions [60, 61], an involved task requiring the technology of twist fields.

3.1 Stability of open-string orbifold models

Let us begin with the description of the supersymmetric model which constitute the basis of the work presented here: The Bianchi-Sagnotti-Gimon-Polchinski (BSGP) model [158–160] compactified to four dimensions.

3.1.1 Supersymmetric setup

The model is the orientifold projection of type IIB with the following background:

$$\mathbb{R}^{1,3} \times T^2 \times \frac{T^4}{\mathbb{Z}_2} \ . \tag{3.1.1}$$

The $\mathbb{Z}_2$ orbifold is non-freely acting on the T^4 along directions X^6, X^7, X^8, X^9 with a generator g,

$$g: \ (X^6, X^7, X^8, X^9) \longrightarrow (-X^6, -X^7, -X^8, -X^9) \ . \tag{3.1.2}$$

Two kinds of orientifold planes are present: An O9$_-$-plane which is the fixed point of the orientifold projection Ω and 16 O5$_-$-planes which are the fixed points of Ωg (modulo the periodicities inside T^4). Two kinds of branes need to be added to cancel the tadpoles: 32 D9-branes and 32 D5-branes orthogonal to the internal $T^4/\mathbb{Z}_2$. The gauge groups carried by both kinds of branes are unitary so that the biggest gauge group that can be achieved without introducing Wilson lines or non-trivial brane positions is $\mathrm{U}(16) \times \mathrm{U}(16)$. Note that the directions spanning the T^2 are denoted X^4 and X^5. The four-dimensional extended spacetime is described by the remaining directions X^0, X^1, X^2 and X^3.

The goal of the work presented here is to study the stability at one loop after supersymmetry breaking of all possible deformations of the model. The moduli under consideration are:

- The positions of the D5-branes along the internal $T^4/\mathbb{Z}_2$.
- The Wilson lines along the T^2 for the gauge group supported by the D5-branes.
- The Wilson lines along the whole internal space for the gauge group supported by the D9-branes.
- Scalars in the Neumann–Dirichlet (ND) sector of the theory, whose stability analysis requires more work and is carried out in the last section of this chapter.
- In the closed-string sector, there are the usual NS-NS moduli: The internal metric denoted $G_{\mathcal{I}\mathcal{J}}$ where calligraphic indices refer to all the internal directions ($\mathcal{I}, \mathcal{J} \in \{4, \ldots, 9\}$) and the dilaton. The antisymmetric tensor is projected out by the orientifold.
- In the R-R sector, there are moduli associated with the surviving two-form $C_{\mathcal{I}\mathcal{J}}$.
- There is also a twisted closed-string sector which contains 16 quaternionic moduli, localized at the fixed points of $T^4/\mathbb{Z}_2$.

It is useful to have a geometric representation of the first three items *i.e.* the open-string moduli in the Neumann–Neumann (NN) and Dirichlet–Dirichlet (DD) sectors. The D5-branes already have a geometric interpretation with their positions inside the $T^4/\mathbb{Z}_2$. To convert the Wilson lines along the T^2 into positions as well, we can consider the theory where this T^2 is T-dualized to a $\tilde{T}^2$ with coordinates $\tilde{X}^4$ and $\tilde{X}^5$ on which the orientifold now acts with an additional parity I_{45} creating fixed points. In this T-dual picture, the original D5-branes are D3-branes and their positions completely characterize the moduli in the DD sector. Fig. 3.1a shows such a geometric configuration. The four fixed points of the $\tilde{T}^2/I_{45}$ are represented while schematically, only two fixed points along the $T^4/\mathbb{Z}_2$ are drawn (in total $4 \times 2 = 8$ fixed points are represented). Anticipating on the sequel, the D3-branes are localized at the fixed points of the whole internal space $T^4 \times \tilde{T}^2/I_{45}$ and the direction $\tilde{X}^5$ is referred to as the Scherk–Schwarz direction. To convert the Wilson lines associated with the D9-branes into positions, we define another T-dual theory where the whole internal space is T-dualized to $\tilde{T}^2/I_{45} \times \tilde{T}^4/\mathbb{Z}_2$. The original D9-branes also become D3-branes in this theory and the positions completely describe the moduli in the NN sector. Fig. 3.1b represents such a configuration. Even if it is somewhat abusive because the two pictorial representations for the original D5-branes and D9-branes are not in the same T-dual theory, we will draw brane/Wilson lines configurations on a single picture like in Fig. 3.1c. With the appropriate interpretation we just gave for such representations, this is fully correct and it highly facilitates the manipulation of brane configurations/Wilson lines.

The geometrical representations are useful to understand what are the true dynamical degrees of freedom of the brane positions and thus the true dynamical Wilson lines compared to the discrete ones. Along the $T^4/\mathbb{Z}_2$, the actions of the orientifold projection and the non-freely-acting orbifold divide by 4 the maximum number of dynamical brane positions. The branes are associated by pairs and can only move by packets of four, symmetrically around the fixed points of $T^4/\mathbb{Z}_2$. We thus conclude that if $2n + 2$, $n \in \mathbb{N}$, branes sit at a fixed point, two of them are rigid and cannot move. There is a maximum of 8 independent positions along $T^4/\mathbb{Z}_2$ when all stacks are multiple of four and a minimum of 0 dynamical degrees of freedom if the branes are all isolated by stacks of two. Along the T^2, there is no action of the orbifold so that the maximum number of degrees of freedom is 16 and the branes also move by mirror pairs. Actually, this number cannot be decreased by isolating single branes on fixed points since this would be inconsistent with the unitary gauge groups supported by the branes[1].

The configurations of interest to us correspond to D3-branes placed at fixed points in the appropriate T-dual pictures since, as we will see later, they correspond to extrema of the effective potential in presence of supersymmetry breaking. We thus introduce a specific labelling for these 64 fixed points. A fixed point is denote ii' where $i \in \{1, \dots, 16\}$ indicates one of the 16 fixed points along the $T^4/\mathbb{Z}_2$ and $i' \in \{1, \dots, 4\}$ denotes one of the four T^2 fixed points. Anticipating on the supersymmetry breaking, it is useful to follow a specific convention for the labelling of the T^2 fixed points in order to distinguish those that are at the origin along direction $\tilde{X}^5$ and those that are at $\pi\sqrt{G_{55}}$. The index i' is thus chosen to be odd for points at the origin and even for the others. Fig. 3.1d schematically represents this labelling. Restricting to brane configurations (in the appropriate T-dual picture) with branes located at the fixed points, we define $N_{ii'}$ and $D_{ii'}$ the number of D3-branes, T-dual to D9-branes and D5-branes respectively, sitting at fixed point ii'. As we saw, each fixed point carries zero or at least two D3-branes so that these numbers are

[1]It would be possible with an orthogonal group. This is what is used to uplift the potential without introducing instabilities in [58].

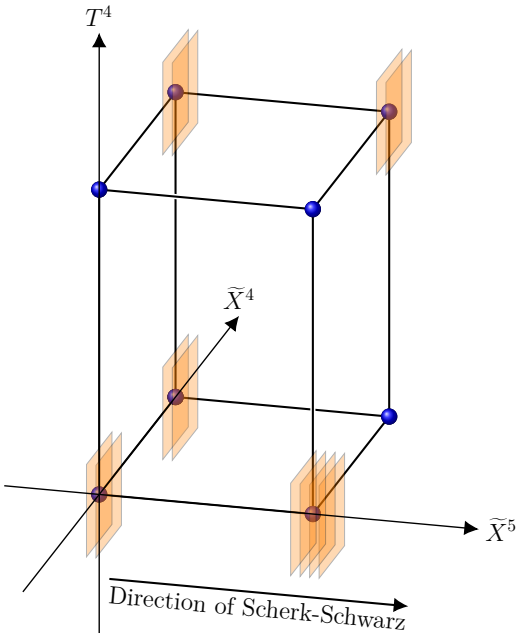

(a) A configuration of D3-branes associated with the D5-branes of the initial type I theory, once T^2 is T-dualized. In this example, the D3-branes sit on O3-planes.

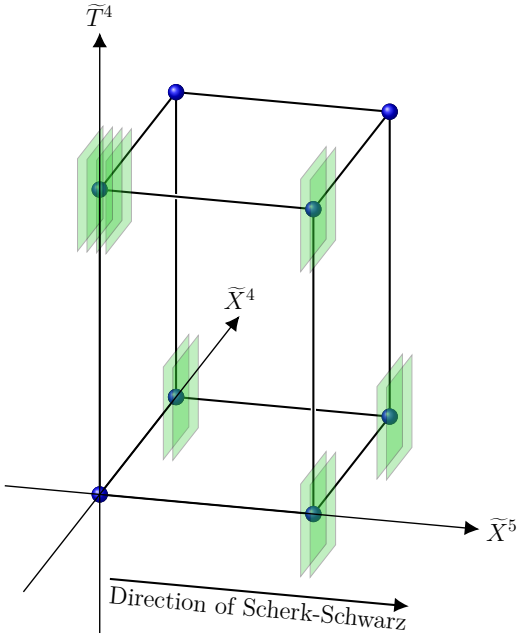

(b) A configuration of D3-branes associated with the D9-branes of the initial type I theory, once both T^2 and $T^4/\mathbb{Z}_2$ are T-dualized. In this example, the D3-branes sit on O3-planes.

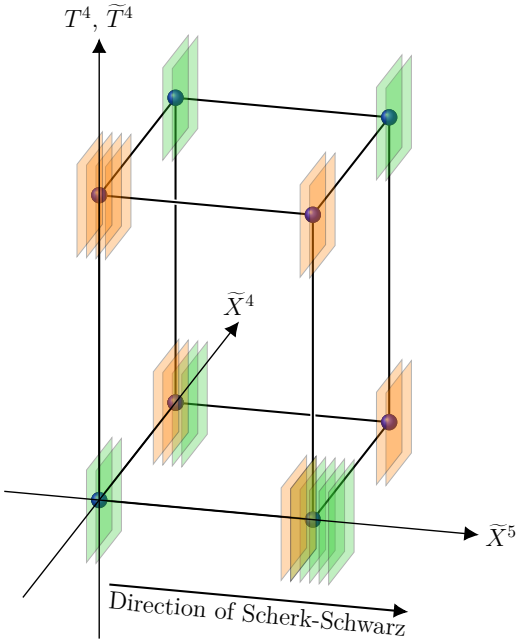

(c) Superposition of pictures (a) and (b). D3-branes associated with the D5-branes (D9-branes) of the initial type I theory are shown in orange (green).

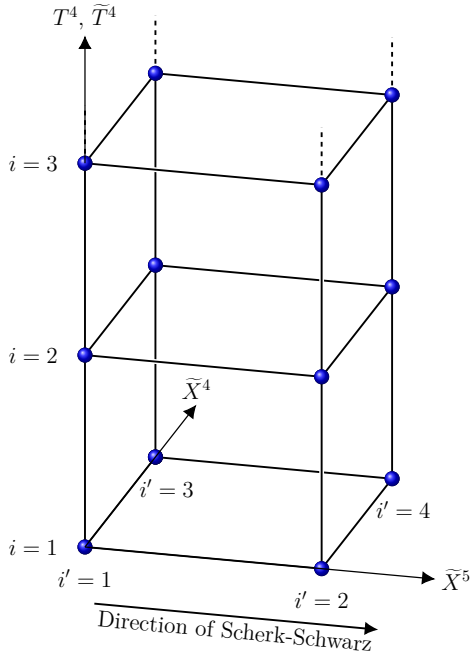

(d) Labelling of the $\tilde{T}^2$ fixed points $i' = 1, 2, 3, 4$, and schematic labelling of the $T^4/\mathbb{Z}_2$ or $\tilde{T}^4/\mathbb{Z}_2$ fixed points $i = 1, \ldots, 16$. Odd i' correspond to points located at $\tilde{X}^5 = 0$, while even i' are associated with points at $\tilde{X}^5 = \pi\sqrt{G_{55}}$, where $\tilde{X}^5$ is the coordinate T-dual to the direction along which the Scherk–Schwarz mechanism is implemented.

Figure 3.1: Geometric T-dual description of the moduli arising from the NN and DD sectors of the orientifold theory.

even and consequently written as $N_{ii'} \equiv 2n_{ii'}$ and $D_{ii'} \equiv 2d_{ii'}$. With these definitions, the tadpole cancellation condition is

$$\sum_{i,i'} N_{ii'} = 32 \iff \sum_{i,i'} n_{ii'} = 16 \ , \qquad \sum_{i,i'} D_{ii'} = 32 \iff \sum_{i,i'} d_{ii'} = 16 \ , \tag{3.1.3}$$

and the open-string gauge group $\mathcal{G}_{\rm open}$ of the model reads (it is understood that if $n_{ii'}$ or $d_{ii'}$ is zero, it does not produce any gauge group)

$$\mathcal{G}_{\rm open} = \prod_{i,i'} {\rm U}(n_{ii'}) \times {\rm U}(d_{ii'}) \ . \tag{3.1.4}$$

For such configurations, the D3-branes positions in the appropriate T-dual pictures (normalized by the internal radii), take values $2\pi\vec{a}_{ii'}$ for the D3-branes T-dual to the D9-branes and $2\pi\vec{b}_{ii'}$ for the D3-branes T-dual to the D5-branes. The vector $\vec{a}_{ii'} \equiv (\vec{a}_{i'}, \vec{a}_i)$, where $\vec{a}_{i'}$ and $\vec{a}_i$ are two- and four-dimensional vectors, has components which take values 0 or $\frac{1}{2}$.

Note that there are non-perturbative constraints for the consistency of the BSGP model [160]. In the original model in only six dimensions, the moduli space has several disconnected components defined by the even number $\mathcal{R} = 0, 2, \ldots, 16$ of pairs of D5-branes that have rigid positions along the $T^4/\mathbb{Z}_2$. The constraint is on the allowed values for $\mathcal{R}$ that can only be equal to 0, 8 or 16. Moreover, when $\mathcal{R} = 8$, the 8 rigid pairs of branes must be on one of the hyperplanes $X^I = 0$ or $X^I = \pi\sqrt{G_{II}}$, $I \in \{6, \ldots, 9\}$. Same constraints arise for the D9-branes, viewed as D5-branes in the theory where the $T^4/\mathbb{Z}_2$ is T-dualized. This defines $\tilde{\mathcal{R}} = 0$, 8 or 16. Up to a T-duality, this gives rise to 6 consistent disconnected parts for the moduli space:

$$(\mathcal{R}, \tilde{\mathcal{R}}) = (0,0),\ (0,8),\ (0,16),\ (8,8),\ (8,16),\ (16,16) \ . \tag{3.1.5}$$

Note that these parts of moduli space are actually connected by deformations of the $T^4/\mathbb{Z}_2$ into smooth $K3$ manifolds [160]. Compactifying the model further on an additional T^2 does not bring new consistency constraints.

3.1.2 Breaking, amplitudes and spectrum

Supersymmetry breaking

We now perform the Scherk–Schwarz mechanism (see Sect. 1.3.1) along direction X^5 and build the one-loop partition functions of the model. The freely-acting orbifold along X^5 coupled to $(-1)^F$ produces an $\mathcal{N} = 2 \to \mathcal{N} = 0$ spontaneous supersymmetry breaking with scale M which reads

$$M = \frac{\sqrt{G^{55}}}{2} M_{\rm s} \ . \tag{3.1.6}$$

In the closed sector, this produces the usual shift for the momentum number m_5. Defining $\vec{m}' \equiv (m_4, m_5)$ and the shift vector $\vec{a}'_{\rm S} \equiv (0, \frac{1}{2})$, the deformation of the original supersymmetric model is

$$\text{Closed sector: } \vec{m}' \longrightarrow \vec{m}' + F\vec{a}'_{\rm S} \ . \tag{3.1.7}$$

Crucially, in the open sector, the Scherk–Schwarz shift combines with the Wilson lines along T^2 which take discrete values proportional to $\vec{a}_{i'}$. The deformation of the original model is

$$\text{Open sector: } \vec{m}' \longrightarrow \vec{m}' + F\vec{a}'_{\rm S} + \vec{a}_{i'} - \vec{a}_{j'} \ , \tag{3.1.8}$$

for string stretched between branes located at the fixed points ii' and jj'. This has dramatic consequences since the Scherk–Scwharz mass can be given to fermions or bosons depending on the Wilson lines. If i' and j' refer to fixed points at the same position along the Scherk–Schwarz direction X^5, the fermions get a mass. But if they refer to fixed points at opposite positions along X^5, it is now the bosons that get a mass. We will see soon precisely how this affects the massless spectrum of the model.

One-loop amplitudes

We can now write the partition functions of the theory. They are defined as the usual traces with the additional projections associated with the non-freely-acting $\mathbb{Z}_2$ orbifold and with the Scherk–Schwarz orbifold. The torus amplitude thus contains the action of the $\mathbb{Z}_2$ orbifold, the action of the Scherk–Schwarz orbifold and the combination of the two. This creates three twisted sectors and thus a lot of terms. For the sake of compactness, the torus partition function is not displayed in the main text and can be found in Appendix B.1. The internal six-dimensional zero-mode lattice with arbitrary metric tensor is

$$\begin{aligned}&\Lambda^{(6,6)}_{\vec{M},\vec{N}}(\tau) = q^{\frac{\alpha'}{4}P^L_{\mathcal{I}}G^{\mathcal{I}\mathcal{J}}P^L_{\mathcal{J}}}\,\bar{q}^{\frac{\alpha'}{4}P^R_{\mathcal{I}}G^{\mathcal{I}\mathcal{J}}P^R_{\mathcal{J}}}\ ,\\ &P^L_{\mathcal{I}} = m_{\mathcal{I}} + G_{\mathcal{I}\mathcal{J}}n_{\mathcal{J}}\ ,\quad P^R_{\mathcal{I}} \;=\; m_{\mathcal{I}} - G_{\mathcal{I}\mathcal{J}}n_{\mathcal{J}}\ ,\quad \mathcal{I}=4,\dots,9\ ,\end{aligned} \tag{3.1.9}$$

and can be split into a four-dimensional lattice along T^4 and a two-dimensional one along T^2,

$$\Lambda^{(6,6)}_{\vec{M},\vec{N}}(\tau) \equiv \Lambda^{(2,2)}_{\vec{m}',\vec{n}'}(\tau)\Lambda^{(4,4)}_{\vec{m},\vec{n}}(\tau) = q^{\frac{\alpha'}{4}P^L_{I'}G^{I'J'}P^L_{J'}}\,\bar{q}^{\frac{\alpha'}{4}P^R_{I'}G^{I'J'}P^R_{J'}} \times q^{\frac{\alpha'}{4}P^L_{I}G^{IJ}P^L_{J}}\,\bar{q}^{\frac{\alpha'}{4}P^R_{I}G^{IJ}P^R_{J}}\ . \tag{3.1.10}$$

The unprimed latin indices I, J take values in $\{6,\dots,9\}$ and the primed indices take values in $\{4,5\}$. For the Klein-bottle and the open-string amplitudes, we define

$$P^{(4)}_{\vec{m}} \equiv \Lambda^{(4,4)}_{\vec{m},\vec{0}},\qquad W^{(4)}_{\vec{n}} \equiv \Lambda^{(4,4)}_{\vec{0},\vec{n}},\qquad P^{(2)}_{\vec{m}'} \equiv \Lambda^{(2,2)}_{\vec{m}',\vec{0}},\qquad W^{(2)}_{\vec{n}'} \equiv \Lambda^{(2,2)}_{\vec{0},\vec{n}'}\ . \tag{3.1.11}$$

The Klein bottle is much simpler since only left-right symmetric states contribute. It reads

$$\begin{aligned}\mathcal{K} = \frac{1}{4}\int_0^{+\infty}\frac{\mathrm{d}\tau_2}{\tau_2^3}\Bigg\{&\left(V_4O_4+O_4V_4\right)\left(\frac{P^{(4)}_{\vec{m}}}{\eta^4}+\frac{W^{(4)}_{\vec{n}}}{\eta^4}\right)+32\left(O_4C_4+V_4S_4\right)\left(\frac{\eta}{\vartheta_4}\right)^2\\ &-\left(S_4S_4+C_4C_4\right)\left(\frac{P^{(4)}_{\vec{m}}}{\eta^4}+\frac{W^{(4)}_{\vec{n}}}{\eta^4}\right)-32\left(S_4O_4+C_4V_4\right)\left(\frac{\eta}{\vartheta_4}\right)^2\Bigg\}\frac{P^{(2)}_{\vec{m}'}}{\eta^4}\ .\end{aligned} \tag{3.1.12}$$

For the open amplitudes, we need to define matrices γ acting on the Chan-Paton indices both for the orientifold action (as in (1.2.15)) and the orbifold action (without exchange of the Chan-Paton indices). For practical purpose, we also define matrices for the action without any generator insertion which are just identity matrices. We define such matrices both for the Neumann and Dirichlet sectors, indicated as a subscript, and for each fixed point ii' of the appropriate T-dual theory, indicated as a superscript. This choice leads to the use of "small matrices" whose sizes are given by the numbers $N_{ii'}$ or $D_{ii'}$. This contrasts with [159,160] where they always manipulate "big" 32×32 matrices but consider traces of submatrices. The precise dictionary between our notations and theirs can be found in Appendix B.2. The matrices for the actions of the generators 1, g, Ω and Ωg, displayed as subscripts, are [159]

$$\begin{aligned}&\gamma^{ii'}_{\mathrm{N},1} = I_{N_{ii'}}\ ,\qquad &&\gamma^{ii'}_{\mathrm{N},g} = J_{N_{ii'}}\ ,\qquad &&\gamma^{ii'}_{\mathrm{N},\Omega} = I_{N_{ii'}}\ ,\qquad &&\gamma^{ii'}_{\mathrm{N},\Omega g} = J_{N_{ii'}}\ ,\\ &\gamma^{ii'}_{\mathrm{D},1} = I_{D_{ii'}}\ ,\qquad &&\gamma^{ii'}_{\mathrm{D},g} = J_{D_{ii'}}\ ,\qquad &&\gamma^{ii'}_{\mathrm{D},\Omega} = J_{D_{ii'}}\ ,\qquad &&\gamma^{ii'}_{\mathrm{D},\Omega g} = I_{D_{ii'}}\ ,\end{aligned} \tag{3.1.13}$$

where I_k is the $k \times k$ identity matrix and for k even,

$$J_k = \begin{pmatrix} 0 & I_{\frac{k}{2}} \\ -I_{\frac{k}{2}} & 0 \end{pmatrix}. \tag{3.1.14}$$

Note the following subtlety: The matrices describing the action of the orientifold Ω and the action of the combination Ωg are exchanged between the Neumann and Dirichlet sectors. There is another subtlety when writing the amplitudes in the ND and DN sectors with action of the orbifold. Indeed, one has to multiply all Neumann matrices by signs following the transformation rule,

$$\gamma^{ii'}_{\mathrm{N},g} \quad \longrightarrow \quad e^{4i\pi\vec{a}_i\cdot\vec{a}_j}\gamma^{ii'}_{\mathrm{N},g}\ , \tag{3.1.15}$$

where the index j refers to the fixed point of $T^4/\mathbb{Z}_2$ where the stack of D5-branes sits. This is explained in [160] and the demonstration for the translation into our notations can be found in Appendix B.2. Thanks to all these definitions, the annulus and Möbius strip amplitudes read

$$\begin{aligned}
\mathcal{A} = \frac{1}{4}\int_0^{+\infty}\frac{\mathrm{d}\tau_2}{\tau_2^3}\sum_{\substack{i,i'\\j,j'}}\Bigg\{\Bigg[&(V_4O_4+O_4V_4)\left(\mathrm{tr}(\gamma^{ii'}_{\mathrm{N},1})\mathrm{tr}(\gamma^{jj'\,-1}_{\mathrm{N},1})\frac{P^{(4)}_{\vec{m}+\vec{a}_i-\vec{a}_j}}{\eta^4}+\mathrm{tr}(\gamma^{ii'}_{\mathrm{D},1})\mathrm{tr}(\gamma^{jj'\,-1}_{\mathrm{D},1})\frac{W^{(4)}_{\vec{n}+\vec{a}_i-\vec{a}_j}}{\eta^4}\right)\\
&-(V_4O_4-O_4V_4)\,\delta_{ij}\left(\mathrm{tr}(\gamma^{ii'}_{\mathrm{N},g})\mathrm{tr}(\gamma^{jj'\,-1}_{\mathrm{N},g})+\mathrm{tr}(\gamma^{ii'}_{\mathrm{D},g})\mathrm{tr}(\gamma^{jj'\,-1}_{\mathrm{D},g})\right)\left(\frac{2\eta}{\vartheta_2}\right)^2\\
&+(O_4C_4+V_4S_4)\big(\mathrm{tr}(\gamma^{ii'}_{\mathrm{N},1})\mathrm{tr}(\gamma^{jj'\,-1}_{\mathrm{D},1})+\mathrm{tr}(\gamma^{ii'}_{\mathrm{D},1})\mathrm{tr}(\gamma^{jj'\,-1}_{\mathrm{N},1})\big)\left(\frac{\eta}{\vartheta_4}\right)^2\\
&-(O_4C_4-V_4S_4)\,e^{4i\pi\vec{a}_i\cdot\vec{a}_j}\big(\mathrm{tr}(\gamma^{ii'}_{\mathrm{N},g})\mathrm{tr}(\gamma^{jj'\,-1}_{\mathrm{D},g})+\mathrm{tr}(\gamma^{ii'}_{\mathrm{D},g})\mathrm{tr}(\gamma^{jj'\,-1}_{\mathrm{N},g})\big)\left(\frac{\eta}{\vartheta_3}\right)^2\Bigg]\frac{P^{(2)}_{\vec{m}'+\vec{a}_{i'}-\vec{a}_{j'}}}{\eta^4}\\
-\Bigg[&(S_4S_4+C_4C_4)\left(\mathrm{tr}(\gamma^{ii'}_{\mathrm{N},1})\mathrm{tr}(\gamma^{jj'\,-1}_{\mathrm{N},1})\frac{P^{(4)}_{\vec{m}+\vec{a}_i-\vec{a}_j}}{\eta^4}+\mathrm{tr}(\gamma^{ii'}_{\mathrm{D},1})\mathrm{tr}(\gamma^{jj'\,-1}_{\mathrm{D},1})\frac{W^{(4)}_{\vec{n}+\vec{a}_i-\vec{a}_j}}{\eta^4}\right)\\
&-(C_4C_4-S_4S_4)\,\delta_{ij}\left(\mathrm{tr}(\gamma^{ii'}_{\mathrm{N},g})\mathrm{tr}(\gamma^{jj'\,-1}_{\mathrm{N},g})+\mathrm{tr}(\gamma^{ii'}_{\mathrm{D},g})\mathrm{tr}(\gamma^{jj'\,-1}_{\mathrm{D},g})\right)\left(\frac{2\eta}{\vartheta_2}\right)^2\\
&+(S_4O_4+C_4V_4)\big(\mathrm{tr}(\gamma^{ii'}_{\mathrm{N},1})\mathrm{tr}(\gamma^{jj'\,-1}_{\mathrm{D},1})+\mathrm{tr}(\gamma^{ii'}_{\mathrm{D},1})\mathrm{tr}(\gamma^{jj'\,-1}_{\mathrm{N},1})\big)\left(\frac{\eta}{\vartheta_4}\right)^2\\
&-(S_4O_4-C_4V_4)\,e^{4i\pi\vec{a}_i\cdot\vec{a}_j}\big(\mathrm{tr}(\gamma^{ii'}_{\mathrm{N},g})\mathrm{tr}(\gamma^{jj'\,-1}_{\mathrm{D},g})+\mathrm{tr}(\gamma^{ii'}_{\mathrm{D},g})\mathrm{tr}(\gamma^{jj'\,-1}_{\mathrm{N},g})\big)\left(\frac{\eta}{\vartheta_3}\right)^2\Bigg]\frac{P^{(2)}_{\vec{m}'+\vec{a}'_{\mathrm{S}}+\vec{a}_{i'}-\vec{a}_{j'}}}{\eta^4}\Bigg\}\ .
\end{aligned} \tag{3.1.16}$$

and

$$\begin{aligned}
\mathcal{M} = -\frac{1}{4}\int_0^{+\infty}\frac{\mathrm{d}\tau_2}{\tau_2^3}\sum_{i,i'}\Bigg\{\Bigg[&(\hat{V}_4\hat{O}_4+\hat{O}_4\hat{V}_4)\left(\mathrm{tr}(\gamma^{ii'\,\mathrm{T}}_{\mathrm{N},\Omega}\gamma^{ii'\,-1}_{\mathrm{N},\Omega})\frac{P^{(4)}_{\vec{m}}}{\hat{\eta}^4}+\mathrm{tr}(\gamma^{ii'\,\mathrm{T}}_{\mathrm{D},\Omega g}\gamma^{ii'\,-1}_{\mathrm{D},\Omega g})\frac{W^{(4)}_{\vec{n}}}{\hat{\eta}^4}\right)\\
&-(\hat{V}_4\hat{O}_4-\hat{O}_4\hat{V}_4)\big(\mathrm{tr}(\gamma^{ii'\,\mathrm{T}}_{\mathrm{N},\Omega g}\gamma^{ii'\,-1}_{\mathrm{N},\Omega g})+\mathrm{tr}(\gamma^{ii'\,\mathrm{T}}_{\mathrm{D},\Omega}\gamma^{ii'\,-1}_{\mathrm{D},\Omega})\big)\left(\frac{2\hat{\eta}}{\hat{\vartheta}_2}\right)^2\Bigg]\frac{P^{(2)}_{\vec{m}'}}{\hat{\eta}^4}\\
-\Bigg[&(\hat{C}_4\hat{C}_4+\hat{S}_4\hat{S}_4)\left(\mathrm{tr}(\gamma^{ii'\,\mathrm{T}}_{\mathrm{N},\Omega}\gamma^{ii'\,-1}_{\mathrm{N},\Omega})\frac{P^{(4)}_{\vec{m}}}{\hat{\eta}^4}+\mathrm{tr}(\gamma^{ii'\,\mathrm{T}}_{\mathrm{D},\Omega g}\gamma^{ii'\,-1}_{\mathrm{D},\Omega g})\frac{W^{(4)}_{\vec{n}}}{\hat{\eta}^4}\right)\\
&-(\hat{C}_4\hat{C}_4-\hat{S}_4\hat{S}_4)\big(\mathrm{tr}(\gamma^{ii'\,\mathrm{T}}_{\mathrm{N},\Omega g}\gamma^{ii'\,-1}_{\mathrm{N},\Omega g})+\mathrm{tr}(\gamma^{ii'\,\mathrm{T}}_{\mathrm{D},\Omega}\gamma^{ii'\,-1}_{\mathrm{D},\Omega})\big)\left(\frac{2\hat{\eta}}{\hat{\vartheta}_2}\right)^2\Bigg]\frac{P^{(2)}_{\vec{m}'+\vec{a}'_{\mathrm{S}}}}{\hat{\eta}^4}\Bigg\}\ ,
\end{aligned} \tag{3.1.17}$$

Massless spectrum

From these one-loop amplitudes, we can uncover the structure of the massless spectrum of the model. In the open sector, the origin of the T^2 lattice (3.1.8) tells us what kind of strings are massless depending on their spacetime fermion number. For bosons *i.e.* when $F = 0$, massless states arise if, in the D3-brane pictures, the ends of the strings are attached to branes located at the fixed points ii' and jj' satisfying

$$\text{Massless bosons:} \quad \vec{a}_{i'} - \vec{a}_{j'} = \vec{0} \iff i' = j' \ . \tag{3.1.18}$$

For fermions *i.e.* when $F = 1$, the condition becomes

$$\text{Massless fermions:} \quad \vec{a}_{i'} - \vec{a}_{j'} = \mp\vec{a}'_{\rm S} \iff \begin{cases} i' = 2i'' - 1 \ , \ j' = 2i'' \\ \text{or} \\ i' = 2i'' \ , \ j' = 2i'' - 1 \end{cases} , \quad i'' = 1, 2 \ . \tag{3.1.19}$$

In the NN and DD sectors, massless states also correspond to the origin of the T^4 lattice. The condition reads

$$\text{Massless NN or DD states:} \quad \vec{a}_i - \vec{a}_j = \vec{0} \iff i = j \ , \tag{3.1.20}$$

while in the ND or DN sector, the T^4 is not involved and no special condition must hold:

$$\text{Massless ND states:} \quad i, j \ \text{ arbitrary} \ . \tag{3.1.21}$$

From this we conclude that massless NN and DD states correspond to strings stretched between branes that are at the same $T^4/\mathbb{Z}_2$ fixed point. Moreover, if the string ends are attached to the same stack of branes, this gives a massless boson while if the string crosses the T-dual Scherk–Schwarz direction $\tilde{X}^5$ to end on the facing stack, this produces a massless fermion. For ND states, the conclusions apply but without the constraint for the strings to be stretched between branes that are at the same $T^4/\mathbb{Z}_2$ fixed point. We can make use of our somewhat abusive pictorial representation shown in Fig. 3.1c to draw such massless states in Fig. 3.2.

To interpret the representations in which the massless spectrum lives, we evaluate the traces appearing in the one-loop amplitudes with the following definitions

$$\begin{aligned} N_{ii'} &\equiv n_{ii'} + \bar{n}_{ii'} = \mathrm{tr}\gamma_{\mathrm{N},1}^{ii'} = \mathrm{tr}\gamma_{\mathrm{N},1}^{ii'\,-1} = \mathrm{tr}(\gamma_{\mathrm{N},\Omega}^{ii'\,T}\gamma_{\mathrm{N},\Omega}^{ii'\,-1}) = \mathrm{tr}(\gamma_{\mathrm{N},\Omega_g}^{ii'\,T}\gamma_{\mathrm{N},\Omega_g}^{ii'\,-1}) \ , \\ D_{ii'} &\equiv d_{ii'} + \bar{d}_{ii'} = \mathrm{tr}\gamma_{\mathrm{D},1}^{ii'} = \mathrm{tr}\gamma_{\mathrm{D},1}^{ii'\,-1} = \mathrm{tr}(\gamma_{\mathrm{D},\Omega_g}^{ii'\,T}\gamma_{\mathrm{D},\Omega_g}^{ii'\,-1}) = \mathrm{tr}(\gamma_{\mathrm{D},\Omega}^{ii'\,T}\gamma_{\mathrm{D},\Omega}^{ii'\,-1}) \ , \end{aligned} \tag{3.1.22}$$

and

$$\begin{aligned} 0 &\equiv i(n_{ii'} - \bar{n}_{ii'}) = \mathrm{tr}\gamma_{\mathrm{N},g}^{ii'} = -\mathrm{tr}\gamma_{\mathrm{N},g}^{ii'\,-1} \ , \\ 0 &\equiv i(d_{ii'} - \bar{d}_{ii'}) = \mathrm{tr}\gamma_{\mathrm{D},g}^{ii'} = -\mathrm{tr}\gamma_{\mathrm{D},g}^{ii'\,-1} \ . \end{aligned} \tag{3.1.23}$$

The traces whose value is zero are expressed as a difference $i(n_{ii'} - \bar{n}_{ii'})$ or $i(d_{ii'} - \bar{d}_{ii'})$ using the fact the matrix J_k has an equal number of eigenvalues i and $-i$. In $\mathcal{A} + \mathcal{M}$, we read the following field-theory spectrum:

$$
\begin{aligned}
\text{Bosons:}\quad & \sum_{i,i'}\Bigg\{ \left[n_{ii'}\bar{n}_{ii'}+d_{ii'}\bar{d}_{ii'}\right]\frac{V_4O_4}{\eta^8}\bigg|_0 \\
& + \left[\frac{n_{ii'}(n_{ii'}-1)}{2}+\frac{\bar{n}_{ii'}(\bar{n}_{ii'}-1)}{2}+\frac{d_{ii'}(d_{ii'}-1)}{2}+\frac{\bar{d}_{ii'}(\bar{d}_{ii'}-1)}{2}\right]\frac{O_4V_4}{\eta^8}\bigg|_0 \\
& + \sum_j\left[\frac{1-e^{4i\pi\vec{a}_i\cdot\vec{a}_j}}{2}\left(n_{ii'}d_{ji'}+\bar{n}_{ii'}\bar{d}_{ji'}\right)+\frac{1+e^{4i\pi\vec{a}_i\cdot\vec{a}_j}}{2}\left(n_{ii'}\bar{d}_{ji'}+\bar{n}_{ii'}d_{ji'}\right)\right]\frac{O_4C_4}{\eta^8}\bigg|_0\Bigg\}\,, \\
\text{Fermions:}\quad & \sum_{i,i''}\Bigg\{ \left[n_{i,2i''-1}\bar{n}_{i,2i''}+\bar{n}_{i,2i''-1}n_{i,2i''}+d_{i,2i''-1}\bar{d}_{i,2i''}+\bar{d}_{i,2i''-1}d_{i,2i''}\right]\frac{C_4C_4}{\eta^8}\bigg|_0 \\
& + \left[n_{i,2i''-1}n_{i,2i''}+\bar{n}_{i,2i''-1}\bar{n}_{i,2i''}+d_{i,2i''-1}d_{i,2i''}+\bar{d}_{i,2i''-1}\bar{d}_{i,2i''}\right]\frac{S_4S_4}{\eta^8}\bigg|_0 \\
& + \sum_j\left[\frac{1-e^{4i\pi\vec{a}_i\cdot\vec{a}_j}}{2}\left(n_{i,2i''-1}d_{j,2i''}+\bar{n}_{i,2i''-1}\bar{d}_{j,2i''}+n_{i,2i''}d_{j,2i''-1}+\bar{n}_{i,2i''}\bar{d}_{j,2i''-1}\right)\right. \\
& \left.+\frac{1+e^{4i\pi\vec{a}_i\cdot\vec{a}_j}}{2}\left(n_{i,2i''-1}\bar{d}_{j,2i''}+\bar{n}_{i,2i''-1}d_{j,2i''}+n_{i,2i''}\bar{d}_{j,2i''-1}+\bar{n}_{i,2i''}d_{j,2i''-1}\right)\right]\frac{S_4O_4}{\eta^8}\bigg|_0\Bigg\}\,.
\end{aligned}
\tag{3.1.24}
$$

In products of SO(4) characters, the first factor indicates the Lorentz structure of the state while the second acts like a multiplicity. For bosons, we thus read in the first line the bosonic parts of an $\mathcal{N}=2$ vector multiplet in the adjoint representation of the open-string gauge group (3.1.4). The second line corresponds to scalars of an hypermultiplet living in the antisymmetric $\oplus$ $\overline{\text{antisymmetric}}$ representation of each unitary factor. The last line corresponds to scalars of an hypermultiplet living in the fundamental $\otimes$ fundamental or fundamental $\otimes$ $\overline{\text{fundamental}}$ of $\mathrm{U}(n_{ii'})\times\mathrm{U}(d_{ji'})$ depending on the sign $e^{4i\pi\vec{a}_i\cdot\vec{a}_j}$. The fermions are all parts of hypermultiplets in the fundamental $\otimes$ fundamental or fundamental $\otimes$ $\overline{\text{fundamental}}$ of products of unitary factors "facing each other" along the Scherk–Schwarz direction $\tilde{X}^5$. As we saw, these factors are at the same $T^4/\mathbb{Z}_2$ or $\tilde{T}^4/\mathbb{Z}_2$ fixed points for NN and DD states and at arbitrary fixed points for ND and DN states. In total, we can count the number of massless bosonic and fermionic degrees of freedom in the open sector:

$$
\begin{aligned}
n_{\mathrm{B}}^{\text{open}} &= 4\left[2\sum_{ii'}\left(n_{ii'}^2+d_{ii'}^2\right)+\sum_{i,i',j}n_{ii'}d_{ji'}-32\right]\,, \\
n_{\mathrm{F}}^{\text{open}} &= 4\left[4\sum_{i,i''}\left(n_{i,2i''-1}n_{i,2i''}+d_{i,2i''-1}d_{i,2i''}\right)+\sum_{i,i'',j}\left(n_{i,2i''-1}d_{j,2i''}+n_{i,2i''}d_{j,2i''-1}\right)\right]\,.
\end{aligned}
\tag{3.1.25}
$$

We end this section by mentioning the closed-string massless spectrum. The Scherk–Schwarz mechanism gives a mass to all fermions since, contrary to the open sector with the Wilson lines, nothing can compensate the shift. The massless spectrum is thus the bosonic part of the BSGP spectrum. From a six-dimensional point of view, there are the $(6-2)\times(6-2)$ on-shell degrees of freedom associated with $G+C$ along the extended dimensions and the 4×4 degrees of freedom associated with $G+C$ along the four internal directions. In addition, there are 4 scalars in each of the 16 twisted hypermultiplets. This yields

$$
n_{\mathrm{B}}^{\text{closed}} = 4\times(4+4+16)\,, \qquad n_{\mathrm{F}}^{\text{closed}} = 0\,. \tag{3.1.26}
$$

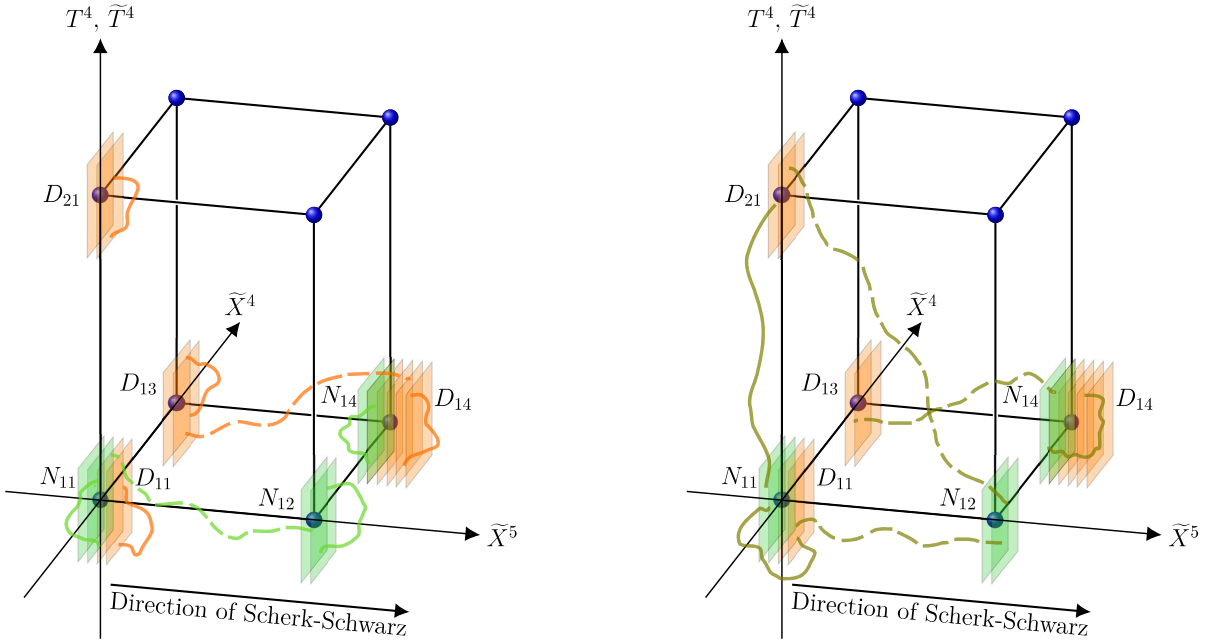

(a) Bosonic NN and DD states (solid strings) are massless when they correspond in the D3-brane picture to strings with both ends attached to the same stack of branes. By contrast, fermionic NN and DD states (dashed strings) are massless when they correspond to strings stretched between corners of the six-dimensional box that are adjacent along the T-dual Scherk–Schwarz direction.

(b) ND states correspond to strings stretched between a stack of D3-branes T-dual to D9-branes and a stack of D3-branes T-dual to D5-branes. Bosonic ND states (solid strings) are massless when the stacks are located on corners with common coordinates in $\tilde{T}^2/I_{45}$. Fermionic ND states (dashed strings) are massless when the corners have common coordinate $\tilde{X}^4$ and distinct coordinate $\tilde{X}^5$.

Figure 3.2: Open-string massless modes.

The total number of bosonic and fermionic degrees of freedom in the model, taking into account both the open- and closed-string sector, is

$$n_{\mathrm{F}} - n_{\mathrm{B}} = 4\Big[8 - 2\sum_{i,i''}\left(n_{i,2i''-1} - n_{i,2i''}\right)^2 - 2\sum_{i,i''}\left(d_{i,2i''-1} - d_{i,2i''}\right)^2 - \sum_{i,i'',j}\left(n_{i,2i''-1} - n_{i,2i''}\right)\left(d_{j,2i''-1} - d_{j,2i''}\right)\Big] \,. \tag{3.1.27}$$

As it will be useful in the next subsection, let us summarize all degrees of freedom and their representations under the gauge groups $\mathrm{U}(n_{i,2i''-1})$ and $\mathrm{U}(n_{i,2i''})$ for $i \in \{1,\ldots,16\}$ and $i' \in \{1,2\}$ (the counting for $\mathrm{U}(d_{i,2i''-1})$ and $\mathrm{U}(d_{i,2i''})$ is the same up to the exchange $n \leftrightarrow d$). The summary is given in Table. 3.1.

3.1.3 Stability conditions

In this section, we compute the masses of the moduli in the NN and DD sector and describe a generalized Green–Schwarz mechanism occurring in our setup. The signs of the masses can be computed in a quick way with the sole knowledge of the massless spectrum and the various representations under which it transforms. A less subtle way to proceed is to Taylor expand the one-loop potential with respect to the moduli and extract the mass term. We will show the two

Massless representations of $\mathrm{U}(n_{i,2i''-1})$

Bosonic degrees of freedom:	**Fermionic degrees of freedom:**
• 4 adjoint • 4 (antisymmetric $\oplus$ $\overline{\text{antisymmetric}}$) • $2\sum_j d_{j,2i''-1}$ (fundamental $\oplus$ $\overline{\text{fundamental}}$)	• $8n_{i,2i''}$ (fundamental $\oplus$ $\overline{\text{fundamental}}$) • $2\sum_j d_{j,2i''}$ (fundamental $\oplus$ $\overline{\text{fundamental}}$)

Massless representations of $\mathrm{U}(n_{i,2i''})$

Bosonic degrees of freedom:	**Fermionic degrees of freedom:**
• 4 adjoint • 4 (antisymmetric $\oplus$ $\overline{\text{antisymmetric}}$) • $2\sum_j d_{j,2i''}$ (fundamental $\oplus$ $\overline{\text{fundamental}}$)	• $8n_{i,2i''-1}$ (fundamental $\oplus$ $\overline{\text{fundamental}}$) • $2\sum_j d_{j,2i''-1}$ (fundamental $\oplus$ $\overline{\text{fundamental}}$)

Table 3.1: Representations of $\mathrm{U}(n_{i,2i''-1})$ and $\mathrm{U}(n_{i,2i''})$ into which the massless degrees of freedom are organized.

derivations and conclude that they fully agree between each other. In our setup, a generalized Green–Schwarz mechanism takes place, that can generate a tree-level mass for some of the NN and DD moduli as well as for some quaternionic scalars, thus improving the global stability of the model. After the description of this mechanism, we give the result for the masses of the scalars in the ND sector of the theory. The detailed computation of these masses thanks to two-point correlation functions is performed in the last section 3.2 of this chapter. The subsection ends with a brief discussion on the moduli in the closed-string sector.

Quick answer with Dynkin indices

As we will see in Chapter 4, one can derive an expression for the one-loop potential in a heterotic framework with arbitrary Wilson lines and supersymmetry breaking *à la* Scherk–Schwarz under the assumption of a low supersymmetry-breaking scale M and absence of lower scales [44, 56, 57]. Let us assume a gauge group $\mathcal{G}$ decomposed into factors like $\mathcal{G} = \prod_\kappa \mathcal{G}_\kappa$. Applied to a four-dimensional setup with breaking along direction X^5 and denoting generically the Wilson lines $y^{\mathcal{I}}_{r_\kappa}$ where $r_\kappa \in \{1, \ldots, \operatorname{rank} \mathcal{G}_\kappa\}$ indicates the Cartan U(1) under consideration for the gauge factor $\mathcal{G}_\kappa$ and $\mathcal{I}$ denotes the internal directions (up to 26 in heterotic string), the expression reads

$$\mathcal{V}_{\text{1-loop}} = \xi_d (n_{\mathrm{F}} - n_{\mathrm{B}}) M^4 \;+\; \xi_{d-2} \sum_\kappa \sum_u \left(T_{\mathcal{R}^{(\kappa)}_{\mathrm{B}u}} - T_{\mathcal{R}^{(\kappa)}_{\mathrm{F}u}} \right) \Big(\sum_{\substack{\mathcal{I}=4 \\ \neq 5}}^{26} \frac{(y^{\mathcal{I}}_{r_\kappa})^2}{3G^{55}} + (y^5_{r_\kappa})^2 \Big) M^4 \;+\; \cdots \;. \tag{3.1.28}$$

In this formula, ξ_d and ξ_{d-2} with $d = 4$ in this case are positive coefficients which capture the contributions of the Kaluza-Klein modes propagating along the Scherk–Schwarz direction. The n_{B} and n_{F} massless degrees of freedom at zero Wilson lines transform into irreducible representations $\mathcal{R}^{(\kappa)}_{\mathrm{B}u}$ and $\mathcal{R}^{(\kappa)}_{\mathrm{F}u}$ labelled by an index u, of the gauge factor $\mathcal{G}_\kappa$. Then, $T_{\mathcal{R}^{(\kappa)}_{\mathrm{B}u}}$ and $T_{\mathcal{R}^{(\kappa)}_{\mathrm{F}u}}$ are the Dynkin indices of these representations. The signs of the masses of the Wilson lines $y^{\mathcal{I}}_{r_\kappa}$ can consequently be extracted from the following formula:

$$\left. \frac{\partial^2 \mathcal{V}}{(\partial y^{\mathcal{I}}_{r_\kappa})^2} \right|_{y=0} \;\propto\; \sum_u T_{\mathcal{R}^{(\kappa)}_{\mathrm{B}u}} - \sum_u T_{\mathcal{R}^{(\kappa)}_{\mathrm{F}u}} \;, \quad r_\kappa = 1, \ldots, \operatorname{rank} \mathcal{G}_\kappa \;, \quad \mathcal{I} = 4, \ldots, 26 \;. \tag{3.1.29}$$

The sole knowledge of the representations and the corresponding Dynkin indices allows to establish the tachyonic nature or not of the Wilson lines. Let us apply this to our model with spectrum (3.1.24).

The Wilson lines along T^2 are true Wilson lines so that the formula can be applied as it is, using the Dynkin indices of unitary groups. They can be found in Table. 3.2. Thanks to the list of representations in Table. 3.1, we conclude that the masses[2] are proportional to

$$\begin{aligned}
&4(n_{i,2i''-1}-n_{i,2i''}-1)+\sum_{j=1}^{16}(d_{j,2i''-1}-d_{j,2i''}) \qquad \text{for} \qquad \mathrm{U}(n_{i,2i''-1})\ ,\\
&4(n_{i,2i''}-n_{i,2i''-1}-1)+\sum_{j=1}^{16}(d_{j,2i''}-d_{j,2i''-1}) \qquad \text{for} \qquad \mathrm{U}(n_{i,2i''})\ ,\\
&4(d_{i,2i''-1}-d_{i,2i''}-1)+\sum_{j=1}^{16}(n_{j,2i''-1}-n_{j,2i''}) \qquad \text{for} \qquad \mathrm{U}(d_{i,2i''-1})\ ,\\
&4(d_{i,2i''}-d_{i,2i''-1}-1)+\sum_{j=1}^{16}(n_{j,2i''}-n_{j,2i''-1}) \qquad \text{for} \qquad \mathrm{U}(d_{i,2i''})\ .
\end{aligned} \tag{3.1.30}$$

The above expressions are valid for unitary factors of rank at least two but can be extended to the U(1) case thanks to the universality of the U(1) charges.

Gauge factor $\mathcal{G}_\kappa$	Representation $\mathcal{R}_u^{(\kappa)}$	$\dim \mathcal{R}_u^{(\kappa)}$	$T_{\mathcal{R}_u}^{(\kappa)}$
SU(q), $q \geq 2$	fundamental	q	1
	$\overline{\text{fundamental}}$	q	1
	adjoint	q^2-1	$2q$
	antisymmetric	$\frac{q(q-1)}{2}$	$q-2$
	$\overline{\text{antisymmetric}}$	$\frac{q(q-1)}{2}$	$q-2$
SO(p), $p \geq 2$	fundamental	p	1
	adjoint	$\frac{p(p-1)}{2}$	$p-2$

Table 3.2: Dimensions and Dynkin indices of representations of special orthogonal and unitary groups. The Dynkin indices of the fundamental representations are normalized to 1 by convention.

One cannot apply directly the method of Dynkin indices for unitary gauge groups to establish the masses of the D3-branes positions along $T^4/\mathbb{Z}_2$ or $\tilde{T}^4/\mathbb{Z}_2$ in the correct T-dual framework. But a careful look at the loop amplitudes $\mathcal{A}$ and $\mathcal{M}$ reveals that such moduli only appear in the NN and DD sectors where the $\mathbb{Z}_2$ orbifold g does not act. This means that up to an overall $\frac{1}{2}$ factor, the contributions of these moduli to the one-loop potential are those of the parent $\mathcal{N}=4 \to \mathcal{N}=0$ theory studied in [58] showing orthogonal gauge groups. In the parent theory, stacks of $N_{i,2i''-1}$ and $N_{i,2i''}$ D3-branes T-dual to original D9-branes produce a gauge group $\mathrm{SO}(N_{i,2i''-1}) \times \mathrm{SO}(N_{i,2i''})$. There are 8 bosons in the adjoint representation of $\mathrm{SO}(N_{i,2i''-1})$ and $8N_{i,2i''}$ in the fundamental coming from bifundamentals of the two gauge factors. The representations of $\mathrm{SO}(N_{i,2i''})$ are the same up to the exchange $N_{i,2i''-1} \leftrightarrow N_{i,2i''}$. With the Dynkin indices for orthogonal groups displayed

[2]Before implementation of the Green–Schwarz mechanism.

in Table. 3.2, we conclude as in [58] that the masses are proportional to

$$\begin{aligned} &N_{i,2i''-1} - N_{i,2i''} - 2 \qquad \text{for} \qquad \mathrm{SO}(N_{i,2i''-1}) \ , \\ &N_{i,2i''} - N_{i,2i''-1} - 2 \qquad \text{for} \qquad \mathrm{SO}(N_{i,2i''}) \ . \end{aligned} \tag{3.1.31}$$

In the $\mathcal{N}=2 \to \mathcal{N}=0$ model, this translates into the following masses for the moduli along $T^4/\mathbb{Z}_2$ or $\tilde{T}^4/\mathbb{Z}_2$ (both for D3-branes T-dual to the original D9-branes or T-dual to the original D5-branes)

$$\begin{aligned} &n_{i,2i''-1} - n_{i,2i''} - 1 \qquad \text{for} \qquad \mathrm{U}(n_{i,2i''-1}) \ , \quad n_{i,2i''-1} \geq 2 \ , \\ &n_{i,2i''} - n_{i,2i''-1} - 1 \qquad \text{for} \qquad \mathrm{U}(n_{i,2i''}) \ , \quad n_{i,2i''} \geq 2 \ , \\ &d_{i,2i''-1} - d_{i,2i''} - 1 \qquad \text{for} \qquad \mathrm{U}(d_{i,2i''-1}) \ , \quad d_{i,2i''-1} \geq 2 \ , \\ &d_{i,2i''} - d_{i,2i''-1} - 1 \qquad \text{for} \qquad \mathrm{U}(d_{i,2i''}) \ , \quad d_{i,2i''} \geq 2 \ . \end{aligned} \tag{3.1.32}$$

These formulas only hold for unitary factors of rank at least two since for U(1)'s, the D3-branes are rigid along $T^4/\mathbb{Z}_2$ or $\tilde{T}^4/\mathbb{Z}_2$.

Taylor expansion of the potential

Let us recover these results by a direct computation of the one-loop potential and a Taylor expansion up to quadratic order with respect to the moduli to obtain their masses. The first step is to express the potential in terms of arbitrary continuous D3-branes positions $2\pi a^{\mathcal{I}}_\alpha$ (for original D9-branes) and $2\pi b^{\mathcal{I}}_\alpha$ (for original D5-branes), $\alpha \in \{1,\dots,32\}$ and $\mathcal{I} \in \{4,\dots,9\}$. These positions are defined as fluctuations $\epsilon^{\mathcal{I}}_\alpha$ and $\xi^{\mathcal{I}}_\alpha$ around the fixed points:

$$a^{\mathcal{I}}_\alpha \ = \ \langle a^{\mathcal{I}}_\alpha \rangle + \epsilon^{\mathcal{I}}_\alpha \ , \qquad \langle a^{\mathcal{I}}_\alpha \rangle \ \in \ \left\{0, \frac{1}{2}\right\}, \qquad b^{\mathcal{I}}_\alpha \ = \ \langle b^{\mathcal{I}}_\alpha \rangle + \xi^{\mathcal{I}}_\alpha \ , \qquad \langle b^{\mathcal{I}}_\alpha \rangle \ \in \ \left\{0, \frac{1}{2}\right\} \ . \tag{3.1.33}$$

The regime in which we perform the computation is characterized by a large Scherk–Schwarz direction and the absence of mass scales below the supersymmetry-breaking scale. More precisely, this translates into

$$G^{55} \ll G_{44}, |G_{IJ}| \ll G_{55} \ , \quad |G_{45}|, |G_{5J}| \ll \sqrt{G_{55}} \ , \quad I,J = 6,\dots,9 \ , \quad G_{55} \gg 1 \ . \tag{3.1.34}$$

The computation of the potential is carried in Appendix. B.3 for a lighter main text and the result takes the following form:

$$\mathcal{V}_{\text{1-loop}} = \frac{\Gamma\left(\frac{5}{2}\right)}{\pi^{\frac{13}{2}}} M^4 \sum_{l_5} \frac{\mathcal{N}_{2l_5+1}(\epsilon,\xi,G)}{|2l_5+1|^5} + \mathcal{O}\left((M_{\mathrm{s}}M)^2 e^{-2\pi c \frac{M_{\mathrm{s}}}{M}}\right) \ , \tag{3.1.35}$$

where c is an order one positive constant and

$$\mathcal{N}_{2l_5+1}(\epsilon,\xi,G) = n^{\text{closed}}_{\mathrm{F}} - n^{\text{closed}}_{\mathrm{B}} + \mathcal{N}^{\text{open}}_{2l_5+1}(\epsilon,\xi,G) \ , \tag{3.1.36}$$

with $\mathcal{N}^{\text{open}}_{2l_5+1}(\epsilon,\xi,G)$ capturing the dependence of the potential on $\epsilon^{\mathcal{I}}_\alpha$ and $\xi^{\mathcal{I}}_\alpha$ and which is displayed in (B.3.14).

Before expanding to quadratic order, the potential must be expressed in terms of the dynamical degrees of freedom only. Denoting such degrees of freedom with an index r, we already explained

that they take the form

$$\begin{aligned}
&\epsilon_r^I\ , && I=6,\dots,9, && r=1,\dots,\sum_{i,i'}\left\lfloor\frac{N_{ii'}}{4}\right\rfloor=\sum_{i,i'}\left\lfloor\frac{n_{ii'}}{2}\right\rfloor\leq 8-\frac{\tilde{\mathcal{R}}}{2}\ ,\\
&\xi_r^I\ , && I=6,\dots,9, && r=1,\dots,\sum_{i,i'}\left\lfloor\frac{D_{ii'}}{4}\right\rfloor=\sum_{i,i'}\left\lfloor\frac{d_{ii'}}{2}\right\rfloor\leq 8-\frac{\mathcal{R}}{2}\ ,\\
&\epsilon_{r'}^{I'}\ ,\ \xi_{r'}^{I'}\ , && I'=4,5, && r'=1,\dots,16\ ,
\end{aligned} \tag{3.1.37}$$

which reflects the fact that 16 fluctuations along T^2 are dynamical while only a maximum of 8 are dynamical along $T^4/\mathbb{Z}_2$ or $\tilde{T}^4/\mathbb{Z}_2$ depending on the numbers $\mathcal{R}$ and $\tilde{\mathcal{R}}$ of frozen D3-branes pairs. We further label by $i(r)i'(r)$ the corner in the appropriate T-dual picture around which the fluctuations occur and by $i(r)\hat{\imath}(r)$ the corner facing $i(r)i'(r)$ along the Scherk–Schwarz direction. We use similar definitions for the index r'. The expansion up to quadratic term yields

$$\begin{aligned}
\mathcal{N}_{2l_5+1}(\epsilon,\xi,G) \;=\; & n_{\rm F}-n_{\rm B}+32\pi^2(2l_5+1)^2\Bigg\{\\
&\sum_r\Big(n_{i(r)i'(r)}-n_{i(r)\hat{\imath}'(r)}-1\Big)\epsilon_r^I\Delta^{IJ}\epsilon_r^J+\sum_r\Big(d_{j(r)j'(r)}-d_{j(r)\hat{\jmath}'(r)}-1\Big)\xi_r^I\Delta_{IJ}\xi_r^J\\
&+\sum_{r'}\left(n_{i(r')i'(r')}-n_{i(r')\hat{\imath}'(r')}-1+\frac{1}{4}\sum_i\big(d_{ii'(r')}-d_{i\hat{\imath}'(r')}\big)\right)\epsilon_{r'}^{I'}\Delta^{I'J'}\epsilon_{r'}^{J'}\\
&+\sum_{r'}\left(d_{j(r')j'(r')}-d_{j(r')\hat{\jmath}'(r')}-1+\frac{1}{4}\sum_j\big(n_{jj'(r')}-n_{j\hat{\jmath}'(r')}\big)\right)\xi_{r'}^{I'}\Delta^{I'J'}\xi_{r'}^{J'}\\
&+\mathcal{O}\big(\epsilon^4,\xi^4\big)\Bigg\}\ .
\end{aligned} \tag{3.1.38}$$

The delta tensors involved in this expression are

$$\Delta^{I'J'}=\frac{1}{3}\left(\frac{G^{I'J'}}{G^{55}}+2\,\frac{G^{5I'}}{G^{55}}\frac{G^{5J'}}{G^{55}}\right)\ ,\qquad \Delta^{IJ}=\frac{2}{3}\frac{G^{IJ}}{G^{55}}\ ,\qquad \Delta_{IJ}=\frac{2}{3}\frac{G_{IJ}}{G^{55}}\ , \tag{3.1.39}$$

and have positive eigenvalues. The signs of the masses are thus given by the signs of the various prefactors which reproduce exactly what we found with the Dynkin indices. The result (3.1.38) also demonstrates that the configurations with D3-branes at fixed points in the T-dual pictures correspond to extremal points for the one-loop potential since there is no linear term.

Generalized Green–Schwarz mechanism

Moduli found to be unstable after the study performed so far may not necessarily be tachyonic after a generalized Green–Schwarz mechanism is taken into account in the model [160]. In the original supersymmetric BSGP $T^4/\mathbb{Z}_2$ model in six dimensions, the anomalies cancel in a non-trivial way. At the level of the effective action, there are tree-level couplings between the R-R fields (the two-form C and the 16 four-form C_4^i, $i\in\{1,\dots,16\}$) and the Cartan U(1)'s of the gauge group which is simply that of the four-dimensional model (3.1.4) but without the primed index:

$$\prod_i \mathrm{U}(n_i)\times\mathrm{U}(d_i)\ , \tag{3.1.40}$$

with the tadpole condition $\sum_i n_i = \sum_i d_i = 16$. Denoting $F_a = \mathrm{d}A_a$, $a = 1, \ldots, 16$ the field strengths of the Cartan U(1)'s of $\prod_i \mathrm{U}(d_i)$ and $F_a = \mathrm{d}A_a$, $a = 17, \ldots, 32$ those of $\prod_i \mathrm{U}(n_i)$, the tree-level couplings are

$$\sum_{i,a} c_{ia} \int C_0^i \wedge F_a^3 + \sum_{i,a} c_{ia} \int C_4^i \wedge F_a = \sum_i \int \left(C_0^i + \sum_a c_{ia} A_a \right) \wedge \star \left(C_0^i + \sum_b c_{ib} A_a \right) \ . \quad (3.1.41)$$

The coefficients c_{ia} have the following expressions:

$$\begin{aligned} c_{ia} &= 4\delta_{a\in i} \ , && \text{for } a = 1, \ldots, 16 \ , \\ c_{ia} &= -e^{4i\pi \vec{a}_i \cdot \vec{a}_{j(a)}} \ , && \text{for } a = 17, \ldots, 32 \ , \end{aligned} \quad (3.1.42)$$

where $\delta_{a\in i} = 1$ when the a-th U(1) belongs to the Cartan subalgebra of $\mathrm{U}(d_i)$, and $\delta_{a\in i} = 0$ otherwise. Moreover, $j(a)$ indicates the fixed point of $\tilde{T}^4/\mathbb{Z}_2$ which supports the Cartan U(1) labelled by $a \in \{17, \ldots, 32\}$ of $\prod_i \mathrm{U}(n_i)$. From (3.1.41), we extract the tree-level mass term generated for the abelian vectors,

$$\frac{1}{2} \sum_{a,b} A_a \mathcal{M}_{ab}^2 A_b \quad \text{where the mass matrix is} \quad \mathcal{M}_{ab}^2 = \sum_i c_{ia} c_{ib} \ . \quad (3.1.43)$$

The non-zero eigenvalues of the mass matrix tell us which combinations of abelian U(1)'s eat a field C_0^i and get a tree-level mass so that they are ensured to be stable at one loop. Supersymmetry implies that as many quaternionic scalars as eaten C_0^i's also get a mass. It is shown [160] that the number of non-zero eigenvalues for the mass matrix is at least 2 and at most 16. This is because if there are fewer than 16 unitary factors (at least two are present in the $\mathrm{U}(16) \times \mathrm{U}(16)$ case), they are all broken to SU groups while if there are more than 16 unitary factors, a maximum of 16 are broken.

Let us write $\mathcal{P}_{ab}$ the orthogonal transformation which diagonalizes the mass matrix such that $A_a \equiv \mathcal{P}_{ab} \hat{A}_b$. When the theory is compactified on an additional T^2, the Wilson lines along this T^2 are $\hat{A}_a^{I'}$, $I' \in \{4, 5\}$. In addition to the mass term generated by the one-loop potential, transformed in the diagonal basis, the Wilson lines $\hat{A}_a^{I'}$ get the tree-level mass contribution $\hat{\mathcal{M}}_a^2$ which is defined to be the a-th eigenvalue of the mass matrix. In total, the mass terms are

$$\hat{A}_a^{I'} \left[\hat{\mathcal{M}}_a^2 \delta_{ab} \delta_{I'J'} + \mathcal{P}_{ca} \frac{\partial \mathcal{V}_{\text{1-loop}}}{\partial \hat{A}_c^{I'} \partial \hat{A}_d^{I'}} \mathcal{P}_{db} \right] \hat{A}_b^{I'} \ . \quad (3.1.44)$$

With our notations (3.1.37), $\hat{A}_a^{I'}$ is simply $\xi_a^{I'}$ when $a \in \{1, \ldots, 16\}$ and $\epsilon_{a-16}^{I'}$ when $a \in \{17, \ldots, 32\}$. The tree-level mass always dominates the one-loop contribution in the regime of low supersymmetry-breaking scale. Hence, the Wilson lines $\hat{A}_a^{I'}$ for which the eigenvalue $\hat{\mathcal{M}}_a^2$ is non-zero can safely be set to zero during the one-loop stability analysis. If we label the remaining non-zero Wilson lines with an index u or v, their stability at one loop depends on the eigenvalues of the submatrix

$$\mathcal{P}_{cu} \frac{\partial \mathcal{V}_{\text{1-loop}}}{\partial \hat{A}_c^{I'} \partial \hat{A}_d^{I'}} \mathcal{P}_{dv} \ . \quad (3.1.45)$$

Non-negative eigenvalues are required to ensure the absence of tachyonic instabilities.

Let us look at the simplest realization of the generalized Green–Scwharz mechanism in (naively) $[\mathrm{U}(16)]_{\mathrm{DD}} \times [\mathrm{U}(16)]_{\mathrm{NN}}$ configurations[3] and see how it affects the Wilson lines along T^2. We will discuss all other moduli in the next subsection since here, we simply want to illustrate the Green–Scwharz mechanism. In each T-dual pictures, the 32 D3-branes are gathered in a single stack. We assume the stack of D3-branes T-dual to D5-branes to sit at fixed point i_0 along $T^4/\mathbb{Z}_2$ and we assume the stack of D3-branes T-dual to D9-branes to sit at fixed point j_0 along $\tilde{T}^4/\mathbb{Z}_2$. In four dimensions, three inequivalent configurations exist depending on the relative positions of the two stacks inside the $\tilde{T}^2/I_{45}$. Mixing the two T-dual pictures, the three configurations are depicted in Fig. 3.3 where orange branes correspond to D3-branes T-dual to D5-branes and the green ones correspond to D3-branes T-dual to D9-branes.

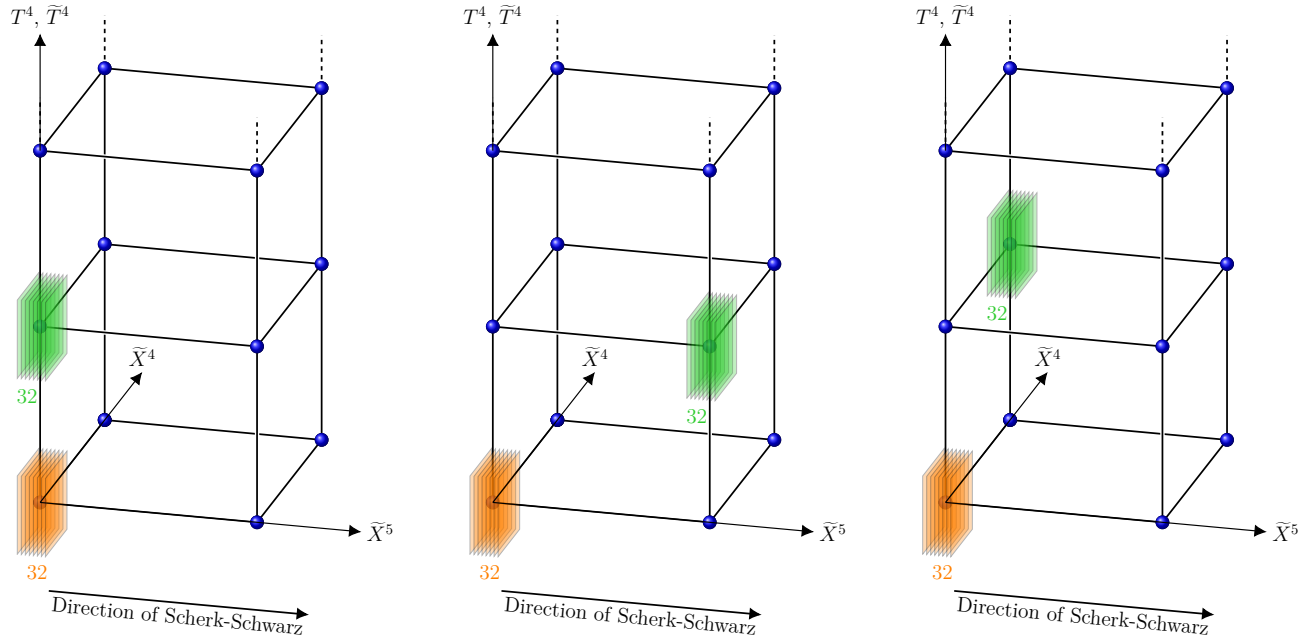

(a) The two stacks of 32 D3-branes T-dual to the D5- or D9-branes have common positions in $\tilde{T}^2/I_{45}$.

(b) The two stacks have the same coordinates along $\tilde{X}^4$ and distinct coordinates along $\tilde{X}^5$.

(c) The two stacks have distinct coordinates along $\tilde{X}^4$.

Figure 3.3: The simplest D3-branes configurations in component $(\mathcal{R}, \tilde{\mathcal{R}}) = (0, 0)$ of the Wilson lines moduli space.

For clarity, let us define $r' \equiv a$ when $a \in \{1, \ldots, 16\}$ and $\tilde{r}' \equiv a - 16$ when $a \in \{17, \ldots, 32\}$ (this means that r' refers to the original D5-branes and $\tilde{r}'$ to the original D9-branes). With these definitions and in such configurations, the c_{ia} coefficients yield the following 32×32 mass matrix $\mathcal{M}^2$ expressed in terms of 16×16 blocks,

$$\mathcal{M}^2 = \left(\begin{array}{c|c} \mathcal{M}^2_{r's'} & \mathcal{M}^2_{r'\tilde{s}'} \\ \hline \mathcal{M}^2_{\tilde{r}'s'} & \mathcal{M}^2_{\tilde{r}'\tilde{s}'} \end{array}\right) , \tag{3.1.46}$$

where the blocks are given by

$$\begin{aligned} \mathcal{M}^2_{r's'} &= 16 \ , & \mathcal{M}^2_{r'\tilde{s}'} &= -4\, e^{4i\pi \vec{a}_{i_0} \cdot \vec{a}_{j_0}} \ , \\ \mathcal{M}^2_{\tilde{r}'s'} &= -4\, e^{4i\pi \vec{a}_{j_0} \cdot \vec{a}_{i_0}} \ , & \mathcal{M}^2_{\tilde{r}'\tilde{s}'} &= 16 \ . \end{aligned} \tag{3.1.47}$$

[3]The subscripts DD or NN indicate if the gauge factors arise from the original D5-branes or D9-branes respectively.

Such a matrix always has 30 zero eigenvalues and 2 strictly positive ones. This indicates that two U(1)'s disappear and the naive U(16) × U(16) gauge group is actually broken to SU(16) × SU(16).

From (3.1.30) or (3.1.38), we conclude that in the three configurations, the Wilson lines along T^2 are massive since the exhibited coefficients are equal to 19, 11 or 16 respectively for the configurations displayed in Figs. 3.3a, 3.3c and 3.3c. Thus, of course, the Green–Schwarz mechanism does not change the stability conclusions for those moduli. But still, it removes two combinations that are deduced from the eigenvectors of the mass matrix associated with the non-zero eigenvalues by allowing us to set them to zero:

$$-\sum_{r'}\xi^{I'}_{r'}+\sum_{\tilde{r}'}\epsilon^{I'}_{\tilde{r}'}=0 \qquad \text{and} \qquad \sum_{r'}\xi^{I'}_{r'}+\sum_{\tilde{r}'}\epsilon^{I'}_{\tilde{r}'}=0\ . \tag{3.1.48}$$

After removal of these two combinations, the resulting 30 × 30 one-loop mass matrix still has only strictly positive eigenvalues of course.

Moduli in the Neumann–Dirichlet sector

As explained before, the computation of the one-loop masses of these moduli is performed in Sect. 3.2. They correspond to strings stretched between stacks of D5-branes and D9-branes in the original picture and they transform in bifundamental representations of gauge groups $\mathrm{U}(n_{ii'})\times\mathrm{U}(d_{ji'})$. Note that the two T^2 indices must be identical to produce massless states at tree level. In our pictorial representations with D3-branes, this means that massless ND scalars arise only if some orange and green stacks share the same position in $\tilde{T}^2/I_{45}$, whatever their positions along $T^4/\mathbb{Z}_2$ or $\tilde{T}^4/\mathbb{Z}_2$.

Here, we only display the sign-dependent part of the final result to be able to fully conclude on the stability of some models in the next subsection. The result is only known up to subdominant corrections of order α'/G^2_{55}. We have

$$M^2_{\mathrm{ND}}\propto(n_{ii'}-n_{i\hat{i}'}-1+d_{ji'}-n_{j\hat{i}'}-1)+\mathcal{O}\left(\frac{\alpha'}{G^2_{55}}\right)\ . \tag{3.1.49}$$

Closed-string moduli

The last moduli that need to be discussed, apart from the ND scalars whose stability study is postponed to the last section of this chapter, are those of the closed-string sector. Thanks to the Green–Schwarz mechanism, at least 2 and up to 16 quaternionic scalars get a mass at tree level. In configurations where some of them do not acquire a tree-level mass, we have not computed their one-loop masses. The closed-sector contribution to the one-loop potential is given in (3.1.35) and depends only on $M=\sqrt{G^{55}}$ up to exponentially suppressed contributions. All other components $G_{\mathcal{I}\mathcal{J}}$ are flat directions at one loop. When $n_{\mathrm{F}}\neq n_{\mathrm{B}}$, M undergoes a runaway while in configurations such that $n_{\mathrm{F}}=n_{\mathrm{B}}$, M is also a flat direction (up to the suppressed contributions).

For the R-R two-form components $C_{\mathcal{I}\mathcal{J}}$, such a straightforward method cannot be followed since the partition function in presence of vacuum expectation values for these fields is unknown. However, they can be argued to be flat directions as well (up to the exponentially small terms), using heterotic-type I duality arguments. Such a duality in four dimensions is a weak/weak correspondence [161–164] and C is mapped to the antisymmetric tensor B on the heterotic side. Without the orbifold action, as explained in Sect. 4.2.1 in Chapter 4, the deformations of the Narain lattice on the

heterotic side are parametrized by $(G+B)_{\mathcal{IJ}}$ as well as Wilson lines of a rank 16 gauge group along the compactified directions. At specific values of $(G+B)_{\mathcal{IJ}}$, symmetry enhancements occur and additional states become massless which contribute to the effective potential when running in the loop. These states have non-trivial winding numbers and produce a dependence of the potential on $(G+B)_{\mathcal{IJ}}$ (see for instance (4.2.6)). On the type I side, these winding states have no non-perturbative counterparts. They are mapped to D1-branes belonging to the non-pertubative spectrum and thus the components $C_{\mathcal{IJ}}$ should be flat directions of the one-loop potential up to exponentially suppressed terms.

Considering now the effect of the $\mathbb{Z}_2$ orbifold on the heterotic side, it turns out that the states in the twisted sector cannot induce symmetry enhancements. Non-trivial winding states in this sector are thus necessarily massive and give exponentially suppressed contributions in the potential so that the previous conclusion about the independence of the potential on $C_{\mathcal{IJ}}$ on the type I side (where the twisted winding states are mapped to "twisted D1-branes") still holds. Moreover, the presence of the Scherk–Schwarz breaking of supersymmetry is expected not to spoil the heterotic-type I equivalence using the adiabatic argument [165].

3.1.4 Stability synthesis

We are now able to conclude on the stability or not of different models.

SU(16) × SU(16) configurations

Let us begin by completing the discussion of the three typical configurations displayed in Fig. 3.3. We saw that two combinations of Wilson lines along T^2 are massive at tree-level and that all the others are massive at one loop. Along T^4, the results (3.1.32) or (3.1.38) show that everything is massive since the coefficients are equal to 15. There are 14 remaining quaternionic scalars whose stability is unknown and the model of Fig. 3.3a contains massless scalars in the ND sector since the two stacks are at the same $\tilde{T}^2/\mathbb{Z}_2$ position. The application of the result (3.1.49) gives a proportionality coefficient 30 for the mass squared of these scalars so that they are massive at one loop. If we define δ such that

- $\delta = +1$ if $i'_0 = j'_0$ (like in Fig. 3.3a),
- $\delta = -1$ if i'_0 and j'_0 are facing each other along $\tilde{X}^5$ (like in Fig. 3.3b),
- $\delta = 0$ if i'_0 and j'_0 do not have the same position along $\tilde{X}^4$ (like in Fig. 3.3c),

then we conclude from (3.1.27) that the model satisfies $n_{\rm F} - n_{\rm B} = -4064 - 1024\delta$ which is strictly negative whatever δ. The breaking scale M thus runs away and as argued in the last subsection, all other untwisted closed-string moduli are flat directions up to suppressed contributions.

A model in the branch $(\mathcal{R}, \tilde{\mathcal{R}}) = (16, 16)$

The models in this branch are characterized by the presence of 16 stacks of two D3-branes associated to D5-branes and 16 stacks of two D3-branes associated to D9-branes spread along the 16 fixed points of $T^4/\mathbb{Z}_2$ and $\tilde{T}^4/\mathbb{Z}_2$. In such configurations, everything is rigid along T^4 and the gauge group before Green–Schwarz mechanism is $[\mathrm{U}(1)^{16}]_{\rm DD} \times [\mathrm{U}(1)^{16}]_{\rm NN}$. The blocks of the mass matrix which takes

the same form (3.1.46) are now

$$\begin{aligned} \mathcal{M}^2_{r's'} &= 16\delta_{r's'} \ , & \mathcal{M}^2_{r'\tilde{s}'} &= -4e^{4i\pi\vec{a}_{i(r')}\cdot\vec{a}_{i(\tilde{s}')}} \ , \\ \mathcal{M}^2_{\tilde{r}'s'} &= -4e^{4i\pi\vec{a}_{i(\tilde{r}')}\cdot\vec{a}_{i(s')}} \ , & \mathcal{M}^2_{\tilde{r}'\tilde{s}'} &= 16\delta_{\tilde{r}'\tilde{s}'} \ . \end{aligned} \tag{3.1.50}$$

The matrix has 16 positive eigenvalues and 16 vanishing ones as expected (16 is the maximum possible positive eigenvalues when the number of unitary factors exceeds 16). Thus, 16 combinations of Wilson lines along T^2 can be set to zero according to the eigenvectors associated with the positive eigenvalues. They can be used for example to eliminate all the $\epsilon^{I'}_{\tilde{r}'}$ degrees of freedom:

$$4\epsilon^{I'}_{\tilde{r}'} = -\sum_{s'} e^{4i\pi\vec{a}_{i(\tilde{r}')}\cdot\vec{a}_{i(s')}}\xi_{s'} \ . \tag{3.1.51}$$

In this case, the whole 16 quaternionic scalars also get a tree-level mass and the gauge group is broken to $\mathrm{U}(1)^{16}$.

Let us study an interesting case where the naive tachyonic instabilities induced by some Wilson lines along T^2 actually disappear thanks to the Green–Schwarz mechanism. The corresponding brane configuration is depicted in Fig. 3.4.

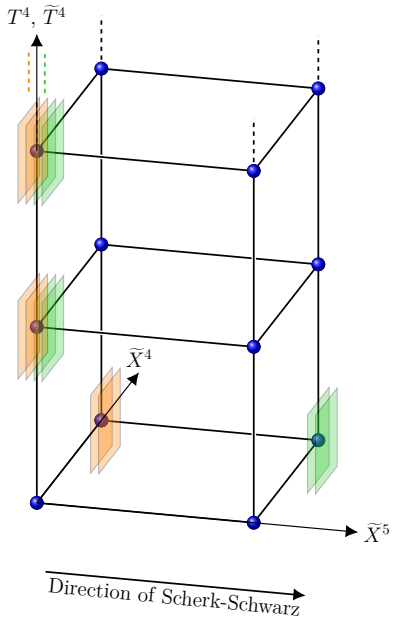

Figure 3.4: 15 pairs of each kind are located at the same $\tilde{T}^2/I_{45}$ fixed point and the remaining pairs, shifted along $\tilde{X}^4$, are facing each other along $\tilde{X}^5$.

We can read from (3.1.30) or (3.1.38) that the mass coefficients associated with the 2×15 pairs of branes are equal to $\frac{15}{4}$ while those associated with the two remaining stacks are equal to $-\frac{1}{4}$. However, the elimination of the $\epsilon^{I'}_{\tilde{r}'}$ thanks to (3.1.51) yields the following 16×16 submatrix of the one-loop mass matrix in the correct basis:

$$\frac{1}{2}\begin{pmatrix} 29 & & & \\ & \ddots & & (0) \\ & & 29 & \\ & (0) & & 13 \end{pmatrix} - \frac{1}{2}\begin{pmatrix} 0 & & & \\ & \ddots & & (1) \\ & & \ddots & \\ & (1) & & 0 \end{pmatrix} \ . \tag{3.1.52}$$

This matrix has only positive eigenvalues so we conclude that the naive instability is washed out by the Green–Schwarz mechanism. In such configurations though, the ND scalars are found to be massless up to the subdominant contributions in (3.1.49). Also, the breaking scale runs away since we have in this case $n_{\rm F} - n_{\rm B} = -1120$.

Models with $n_{\rm F} - n_{\rm B} = 0$

As one can expect from the typical expression of the one-loop potential (3.1.28), uplifting the potential while maintaining stability of the moduli is not easy to achieve. This is because the uplifting requires to increase the number of massless fermions and lower the number of massless bosons while improving stability requires the opposite. In an $\mathcal{N} = 4 \to \mathcal{N} = 0$ framework [58], stable models with zero or positive potential were indeed very rare.

In order to find stable models with a non-negative potential in our setup, we performed a numerical exploration of all possibilities in all consistent non-perturbative branches. The exploration goes as follows:

- For each non-perturbatively consistent component of the moduli space, we loop over all possible distributions of D3-branes in $T^4/\mathbb{Z}_2$ and $\tilde{T}^4/\mathbb{Z}_2$.
- For each such distributions, the tree-level mass matrix $\mathcal{M}^2$ of the Cartan U(1)'s is computed and diagonalized.
- We then loop over all possible distribution of the D3-branes along the $\tilde{T}^2/I_{45}$ and we check that the positions in $T^4/\mathbb{Z}_2$ and $\tilde{T}^4/\mathbb{Z}_2$ given in (3.1.32) or (3.1.38) are non-tachyonic.
- Before going further and apply the Green–Scwharz mechanism to the positions along $\tilde{T}^2/I_{45}$, we reject all distributions for which $n_{\rm F} - n_{\rm B} < 0$ thanks to (3.1.27).
- For each distribution that reaches this step, we compute the naive mass matrix for the Wilson lines along $\tilde{T}^2/I_{45}$ with (3.1.30) or (3.1.38), we go to the basis which diagonalizes $\mathcal{M}^2$, we remove the combinations that get a tree-level mass and we diagonalize again the resulting (smaller) mass matrix. Configurations for which this matrix possesses at least one strictly negative eigenvalue are rejected.

Only eight models are found to pass all these filters among the hundreds of billions of possibilities and three of them have an exponentially suppressed one-loop potential ($n_{\rm F} - n_{\rm B} = 0$). Let us describe theses three models in detail and check the status of the moduli not treated by the numerical exploration. The brane configurations of these three models are drawn in Fig. 3.5.

• The model displayed in Fig. 3.5a contains 16 unitary factors from a six-dimensional point of view (and 17 in four dimensions). Thus, 16 U(1)'s disappear from the naive gauge group $[{\rm U}(1)^7 \times {\rm U}(2) \times {\rm U}(7)]_{\rm DD} \times [{\rm U}(1)^6 \times {\rm U}(5)^2]_{\rm NN}$ to yield

$$\text{Model (a):} \quad {\rm U}(1) \times {\rm SU}(2) \times {\rm SU}(7) \times {\rm SU}(5)^2 \ . \tag{3.1.53}$$

Also, the 16 quaternionic scalars get a tree-level mass. Of course, because the model has survived to all filters, all dynamical D3-branes positions are non-tachyonic and turn out to be strictly massive. No ND scalars exist in this model and, up to suppressed terms, all closed-string moduli are flat

directions of the potential, even the breaking scale M thanks to the Bose/Fermi degeneracy at the massless level. The massless bosons are the bosonic parts of $\mathcal{N}=2$ vector multiplets in the adjoint representations of the groups in (3.1.53) together with the scalars of hypermultiplets in antisymmetric $\oplus$ $\overline{\text{antisymmetric}}$ of the non-abelian factors. This gives $n_{\rm B}^{\rm open}=800$ and the closed sector contributes with $n_{\rm B}^{\rm closed}=96$ for a total of $n_{\rm B}=896$. The massless fermions are the fermionic part of hypermultiplets in the ND sector in bifundamental representations of all pairs of gauge factors (one N and one D) facing each other along $\tilde{X}^5$ in Fig. 3.5a. This gives $n_{\rm F}=4\times14\times16=896$, which exactly compensates the bosonic degrees of freedom.

• The model displayed in Fig. 3.5b also contains 16 unitary factors from a six-dimensional point of view (and 17 in four dimensions). Thus, 16 U(1)'s disappear from the naive gauge group which is slightly different than in model (a), $[\mathrm{U}(1)^7\times\mathrm{U}(3)\times\mathrm{U}(6)]_{\rm DD}\times[\mathrm{U}(1)^6\times\mathrm{U}(5)^2]_{\rm NN}$ to yield

$$\text{Model (b):}\quad \mathrm{U}(1)\times\mathrm{SU}(3)\times\mathrm{SU}(6)\times\mathrm{SU}(5)^2\ . \tag{3.1.54}$$

The 16 quaternionic scalars get a tree-level mass and all dynamical D3-branes positions are strictly massive. No ND scalars exist in this model and all closed-string moduli are flat directions of the potential. In this case, the counting of massless degrees of freedom yields $n_{\rm B}=n_{\rm F}=832$.

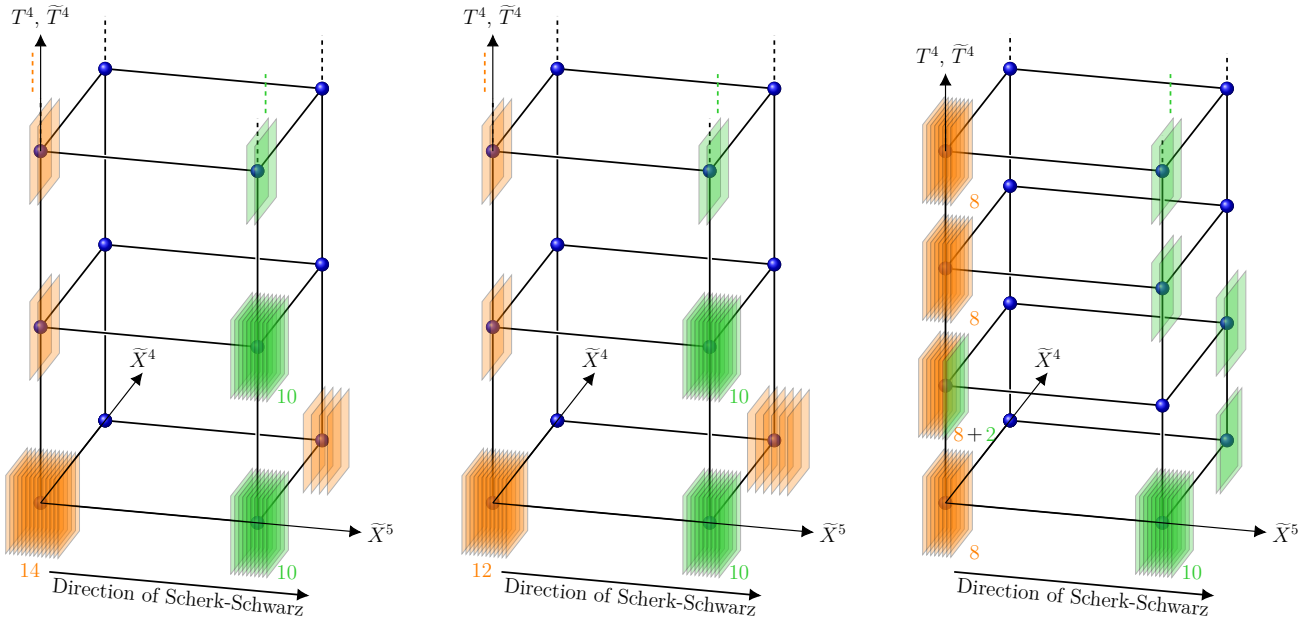

(a) Configuration tachyon-free at one loop with gauge group $\mathrm{U}(1)\times\mathrm{SU}(2)\times\mathrm{SU}(7)\times\mathrm{SU}(5)^2$.

(b) Configuration tachyon-free at one loop with gauge group $\mathrm{U}(1)\times\mathrm{SU}(3)\times\mathrm{SU}(6)\times\mathrm{SU}(5)^2$.

(c) Configuration tachyon-free at one loop with gauge group $\mathrm{U}(1)^2\times\mathrm{SU}(4)^4\times\mathrm{SU}(5)$ up to stability of two quaternionic scalars.

Figure 3.5: Two brane configurations (a) and (b) in component $(\mathcal{R},\tilde{\mathcal{R}})=(8,8)$ of the moduli space, and one configuration (c) in component $(\mathcal{R},\tilde{\mathcal{R}})=(0,8)$. They all have a Bose/Fermi degeneracy at the massless level and thus an exponentially suppressed potential.

• The model displayed in Fig. 3.5c contains only 14 unitary factors from a six-dimensional point of view (and 16 in four dimensions). Thus, 14 U(1)'s disappear from the naive gauge group $[\mathrm{U}(4)^4]_{\rm DD}\times$

$[\mathrm{U}(1)^1 1 \times \mathrm{U}(5)]_{\mathrm{NN}}$ to yield

$$\text{Model (c):} \quad \mathrm{U}(1)^2 \times \mathrm{SU}(4)^4 \times \mathrm{SU}(5) \ . \tag{3.1.55}$$

Only 14 quaternionic scalars get a tree-level mass and the stability status of the remaining two is unknown. All dynamical D3-branes positions are massless except one that is strictly massive. The model contains ND scalars whose "mass" is given by (3.1.49). Applied with $N_{ii'} = 1$, $N_{i\hat{i}'} = 0$ (in Fig. 3.5c, it corresponds to the stack of two green branes mixed with the orange ones) and $D_{ji'} = 8$, $D_{j\hat{i}'} = 0$ (it correspond to one of the four stacks of eight orange branes in the figure), we have

$$(n_{ii'} - n_{i\hat{i}'} - 1 + d_{ji'} - n_{j\hat{i}'} - 1) = 3 > 0 \ . \tag{3.1.56}$$

We thus conclude that the ND scalars are massive. All closed-string moduli are flat directions of the potential and the counting of massless degrees of freedom gives $n_{\mathrm{B}} = n_{\mathrm{F}} = 832$.

3.2 Mass of Neumann–Dirichlet scalars

This section is dedicated to the computation of the mass of scalars in the ND sector of the BSGP model. The followed strategy is to evaluate the one-loop two-point correlation function of such states to extract their mass from it. The difficulty of this evaluation is due to the presence of *boundary-changing fields* [166] in the vertex operators of the ND states that handle the change of boundary conditions from Neumann to Dirichlet on the wolrdsheet. It is the evaluation of correlators of boundary-changing fields involved in the two-point correlation function that constitutes a hard task. The correspondence between these boundary-changing fields and so-called *twist fields* for closed-strings, that are the operators that create states in twisted sectors of non-freely acting orbifolds in the Hilbert space, is a key ingredient to evaluate the correlators of such fields at one loop. Indeed, the boundary-changing and the twist operators share the same OPE's [166, 167] so that their correlation functions are linked. To go from the closed string to the open string at one-loop, it is useful to define the Euler characteristic zero open-string surfaces from doubly-covering tori modded by involutions [115, 162, 168, 169].

In this section, we will derive the full expression of the one-loop two-point correlation function of the scalars in the ND sector and find the field-theory limit of this quite involved result. Note that the Appendix C.1 reviews the twist-field technology at one loop, necessary to evaluate correlators involving the boundary-changing fields by using the correspondence between those two kind of operators. References to this appendix will be done but it has been chosen not to incorporate it in the main text for a less technical manuscript. From the field-theory limit, we will be able to justify the expression (3.1.49) that we used to conclude on the stability of these moduli in the previous section.

3.2.1 Two-point correlation functions of ND moduli

We want to evaluate the one-loop two-point correlations functions of scalars in the ND sector. Such kinds of correlation functions involving Neumann–Dirichlet states have already been computed in the literature in supersymmetric theories, either at tree level [170–175] or at one loop [176–181]. In this subsection, we give a precise definition of what we want to compute and then we express the relevant vertex operators for ND states to derive the two-point correlation function in terms of various correlators whose expressions are given afterwards, in a new subsection, for clarity. The

synthesis of all these results is displayed in a third subsection and we give a full exact result for the one-loop two-point correlation function of ND scalars.

The setup

We are in the context of the BSGP model with broken supersymmetry compactified down to four dimensions, described in Sect 3.1. Massless scalars in the ND sector of the theory correspond to strings stretched between D9-branes and D5-branes in the original picture. For such strings to be massless and with spin zero, the stacks of D3-branes T-dual to the D9-branes or D5-branes in the proper T-dual theories should be located at fixed points with same positions inside $\tilde{T}^2/I_{45}$. Let us call $i_0 i'_0$ the fixed point where the $2n_{i_0 i'_0}$ D3-branes T-dual to the D9-branes are and $j_0 i'_0$ the fixed point where the $2d_{i_0 i'_0}$ D3-branes T-dual to the D5-branes sit. The same primed index ensure the ND states to be massless scalars.

The ND string is characterized by a Chan-Paton index α_0 which refers to one of the $2n_{i_0 i'_0}$ D3-branes T-dual to D9-branes and another index β_0 referring to one of the $2d_{i_0 i'_0}$ D3-branes T-dual to the D5-branes. The two-point function at one loop have two external legs and can have the topology of an annulus of that of a Möbius strip. In the former case, the diagram has two boundaries: One on which the incoming ND state and outgoing DN state are inserted and the other which carries an arbitrary Chan-Paton index γ referring either to the N or D sector. These two cases are depicted in the two first diagrams on the left in Fig. 3.6. The string which is drawn is the state running inside the loop. On the right of the figure, the diagrams are mapped to double-cover tori with Teichmüller parameters $\tau^{\rm dc} \equiv \frac{i\tau_2}{2}$ on which the involution $\mathcal{I}(z) :\ z \to 1 - \bar{z}$ gives back the annulus topology. The two external legs representing the ND state are mapped to vertex operators inserted at z_1 and z_2. In the case of the Möbius strip topology (third figure on the left in Fig. 3.6), there is only one boundary and no free index γ. The double-cover torus has Teichmüller parameter $\tau^{\rm dc} \equiv \frac{1}{2} + \frac{i\tau_2}{2}$. Denoting $V^{\alpha_0\beta_0}(z_1, k)$ the vertex operator inserted at z_1 and $V^{\beta_0\alpha_0}(z_2, -k)$ the one inserted at z_2, what we want to compute is the following quantity

$$\sum_{\Sigma\in\{\mathcal{A},\mathcal{M}\}} \sum_{\alpha_0=1}^{N_{i_0 i'_0}} \sum_{\beta_0=1}^{D_{j_0 i'_0}} \left\langle V^{\alpha_0\beta_0}(z_1, k) V^{\beta_0\alpha_0}(z_2, -k) \right\rangle^{\Sigma} \ . \tag{3.2.1}$$

Let us define additional useful notations. States that transform under the bifundamental representation of $\mathrm{U}(n_{i_0 i'_0}) \times \mathrm{U}(d_{j_0 i'_0})$ are labelled by a matrix λ which takes the following form [159]

$$\lambda \equiv \begin{pmatrix} \Lambda_1 & \Lambda_2 \\ -\Lambda_2 & \Lambda_1 \end{pmatrix}, \tag{3.2.2}$$

where Λ_1 and Λ_2 are arbitrary real $n_{i_0 i'_0} \times d_{j_0 i'_0}$ matrices. Eventually, like in (C.1.1), we define a complex basis both for the bosonic worldsheet coordinates X^μ, $\mu \in \{0, \dots, 3\}$, $X^{I'}$, $I' \in \{4, 5\}$, X^I, $I \in \{6, 7, 8, 9\}$ and for the fermionic fields ψ^μ, $\psi^{I'}$, ψ^I,

$$\begin{aligned} Z^u &\equiv \frac{X^{2u} + iX^{2u+1}}{\sqrt{2}} \ , & \overline{Z}^u &\equiv \frac{X^{2u} - iX^{2u+1}}{\sqrt{2}} \ , \\ \Psi^u &\equiv \frac{\psi^{2u} + i\psi^{2u+1}}{\sqrt{2}} \equiv e^{iH_u} \ , & \overline{\Psi}^u &\equiv \frac{\psi^{2u} - i\psi^{2u+1}}{\sqrt{2}} \equiv e^{-iH_u} \ , \qquad u \in \{0, \dots, 4\} \ , \end{aligned} \tag{3.2.3}$$

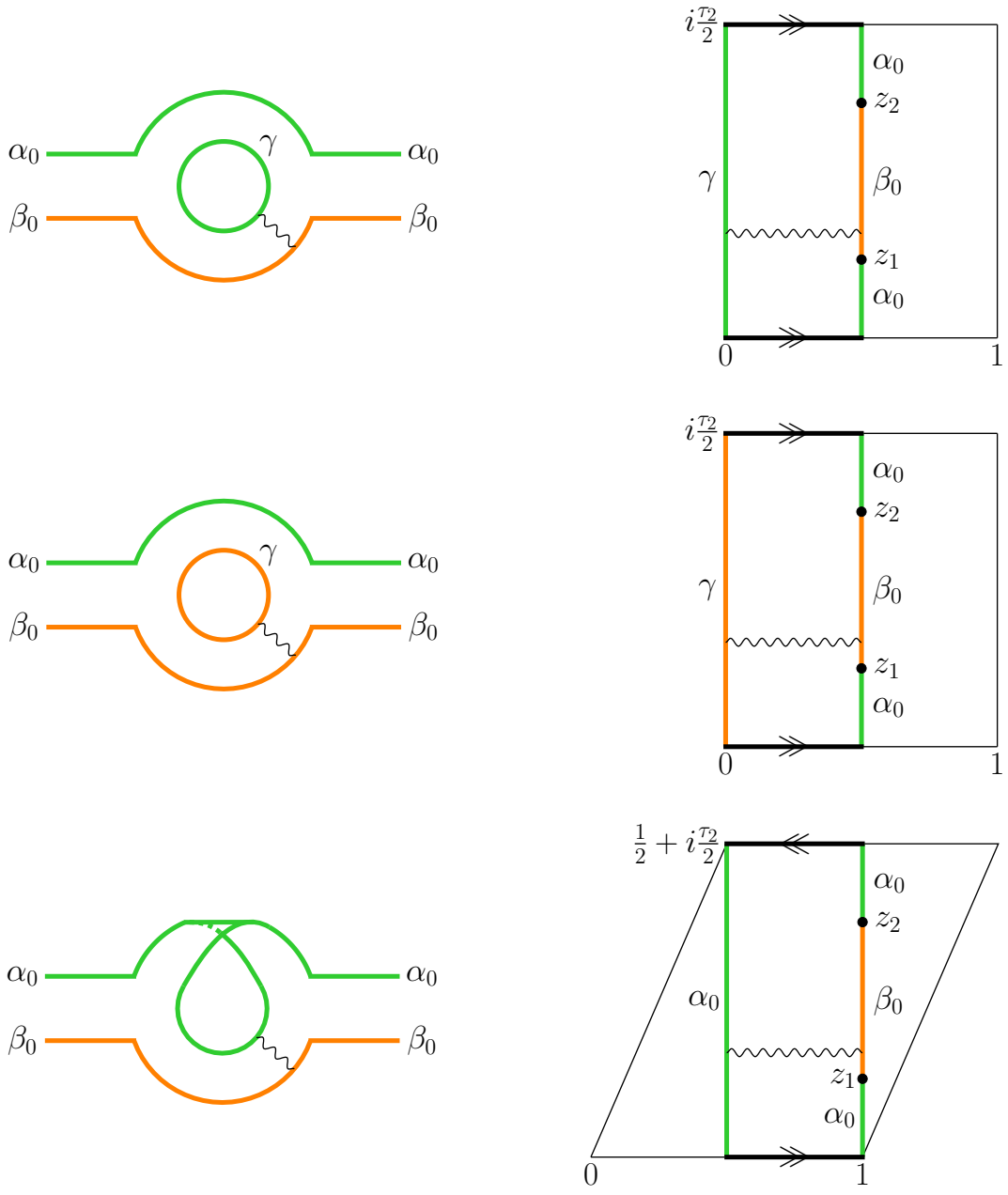

Figure 3.6: Open-string diagrams with two external legs in the ND and DN sectors (left panel). On the double-cover tori (right panel), the external legs are mapped to boundary-changing vertex operators at positions z_1, z_2.

where the scalars H_u are introduced to bosonize the fermionic fields. In the same spirit, it is also useful to define the external complexified momentum K^u for $u \in \{0, 1\}$ from the external momentum k^μ of the ND state like

$$K^u = \frac{k^{2u} + ik^{2u+1}}{\sqrt{2}} \ . \tag{3.2.4}$$

For simplicity in the following, we restrict our analysis to the case where the internal metric, both along the T^2 and T^4 is diagonal with radii R_4, R_5 in the T^2 and R_6, R_7, R_8, R_9 in the T^4.

Vertex operators and amplitudes

Along the boundary of the Möbius strip and along that of the annulus where the vertex operators are inserted, there is a change of boundary condition for the state running in the loop from Neumann to Dirichlet or the contrary at the insertion points. This implies the presence of *boundary-changing field* [166] in the vertex operators to account for this change. In ghost-picture -1 (indicated with a subscript), the vertex operators $V_{-1}^{\alpha_0\beta_0}(z_1,k)$ at z_1 and $V_{-1}^{\beta_0\alpha_0}(z_2,-k)$ at z_2 are

$$\begin{aligned} V_{-1}^{\alpha_0\beta_0}(z_1,k) &= \lambda_{\alpha_0\beta_0}\, e^{-\phi}\, e^{ik\cdot X}\, e^{\frac{i}{2}(H_3-H_4)}\, \sigma^3\sigma^4(z_1)\ , \\ V_{-1}^{\beta_0\alpha_0}(z_2,-k) &= \lambda^{\mathrm{T}}_{\beta_0\alpha_0}\, e^{-\phi}\, e^{-ik\cdot X}\, e^{-\frac{i}{2}(H_3-H_4)}\, \sigma^3\sigma^4(z_2)\ . \end{aligned} \tag{3.2.5}$$

They involve the element $\alpha_0\beta_0$ of the matrix λ and the element $\beta_0\alpha_0$ of its transpose. The field $\phi(z)$ is the scalar ghost coming from the bosonization of the superconformal ghosts. The momentum involved in $e^{ik\cdot X}$ refers to the external momentum k^μ only and the operators $e^{\pm i(H_3-H_4)}$ are *spin fields* to describe states that are spinors from the $T^4/\mathbb{Z}_2$ point of view. Indeed, remember that in Table. 3.1, the ND states are associated with characters O_4C_4 with a spinorial internal structure of negative chirality. Finally, the fields σ^3 and σ^4 are the boundary-changing fields and handle the change of boundary conditions along the complex directions 3 and 4.

To proceed with the evaluation of the correlation function (3.2.1), it is useful to transform the vertex operators to ghost-picture zero with the formulas

$$\begin{aligned} V_0^{\alpha_0\beta_0}(z,k,\epsilon) &= \lim_{w\to z} e^{\phi}\, T_{\mathrm{F}}(w)\, V_{-1}^{\alpha_0\beta_0}(z,k,\epsilon)\ , \\ V_0^{\beta_0\alpha_0}(z,-k,-\epsilon) &= \lim_{w\to z} e^{\phi}\, T_{\mathrm{F}}(w)\, V_{-1}^{\beta_0\alpha_0}(z,-k,-\epsilon)\ , \end{aligned} \tag{3.2.6}$$

where T_{F} is the supercurrent given by

$$T_{\mathrm{F}}(z) = \frac{1}{\sqrt{\alpha'}}\,\partial X^\mu\psi_\mu(z) = \frac{1}{\sqrt{\alpha'}}\big(\partial\overline{Z}^u\Psi^u(z) + \partial Z^u\overline{\Psi}^u(z)\big)\ . \tag{3.2.7}$$

The picture changing requires the use of OPE's between the various involved operators. Most importantly, the OPE's between the fields $\partial Z^u(z)$, $\partial\overline{Z}^u(z)$ and the boundary-changing fields σ^u, $u\in\{3,4\}$ are identical to those of ground-state twist fields in (C.1.2) with $N=2$ and $\frac{\kappa}{N}=\frac{1}{2}$:

$$\begin{aligned} \partial Z^u(z)\sigma^u(w) &\underset{z\to w}{\sim} (z-w)^{-\frac{1}{2}}\,\tau^u(w) + \text{finite}\ , \\ \partial\overline{Z}^u(z)\sigma^u(w) &\underset{z\to w}{\sim} (z-w)^{-\frac{1}{2}}\,\tau'^u(w) + \text{finite}\ . \end{aligned} \tag{3.2.8}$$

This introduces the excited boundary-changing fields τ^u and τ'^u, the counterparts of the excited twist fields.

The vertex operators in ghost-picture zero then naturally split into an "external part" $V_{0,\mathrm{ext}}^{\alpha_0\beta_0}(z_i,\pm k)$ corresponding to the action of the part of the supercurrent with $u=0,1,2$ and an "internal part" $V_{0,\mathrm{int}}^{\alpha_0\beta_0}(z_i,\pm k)$ for the action of the $u=3,4$ terms. In the external parts of the vertex operators, the momentum along complex direction $u=2$ *i.e.* along the T^2 is set to zero since we are interested in massless states at tree level. The total amplitude (3.2.1) splits into an external contribution and

an internal one. For a given α_0 and β_0, the external amplitude is

$$\begin{aligned} A^{\alpha_0\beta_0}_{\text{ext}\Sigma} &\equiv \left\langle V^{\alpha_0\beta_0}_{0,\text{ext}}(z_1,k) V^{\beta_0\alpha_0}_{0,\text{ext}}(z_2,-k)\right\rangle^{\Sigma} \\ &= \alpha' \,\lambda_{\alpha_0\beta_0}\lambda^{\mathrm{T}}_{\beta_0\alpha_0}\,\langle e^{ik\cdot X}(z_1)e^{-ik\cdot X}(z_2)\rangle\,\langle e^{\frac{i}{2}H_3}(z_1)e^{-\frac{i}{2}H_3}(z_2)\rangle\,\langle e^{-\frac{i}{2}H_4}(z_1)e^{\frac{i}{2}H_4}(z_2)\rangle\times \\ &\quad \langle\sigma^3(z_1)\sigma^3(z_2)\rangle\,\langle\sigma^4(z_1)\sigma^4(z_2)\rangle\sum_{u=0}^{1} K^u\overline{K}^u\Big[\langle e^{iH_u}(z_1)e^{-iH_u}(z_2)\rangle + \langle e^{-iH_u}(z_1)e^{iH_u}(z_2)\rangle\Big]\,. \end{aligned} \tag{3.2.9}$$

This amplitude contains the one-loop corrections to the Kähler potential for the ND scalars. It is the internal part that contains the one-loop correction to the mass of these moduli that we want to extract and it reads

$$\begin{aligned} A^{\alpha_0\beta_0}_{\text{int}\Sigma} &\equiv \left\langle V^{\alpha_0\beta_0}_{0,\text{int}}(z_1,k) V^{\beta_0\alpha_0}_{0,\text{int}}(z_2,-k)\right\rangle^{\Sigma} \\ &= \frac{1}{\alpha'}\,\lambda_{\alpha_0\beta_0}\lambda^{\mathrm{T}}_{\beta_0\alpha_0}\,\langle e^{ik\cdot X}(z_1)e^{-ik\cdot X}(z_2)\rangle \\ &\quad\times\Big[\langle e^{-\frac{i}{2}H_3}(z_1)e^{\frac{i}{2}H_3}(z_2)\rangle\,\langle e^{-\frac{i}{2}H_4}(z_1)e^{\frac{i}{2}H_4}(z_2)\rangle\,\langle\tau^3(z_1)\tau'^3(z_2)\rangle\,\langle\sigma^4(z_1)\sigma^4(z_2)\rangle \\ &\quad + \langle e^{\frac{i}{2}H_3}(z_1)e^{-\frac{i}{2}H_3}(z_2)\rangle\,\langle e^{\frac{i}{2}H_4}(z_1)e^{-\frac{i}{2}H_4}(z_2)\rangle\,\langle\sigma^3(z_1)\sigma^3(z_2)\rangle\,\langle\tau'^4(z_1)\tau^4(z_2)\rangle\Big]\,. \end{aligned} \tag{3.2.10}$$

Several things are understood in these formulas: For the annulus topology ($\Sigma = \mathcal{A}$), there is a sum over the other boundary γ and the sums over the spin structures of the fermions Ψ^u are also left implicit. The next step in the computation consists in evaluating the various correlators on the surfaces $\Sigma = \mathcal{A}$ or $\mathcal{M}$ involved in the amplitudes and more particularly the correlators of (excited) boundary-changing fields.

3.2.2 One-loop correlators

Here we express all the correlators involved in the amplitudes. They are given on the double-cover tori of the open-string surfaces before finding their open expressions. To be clear with the notations, we will denote the correlators on the covering tori with a superscript "dc" and without anything for the correlators on the open-string worldsheets. To determine the correlators involving boundary-changing fields and their excited versions, we use the twist-field technology at one-loop [167, 182] reviewed in Appendix C.1.

Ground-state boundary-changing fields correlators

We start with the most complicated correlators involving the boundary-changing fields. We first evaluate the correlators on the double-cover tori $\mathcal{T}$ with Teichmüller parameter τ^{dc} before going to the annulus or Möbius strip topology thanks to the method of images. For correlators of ground-state boundary-changing fields $\langle\sigma^u(z_1)\sigma^u(z_2)\rangle^{\text{dc}}$, $u \in \{3,4\}$, we use the correspondence between these boundary-changing fields and ground-state twist fields of a $\mathbb{Z}_2$ orbifold. As explained in the appendix, the correlator is expressed in terms of a classical action and a quantum correlator. The latter given by (C.1.23) applied with $N=2$, $L=2$, $M=1$ and $\frac{\kappa_1}{N} = \frac{\kappa_2}{N} = \frac{1}{2}$. We thus have

$$\langle\sigma^u(z_1,\bar{z}_1)\sigma^u(z_2,\bar{z}_2)\rangle^{\text{dc}}_{\text{qu}} = f_{\text{dc}}(\tau^{\text{dc}};\tfrac{1}{2},\tfrac{1}{2})\,(\det W)^{-1}\,\vartheta_1(z_1-z_2)^{-\frac{1}{4}}\,\overline{\vartheta_1(z_1-z_2)}^{-\frac{1}{4}}\,, \tag{3.2.11}$$

where the 2×2 cut-period matrix ${W_a}^A$ (see Eq. (C.1.21)) is expressed in terms of a single cut differential ω (see Eq. C.1.15)),

$$\omega(z) = \vartheta_1(z-z_1)^{-\frac{1}{2}}\,\vartheta_1(z-z_2)^{-\frac{1}{2}}\,\vartheta_1\big(z-\frac{z_1+z_2}{2}\big)\,, \tag{3.2.12}$$

integrated over the two cycles of the torus $\gamma_1 :\ z \to z+1$ and $\gamma_2 :\ z \to z+\tau^{\rm dc}$,

$$W = \begin{pmatrix} W_1 & \overline{W}_1 \\ W_2 & \overline{W}_2 \end{pmatrix}, \quad \text{where} \quad W_a = \oint_{\gamma_a} \mathrm{d}z\, \omega\,, \quad a \in \{1,2\}\ . \tag{3.2.13}$$

In this case, the classical action (C.1.27) for directions $u = 3$ and 4 *i.e.* along the internal T^4 is

$$S_{\rm cl}^{\mathcal{T},T^4} = \sum_{u=3}^{4} \frac{1}{4\pi\alpha' \,\mathrm{Im}(\overline{W}_1 W_2)} \left(\left| \overline{W}_2 v_1^u - \overline{W}_1 v_2^u \right|^2 + \left| W_2 v_1^u - W_1 v_2^u \right|^2 \right), \tag{3.2.14}$$

where the displacement vectors v_a^u, $a \in \{1,2\}$ reflects how many times the instantonic solution winds around the internal T^4 when z is transported along the paths γ_1 and γ_2. We define the winding numbers n_I, $I \in \{6,\dots,9\}$ associated with γ_1 and the wrapping numbers l_I associated with γ_2 such that:

$$v_1^u = \frac{2\pi R_{2u} n_{2u} + 2i\pi R_{2u+1} n_{2u+1}}{\sqrt{2}}\ , \qquad v_2^u = \frac{2\pi R_{2u} l_{2u} + 2i\pi R_{2u+1} l_{2u+1}}{\sqrt{2}}\ . \tag{3.2.15}$$

Note that this formalism is fully compatible with the complex direction $u = 2$ describing the T^2 which is not twisted. Along this direction, the cut differential is trivial *i.e.* $\omega(z) = 1$ yielding the trivial cut-period matrix

$$\begin{pmatrix} 1 & 1 \\ \tau^{\rm dc} & \bar{\tau}^{\rm dc} \end{pmatrix}. \tag{3.2.16}$$

Defining the displacements exactly like in (3.2.15), the obtained action is the usual result for a two-torus:

$$S_{\rm cl}^{\mathcal{T},T^2} = \frac{\pi}{\alpha' \,\mathrm{Im}\tau^{\rm dc}} \left(R_4^2 |n_4 \tau^{\rm dc} - l_4|^2 + R_5^2 |n_5 \tau^{\rm dc} - l_5|^2 \right)\ . \tag{3.2.17}$$

A takeaway is that the sum over instantons which appears in (C.1.5) translates into a sum over all the internal winding and wrapping numbers in our case.

For open-string topologies that are of interest in this work, the quantum correlator of ground-state boundary-changing fields is found in [176] using the method of images. The result turns out to be, for $u = 3$ or 4,

$$\langle \sigma^u(z_1) \sigma^u(z_2) \rangle_{\rm qu} = f(\tau^{\rm dc}; \tfrac{1}{2}, \tfrac{1}{2})\, (\det W)^{-\frac{1}{2}}\, \vartheta_1(z_1 - z_2)^{-\frac{1}{4}}\ . \tag{3.2.18}$$

As for the classical action, instantonic worldsheets can have NN, DD, ND or DN boundary conditions for the annulus topology and N or D for the Möbius strip. For NN or N conditions, the winding numbers must vanish while for DD and D conditions, we define T-dual winding numbers that should also vanish. For ND and DN boundary conditions, both winding and wrapping numbers (and their T-dual counterparts) must be zero. In addition, a division by two must be performed compared to the torus action due to the involution that creates the open-string surfaces which halves the wolrdsheet surface. The total classical action on an open-string surface $\Sigma \in \{\mathcal{A}, \mathcal{M}\}$, which is the sum of the T^2 and T^4 contributions then reads

$$S_{\rm cl}^{\Sigma} = \frac{\pi[(R_4 l_4)^2 + (R_5 l_5)^2]}{\alpha' \tau_2} + \frac{|W_1|^2}{4\pi\alpha' \,\mathrm{Im}(\overline{W}_1 W_2)} \times \begin{cases} \displaystyle\sum_{u=3}^{4} |v_2^u|^2 & \text{for NN and N}\ , \\ \displaystyle\sum_{u=3}^{4} |\tilde{v}_2^u|^2 & \text{for DD and D}\ , \\ 0 & \text{for ND and DN}\ , \end{cases} \tag{3.2.19}$$

where v_2^u is defined like in (3.2.15) while the T-dual version denoted with a tilde is defined as

$$\tilde{v}_2^u = \frac{2\pi\frac{\alpha'}{R_{2u}}\,\tilde{l}_{2u} + 2i\pi\frac{\alpha'}{R_{2u+1}}\,\tilde{l}_{2u+1}}{\sqrt{2}} \ , \quad u \in \{3,4\} \ . \tag{3.2.20}$$

Excited boundary-changing fields correlators

To determine the correlator $\langle \tau^u(z_1)\tau'^u(z_2)\rangle^{\rm dc}$ whose open-string version is present in (3.2.10), we apply a technique used in [176, 178–180] which exploits the OPE (3.2.8) between the coordinates derivatives and the boundary-changing fields. This allows to write

$$\langle \tau^u(z_1,\bar{z}_1)\tau'^u(z_2,\bar{z}_2)\,\rangle^{\rm dc}_{\rm qu} = \lim_{\substack{z\to z_1\\ w\to z_2}}\Big[(z-z_1)^{\frac{1}{2}}(w-z_2)^{\frac{1}{2}}\langle\partial Z^u(z)\partial\overline{Z}^u(w)\sigma^u(z_1,\bar{z}_1)\sigma^u(z_2,\bar{z}_2)\rangle^{\rm dc}_{\rm qu}\Big] \ , \tag{3.2.21}$$

which decomposes into two parts $\langle \tau^u(z_1,\bar{z}_1)\tau'^u(z_2,\bar{z}_2)\rangle^{\rm dc,(1)}_{\rm qu}$ and $\langle \tau^u(z_1,\bar{z}_1)\tau'^u(z_2,\bar{z}_2)\rangle^{\rm dc,(2)}_{\rm qu}$ following the decomposition (C.1.4) of the coordinates into the classical background and quantum fluctuations:

$$\begin{aligned}
\langle \tau^u(z_1,\bar{z}_1)\tau'^u(z_2,\bar{z}_2)\rangle^{\rm dc,(1)}_{\rm qu} &= \langle\sigma^u(z_1,\bar{z}_1)\sigma^u(z_2,\bar{z}_2)\rangle^{\rm dc}_{\rm qu}\lim_{\substack{z\to z_1\\ w\to z_2}}\Big[(z-z_1)^{\frac{1}{2}}(w-z_2)^{\frac{1}{2}}\,\partial Z^u_{\rm cl}(z)\partial\overline{Z}^u_{\rm cl}(w)\Big] \ ,\\
\langle \tau^u(z_1,\bar{z}_1)\tau'^u(z_2,\bar{z}_2)\,\rangle^{\rm dc,(2)}_{\rm qu} &= \lim_{\substack{z\to z_1\\ w\to z_2}}\Big[(z-z_1)^{\frac{1}{2}}(w-z_2)^{\frac{1}{2}}\langle\partial Z^u_{\rm qu}(z)\partial\overline{Z}^u_{\rm qu}(w)\sigma^u(z_1,\bar{z}_1)\sigma^u(z_2,\bar{z}_2)\rangle^{\rm dc}_{\rm qu}\Big] \ .
\end{aligned} \tag{3.2.22}$$

Part (1) is found using (C.1.25) in our special case which yields

$$\langle \tau^u(z_1,\bar{z}_1)\tau'^u(z_2,\bar{z}_2)\rangle^{\rm dc,(1)}_{\rm qu} = is\,(W^{-1})_1{}^a v_a^u(\overline{W}^{-1})_2{}^b\bar{v}_b^u\,\frac{\vartheta_1(\frac{z_1-z_2}{2})^2}{\vartheta_1'(0)\,\vartheta_1(z_1-z_2)}\langle\sigma^u(z_1,\bar{z}_1)\sigma^u(z_2,\bar{z}_2)\rangle^{\rm dc}_{\rm qu} \ , \tag{3.2.23}$$

where we have introduced a sign ambiguity s such that

$$s\,i \equiv \left(\frac{z_2-z_1}{z_1-z_2}\right)^{\frac{1}{2}} \ . \tag{3.2.24}$$

To evaluate part (2), we use the Green's function (C.1.11) applied to our case. The expressions (C.1.19) and (C.1.22) take the following form

$$\begin{aligned}
g(z,w) &= g_s(z,w) + C\,\omega(z)\,\omega(w)\\
&= g_s(z,w) - \omega(z)(W^{-1})_1{}^a\oint_{\gamma_a}{\rm d}\zeta\,g_s(\zeta,w) \ ,
\end{aligned} \tag{3.2.25}$$

where we need an explicit expression for $g_{\rm s}(z,w)$ defined in (C.1.18). Such an expression is found in [167] which, in our case, reduces to

$$\begin{aligned}
g_s(z,w) = \gamma(z)\gamma(w)\left(\frac{\vartheta_1'(0)}{\vartheta_1(z-w)}\right)^2\frac{1}{2}\Big[&F_1(z,w)\vartheta_1(w-z_1)\vartheta_1(z-z_2)\\
&+F_1(w,z)\vartheta_1(w-z_2)\vartheta_1(z-z_1)\Big] \ .
\end{aligned} \tag{3.2.26}$$

It is expressed in terms of a unique function γ (see Eq. (C.1.16))

$$\gamma(z) = \vartheta_1(z-z_1)^{-\frac{1}{2}}\,\vartheta_1(z-z_2)^{-\frac{1}{2}}\ , \tag{3.2.27}$$

and the function F_1 is

$$F_1(z,w) = \frac{\vartheta_1(z-w+U_1)}{\vartheta_1(U_1)}\,\frac{\vartheta_1\left(z-w+\frac{z_2-z_1}{2}-U_1\right)}{\vartheta_1\left(\frac{z_2-z_1}{2}-U_1\right)}\ , \quad A\in\{1,2\}\ , \tag{3.2.28}$$
where U_1 is such that $\partial_z F_1(z,w)\big|_{z=w}=0$.

The part (2) eventually reads

$$\langle\tau^u(z_1,\bar z_1)\tau'^u(z_2,\bar z_2)\,\rangle^{\mathrm{dc},(2)}_{\mathrm{qu}} = -is\,\alpha'\langle\sigma^u(z_1,\bar z_1)\sigma^u(z_2,\bar z_2)\rangle^{\mathrm{dc}}_{\mathrm{qu}}\left[C\frac{\vartheta_1(\frac{z_1-z_2}{2})^2}{\vartheta_1'(0)\,\vartheta_1(z_1-z_2)}+\frac{\vartheta_1'(0)\,F_1(z_1,z_2)}{2\,\vartheta_1(z_1-z_2)}\right]\ , \tag{3.2.29}$$

and we can switch to another formulation without C and fully in terms of $g_{\mathrm{s}}(z,w)$ (see Eq. (3.2.25)) thanks to the correspondence

$$C\,\frac{\vartheta_1(\frac{z_1-z_2}{2})^2}{\vartheta_1'(0)\,\vartheta_1(z_1-z_2)} = -\frac{1}{2}\,\vartheta_1'(0)\,\vartheta_1\big(\frac{z_1-z_2}{2}\big)(W^{-1})_1{}^a\oint_{\gamma_a}\mathrm{d}z\,\frac{F_1(z,z_2)}{\vartheta_1(z-z_1)^{\frac{1}{2}}\,\vartheta_1(z-z_2)^{\frac{3}{2}}}\ . \tag{3.2.30}$$

Note that the correlator $\langle\tau'^u(z_1)\tau^u(z_2)\rangle^{\mathrm{dc}}$ is identical up to the exchange $z_1\leftrightarrow z_2$.

When going to the open-string topologies, the correlators involving excited boundary-changing fields keep the same forms since such fields are only excited on their holomorphic sides (see Eq. (C.1.2) or (3.2.8)). To be consistent with the open-string action that displays a division by two compared to the closed-string action, parts (1) of the correlators $\langle\tau^u(z_1)\tau'^u(z_2)\rangle^{\mathrm{dc}}$ and $\langle\tau'^u(z_1)\tau^u(z_2)\rangle^{\mathrm{dc}}$ should be modified with the replacements $|v_2^u|^2\to|v_2^u|^2/2$ and $|\tilde v_2^u|^2\to|\tilde v_2^u|^2/2$. Putting the two parts together, we have, on open-string surfaces,

$$\begin{aligned}\langle\tau^u(z_1)\tau'^u(z_2)\rangle_{\mathrm{qu}} = \langle\tau'^u(z_1)\tau^u(z_2)\rangle_{\mathrm{qu}} = -s\,i\,\langle\sigma^u(z_1)\sigma^u(z_2)\rangle_{\mathrm{qu}}\,\times\\ \left[\left(\alpha' C+\frac{\overline{W}_1^2\,|v_2^u|^2}{8[\mathrm{Im}(\overline{W}_1W_2)]^2}\right)\frac{\vartheta_1(\frac{z_1-z_2}{2})^2}{\vartheta_1'(0)\,\vartheta_1(z_1-z_2)}+\alpha'\frac{\vartheta_1'(0)\,F_1(z_1,z_2)}{2\,\vartheta_1(z_1-z_2)}\right]\ ,\end{aligned} \tag{3.2.31}$$

when the worldsheet has NN or N boundary conditions on the annulus or Möbius strip. For DD or D boundary conditions, the correlators take identical forms up to the change $v_2^u\to\tilde v_2^u$. Finally, for boundary conditions ND or DN on the annulus, the classical displacements vanish and only the pure quantum contributions proportional to α' survive.

Bosonic and fermionic correlators

The other correlators in (3.2.9) and (3.2.10) involving the bosonic fields and the bosonized fermions are given in this paragraph. On the torus, the propagator of spacetime coordinates X^μ is

$$\langle X^\mu(z_1)X_\nu(z_2)\rangle^{\mathrm{dc}} = \delta^\mu_\nu\left[-\frac{\alpha'}{2}\ln\left|\frac{\vartheta_1(z_1-z_2)}{\vartheta_1'(0)}\right|^2+\frac{\alpha'\pi\,[\mathrm{Im}(z_1-z_2)]^2}{\mathrm{Im}\tau^{\mathrm{dc}}}\right]\ , \tag{3.2.32}$$

and the propagator of the bosonized fermions Ψ^u, $u \in \{0,\dots,4\}$, for each spin structure $\nu \in \{1,2,3,4\}$ and arbitrary H_u-charge q is

$$\langle e^{iqH_u}(z_1)e^{-iqH_u}(z_2)\rangle_\nu^{\rm dc} = K_{\nu,|q|}\,\vartheta_\nu(q(z_1-z_2))\,\vartheta_1(z_1-z_2)^{-q^2}\ , \tag{3.2.33}$$

with $K_{\nu,|q|}$ a normalization factor which depends on $\tau^{\rm dc}$.

The bosonic correlator on the annulus and Möbius strip is obtained by symmetrizing the double-cover torus correlator with respect to the involution $\mathcal{I}(z):\ z\to 1-\bar z$,

$$\begin{aligned}\langle X^\mu(z_1)X_\nu(z_2)\rangle &= \frac{1}{2}\Big[\langle X^\mu(z_1)X_\nu(z_2)\rangle^{\rm dc} + \langle X^\mu(z_1)X_\nu(\mathcal{I}(z_2))\rangle^{\rm dc}\\ &\qquad + \langle X^\mu(\mathcal{I}(z_1))X_\nu(z_2)\rangle^{\rm dc} + \langle X^\mu(\mathcal{I}(z_1))X_\nu(\mathcal{I}(z_2))\rangle^{\rm dc}\Big]\\ &= \delta^\mu_\nu\bigg[-\alpha'\ln\left|\frac{\vartheta_1(z_1-z_2)}{\vartheta_1'(0)}\right|^2 + \frac{4\pi\alpha'\,[{\rm Im}(z_1-z_2)]^2}{\tau_2}\bigg]\ .\end{aligned} \tag{3.2.34}$$

From this formula, we deduce the following correlator of interest to us:

$$\langle e^{ik\cdot X}(z_1)e^{-ik\cdot X}(z_2)\rangle = \left(\left|\frac{\vartheta_1(z_1-z_2)}{\vartheta_1'(0)}\right| e^{-\frac{2\pi[{\rm Im}(z_1-z_2)]^2}{\tau_2}}\right)^{-2\alpha' k^2}\ . \tag{3.2.35}$$

As for the correlators of the bosonized fermions on the open-string worldsheets, it is shown [176] that they are identical to those on the double-cover tori:

$$\langle e^{iqH_u}(z_1)e^{-iqH_u}(z_2)\rangle_\nu = \langle e^{iqH_u}(z_1)e^{-iqH_u}(z_2)\rangle_\nu^{\rm dc} = K_{\nu,|q|}\,\vartheta_\nu(q(z_1-z_2))\,\vartheta_1(z_1-z_2)^{-q^2}\ . \tag{3.2.36}$$

3.2.3 Final result

In this subsection, we use the results (3.2.18), (3.2.19), (3.2.31), (3.2.35) and (3.2.36) to express the amplitudes (3.2.9) and (3.2.10). They are derived up to an instanton-dependent normalization that we will have to determine using the coalescence limit and the collapse of the amplitudes to the partition function in this regime. The external amplitude is

$$\begin{aligned}A^{\alpha_0\beta_0}_{{\rm ext}\Sigma} &= \alpha' k^2\,\lambda_{\alpha_0\beta_0}\lambda^{\rm T}_{\beta_0\alpha_0}\left[\left|\frac{\vartheta_1(z_{12})}{\vartheta_1'(0)}\right| e^{-\frac{2\pi}{\tau_2}[{\rm Im}(z_{12})]^2}\right]^{-2\alpha' k^2}\frac{1}{\det W\,\vartheta_1(z_{12})^2}\\ &\quad\times\sum_{\nu_{\rm ext}\neq 1} K_{\nu_{\rm ext},1}\,\vartheta_{\nu_{\rm ext}}(z_{12})\sum_{\nu_{\rm int}}(-1)^{\delta_{\nu_{\rm int},1}}\,\vartheta_{\nu_{\rm int}}\big(\frac{z_{12}}{2}\big)^2\\ &\quad\times\sum_{\vec{l}'} e^{-\frac{\pi}{\alpha'\tau_2}\sum_{I'}(R_{I'}l_{I'})^2}\left[\sum_{\vec{l}} e^{-\frac{|W_1|^2(|v_2^3|^2+|v_2^4|^2)}{4\pi\alpha'{\rm Im}(\overline{W}_1W_2)}}\mathcal{C}^{\Sigma\vec{l}'\vec{l}}_{\nu_{\rm int}} + \sum_{\vec{\tilde l}} e^{-\frac{|W_1|^2(|\tilde v_2^3|^2+|\tilde v_2^4|^2)}{4\pi\alpha'{\rm Im}(\overline{W}_1W_2)}}\tilde{\mathcal{C}}^{\Sigma\vec{l}'\vec{\tilde l}}_{\nu_{\rm int}}\right]\ ,\end{aligned} \tag{3.2.37}$$

where the index I' takes values in $\{4,5\}$ and $\vec{l}'\equiv(l_4,l_5)$. The vectors $\vec{l}$ and $\vec{\tilde l}$ are the four-vectors with components l_I and $\tilde l_I$, $I\in\{6,\dots,9\}$. The expression displays a sum over the "external" spin structure $\nu_{\rm ext}$ of the complex fermions Ψ^0, Ψ^1 and Ψ^2 and over the "internal" spin structure $\nu_{\rm int}$ of Ψ^3 and Ψ^4. The normalization factor $K_{\nu_{\rm ext},1}$ is given by [95]

$$K_{\nu_{\rm ext},1} = \frac{\vartheta_1'(0)}{\vartheta_{\nu_{\rm ext}}(0)}\ ,\quad \nu_{\rm ext}\in\{2,3,4\}\ . \tag{3.2.38}$$

We also defined $z_{12} \equiv z_1 - z_2$. Eventually, the coefficients $\mathcal{C}_{\nu_{\rm int}}^{\Sigma\vec{l}\vec{l}}$ and $\tilde{\mathcal{C}}_{\nu_{\rm int}}^{\Sigma\vec{l}'\vec{l}}$ are instanton-dependent normalization functions arising from the various normalizations in the correlators. For the annulus, we also expect them to contain a sum over the free boundary condition γ. Similarly, the internal amplitude is

$$\begin{aligned} A_{{\rm int}\Sigma}^{\alpha_0\beta_0} = -\frac{s\,i}{\alpha'}\,\lambda_{\alpha_0\beta_0}\lambda^{\rm T}_{\beta_0\alpha_0}\left[\left|\frac{\vartheta_1(z_{12})}{\vartheta_1'(0)}\right| e^{-\frac{2\pi}{\tau_2}[{\rm Im}(z_{12})]^2}\right]^{-2\alpha' k^2} \frac{\vartheta_1(\frac{z_{12}}{2})^2}{\det W\,\vartheta_1(z_{12})^2\,\vartheta_1'(0)} \\ \times 4\sum_{\nu_{\rm int}}\vartheta_{\nu_{\rm int}}(\frac{z_{12}}{2})^2\sum_{\vec{l}'} e^{-\frac{\pi}{\alpha'\tau_2}\sum_{I'}(R_{I'}l_{I'})^2} \\ \times\left\{\sum_{\vec{l}} e^{-\frac{|W_1|^2(|v_2^3|^2+|v_2^4|^2)}{4\pi\alpha'{\rm Im}(\overline{W}_1W_2)}}\mathcal{C}_{\nu_{\rm int}}^{\Sigma\vec{l}'\vec{l}}\left[\frac{\overline{W}_1^2\,(|v_2^3|^2+|v_2^4|^2)}{8[{\rm Im}(\overline{W}_1W_2)]^2}+2\alpha'(C+\hat{C})\right]\right. \\ \left.+\sum_{\vec{\tilde{l}}} e^{-\frac{|W_1|^2(|\tilde{v}_2^3|^2+|\tilde{v}_2^4|^2)}{4\pi\alpha'{\rm Im}(\overline{W}_1W_2)}}\tilde{\mathcal{C}}_{\nu_{\rm int}}^{\Sigma\vec{l}'\vec{\tilde{l}}}\left[\frac{\overline{W}_1^2\,(|\tilde{v}_2^3|^2+|\tilde{v}_2^4|^2)}{8[{\rm Im}(\overline{W}_1W_2)]^2}+2\alpha'(C+\hat{C})\right]\right\}, \end{aligned} \tag{3.2.39}$$

where for compactness we have defined

$$\hat{C} \equiv \frac{\vartheta_1'(0)^2}{2\,\vartheta_1(\frac{z_{12}}{2})^2}\,F_1(z_1,z_2)\ . \tag{3.2.40}$$

The evaluation of the normalization functions is a crucial step to determine the full expressions of the amplitudes. To do this, we use the fact that in the coalescence limit $z_1 \to z_2$, the ground-state boundary-changing fields compensate each other so that the external part of the amplitude reduces to pieces of the partition function, up to multiplicative factors. It is important to determine precisely which pieces we should find to correctly identify the normalization factors. To help us in this task, we redraw the double-cover diagrams of Fig. 3.6 in the coalescence limit. Note that assuming z_1 fixed, we can either imagine z_2 descending down to z_1 or alternatively going up along the boundary, reappearing at the bottom and reach z_2 from below. For each diagram, this yields two contributions to the limit that we have drawn in Fig. 3.7.

In the coalescence limit, the cut differential (3.2.12) becomes also trivial in directions $u = 3$ and 4 ($\omega(z) \to 1$) and the cut-period matrix takes the same form as for direction $u = 2$ (see Eq. (3.2.16)). The external amplitude in the limit is then to be identified with (up to pre-factors not written here)

$$\begin{aligned} &\sum_{\gamma=1}^{32+32}\ \underset{\alpha_0\gamma+\beta_0\gamma}{\rm Str}\ \frac{1}{2}\,\frac{1+g}{2}\,q^{\frac{1}{2}(L_0-1)} \qquad \text{for } \mathcal{A}\,, \\ \text{and}\qquad &\underset{\alpha_0\alpha_0+\beta_0\beta_0}{\rm Str}\ \frac{\Omega}{2}\,\frac{1+g}{2}\,q^{\frac{1}{2}(L_0-1)} \qquad \text{for } \mathcal{M}\,. \end{aligned} \tag{3.2.41}$$

The traces are restricted to the contributions drawn in Fig. 3.7 *i.e.* to states with Chan-Paton indices $\alpha_0\gamma$ or $\gamma\beta_0$ in the annulus, with a sum over the free boundary γ, and to the state with indices $\alpha_0\beta_0$ in the Möbius strip. We can extract these contributions from the full annulus and Möbius strip one-loop amplitudes of our model written in (3.1.16) and (3.1.17) by picking the correct terms in the various traces involving the matrices which act on the Chan-Paton indices. In the annulus, we extract the following contributions in the NN and ND sectors, which correspond to the two annulus diagrams on the left of Fig. 3.7 (the contributions of the DD and DN sector easily found by exchanging $N \leftrightarrow D$ and $\alpha_0 \leftrightarrow \beta_0$),

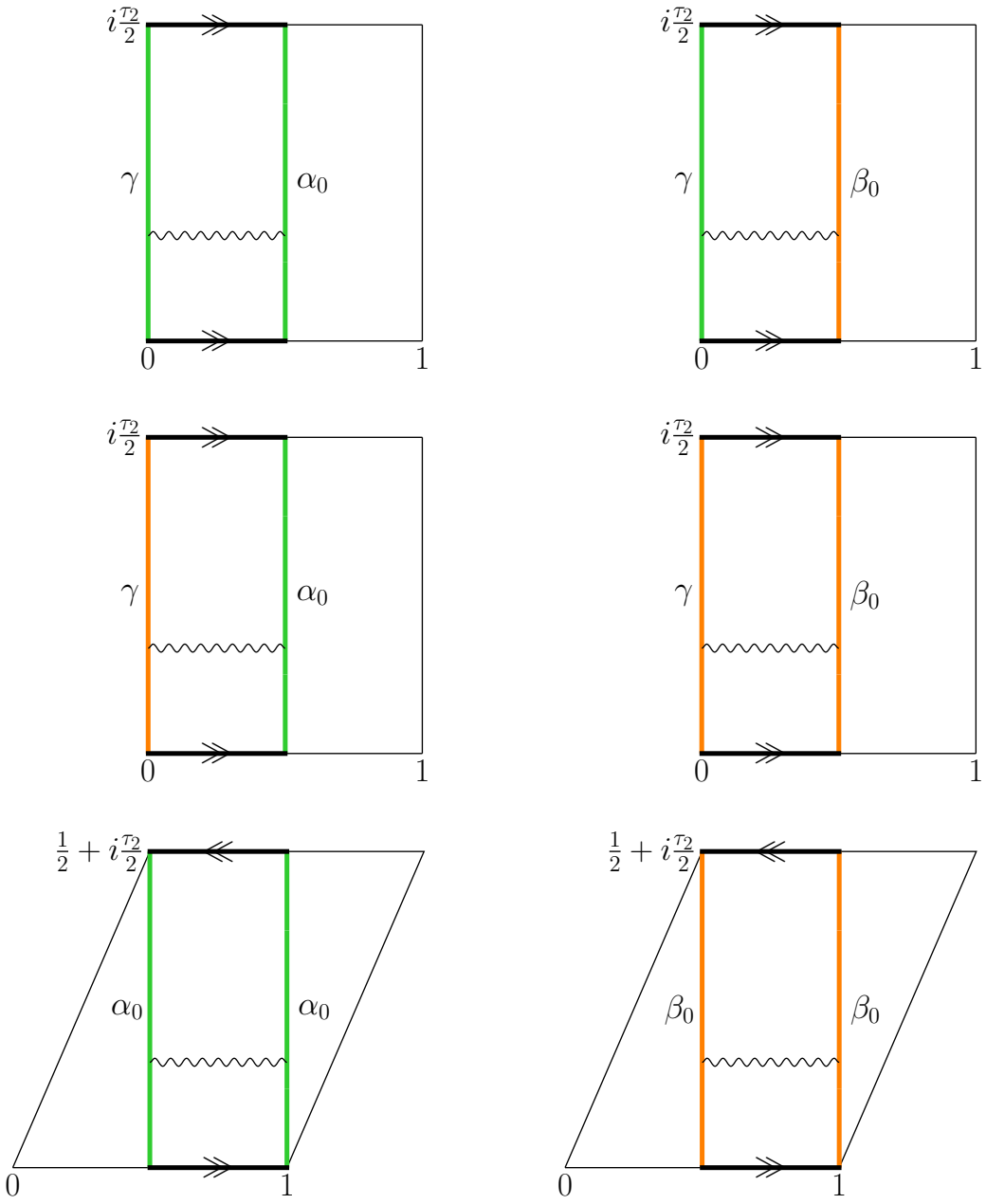

Figure 3.7: Open-string diagrams of Fig. 3.6 in the limit $z_1 \to z_2$.

$$
\begin{aligned}
\text{NN:}\quad & \sum_{i,i';j,j'} \mathrm{tr}(\gamma_{\mathrm{N},1}^{ii'})\mathrm{tr}(\gamma_{\mathrm{N},1}^{jj'\,-1}) \;\longrightarrow\; (\gamma_{\mathrm{N},1}^{i_0i'_0})_{\alpha_0\alpha_0} \sum_{j,j'} \sum_{\gamma=1}^{N_{jj'}} (\gamma_{\mathrm{N},1}^{jj'\,-1})_{\gamma\gamma} = \sum_{j,j'} N_{jj'} \ , \\
& \sum_{i,i';j,j'} \mathrm{tr}(\gamma_{\mathrm{N},g}^{ii'})\mathrm{tr}(\gamma_{\mathrm{N},g}^{jj'\,-1}) \;\longrightarrow\; (\gamma_{\mathrm{N},g}^{i_0i'_0})_{\alpha_0\alpha_0} \sum_{j,j'} \sum_{\gamma=g}^{N_{jj'}} (\gamma_{\mathrm{N},g}^{jj'\,-1})_{\gamma\gamma} = 0 \ , \\
\text{ND:}\quad & \sum_{i,i';j,j'} \mathrm{tr}(\gamma_{\mathrm{N},1}^{ii'})\mathrm{tr}(\gamma_{\mathrm{D},1}^{jj'\,-1}) \;\longrightarrow\; (\gamma_{\mathrm{N},1}^{i_0i'_0})_{\alpha_0\alpha_0} \sum_{j,j'} \sum_{\gamma=1}^{D_{jj'}} (\gamma_{\mathrm{D},1}^{jj'\,-1})_{\gamma\gamma} = \sum_{j,j'} D_{jj'} \ , \\
& \sum_{i,i';j,j'} \mathrm{tr}(\gamma_{\mathrm{N},g}^{ii'})\mathrm{tr}(\gamma_{\mathrm{D},g}^{jj'\,-1}) \;\longrightarrow\; (\gamma_{\mathrm{N},g}^{i_0i'_0})_{\alpha_0\alpha_0} \sum_{j,j'} \sum_{\gamma=1}^{D_{jj'}} (\gamma_{\mathrm{D},g}^{jj'\,-1})_{\gamma\gamma} = 0 \ .
\end{aligned}
\tag{3.2.42}
$$

In the Möbius strip partition function, we extract the following terms, both in the N and D sectors which correspond respectively to the bottom-left and bottom-right Möbius diagrams in Fig. 3.7,

$$\begin{aligned}
\text{N:}\quad & \mathrm{tr}(\gamma^{ii'\,\mathrm{T}}_{\mathrm{N},\Omega}\gamma^{jj'\,-1}_{\mathrm{N},\Omega}) \quad\longrightarrow\quad (\gamma^{i_0i'_0\,\mathrm{T}}_{\mathrm{N},\Omega})_{\alpha_0\alpha_0}(\gamma^{jj'\,-1}_{\mathrm{N},\Omega})_{\alpha_0\alpha_0} = 1\ , \\
& \mathrm{tr}(\gamma^{ii'\,\mathrm{T}}_{\mathrm{N},\Omega g}\gamma^{jj'\,-1}_{\mathrm{N},\Omega g}) \quad\longrightarrow\quad (\gamma^{i_0i'_0\,\mathrm{T}}_{\mathrm{N},\Omega g})_{\alpha_0\alpha_0}(\gamma^{jj'\,-1}_{\mathrm{N},\Omega g})_{\alpha_0\alpha_0} = 0\ , \\
\text{D:}\quad & \mathrm{tr}(\gamma^{ii'\,\mathrm{T}}_{\mathrm{D},\Omega}\gamma^{jj'\,-1}_{\mathrm{D},\Omega}) \quad\longrightarrow\quad (\gamma^{i_0i'_0\,\mathrm{T}}_{\mathrm{D},\Omega})_{\alpha_0\alpha_0}(\gamma^{jj'\,-1}_{\mathrm{D},\Omega})_{\alpha_0\alpha_0} = 0\ , \\
& \mathrm{tr}(\gamma^{ii'\,\mathrm{T}}_{\mathrm{D},\Omega g}\gamma^{jj'\,-1}_{\mathrm{D},\Omega g}) \quad\longrightarrow\quad (\gamma^{i_0i'_0\,\mathrm{T}}_{\mathrm{D},\Omega g})_{\alpha_0\alpha_0}(\gamma^{jj'\,-1}_{\mathrm{D},\Omega g})_{\alpha_0\alpha_0} = 1\ .
\end{aligned} \tag{3.2.43}$$

Notice that in the Möbius, the non-zero contributions come from the action of Ω in the N sector and from the action of Ωg in the D sector. For a lighter main text, the results of the identifications and some details are only presented in Appendix C.2.

The expression (3.2.39) together with formulas (C.2.4) and (C.2.6), up to the sum over α_0 and β_0 that just produces a trace $\mathrm{tr}(\lambda\lambda^{\mathrm{T}})$, is the final result for the computation of the correlation functions defined in (3.2.1). To obtain the true two-point function, one needs to perform a last step, namely to integrate over the moduli of the open-string surfaces *i.e.* on the imaginary parts of the double-cover tori and on the vertex operators insertion points modulo the conformal Killing group [91]. Instead of integrating over all positions z_1 and z_2 and then dividing by the volume of the group, we fix $z_2 \equiv \frac{1}{2}$ and integrate only on the position z_1. For the annulus, z_1 must be on the same boundary as z_2 so we write $z_1 \equiv \frac{1}{2} + iy_1$ and integrate over the imaginary part y_1, from 0 to $\mathrm{Im}\tau^{\mathrm{dc}}$. For the Möbius strip topology, because there is only one boundary, we have either $z_1 = \frac{1}{2} + iy_1$ or $z_1 = iy_1$ and we integrate y_1 from 0 to $\mathrm{Im}\tau^{\mathrm{dc}}$ for both cases. Denoting the integrated internal amplitudes with calligraphic letters, we have

$$\begin{aligned}
\mathcal{A}^{\alpha_0\beta_0}_{\mathrm{int}\mathcal{A}} &= \int_0^{+\infty} \mathrm{d}\,\mathrm{Im}\tau^{\mathrm{dc}} \int_0^{\mathrm{Im}\tau^{\mathrm{dc}}} \mathrm{d}y_1\ A^{\alpha_0\beta_0}_{\mathrm{int}\mathcal{A}}\Big|_{z_1=\frac{1}{2}+iy_1,z_2=\frac{1}{2}}\ , \\
\mathcal{A}^{\alpha_0\beta_0}_{\mathrm{int}\mathcal{M}} &= \int_0^{+\infty} \mathrm{d}\,\mathrm{Im}\tau^{\mathrm{dc}} \int_0^{\mathrm{Im}\tau^{\mathrm{dc}}} \mathrm{d}y_1 \left(A^{\alpha_0\beta_0}_{\mathrm{int}\mathcal{M}}\Big|_{z_1=\frac{1}{2}+iy_1,z_2=\frac{1}{2}} + A^{\alpha_0\beta_0}_{\mathrm{int}\mathcal{M}}\Big|_{z_1=iy_1,z_2=\frac{1}{2}}\right)\ .
\end{aligned} \tag{3.2.44}$$

3.2.4 Field-theory limit and low breaking scale

The full result without approximation for the one-loop two-point function of the ND scalars is quite involved and hard to exploit. In the same spirit as for the other moduli, we want to take a limit where we can throw out all states other than the Kaluza–Klein modes along the Scherk–Schwarz direction by making them supermassive. To throw out the string modes, we consider the field-theory limit $\alpha' \to 0$. In order to implement it, we rescale the Teichmüller parameters of the covering tori of the annulus and Möbius strip like

$$\mathrm{Im}\tau^{\mathrm{dc}} = \frac{\tau_2}{2} \equiv \frac{t}{2\pi\alpha'} \gg 1\,, \qquad \text{where} \qquad t \in (0,+\infty)\ . \tag{3.2.45}$$

In the $\alpha' \to 0$, the non-trivial string oscillators become supermassive and from practical point of view, all Jacobi theta functions can be restricted to their dominant terms up to exponentially suppressed contributions.

For all mass scales other than the supersymmetry-breaking scale to be very large, we assume the radii R_4 and R_I, $I \in \{6,\dots,9\}$ as well as their T-dual counterparts α'/R_I to be small. Defining

dimensionless radii r_4 and r_I like

$$R_4 = r_4\sqrt{\alpha'}\,, \qquad R_I = r_I\sqrt{\alpha'}\,, \qquad \frac{\alpha'}{R_I} = \frac{\sqrt{\alpha'}}{r_I}\,, \tag{3.2.46}$$

we see that both the torus T^4 and T-dual torus $\tilde{T}^4$ become small in the $\alpha' \to 0$ limit. In such a regime, it is convenient to perform a Poisson summation over the indices l_4, $\vec{l}$ and $\vec{\tilde{l}}$ before throwing out exponentially suppressed terms. The dominant contributions come from terms with trivial resummed indices $m_4 = 0$ and $\vec{m} = \vec{n} = \vec{0}$. Moreover in the annulus, only specific fixed points ii' in the sum yield non-exponentially small contributions. One must have $i = i_0$ or $i = j_0$ and i' can be either i'_0 or the opposite fixed point along $\tilde{X}^5$ denoted $\hat{\imath}_0$. Defining $u \equiv |y_1 - y_2|/\mathrm{Im}\tau^{\mathrm{dc}} \in (0,1)$, we obtain

$$\begin{aligned}
A_{\mathrm{int}\mathcal{A}}^{\alpha_0\beta_0} =& -16\mathcal{C}s\sqrt{\pi}\,\lambda_{\alpha_0\beta_0}\lambda^{\mathrm{T}}_{\beta_0\alpha_0}\,\frac{\alpha'^3 R_5}{t^{\frac{7}{2}}}\sum_{l_5} e^{-\frac{\pi^2}{t}R_5^2(2l_5+1)^2}\left(N_{i_0i'_0} - N_{i_0\hat{\imath}'_0} + D_{j_0i'_0} - D_{j_0\hat{\imath}'_0}\right)\\
&\times\left\{2\pi^3 + 2\pi\left[\frac{t(1-u)}{\alpha'} + 2\ln 4 + \cdots\right](C+\hat{C})\right\} + \cdots\,,\\
A_{\mathrm{int}\mathcal{M}}^{\alpha_0\beta_0} =& \;16\mathcal{C}s\sqrt{\pi}\,\lambda_{\alpha_0\beta_0}\lambda^{\mathrm{T}}_{\beta_0\alpha_0}\,\frac{\alpha'^3 R_5}{t^{\frac{7}{2}}}\sum_{l_5} e^{-\frac{\pi^2}{t}R_5^2(2l_5+1)^2}\,(1+1)\\
&\times\left\{2\pi^3 + 2\pi\left[\frac{t(1-u)}{\alpha'} + 2\ln 4 + \cdots\right](C+\hat{C})\right\} + \cdots\,,
\end{aligned} \tag{3.2.47}$$

where the dots represent exponentially small contributions. In the limit, the integrals (3.2.44) over $\mathrm{Im}\tau^{\mathrm{dc}}$ and y_1 translate into integrals over the parameters t and u,

$$\int_0^{+\infty}\mathrm{d}\,\mathrm{Im}\tau^{\mathrm{dc}}\int_0^{\mathrm{Im}\tau^{\mathrm{dc}}}\mathrm{d}y_1 = \frac{1}{(2\pi\alpha')^2}\int_0^{+\infty} t\,\mathrm{d}t\int_0^1\mathrm{d}u_1\,. \tag{3.2.48}$$

The evaluation of C and $\hat{C}$, whose origin lies in the correlators of excited boundary-changing fields, in the limit of small α' is not an easy task. One must find an explicit expression for the function F_1 defined in (3.2.28) in the field-theory limit and compute the integrals over the torus cycles involved in C (see Eq. 3.2.30). The result turns out to yield (the details are presented in Appendix C.3)

$$2\pi\left[\frac{t(1-u)}{\alpha'} + 2\ln 4 + \cdots\right](C+\hat{C}) = -4\pi^3 + \cdots\,. \tag{3.2.49}$$

Note that the evaluations of these limits and everything that has been said so fare is valid for generic values of the insertion points locations, excluding the special values at 0 and $\mathrm{Im}\tau^{\mathrm{dc}}$ for the imaginary parts. In these particular cases, some contributions in the ellipses are actually no more exponentially suppressed. In the strict limit $\alpha' = 0$, the contributions have a zero measure in the integrals over t and u but at small and finite α', they contribute with subdominant terms in powers of α'/R_5^2. The integration thus gives

$$\begin{aligned}
\mathcal{A}_{\mathrm{int}\mathcal{A}}^{\alpha_0\beta_0} + \mathcal{A}_{\mathrm{int}\mathcal{M}}^{\alpha_0\beta_0} =& \frac{4}{\pi}\,\mathcal{C}s\,\lambda_{\alpha_0\beta_0}\lambda^{\mathrm{T}}_{\beta_0\alpha_0}\sum_{l_5}\frac{1}{|2l_5+1|^3}\\
&\times\frac{\alpha'}{R_5^2}\left(N_{i_0i'_0} - N_{i_0\hat{\imath}'_0} - 2 + D_{j_0i'_0} - D_{j_0\hat{\imath}'_0} - 2\right) + \mathcal{O}\left(\frac{\alpha'^2}{R_5^4}\right)\,.
\end{aligned} \tag{3.2.50}$$

To extract the mass $M^2_{\rm ND}$ acquired at one loop by the ND states, we divide by α' and sum over the indices α_0 and β_0. This yields

$$\begin{aligned} M^2_{\rm ND} &= \frac{1}{\alpha'} \sum_{\alpha_0=1}^{N_{i_0 i'_0}} \sum_{\beta_0=1}^{D_{j_0 i'_0}} \left(\mathcal{A}^{\alpha_0\beta_0}_{\text{int}\mathcal{A}} + \mathcal{A}^{\alpha_0\beta_0}_{\text{int}\mathcal{M}} \right) \\ &= \frac{32}{\pi} \mathcal{C}s \sum_{l_5} \frac{1}{|2l_5+1|^3} \operatorname{tr}(\lambda\lambda^{\rm T})\, M^2 \left(n_{i_0 i'_0} - n_{i_0 \hat{i}'_0} - 1 + d_{j_0 i'_0} - d_{j_0 \hat{i}'_0} - 1 \right) + \mathcal{O}\left(\alpha' M^4\right) \ . \end{aligned} \tag{3.2.51}$$

Because $\operatorname{tr}(\lambda\lambda^{\rm T}) > 0$ and because from a field-theory point of view we expect bosons running in the loop to contribute positively and fermions to contribute negatively, we deduce that $\mathcal{C}s > 0$. The sign of the mass squared is thus given by the terms insides the brackets.

3.3 Conclusions

In this second part of the thesis, we explored the one-loop stability of moduli in type I string theory showing an $\mathcal{N} = 2 \to \mathcal{N} = 0$ spontaneous breaking of supersymmetry. Different techniques have been used to treat the variety of moduli present in the model. The NN and DD moduli masses at one loop could be determined equivalently with two methods: An algebraic computation with Dynkin indices and the sole knowledge of the massless spectrum and the representations in which it transforms, and a more direct evaluation by Taylor expanding the effective Coleman–Weinberg potential up to quadratic order. We saw however that the stability conclusions drawn at this stages are not complete since a generalized Green–Schwarz mechanism that gives a tree-level mass to some moduli is to be taken into account and improves the stability. The mechanism also generates a mass to some, and sometimes every, quaternionic scalars of the twisted closed-string sector.

The computation of the Coleman–Weinberg potential demonstrates that up to exponentially suppressed contributions, it does not depend on the NS-NS metric except the breaking scale. In generic models, the scale runs away except in special cases where a Bose/Fermi degeneracy is present at the massless level. In this case, the one-loop potential is exponentially small. To conclude on the independence of the potential on the R-R two-form, we invoked weak/weak duality arguments between type I string theory and heterotic strings.

Eventually, to determine the masses of the moduli lying in the ND sector of the theory, we have computed their two-point correlation functions at one loop. Most importantly, this computation involves boundary-changing fields present in the vertex operators of the ND states that handle the change from Neumann to Dirichlet conditions on the worldsheet. Thanks to a correspondence between such operators and closed-string twist fields that create states in twisted sectors of $\mathbb{Z}_N$ orbifolds, we could make use of the technology developed for them in the literature in our case.

With all the stability conditions in our hands, we numerically searched for fully stable brane configurations showing an exponentially suppressed potential. Among the $\mathcal{O}(10^{12})$ possibilities, only three satisfy all the criteria.

4 Cosmological considerations

The last part of the tryptich concerns the study of the cosmology induced by the one-loop potential created by the Scherk–Schwarz mechanism in a heterotic string context. In a first work, we take seriously the dynamical consequences of the one-loop potential and study its backreaction on the cosmological equations of motion of no-scale models [78–81]. These classical models show a spontaneously broken supersymmetry in flat space with a scale that is a flat direction of the classical potential. Of course, such no-scale structures are expected not to hold once quantum corrections are taken into account except in specific models in type II theories [82–85], open-string theories [86, 87] or in heterotic string models showing a Bose/Fermi degeneracy at the massless level [45–47, 56, 57] to yield so-called "super no-scale models".

In a toy model where the dynamics of a restricted number of moduli is considered, we show the existence of an attractor towards FLRW expanding universes whose asymptotic cosmological behaviour is identical to that of an exact no-scale model. We refer to this asymptotic regime as a "quantum no-scale regime", where flatness of the Minkowski spacetime is not destabilized by the quantum corrections. We will show that the derived cosmologies depend on subsets of initial conditions as well as on the characteristic of the one-loop potential and more precisely on its sign, given by the number of massless bosonic and fermionic degrees of freedom.

In the continuity of this work, we turn on Wilson lines and study their dynamics to determine how the previous conclusions are affected. To do this, we first briefly review the computation of the one-loop potential around backgrounds where no mass scale is present below the supersymmetry-breaking scale and then focus on configurations where we can consistently freeze to zero the vast majority of the Wilson lines and restrict to those along two directions comprising the Scherk–Schwarz one. We will demonstrate that quantum no-scale regimes still exist and that global attractor mechanisms are present under some conditions on the one-loop potential. All the results derived analytically will be confirmed with numerical simulations.

Eventually, in a third work, we develop a new mechanism for the creation of a cold dark-matter relic density, a necessary ingredient to tell a realistic cosmological story. This is done at finite temperature and the mechanism exploits the condensation of a modulus along a cosmological attractor that gives a sudden mass to some dark-matter candidate particle [88, 89].

4.1 Cosmological stability of the no-scale structure: A toy model

We begin with the cosmological study of a toy model where only the dynamics of a restricted number of fields is considered. In a first subsection, we describe the setup of our study and derive the equations of motion of the relevant fields. Then, we comment on the solutions of these equations by exhibiting several behaviours depending on the values of various integration constants. In some

of these cases, we will find and define the "quantum no-scale regimes" where the cosmological evolution converges towards that of a no-scale model.

4.1.1 Setup

We consider the heterotic string in arbitrary dimension $d \geq 3$ compactified on n circles of radii R_i, $i \in \{d, \dots, d+n-1\}$ and on a $(10-d-n)$-dimensional torus. The background is thus

$$\prod_{i=1}^{d+n-1} S^1(R_i) \times T^{10-d-n} \ . \tag{4.1.1}$$

All the n circles are used to perform the Scherk–Schwarz mechanism. This a bit different of what we encountered so far in this thesis but it is just a simple generalization of the use of only one circle. In this case, the supersymmetry-breaking scale denoted $M_{(\sigma)}$ involves all the radii and read[1],

$$M_{(\sigma)} \equiv \frac{M_{\rm s}}{\left(\prod_{i=1}^{d+n-1} R_i\right)^{\frac{1}{n}}} \ . \tag{4.1.2}$$

We use the subscript "(σ)" to refer to the breaking scale in sigma-model frame. Because we will study cosmological equations of motion, we will almost always work in Einstein frame and thus for the sake of simplicity, we prefer to use the notation M without any subscript to describe the breaking scale in this case. As explained in Chapter 1, if we assume the Scherk-Schwarz radii R_i to be large to have a small breaking scale and the volume of the torus T^{10-d-n} to be intermediate in order to ensure the absence of intermediate mass scales below $M_{(\sigma)}$, the one-loop potential in sigma-model frame $\mathcal{V}^{(\sigma)}_{\text{1-loop}}$ takes the generic form (1.3.11)

$$\mathcal{V}^{(\sigma)}_{\text{1-loop}} = \xi_{d,n}(n_{\rm F} - n_{\rm B}) M^d_{(\sigma)} + \mathcal{O}\left((M_{\rm s} M_{(\sigma)})^{\frac{d}{2}} e^{-2\pi c \frac{M_{\rm s}}{M_{(\sigma)}}} \right) \ . \tag{4.1.3}$$

The positive constant $\xi_{d,n}$ is denoted with an additional subscript n because in addition to depend on the dimension d, it depends on the $n-1$ complex structure moduli R_i/R_d, $i \in \{i = d+1, \dots, d+n-1\}$. Decomposing the dilaton field $\phi_{\rm dil}$ into a background value $\langle \phi_{\rm dil} \rangle$ and a fluctuation ϕ, the low-energy effective action S at one loop, restricted to the graviton, the dilaton fluctuation ϕ and the circles radii reads

$$S = \frac{1}{\kappa^2} \int {\rm d}^d x \sqrt{-g} \left[\frac{\mathcal{R}}{2} - \frac{2}{d-2} (\partial\phi)^2 - \frac{1}{2} \sum_{i=d}^{d+n-1} \left(\frac{\partial R_i}{R_i} \right)^2 - \kappa^2 \mathcal{V}_{\text{1-loop}} \right] , \tag{4.1.4}$$

where $\mathcal{R}$ is the Ricci curvature, $\kappa^2 = e^{2\langle \phi_{\rm dil} \rangle}/M_{\rm s}^{d-2}$ is the Einstein constant and the one-loop potential is written in Einstein frame with a dilaton-dependent dressing:

$$\mathcal{V}_{\text{1-loop}} \equiv e^{\frac{2d}{d-2}\phi} \mathcal{V}^{(\sigma)}_{\text{1-loop}} \simeq \xi_{d,n}(n_{\rm F} - n_{\rm B}) M^d \qquad \text{where} \qquad M \equiv e^{\frac{2}{d-2}\phi} M_{(\sigma)} \ . \tag{4.1.5}$$

[1] Note that we assume the complex structures *i.e.* the ratios of the radii to be close to unity so that all radii are equivalent. The expression (4.1.2) for the supersymmetry-breaking scale is then arbitrary but chosen for its explicit invariance under the exchange of the radii.

It is useful to perform some field redefinitions for the action to be expressed in terms of fields that have canonical kinetic terms. To this end, we define Φ, $\Phi_\perp$ and φ_k, $k \in \{1, \dots, n-1\}$ like

$$\begin{aligned} \alpha\Phi &\equiv \frac{2}{d-2}\phi - \frac{1}{n}\sum_{i=d}^{d+n-1} \ln R_i \ , \qquad & \Phi_\perp &\equiv \frac{1}{\sqrt{d-2+n}}\left(2\phi + \sum_{i=d}^{d+n-1} \ln R_i\right) \\ \varphi_k &\equiv \frac{1}{\sqrt{k(k+1)}}\left(k \ln R_{d+k} - \sum_{i=d}^{d+n-1} \ln R_i\right) \ , \text{ for } k \in \{1, \dots, n-1\} \ , \end{aligned} \tag{4.1.6}$$

where α is a constant defined like $\alpha \equiv \sqrt{\frac{1}{d-2} + \frac{1}{n}}$. These definitions ensure that the breaking scale M depends only on the field Φ, called the "no-scale modulus":

$$M = e^{\Phi} M_{\rm s} \ , \tag{4.1.7}$$

and the effective action takes the form

$$S = \frac{1}{\kappa^2}\int \mathrm{d}^d x \, \sqrt{-g}\left[\frac{\mathcal{R}}{2} - \frac{1}{2}(\partial\Phi)^2 - \frac{1}{2}(\partial\Phi_\perp)^2 - \frac{1}{2}\sum_{k=1}^{n-1}(\partial\varphi_k)^2 - \kappa^2 \mathcal{V}_{\text{1-loop}}\right] \ , \tag{4.1.8}$$

where the one-loop potential in terms of the redefined fields is

$$\mathcal{V}_{\text{1-loop}} = \xi_{d,n}(n_{\rm F} - n_{\rm B}) e^{d\alpha\Phi} M_{\rm s}^d \ . \tag{4.1.9}$$

To further simplify the problem, we assume the complex structure moduli φ_k to be constants so that the only dynamical degree of freedom coming from the circles is the volume $\prod_{i=d}^{d+n-1} R_i$ involved in Φ and $\Phi_\perp$. Because we are interested in homogeneous and isotropic cosmological evolutions in flat space, we assume a FLRW metric with lapse function N and scale factor a

$$\mathrm{d}s^2 = -N(x^0)^2(\mathrm{d}x^0)^2 + a(x^0)\left[(\mathrm{d}x^1)^2 + \cdots + (\mathrm{d}x^{d-1})^2\right] \ , \tag{4.1.10}$$

and we suppose the fields Φ and $\Phi_\perp$ to depend on the timelike coordinate x^0 only. In the gauge $N \equiv 1$, $x^0 = t$, the cosmic time. In this case, the two Einstein equations are the ones displayed in (1.4.2) in the case $k = 0$ and where the density and pressure for the scalar fields Φ and $\Phi_\perp$ are simply their kinetic energies $\mathcal{K}$. The cosmological constant Λ is not there and is instead replaced by the one-loop potential. In addition, varying the action with respect to Φ and $\Phi_\perp$ yields two more equations. Overall we have

$$\frac{1}{2}(d-1)(d-2)\,H^2 = \mathcal{K} + \kappa^2 \mathcal{V}_{\text{1-loop}} \ , \qquad \mathcal{K} \equiv \frac{1}{2}\dot\Phi^2 + \frac{1}{2}\dot\Phi_\perp^2 \ , \tag{4.1.11}$$

$$(d-2)\,\dot H + \frac{1}{2}(d-1)(d-2)\,H^2 = -\mathcal{K} + \kappa^2 \mathcal{V}_{\text{1-loop}} \ , \tag{4.1.12}$$

$$\ddot\Phi + (d-1)\,H\,\dot\Phi = -d\alpha\kappa^2 \mathcal{V}_{\text{1-loop}} \ , \tag{4.1.13}$$

$$\ddot\Phi_\perp + (d-1)\,H\,\dot\Phi_\perp = 0 \ . \tag{4.1.14}$$

Let us manipulate these equations a bit. Firstly, we can suitably combine the three first equations (4.1.11), (4.1.12) and (4.1.13) to eliminate both $\mathcal{K}$ and $\mathcal{V}_{\text{1-loop}}$ in the right-hand side. The result is a free-field equation identical to the one satisfied by $\Phi_\perp$,

$$\left(\alpha\dot\Phi + \frac{\alpha^2}{2}\,d(d-2)\,H\right)^{\cdot} + (d-1)\,H\left(\alpha\dot\Phi + \frac{\alpha^2}{2}\,d(d-2)\,H\right) = 0 \ . \tag{4.1.15}$$

Integrating this equation and (4.1.14) yields

$$\dot{\Phi}_\perp = \sqrt{2}\,\frac{c_\perp}{a^{d-1}}\,, \qquad\qquad \alpha\dot{\Phi} + \frac{\alpha^2}{2}\,d(d-2)\,H = \frac{c_\Phi}{a^{d-1}}\,, \tag{4.1.16}$$

where $c_\perp$ and c_Φ are arbitrary integration constants which acquire a minus sign upon time reversal. The one-loop potential can be eliminated from the two first equations (4.1.11) and (4.1.12) to give

$$\frac{1}{2}(d-2)\dot{H} = -\mathcal{K}\,. \tag{4.1.17}$$

The insertion of the solutions (4.1.16) in this equation then gives a differential equation on the scale factor a only. If $c_\Phi \neq 0$, we can define a dimensionless time variable τ like

$$\tau \equiv \frac{2A}{dc_\Phi}\,\dot{a}\,a^{d-2} \quad \text{with} \quad A = \frac{\omega}{4}\,d^2(d-2)\alpha^2 \quad \text{and} \quad \omega = 1 - \frac{4(d-1)}{d^2(d-2)\alpha^2} \in (0,1)\,. \tag{4.1.18}$$

With this definition, the obtained differential equation takes the simple form

$$\tau \mathrm{d}\tau = -A\,\mathcal{P}(\tau)\,\frac{\mathrm{d}a}{a} \quad \text{where} \quad \mathcal{P}(\tau) = \tau^2 - 2\tau + \omega\Big[1 + 2\alpha^2\Big(\frac{c_\perp}{c_\Phi}\Big)^2\Big]\,. \tag{4.1.19}$$

Eventually, the solutions (4.1.16) injected in the Friedmann equation (4.1.11) gives the breaking scale M as a function of a and τ:

$$(n_\mathrm{F} - n_\mathrm{B})\,\xi_n\,\kappa^2 M^d = -\frac{c_\Phi^2}{2\alpha^2\omega}\,\frac{\mathcal{P}(\tau)}{a^{2(d-1)}}\,. \tag{4.1.20}$$

The characteristics of the polynomial $\mathcal{P}(\tau)$ is of crucial importance in the form of the solutions for the scale factor and the breaking scale. It can have zero, one or two real roots depending on the value of $c_\perp/c_\Phi$. Defining the critical value

$$\gamma_\mathrm{c} = \sqrt{\frac{1-\omega}{2\alpha^2\omega}}\,, \tag{4.1.21}$$

we have

$$\begin{aligned}
&\text{Supercritical case:} && \Big|\frac{c_\perp}{c_\Phi}\Big| > \gamma_\mathrm{c}\,, && \text{no real roots,} && \mathcal{P}(\tau) > 0\,,\\
&\text{Subcritical case:} && \Big|\frac{c_\perp}{c_\Phi}\Big| < \gamma_\mathrm{c}\,, && \text{two real roots,} &&\\
&\text{Critical case:} && \Big|\frac{c_\perp}{c_\Phi}\Big| = \gamma_\mathrm{c}\,, && \text{one real root,} && \mathcal{P}(\tau) \geq 0\,.
\end{aligned} \tag{4.1.22}$$

The three next subsections treat the cosmologies arising from these three cases and we will not describe the case when $c_\Phi = 0$ for brevity.

Note that to control the validity of string perturbation theory, it is useful to determine the evolution of the dilaton ϕ which by definition is

$$e^{2d\alpha^2\phi} = \left(\frac{M}{M_\mathrm{s}}\right)^{d\alpha} e^{\frac{d}{n}\sqrt{d-2+n}\,\Phi_\perp}\,, \tag{4.1.23}$$

and is deduced from the evolution of M and also $\Phi_\perp$ whose behaviour is dictated by the equation

$$\frac{\mathrm{d}\Phi_\perp}{\mathrm{d}\tau}\mathcal{P}(\tau) = -\frac{2\sqrt{2}}{d}\frac{c_\perp}{c_\Phi}\,. \tag{4.1.24}$$

It is also useful to relate the parameter τ with the cosmic time t through the differential equation

$$\frac{\mathrm{d}\tau}{\mathrm{d}t} = -\frac{d}{2}\frac{c_\Phi}{a^{d-1}}\mathcal{P}(\tau)\,. \tag{4.1.25}$$

4.1.2 Supercritical case

As we already said, in this case $\mathcal{P}(\tau)$ has no real roots and it is always positive. We deduce from (4.1.20) that the supercritical case can only arise for models with $n_{\mathrm{F}} - n_{\mathrm{B}} < 0$. We also conclude that the classical limit $\kappa^2 \to 0$ is not allowed. This means that in this case, the cosmological evolution of the universe is intrinsically quantum and the one-loop potential can never be neglected. The integration of (4.1.19) gives the following behaviour for the scale factor,

$$a = a_0 \, \frac{e^{-\frac{1}{As}\arctan(\frac{\tau-1}{s})}}{\mathcal{P}(\tau)^{\frac{1}{2A}}} \ , \qquad \text{where} \qquad s \equiv \sqrt{1-\omega}\,\sqrt{\Big(\frac{c_\perp}{\gamma_{\mathrm{c}} c_\Phi}\Big)^2 - 1} \ , \tag{4.1.26}$$

and where a_0 is some positive integration constant. Inserting this expression in (4.1.20) yields

$$M^d = -\frac{c_\Phi^2}{2\alpha^2\omega\kappa^2} \, \frac{a_0^{2A}}{(n_{\mathrm{F}} - n_{\mathrm{B}})\, v_{d,n}} \, \frac{e^{-\frac{2}{s}\arctan(\frac{\tau-1}{s})}}{a^{2(A+d-1)}} \ . \tag{4.1.27}$$

The shape of the scale factor as a function of τ is drawn in Fig. 4.1a. As explained in the legend of the whole figure, the black arrow shows the direction of evolution for $c_\Phi > 0$ and the red arrow indicates a remarkable tangent. In the supercritical case, all the solutions describe an expanding universe that reaches a maximum size before contracting.

In the limits of high τ in absolute value: $\tau \to \epsilon\infty$ with $\epsilon = \pm 1$, the scale factor expressed in terms of the cosmic time t thanks to (4.1.25) is

$$a(t) \sim \left[\frac{d(A+d-1)}{2A} \, a_0^A \, e^{-\frac{\epsilon\pi}{2s}} \, \epsilon c_\Phi (t - t_\epsilon)\right]^{\frac{1}{A+d-1}} \ , \tag{4.1.28}$$

where t_ϵ is an integration constant. If $\epsilon c_\Phi > 0$, it describes a Big Bang at $t \gtrsim t_\epsilon$ and a Big Crunch at $t \lesssim t_\epsilon$ if $\epsilon c_\Phi < 0$. Comparing the magnitude of the energy sources, we have

$$H^2 \sim \#\,\dot\Phi^2 \sim \#\,\kappa^2 \mathcal{V}_{\text{1-loop}} \sim \#\,\frac{a_0^{2A} c_\Phi^2}{a^{2(A+d-1)}} \gg \frac{1}{2}\,\dot\Phi_\perp^2 = \frac{c_\perp^2}{a^{2(d-1)}} \ , \tag{4.1.29}$$

from which we see that the kinetic energy of the no-scale modulus Φ is of the same order as the one-loop potential and it dominates the kinetic energy of the orthogonal combination. When a reaches its maximum value, the potential exactly compensates the kinetic energy.

The validity of perturbation theory is given by the evolution of the dilaton ϕ. In the limits $\tau \to \pm\infty$, Eq. (4.1.24) shows that $\Phi_\perp$ converges to a constant which, when inserted in (4.1.23), gives the behaviour

$$e^{2d\alpha^2\phi} \sim \#|\tau|^{\frac{2}{\omega}} \to +\infty \ , \tag{4.1.30}$$

which shows that the dilaton diverges. In addition, the scale factor is supposed to be large enough for the kinetic energies to be small compared to the string scale. If not, higher derivative terms should be incorporated to the effective action. For these two reasons, we thus conclude that our one-loop analysis is only valid far enough in time from the Big Bang and Big Crunch.

The supercritical case described here realizes a universe entirely driven by quantum effects and which is sentenced to live for only a finite cosmic time. We interpret this situation as an "unstable flat FLRW universe" since quantum effects destroy the classical conclusions on the cosmology. Note that because perturbation theory cannot be trusted until the Big Crunch, a correct analysis there may resolve the singularity.

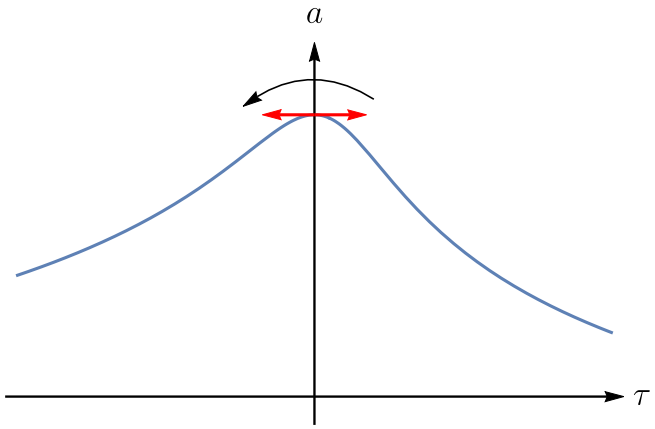

(a) This is the evolution of a in the supercritical case. It reaches a maximum value before contracting and is only allowed for models with $n_{\mathrm{F}} - n_{\mathrm{B}} < 0$.

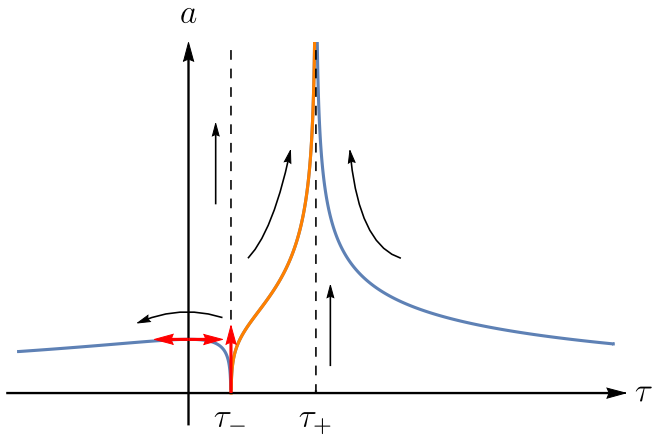

(b) The subcritical case allows for three different branches depending on the sign of the one-loop potential. The two blue branches are possible when $n_{\mathrm{F}} - n_{\mathrm{B}} < 0$ while the orange branch is allowed when $n_{\mathrm{F}} - n_{\mathrm{B}} > 0$.

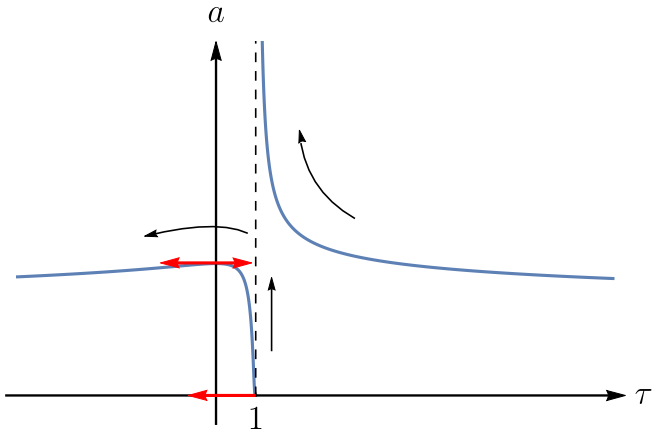

(c) In the critical case, the two roots of the polynomial $\mathcal{P}(\tau)$ are 1 and the two possible branches correspond to $n_{\mathrm{F}} - n_{\mathrm{B}} < 0$. It is not obvious here but the tangent at 1 from the left is horizontal. The plot on the right of this one displays a zoom near $\tau = 1$.

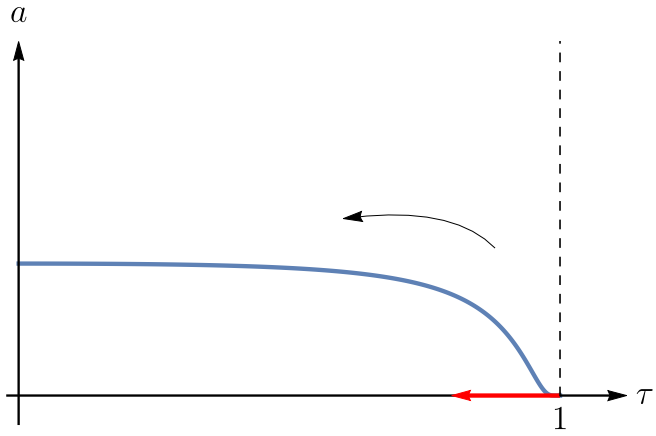

(d) In the critical case, zoom near $\tau = 1$. The tangent is horizontal.

Figure 4.1: Behaviours of the different branches of the scale factor a as a function of τ in the three cases, supercritical, subcritical and critical for $d = 4$ and $n = 1$. Remarkable tangents are drawn with red arrows and the black arrows show the direction of evolution along the various branches for $c_\Phi > 0$.

4.1.3 Subcritical case

The subcritical case turns out to be very rich. Now the polynomial $\mathcal{P}(\tau)$ has two real roots

$$\tau_\pm = 1 \pm r \ , \qquad \text{where} \qquad r \equiv \sqrt{1-\omega}\,\sqrt{1-\left(\frac{c_\perp}{\gamma_{\mathrm{c}} c_\Phi}\right)^2} \ . \tag{4.1.31}$$

All signs for the potential are allowed and the massless content of the models determines the allowed branches for the variations of τ:

$$\begin{aligned} n_{\rm F} - n_{\rm B} < 0 \qquad &\Longrightarrow \qquad \tau < \tau_- \quad \text{or} \quad \tau > \tau_+ \ , \\ n_{\rm F} - n_{\rm B} = 0 \qquad &\Longrightarrow \qquad \tau \equiv \tau_- \quad \text{or} \quad \tau \equiv \tau_+ \ , \\ n_{\rm F} - n_{\rm B} > 0 \qquad &\Longrightarrow \qquad \tau_- < \tau < \tau_+ \ . \end{aligned} \tag{4.1.32}$$

The classical trajectories for which $\kappa^2 \to 0$ correspond to $\tau(t) = \tau_\pm$ and are identical to the quantum evolutions of super no-scale models characterized by $n_{\rm F} = n_{\rm B}$. Let us describe these particular evolutions before studying the generic case with arbitrary $n_{\rm F} - n_{\rm B}$.

Super no-scale case

When $\tau = \tau_\pm$, it is trivial to obtain for the two possibilities

$$a = \left[\frac{d(d-1)}{2A} \, (1 \pm r) \, c_\Phi (t - t_\pm) \right]^{\frac{1}{d-1}} \ , \tag{4.1.33}$$

where $t_\pm$ are integration constants. With $c_\Phi > 0$, it describes a never-ending era of expansion starting with a Big Bang at $t_\pm$. By time reversal, one obtains contracting solutions down to a Big Crunch at $t_\pm$. The breaking scale satisfies

$$M^d = \frac{e^{d\alpha\Phi_\pm}}{a^{2(d-1)+K_\pm}} \, M_{\rm s}^d \ , \qquad \text{where} \qquad K_\pm \equiv \pm \frac{2Ar}{1 \pm r} \ , \tag{4.1.34}$$

and $\Phi_\pm$ are two integration constants. The kinetic energies of Φ and $\Phi_\perp$ are of the same order and dominate the cosmology

$$H^2 \sim \# \dot\Phi_\perp^2 \sim \# \dot\Phi \sim \# \frac{c_\Phi^2}{a^{2(d-1)}} \ . \tag{4.1.35}$$

From the study of the dilaton, the conditions for perturbative consistency in the large scale factor limit along the solution $\tau = \tau_+$ translate into constraints on the initial condition $\frac{c_\perp}{c_\Phi}$ and read

$$-\gamma_{\rm c} < \frac{c_\perp}{c_\Phi} < \gamma_+ \quad \text{when} \quad n < \frac{d^2(d-2)}{4(d-1)} \ , \qquad -\gamma_{\rm c} < \frac{c_\perp}{c_\Phi} < \gamma_{\rm c} \quad \text{when} \quad n > \frac{d^2(d-2)}{4(d-1)} \ , \tag{4.1.36}$$

where

$$\gamma_\pm \equiv \frac{(1-\omega)\sqrt{\frac{2(d-2)}{n}} \pm \alpha \sqrt{2(1-\omega)(d-2)}}{2\alpha(\omega \frac{d-2}{n} + 1)} \ . \tag{4.1.37}$$

In a similar way, the solution $\tau = \tau_-$ is perturbative in the small scale factor limit if and only if

$$\gamma_- < \frac{c_\perp}{c_\Phi} < \gamma_{\rm c} \quad \text{when} \quad n < \frac{d^2(d-2)}{4(d-1)} \ , \qquad \gamma_- < \frac{c_\perp}{c_\Phi} < \gamma_+ \quad \text{when} \quad n > \frac{d^2(d-2)}{4(d-1)} \ . \tag{4.1.38}$$

Generic case

The scale factor takes the form

$$a = \frac{a_0}{|\tau - \tau_-|^{\frac{1}{K_-}} |\tau - \tau_+|^{\frac{1}{K_+}}} \ , \tag{4.1.39}$$

and the breaking scale reads

$$M^d = \frac{M_+^d}{a^{2(d-1)+K_+}} \left|\tau - \tau_-\right|^{\frac{2}{\tau_+}} \quad \text{where} \quad M_+^d = \frac{c_\Phi^2}{2\alpha^2\omega\kappa^2} \frac{a_0^{K_+}}{\left|n_\mathrm{F} - n_\mathrm{B}\right| v_{d,n}} \ . \tag{4.1.40}$$

The evolution of a as a function of τ is shown in Fig. 4.1b. The ranges $\tau < \tau_-$ and $\tau > \tau_+$, where the polynomial $\mathcal{P}(\tau)$ is positive, define two allowed branches (blue trajectories) satisfying $n_\mathrm{F} - n_\mathrm{B} < 0$. The range $\tau_- < \tau < \tau_+$ defines a single allowed trajectory (in orange) corresponding to $n_\mathrm{F} - n_\mathrm{B} > 0$. Like before, the arrows indicate the direction of evolution for a positive constant c_Φ.

Crucially, it is possible in all branches to approach the super no-scale solutions $\tau = \tau_\pm$. In this regime, the scale factor evolution is identical to that found in the super no-scale case (4.1.33) and the breaking scale also behaves like (4.1.34). We conclude that the cosmological evolution of the universe as a whole and the behaviours of the scalar fields approach the super no-scale evolution where $n_\mathrm{F} = n_\mathrm{B}$ *i.e.* for an exponentially suppressed one-loop potential. We thus define these limits $\tau \to \tau_\pm$ as *"quantum no-scale regimes"* since the classical no-scale structure is not spoiled by the quantum potential. The magnitudes of the kinetic energies are the same as in (4.1.35) and here they dominate the one-loop potential:

$$H^2 \sim \#\dot{\Phi}_\perp^2 \sim \#\dot{\Phi} \sim \#\frac{c_\Phi^2}{a^{2(d-1)}} \gg \kappa^2 \left|\mathcal{V}_{\text{1-loop}}\right| \sim \#\frac{a_0^{K_\pm} c_\Phi^2}{a^{2(d-1)+K_\pm}} \ . \tag{4.1.41}$$

Note that the left branch describes an evolution similar to the supercritical case with a scale factor that reaches a maximum before contracting and an energy content similar to (4.1.29), intrinsically quantum.

The conditions for perturbative consistency in the quantum no-scale regimes are the same as in the super no-scale case (4.1.36) and (4.1.38). In particular, the branch with $n_\mathrm{F} - n_\mathrm{B} > 0$ (the orange branch on Fig. 4.1b), is all the way perturbative from τ_- to τ_+ regardless of d and n if $\gamma_- < \frac{c_\perp}{c_\Phi} < \gamma_+$. The one-loop potential is dominated everywhere except near $\tau = 1$ where it induces the transition from a quantum no-scale regime to the other. Finally, as before, the behaviours at $\tau \to \pm\infty$ can only be trusted up to a certain time.

The subcritical case is also interesting from the point of view of the dynamics of the breaking scale. If we assume $c_\Phi > 0$, three distinct behaviours arise:

- If $\sqrt{\omega}\gamma_\mathrm{c} < |c_\perp/c_\Phi| < \gamma_\mathrm{c}$, the evolution of the breaking scale as a function of τ is displayed in Fig. 4.2a in the three branches (the two blue ones allowed when $n_\mathrm{F} - n_\mathrm{B} < 0$ and the orange one when $n_\mathrm{F} - n_\mathrm{B} > 0$). The black arrows show the directions of evolution. Along the branch on the right where $\tau > \tau_+$, we saw that the universe is attracted to the ever-expanding quantum no-scale regime but the figure shows that M decreases *i.e.* it forever climbs its negative potential [183]. In the other branches, the situation is more natural at late times since M is either attracted to large values when the potential is negative after a phase of decreasing (along the blue branch on the left) or drops along its positive potential along the orange branch.

- If $|c_\perp/c_\Phi| < \sqrt{\omega}\gamma_\mathrm{c}$, the evolution of M is displayed in Fig. 4.2b. Along the branch $\tau > \tau_+$ the same unnatural behaviour occurs and M climbs its negative potential while for $\tau < \tau_-$, M drops along its negative potential and reaches large values. Along the orange branch $\tau_- < \tau < \tau_+$, the breaking scale starts climbing its positive potential and then drops. The turning point is

at $\tau = \omega$ and there we have $\dot{\Phi} = 0$ and $\mathcal{V}_{\text{1-loop}} > 0$ which allows an acceleration phase for the scale factor [184–205] but which turns out not to yield a big enough e-folding number.

- If $|c_\perp/c_\Phi| = \sqrt{\omega}\gamma_c$, then the situation is the same as in the previous case with $\omega = \tau_-$. The conclusions are easily found from the evolution of M shown in Fig. 4.2c.

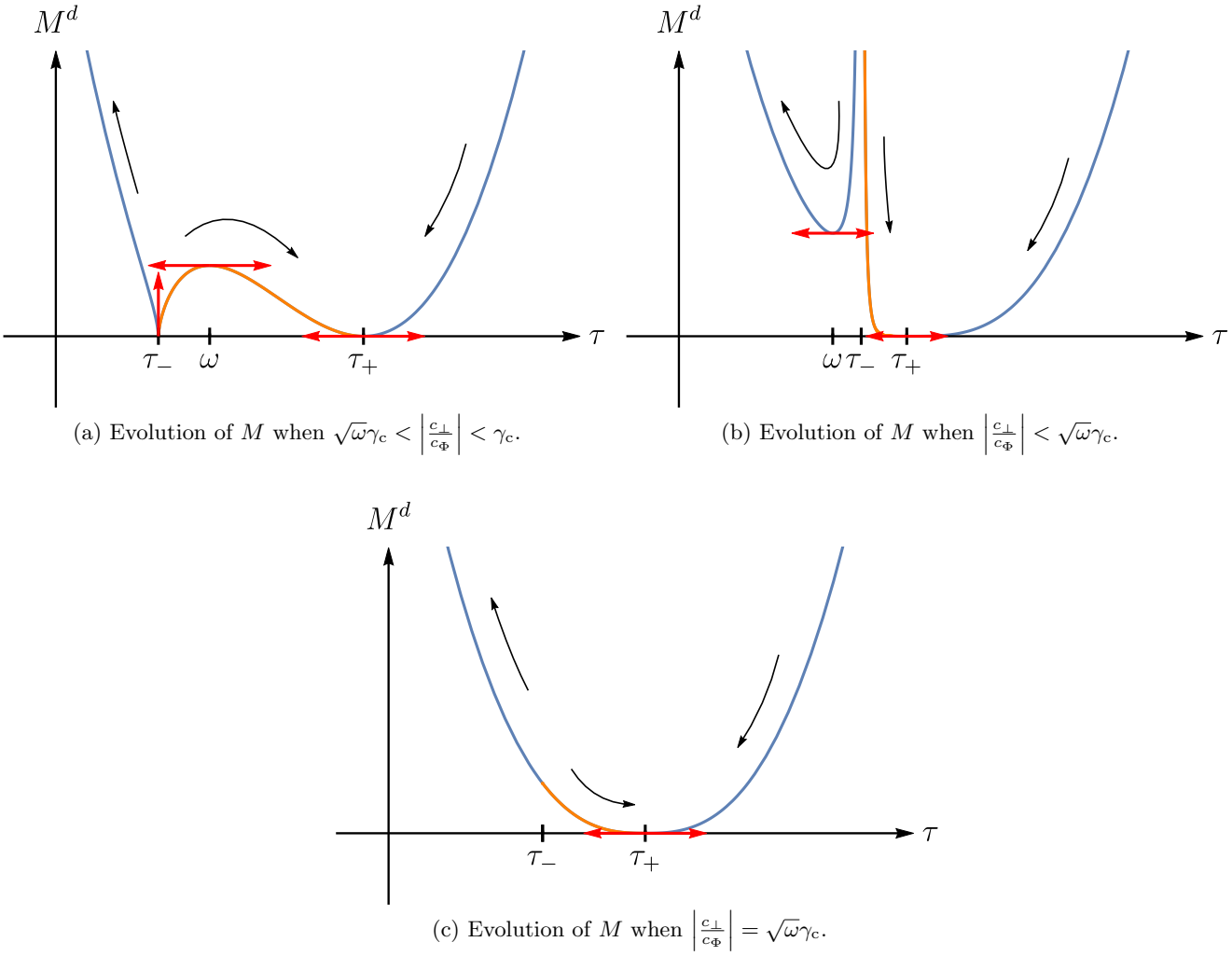

(a) Evolution of M when $\sqrt{\omega}\gamma_c < \left|\frac{c_\perp}{c_\Phi}\right| < \gamma_c$.

(b) Evolution of M when $\left|\frac{c_\perp}{c_\Phi}\right| < \sqrt{\omega}\gamma_c$.

(c) Evolution of M when $\left|\frac{c_\perp}{c_\Phi}\right| = \sqrt{\omega}\gamma_c$.

Figure 4.2: Evolution of M in the three allowed branches in the subcritical case with $c_\phi > 0$ for three different ranges of the initial condition $\left|\frac{c_\perp}{c_\Phi}\right|$. The directions of evolution are indicated by the black arrows and the red arrows show remarkable tangents.

4.1.4 Critical case

The evolution of the scale factor in the critical case is displayed in Fig. 4.1c and the conclusions on the behaviours of the cosmological evolutions are similar to those of the subcritical case. We thus do not say more on this case. Note that the zoom near $\tau = 1$ in Fig. 4.1d shows an horizontal tangent for the branch $\tau < 1$. However, in terms of the cosmic time t, the tangent is vertical as in a classical Big Bang/Big Crunch.

4.1.5 Summary

Let us summarize the different cosmologies taking place in our setup *i.e.* in heterotic no-scale models compactified down to arbitrary $d \geq 3$ dimensions on tori where the one-loop potential induced by a Scherk–Schwarz mechanism backreacts on the classical background. We have reduced the analysis to a restricted number of fields: The scale factor $a(t)$ of an homogeneous and isotropic FLRW universe, the no-scale modulus $\Phi(t)$ driving the breaking scale and the free field $\Phi_\perp(t)$. We can parametrize the space of solutions by the couple $(\frac{c_\perp}{c_\Phi}, \tau_i)$ where $c_\perp$ and c_Φ are integration constants and τ_i is the initial value of the parameter τ, a dimensionless time variable defined in (4.1.18). Note that the interpretation as a time variable is correct for all trajectories except those with constant $\tau = \tau_\pm$ along which the cosmic time t keeps flowing. The partition of the $\mathbb{R}^2$-plane $(\frac{c_\perp}{c_\Phi}, \tau_i)$ depicted in Fig. 4.3 shows five distinct regions in which the cosmologies have specific behaviours.

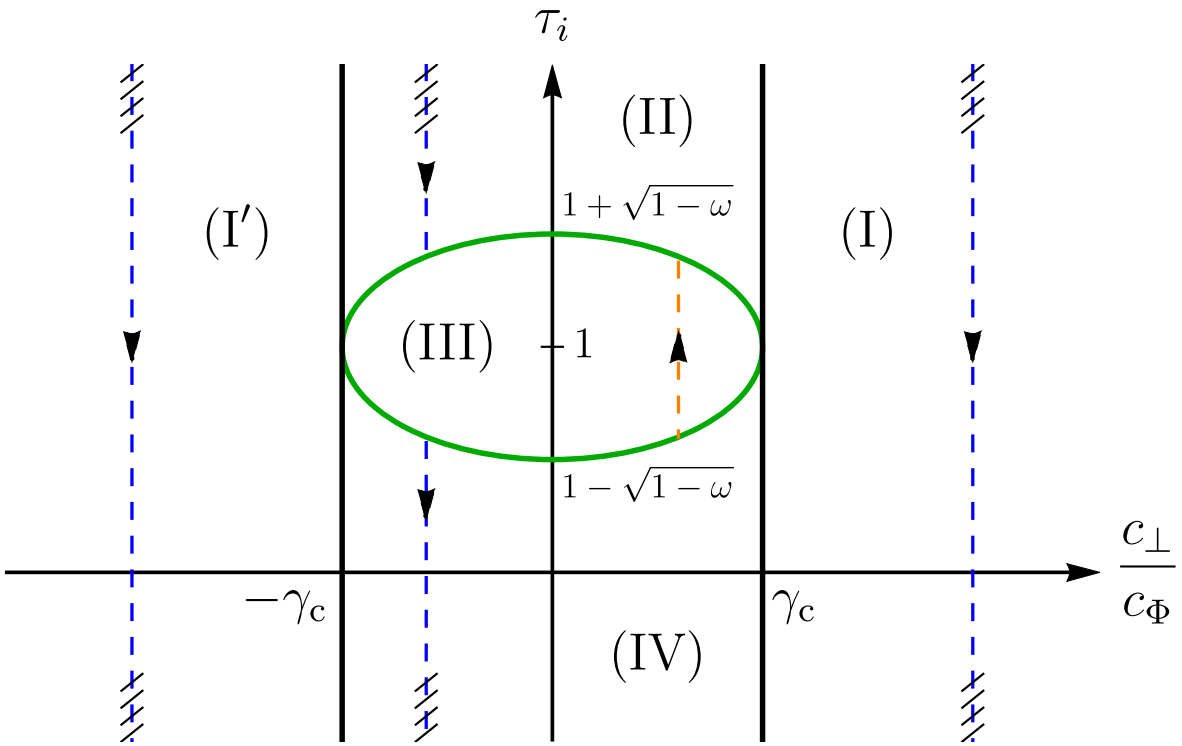

Figure 4.3: Partition of the $\mathbb{R}^2$-plane $(c_\perp/c_\Phi, \tau_i)$ of cosmological solutions. The supercritical regions satisfy $|c_\perp/c_\Phi| > \gamma_c$ and $n_F - n_B < 0$. The subcritical region, $|c_\perp/c_\Phi| < \gamma_c$, contains an ellipse $\tau_- < \tau_i < \tau_+$, the interior (exterior) of it corresponding to models satisfying $n_F - n_B > 0$ (< 0). The trajectories $\tau(t)$ for increasing cosmic time t are represented by dashed lines, for $c_\Phi > 0$. The hatches indicate where perturbative consistency is expected to break down.

Regions (I) and (I′) correspond to the supercritical case where $|c_\perp/c_\Phi|$ is bigger than a critical value γ_c. In these regions, the dashed-blue trajectories whose directions of evolution for $c_\Phi > 0$ are indicated with a black arrow describe intrinsically quantum universes. The dynamics is always dominated both by the kinetic energy of the no-scale modulus and by the one-loop potential that can never be neglected. In this situation, the universe starts with a Big Bang, grows, reaches a maximal size and ends with a Big Crunch. However, the singular behaviours at too early or too late times cannot be trusted since perturbative consistency breaks down. This is illustrated with

hatches on the figure.

Inside the subcritical area in which $|c_\perp/c_\Phi| < \gamma_c$, the interior of the green ellipse corresponds to a parameter τ confined between the particular values τ_- (bottom of the ellipse) and τ_+ (top of the ellipse) and thus to the orange trajectories of Figs. 4.1b and 4.2. There, the potential is positive ($n_F - n_B > 0$) and for $c_\Phi > 0$, the dashed-orange trajectory goes from a Big Crunch at τ_- to an ever-expanding era at τ_+. Asymptotically near these values, the dynamics is identical to that of a super no-scale model where the one-loop potential vanishes up to exponentially suppressed contributions. The classical no-scale structure is preserved in the sense that quantum corrections do not disturb the asymptotic cosmological evolution and we thus define these cosmologies as "quantum no-scale regimes". In these regimes, the dynamics is driven by the kinetic energies of Φ and $\Phi_\perp$, which dominate the one-loop potential. Moreover, depending on their locations in region (III), such orange trajectories in Fig. 4.3 can easily be consistent with perturbation theory. The endless expansion and flatness of the universe near τ_+ is not destabilized by quantum corrections.

In region (II) outside the ellipse and thus with a negative potential, the dashed-blue trajectory comes from a Big Crunch at $\tau \to +\infty$ (where pertubation theory cannot be trusted) and ends in an ever-expanding quantum no-scale regime near τ_+ where perturbative consistency can be achieved. In region (IV), the potential is also negative and the cosmology is that of Big Bang in a quantum no-scale regime near τ_- and a Big Crunch at $\tau \to -\infty$, where the universe is intrinsically quantum like in regions (I) and (I′) and whose behaviour cannot be trusted at too late times.

4.2 Cosmological stability of the no-scale structure: Influence of deformations

The goal of this subsection is to study the influence of the dynamics of marginal deformations on the emergence of quantum no-scale regimes. We will see new effects occurring due to the presence of non-trivial deformations and the existence of enhanced symmetry points. The first subsection will briefly review how more involved Scherk–Schwarz mechanisms can be implemented to yield richer breaking patterns in the presence of deformations and the generic form of the one-loop potential in the regime of low supersymmetry-breaking scale in such context, already encountered in (3.1.28), will be presented. Next, we will consider a setup with a specific background and a restricted number of small deformations to see if quantum no-scale regimes are still allowed in the presence of the deformations. We will end the section with a discussion on the existence of global attractors by relaxing the smallness assumption of the deformations.

4.2.1 Arbitrary deformations and one-loop potential

This subsection will not be exhaustive at all about the deformed partition function of the heterotic string and the derivation of the one-loop potential in the low breaking scale limit. Lots of details can be found in the self-contained appendix of [44]. The most general modular invariant one-loop amplitude in d dimensions, for arbitrary internal metric and antisymmetric tensors G and B and deformations $\vec{Y}$ (more details on them soon) takes the form [18–22, 44, 56, 57, 206]

$$\mathcal{T} = \int_{\mathcal{F}} \frac{\mathrm{d}^2\tau}{\tau_2^{\frac{d}{2}+1}} \frac{1}{\eta^{12}\bar{\eta}^{24}} \frac{1}{|\Xi|} \sum_{\vec{a},\vec{b}\in\Xi} \mathcal{C}\left[\begin{smallmatrix}\vec{a}\\ \vec{b}\end{smallmatrix}\right] \mathcal{Z}[\vec{a},\vec{b},G,B,\vec{Y}] \ , \tag{4.2.1}$$

where Ξ is the set of spin structures $\vec{a} \equiv (\vec{a}^{\,\mathrm{L}}, \vec{a}^{\,\mathrm{R}})$ and $\vec{b} \equiv (\vec{b}^{\,\mathrm{L}}, \vec{b}^{\,\mathrm{R}})$ of the 10 left-moving complex fermions and the 16 right-moving ones along the two cycles of the torus. The factor $\mathcal{C}\left[\begin{smallmatrix}\vec{a}\\ \vec{b}\end{smallmatrix}\right]$ is a phase such that the partition function at $\vec{Y} = \vec{0}$ is modular invariant and $\mathcal{Z}$ is

$$\mathcal{Z}[\vec{a},\vec{b},G,B,\vec{Y}] = \frac{\sqrt{\det G}}{\tau_2^{\frac{10-d}{2}}} \sum_{\substack{\tilde{m}_d,\dots,\tilde{m}_9\\ n_d,\dots,n_9}} e^{-\frac{\pi}{\tau_2}(\tilde{m}_I+n_I\bar{\tau})(G+B)_{IJ}(\tilde{m}_I+n_I\tau)} \times e^{i\pi n_I \vec{Y}_I\cdot(\vec{b}-\tilde{m}_J\vec{Y}_J)} \prod_{\mathcal{A}=1}^{4} \theta\left[\begin{smallmatrix} a^L_{\mathcal{A}}-2n_I Y^L_{I\mathcal{A}} \\ b^L_{\mathcal{A}}-2\tilde{m}_I Y^L_{I\mathcal{A}}\end{smallmatrix}\right](\tau) \prod_{\mathcal{J}=10}^{25} \bar{\theta}\left[\begin{smallmatrix} a^R_{\mathcal{J}}-2n_I Y^R_{I\mathcal{J}} \\ b^R_{\mathcal{J}}-2\tilde{m}_I Y^R_{I\mathcal{J}}\end{smallmatrix}\right](\bar{\tau}) \ . \quad (4.2.2)$$

The sum in the first line is the contribution of the bosonic zero modes on the internal torus T^{10-d} with tensors G_{IJ} and B_{IJ}, $I \in \{d,\dots,9\}$ in Lagrangian form. In the second line, the holomorphic Jacobi theta functions describe the left-moving fermions with spin structures $a^{\mathrm{L}}_1 = \cdots = a^{\mathrm{L}}_4$ and $b^{\mathrm{L}}_1 = \cdots = b^{\mathrm{L}}_4$ for a maximally supersymmetric background. The antiholomorphic Jacobi functions describe the right-moving fermions with arbitrary spin structures $a^{\mathrm{R}}_{\mathcal{J}}$ and $b^{\mathrm{R}}_{\mathcal{J}}$, $\mathcal{J} \in \{10,\dots,25\}$ before deformation. The $Y^{\mathrm{L}}_{I\mathcal{A}} \in \mathbb{Z}$, $I \in \{d,\dots,9\}$, $\mathcal{A} \in \{1,\dots,4\}$ are deformations of the left superconformal theory. They take integer values for the holomorphic supercurrent to be conserved. The $Y^{\mathrm{R}}_{I\mathcal{J}}$, $I \in \{d,\dots,9\}$, $\mathcal{J} \in \{10,\dots,25\}$ are arbitrary deformations of the right conformal theory, interpreted as Wilson lines of a rank 16 gauge group along the internal right torus. We define $\vec{Y}_I \equiv (\vec{Y}^{\mathrm{L}}_I, \vec{Y}^{\mathrm{R}}_I) \equiv (Y_{I\Upsilon}, \Upsilon \in \{d,\dots,25\})$ that can be interpreted as Wilson lines along T^{10-d} of a rank 16 gauge group. Eventually, the phase in the second line ensures that the modular transformations of $\mathcal{Z}$ are independent of the deformations so that if the partition function is modular invariant at zero deformations, it remains consistent when they are turned on. Note that the scalar product involved in the phase dresses the left part with a plus sign and the right part with a minus sign.

These expressions are the most general formulas of which the supersymmetric $\mathrm{Spin}(32)/\mathbb{Z}_2$ and $\mathrm{E}_8 \times \mathrm{E}_8$ heterotic string theories as well as Scherk–Schwarz realizations are just particular cases. Let us see precisely how to recover: (1) The undeformed heterotic string compactified on T^{10-d} (2) The simplest Scherk–Schwarz realization along the single direction X^d (3) A more involved pattern involving large discrete deformations as a background which yield an $n_{\mathrm{F}} - n_{\mathrm{B}}$ of arbitrary sign depending on the location in moduli space and eventually (4) How a discrete background for the antisymmetric tensor can change the nature of the states that become massless at enhancement points.

- The compactified $\mathrm{Spin}(32)/\mathbb{Z}_2$ heterotic string corresponds to

$$\begin{aligned} &\Xi = \left\{(4,16)\text{-tuples } (a,\dots,a;\gamma,\dots,\gamma)\,, \quad \text{where} \quad a,\gamma \in \mathbb{Z}_2\right\}\,,\\ &\mathcal{C}\left[\begin{smallmatrix}a;\gamma\\ b;\delta\end{smallmatrix}\right] = (-1)^{a+b+ab}\,,\\ &\vec{Y}^{\mathrm{L}}_I = \vec{0}\,,\ \vec{Y}^{\mathrm{R}}_I = \vec{0}\,, \quad I \in \{d,\dots,9\}\,. \end{aligned} \quad (4.2.3)$$

  The Y's are all set to zero and the phase $\mathcal{C}$ is the standard one. Going to the Hamiltonian form by Poisson summation over the $\tilde{m}_I$, $I \in \{d,\dots,9\}$, the light spectrum is found to be a supergravity multiplet in d dimensions coupled to a vector multiplet in the adjoint representation of $\mathcal{G}_{10-d} \times \mathrm{Spin}(32)/\mathbb{Z}_2$ where $\mathcal{G}_{10-d}$ is a rank $10-d$ group arising from compactification (this gauge factor can have symmetry enhancements for special values of G as evoked in Chapter 1). To obtain the group $\mathrm{E}_8 \times \mathrm{E}_8$ instead of $\mathrm{Spin}(32)/\mathbb{Z}_2$, one needs to consider

$$\Xi = \left\{(4,8+8)\text{-tuples } (a,\dots,a;\gamma,\dots,\gamma,\gamma',\dots,\gamma')\,, \quad \text{where} \quad a,\gamma,\gamma' \in \mathbb{Z}_2\right\}\,. \quad (4.2.4)$$

- From these undeformed theories, the simplest Scherk–Schwarz mechanism implemented along direction X^d amounts to take $Y^{\mathrm{L}}_{I\mathcal{A}} = \delta_{Id}\delta_{\mathcal{A}1}$, $I \in \{d,\dots,9\}$, $\mathcal{A} \in \{1,\dots,4\}$. The phase in the second line of (4.2.2) combined with the shift of argument of the holomorphic theta functions gives an overall modular invariant phase $(-1)^{\tilde{m}_d a + n_d b + \tilde{m}_d n_d}$. Because it depends on a, which determines the NS or R boundary conditions of the fermions, it introduces a $\frac{1}{2}$ shift to the Hamiltonian momentum number m_d only to the fermions which yields a theory with only bosonic light states. The gauge group $\mathcal{G}_{10-d}$ is broken to $\mathrm{U}(1) \times \mathcal{G}_{9-d}$ in this case.

- Something very interesting occurs if in addition one considers large discrete deformations $Y^{\mathrm{R}}_{I\mathcal{J}} = \delta_{Id}\eta^{\mathrm{R}}_{\mathcal{J}}$, $I \in \{d,\dots,9\}$, $\mathcal{J} \in \{10,\dots,25\}$ with $\vec{\eta}^{\mathrm{R}} \cdot \vec{a}^{\mathrm{R}} \equiv \eta \in \mathbb{Z}$. Now the bosonic or fermionic nature of the light states depends on η. If η is even, the fermions acquire the mass shift as usual whereas for η odd, it is the bosons that get the mass shift and the fermions that remain light. Starting from the $\mathrm{E}_8 \times \mathrm{E}_8$ theory, a suitable choice for $\vec{\eta}^{\mathrm{R}}$ breaks the group to $\mathrm{SO}(16) \times \mathrm{SO}(16)$ with massless bosons in the adjoint representation and massless fermions in the spinorial one. If we call d_{en} the number of roots of the enhanced U(1)'s in $\mathcal{G}_{9-d}$, we obtain

$$n_{\mathrm{B}} = 8 \times (8 + 120 + 120 + d_{\mathrm{en}}) \qquad \text{and} \qquad n_{\mathrm{F}} = 8 \times (128 + 128)\ . \tag{4.2.5}$$

  Simply by considering SU(2) enhancements, depending on how many are present in the group $\mathcal{G}_{9-d}$, we see that $n_{\mathrm{F}} - n_{\mathrm{B}}$ can be negative, vanishing or positive.

- Finally, when a Scherk–Schwarz mechanism is implemented along X^d, the generalized momentum P_d along that direction becomes

$$P_d \equiv m_d + \frac{1}{2}\left[F + 2(G+B)_{dj}n_j\right]\ . \tag{4.2.6}$$

  At enhancement points in moduli space where vector multiplets with windings $n_j = \pm 1$, $j \in \{d+1,\dots,9\}$ become massless in a supersymmetric theory, we see that for an even background integer value for $2(G+B)_{dj}n_j$, the bosonic part is indeed massless while the fermionic one get a mass. In this case, the gauge symmetry is still enhanced like in the supersymmetric case. However, an odd background integer value for $2(G+B)_{dj}n_j$ produces a mass shift for the bosonic part of the multiplet and keeps the fermionic part massless. In this case the gauge symmetry is not enhanced.

Defining small deformations $y_{I\Upsilon}$, $I \in \{d,\dots,9\}$, $\Upsilon \in \{d,\dots,25\}$ around a Scherk–Schwarz background (using only direction X^d) with an enhanced massless spectrum where n_{F} and n_{B} light fermions and bosons are present and where the supersymmetry-breaking scale in sigma-model frame $M_{(\sigma)} = \sqrt{G^{dd}}M_{\mathrm{s}}$ is the lowest scale, the one-loop potential $\mathcal{V}^{(\sigma)}_{\text{1-loop}}$ in the regime of low breaking scale and up to quadratic order in the $y_{I\Upsilon}$'s is [44, 56, 57]

$$\begin{aligned}\mathcal{V}^{(\sigma)}_{\text{1-loop}} = {}& \xi_d(n_{\mathrm{F}} - n_{\mathrm{B}})M^d_{(\sigma)} + \frac{\xi_{d-2}}{2\pi}\sum_{\Upsilon=d+1}^{25} c_\Upsilon \left[(d-1)y^2_{d\Upsilon} + \frac{1}{G^{dd}}\sum_{i=d+1}^{9} y^2_{i\Upsilon}\right] M^d_{(\sigma)} + \cdots \\ & + \mathcal{O}\left((cM_{\mathrm{s}}M_{(\sigma)})^{\frac{d}{2}} e^{-2\pi c M_{\mathrm{s}}/M_{(\sigma)}}\right)\ .\end{aligned} \tag{4.2.7}$$

The constant c is of order one and ξ_d, already encountered several times and never given explicitly, is

$$\xi_d = \frac{\Gamma\left(\frac{d+1}{2}\right)\zeta(d+1)}{2^{d-1}\pi^{\frac{3d+1}{2}}}\left(1 - 2^{-(d+1)}\right)\ . \tag{4.2.8}$$

The coefficient c_Υ determines whether the Wilson lines $y_{i\Upsilon}$ are massive, massless or tachyonic at one loop[2] and is related to the Dynkin indices in which the massless background spectrum transforms, as mentioned around Eq. (3.1.28).

4.2.2 Dynamics with a restricted number of small deformations

Setup and objectives

In the sequel, we study the cosmology of models with the specific following deformations along directions d and $d+1$:

$$(G+B)_{Ij} = \begin{pmatrix} R_d^2/\alpha' & \frac{\epsilon}{2}+\sqrt{2}y_{d,d+1} \\ -\frac{\epsilon}{2}+\sqrt{2}y_{d+1,d} & 1+\sqrt{2}y_{d+1,d+1} \end{pmatrix}, \qquad I,j \in \{d,d+1\} \ . \tag{4.2.9}$$

The internal metric and antisymmetric tensors along the remaining $8-d$ internal directions are arbitrary and we freeze for simplicity all other deformations

$$y_{I,d+2} = \cdots = y_{I,25} = 0 \ , \ I \in \{d,\ldots,9\} \quad \text{and} \quad y_{Id} = y_{I,d+1} = 0 \ , \ I \in \{d+2,\ldots,9\} \ . \tag{4.2.10}$$

As mentioned in the previous subsection, the parity of ϵ determines if the additional massless states arising at $R_{d+1,d+1} = \sqrt{\alpha'}$ are bosons with an enhancement from U(1) to SU(2) or fermions without enhancement. In Eq. (4.2.7) applied to this case, the coefficient c_Υ is then accordingly either $+16$ for ϵ even and -16 for ϵ odd.

In this subsection, we only want to show that quantum no-scale regimes exist in the presence of the deformations $y_{d,d+1}$, $y_{d+1,d}$ and $y_{d+1,d+1}$ so that it is enough to assume them to be small, $|y_{d,d+1}|, |y_{d+1,d}| \ll 1$ and $|y_{d+1,d+1}| \ll \sqrt{G^{dd}} \ll 1$. Denoting $n_{\rm F}$ and $n_{\rm B}$ the number of background massless fermionic and bosonic degrees of freedom without counting those arising at $R_{d+1,d+1} = \sqrt{\alpha'}$, we have from (4.2.7),

$$\mathcal{V}^{(\sigma)}_{\text{1-loop}} = \xi_d(n_{\rm F} - n_{\rm B} + (-1)^\epsilon 8\times 2) M^d_{(\sigma)} + (-1)^\epsilon \frac{8}{\pi}\xi_{d-2}\left((d-1)y^2_{d,d+1} + \frac{y^2_{d+1,d+1}}{G^{dd}}\right) M^d_{(\sigma)} + \cdots \ . \tag{4.2.11}$$

Up to quadratic order in the y's, the one-loop effective action we consider takes the form

$$\begin{aligned} S = \frac{1}{\kappa^2}\int \mathrm{d}^d x\sqrt{-g}\Big[\frac{\mathcal{R}}{2} - \frac{1}{2}(\partial\Phi)^2 - \frac{1}{2}(\partial\Phi_\perp)^2 - \frac{1}{4}(\partial y_{d+1,d+1})^2 \\ - \frac{G^{dd}}{4}(\partial y_{d,d+1})^2 - \frac{G^{dd}}{4}(\partial y_{d+1,d})^2 + \cdots - \kappa^2 \mathcal{V}_{\text{1-loop}}\Big] \ , \end{aligned} \tag{4.2.12}$$

where $\mathcal{V}_{\text{1-loop}} \equiv e^{d\alpha\Phi}\mathcal{V}^{(\sigma)}_{\text{1-loop}}$. Like before, we assume a FLRW metric (4.1.10) and we assume the fields to depend only on x^0. The equations of motion for the lapse N and scale factor a have the same forms as before (Eqs. (4.1.11) and (4.1.12)), with the new expression for $\mathcal{V}_{\text{1-loop}}$ and a kinetic energy K given by

$$\mathcal{K} = \frac{1}{2}\dot\Phi^2 + \frac{1}{2}\dot\Phi_\perp^2 + \frac{G^{dd}}{4}\dot y^2_{d,d+1} + \frac{G^{dd}}{4}\dot y^2_{d+1,d} + \frac{1}{4}\dot y^2_{d+1,d+1} \ . \tag{4.2.13}$$

We are looking for quantum no-scale regimes and thus for solutions where the scale factor diverges at $t \to +\infty$ or goes to zero at $t \to t_-$ and where the effective potential is dominated by H^2. Defining

[2] If we forget the runaway of $M_{(\sigma)}$.

constants $\kappa_\pm$ such that $\pm\kappa_\pm > 0$ that are to be determined by consistency, we look for solutions

$$a(t) \underset{t\to+\infty}{\longrightarrow} +\infty \qquad \text{or} \qquad a(t) \underset{t\to t_-}{\longrightarrow} 0 \qquad \text{where} \qquad \kappa^2 M_{\rm s}^d e^{d\alpha\Phi} = \mathcal{O}\left(\frac{H^2}{a^{\kappa_\pm}}\right) . \tag{4.2.14}$$

Resolution of the equations of motion

The above assumptions to find a quantum no-scale regime imply a behaviour for the scale factor like $a \sim t^{\frac{1}{d-1}}$ or $a \sim |t-t_-|^{\frac{1}{d-1}}$. The sign $(-1)^\epsilon$ inside the potential before the quadratic terms in y's turns out to be irrelevant in the equations of motion for $y_{d+1,d}$ and $y_{d,d+1}$ so that

$$\dot{y}_{d+1,d} \sim \dot{y}_{d,d+1} \sim \frac{1}{a^{d-1}G^{dd}} . \tag{4.2.15}$$

Injecting these expressions in the kinetic energy gives a constraint on the behaviour of G^{dd} for the Friedmann equation (4.1.11) to be consistent with $H^2 \sim t^{-2}$ or $H^2 \sim (t-t_-)^{-2}$. We thus assume $G^{dd} \sim t^{J_+}$ or $G^{dd} \sim (t-t_-)^{J_-}$ with constants $J_\pm$ to be determined and that must satisfy $\pm J_\pm > 0$. With this assumption, we conclude from (4.2.15) that the fields $y_{d,d+1}$ and $y_{d+1,d}$ converge to small arbitrary constants. Notice that even when the "mass term" is negative when ϵ is odd, the deformations do not automatically reach large expectation values that would destabilize the initial background. The equation of motion for $y_{d+1,d+1}$ yields, with c_y an integration constant,

$$\dot{y}_{d+1,d+1} \sim \frac{2c_y}{a^{d-1}} \quad \Longrightarrow \quad |y_{d+1,d+1}| \sim |\ln(t)| \quad \text{or} \quad |\ln(t-t_-)| \ll \sqrt{G^{dd}} . \tag{4.2.16}$$

The logarithm behaviour is not inconsistent with the smallness of $y_{d+1,d+1}$ since the behaviour of G^{dd} with $\pm J_\pm > 0$ ensures that $|y_{d+1,d+1}|/\sqrt{G^{dd}}$ decreases. The dominant behaviours of Φ and $\Phi_\perp$ are the same as the exact ones in (4.1.16) with two integration constants $c_\perp$ and c_Φ. Eventually, going back to Friedmann equation, it is consistent only if $c_\perp$, c_Φ and c_y satisfy a subcriticality condition similar to the one in the underformed analysis

$$\left(\frac{c_\perp}{\gamma_{\rm c} c_\Phi}\right)^2 + \left(\frac{c_y}{\gamma_{\rm c} c_\Phi}\right)^2 \leq 1 \tag{4.2.17}$$

where the critical value $\gamma_{\rm c}$ is the same as before (see Eq. (4.1.21)) with $n = 1$. The subcritical region is thus now the disk of radius one in the plane $(\frac{c_\perp}{\gamma_{\rm c} c_\Phi}, \frac{c_y}{\gamma_{\rm c} c_\Phi})$ instead of being just the segment $\left|\frac{c_\perp}{\gamma_{\rm c} c_\Phi}\right| \leq 1$.

Consistency of the analysis requires to determine $\kappa_\pm$ and $J_\pm$ and check if they indeed satisfy $\pm\kappa_\pm > 0$ and $\pm J_\pm > 0$. It turns out that $\kappa_\pm$ does not introduce any constraint in the subcritical region depicted in Fig. 4.4 while $J_\pm$ restrict $(\frac{c_\perp}{\gamma_{\rm c} c_\Phi}, \frac{c_y}{\gamma_{\rm c} c_\Phi})$ to lie in the schematic blue shaded regions. The left crescent yields a quantum no-scale regime $a \to +\infty$ which is always perturbative while the right one gives rise to a quantum no-scale regime $a \to 0$ perturbative everywhere except at the tips of the crescent.

We thus conclude that quantum no-scale regimes exist even when the dynamics of internal moduli fields is considered. It is important to note that Fig. 4.4 is only schematic and that for $3 \leq d \leq 9$, the width of the left crescent along the horizontal axis is actually very small. It approximately ranges from 10^{-3} to 10^{-2}. We should not conclude that some fine tuning is required for ever-expanding quantum no-scale regimes to exist since global attractor may be present. This analysis is the purpose of the next subsection.

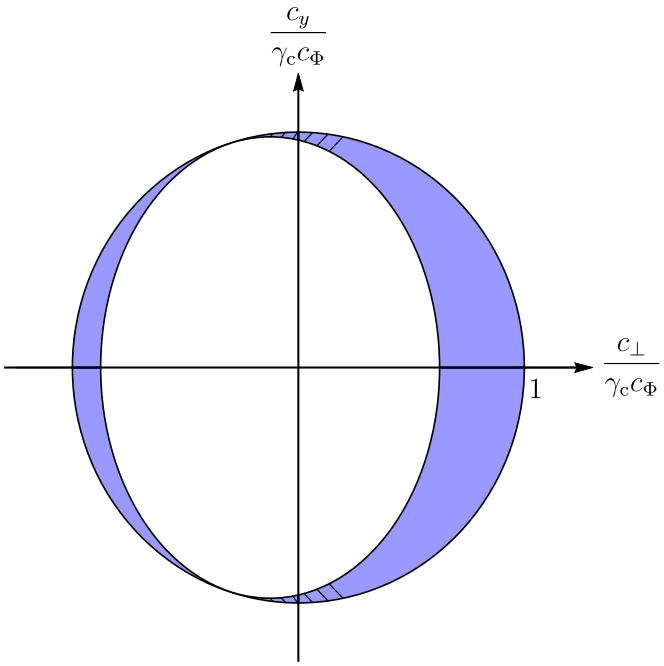

Figure 4.4: The points $(\frac{c_\perp}{\gamma_c c_\Phi}, \frac{c_y}{\gamma_c c_\Phi})$ of the disk of radius 1 that lie in the shaded regions yield quantum no-scale regimes. The universe is forever expanding in the left crescent and goes to a Big Crunch in the right crescent. The hatches schematically indicate where perturbative consistency breaks down.

4.2.3 Global attractor mechanism

We use numerical tools to investigate if global attractors towards quantum no-scale regimes with $a \to +\infty$ exist in order to avoid the fine tuning of the integration constants. We are particularly interested in the evolutions of the simulated quantities in $d = 4$ dimensions

$$c_\perp^{\text{sim}} = \frac{a^{d-1}}{\sqrt{2}}\dot{\Phi}_\perp \ , \quad c_\Phi^{\text{sim}} = a^{d-1}\left(\alpha\dot{\Phi} + \frac{\alpha^2}{2}d(d-2)H\right) \ , \quad c_y^{\text{sim}} = \frac{a^{d-1}}{2}\dot{y}_{55} \ . \tag{4.2.18}$$

Note that before simulating the whole system, we checked that starting from the tiny left crescent indeed yields a quantum no-scale regime where the above simulated quantities freeze. We also observed the expected non-trivial behaviours: The climbing of M of its negative potential and the stabilization of the y's even when they have negative "mass terms" in the potential.

To simulate the whole system and allow for the y's to reach arbitrary large values, the exact potential without approximation to quadratic order in the y's needs to be implemented [44]. For simplicity, the simulations have been performed with $y_{55} = 0 \Rightarrow c_y = 0$. Note that the parity of ϵ is no more relevant in this context since the exploration of a large range of values by the moduli fields interpolates between different values for $n_{\text{F}} - n_{\text{B}} + (-1)^\epsilon 8 \times 2$. An important feature of the exact potential in our specific setup is that depending on $n_{\text{F}} - n_{\text{B}}$, its sign can be always positive for all values of $y_{d,d+1}$, always negative or without a definite sign. The results of the simulations are the following:

- When $\mathcal{V}_{\text{1-loop}} < 0$ for some values of y_{45}, the universe collapses after a certain time unless the trajectory happens to sit in the tiny left crescent. In this case, the dynamics of the Wilson lines thus drastically impacts the possibility of emergence of quantum no-scale regimes compared to the toy model.

- When $\mathcal{V}_{\text{1-loop}} \geq 0$ for all values of y_{45}, the quantity $\frac{c_{\perp}^{\text{sim}}}{\gamma_c c_{\Phi}^{\text{sim}}}$ is always attracted inside the tiny crescent where it freezes and the system enters a quantum no-scale regime. This global attractor makes a flat expanding universe much more likely when the one-loop potential is positive rather than negative where fine tuning is required for the universe not to collapse.

It is interesting to see how the system evolves before reaching a quantum no-scale regime when $\mathcal{V}_{\text{1-loop}} \geq 0$. Remember that in such a regime, the scale factor satisfies $a^{d-1} \sim t$ so that $(a^{d-1})^{\cdot}$ is constant. Fig. 4.5a shows the evolution of $(a^{d-1})^{\cdot}$ for a set of small initial velocities for y_{45} and y_{54}. We observe that a structure of plateaux arises, that can be understood as follows:

- For small velocities, the dynamics temporarily matches the one of the toy model where we have shown that the system always enters a quantum no-scale regime since $\mathcal{V}_{\text{1-loop}} \geq 0$. That is why $(a^{d-1})^{\cdot}$ follows a first plateau.
- It is unlikely that the system initially sits in the tiny crescent and thus the value of J_{+}^{sim} (which is dynamical at this stage) is almost certainly negative. The kinetic energies of y_{45} and y_{54} inevitably end up dominating in Friedmann equation and destabilize the initial approximate quantum no-scale regime. Thanks to the positivity of the one-loop potential, the quantity $(a^{d-1})^{\cdot}$ starts increasing.
- The kinetic energies of y_{45} and y_{54} cannot dominate forever since no such asymptotic solutions exist. The energy must be released at some point and the system reaches a new approximate quantum no-scale regime.
- At each plateaux, the dynamical value of J_{+}^{sim} gets closer to the tiny crescent and after enough plateaux, it stabilizes to a positive value (see Fig. 4.5b).
- This convergence to the tiny crescent can be checked by plotting $\frac{c_{\perp}^{\text{sim}}}{\gamma_c c_{\Phi}^{\text{sim}}}$ in Figs. 4.5c and 4.5d.
- Once this is the case, the universe stays in this final quantum no-scale regime forever.

4.3 Thermal cosmology: A model for dark-matter relic generation

Inspired by the effect of a discrete antisymmetric tensor on the bosonic or fermionic nature of the additional massless states at specific points in moduli space, we describe how it can affect the cosmology considered at finite temperature $T_{(\sigma)}$ in sigma-model frame. We exhibit a mechanism where a cosmological attractor triggers a phase transition and implies the condensation of initially massless scalars. Assuming such states to be dark-matter candidates, we study how this sudden mass increase affects the standard freeze-out scenario of dark matter presented in Chapter. 1.

This study is again performed in a heterotic string framework in d dimensions with spontaneously broken supersymmetry *à la* Scherk–Schwarz in the low breaking scale regime and this time with the additional implementation of finite temperature. In a first subsection, we express the one-loop thermal potential $\mathcal{V}_{\text{1-loop}}^{\text{th},(\sigma)}$ in our setup. We then briefly define and review the existence of an attractor to a so-called "radiation-like era" in this configuration [38–42]. After that, we show how the evolution of the universe along such an attractor can trigger a destabilization of some initially massless states before entering a second radiation-like era. In a fourth and last subsection, we describe how this mechanism impacts the standard freeze-out scenario to yield a relic density of dark matter at late times.

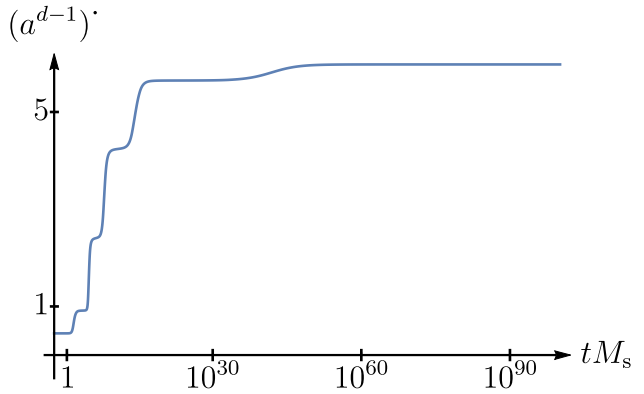

(a) Convergence of $(a^{d-1})^{\cdot}$ towards a constant, signalling the entrance of the universe in a quantum no-scale regime. The plateaux correspond to approximate intermediate quantum no-scale regimes before reaching the exact final one.

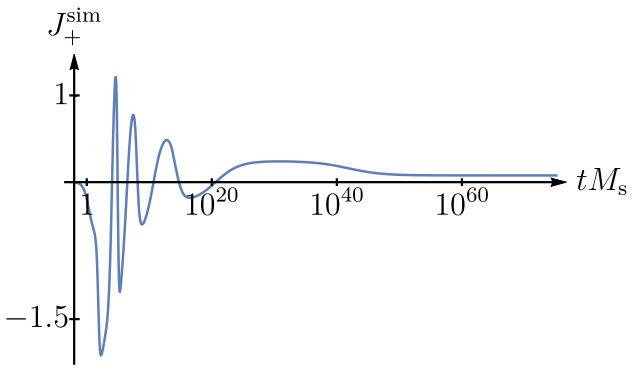

(b) Evolution of J_+^{sim}. It oscillates between positive and negative values before stabilizing at a positive value when the final exact quantum no-scale regime is reached.

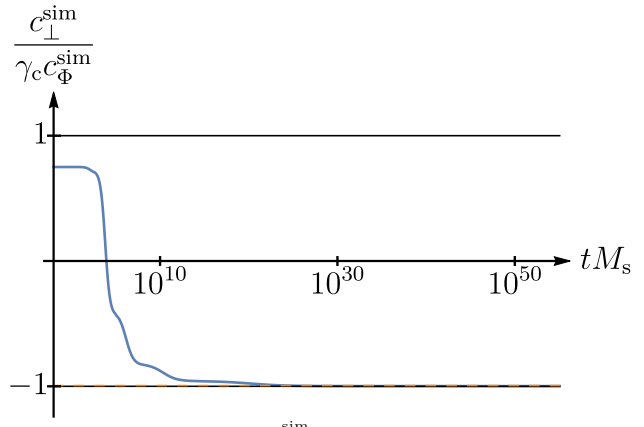

(c) Convergence of $\frac{c_\perp^{\mathrm{sim}}}{\gamma_{\mathrm{c}} c_\Phi^{\mathrm{sim}}}$ towards the tiny range $[-1, -0.9941]$. The next plot on the right zooms over this range to better see the convergence.

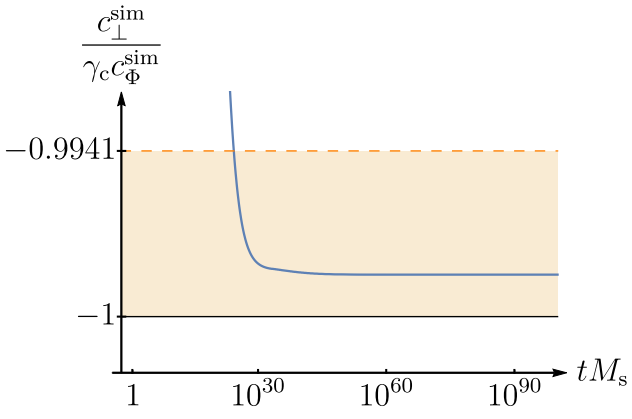

(d) Zoom over the entrance of $\frac{c_\perp^{\mathrm{sim}}}{\gamma_{\mathrm{c}} c_\Phi^{\mathrm{sim}}}$ into the tiny range $[-1, -0.9941]$ represented by the orange shaded area.

Figure 4.5: Evolution of the simulated quantities $(a^{d-1})^{\cdot}$, J_+^{sim} and $\frac{c_\perp^{\mathrm{sim}}}{\gamma_{\mathrm{c}} c_\Phi^{\mathrm{sim}}}$ as a function of time with $d = 4$.

4.3.1 Thermal potential at one loop

We consider the $\mathrm{E}_8 \times \mathrm{E}_8$ heterotic string compactified on

$$S^1_{\mathrm{E}}(R_0) \times \mathbb{R}^{d-1} \times S^1(R_d) \times T^{8-d} \times S^1(R_9) \ . \tag{4.3.1}$$

The first circle of radius R_0 is the compactified Euclidean time that implements the finite temperature [22]. The temperature is then proportional to the inverse of the radius R_0 and the associated Matsubara excitations have a momentum m_0 which is unshifted for boson and shifted for fermions:

$$T_{(\sigma)} \equiv \frac{1}{2\pi R_0} \qquad \text{and} \qquad m_0 \longrightarrow \frac{m_0 + \frac{F}{2}}{R_0} \ , m_0 \in \mathbb{Z} \ . \tag{4.3.2}$$

Note the following difference of notation compared to the other studies presented in this thesis: We will perform the Scherk–Schwarz mechanism responsible for the spontaneous breaking of supersymmetry along the direction X^9 with radius R_9. The radius R_d of the other factorized circle will play

the role of the (de)-stabilized modulus throughout the cosmological evolution of the universe. To have more flexibility for the possible values of $n_{\rm F} - n_{\rm B}$, we break $\mathrm{E}_8 \times \mathrm{E}_8$ to $\mathrm{SO}(16) \times \mathrm{SO}(16)$ as explained in Subsect. 4.2.1. Note that here, we define $d_{\rm en}$ to be the number of roots of the enhanced U(1)'s excluding direction X^d. We then define $n_{\rm F}$ and $n_{\rm B}$ to be the massless degrees of freedom which do not contain the possible additional states coming from direction X^d,

$$n_{\rm B} = 8 \times (8 + 120 + 120 + d_{\rm en}) \qquad \text{and} \qquad n_{\rm F} = 8 \times (128 + 128) \ . \tag{4.3.3}$$

As described in the same subsection, we also turn on a discrete background value for $2B_{d9} \equiv \epsilon$ so that its parity determines if the additional massless states at the self-dual radius $R_d = \sqrt{\alpha'}$ are bosons (producing a gauge symmetry enhancement) or fermions. This will be very important to trigger or not a phase transition as the universe evolves. More precisely, the whole Kaluza-Klein tower along X^9 with momentum $m_9 \in \mathbb{Z}$ and with momentum and winding numbers along X^d satisfying $m_d = \pm n_d = \pm 1$ has squared mass

$$\left(\frac{R_d}{\alpha'} - \frac{1}{R_d}\right)^2 + \left(\frac{m_9 + \frac{F + 2B_{d9} n_d}{2}}{R_9}\right)^2 = \left(\frac{R_d}{\alpha'} - \frac{1}{R_d}\right)^2 + \left(\frac{m_9 + \frac{F \pm \epsilon}{2}}{R_9}\right)^2 \ . \tag{4.3.4}$$

Denoting $\tilde{n}_{\rm B}$ and $\tilde{n}_{\rm F}$ the additional numbers of bosonic and fermionic degrees of freedom at the self-dual radius, we have

$$\tilde{n}_{\rm B} = 8 \times 2(1 - \epsilon) \qquad \text{and} \qquad \tilde{n}_{\rm F} = 8 \times 2\epsilon \ . \tag{4.3.5}$$

To proceed, we define the following quantities,

$$\zeta \equiv \ln\left(\frac{R_d}{\alpha'}\right) \ , \qquad z \equiv \ln\left(\frac{R_0}{R_9}\right) = \ln\left(\frac{M_{(\sigma)}}{T_{(\sigma)}}\right) \ . \tag{4.3.6}$$

We do not write the full result for $\mathcal{V}^{\rm th,(\sigma)}_{\text{1-loop}}$ that can be found in [39] but we display its Taylor expansion up to quadratic order around $\zeta = 0$:

$$\begin{aligned} \mathcal{V}^{\rm th,(\sigma)}_{\text{1-loop}} = T^4_{(\sigma)} \Big[&-(N_{\rm F} + N_{\rm B}) f^{(d)}_{\rm T}(z) + (N_{\rm F} - N_{\rm B}) f^{(d)}_{\rm V}(z) \Big] \\ &+ \frac{T^{d-2}_{(\sigma)} \zeta^2}{\pi} (\tilde{n}_{\rm F} + \tilde{n}_{\rm B}) \Big[f^{(d-2)}_{\rm T}(z) + (-1)^\epsilon f^{(d-2)}_{\rm V}(z) \Big] + \mathcal{O}(\zeta^4) \ , \end{aligned} \tag{4.3.7}$$

where $N_{\rm F} = n_{\rm F} + \tilde{n}_{\rm F}$ and $N_{\rm B} = n_{\rm B} + \tilde{n}_{\rm B}$ are the total number of fermionic and bosonic degrees of freedom at $\zeta = 0$ and the function $f_{\rm T}$ and $f_{\rm V}$ are

$$f^{(d)}_{\rm T}(z) = \frac{\Gamma\left(\frac{d+1}{2}\right)}{\pi^{\frac{d+1}{2}}} \sum_{\tilde{k}_0, \tilde{k}_9 \in \mathbb{Z}} \frac{e^{dz}}{\left[e^{2z}(2\tilde{k}_0 + 1)^2 + (2\tilde{k}_9)^2\right]^{\frac{d+1}{2}}} \ , \qquad f^{(d)}_{\rm V}(z) = e^{(d-1)z} f^{(d)}_{\rm T}(-z) \ . \tag{4.3.8}$$

Note that at $\zeta = 0$, we see that the thermal one-loop potential displays a competition between the thermal effects in $f^{(d)}_{\rm T}(z)$ and the usual quantum effects in $f^{(d)}_{\rm V}(z)$. When the temperature is dominated by the supersymmetry-breaking scale ($z \to +\infty$), the expression of $\mathcal{V}^{\rm th,(\sigma)}_{\text{1-loop}}$ matches the one of $\mathcal{V}^{(\sigma)}_{\text{1-loop}}$ (Eq. 1.3.11). On the contrary, when the temperature dominates ($z \to -\infty$), $\mathcal{V}^{\rm th}_{\text{1-loop}}$ reduces to the first thermal term. Notice also that the thermal contribution is always negative with a pre-factor $-(N_{\rm F} + N_{\rm B})$ while the quantum effects are dressed with the usual $(N_{\rm F} - N_{\rm B})$ factor that can be of arbitrary sign and can potentially compensate the thermal part when $N_{\rm F} > N_{\rm B}$.

4.3.2 Attraction to a radiation-like era

When ϵ is even, the shape of the thermal potential as a function of ζ is drawn in Fig. 4.6. It is drawn in the case $T_{(\sigma)} > M_{(\sigma)}$ but the qualitative shape is the same if $T_{(\sigma)} < M_{(\sigma)}$ up to the replacement $R_0 \to R_9$ in the figure. We see that there is a local minimum at $\zeta = 0$ and we can naively expect a stabilization. The well centred at the origin is surrounded by two plateaux where the contributions to the thermal potential of the $\tilde{n}_{\rm B}$ and $\tilde{n}_{\rm F}$ states become exponentially suppressed so that it does not depend on ζ any more. If the the radius R_d is too big ($R_d \gtrsim R_0$) or to small ($R_d \lesssim 1/R_0$), the Kaluza–Klein modes or winding modes contribute significantly and produce an exponential behaviour that can be decreasing or increasing depending on the sign $n_{\rm F} - n_{\rm B}$ and the value of z.

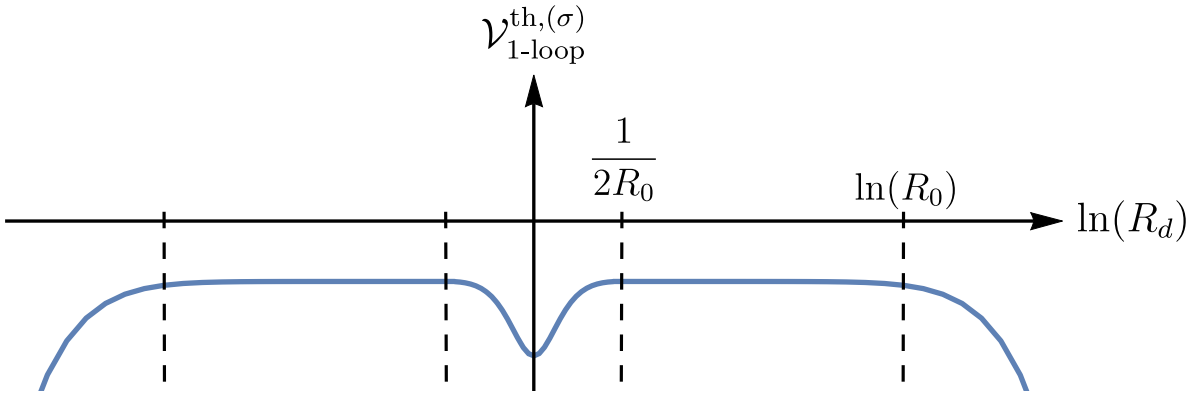

Figure 4.6: Qualitative shape of the thermal potential as a function of $\zeta = \ln(R_d)$ in the case ϵ even and $T_{(\sigma)} > M_{(\sigma)}$. If $T_{(\sigma)} < M_{(\sigma)}$, the shape is the same up to the change $R_0 \to R_9$.

In this case, it has been shown in [41] that the naive expectation for a stabilization of ζ is indeed correct and the dynamics shows a peculiar cosmological behaviour. With the usual definitions (4.1.6) applied with $n = 1$ for the no-scale modulus Φ and the orthogonal combination $\Phi_\perp$ in function of R_9 and the dilaton ϕ, the action in Einstein frame reads

$$S = \int \mathrm{d}^d x \sqrt{-g} \left[\frac{\mathcal{R}}{2} - \frac{1}{2}(\partial\Phi)^2 - \frac{1}{2}(\partial\Phi_\perp)^2 - \frac{1}{2}(\partial\zeta)^2 - \mathcal{V}^{\text{th}}_{\text{1-loop}} \right] , \tag{4.3.9}$$

where $\mathcal{V}^{\text{th}}_{\text{1-loop}} \equiv e^{\frac{2d}{d-2}\phi} \mathcal{V}^{\text{th},(\sigma)}_{\text{1-loop}}$. The temperature and supersymmetry-breaking scale in Einstein frame without subscript (σ) are defined from the expression in sigma-model frame with the multiplicative factor $e^{\frac{2}{d-2}\phi}$. It is also convenient to define $\beta = 1/T$. With a FLRW ansatz,

$$\mathrm{d}s^2 = -\beta(x^0)^2(\mathrm{d}x^0)^2 + a(x^0)^2 \sum_{i=1}^{d-1} (\mathrm{d}x^i)^2 , \quad \Phi(x^0) , \quad \Phi_\perp(x^0) , \quad \zeta(x^0) , \tag{4.3.10}$$

and the definition of a cosmic time $t \equiv \beta x^0$, the equations of motion for β, the scale factor a and the fields Φ, $\Phi_\perp$ and ζ can be worked out. Provided that the massless spectrum satisfies

$$0 < \frac{N_{\rm F} - N_{\rm B}}{N_{\rm F} + N_{\rm B}} < \frac{1}{2^d - 1} , \tag{4.3.11}$$

they admit as a solution a behaviour where $\zeta = 0$, $\Phi_\perp = \phi_{\perp 0} = \text{cst}$ and z keeps a constant value $\tilde{z}_{\rm c}$ that can range from $-\infty$ to $+\infty$ depending on the precise values of $N_{\rm F}$ and $N_{\rm B}$. In such a

solution, ζ does not move and the the breaking scale M is proportional to the temperature T with proportionality constant equal to $e^{\tilde{z}_c}$. Both M and T decrease like the inverse of the scale factor which itself grows like $t^{\frac{d}{2}}$. The cosmology then looks like that of a universe filled only by radiation with $H^2 \propto T^d$. Of course, the energy density ρ and pressure P derived from the thermal potential do not satisfy the state equation of pure radiation $\rho = (d-1)P$ but when the kinetic energy of the no-scale modulus Φ is taken into account, the total energy density ρ_{tot} and pressure P_{tot} indeed verify $\rho_{\text{tot}} = (d-1)P_{\text{tot}}$. This is the reason why this cosmological behaviour is called "radiation-like".

This solution has been shown to be robust to small fluctuations in $d \geq 4$ [39] so that the generic evolution of a trajectory not too far from the critical behaviour converges towards the critical evolution. In the transient regime, the value of z can oscillate or not while ζ undergoes damped oscillations around zero. Such oscillating scalars usually give rise to the so-called "cosmological moduli problem" since their energies do not dilute fast enough as the universe expands and do not stabilize. Some authors invoked decays of the scalars to solve the problem but this gives rise to new difficulties such as an excessive entropy production [207, 208]. Note that our setup avoids the cosmological moduli problem and ζ indeed stabilizes thanks to the drop of its mass as the universe evolves.

If ζ starts too far from zero along one of the plateaux in Fig. 4.6, the setup is the same as before but without the additional $\tilde{n}_{\text{F}}$ and $\tilde{n}_{\text{B}}$ massless states contributing. A local attractor again exists [39], very similar to the previous one but this time with $\zeta = \zeta_0 = \text{cst}$ and a new critical value z_{c} provided that now

$$0 < \frac{n_{\text{F}} - n_{\text{B}}}{n_{\text{F}} + n_{\text{B}}} < \frac{1}{2^d - 1} \, . \tag{4.3.12}$$

Notice also that when ζ starts on the exponential part of the potential in Fig. 4.6, even if this part is exponentially decreasing, the plateau width is dynamical and always ends up catching ζ, preventing it from eternally falling out.

4.3.3 Conditions for a dynamical phase transition

Let us now look at the qualitative shape of the potential as a function of ζ in the case where ϵ is odd. When the temperature dominates the supersymmetry-breaking scale, the shape is the same as in Fig. 4.6. However, when the ratio M/T becomes greater than one, the well centered at the origin becomes a bump as can be seen from Fig. 4.7.

We want to use this change of behaviour as the temperature drops to trigger a phase transition responsible for the generation of a large mass to some states that will be interpreted as dark-matter candidates. In this subsection, we describe qualitatively what we naively expect to happen and then check these conclusions thanks to numerical simulations.

Expected behaviour

- At large temperature, we assume ζ to sit not too far from the origin inside the well formed by its potential and we assume condition (4.3.11) to be valid. We then expect the cosmological evolution to converge towards the critical solution with $z = \tilde{z}_{\text{c}}$.
- If $e^{\tilde{z}_c} = M/T < 1$, the temperature never drops below the breaking scale and the potential keeps its well shape as in Fig. 4.6 forever and nothing special happens.

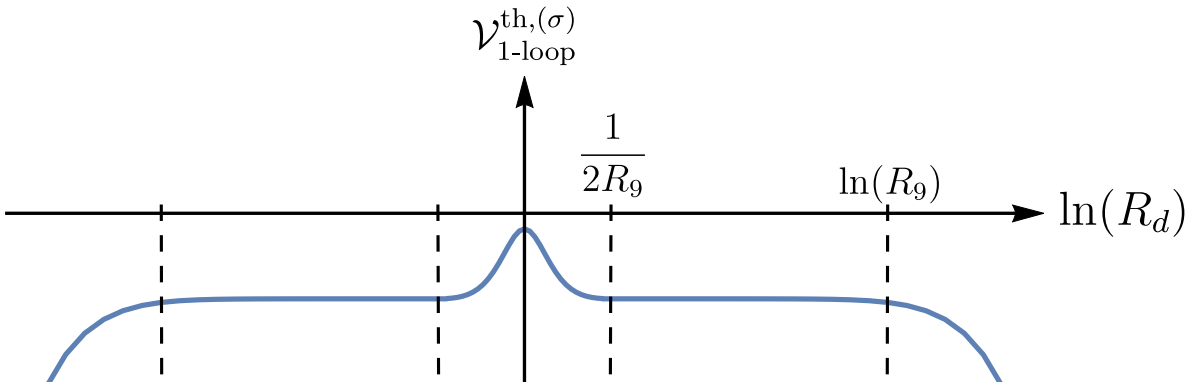

Figure 4.7: Qualitative shape of the thermal potential as a function of $\zeta = \ln(R_d)$ in the case ϵ odd and $T_{(\sigma)} < M_{(\sigma)}$. When $T_{(\sigma)} > M_{(\sigma)}$, the shape is the same as the one drawn in Fig. 4.6.

- However, if $e^{\tilde{z}_c} > 1$, at the inevitable moment when the breaking scale starts to dominate the temperature, the potential develops a bump and ζ is destabilized.
- We then expect ζ to slide along the bump until it freezes along the plateau. From there, if condition (4.3.12) is satisfied, the universe follows another radiation-like critical solution with $z = z_c > 1$.

For this expected scenario to take place in our setup, the three following conditions must hold:

$$\begin{aligned} &(i)\ 0 < \frac{n_F - n_B}{n_F + n_B}, \frac{N_F - N_B}{N_F + N_B} < \frac{1}{2^d - 1} && (z_c \text{ and } \tilde{z}_c \text{ exist}), \\ &(ii)\ \epsilon \in 2\mathbb{Z} + 1 && (\text{necessary for a possible destabilization of } \zeta), \\ &(iii)\ \tilde{z}_c > 0 && (\zeta \text{ indeed becomes tachyonic}). \end{aligned} \tag{4.3.13}$$

We thus choose ϵ odd and condition (i) can be written like

$$0 < \frac{8 - d_{en}}{504 + d_{en}}, \frac{10 - d_{en}}{506 + d_{en}} < \frac{1}{2^d - 1}\ . \tag{4.3.14}$$

Condition (iii) can be checked by determining $\tilde{z}_c$ explicitly [41],

$$\tilde{z}_c \text{ is the unique root of the equation } \frac{N_F - N_B}{N_F + N_B} - \frac{f_T^{(d)} + \partial_z f_T^{(d)}}{f_V^{(d)} + \partial_z f_V^{(d)}} = 0\ . \tag{4.3.15}$$

We find that:

- For $d = 3$ and $d = 4$, condition (i) holds with $d_{en} = 0, 2, 4, 6$ and also $d_{en} = 8$ if we allow the critical value z_c to be $+\infty$. The critical value $\tilde{z}_c$ is positive in all cases so condition (iii) is also verified and the phase transition occurs.
- For $d = 5$, condition (i) holds with $d_{en} = 0, 2, 4, 6$ (and 8) but $\tilde{z}_c$ turns out to be positive only for $d_{en} = 4, 6$ (and 8).
- For $d = 6$, condition (i) implies $d_{en} = 2, 4, 6$ (and 8) but $\tilde{z}_c$ is always negative.
- For $d = 7$ and 8, condition (i) can no more be satisfied.

Numerical simulations

To confirm all these expectations, we have numerically simulated the system of differential equations to see if the phase transition indeed occurs during a transient regime. We choose initial conditions with an expanding universe ($\dot{a}(0) > 0$) and a temperature higher than the supersymmetry-breaking scale ($z(0) < 0$). We also choose $\zeta(0)$ to be inside the well of the potential and with a low enough initial velocity. Note that a medium size for the initial radius R_0 (few units of $\sqrt{\alpha'}$) is enough to throw out the exponentially suppressed contributions and gives a well width large enough not to require an important initial fine tuning.

The simulated evolutions of the fields $\zeta(t)$, $z(t)$, $\Phi_\perp(t)$ and $a(t)T(t)$ in dimension $d = 4$ are depicted in Fig. 4.8a. We observe that $\zeta(t)$ (blue curve) undergoes damped oscillations around the origin at the beginning. In the meantime, $z(t)$ (orange curve) increases from its initial negative value to try to approach the positive value $\tilde{z}_c$. Once $z(t)$ becomes positive, the potential well becomes a bump as we saw and as expected, $\zeta(t)$ slides along this bump before freezing somewhere. The field $z(t)$ converges to the new critical value z_c and $\Phi_\perp(t)$ also freezes. The final regime is indeed radiation-like as the product $a(t)T(t)$ becomes constant. It could be surprising at first sight that the absolute value of the constant reached by $\zeta(t)$ is lower than the initial one since one could naively think that it remains stuck on top of the bump. Actually, the bump width is dynamical and decreases with time as shown in Fig. 4.8b. We see that the end value of $\zeta(t)$ is indeed far away from the bump. In the simulation, the mass acquired by the $\tilde{n}_F$ states is roughly 2% of the string scale, which is much larger than $T_{(\sigma)}$ and $M_{(\sigma)}$ that keeps decreasing.

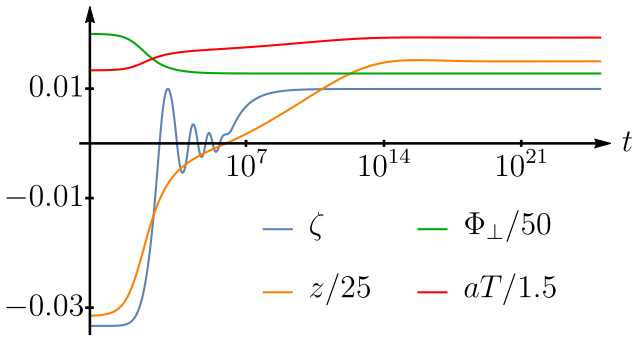

(a) Evolution of $\zeta(t)$, $z(t)$, $\Phi_\perp(t)$ and $a(t)T(t)$ in a model that realizes the dynamical phase transition.

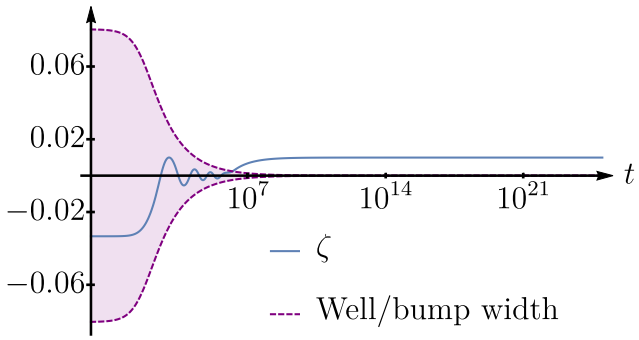

(b) Evolution of the dynamical well/bump width (purple shaded area). The oscillations at the beginning are within the well and the ζ eventually freezes away from the bump.

Figure 4.8: Numerical simulations of the phase transition for $d = 4$.

4.3.4 Dark-matter freeze-out and relic density

In this subsection, we want to show how the phase transition exhibited so far, which suddenly gives a large mass compared to the temperature to some particles, can produce a non-trivial relic density of cold (non-relativistic) dark matter[3]. More particularly, we will see how it affects the standard thermal freeze-out scenario presented in Chapter 1. In order to describe qualitatively what happens, we assume the mass jump from 0 to m_{DM} of the dark-matter particles mass $m(T)$ occurring at the

[3]The identification of the enhanced states with dark-matter candidates is very formal here since we did not even talk about the standard model. For a good candidate, the gauge group should be decoupled enough from the standard model, either with weakly interacting particles or states only coupled to gravity yielding a more complex dark sector.

critical temperature T_c to be very quick compared to all other processes so that we can write

$$m(T) = \begin{cases} 0 & \text{for } T > T_c \\ m_{\rm DM} & \text{for } T < T_c \end{cases} . \tag{4.3.16}$$

Different behaviours arise for the evolution of the dark-matter yield depending on the value of the critical temperature T_c and more precisely depending on the value of the equilibrium density for particles of mass $m_{\rm DM}$ compared to the curve $n_{\rm DM}\langle\sigma_{\rm DM\leftrightarrow SM}v\rangle = (d-1)H$ at T_c, which indicates if the expansion rate of the universe dominates in Boltzmann equation (1.4.3) or not. We distinguish three qualitatively different evolutions, drawn in Fig. 4.9:

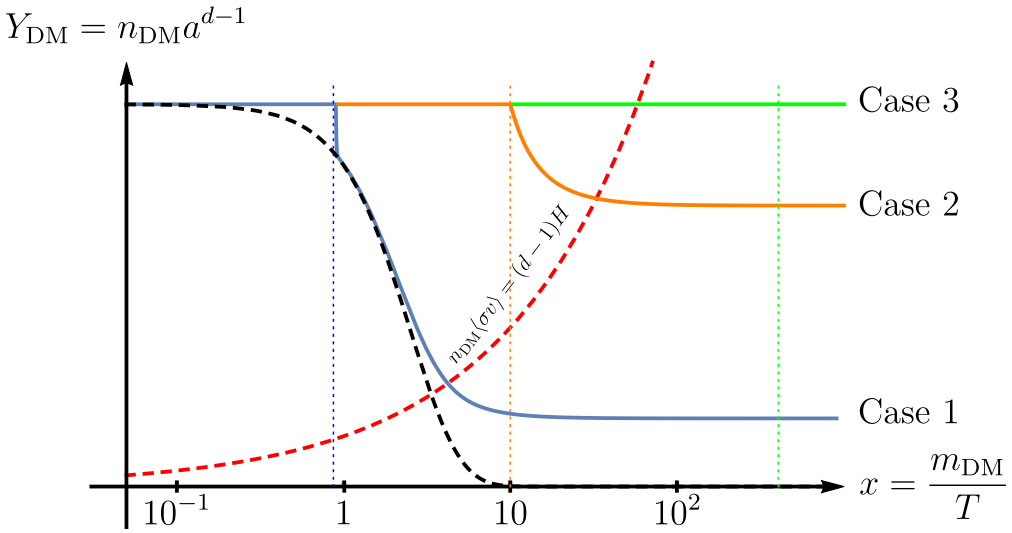

Figure 4.9: Evolution of the dark-matter yield before and after the phase transition in three cases differing by the moment (or temperature) when the transition occurs.

- Case 1: At $x_c \equiv m_{\rm DM}/T_c$, indicated by the vertical blue dotted line, the Boltzmann equilibrium for particles of mass $m_{\rm DM}$ (black dashed curve) is above the red dashed curve representing $n_{\rm DM}\langle\sigma_{\rm DM\leftrightarrow SM}v\rangle = (d-1)H$. The dark matter being initially massless, the yield (blue curve) at the beginning is constant. After the phase transition, the yield has enough time to reach the equilibrium before the expansion rate dominates and this gives a relic density identical to the standard freeze-out mechanism.

- Case 2: At $x_c \equiv m_{\rm DM}/T_c$, indicated by the vertical orange dotted line, the Boltzmann equilibrium for particles of mass $m_{\rm DM}$ (black dashed curve) is below the red dashed curve. The yield (orange curve) starts to decrease but is frozen out before being able to reach the equilibrium. This produces a higher relic density compared to the standard case.

- Case 3: At $x_c \equiv m_{\rm DM}/T_c$, indicated by the vertical green dotted line, the Boltzmann equilibrium for particles of mass $m_{\rm DM}$ (black dashed curve) is well below the red dashed curve and the initial constant yield (green line) is also already below it. This means that the chemical decoupling has already occurred when the dark-matter particles acquire their masses. The yield thus remains constant after the transition and in this case we have a hot (relativistic)

dark-matter relic density. Note that such a hot scenario is what is thought to have happened for the actual neutrino relic density.

4.4 Conclusions

In the last part of this thesis, we investigated the cosmology derived in heterotic models with spontaneous breaking of supersymmetry. We wanted to analyze the quantum backreaction of the one-loop potential generated by the supersymmetry breaking on the no-scale structure of classical models. In a simplified model where only the dynamics of few moduli is taken into account, we showed, under some conditions, the existence of quantum no-scale regimes characterized by a dominated potential and a cosmology identical to that of a classical no-scale model. In such universes, the flat and expanding Minkowski dynamics is not spoiled by quantum effects. This contrasts with some cosmologies put forward in the setup where the universe evolution is intrinsically quantum and driven by the one-loop potential. In these cases, the universe is inexorably sentenced to undergo a Big Crunch.

After this work, it was natural to study the effect of the addition of other deformations on the previous conclusions. In a framework with a specific background and three additional deformations of the internal metric and antisymmetric tensor, assumed to be small, we showed the existence of local attractors towards quantum no-scale regimes. It turned out that the allowed parameter space for a quantum no-scale regime describing an ever-expanding universe is very tiny. However, a numerical study of the dynamics with deformations of arbitrary magnitude exhibited the existence of global attractors towards such evolutions. These global attractors exist when the one-loop potential is positive for all values of the deformations. This makes stability of flat Minkowski spacetime much more natural in this case compared to when the potential can be negative and where some fine tuning is required to avoid a collapse of the universe.

In a third project, we studied the cosmology of heterotic models at finite temperature, motivated by the purpose of generating a dark-matter relic density, a crucial ingredient of the standard model of cosmology. Thanks to the condensation of a modulus during the universe evolution, some states (dark-matter candidates) initially massless acquire a big mass. While massless, the dark-matter particles can be abundantly created and the moment when they acquire their mass drastically impacts the usual freeze-out scenario for dark-matter relic production and can for instance yield a much higher relic density.

5 | Outlook: The challenges of string theory

This thesis delved into three different aspects of string theory with firstly, the very elaboration of supersymmetry breaking mechanisms at the perturbative string level in the framework of orientifold models. Secondly, we studied "moduli stability" in models with spontaneously broken supersymmetry. Talking about stability from the sole investigation of the one-loop potential and its dependences on the moduli is a bit naive since it is the cosmological dynamics that truly stabilizes the scalars or not. It was the object of the third aspect treated in this work to study cosmological implications of the potential generated at one loop by supersymmetry breaking.

Of course, this thesis is just a modest exploration of these various aspects through the study of specific mechanisms which do not pretend to solve the big questions of modern theoretical physics. String theory has not yet been able to prove that it is indeed a good theory to describe the fundamental degrees of freedom of our world and their interactions, despite a lot of theoretically appealing facets. For now, even if great theoretical successes have been achieved, the theory remains too flexible and cannot satisfyingly explain the black-hole information loss paradox or the de Sitter nature of our universe. Moreover, it faces the big difficulty of collecting data, both from particle physics and from cosmological observations, to constrain the models and parameters. This difficulty can have two distinct origins: Because the energy scale at which new physics appears is much higher than what we can experimentally achieve and does not leave big enough effects in precision experiments ; Or because of the environmental nature of some parameters that may have specific values for no specific reasons inside a multiverse.

In the seek of constraints for string theory, the swampland program initiated quite recently tries to establish criteria that field theories must satisfy to consistently be effective low-energy limits of quantum theories of gravity. Among the whole ensemble of field theories, those that can indeed be consistent low-energy limits are part of the "landscape" while the others form the "swampland". In this bottom-up approach, the delineation of the landscape and the features of the theories inside it could provide constraints for the "up" part *i.e.* at the string-theory level. The landscape is now full of conjectures about effective field theories that have been shown to be related to each other as a complex web of features that are expected in consistent theories.

More work in the future, both from the theoretical physics community, the experimentalists and the engineers, will hopefully bring answers to the deepest questions of fundamental physics and unravel the description of quantum gravity.

A Conventions and notations for the characters

Our definitions of the Jacobi modular forms and Dedekind function are

$$\vartheta\left[\begin{smallmatrix}\alpha\\ \beta\end{smallmatrix}\right](z|\tau)=\sum_m q^{\frac{1}{2}(m+\alpha)^2}e^{2i\pi(z+\beta)(m+\alpha)}\ ,\qquad \eta(\tau)=q^{\frac{1}{24}}\prod_{n=1}^{+\infty}(1-q^n)\ . \tag{A.0.1}$$

It is standard to denote

$$\vartheta\left[\begin{smallmatrix}0\\ 0\end{smallmatrix}\right](z|\tau)=\vartheta_3(z|\tau)\ ,\ \ \vartheta\left[\begin{smallmatrix}0\\ \frac{1}{2}\end{smallmatrix}\right](z|\tau)=\vartheta_4(z|\tau)\ ,\ \ \vartheta\left[\begin{smallmatrix}\frac{1}{2}\\ 0\end{smallmatrix}\right](z|\tau)=\vartheta_2(z|\tau)\ ,\ \ \vartheta\left[\begin{smallmatrix}\frac{1}{2}\\ \frac{1}{2}\end{smallmatrix}\right](z|\tau)=\vartheta_1(z|\tau)\ , \tag{A.0.2}$$

and to keep implicit both arguments when $z=0$. In these notations, the SO($2n$) affine characters can be written as

$$O_{2n}=\frac{\vartheta_3^n+\vartheta_4^n}{2\eta^n}\ ,\qquad V_{2n}=\frac{\vartheta_3^n-\vartheta_4^n}{2\eta^n}\ ,\qquad S_{2n}=\frac{\vartheta_2^n+i^{-n}\vartheta_1^n}{2\eta^n}\ ,\qquad C_{2n}=\frac{\vartheta_2^n-i^{-n}\vartheta_1^n}{2\eta^n}\ . \tag{A.0.3}$$

They satisfy the following modular properties:

$$\begin{aligned}
&\begin{pmatrix}O_{2n}\\ V_{2n}\\ S_{2n}\\ C_{2n}\end{pmatrix}(\tau+1)=e^{-in\pi/12}\mathrm{diag}\big(1,-1,e^{in\pi/4},e^{in\pi/4}\big)\begin{pmatrix}O_{2n}\\ V_{2n}\\ S_{2n}\\ C_{2n}\end{pmatrix}(\tau)\ ,\\
&\begin{pmatrix}O_{2n}\\ V_{2n}\\ S_{2n}\\ C_{2n}\end{pmatrix}\Big(-\frac{1}{\tau}\Big)=\frac{1}{2}\begin{pmatrix}1&1&1&1\\ 1&1&-1&-1\\ 1&-1&i^{-n}&-i^{-n}\\ 1&-1&-i^{-n}&i^{-n}\end{pmatrix}\begin{pmatrix}O_{2n}\\ V_{2n}\\ S_{2n}\\ C_{2n}\end{pmatrix}(\tau)\ ,
\end{aligned} \tag{A.0.4}$$

which are relevant for the amplitudes $\mathcal{T}$, $\mathcal{K}$ and $\mathcal{A}$. For the Möbius strip, it is convenient to switch from the characters χ to the real "hatted" characters $\hat{\chi}$ defined by [115, 116]

$$\hat{\chi}\Big(\frac{1}{2}+i\tau_2\Big)=e^{-i\pi(h-\frac{c}{24})}\,\chi\Big(\frac{1}{2}+i\tau_2\Big)\ , \tag{A.0.5}$$

where h is the weight of the associated primary state and c is the central charge. The so-called P-transformation then takes the form

$$\begin{pmatrix}\hat{O}_{2n}\\ \hat{V}_{2n}\\ \hat{S}_{2n}\\ \hat{C}_{2n}\end{pmatrix}\Big(\frac{1}{2}+\frac{i}{2\tau_2}\Big)=\begin{pmatrix}c&s&0&0\\ s&-c&0&0\\ 0&0&\zeta c&i\zeta s\\ 0&0&i\zeta s&\zeta c\end{pmatrix}\begin{pmatrix}\hat{O}_{2n}\\ \hat{V}_{2n}\\ \hat{S}_{2n}\\ C_{2n}\end{pmatrix}\Big(\frac{1}{2}+i\frac{\tau_2}{2}\Big)\ ,\quad \hat{\eta}\Big(\frac{1}{2}+\frac{i}{2\tau_2}\Big)=\sqrt{\tau_2}\,\hat{\eta}\Big(\frac{1}{2}+i\frac{\tau_2}{2}\Big)\ . \tag{A.0.6}$$

where $c = \cos(n\pi/4)$, $s = \sin(n\pi/4)$ and $\zeta = e^{-in\pi/4}$. Throughout this work, the implicit arguments of the characters are τ, $2i\tau_2$, $i\tau_2/2$ and $(1 + i\tau_2)/2$ for the torus, Klein bottle, annulus and Möbius strip amplitudes respectively.

B | BSGP model with Scherk–Schwarz mechanism

Appendix B.1: Torus partition function

Given the notations defined in the main text and the conventions for characters defined in Appendix A, the torus amplitude of the BSGP model with Scherk–Schwarz mechanism along direction X^5 takes the following form,

$$
\begin{aligned}
\mathcal{T} = \frac{1}{4}\int \frac{\mathrm{d}^2\tau}{\tau_2^3} \Bigg\{ \Bigg[& \left(|V_4O_4 + O_4V_4|^2 + |S_4S_4 + C_4C_4|^2\right) \frac{\Lambda^{(4,4)}_{\vec{m},\vec{n}}}{|\eta^4|^2} \\
& + \left(|V_4O_4 - O_4V_4|^2 + |S_4S_4 - C_4C_4|^2\right) \left|\frac{2\eta}{\vartheta_2}\right|^4 \\
& + 16\left(|O_4C_4 + V_4S_4|^2 + |S_4O_4 + C_4V_4|^2\right) \left|\frac{\eta}{\vartheta_4}\right|^4 \\
& + 16\left(|O_4C_4 - V_4S_4|^2 + |S_4O_4 - C_4V_4|^2\right) \left|\frac{\eta}{\vartheta_3}\right|^4 \Bigg] \frac{\Lambda^{(2,2)}_{\vec{m}',(n_4,2n_5)}}{|\eta^4|^2} \\
- \Bigg[& \left((V_4O_4 + O_4V_4)(\bar{S}_4\bar{S}_4 + \bar{C}_4\bar{C}_4) + (S_4S_4 + C_4C_4)(\bar{V}_4\bar{O}_4 + \bar{O}_4\bar{V}_4)\right) \frac{\Lambda^{(4,4)}_{\vec{m},\vec{n}}}{|\eta^4|^2} \\
& + \left((V_4O_4 - O_4V_4)(\bar{S}_4\bar{S}_4 - \bar{C}_4\bar{C}_4) + (S_4S_4 - C_4C_4)(\bar{V}_4\bar{O}_4 - \bar{O}_4\bar{V}_4)\right) \left|\frac{2\eta}{\vartheta_2}\right|^4 \\
& + 16\left((O_4C_4 + V_4S_4)(\bar{S}_4\bar{O}_4 + \bar{C}_4\bar{V}_4) + (S_4O_4 + C_4V_4)(\bar{O}_4\bar{C}_4 + \bar{V}_4\bar{S}_4)\right) \left|\frac{\eta}{\vartheta_4}\right|^4 \\
& + 16\left((O_4C_4 - V_4S_4)(\bar{S}_4\bar{O}_4 - \bar{C}_4\bar{V}_4) + (S_4O_4 - C_4V_4)(\bar{O}_4\bar{C}_4 - \bar{V}_4\bar{S}_4)\right) \left|\frac{\eta}{\vartheta_3}\right|^4 \Bigg] \frac{\Lambda^{(2,2)}_{\vec{m}'+\vec{a}'_{\mathrm{S}},(n_4,2n_5)}}{|\eta^4|^2} \\
+ \Bigg[& \left(|O_4O_4 + V_4V_4|^2 + |C_4S_4 + S_4C_4|^2\right) \frac{\Lambda^{(4,4)}_{\vec{m},\vec{n}}}{|\eta^4|^2} + \left(|O_4O_4 - V_4V_4|^2 + |S_4C_4 - C_4S_4|^2\right) \left|\frac{2\eta}{\vartheta_2}\right|^4 \\
& + 16\left(|O_4S_4 + V_4C_4|^2 + |S_4V_4 + C_4O_4|^2\right) \left|\frac{\eta}{\vartheta_4}\right|^4 \\
& + 16\left(|O_4S_4 - V_4C_4|^2 + |S_4V_4 - C_4O_4|^2\right) \left|\frac{\eta}{\vartheta_3}\right|^4 \Bigg] \frac{\Lambda^{(2,2)}_{\vec{m}',(n_4,2n_5+1)}}{|\eta^4|^2} \\
- \Bigg[& \left((O_4O_4 + V_4V_4)(\bar{C}_4\bar{S}_4 + \bar{S}_4\bar{C}_4) + (C_4S_4 + S_4C_4)(\bar{O}_4\bar{O}_4 + \bar{V}_4\bar{V}_4)\right) \frac{\Lambda^{(4,4)}_{\vec{m},\vec{n}}}{|\eta^4|^2}
\end{aligned}
\tag{B.1.1}
$$

$$
\begin{aligned}
&+\Big((O_4O_4-V_4V_4)(\bar S_4\bar C_4-\bar C_4\bar S_4)+(S_4C_4-C_4S_4)(\bar O_4\bar O_4-\bar V_4\bar V_4)\Big)\left|\frac{2\eta}{\vartheta_2}\right|^4\\
&+16\Big((O_4S_4+V_4C_4)(\bar S_4\bar V_4+\bar C_4\bar O_4)+(S_4V_4+C_4O_4)(\bar O_4\bar S_4+\bar V_4\bar C_4)\Big)\left|\frac{\eta}{\vartheta_4}\right|^4\\
&+16\Big((O_4S_4-V_4C_4)(\bar S_4\bar V_4-\bar C_4\bar O_4)+(S_4V_4-C_4O_4)(\bar O_4\bar S_4-\bar V_4\bar C_4)\Big)\left|\frac{\eta}{\vartheta_3}\right|^4\Big]\frac{\Lambda^{(2,2)}_{\vec m'+\vec a'_{\rm S},(n_4,2n_5+1)}}{|\eta^4|^2}\Bigg\}\ .
\end{aligned}
$$

The sums over the momentum and winding numbers are implicit, as usual in this thesis.

Appendix B.2: Conventions of matrix actions on Chan–Paton indices

In [160], the actions of the group elements $G\in\{1,g,\Omega,\Omega g\}$ on the Dirichlet or Neumann Chan–Paton indices $\alpha\in\{1,\dots,32\}$ are always represented by 32×32 matrices. If needed, they define traces with an index I (that would be denoted i in our notations) labelling a fixed point of $T^4/\mathbb{Z}_2$ to indicate when they restrict to the matrix entries associated with the fixed point I (see their Eq. (2.22)). In our conventions, we work directly with smaller matrices, one for each fixed point ii' of $\tilde T^2\times T^4/\mathbb{Z}_2$ or $\tilde T^2\times\tilde T^4/\mathbb{Z}_2$, which are submatrices of those used in [160]. In this appendix, we give a detailed correspondence between their notations and ours for the traces appearing in the open-string one-loop amplitudes.

Let us focus on the matrices acting on the Neumann Chan–Paton factors. In order to avoid any ambiguity, we first define the sets of indices $\mathcal{H}_{ii'}$ associated with the fixed points ii' that are used to generate the submatrices from the big ones. To this end, we label the fixed points in lexicographical order, $(11,12,13,14,21,\dots)$, and introduce a function $p(i,i')$ that gives the predecessor in this list,

$$
p(i,i')=\begin{cases} i,i'-1 & \text{if } i'\in\{2,3,4\}\\ i-1,4 & \text{if } i'=1\end{cases}\ . \tag{B.2.1}
$$

The sets are then

$$
\mathcal{H}_{11}=\begin{cases}\varnothing & \text{if } N_{11}=0\\ \{1,\dots,\frac{N_{11}}{2}\}\cup\{17,\dots,16+\frac{N_{11}}{2}\} & \text{if } N_{11}\neq0\end{cases}\ . \tag{B.2.2}
$$

and for $ii'\neq11$,

$$
\mathcal{H}_{ii'}=\begin{cases}\varnothing & \text{if } N_{ii'}=0\\ \left\{\frac{N_{p(i,i')}}{2}+1,\dots,\frac{N_{p(i,i')}}{2}+\frac{N_{ii'}}{2}\right\}\cup\left\{\frac{N_{p(i,i')}}{2}+17,\dots,16+\frac{N_{p(i,i')}}{2}+\frac{N_{ii'}}{2}\right\} & \text{if } N_{ii'}\neq0\end{cases}\ . \tag{B.2.3}
$$

Our $N_{ii'}\times N_{ii'}$ matrices $\gamma^{ii'}_{\mathrm{N},G}$ are formed from 32×32 matrices $\gamma_{\mathrm{N},G}$ as follows,

$$
\gamma^{ii'}_{\mathrm{N},G}=\gamma_{\mathrm{N},G}|_{\mathcal{H}_{ii'}}\ , \tag{B.2.4}
$$

where the notation in the right-hand side means that we form submatrices by keeping the rows and columns $\alpha\in\mathcal{H}_{ii'}$. The traces of 32×32 matrices can then be expressed as

$$
\begin{aligned}
\mathrm{tr}(\gamma_{\mathrm{N},G})&=\sum_{\alpha=1}^{32}(\gamma_{\mathrm{N},G})_{\alpha\alpha}=\sum_{i,i'}\sum_{\alpha\in\mathcal{H}_{ii'}}(\gamma_{\mathrm{N},G})_{\alpha\alpha}=\sum_{i,i'}\mathrm{tr}(\gamma_{\mathrm{N},G}|_{\mathcal{H}_{ii'}})\\
&=\sum_{i,i'}\mathrm{tr}(\gamma^{ii'}_{\mathrm{N},G})\ ,
\end{aligned} \tag{B.2.5}
$$

and similarly for the matrices associated with the Dirichlet sector.

Moreover, in order to justify the replacement (3.1.15), let us define in our notations the 32×32 matrix $\mathcal{W}_j$ that is denoted W_I and appears in Eq. (2.22) of [160],

$$\mathcal{W}_j = \prod_{I=6}^{9} \mathcal{W}_I^{2a_j^I} \ , \quad \text{where} \quad \mathcal{W}_I = I_2 \otimes \begin{pmatrix} e^{2i\pi a_1^I} I_{\frac{N_1}{2}} & & 0 \\ & \ddots & \\ 0 & & e^{2i\pi a_{16}^I} I_{\frac{N_{16}}{2}} \end{pmatrix}, \quad N_i \equiv \sum_{i'} N_{ii'} \ . \tag{B.2.6}$$

For $G = g$ we have to compute

$$\begin{aligned} \mathrm{tr}(\mathcal{W}_j \gamma_{\mathrm{N},g}) &= \sum_{\alpha=1}^{32} (\mathcal{W}_j \gamma_{\mathrm{N},g})_{\alpha\alpha} = \sum_{\alpha=1}^{32} \sum_{\beta=1}^{32} (\mathcal{W}_j)_{\alpha\beta} (\gamma_{\mathrm{N},g})_{\beta\alpha} = \sum_{\alpha=1}^{32} (\mathcal{W}_j)_{\alpha\alpha} (\gamma_{\mathrm{N},g})_{\alpha\alpha} \\ &= \sum_{i,i'} \sum_{\alpha \in \mathcal{H}_{ii'}} (\mathcal{W}_j)_{\alpha\alpha} (\gamma_{\mathrm{N},g})_{\alpha\alpha} = \sum_{i,i'} e^{4i\pi \vec{a}_i \cdot \vec{a}_j} \sum_{\alpha \in \mathcal{H}_{ii'}} (\gamma_{\mathrm{N},g})_{\alpha\alpha} \\ &= \sum_{i,i'} e^{4i\pi \vec{a}_i \cdot \vec{a}_j} \mathrm{tr}(\gamma_{\mathrm{N},g}^{ii'}) \ . \end{aligned} \tag{B.2.7}$$

In this derivation, we have used the fact that the matrix $\mathcal{W}_j$ is diagonal and that its components $\alpha\alpha$ for $\alpha \in \mathcal{H}_{ii'}$ are $e^{4i\pi \vec{a}_i \cdot \vec{a}_j}$.

Appendix B.3: One-loop potential

In this section, we express the one-loop potential of the model for arbitrary deformations in a regime where the Scherk–Schwarz radius is large and where there is no mass scale lower than the supersymmetry-breaking scale. The final result is meant to be developed up to quadratic order in order to determine the masses of the Wilson lines.

In terms of arbitrary D3-branes positions (not necessarily independent) $2\pi a_\alpha^{\mathcal{I}}$ (for original D9-branes) and $2\pi b_\alpha^{\mathcal{I}}$ (for original D5-branes), $\alpha \in \{1, \ldots, 32\}$, the annulus and Möbius strip one-loop amplitudes are numerically

$$\begin{aligned} \mathcal{A} = \frac{1}{4} \int_0^{+\infty} \frac{\mathrm{d}\tau_2}{\tau_2^3} \sum_{\alpha,\beta} \sum_{\vec{m}'} \Bigg\{ & \frac{(V_4 O_4 + O_4 V_4)}{\eta^8} \left(P^{(4)}_{\vec{m}+\vec{a}_\alpha-\vec{a}_\beta} P^{(2)}_{\vec{m}'+\vec{a}'_\alpha-\vec{a}'_\beta} + W^{(4)}_{\vec{n}+\vec{b}_\alpha-\vec{b}_\beta} P^{(2)}_{\vec{m}'+\vec{b}'_\alpha-\vec{b}'_\beta} \right) \\ & + 2(O_4 C_4 + V_4 S_4) \left(\frac{\eta}{\vartheta_4} \right)^2 \frac{P^{(2)}_{\vec{m}'+\vec{a}'_\alpha-\vec{b}'_\beta}}{\eta^4} \\ & - \Bigg[\frac{(S_4 S_4 + C_4 C_4)}{\eta^8} \left(P^{(4)}_{\vec{m}+\vec{a}_\alpha-\vec{a}_\beta} P^{(2)}_{\vec{m}'+\vec{a}'_{\mathrm{S}}+\vec{a}'_\alpha-\vec{a}'_\beta} + W^{(4)}_{\vec{n}+\vec{b}_\alpha-\vec{b}_\beta} P^{(2)}_{\vec{m}'+\vec{a}'_{\mathrm{S}}+\vec{b}'_\alpha-\vec{b}'_\beta} \right) \\ & + 2(S_4 O_4 + C_4 V_4) \left(\frac{\eta}{\vartheta_4} \right)^2 \frac{P^{(2)}_{\vec{m}'+\vec{a}'_{\mathrm{S}}+\vec{a}'_\alpha-\vec{b}'_\beta}}{\eta^4} \Bigg] \Bigg\} \ . \end{aligned} \tag{B.3.1}$$

and

$$\begin{aligned} \mathcal{M} = -\frac{1}{4} \int_0^{+\infty} \frac{\mathrm{d}\tau_2}{\tau_2^3} \sum_{\alpha} \sum_{\vec{m}'} \Bigg\{ & \frac{(\hat{V}_4 \hat{O}_4 + \hat{O}_4 \hat{V}_4)}{\hat{\eta}^8} \left(P^{(4)}_{\vec{m}+2\vec{a}_\alpha} P^{(2)}_{\vec{m}'+2\vec{a}'_\alpha} + W^{(4)}_{\vec{n}+2\vec{b}_\alpha} P^{(2)}_{\vec{m}'+2\vec{b}'_\alpha} \right) \\ & - \frac{(\hat{C}_4 \hat{C}_4 + \hat{S}_4 \hat{S}_4)}{\hat{\eta}^8} \left(P^{(4)}_{\vec{m}+2\vec{a}_\alpha} P^{(2)}_{\vec{m}'+\vec{a}'_{\mathrm{S}}+2\vec{a}'_\alpha} + W^{(4)}_{\vec{n}+2\vec{b}_\alpha} P^{(2)}_{\vec{m}'+\vec{a}'_{\mathrm{S}}+2\vec{b}'_\alpha} \right) \Bigg\} \ . \end{aligned} \tag{B.3.2}$$

The characters are expanded like

$$\begin{aligned}
&\frac{V_4O_4+O_4V_4}{\eta^8}=\frac{C_4C_4+S_4S_4}{\eta^8}=8\sum_{k\geq 0}c_k e^{-\pi k\tau_2}\ ,\\
&\frac{\hat{V}_4\hat{O}_4+\hat{O}_4\hat{V}_4}{\hat{\eta}^8}=\frac{\hat{C}_4\hat{C}_4+\hat{S}_4\hat{S}_4}{\hat{\eta}^8}=8\sum_{k\geq 0}(-1)^k c_k e^{-\pi k\tau_2}\ ,\\
&2(O_4C_4+V_4S_4)\left(\frac{\eta}{\vartheta_4}\right)^2\frac{1}{\eta^4}=2(S_4O_4+C_4V_4)\left(\frac{\eta}{\vartheta_4}\right)^2\frac{1}{\eta^4}=4\sum_{k\geq 0}d_k e^{-\frac{\pi}{2}k\tau_2}\ ,
\end{aligned}\tag{B.3.3}$$

where $c_0=d_0=1$, to yield

$$\begin{aligned}
\mathcal{A}=2\int_0^{+\infty}\frac{\mathrm{d}\tau_2}{\tau_2^3}\sum_{k\geq 0}\sum_{\alpha,\beta}\sum_{\vec{m}'}\Bigg\{c_k e^{-\pi k\tau_2}\Bigg[\sum_{\vec{m}}P^{(4)}_{\vec{m}+\vec{a}_\alpha-\vec{a}_\beta}\left(P^{(2)}_{\vec{m}'+\vec{a}'_\alpha-\vec{a}'_\beta}-P^{(2)}_{\vec{m}'+\vec{a}'_{\mathrm{S}}+\vec{a}'_\alpha-\vec{a}'_\beta}\right)\\
+\sum_{\vec{n}}W^{(4)}_{\vec{n}+\vec{b}_\alpha-\vec{b}_\beta}\left(P^{(2)}_{\vec{m}'+\vec{b}'_\alpha-\vec{b}'_\beta}-P^{(2)}_{\vec{m}'+\vec{a}'_{\mathrm{S}}+\vec{b}'_\alpha-\vec{b}'_\beta}\right)\Bigg]\\
+d_k e^{-\frac{\pi}{2}k\tau_2}\left(P^{(2)}_{\vec{m}'+\vec{a}'_\alpha-\vec{b}'_\beta}-P^{(2)}_{\vec{m}'+\vec{a}'_{\mathrm{S}}+\vec{a}'_\alpha-\vec{b}'_\beta}\right)\Bigg\}\ ,
\end{aligned}\tag{B.3.4}$$

and

$$\begin{aligned}
\mathcal{M}=-2\int_0^{+\infty}\frac{\mathrm{d}\tau_2}{\tau_2^3}\sum_{k\geq 0}\sum_{\alpha}\sum_{\vec{m}'}\Bigg\{(-1)^k c_k\Bigg[\sum_{\vec{m}}P^{(4)}_{\vec{m}+2\vec{a}_\alpha}\left(P^{(2)}_{\vec{m}'+2\vec{a}'_\alpha}-P^{(2)}_{\vec{m}'+\vec{a}'_{\mathrm{S}}+2\vec{a}'_\alpha}\right)\\
+\sum_{\vec{n}}W^{(4)}_{\vec{n}+2\vec{b}_\alpha}\left(P^{(2)}_{\vec{m}'+2\vec{b}'_\alpha}-P^{(2)}_{\vec{m}'+\vec{a}'_{\mathrm{S}}+2\vec{b}'_\alpha}\right)\Bigg]\Bigg\}\ .
\end{aligned}\tag{B.3.5}$$

In the regime (3.1.34) we are interested in, a Poisson summation over the index m_5 which becomes l_5 is useful. The amplitudes become

$$\begin{aligned}
\mathcal{A}=&\left(G^{55}\right)^2\frac{\Gamma\left(\frac{5}{2}\right)}{\pi^{\frac{5}{2}}}4\sum_{k\geq 0}\sum_{\alpha,\beta}\sum_{m_4}\sum_{l_5}\frac{1}{|2l_5+1|^5}\\
&\Bigg\{\sum_{\vec{m}}c_k\cos\left[2\pi|2l_5+1|\left(a^5_\alpha-a^5_\beta+\frac{G^{54}}{G^{55}}(m_4+a^4_\alpha-a^4_\beta)\right)\right]\mathcal{H}_{\frac{5}{2}}\left(\pi|2l_5+1|\frac{\mathcal{M}_{\mathcal{A}_1}}{\sqrt{G^{55}}}\right)\\
&+\sum_{\vec{n}}c_k\cos\left[2\pi|2l_5+1|\left(b^5_\alpha-b^5_\beta+\frac{G^{54}}{G^{55}}(m_4+b^4_\alpha-b^4_\beta)\right)\right]\mathcal{H}_{\frac{5}{2}}\left(\pi|2l_5+1|\frac{\mathcal{M}_{\mathcal{A}_2}}{\sqrt{G^{55}}}\right)\\
&+\frac{d_k}{2}\cos\left[2\pi|2l_5+1|\left(a^5_\alpha-b^5_\beta+\frac{G^{54}}{G^{55}}(m_4+a^4_\alpha-b^4_\beta)\right)\right]\mathcal{H}_{\frac{5}{2}}\left(\pi|2l_5+1|\frac{\mathcal{M}_{\mathcal{A}_3}}{\sqrt{G^{55}}}\right)\Bigg\}\ ,
\end{aligned}\tag{B.3.6}$$

and

$$\begin{aligned}
\mathcal{M}=&-\left(G^{55}\right)^2\frac{\Gamma\left(\frac{5}{2}\right)}{\pi^{\frac{5}{2}}}4\sum_{k\geq 0}(-1)^k c_k\sum_{\alpha}\sum_{m_4}\sum_{l_5}\frac{1}{|2l_5+1|^5}\\
&\Bigg\{\sum_{\vec{m}}\cos\left[2\pi|2l_5+1|\left(2a^5_\alpha+\frac{G^{54}}{G^{55}}(m_4+2a^4_\alpha)\right)\right]\mathcal{H}_{\frac{5}{2}}\left(\pi|2l_5+1|\frac{\mathcal{M}_{\mathcal{M}_1}}{\sqrt{G^{55}}}\right)\\
&+\sum_{\vec{n}}\cos\left[2\pi|2l_5+1|\left(2b^5_\alpha+\frac{G^{54}}{G^{55}}(m_4+2b^4_\alpha)\right)\right]\mathcal{H}_{\frac{5}{2}}\left(\pi|2l_5+1|\frac{\mathcal{M}_{\mathcal{M}_2}}{\sqrt{G^{55}}}\right)\Bigg\}\ ,
\end{aligned}\tag{B.3.7}$$

where the function $\mathcal{H}_\nu$ is expressed in terms of the modified Bessel function K_ν:

$$\mathcal{H}_\nu(z) = \frac{1}{\Gamma(\nu)} \int_0^{+\infty} \frac{dx}{x^{1+\nu}}\, e^{-\frac{1}{x} - z^2 x} = \frac{2}{\Gamma(\nu)}\, z^\nu K_\nu(2z) \ , \tag{B.3.8}$$

whose arguments are given by characteristic mass scales $\mathcal{M}_{\mathcal{A}_1}$, $\mathcal{M}_{\mathcal{A}_2}$, $\mathcal{M}_{\mathcal{A}_3}$ and $\mathcal{M}_{\mathcal{M}_1}$, $\mathcal{M}_{\mathcal{M}_2}$ which depend on the sector (NN, DD or ND and DN).

In the annulus, we have

$$\begin{aligned}
\mathcal{M}^2_{\mathcal{A}_1} &= (m_I + a^I_\alpha - a^I_\beta) G^{IJ} (m_J + a^J_\alpha - a^J_\beta) + (m_4 + a^4_\alpha - a^4_\beta)^2 \hat{G}^{44} + k \ , \\
\mathcal{M}^2_{\mathcal{A}_2} &= (n_I + b^I_\alpha - b^I_\beta) G_{IJ} (n_J + b^J_\alpha - b^J_\beta) + (m_4 + b^4_\alpha - b^4_\beta)^2 \hat{G}^{44} + k \ , \\
\mathcal{M}^2_{\mathcal{A}_3} &= (m_4 + a^4_\alpha - b^4_\beta)^2 \hat{G}^{44} + \frac{k}{2} \ ,
\end{aligned} \tag{B.3.9}$$

where $\hat{G}^{44} = G^{44} - \frac{G^{45}}{G^{55}}\, G^{55}\, \frac{G^{54}}{G^{55}}$. With the decomposition of the Wilson lines into fluctuations around fixed points displayed in (3.1.33), the characteristic masses (B.3.9) are either of order one, yielding exponentially suppressed corrections, or proportional to the fluctuations and thus contributing significantly to the result. The non-suppressed contributions arise for $k = 0$, $\vec{m} = \vec{0}$, $m_4 = 0$ and specific values of α and β depending on the characteristic mass under considerations. We denote the sets of couples (α, β) for which $\mathcal{M}_{\mathcal{A}_1}$, $\mathcal{M}_{\mathcal{A}_2}$ and $\mathcal{M}_{\mathcal{A}_3}$ yield non-suppressed contributions respectively by $L_{\rm NN}$, $L_{\rm DD}$ and $L_{\rm ND}$.

The set $L_{\rm NN}$ is such that the D3-branes α, β T-dual to D9-branes

- belong to the same stack of $N_{ii'}$ branes, $i = 1, \ldots, 16$, $i' = 1, \ldots, 4$,
- or belong respectively to stacks of $N_{i,2i''-1}$ and $N_{i,2i''}$ branes, $i = 1, \ldots, 16$, $i'' = 1, 2$,
- or belong respectively to stacks of $N_{i,2i''}$ and $N_{i,2i''-1}$ branes, $i = 1, \ldots, 16$, $i'' = 1, 2$.

The set $L_{\rm DD}$ is such that the D3-branes α, β T-dual to D5-branes

- belong to the same stack of $D_{ii'}$ branes, $i = 1, \ldots, 16$, $i' = 1, \ldots, 4$,
- or belong respectively to stacks of $D_{i,2i''-1}$ and $D_{i,2i''}$ branes, $i = 1, \ldots, 16$, $i'' = 1, 2$,
- or belong respectively to stacks of $D_{i,2i''}$ and $D_{i,2i''-1}$ branes, $i = 1, \ldots, 16$, $i'' = 1, 2$.

The set $L_{\rm ND}$ such that the D3-branes α, β T-dual to a D9-brane and a D5-brane

- belong respectively to stacks of $N_{ii'}$ and $D_{ji'}$ branes, $i, j = 1, \ldots, 16$, $i' = 1, \ldots, 4$,
- or belong respectively to stacks of $N_{i,2i''-1}$ and $D_{j,2i''}$ branes, $i, j = 1, \ldots, 16$, $i'' = 1, 2$,
- or belong respectively to stacks of $N_{j,2i''}$ and $D_{i,2i''-1}$ branes, $i, j = 1, \ldots, 16$, $i'' = 1, 2$.

Similarly, the characteristic masses involved in the Möbius are

$$\begin{aligned}
\mathcal{M}^2_{\mathcal{M}_1} &= (m_I + 2a^I_\alpha) G^{IJ} (m_J + 2a^J_\alpha) + (m_4 + 2a^4_\alpha)^2 \hat{G}^{44} + k \ , \\
\mathcal{M}^2_{\mathcal{M}_2} &= (n_I + 2b^I_\alpha) G_{IJ} (n_J + 2b^J_\alpha) + (m_4 + 2b^4_\alpha)^2 \hat{G}^{44} + k \ ,
\end{aligned} \tag{B.3.10}$$

and yield non-suppressed terms when $k = 0$, $m_I = -2\langle a^I_\alpha \rangle$, $m_4 = -2\langle a^4_\alpha \rangle$, or $n_I = -2\langle b^I_\alpha \rangle$, $m_4 = -2\langle b^4_\alpha \rangle$.

The closed-sector contribution to the one-loop effective $\mathcal{V}_{\text{1-loop}}$ defined as

$$\mathcal{V}_{\text{1-loop}} \equiv -\frac{M_{\text{s}}^4}{2(2\pi)^4}\left(\mathcal{T}+\mathcal{K}+\mathcal{A}+\mathcal{M}\right) , \tag{B.3.11}$$

is just $n_{\text{F}}^{\text{closed}} - n_{\text{B}}^{\text{closed}}$ up to exponentially suppressed terms. The end result can thus be written like

$$\mathcal{V}_{\text{1-loop}} = \frac{\Gamma\left(\frac{5}{2}\right)}{\pi^{\frac{13}{2}}} M^4 \sum_{l_5} \frac{\mathcal{N}_{2l_5+1}(\epsilon,\xi,G)}{|2l_5+1|^5} + \mathcal{O}\left((M_{\text{s}}M)^2 e^{-2\pi c\frac{M_{\text{s}}}{M}}\right) , \tag{B.3.12}$$

where

$$\mathcal{N}_{2l_5+1}(\epsilon,\xi,G) = n_{\text{F}}^{\text{closed}} - n_{\text{B}}^{\text{closed}} + \mathcal{N}_{2l_5+1}^{\text{open}}(\epsilon,\xi,G) , \tag{B.3.13}$$

and

$$\begin{aligned}
\mathcal{N}_{2l_5+1}^{\text{open}}(\epsilon,\xi,G) = 2\Bigg\{ & -\sum_{(\alpha,\beta)\in L_{\text{NN}}} (-)^F \cos\left[2\pi|2l_5+1|\frac{G^{5I'}}{G^{55}}\left(\epsilon_\alpha^{I'}-\epsilon_\beta^{I'}\right)\right] \\
& \qquad \times \mathcal{H}_{\frac{5}{2}}\left(\pi|2l_5+1|\frac{\left[(\epsilon_\alpha^I-\epsilon_\beta^I)G^{IJ}(\epsilon_\alpha^J-\epsilon_\beta^J)+(\epsilon_\alpha^4-\epsilon_\beta^4)^2\hat{G}^{44}\right]^{\frac{1}{2}}}{\sqrt{G^{55}}}\right) \\
& -\sum_{(\alpha,\beta)\in L_{\text{DD}}} (-)^F \cos\left[2\pi|2l_5+1|\frac{G^{5I'}}{G^{55}}\left(\xi_\alpha^{I'}-\xi_\beta^{I'}\right)\right] \\
& \qquad \times \mathcal{H}_{\frac{5}{2}}\left(\pi|2l_5+1|\frac{\left[(\xi_\alpha^I-\xi_\beta^I)G_{IJ}(\xi_\alpha^J-\xi_\beta^J)+(\xi_\alpha^4-\xi_\beta^4)^2\hat{G}^{44}\right]^{\frac{1}{2}}}{\sqrt{G^{55}}}\right) \\
& -\frac{1}{2}\sum_{(\alpha,\beta)\in L_{\text{ND}}} (-)^F \cos\left[2\pi|2l_5+1|\frac{G^{5I'}}{G^{55}}\left(\epsilon_\alpha^{I'}-\xi_\beta^{I'}\right)\right] \mathcal{H}_{\frac{5}{2}}\left(\pi|2l_5+1|\frac{\left[(\epsilon_\alpha^4-\xi_\beta^4)^2\hat{G}^{44}\right]^{\frac{1}{2}}}{\sqrt{G^{55}}}\right) \\
& +\sum_\alpha \cos\left[4\pi|2l_5+1|\frac{G^{5I'}}{G^{55}}\epsilon_\alpha^{I'}\right] \mathcal{H}_{\frac{5}{2}}\left(2\pi|2l_5+1|\frac{\left[\epsilon_\alpha^I G^{IJ}\epsilon_\alpha^J+\left(\epsilon_\alpha^4\right)^2\hat{G}^{44}\right]^{\frac{1}{2}}}{\sqrt{G^{55}}}\right) \\
& +\sum_\alpha \cos\left[4\pi|2l_5+1|\frac{G^{5I'}}{G^{55}}\xi_\alpha^{I'}\right] \mathcal{H}_{\frac{5}{2}}\left(2\pi|2l_5+1|\frac{\left[\xi_\alpha^I G_{IJ}\xi_\alpha^J+\left(\xi_\alpha^4\right)^2\hat{G}^{44}\right]^{\frac{1}{2}}}{\sqrt{G^{55}}}\right)\Bigg\} .
\end{aligned} \tag{B.3.14}$$

C | Two-point functions of Neumann–Dirichlet states at one loop

Appendix C.1: Twist-field technology

In [167], the authors derive arbitrary genus-g correlators of an arbitrary product of twist fields associated with a $\mathbb{Z}_N$ orbifold. Here, we first give some definitions and then explain the followed strategy in [167] to derive the correlators. We end by showing the result for our case of interest *i.e.* for a genus-1 Riemann surface.

C.1.1 Definitions

The twist fields $\sigma_\kappa(z,\bar{z})$ create ground states in the κ-th twisted sector of the orbifold with $\kappa \in \{1,\dots,N-1\}$. It is useful to define a new complex basis for the bosonic fields $X^\mu(z,\bar{z})$, $\mu \in \{0,\dots,9\}$ as follows:

$$Z^u(z,\bar{z}) \equiv \frac{X^{2u}+iX^{2u+1}}{\sqrt{2}} \quad \text{and} \quad \overline{Z}^u(z,\bar{z}) \equiv \frac{X^{2u}-iX^{2u+1}}{\sqrt{2}}\,, \quad u \in \{0,\dots,4\}\,. \tag{C.1.1}$$

To make contact with our setup, we will assume a six-dimensional model, compactified on $T^4/\mathbb{Z}_N$ along directions X^6, X^7, X^8, X^9. The twist fields $\sigma_\kappa(z,\bar{z})$ thus decompose into the complex directions $u \in \{3,4\}$. From now on, we only focus on one given direction u and twist fields along this direction $\sigma^u_\kappa(z,\bar{z})$. The OPE's between the derivative fields $\partial Z^u(z)$ and $\partial\overline{Z}^u(z)$ (and $\bar{\partial}Z^u(\bar{z})$ and $\bar{\partial}\overline{Z}^u(\bar{z})$) are determined by the annihilations of the twisted ground states by the positive frequency modes of the coordinates:

$$\begin{aligned}
\partial Z^u(z)\sigma^u_\kappa(w,\bar{w}) &\underset{z\to w}{\sim} (z-w)^{-(1-\kappa/N)}\,\tau^u_\kappa(w,\bar{w}) &&+\text{finite}\,,\\
\partial \bar{Z}^u(z)\sigma^u_\kappa(w,\bar{w}) &\underset{z\to w}{\sim} (z-w)^{-\kappa/N}\,\tau'^u_\kappa(w,\bar{w}) &&+\text{finite}\,,\\
\bar{\partial} Z^u(\bar{z})\sigma^u_\kappa(w,\bar{w}) &\underset{\bar{z}\to \bar{w}}{\sim} (\bar{z}-\bar{w})^{-\kappa/N}\,\tilde{\tau}^u_\kappa(w,\bar{w}) &&+\text{finite}\,,\\
\bar{\partial}\bar{Z}^u(\bar{z})\sigma^u_\kappa(w,\bar{w}) &\underset{\bar{z}\to \bar{w}}{\sim} (\bar{z}-\bar{w})^{-(1-\kappa/N)}\,\tilde{\tau}'^u_\kappa(w,\bar{w}) &&+\text{finite}\,.
\end{aligned} \tag{C.1.2}$$

The fields τ^u_κ, τ'^u_κ, $\tilde{\tau}^u_\kappa$ and $\tilde{\tau}'^u_\kappa$ appearing in the right-hand sides create excited states in the κ-th twisted sector of the Hilbert space. These OPE's capture the local behaviour of the coordinate Z^u which undergoes a $\mathbb{Z}_N$ rotation $Z^u \longrightarrow e^{2i\pi\kappa/N}Z^u$ upon parallel transport. However, they are blind to the translation $Z^u \longrightarrow Z^u + v^u$ induced by the transport where v^u is a displacement vector implementing the periodicity along internal direction u. This data is recovered by imposing *global monodromy conditions* which describe how the coordinates change when they are carried around a

set of twist fields $\sigma^u_{\kappa_i}(z,\bar z)$, $i\in\{1,\dots,n\}$ with vanishing total twist *i.e.* with $\sum_{i=1}^n\kappa_i=0 \bmod N$, following a loop γ:

$$\oint_\gamma \mathrm{d}z\partial Z^u+\oint_\gamma \mathrm{d}\bar z\bar\partial Z=v^u_\gamma\ . \tag{C.1.3}$$

If we split the coordinates into a classical background $Z_{\rm cl}$ and quantum fluctuations $Z_{\rm qu}$ like

$$Z^u(z,\bar z)\equiv Z^u_{\rm cl}(z,\bar z)+Z^u_{\rm qu}(z,\bar z)\ , \tag{C.1.4}$$

then the displacement only arises from the classical part and the global monodromy condition for $Z_{\rm qu}$ is trivial.

The correlator of $L\geq 2$ twist fields $\sigma_{\kappa_A}(z_A,\bar z_A)$, $A\in\{1,\dots,L\}$ with zero net twist *i.e.* with $\sum_{A=1}^L\kappa_A=0 \bmod N$ on a Riemann surface R of genus $g\geq 0$ takes the form

$$\left\langle\prod_{A=1}^L\sigma_{\kappa_A}(z_A,\bar z_A)\right\rangle=\sum_{Z_{\rm cl}}e^{-S^R_{\rm cl}}\prod_{u=3}^4\left\langle\prod_{A=1}^L\sigma^u_{\kappa_A}(z_A,\bar z_A)\right\rangle_{\rm qu}\ , \tag{C.1.5}$$

where for each instanton $Z_{\rm cl}$, the classical worldsheet action $S^R_{\rm cl}$ is

$$S^R_{\rm cl}=\frac{i}{2\pi\alpha'}\int_R\mathrm{d}z\wedge\mathrm{d}\bar z\sum_{u=3}^4\left(\partial Z^u_{\rm cl}\bar\partial\overline{Z}^u_{\rm cl}+\partial\overline{Z}^u_{\rm cl}\bar\partial Z^u_{\rm cl}\right)\ . \tag{C.1.6}$$

C.1.2 Stress-tensor method

For a given u, the quantum part of the correlator $\left\langle\prod_{A=1}^L\sigma^u_{\kappa_A}(z_A,\bar z_A)\right\rangle_{\rm qu}$ is found using the *stress-tensor method*. The idea is to exploit the form of the OPE's between the stress tensor $T^u(z)$ and primary fields. For twist fields $\sigma_{\kappa_A}(z_A,\bar z_A)$ with conformal weight $h_A=\frac12\frac{\kappa_A}{N}(1-\frac{\kappa_A}{N})$, the OPE is

$$T^u(z)\sigma^u_{\kappa_A}(z_A,\bar z_A)\underset{z\to z_A}{\sim}\frac{h_A}{(z-z_A)^2}\,\sigma^u_{\kappa_A}(z_A,\bar z_A)+\frac{1}{z-z_A}\,\partial_{z_A}\sigma^u_{\kappa_A}(z_A,\bar z_A)+\text{finite}\ . \tag{C.1.7}$$

The goal is to find a set of differential equations satisfied by the quantum part of the correlator. If one considers the quantity

$$\langle\langle T^u(z)\rangle\rangle\equiv\frac{\left\langle T^u(z)\prod_A\sigma^u_{\kappa_A}(z_A,\bar z_A)\right\rangle_{\rm qu}}{\left\langle\prod_A\sigma^u_{\kappa_A}(z_A,\bar z_A)\right\rangle_{\rm qu}}\ , \tag{C.1.8}$$

then, thanks to (C.1.7), a set of differential equations is found by subtracting the double pole of $\langle\langle T^u(z)\rangle\rangle$ when $z\to z_B$ for $B\in\{1,\dots,L\}$:

$$\partial_{z_B}\ln\Big\langle\prod_A\sigma^u_A(z_A,\bar z_A)\Big\rangle_{\rm qu}=\lim_{z\to z_B}\left[(z-z_B)\,\langle\langle T^u(z)\rangle\rangle-\frac{h_B}{(z-z_B)}\right]\ . \tag{C.1.9}$$

One thus needs to evaluate $\langle\langle T^u(z)\rangle\rangle$. For this, a useful OPE is

$$-\frac{1}{\alpha'}\,\partial Z^u_{\rm qu}(z)\,\partial\overline{Z}^u_{\rm qu}(w)\underset{z\to w}{\sim}\frac{1}{(z-w)^2}+T^u(w)+\mathcal{O}(z-w)\ . \tag{C.1.10}$$

Defining the *Green's function in presence of twist fields* $g(z,w)$ like

$$g(z,w)\equiv\frac{\langle-\partial Z^u_{\rm qu}(z)\,\partial\overline{Z}^u_{\rm qu}(w)\prod_A\sigma^u_{\kappa_A}(z_A,\bar z_A)\rangle_{\rm qu}}{\alpha'\,\langle\prod_A\sigma^u_{\kappa_A}(z_A,\bar z_A)\rangle_{\rm qu}}\ , \tag{C.1.11}$$

then the quantity $\langle\langle T^u(z)\rangle\rangle$ is given by subtracting the double pole of the Green's function,

$$\langle\langle T^u(z)\rangle\rangle = \lim_{w\to z}\left[g(z,w) - \frac{1}{(z-w)^2}\right] . \tag{C.1.12}$$

The starting point of the method is thus to evaluate the Green's function in presence of twist fields (C.1.11). This is done by writing the most general possible formula with the appropriate local and global behaviours. Once the expression is obtained, $\langle\langle T^u(z)\rangle\rangle$ is deduced and from it, a set of differential equations is found. Eventually, the final result is obtained by solving these differential equations.

C.1.3 Genus-1 result: Quantum correlator

Let us review the process for the correlator at one loop where the Riemann surface R is simply a torus of Teichmüller parameter denoted[1] τ^{dc}. As mentioned above, the first step consists in writing the most general expression for the Green's function in presence of twist fields (C.1.11) as well as for the *auxiliary Green's function* $h(\bar z, w)$ defined as

$$h(\bar z, w) \equiv \frac{\langle -\bar\partial Z^u_{\mathrm{qu}}(\bar z)\,\partial\overline{Z}^u_{\mathrm{qu}}(w)\prod_A \sigma^u_{\kappa_A}(z_A,\bar z_A)\rangle_{\mathrm{qu}}}{\alpha'\,\langle\prod_A \sigma^u_{\kappa_A}(z_A,\bar z_A)\rangle_{\mathrm{qu}}} . \tag{C.1.13}$$

The expressions $g(z,w)$ and $h(\bar z,w)$ must be doubly periodic on the torus. This means that they should be invariant under $z\to z+1$ and $z\to z+\tau^{\mathrm{dc}}$ (or $\bar z\to\bar z+1$ and $\bar z\to\bar z+\tau^{\mathrm{dc}}$ for h) and $w\to w+1$ and $w\to w+\tau^{\mathrm{dc}}$. They should also have the correct behaviours dictated by (C.1.2) when z (or $\bar z$) and w tend to the z_A's (or $\bar z_A$'s). From (C.1.10), we see that g should have a double pole when $z\to w$ and the OPE $\bar\partial Z^u_{\mathrm{qu}}(\bar z)\,\partial\overline{Z}^u_{\mathrm{qu}}(w) \underset{z\to w}{\sim}$ finite imposes finiteness of h when $z\to w$. Moreover, g and h must be consistent with the trivial global monodromy condition for Z_{qu}.

To satisfy the local behaviours, the authors of [167] define a basis of L holomorphic one-forms on the torus with appropriate local properties called *cut differentials* and express g and h in this basis. To proceed, we define

$$M \equiv \sum_{A=1}^{L}\frac{\kappa_A}{N} , \tag{C.1.14}$$

which is an integer taking values in the set $\{0,\dots,L-1\}$ (because the fields in the correlator have a zero net twist). Choosing arbitrarily two subsets $\{z_{\alpha_1},\dots,z_{\alpha_{L-M}}\}$ and $\{z_{\beta_1},\dots,z_{\beta_M}\}$ among the insertion points, the basis is given by the functions

$$\begin{aligned}
\omega^{\alpha_A}_{N-\kappa}(z) &= \gamma_{N-\kappa}(z)\,\vartheta_1(z-z_{\alpha_A}-y_{N-\kappa})\prod_{B\neq A}^{L-M}\vartheta_1(z-z_{\alpha_B}) , \quad A\in\{1,\dots,L-M\} ,\\
\omega^{\beta_A}_{\kappa}(z) &= \gamma_{\kappa}(z)\,\vartheta_1(z-z_{\beta_A}-y_{\kappa})\prod_{B\neq A}^{M}\vartheta_1(z-z_{\beta_B}) , \qquad A\in\{1,\dots,M\} ,
\end{aligned} \tag{C.1.15}$$

where

$$\gamma_{N-\kappa}(z)\equiv\prod_{A=1}^{L}\vartheta_1(z-z_A)^{-(1-\kappa_A/N)} , \qquad \gamma_{\kappa}(z)\equiv\prod_{A=1}^{L}\vartheta_1(z-z_A)^{-\kappa_A/N} , \tag{C.1.16}$$

[1] The superscript "dc" stands for "double cover". It will be useful later.

and

$$y_{N-\kappa} \equiv \sum_{A=1}^{L} \left(1 - \frac{k_A}{N}\right) z_A - \sum_{B=1}^{L-M} z_{\alpha_B} \,, \qquad y_\kappa \equiv \sum_{A=1}^{L} \frac{\kappa_A}{N} z_A - \sum_{B=1}^{M} z_{\beta_B} \,. \tag{C.1.17}$$

Note that the subscripts $N-\kappa$ and κ are just names and do not refer to varying indices. Using this basis is not enough for g to satisfy all local properties since the double pole when $z \to w$ must be handled separately. For this, we define the function $g_{\mathrm{s}}(z,w)$, doubly periodic on the torus in both variables and with the correct double-pole structure [167]:

$$g_s(z,w) \equiv \gamma_{N-\kappa}(z)\,\gamma_\kappa(w) \left(\frac{\vartheta_1'(0)}{\vartheta_1(z-w)}\right)^2 P(z,w) \,, \tag{C.1.18}$$

where the function $P(z,w)$, which must satisfy correct conditions, turns out not to appear in the final result so that an explicit knowledge of it is unnecessary. This function plays a role in the correlator of excited twist fields though, and we will need to have an explicit expression for it. This expression will be shown later in the particular case of interest for this thesis with only two twist fields in the correlator. The Green's functions can then generically be written in the basis of cut differentials with components C_{AB} and B_{AB} (they depend on τ^{dc} and on the insertion points) like

$$\begin{aligned} g(z,w) &= g_s(z,w) + \sum_{A=1}^{L-M}\sum_{B=1}^{M} C_{AB}\,\omega_{N-\kappa}^{\alpha_A}(z)\,\omega_\kappa^{\beta_B}(w) \,, \\ h(\bar z,w) &= \sum_{A=1}^{M}\sum_{B=1}^{M} B_{AB}\,\bar\omega_\kappa^{\beta_A}(\bar z)\,\omega_\kappa^{\beta_B}(w) \,, \end{aligned} \tag{C.1.19}$$

Only the global behaviour remains to be handled by consistency with the trivial monodromy condition for Z_{qu}. We can restrict to loops γ_a which form a basis of the homology group of the Riemann surface under considerations with L punctures. For a genus-g surface, the cardinal of such a basis is $L+2g-2$ [167] which gives L loops in the torus case. The conditions on g and h are thus

$$\oint_{\gamma_a} \mathrm{d}z\, g(z,w) + \oint_{\gamma_a} \mathrm{d}\bar z\, h(\bar z,w) = 0 \,, \quad a \in \{1,\dots,L\} \,. \tag{C.1.20}$$

It is convenient to define an $L \times L$ *cut-period matrix* ${W_a}^A$ like

$$\begin{aligned} {W_a}^A &\equiv \oint_{\gamma_a} \mathrm{d}z\,\omega_{N-\kappa}^{\alpha_A}(z) \,, \quad A \in \{1,\dots,L-M\} \,, \\ {W_a}^{L-M+A} &\equiv \oint_{\gamma_a} \mathrm{d}\bar z\,\bar\omega_\kappa^{\beta_A}(\bar z) \,, \qquad A \in \{1,\dots,M\} \,, \end{aligned} \tag{C.1.21}$$

from which the Green's functions, satisfying both local and global properties, can be written:

$$\begin{aligned} g(z,w) &= g_s(z,w) - \sum_{A=1}^{L-M} \omega_{N-\kappa}^{\alpha_A}(z) \sum_{a=1}^{L} {(W^{-1})_A}^a \oint_{\gamma_a} \mathrm{d}\zeta\, g_s(\zeta,w) \,, \\ h(\bar z,w) &= -\sum_{A=1}^{M} \omega_\kappa^{\beta_A}(\bar z) \sum_{a=1}^{L} {(W^{-1})_{L-M+A}}^a \oint_{\gamma_a} \mathrm{d}\zeta\, g_s(\zeta,w) \,. \end{aligned} \tag{C.1.22}$$

Finding these explicit expressions for the Green's function is the first step of the stress-tensor method. From them, $\langle\langle T^u(z)\rangle\rangle$ can be derived to be ready to express the differential equations.

It turns out that the equations involving the derivative of the correlator with respect to insertion points that are in the subset $\{z_{\alpha_1},\dots,z_{\alpha_{L-M}}\}$ are easier to determine. Moreover, the function $P(z,w)$ can be eliminated from those differential equations. After integration of this subset of differential equations, it can be shown that the result actually contains the full dependence on all the insertion points so that considering the remaining equations is unnecessary. The last step consists in performing the exact same computations using the Green's functions $\bar{g}(\bar{z},\bar{w})$ and $\bar{h}(z,\bar{w})$ to find the antiholomorphic dependence of the correlator. For a given complex direction $u\in\{3,4\}$, the final result is [167]

$$\begin{aligned}\left\langle\prod_{A=1}^{L}\sigma_{\kappa_A}^{u}(z_A,\bar{z}_A)\right\rangle_{\text{qu}} &= f(\tau^{\text{dc}};\kappa_1,\dots,\kappa_L)\,\frac{1}{\det W}\,\vartheta_1(y_{N-\kappa})^{L-M-1}\,\overline{\vartheta_1(y_\kappa)}^{M-1}\\ &\times\prod_{\substack{A,B=1\\A<B}}^{L-M}\vartheta_1(z_{\alpha_A}-z_{\alpha_B})\prod_{\substack{A,B=1\\A<B}}^{M}\overline{\vartheta_1(z_{\beta_A}-z_{\beta_B})}\\ &\times\prod_{\substack{A,B=1\\A<B}}^{L}\vartheta_1(z_A-z_B)^{-(1-\kappa_A/N)(1-\kappa_B/N)}\,\overline{\vartheta_1(z_A-z_B)}^{-(\kappa_A/N)(\kappa_B/N)}\ ,\end{aligned}\tag{C.1.23}$$

where $f(\tau^{\text{dc}};\kappa_1,\dots,\kappa_L)$ is an integration constant that can be determined in the coalescence of all insertion points in which the left-hand side reduces to the partition function $\langle 1\rangle$.

C.1.4 Genus-1 result: Classical action

To determine the full correlator, the classical action (C.1.6) present in (C.1.5) must be computed. For this, we need to express the fields $\partial Z_{\text{cl}}^u(z)$ and $\bar{\partial}Z_{\text{cl}}^u(\bar{z})$ that satisfy the global monodromy condition

$$\oint_{\gamma_a}\mathrm{d}z\partial Z_{\text{cl}}^u+\oint_{\gamma_a}\mathrm{d}\bar{z}\bar{\partial}Z_{\text{cl}}=v_a^u\ ,\quad a\in\{1,\dots,L\}\ .\tag{C.1.24}$$

Moreover, the fields must be linear combination of the cut-differentials and the monodromy condition constrains the coefficients. Solving it yields

$$\partial Z_{\text{cl}}^u(z)=\omega_{A'}(z)\,(W^{-1})_{A'}{}^{a}\,v_a^u\ ,\qquad \bar{\partial}Z_{\text{cl}}^u(\bar{z})=\bar{\omega}_{A''}(\bar{z})\,(W^{-1})_{A''}{}^{a}\,v_a^u\ ,\tag{C.1.25}$$

where the index A' is summed from 1 to $L-M$ while A'' is summed from $L-M+1$ to L. Written like this, the cut differentials with an index A' lower than $L-M$ are defined to be the $\omega_{N-\kappa}^{\alpha_{A'}}(z)$ while those with an index A'' higher than $L-M+1$ are defined to be the $\omega_{\kappa}^{\beta_{A''-L+M}}(z)$. With the following definition of the Hermitian inner product for differential forms

$$(\omega_A,\omega_B)\equiv i\int_R\mathrm{d}z\wedge\mathrm{d}\bar{z}\omega_A(z)\bar{\omega}_B(\bar{z})\ ,\tag{C.1.26}$$

the classical action reads

$$S_{\text{cl}}^R=\sum_{u=3}^{4}\frac{v_a^u\bar{v}_b^u}{2\pi\alpha'}\Big[(W^{-1})_{A'}{}^{a}\,(W^{-1})_{B'}{}^{b}\,(\omega_{A'},\omega_{B'})+(W^{-1})_{A''}{}^{a}\,(W^{-1})_{B''}{}^{b}\,(\omega_{A''},\omega_{B''})\Big]\ .\tag{C.1.27}$$

Appendix C.2: Normalization coefficients in the amplitudes

In the coalescence limit, the external amplitude (3.2.37) becomes

$$\begin{aligned} A_{\mathrm{ext}\Sigma}^{\alpha_0\beta_0} \underset{z_{12}\to 0}{\sim} \frac{3}{2i\pi}\,\alpha' k^2\,\lambda_{\alpha_0\beta_0}\lambda^{\mathrm{T}}_{\beta_0\alpha_0}\,\frac{1}{z_{12}^2}\,\frac{1}{\tau_2\eta^3}\sum_{\nu_{\mathrm{int}}}(-1)^{\delta_{\nu_{\mathrm{int}},1}}\,\vartheta_{\nu_{\mathrm{int}}}^2\,\times \\ \sum_{\vec{l}'} e^{-\frac{\pi}{\alpha'\tau_2}\sum_{I'}(R_{I'}l_{I'})^2}\left[\sum_{\vec{l}} e^{-\frac{\pi}{\alpha'\tau_2}\sum_I(R_I l_I)^2}\mathcal{C}^{\Sigma\vec{l}'\vec{l}}_{\nu_{\mathrm{int}}} + \sum_{\vec{\tilde{l}}} e^{-\frac{\pi\alpha'}{\tau_2}\sum_I(\tilde{l}_I/R_I)^2}\tilde{\mathcal{C}}^{\Sigma\vec{l}'\vec{\tilde{l}}}_{\nu_{\mathrm{int}}}\right]. \end{aligned} \tag{C.2.1}$$

Factorizing all unwanted prefactors and up to a constant $\mathcal{C}$, this is to be identified with

$$\begin{aligned} &\frac{3}{2i\pi}\,\alpha' k^2\,\lambda_{\alpha_0\beta_0}\lambda^{\mathrm{T}}_{\beta_0\alpha_0}\,\frac{8\mathcal{C}}{z_{12}^2}\times\frac{1}{\tau_2^2}\sum_{\gamma=1}^{32+32}\underset{\alpha_0\gamma+\beta_0\gamma}{\mathrm{Str}}\frac{1}{2}\,\frac{1+g}{2}\,q^{\frac{1}{2}(L_0-1)} \qquad \text{for } \mathcal{A}\,, \\ \text{and}\quad &\frac{3}{2i\pi}\,\alpha' k^2\,\lambda_{\alpha_0\beta_0}\lambda^{\mathrm{T}}_{\beta_0\alpha_0}\,\frac{8\mathcal{C}}{z_{12}^2}\times\frac{1}{\tau_2^2}\underset{\alpha_0\alpha_0+\beta_0\beta_0}{\mathrm{Str}}\frac{\Omega}{2}\,\frac{1+g}{2}\,q^{\frac{1}{2}(L_0-1)} \qquad \text{for } \mathcal{M}\,. \end{aligned} \tag{C.2.2}$$

The details on how to identify the correct relevant parts of the partition functions are given in the main text. To be able to identify these contributions with the external amplitude, we must transform the T^2 and T^4 lattices in the partition functions to Hamiltonian form thanks to Poisson summation over the momentum numbers $\vec{m}'$ (which become $\vec{l}'$), over the momentum numbers $\vec{m}$ (which become $\vec{l}$) and over the winding numbers $\vec{n}$ (which become $\tilde{l}$),

$$\begin{aligned} \sum_{\vec{m}} P^{(4)}_{\vec{m}+\vec{a}_i-\vec{a}_j} &= \frac{\mathrm{v}_4}{\alpha'^2\,\tau_2^2}\sum_{\vec{l}} e^{-\frac{\pi}{\alpha'\tau_2}\sum_I(R_I l_I)^2}e^{2i\pi\vec{l}\cdot(\vec{a}_i-\vec{a}_j)}\,, \\ \sum_{\vec{m}} W^{(4)}_{\vec{n}+\vec{a}_i-\vec{a}_j} &= \frac{\alpha'^2}{\mathrm{v}_4\,\tau_2^2}\sum_{\vec{\tilde{l}}} e^{-\frac{\pi\alpha'}{\tau_2}\sum_I(\tilde{l}_I/R_I)^2}e^{2i\pi\vec{\tilde{l}}\cdot(\vec{a}_i-\vec{a}_j)}\,, \\ \sum_{\vec{m}'} P^{(2)}_{\vec{m}'+F\vec{a}'_{\mathrm{S}}+\vec{a}_{i'}-\vec{a}_{j'}} &= \frac{\mathrm{v}_2}{\alpha'\,\tau_2}\sum_{\vec{l}'} e^{-\frac{\pi}{\alpha'\tau_2}\sum_I(R_{I'}l_{I'})^2}e^{2i\pi\vec{l}'\cdot(\vec{a}_{i'}-\vec{a}_{j'})}e^{2i\pi F\vec{l}'\cdot\vec{a}'_{\mathrm{S}}}\,, \end{aligned} \tag{C.2.3}$$

where $\mathrm{v}_4\equiv R_6R_7R_8R_9$ and $\mathrm{v}_2\equiv R_4R_5$. For the annulus, the identification then yields

$$\begin{aligned} \mathcal{C}_1^{\mathcal{A}\vec{l}'\vec{l}} &= \frac{\mathcal{C}}{\tau_2^2\,\eta^3}\,f^{\mathcal{A}\vec{l}'\vec{l}}_{\alpha_0\mathrm{D}}\,, & \tilde{\mathcal{C}}_1^{\mathcal{A}\vec{l}'\vec{\tilde{l}}} &= \frac{\mathcal{C}}{\tau_2^2\,\eta^3}\,f^{\mathcal{A}\vec{l}'\vec{\tilde{l}}}_{\beta_0\mathrm{N}}\,, \\ \mathcal{C}_2^{\mathcal{A}\vec{l}'\vec{l}} &= \frac{\mathcal{C}}{\tau_2^2\,\eta^3}\,\frac{\vartheta_3^2}{\vartheta_4^2}\,f^{\mathcal{A}\vec{l}'\vec{l}}_{\alpha_0\mathrm{D}} - \frac{\mathcal{C}\,\vartheta_2^2}{\tau_2^4\,\eta^9}\,f^{\mathcal{A}\vec{l}'\vec{l}}_{\alpha_0\mathrm{N}}\,e^{2i\pi\vec{l}'\cdot\vec{a}'_{\mathrm{S}}}\,, & \tilde{\mathcal{C}}_2^{\mathcal{A}\vec{l}'\vec{\tilde{l}}} &= \frac{\mathcal{C}}{\tau_2^2\,\eta^3}\,\frac{\vartheta_3^2}{\vartheta_4^2}\,f^{\mathcal{A}\vec{l}'\vec{\tilde{l}}}_{\beta_0\mathrm{N}} - \frac{\mathcal{C}\,\vartheta_2^2}{\tau_2^4\,\eta^9}\,f^{\mathcal{A}\vec{l}'\vec{\tilde{l}}}_{\beta_0\mathrm{D}}\,e^{2i\pi\vec{l}'\cdot\vec{a}'_{\mathrm{S}}}\,, \\ \mathcal{C}_3^{\mathcal{A}\vec{l}'\vec{l}} &= \frac{\mathcal{C}\,\vartheta_3^2}{\tau_2^4\,\eta^9}\,f^{\mathcal{A}\vec{l}'\vec{l}}_{\alpha_0\mathrm{N}} - \frac{\mathcal{C}}{\tau_2^2\,\eta^3}\,\frac{\vartheta_2^2}{\vartheta_4^2}\,f^{\mathcal{A}\vec{l}'\vec{l}}_{\alpha_0\mathrm{D}}\,e^{2i\pi\vec{l}'\cdot\vec{a}'_{\mathrm{S}}}\,, & \tilde{\mathcal{C}}_3^{\mathcal{A}\vec{l}'\vec{\tilde{l}}} &= \frac{\mathcal{C}\,\vartheta_3^2}{\tau_2^4\,\eta^9}\,f^{\mathcal{A}\vec{l}'\vec{\tilde{l}}}_{\beta_0\mathrm{D}} - \frac{\mathcal{C}}{\tau_2^2\,\eta^3}\,\frac{\vartheta_2^2}{\vartheta_4^2}\,f^{\mathcal{A}\vec{l}'\vec{\tilde{l}}}_{\beta_0\mathrm{N}}\,e^{2i\pi\vec{l}'\cdot\vec{a}'_{\mathrm{S}}}\,, \\ \mathcal{C}_4^{\mathcal{A}\vec{l}'\vec{l}} &= -\frac{\mathcal{C}\,\vartheta_4^2}{\tau_2^4\,\eta^9}\,f^{\mathcal{A}\vec{l}'\vec{l}}_{\alpha_0\mathrm{N}}\,, & \tilde{\mathcal{C}}_4^{\mathcal{A}\vec{l}'\vec{\tilde{l}}} &= -\frac{\mathcal{C}\,\vartheta_4^2}{\tau_2^4\,\eta^9}\,f^{\mathcal{A}\vec{l}'\vec{\tilde{l}}}_{\beta_0\mathrm{D}}\,, \end{aligned} \tag{C.2.4}$$

where

$$\begin{aligned} f^{\mathcal{A}\vec{l}'\vec{l}}_{\alpha_0\mathrm{N}} &\equiv \frac{\mathrm{v}_2\mathrm{v}_4}{\alpha'^3}\sum_{i,i'} N_{ii'}\,e^{2i\pi\vec{l}\cdot(\vec{a}_{i_0}-\vec{a}_i)}e^{2i\pi\vec{l}'\cdot(\vec{a}_{i'_0}-\vec{a}_{i'})}, & f^{\mathcal{A}\vec{l}'\vec{\tilde{l}}}_{\beta_0\mathrm{D}} &\equiv \frac{\mathrm{v}_2\,\alpha'^2}{\alpha'\,\mathrm{v}_4}\sum_{i,i'} D_{ii'}\,e^{2i\pi\vec{\tilde{l}}\cdot(\vec{a}_{j_0}-\vec{a}_i)}e^{2i\pi\vec{l}'\cdot(\vec{a}_{i'_0}-\vec{a}_{i'})}\,, \\ f^{\mathcal{A}\vec{l}'\vec{l}}_{\alpha_0\mathrm{D}} &\equiv \delta_{\vec{l},\vec{0}}\,\frac{\mathrm{v}_2}{\alpha'}\sum_{i,i'} D_{ii'}\,e^{2i\pi\vec{l}'\cdot(\vec{a}_{i'_0}-\vec{a}_{i'})}, & f^{\mathcal{A}\vec{l}'\vec{\tilde{l}}}_{\beta_0\mathrm{N}} &\equiv \delta_{\vec{\tilde{l}},\vec{0}}\,\frac{\mathrm{v}_2}{\alpha'}\sum_{i,i'} N_{ii'}\,e^{2i\pi\vec{l}'\cdot(\vec{a}_{i'_0}-\vec{a}_{i'})}\,. \end{aligned} \tag{C.2.5}$$

For the Möbius strip we find

$$\begin{aligned}
\mathcal{C}_1^{\mathcal{M}\vec{l}'\vec{l}} &= 0\ , & \tilde{\mathcal{C}}_1^{\mathcal{M}\vec{l}'\vec{l}} &= 0\ ,\\
\mathcal{C}_2^{\mathcal{M}\vec{l}'\vec{l}} &= \frac{\mathcal{C}\,\vartheta_2^2}{\tau_2^4\,\eta^9}\,\frac{\mathrm{v}_2\mathrm{v}_4}{\alpha'^3}\,e^{2i\pi\vec{l}'\cdot\vec{a}'_{\mathrm{S}}}\ , & \tilde{\mathcal{C}}_2^{\mathcal{M}\vec{l}'\vec{l}} &= \frac{\mathcal{C}\,\vartheta_2^2}{\tau_2^4\,\eta^9}\,\frac{\mathrm{v}_2\,\alpha'^2}{\alpha'\,\mathrm{v}_4}\,e^{2i\pi\vec{l}'\cdot\vec{a}'_{\mathrm{S}}}\ ,\\
\mathcal{C}_3^{\mathcal{M}\vec{l}'\vec{l}} &= -\frac{\mathcal{C}\,\vartheta_3^2}{\tau_2^4\,\eta^9}\,\frac{\mathrm{v}_2\mathrm{v}_4}{\alpha'^3}\ , & \tilde{\mathcal{C}}_3^{\mathcal{M}\vec{l}'\vec{l}} &= -\frac{\mathcal{C}\,\vartheta_3^2}{\tau_2^4\,\eta^9}\,\frac{\mathrm{v}_2\,\alpha'^2}{\alpha'\,\mathrm{v}_4}\ ,\\
\mathcal{C}_4^{\mathcal{M}\vec{l}'\vec{l}} &= \frac{\mathcal{C}\,\vartheta_4^2}{\tau_2^4\,\eta^9}\,\frac{\mathrm{v}_2\mathrm{v}_4}{\alpha'^3}\ , & \tilde{\mathcal{C}}_4^{\mathcal{M}\vec{l}'\vec{l}} &= \frac{\mathcal{C}\,\vartheta_4^2}{\tau_2^4\,\eta^9}\,\frac{\mathrm{v}_2\,\alpha'^2}{\alpha'\,\mathrm{v}_4}\ .
\end{aligned} \tag{C.2.6}$$

Appendix C.3: Field-theory limit of the excited boundary-changing fields correlators

The correlators of excited boundary-changing fields involved in the two-point functions of ND scalars imply the presence of the terms C and $\hat{C}$ in (3.2.39). These terms contain the function F_1 implicitly defined in (3.2.28) and integrals of this function over the torus cycles (see Eq. (3.2.30)). In this appendix, we derive the $\alpha' \to 0$ limit of C and $\hat{C}$.

C.3.1 Explicit expressions for F_1

Lots of Jacobi functions ϑ_1 are involved in the computations. In the $\alpha' \to 0$ limit, we can write

$$\begin{aligned}
\vartheta_1(z) &\equiv -2\,q_{\mathrm{dc}}^{\frac{1}{8}}\sin(\pi z)\prod_{n\geq 1}\left[(1-q_{\mathrm{dc}}^n)(1-q_{\mathrm{dc}}^n z^{-2i\pi z})(1-q_{\mathrm{dc}}^n z^{2i\pi z})\right]\ , \quad q_{\mathrm{dc}} \equiv e^{2i\pi\tau^{\mathrm{dc}}}\ ,\\
&= -2\,q_{\mathrm{dc}}^{\frac{1}{8}}\sin(\pi z)(1+\cdots)\ , \qquad \text{when} \qquad |\mathrm{Im}z| < \mathrm{Im}\tau^{\mathrm{dc}}\ ,
\end{aligned} \tag{C.3.1}$$

which is only valid for $|\mathrm{Im}z| < \mathrm{Im}\tau^{\mathrm{dc}}$. If it is not the case, one has to shift the argument before applying the formula. In the following, we will consider τ^{dc} to be arbitrary and z_1 and z_2 are taken anywhere inside the fundamental cell of the torus *i.e.* the parallelogram with corner 0, 1 and τ^{dc}.

We want to determine explicitly the function F_1 defined in (3.2.28). This amounts to find the parameter U_1 defined as a root of

$$\Gamma(U) \equiv \partial_z F_1(z,w)|_{z=w} = \frac{\vartheta_1'}{\vartheta_1}(U) + \frac{\vartheta_1'}{\vartheta_1}(Y_1 - U)\ , \qquad \text{where} \qquad Y_1 = -\frac{z_{12}}{2}\ . \tag{C.3.2}$$

The function Γ is doubly periodic on the torus and because it is meromorphic with two simple poles at $U = 0$ and $U = Y_1$, it has two simple zeros inside the fundamental cell. We write these zeros U_1 and $Y_1 - U_1$. Because we have

$$-\frac{3}{2}\,\mathrm{Im}\tau^{\mathrm{dc}} < \mathrm{Im}(Y_1 - U_1) < \frac{1}{2}\,\mathrm{Im}\tau^{\mathrm{dc}}\ , \tag{C.3.3}$$

we cannot use directly (C.3.1) and we must proceed in two steps:

- If $0 < \mathrm{Im}Y_1 < \frac{1}{2}\mathrm{Im}\tau^{\mathrm{dc}}$, (C.3.1) can be applied and the equation $\Gamma(U) = 0$ becomes

$$\pi\,\frac{\sin(\pi Y_1)}{\sin(\pi U_1)\sin[\pi(Y_1 - U_1)]} + 2i\pi q_{\mathrm{dc}} e^{-2i\pi U_1} + \cdots = 0\ . \tag{C.3.4}$$

We wrote the first subdominant term in the left-hand side because looking at the dominant term only tells us that U_1 should be such that $\mathrm{Im}\, U_1 \to +\infty$ and $\mathrm{Im}(Y_1 - U_1) < 0$. The subdominant contribution allows us to refine these conclusions. The equation implies the following asymptotic equivalence

$$-\, e^{-i\pi Y_1} \underset{\alpha'\to 0}{\sim} e^{-i\pi U_1}\, e^{i\pi(Y_1-U_1)}\, q_{\rm dc}\, e^{-2i\pi U_1} \ , \tag{C.3.5}$$

which leads us to redefine

$$U_1 \equiv \frac{\tau^{\rm dc}+Y_1}{2} + \frac{1}{4} + \frac{m}{2} + \varepsilon \quad \text{for some } m \in \mathbb{Z} \ , \qquad \text{with} \qquad |\mathrm{Re}\,\varepsilon| < \frac{1}{2} \ , \tag{C.3.6}$$

and $\epsilon \to 0$ in the limit to satisfy the asymptotic equivalence.

- If $-\frac{1}{2}\mathrm{Im}\tau^{\rm dc} < \mathrm{Im}Y_1 < 0$, the redefinition yields

$$-\frac{3}{4}\,\mathrm{Im}\tau^{\rm dc} - \mathrm{Im}\,\varepsilon < \mathrm{Im}(Y_1 - U_1) < -\frac{1}{2}\,\mathrm{Im}\tau^{\rm dc} - \mathrm{Im}\,\varepsilon \ , \tag{C.3.7}$$

that allows to use (C.3.1) for sufficiently small α' if we suppose ϵ to be bounded. This yields to an equation equivalent to (C.3.5) from which we conclude that again $\epsilon \to 0$ and the boundedness assumption was correct.

The two roots of Γ inside the fundamental cell of the torus are thus

$$U_1 = \frac{\tau^{\rm dc}+Y_1}{2} + \frac{1}{4} + \cdots \quad \text{or} \quad \frac{\tau^{\rm dc}+Y_1}{2} + \frac{3}{4} + \cdots \ . \tag{C.3.8}$$

Now that we know U_1, we can express $F_1(z,z_2)$ and $F_1(z_1,z_2)$ involved in C and $\hat{C}$. We have

$$F_1(z,z_2) = \frac{\vartheta_1\big(z + \frac{\tau^{\rm dc}}{2} - \frac{1}{4}\,z_1 - \frac{3}{4}\,z_2 + \frac{1}{4} + \cdots\big)\,\vartheta_1\big(z - \frac{\tau^{\rm dc}}{2} - \frac{1}{4}\,z_1 - \frac{3}{4}\,z_2 - \frac{1}{4} + \cdots\big)}{\vartheta_1\big(\frac{\tau^{\rm dc}}{2} - \frac{z_{12}}{4} + \frac{1}{4} + \cdots\big)\,\vartheta_1\big(-\frac{\tau^{\rm dc}}{2} - \frac{z_{12}}{4} - \frac{1}{4} + \cdots\big)} \ . \tag{C.3.9}$$

Several cases must be handled depending on the value of $\frac{1}{2}y_1 + \frac{3}{2}y_2$ and $\mathrm{Im}z$ to apply correctly (C.3.1). We obtain

- when $\quad 0 < \frac{1}{2}\,y_1 + \frac{3}{2}\,y_2 < \mathrm{Im}\tau^{\rm dc} \ , \quad$ then $\tag{C.3.10}$

$$F_1(z,z_2) = \begin{cases} 1 + \cdots & \text{if } \ 0 < y < \frac{1}{2}\,\mathrm{Im}\tau^{\rm dc} + \frac{1}{4}\,y_1 + \frac{3}{4}\,y_2 \ , \\ e^{-4i\pi(z - \frac{\tau^{\rm dc}}{2} - \frac{1}{4}z_1 - \frac{3}{4}z_2)}\,(1+\cdots) & \text{if } \ \frac{1}{2}\,\mathrm{Im}\tau^{\rm dc} + \frac{1}{4}\,y_1 + \frac{3}{4}\,y_2 < y < \mathrm{Im}\tau^{\rm dc} \ . \end{cases}$$

and

- when $\quad \mathrm{Im}\tau^{\rm dc} < \frac{1}{2}\,y_1 + \frac{3}{2}\,y_2 < 2\,\mathrm{Im}\tau^{\rm dc} \ , \quad$ then $\tag{C.3.11}$

$$F_1(z,z_2) = \begin{cases} e^{4i\pi(z - \frac{1}{4}z_1 - \frac{3}{4}z_2 + \frac{\tau^{\rm dc}}{2})}\,(1+\cdots) & \text{if } \ 0 < y < \frac{1}{4}\,y_1 + \frac{3}{4}\,y_2 - \frac{1}{2}\,\mathrm{Im}\tau^{\rm dc} \ , \\ 1 + \cdots & \text{if } \ \frac{1}{4}\,y_1 + \frac{3}{4}\,y_2 - \frac{1}{2}\,\mathrm{Im}\tau^{\rm dc} < y < \mathrm{Im}\tau^{\rm dc} \ . \end{cases}$$

From these formulas, we deduce

$$F_1(z_1,z_2) = \begin{cases} e^{2i\pi(\tau^{\rm dc} - \frac{3}{2}z_{12})}(1+\cdots) & \text{if } \ \ \frac{2}{3}\,\mathrm{Im}\tau^{\rm dc} < \mathrm{Im}z_{12} < \mathrm{Im}\tau^{\rm dc} \ , \\ (1+\cdots) & \text{if } \ -\frac{2}{3}\,\mathrm{Im}\tau^{\rm dc} < \mathrm{Im}z_{12} < \frac{2}{3}\,\mathrm{Im}\tau^{\rm dc} \ , \\ e^{2i\pi(\tau^{\rm dc} + \frac{3}{2}z_{12})}(1+\cdots) & \text{if } \ \ -\mathrm{Im}\tau^{\rm dc} < \mathrm{Im}z_{12} < -\frac{2}{3}\,\mathrm{Im}\tau^{\rm dc} . \end{cases} \tag{C.3.12}$$

C.3.2 Limit of $\hat{C}$

From (C.3.12), we directly conclude that the contributions in the amplitudes (3.2.47) proportional to C are

$$2\pi\Big[\frac{t(1-u)}{\alpha'}+2\ln 4+\cdots\Big]\hat{C}=-4\pi^3\Big[\frac{t(1-u)}{\alpha'}+2\ln 4+\cdots\Big]\times \\ \begin{cases} e^{2i\pi(\tau^{\rm dc}-z_{12})}(1+\cdots) & \text{if} \quad \frac{2}{3}\,{\rm Im}\tau^{\rm dc}<{\rm Im}z_{12}<{\rm Im}\tau^{\rm dc}\ , \\ e^{i\pi z_{12}}(1+\cdots) & \text{if} \quad 0<{\rm Im}z_{12}<\frac{2}{3}\,{\rm Im}\tau^{\rm dc}\ , \\ e^{-i\pi z_{12}}(1+\cdots) & \text{if} \quad -\frac{2}{3}\,{\rm Im}\tau^{\rm dc}<{\rm Im}z_{12}<0\ , \\ e^{2i\pi(\tau^{\rm dc}+z_{12})}(1+\cdots) & \text{if} \quad -{\rm Im}\tau^{\rm dc}<{\rm Im}z_{12}<-\frac{2}{3}\,{\rm Im}\tau^{\rm dc}\ , \end{cases} \\ =\cdots\ , \tag{C.3.13}$$

which is exponentially suppressed for generic values of ${\rm Im}z_{12}$. Thus, only C contributes to the result.

C.3.3 Limit of C

Using the integral form of C displayed in (3.2.30), the contributions in the amplitudes (3.2.47) proportional to $\hat{C}$ are

$$2\pi\Big[\frac{t(1-u)}{\alpha'}+2\ln 4+\cdots\Big]C=-2i\pi^4\cos\Big(\frac{\pi}{2}\,z_{12}\Big)\big[\overline{W}_2\,\mathcal{F}_1-\mathcal{F}_2\big]\ , \\ \text{where}\quad \mathcal{F}_a=\oint_{\gamma_a}{\rm d}z\,\frac{F_1(z,z_2)\,(1+\cdots)}{\sin[\pi(z-z_1)]^{\frac{1}{2}}\sin[\pi(z-z_2)]^{\frac{3}{2}}}\ ,\quad a\in\{1,2\}\ , \tag{C.3.14}$$

To evaluate $\mathcal{F}_1$, we parametrize the cycle γ with ${\rm Im}z\equiv\frac{1}{2}{\rm Im}\tau^{\rm dc}$. The integral becomes

$$\mathcal{F}_1=\int_0^1{\rm d}x\,\frac{1+\cdots}{\sin[\pi(x+\frac{\tau^{\rm dc}}{2}-z_1)]^{\frac{1}{2}}\sin[\pi(x+\frac{\tau^{\rm dc}}{2}-z_2)]^{\frac{3}{2}}}\ . \tag{C.3.15}$$

Using a primitive, the integral with 1 in the denominator gives an identically zero result. To conclude, we need to look at the ellipsis that can possibly be large once multiplied by the cosine $\cos(\pi z_{12}/2)$. Depending on the signs of $\frac{1}{2}{\rm Im}\tau^{\rm dc}-y_1$, $\frac{1}{2}{\rm Im}\tau^{\rm dc}-y_2$ and y_1-y_2, we can find upper bounds for the integrand by approximating the sines with exponentials and show that the integral multiplied by the cosine always gives an exponentially suppressed result.

The evaluation of $\mathcal{F}_2$ requires to consider two cases: When $0<\frac{1}{2}y_1+\frac{3}{2}y_2<{\rm Im}\tau^{\rm dc}$ and when ${\rm Im}\tau^{\rm dc}<\frac{1}{2}y_1+\frac{3}{2}y_2<2{\rm Im}\tau^{\rm dc}$. Let us describe in details the former case. The expression (C.3.10) for $F(z,z_2)$ allows us to split the integral into two pieces,

$$\mathcal{F}_2=\mathcal{F}_2^{(1)}+\mathcal{F}_2^{(2)}\ , \\ \text{where}\quad \mathcal{F}_2^{(1)}=\int_0^{\frac{\tau^{\rm dc}}{2}+\frac{1}{4}z_1+\frac{3}{4}z_2}{\rm d}z\,\frac{1+\cdots}{\sin[\pi(z-z_1)]^{\frac{1}{2}}\sin[\pi(z-z_2)]^{\frac{3}{2}}}\ , \\ \mathcal{F}_2^{(2)}=\int_{\frac{\tau^{\rm dc}}{2}+\frac{1}{4}z_1+\frac{3}{4}z_2}^{\tau^{\rm dc}}{\rm d}z\,\frac{e^{-4i\pi(z-\frac{\tau^{\rm dc}}{2}-\frac{1}{4}z_1-\frac{3}{4}z_2)}\,(1+\cdots)}{\sin[\pi(z-z_1)]^{\frac{1}{2}}\sin[\pi(z-z_2)]^{\frac{3}{2}}}\ . \tag{C.3.16}$$

Using a primitive for $\mathcal{F}_2^{(1)}$, two subcases arise, namely $(a):\ y_1-y_2>\frac{2}{3}{\rm Im}\tau^{\rm dc}$ and $(b):\ y_1-y_2>$

$\frac{2}{3}\mathrm{Im}\tau^{\mathrm{dc}}$, but they give the same result in the $\alpha' \to 0$ limit which is

$$\cos\Big(\frac{\pi}{2}\,z_{12}\Big)\int_0^{\frac{\tau^{\mathrm{dc}}}{2}+\frac{1}{4}z_1+\frac{3}{4}z_2}\mathrm{d}z\,\frac{1}{\sin[\pi(z-z_1)]^{\frac{1}{2}}\sin[\pi(z-z_2)]^{\frac{3}{2}}}=\frac{2i}{\pi}+\cdots\ . \tag{C.3.17}$$

We can show that the contribution coming from the ellipsis is dominated by this finite result. This is not obvious since the dominant term in the ellipsis in $\mathcal{F}_2^{(1)}$ turns out to be 1 at the upper bound of the integral. However, if we split the integration region from 0 to some z_0 and from z_0 to the upper bound, with z_0 such that the sines in the denominator can be replaced by their dominant exponentials in the second domain, then the first piece can be trivially bounded by an exponentially suppressed majorant while the second piece is easily integrable and yields an exponentially suppressed result.

For $\mathcal{F}_2^{(2)}$, the sine $\sin[\pi(z-z_2)]$ can always be replaced by the dominant exponential. For the other sine $\sin[\pi(z-z_1)]$, it depends on if we consider the subcase (a) or (b). In subcase (a), the integration domain does not contain z_1 so that the second sine can also be replaced by an exponential. The integration is then easy to perform and is exponentially suppressed. In subcase (b), the sine $\sin[\pi(z-z_1)]$ cannot be substituted. However, the piece with 1 in the numerator can be integrated using a primitive. It is exponentially suppressed and can be shown to dominate the integral of the ellipsis with the same method as for $\mathcal{F}_2^{(1)}$. We then conclude that $\mathcal{F}_2^{(2)}$ does not contribute to the result. In the second case $\mathrm{Im}\tau^{\mathrm{dc}} < \frac{1}{2}y_1+\frac{3}{2}y_2 < 2\mathrm{Im}\tau^{\mathrm{dc}}$, the splitting of the integral is different but the logic is the same and so is the final result.

Gathering everything, we eventually obtain

$$2\pi\left[\frac{t(1-u)}{\alpha'}+2\ln 4+\cdots\right](C+\hat{C})=-4\pi^3+\cdots\ , \tag{C.3.18}$$

where the finite contribution only comes from $\mathcal{F}_2^{(1)}$ in C.

Bibliography

[1] Y. Fukuda *et al.* [Super-Kamiokande], "Measurements of the solar neutrino flux from Super-Kamiokande's first 300 days," Phys. Rev. Lett. **81** (1998), 1158-1162 [erratum: Phys. Rev. Lett. **81** (1998), 4279] [arXiv:hep-ex/9805021 [hep-ex]].

[2] Q. R. Ahmad *et al.* [SNO], "Measurement of the rate of $\nu_e + d \to p + p + e^-$ interactions produced by ^{8}B solar neutrinos at the Sudbury Neutrino Observatory," Phys. Rev. Lett. **87** (2001), 071301 [arXiv:nucl-ex/0106015 [nucl-ex]].

[3] J. K. Ahn *et al.* [RENO], "Observation of Reactor Electron Antineutrino Disappearance in the RENO Experiment," Phys. Rev. Lett. **108** (2012), 191802 [arXiv:1204.0626 [hep-ex]].

[4] B. Abi *et al.* [Muon g-2], "Measurement of the Positive Muon Anomalous Magnetic Moment to 0.46 ppm," Phys. Rev. Lett. **126** (2021) no.14, 141801 [arXiv:2104.03281 [hep-ex]].

[5] R. Aaij *et al.* [LHCb], "Measurement of the ratio of branching fractions $\mathcal{B}(\bar{B}^0 \to D^{*+}\tau^-\bar{\nu}_\tau)/\mathcal{B}(\bar{B}^0 \to D^{*+}\mu^-\bar{\nu}_\mu)$," Phys. Rev. Lett. **115** (2015) no.11, 111803 [erratum: Phys. Rev. Lett. **115** (2015) no.15, 159901] [arXiv:1506.08614 [hep-ex]].

[6] M. Aaboud *et al.* [ATLAS], "Study of the rare decays of B_s^0 and B^0 mesons into muon pairs using data collected during 2015 and 2016 with the ATLAS detector," JHEP **04** (2019), 098 [arXiv:1812.03017 [hep-ex]].

[7] C. A. Baker, D. D. Doyle, P. Geltenbort, K. Green, M. G. D. van der Grinten, P. G. Harris, P. Iaydjiev, S. N. Ivanov, D. J. R. May and J. M. Pendlebury, *et al.* "An Improved experimental limit on the electric dipole moment of the neutron," Phys. Rev. Lett. **97** (2006), 131801 [arXiv:hep-ex/0602020 [hep-ex]].

[8] J. M. Pendlebury, S. Afach, N. J. Ayres, C. A. Baker, G. Ban, G. Bison, K. Bodek, M. Burghoff, P. Geltenbort and K. Green, *et al.* "Revised experimental upper limit on the electric dipole moment of the neutron," Phys. Rev. D **92** (2015) no.9, 092003 [arXiv:1509.04411 [hep-ex]].

[9] A. Hook, "TASI Lectures on the Strong CP Problem and Axions," PoS **TASI2018** (2019), 004 [arXiv:1812.02669 [hep-ph]].

[10] F. Zwicky, "On the Masses of Nebulae and of Clusters of Nebulae," Astrophys. J. **86** (1937), 217-246.

[11] V. C. Rubin and W. K. Ford, Jr., "Rotation of the Andromeda Nebula from a Spectroscopic Survey of Emission Regions," Astrophys. J. **159** (1970), 379-403.

[12] V. C. Rubin, N. Thonnard and W. K. Ford, Jr., "Rotational properties of 21 SC galaxies with a large range of luminosities and radii, from NGC 4605 /R = 4kpc/ to UGC 2885 /R = 122 kpc/," Astrophys. J. **238** (1980), 471.

[13] A. G. Riess *et al.* [Supernova Search Team], "Observational evidence from supernovae for an accelerating universe and a cosmological constant," Astron. J. **116** (1998), 1009-1038 [arXiv:astro-ph/9805201 [astro-ph]].

[14] S. Perlmutter *et al.* [Supernova Cosmology Project], "Measurements of Ω and Λ from 42 high redshift supernovae," Astrophys. J. **517** (1999), 565-586 [arXiv:astro-ph/9812133 [astro-ph]].

[15] N. Aghanim *et al.* [Planck], "Planck 2018 results. VI. Cosmological parameters," Astron. Astrophys. **641** (2020), A6 [arXiv:1807.06209 [astro-ph.CO]].

[16] J. Scherk and J. H. Schwarz, "Spontaneous breaking of supersymmetry through dimensional reduction," Phys. Lett. B **82** (1979), 60.

[17] J. Scherk and J. H. Schwarz, "How to Get Masses from Extra Dimensions," Nucl. Phys. B **153** (1979), 61-88.

[18] R. Rohm, "Spontaneous supersymmetry breaking in supersymmetric string theories," Nucl. Phys. B **237** (1984), 553.

[19] C. Kounnas and M. Porrati, "Spontaneous supersymmetry breaking in string theory," Nucl. Phys. B **310** (1988), 355.

[20] S. Ferrara, C. Kounnas and M. Porrati, "Superstring solutions with spontaneously broken four-dimensional supersymmetry," Nucl. Phys. B **304** (1988), 500.

[21] S. Ferrara, C. Kounnas, M. Porrati and F. Zwirner, "Superstrings with spontaneously broken supersymmetry and their effective theories," Nucl. Phys. B **318** (1989), 75.

[22] C. Kounnas and B. Rostand, "Coordinate-dependent compactifications and discrete symmetries," Nucl. Phys. B **341** (1990), 641.

[23] R. Hagedorn, "Statistical thermodynamics of strong interactions at high-energies," Nuovo Cim. Suppl. **3** (1965), 147-186 CERN-TH-520.

[24] S. Fubini and G. Veneziano, "Level structure of dual-resonance models," Nuovo Cim. A **64** (1969), 811-840.

[25] K. Huang and S. Weinberg, "Ultimate temperature and the early universe," Phys. Rev. Lett. **25** (1970), 895-897.

[26] J. J. Atick and E. Witten, "The Hagedorn Transition and the Number of Degrees of Freedom of String Theory," Nucl. Phys. B **310** (1988), 291-334.

[27] M. Axenides, S. D. Ellis and C. Kounnas, "Universal Behavior of D-dimensional Superstring Models," Phys. Rev. D **37** (1988), 2964.

[28] D. Kutasov and N. Seiberg, "Number of degrees of freedom, density of states and tachyons in string theory and CFT," Nucl. Phys. B **358** (1991), 600-618.

[29] B. Sathiapalan, "Vortices on the String World Sheet and Constraints on Toral Compactification," Phys. Rev. D **35** (1987), 3277.

[30] Y. I. Kogan, "Vortices on the World Sheet and String's Critical Dynamics," JETP Lett. **45** (1987), 709-712 ITEP-87-110.

[31] I. Antoniadis and C. Kounnas, "Superstring phase transition at high temperature," Phys. Lett. B **261** (1991), 369-378.

[32] I. Antoniadis, J. P. Derendinger and C. Kounnas, "Nonperturbative temperature instabilities in $\mathcal{N} = 4$ strings," Nucl. Phys. B **551** (1999), 41-77 [arXiv:hep-th/9902032 [hep-th]].

[33] H. Partouche and B. de Vaulchier, "Hagedorn-like transition at high supersymmetry breaking scale," JHEP **08** (2019), 155 [arXiv:1903.09116 [hep-th]].

[34] H. Partouche and B. de Vaulchier, "Phase transition at high supersymmetry breaking scale in string theory," Springer Proc. Math. Stat. **335** (2019), 265-274 [arXiv:1911.06558 [hep-th]].

[35] E. Dudas and C. Timirgaziu, "Nontachyonic Scherk–Schwarz compactifications, cosmology and moduli stabilization," JHEP **03** (2004), 060 [arXiv:hep-th/0401201 [hep-th]].

[36] C. Angelantonj, H. Partouche and G. Pradisi, "Heterotic − type I dual pairs, rigid branes and broken SUSY," Nucl. Phys. B **954** (2020), 114976 [arXiv:1912.12062 [hep-th]].

[37] C. Angelantonj, M. Cardella and N. Irges, "An alternative for moduli stabilisation," Phys. Lett. B **641** (2006), 474-480 [arXiv:hep-th/0608022 [hep-th]].

[38] T. Catelin-Jullien, C. Kounnas, H. Partouche and N. Toumbas, "Thermal/quantum effects and induced superstring cosmologies," Nucl. Phys. B **797** (2008), 137 [arXiv:0710.3895 [hep-th]].

[39] T. Catelin-Jullien, C. Kounnas, H. Partouche and N. Toumbas, "Induced superstring cosmologies and moduli stabilization," Nucl. Phys. B **820** (2009), 290 [arXiv:0901.0259 [hep-th]].

[40] F. Bourliot, C. Kounnas and H. Partouche, "Attraction to a radiation-like era in early superstring cosmologies," Nucl. Phys. B **816** (2009), 227 [arXiv:0902.1892 [hep-th]].

[41] F. Bourliot, J. Estes, C. Kounnas and H. Partouche, "Cosmological phases of the string thermal effective potential," Nucl. Phys. B **830** (2010), 330 [arXiv:0908.1881 [hep-th]].

[42] J. Estes, C. Kounnas and H. Partouche, "Superstring cosmology for $\mathcal{N}_4 = 1 \to 0$ superstring vacua," Fortsch. Phys. **59** (2011), 861 [arXiv:1003.0471 [hep-th]].

[43] T. Coudarchet, C. Fleming and H. Partouche, "Quantum no-scale regimes in string theory," Nucl. Phys. B **930** (2018), 235 [arXiv:1711.09122 [hep-th]].

[44] T. Coudarchet and H. Partouche, "Quantum no-scale regimes and moduli dynamics," Nucl. Phys. B **933** (2018), 134 [arXiv:1804.00466 [hep-th]].

[45] H. Itoyama and T. R. Taylor, "Supersymmetry restoration in the compactified $\mathrm{O}(16) \times \mathrm{O}(16)'$ heterotic string theory," Phys. Lett. B **186** (1987), 129.

[46] S. Abel, K. R. Dienes and E. Mavroudi, "Towards a non-supersymmetric string phenomenology," Phys. Rev. D **91** (2015), 126014 [arXiv:1502.03087 [hep-th]].

[47] I. Florakis and J. Rizos, "Chiral heterotic strings with positive cosmological constant," Nucl. Phys. B **913** (2016), 495 [arXiv:1608.04582 [hep-th]].

[48] S. Abel and R. J. Stewart, "On exponential suppression of the cosmological constant in non-SUSY strings at two loops and beyond," Phys. Rev. D **96** (2017), 106013 [arXiv:1701.06629 [hep-th]].

[49] H. Itoyama and S. Nakajima, "Exponentially suppressed cosmological constant with enhanced gauge symmetry in heterotic interpolating models," PTEP **2019** (2019) no.12, 123B01 [arXiv:1905.10745 [hep-th]].

[50] H. Itoyama and S. Nakajima, "Stability, enhanced gauge symmetry and suppressed cosmological constant in 9D heterotic interpolating models," Nucl. Phys. B **958** (2020), 115111 [arXiv:2003.11217 [hep-th]].

[51] H. Itoyama and S. Nakajima, "Marginal deformations of heterotic interpolating models and exponential suppression of the cosmological constant," [arXiv:2101.10619 [hep-th]].

[52] R. Iengo and C. J. Zhu, "Evidence for nonvanishing cosmological constant in nonSUSY superstring models," JHEP **04** (2000), 028 [arXiv:hep-th/9912074 [hep-th]].

[53] K. Aoki, E. D'Hoker and D. H. Phong, "Two loop superstrings on orbifold compactifications," Nucl. Phys. B **688** (2004), 3-69 [arXiv:hep-th/0312181 [hep-th]].

[54] S. Abel and R. J. Stewart, "Exponential suppression of the cosmological constant in non-supersymmetric string vacua at two loops and beyond," Phys. Rev. D **96** (2017) no.10, 106013 [arXiv:1701.06629 [hep-th]].

[55] S. Groot Nibbelink, O. Loukas, A. Mütter, E. Parr and P. K. S. Vaudrevange, "Tension Between a Vanishing Cosmological Constant and Non-Supersymmetric Heterotic Orbifolds," Fortsch. Phys. **68** (2020) no.7, 2000044 [arXiv:1710.09237 [hep-th]].

[56] C. Kounnas and H. Partouche, "Super no-scale models in string theory," Nucl. Phys. B **913** (2016), 593 [arXiv:1607.01767 [hep-th]].

[57] C. Kounnas and H. Partouche, "$\mathcal{N} = 2 \to 0$ super no-scale models and moduli quantum stability," Nucl. Phys. B **919** (2017), 41 [arXiv:1701.00545 [hep-th]].

[58] S. Abel, E. Dudas, D. Lewis and H. Partouche, "Stability and vacuum energy in open string models with broken supersymmetry," JHEP **10** (2019), 226 [arXiv:1812.09714 [hep-th]].

[59] S. Abel, T. Coudarchet and H. Partouche, "On the stability of open-string orbifold models with broken supersymmetry," Nucl. Phys. B **957** (2020), 115100 [arXiv:2003.02545 [hep-th]].

[60] T. Coudarchet and H. Partouche, "One-loop masses of Neumann-Dirichlet open strings and boundary-changing vertex operators," [arXiv:2011.13725 [hep-th]].

[61] T. Coudarchet and H. Partouche, "Two-point functions of Neumann-Dirichlet open-string sector moduli," [arXiv:2012.14442 [hep-th]].

[62] S. Sugimoto, "Anomaly cancellations in type I D9-D9-bar system and the USp(32) string theory," Prog. Theor. Phys. **102** (1999), 685 [arXiv:hep-th/9905159].

[63] I. Antoniadis, E. Dudas and A. Sagnotti, "Brane supersymmetry breaking," Phys. Lett. B **464** (1999), 38 [arXiv:hep-th/9908023].

[64] C. Angelantonj, "Comments on open-string orbifolds with a non-vanishing B_{ab}," Nucl. Phys. B **566** (2000), 126 [arXiv:hep-th/9908064].

[65] G. Aldazabal and A. M. Uranga, "Tachyon-free non-supersymmetric type IIB orientifolds *via* brane-antibrane systems," JHEP **9910** (1999), 024 [arXiv:hep-th/9908072].

[66] C. Angelantonj, I. Antoniadis, G. D'Appollonio, E. Dudas and A. Sagnotti, "Type I vacua with brane supersymmetry breaking," Nucl. Phys. B **572** (2000), 36 [arXiv:hep-th/9911081].

[67] For a recent review of the state of the art, see J. Mourad and A. Sagnotti, "An update on brane supersymmetry breaking," [arXiv:1711.11494 [hep-th]].

[68] E. Dudas and J. Mourad, "Consistent gravitino couplings in nonsupersymmetric strings," Phys. Lett. B **514** (2001), 173 [hep-th/0012071].

[69] G. Pradisi and F. Riccioni, "Geometric couplings and brane supersymmetry breaking," Nucl. Phys. B **615** (2001), 33 [hep-th/0107090].

[70] W. Fischler and L. Susskind, "Dilaton tadpoles, string condensates and scale invariance," Phys. Lett. B **171** (1986), 383-389.

[71] W. Fischler and L. Susskind, "Dilaton tadpoles, string condensates and scale invariance. 2.," Phys. Lett. B **173** (1986), 262-264.

[72] E. Dudas, G. Pradisi, M. Nicolosi and A. Sagnotti, "On tadpoles and vacuum redefinitions in string theory," Nucl. Phys. B **708** (2005), 3-44 [arXiv:hep-th/0410101 [hep-th]].

[73] R. Pius, A. Rudra and A. Sen, "String perturbation theory around dynamically shifted vacuum," JHEP **10** (2014), 070 [arXiv:1404.6254 [hep-th]].

[74] E. S. Fradkin and A. A. Tseytlin, "Nonlinear Electrodynamics from Quantized Strings," Phys. Lett. B **163** (1985), 123-130.

[75] A. Abouelsaood, C. G. Callan, Jr., C. R. Nappi and S. A. Yost, "Open Strings in Background Gauge Fields," Nucl. Phys. B **280** (1987), 599-624.

[76] C. Bachas, "A Way to break supersymmetry," [arXiv:hep-th/9503030 [hep-th]].

[77] T. Coudarchet, E. Dudas and H. Partouche, "Geometry of orientifold vacua and supersymmetry breaking," [arXiv:2105.06913 [hep-th]].

[78] E. Cremmer, S. Ferrara, C. Kounnas and D. V. Nanopoulos, "Naturally Vanishing Cosmological Constant in $\mathcal{N} = 1$ Supergravity," Phys. Lett. B **133** (1983), 61.

[79] J. R. Ellis, C. Kounnas and D. V. Nanopoulos, "Phenomenological SU(1,1) Supergravity," Nucl. Phys. B **241** (1984), 406-428.

[80] J. R. Ellis, A. B. Lahanas, D. V. Nanopoulos and K. Tamvakis, "No-Scale Supersymmetric Standard Model," Phys. Lett. B **134** (1984), 429.

[81] J. R. Ellis, C. Kounnas and D. V. Nanopoulos, Nucl. Phys. B **247** (1984), 373-395.

[82] S. Kachru, J. Kumar and E. Silverstein, "Vacuum energy cancellation in a nonsupersymmetric string," Phys. Rev. D **59** (1999), 106004 [arXiv:hep-th/9807076 [hep-th]].

[83] G. Shiu and S. H. H. Tye, "Bose-Fermi degeneracy and duality in nonsupersymmetric strings," Nucl. Phys. B **542** (1999), 45-72 [arXiv:hep-th/9808095 [hep-th]].

[84] Y. Satoh, Y. Sugawara and T. Wada, "Non-supersymmetric Asymmetric Orbifolds with Vanishing Cosmological Constant," JHEP **02** (2016), 184 [arXiv:1512.05155 [hep-th]].

[85] Y. Sugawara and T. Wada, "More on Non-supersymmetric Asymmetric Orbifolds with Vanishing Cosmological Constant," JHEP **08** (2016), 028 [arXiv:1605.07021 [hep-th]].

[86] C. Angelantonj, I. Antoniadis and K. Forger, "Nonsupersymmetric type I strings with zero vacuum energy," Nucl. Phys. B **555** (1999), 116-134 [arXiv:hep-th/9904092 [hep-th]].

[87] R. Blumenhagen and L. Gorlich, "Orientifolds of nonsupersymmetric asymmetric orbifolds," Nucl. Phys. B **551** (1999), 601-616 [arXiv:hep-th/9812158 [hep-th]].

[88] T. Coudarchet, L. Heurtier and H. Partouche, "Spontaneous dark-matter mass generation along cosmological attractors in string theory," JHEP **03** (2019), 117 [arXiv:1812.10134 [hep-th]].

[89] T. Coudarchet, L. Heurtier and H. Partouche, "Spontaneous Freeze Out of Dark Matter," PoS **CORFU2019** (2020), 136 [arXiv:1912.10276 [hep-th]].

[90] K. Becker, M. Becker and J. H. Schwarz, "String theory and M-theory: A modern introduction."

[91] J. Polchinski, "String theory. Vol. 1: An introduction to the bosonic string."

[92] J. Polchinski, "String theory. Vol. 2: Superstring theory and beyond."

[93] M. B. Green, J. H. Schwarz and E. Witten, "SUPERSTRING THEORY. VOL. 1: INTRODUCTION."

[94] D. Tong, "String Theory," [arXiv:0908.0333 [hep-th]].

[95] E. Kiritsis, "String theory in a nutshell."

[96] R. Blumenhagen, D. Lüst and S. Theisen, "Basic concepts of string theory,".

[97] Y. Nambu, "Duality and Hadrodynamics," Notes prepared for the Copenhagen High Energy Symposium (1970).

[98] T. Goto, "Relativistic quantum mechanics of one-dimensional mechanical continuum and subsidiary condition of dual resonance model," Prog. Theor. Phys. **46** (1971), 1560-1569.

[99] L. Brink, P. Di Vecchia and P. S. Howe, "A Locally Supersymmetric and Reparametrization Invariant Action for the Spinning String," Phys. Lett. B **65** (1976), 471-474.

[100] S. Deser and B. Zumino, "A Complete Action for the Spinning String," Phys. Lett. B **65** (1976), 369-373.

[101] A. M. Polyakov, "Quantum Geometry of Bosonic Strings," Phys. Lett. B **103** (1981), 207-210.

[102] P. Ramond, "Dual Theory for Free Fermions," Phys. Rev. D **3** (1971), 2415-2418.

[103] A. Neveu and J. H. Schwarz, "Factorizable dual model of pions," Nucl. Phys. B **31** (1971), 86-112.

[104] M. B. Green and J. H. Schwarz, "Supersymmetrical String Theories," Phys. Lett. B **109** (1982), 444-448.

[105] M. B. Green and J. H. Schwarz, "Supersymmetrical Dual String Theory. 2. Vertices and Trees," Nucl. Phys. B **198** (1982), 252-268.

[106] M. B. Green and J. H. Schwarz, "Supersymmetrical String Theories," Phys. Lett. B **109** (1982), 444-448.

[107] J. E. Paton and H. M. Chan, "Generalized veneziano model with isospin," Nucl. Phys. B **10** (1969), 516-520.

[108] F. Gliozzi, J. Scherk and D. I. Olive, "Supergravity and the Spinor Dual Model," Phys. Lett. B **65** (1976), 282-286.

[109] F. Gliozzi, J. Scherk and D. I. Olive, "Supersymmetry, Supergravity Theories and the Dual Spinor Model," Nucl. Phys. B **122** (1977), 253-290.

[110] D. J. Gross, J. A. Harvey, E. J. Martinec and R. Rohm, "The Heterotic String," Phys. Rev. Lett. **54** (1985), 502-505.

[111] D. J. Gross, J. A. Harvey, E. J. Martinec and R. Rohm, "Heterotic String Theory. 1. The Free Heterotic String," Nucl. Phys. B **256** (1985), 253.

[112] D. J. Gross, J. A. Harvey, E. J. Martinec and R. Rohm, "Heterotic String Theory. 2. The Interacting Heterotic String," Nucl. Phys. B **267** (1986), 75-124.

[113] K. S. Narain, "New Heterotic String Theories in Uncompactified Dimensions < 10," Phys. Lett. B **169** (1986), 41-46.

[114] K. S. Narain, M. H. Sarmadi and E. Witten, "A Note on Toroidal Compactification of Heterotic String Theory," Nucl. Phys. B **279** (1987), 369-379.

[115] C. Angelantonj and A. Sagnotti, "Open strings," Phys. Rept. **371** (2002) 1 [Erratum-ibid. **376** (2003) 339] [arXiv:hep-th/0204089].

[116] E. Dudas, "Theory and phenomenology of type I strings and M-theory," Class. Quant. Grav. **17** (2000) R41 [arXiv:hep-ph/0006190].

[117] A. Neveu and J. Scherk, "Connection between Yang-Mills fields and dual models," Nucl. Phys. B **36** (1972), 155-161.

[118] E. Witten, "Bound states of strings and p-branes," Nucl. Phys. B **460** (1996), 335-350 [arXiv:hep-th/9510135 [hep-th]].

[119] A. Sagnotti, "Open Strings and their Symmetry Groups," [arXiv:hep-th/0208020 [hep-th]].

[120] M. B. Green and J. H. Schwarz, "Infinity Cancellations in SO(32) Superstring Theory," Phys. Lett. B **151** (1985), 21-25.

[121] N. Marcus and A. Sagnotti, "Group Theory from Quarks at the Ends of Strings," Phys. Lett. B **188** (1987), 58-64.

[122] S. Weinberg, "Cancellation of One Loop Divergences in SO(8192) String Theory," Phys. Lett. B **187** (1987), 278-282.

[123] M. R. Douglas and B. Grinstein, "Dilaton Tadpole for the Open Bosonic String," Phys. Lett. B **183** (1987), 52 [erratum: Phys. Lett. B **187** (1987), 442].

[124] J. Polchinski and Y. Cai, "Consistency of Open Superstring Theories," Nucl. Phys. B **296** (1988), 91-128.

[125] I. Antoniadis, E. Dudas and A. Sagnotti, "Supersymmetry breaking, open strings and M theory," Nucl. Phys. B **544** (1999), 469-502 [arXiv:hep-th/9807011 [hep-th]].

[126] I. Antoniadis, G. D'Appollonio, E. Dudas and A. Sagnotti, "Partial breaking of supersymmetry, open strings and M theory," Nucl. Phys. B **553** (1999), 133-154 [arXiv:hep-th/9812118 [hep-th]].

[127] Z. Kakushadze and S. H. H. Tye, "Brane world," Nucl. Phys. B **548** (1999), 180-204 [arXiv:hep-th/9809147 [hep-th]].

[128] D. Baumann, "Inflation," [arXiv:0907.5424 [hep-th]].

[129] M. Viel, J. Lesgourgues, M. G. Haehnelt, S. Matarrese and A. Riotto, "Constraining warm dark matter candidates including sterile neutrinos and light gravitinos with WMAP and the Lyman-alpha forest," Phys. Rev. D **71** (2005) 063534 [astro-ph/0501562].

[130] L. McAllister and E. Silverstein, "String Cosmology: A Review," Gen. Rel. Grav. **40** (2008), 565-605 [arXiv:0710.2951 [hep-th]].

[131] D. Baumann and L. McAllister, "Advances in Inflation in String Theory," Ann. Rev. Nucl. Part. Sci. **59** (2009), 67-94 [arXiv:0901.0265 [hep-th]].

[132] C. Angelantonj and M. Cardella, "Vanishing perturbative vacuum energy in nonsupersymmetric orientifolds," Phys. Lett. B **595** (2004), 505-512 [arXiv:hep-th/0403107 [hep-th]].

[133] A. Sagnotti, in Cargese '87, "Non-perturbative quantum field theory", eds. G. Mack et al (Pergamon Press, 1988), p. 521, "Open strings and their symmetry groups," arXiv:hep-th/0208020.

[134] G. Pradisi and A. Sagnotti, "Open string orbifolds," Phys. Lett. B **216** (1989), 59.

[135] P. Horava, "Strings on world sheet orbifolds," Nucl. Phys. B **327** (1989), 461.

[136] P. Horava, "Background duality of open string models," Phys. Lett. B **231** (1989), 251.

[137] M. Bianchi and A. Sagnotti, "On the systematics of open string theories," Phys. Lett. B **247** (1990), 517.

[138] M. Bianchi and A. Sagnotti, "Twist symmetry and open string Wilson lines," Nucl. Phys. B **361** (1991) 519.

[139] A. Sagnotti, "A note on the Green–Schwarz mechanism in open string theories," Phys. Lett. B **294** (1992), 196 [arXiv:hep-th/9210127].

[140] M. Bianchi, G. Pradisi and A. Sagnotti, "Toroidal compactification and symmetry breaking in open string theories," Nucl. Phys. B **376** (1992), 365-386.

[141] M. Bianchi, "A note on toroidal compactifications of the type I superstring and other superstring vacuum configurations with sixteen supercharges," Nucl. Phys. B **528** (1998), 73-94 [arXiv:hep-th/9711201 [hep-th]].

[142] G. Pradisi, "Magnetic fluxes, NS-NS B field and shifts in four-dimensional orientifolds," [arXiv:hep-th/0310154 [hep-th]].

[143] E. Witten, "Toroidal compactification without vector structure," JHEP **02** (1998), 006 [arXiv:hep-th/9712028 [hep-th]].

[144] R. Minasian and G. W. Moore, "K theory and Ramond–Ramond charge," JHEP **11** (1997), 002 [arXiv:hep-th/9710230 [hep-th]].

[145] E. Witten, "D-branes and K theory," JHEP **12** (1998), 019 [arXiv:hep-th/9810188 [hep-th]].

[146] E. Witten, "An SU(2) anomaly," Phys. Lett. B **117** (1982), 324-328.

[147] A. M. Uranga, "D-brane probes, RR tadpole cancellation and K theory charge," Nucl. Phys. B **598** (2001), 225-246 [arXiv:hep-th/0011048 [hep-th]].

[148] A. Sen, "NonBPS states and Branes in string theory," [arXiv:hep-th/9904207 [hep-th]].

[149] E. Dudas, J. Mourad and A. Sagnotti, "Charged and uncharged D-branes in various string theories," Nucl. Phys. B **620** (2002), 109-151 [arXiv:hep-th/0107081 [hep-th]].

[150] N. Cribiori, D. Lüst and M. Scalisi, "The gravitino and the swampland," [arXiv:2104.08288 [hep-th]].

[151] A. Castellano, A. Font, A. Herráez and L. E. Ibáñez, "A gravitino distance conjecture," [arXiv:2104.10181 [hep-th]].

[152] E. Dudas, M. A. G. Garcia, Y. Mambrini, K. A. Olive, M. Peloso and S. Verner, "Slow and safe gravitinos," [arXiv:2104.03749 [hep-th]].

[153] E. W. Kolb, A. J. Long and E. Mcdonough, "Catastrophic production of slow gravitinos," [arXiv:2102.10113 [hep-th]].

[154] E. W. Kolb, A. J. Long and E. Mcdonough, "The gravitino swampland conjecture," [arXiv:2103.10437 [hep-th]].

[155] Y. Ema, K. Mukaida, K. Nakayama and T. Terada, "Nonthermal gravitino production after large field inflation," JHEP **11** (2016), 184 [arXiv:1609.04716 [hep-ph]].

[156] T. Terada, "Minimal supergravity inflation without slow gravitino," [arXiv:2104.05731 [hep-th]].

[157] I. Antoniadis, K. Benakli and W. Ke, "Salvage of too slow gravitinos," [arXiv:2105.03784 [hep-th]].

[158] M. Bianchi and A. Sagnotti, "Twist symmetry and open string Wilson lines," Nucl. Phys. **B 361** (1991) 519.

[159] E. G. Gimon and J. Polchinski, "Consistency conditions for orientifolds and D-manifolds," Phys. Rev. D **54** (1996) 1667 [hep-th/9601038].

[160] M. Berkooz, R. G. Leigh, J. Polchinski, J. H. Schwarz, N. Seiberg and E. Witten, "Anomalies, dualities, and topology of $D = 6$ $\mathcal{N} = 1$ superstring vacua," Nucl. Phys. B **475** (1996) 115 [hep-th/9605184].

[161] C. Angelantonj, M. Bianchi, G. Pradisi, A. Sagnotti and Y. S. Stanev, "Comments on Gepner models and type I vacua in string theory," Phys. Lett. B **387** (1996), 743-749 [arXiv:hep-th/9607229 [hep-th]].

[162] I. Antoniadis, C. Bachas, C. Fabre, H. Partouche and T. R. Taylor, "Aspects of type I - type II - heterotic triality in four-dimensions," Nucl. Phys. B **489** (1997) 160 [hep-th/9608012].

[163] I. Antoniadis, H. Partouche and T. R. Taylor, "Duality of $\mathcal{N} = 2$ heterotic type I compactifications in four-dimensions," Nucl. Phys. B **499** (1997), 29-44 [arXiv:hep-th/9703076 [hep-th]].

[164] I. Antoniadis, H. Partouche and T. R. Taylor, "Lectures on heterotic type I duality," Nucl. Phys. B Proc. Suppl. **61** (1998), 58-71 [arXiv:hep-th/9706211 [hep-th]].

[165] C. Vafa and E. Witten, "Dual string pairs with N=1 and N=2 supersymmetry in four-dimensions," Nucl. Phys. B Proc. Suppl. **46** (1996), 225-247 [arXiv:hep-th/9507050 [hep-th]].

[166] A. Hashimoto, "Dynamics of Dirichlet-Neumann open strings on D-branes," Nucl. Phys. B **496** (1997), 243-258 [arXiv:hep-th/9608127 [hep-th]].

[167] J. J. Atick, L. J. Dixon, P. A. Griffin and D. Nemeschansky, "Multiloop twist field correlation functions for $\mathbb{Z}_N$ orbifolds," Nucl. Phys. B **298** (1988) 1.

[168] C. P. Burgess and T. R. Morris, "Open and unoriented strings à la Polyakov," Nucl. Phys. B **291** (1987), 256-284.

[169] C. P. Burgess and T. R. Morris, "Open superstrings à la Polyakov," Nucl. Phys. B **291** (1987), 285-333.

[170] M. Cvetic and I. Papadimitriou, "Conformal field theory couplings for intersecting D-branes on orientifolds," Phys. Rev. D **68** (2003), 046001 [erratum: Phys. Rev. D **70** (2004), 029903] [arXiv:hep-th/0303083 [hep-th]].

[171] S. A. Abel and A. W. Owen, "Interactions in intersecting brane models," Nucl. Phys. B **663** (2003), 197-214 [arXiv:hep-th/0303124 [hep-th]].

[172] S. A. Abel and A. W. Owen, "N-point amplitudes in intersecting brane models," Nucl. Phys. B **682** (2004), 183-216 [arXiv:hep-th/0310257 [hep-th]].

[173] J. Frohlich, O. Grandjean, A. Recknagel and V. Schomerus, "Fundamental strings in Dp - Dq brane systems," Nucl. Phys. B **583** (2000), 381-410 [arXiv:hep-th/9912079 [hep-th]].

[174] P. Anastasopoulos, M. Bianchi and R. Richter, "On closed-string twist-field correlators and their open-string descendants," [arXiv:1110.5359 [hep-th]].

[175] L. Mattiello and I. Sachs, "$\mathbb{Z}_2$ boundary twist fields and the moduli space of D-branes," JHEP **07** (2018), 099 [arXiv:1803.07500 [hep-th]].

[176] S. A. Abel and B. W. Schofield, "One-loop Yukawas on intersecting branes," JHEP **06** (2005), 072 [arXiv:hep-th/0412206 [hep-th]].

[177] B. Schofield, "One-loop phenomenology in brane models," Durham thesis, Durham University, Ph.D. Thesis.

[178] S. A. Abel and M. D. Goodsell, "Intersecting brane worlds at one loop," JHEP **02** (2006), 049 [arXiv:hep-th/0512072 [hep-th]].

[179] S. A. Abel and M. D. Goodsell, "Realistic Yukawa couplings through instantons in intersecting brane worlds," JHEP **10** (2007), 034 [arXiv:hep-th/0612110 [hep-th]].

[180] M. D. Goodsell, "One loop phenomenology of type II string theory: intersecting d-branes and noncommutativity," Durham thesis, Durham University,Ph.D. Thesis.

[181] K. Benakli and M. D. Goodsell, "Two-point functions of chiral fields at one loop in Type II," Nucl. Phys. B **805** (2008), 72-103 [arXiv:0805.1874 [hep-th]].

[182] L. J. Dixon, D. Friedan, E. J. Martinec and S. H. Shenker, "The conformal field theory of orbifolds," Nucl. Phys. B **282** (1987) 13.

[183] E. Dudas, N. Kitazawa and A. Sagnotti, "On climbing scalars in string theory," Phys. Lett. B **694** (2011) 80 [arXiv:1009.0874 [hep-th]].

[184] J. J. Halliwell, "Scalar fields in cosmology with an exponential potential," Phys. Lett. B **185** (1987) 341.

[185] A. B. Burd and J. D. Barrow, "Inflationary models with exponential potentials," Nucl. Phys. B **308** (1988) 929, Erratum: [Nucl. Phys. B **324** (1989) 276].

[186] L. P. Chimento, "General solution to two-scalar field cosmologies with exponential potentials," Class. Quant. Grav. **15** (1998) 965.

[187] I. P. C. Heard and D. Wands, "Cosmology with positive and negative exponential potentials," Class. Quant. Grav. **19** (2002) 5435 [gr-qc/0206085]

[188] Z. K. Guo, Y. S. Piao and Y. Z. Zhang, "Cosmological scaling solutions and multiple exponential potentials," Phys. Lett. B **568** (2003) 1 [hep-th/0304048].

[189] P. K. Townsend, "Cosmic acceleration and M-theory," hep-th/0308149.

[190] I. P. Neupane, "Accelerating cosmologies from exponential potentials," Class. Quant. Grav. **21** (2004) 4383 [hep-th/0311071].

[191] P. Vieira, "Late-time cosmic dynamics from M-theory," Class. Quant. Grav. **21** (2004) 2421 [hep-th/0311173].

[192] E. Bergshoeff, A. Collinucci, U. Gran, M. Nielsen and D. Roest, "Transient quintessence from group manifold reductions or how all roads lead to Rome," Class. Quant. Grav. **21** (2004) 1947 [hep-th/0312102].

[193] J. G. Russo, "Exact solution of scalar tensor cosmology with exponential potentials and transient acceleration," Phys. Lett. B **600** (2004) 185 [hep-th/0403010].

[194] L. Jarv, T. Mohaupt and F. Saueressig, "Quintessence cosmologies with a double exponential potential," JCAP **0408** (2004) 016 [hep-th/0403063].

[195] P. K. Townsend and M. N. R. Wohlfarth, "Cosmology as geodesic motion," Class. Quant. Grav. **21** (2004) 5375 [hep-th/0404241].

[196] A. Collinucci, M. Nielsen and T. Van Riet, "Scalar cosmology with multi-exponential potentials," Class. Quant. Grav. **22** (2005) 1269 [hep-th/0407047].

[197] P. K. Townsend and M. N. R. Wohlfarth, "Accelerating cosmologies from compactification," Phys. Rev. Lett. **91** (2003) 061302 [hep-th/0303097].

[198] N. Ohta, "Accelerating cosmologies from S-branes," Phys. Rev. Lett. **91** (2003) 061303 [hep-th/0303238].

[199] S. Roy, "Accelerating cosmologies from M/string theory compactifications," Phys. Lett. B **567** (2003) 322 [hep-th/0304084].

[200] M. N. R. Wohlfarth, "Accelerating cosmologies and a phase transition in M-theory," Phys. Lett. B **563** (2003) 1 [hep-th/0304089].

[201] R. Emparan and J. Garriga, "A Note on accelerating cosmologies from compactifications and S-branes," JHEP **0305** (2003) 028 [hep-th/0304124].

[202] N. Ohta, "A Study of accelerating cosmologies from superstring/M theories," Prog. Theor. Phys. **110** (2003) 269 [hep-th/0304172].

[203] C. M. Chen, P. M. Ho, I. P. Neupane and J. E. Wang, "A Note on acceleration from product space compactification," JHEP **0307** (2003) 017 [hep-th/0304177].

[204] C. M. Chen, P. M. Ho, I. P. Neupane, N. Ohta and J. E. Wang, "Hyperbolic space cosmologies," JHEP **0310** (2003) 058 [hep-th/0306291].

[205] M. N. R. Wohlfarth, "Inflationary cosmologies from compactification?," Phys. Rev. D **69** (2004) 066002 [hep-th/0307179].

[206] E. Kiritsis and C. Kounnas, "Perturbative and nonperturbative partial supersymmetry breaking: $\mathcal{N} = 4 \longrightarrow \mathcal{N} = 2 \longrightarrow \mathcal{N} = 1$," Nucl. Phys. B **503** (1997), 117-156 [arXiv:hep-th/9703059 [hep-th]].

[207] B. de Carlos, J. A. Casas, F. Quevedo and E. Roulet, "Model independent properties and cosmological implications of the dilaton and moduli sectors of 4-d strings," Phys. Lett. B **318** (1993), 447-456 [arXiv:hep-ph/9308325 [hep-ph]].

[208] G. D. Coughlan, R. Holman, P. Ramond and G. G. Ross, "Supersymmetry and the Entropy Crisis," Phys. Lett. B **140** (1984), 44-48.

Publications

The works produced and published during the thesis are appended here. Note that from here, the page numbering is inconsistent since the pdf files of the articles have been inserted without modifications.

Available online at www.sciencedirect.com

ScienceDirect

Nuclear Physics B 930 (2018) 235–254

NUCLEAR PHYSICS B

www.elsevier.com/locate/nuclphysb

Quantum no-scale regimes in string theory

Thibaut Coudarchet, Claude Fleming, Hervé Partouche *

Centre de Physique Théorique, Ecole Polytechnique [1]*, F–91128 Palaiseau cedex, France*

Received 14 December 2017; accepted 7 March 2018
Available online 10 March 2018
Editor: Stephan Stieberger

Abstract

We show that in generic no-scale models in string theory, the flat, expanding cosmological evolutions found at the quantum level can be attracted to a "quantum no-scale regime", where the no-scale structure is restored asymptotically. In this regime, the quantum effective potential is dominated by the classical kinetic energies of the no-scale modulus and dilaton. We find that this natural preservation of the classical no-scale structure at the quantum level occurs when the initial conditions of the evolutions sit in a subcritical region of their space. On the contrary, supercritical initial conditions yield solutions that have no analogue at the classical level. The associated intrinsically quantum universes are sentenced to collapse and their histories last finite cosmic times. Our analysis is done at 1-loop, in perturbative heterotic string compactified on tori, with spontaneous supersymmetry breaking implemented by a stringy version of the Scherk–Schwarz mechanism.

1. Introduction

Postulating the classical Lagrangian of the Standard Model in rigid Minkowski spacetime proved to be a very efficient starting point for computing quantum corrections. However, beyond this Standard Model, theories sometimes admit a gravitational origin. In particular, considering $\mathcal{N} = 1$ supergravity models in dimension $d = 4$, where local supersymmetry is spontaneously

* Corresponding author.
E-mail addresses: thibaut.coudarchet@ens-lyon.fr (T. Coudarchet), claude.fleming@polytechnique.edu (C. Fleming), herve.partouche@polytechnique.edu (H. Partouche).
[1] Unité mixte du CNRS et de l'Ecole Polytechnique, UMR 7644.

https://doi.org/10.1016/j.nuclphysb.2018.03.002

broken in flat space, and restricting the Lagrangians to the relevant operators gives renormalizable classical field theories in rigid Minkowski spacetime, where supersymmetry is softly broken [1]. In that case, consistency of the picture should imply the possibility to commute the order of the above operations, namely first computing quantum corrections and then decoupling gravity.

To explore this alternative point of view in arbitrary dimension d, the classical supergravity theories may be viewed in the framework of no-scale models [2] in string theory, for loop corrections to be unambiguously evaluated. By definition, the no-scale models are classical theories where local (extended) supersymmetry is (totally) spontaneously broken in flat space. In this context, the supersymmetry breaking scale is a scalar field which is a flat direction of a positive semi-definite classical potential. Therefore, if its vacuum expectation value is undetermined classically, a common wisdom is that this no-scale structure breaks down at the quantum level (see *e.g.* [3]).

One way to implement a spontaneous breaking of supersymmetry in string theory is *via* coordinate-dependent compactification [4,5], a stringy version of the Scherk–Schwarz mechanism [6]. An effective potential is generated at 1-loop and is generically of order $\mathcal{O}(M^d)$, where M is the supersymmetry breaking scale measured in Einstein frame. Assuming a mechanism responsible for the stabilization of M (above 10 TeV for $d = 4$) to exist, one then expects the quantum vacuum to be anti-de Sitter- or de Sitter-like, with no way to obtain a theory in rigid Minkowski space, once gravity is decoupled. Exceptions may however exist. In type II [7] and open [8] string theory, the 1-loop effective potential $\mathcal{V}_{\text{1-loop}}$ of some models vanishes at specific points in moduli space. In heterotic string, the closest analogous models [9] are characterized by equal numbers of *massless* bosons and fermions (observable and hidden sectors included), so that $\mathcal{V}_{\text{1-loop}}$ is exponentially suppressed when $M_{(\sigma)}$, the supersymmetry breaking scale measured in σ-model frame, is below the string scale M_{s} [10–12]. These theories, sometimes referred as super no-scale models, can even be dual to the former, where $\mathcal{V}_{\text{1-loop}}$ vanishes [13]. However, all these particular type II, orientifold or heterotic models are expected to admit non-vanishing or non-exponentially suppressed higher order loop corrections [14], in which case they may lead to conclusions similar to those stated in the generic case. Moreover, the particular points in moduli space where $\mathcal{V}_{\text{1-loop}}$ vanishes or is exponentially small are in most cases saddle points. As a consequence, moduli fields are destabilized and, even if their condensations induce a small mass scale $M_H < M$ such as the electroweak scale, the order of magnitude of $\langle \mathcal{V}_{\text{1-loop}} \rangle$ ends up being of order $\mathcal{O}(M^{d-2} M_H^2)$ [11], which is still far too large to be compatible with flat space.

In the present work, we will not assume the existence of a mechanism of stabilization of M that would lead (artificially) to an extremely small cosmological constant. Instead, we take seriously the time-dependance of M induced by the effective potential, in a cosmological setting. We show the existence of an attractor mechanism towards flat Friedmann–Lemaître–Robertson–Walker (FLRW) expanding universes, where the effective potential is dominated by the kinetic energies of M and ϕ, the dilaton field. Asymptotically, the cosmological evolution converges to that found in the classical limit, where the no-scale structure is exact. For this reason, we refer to this mechanism as an attraction to a "quantum no-scale regime". In these circumstances, flatness of the universe is not destabilized by quantum corrections, which justifies that rigid Minkowski spacetime can be postulated in quantum field theory. We stress that even if the effective potential, which scales like M^d, is negligible from a cosmological point of view, the net value of the supersymmetry breaking scale M remains a fundamental ingredient of the theory in rigid spacetime, since it determines the order of magnitude of all soft breaking terms. Note however that the analysis of the constraints raised by astrophysical observations about the constancy of couplings

and masses, or the validity of the equivalence principle, stand beyond the scope of the present work [15].

The above statements are shown in heterotic string compactified on a torus, with the total spontaneous breaking of supersymmetry implemented by a stringy Scherk–Schwarz mechanism [4,5]. Actually, we analyze a simplified model presented in Sect. 2, where only a small number of degrees of freedom are taken into account. To be specific, we consider in a perturbative regime the 1-loop effective action restricted to the scale factor a, as well as M and ϕ. In terms of canonical fields, the scalars can be described by a "no-scale modulus" Φ with exponential potential, and a free scalar $\phi_\perp$. Notice that numerous works have already analyzed such systems, namely scalar fields with exponential potentials [16,17], sometimes as autonomous dynamical systems or by finding explicit solutions. Motivated by different goals, these studies often stress the onset of transient periods of accelerated cosmology. Such models have been realized by classical compactifications involving compact hyperbolic spaces, S-branes or non-trivial fluxes (field strengths) [18].

In the present paper, we find that the space of initial conditions of the equations of motion can be divided into two parts, and we present explicitly the resulting cosmologies in Sects. 3–6.[2] In the first region, which is referred as supercritical and exists only if $\mathcal{V}_{1\text{-loop}}$ is negative, no classical limit exists. Thus, the universe is intrinsically quantum and its existence is found to be limited to a finite lapse of cosmic time. On the contrary, when the initial conditions sit in the so-called subcritical second region, the perturbative solutions can be seen as deformations of classical counterparts. It is in this case that attractions to quantum no-scale regimes take place. If, as mentioned before, the latter can correspond to flat expanding evolutions, we also find that other quantum no-scale regimes exist, which describe a Big Bang (or Big Crunch by time reversal). Moreover, when $\mathcal{V}_{1\text{-loop}}$ is positive, a short period of accelerated expansion can occur during the intermediate era that connects no-scale regimes of the two previous natures [18]. Whereas when $\mathcal{V}_{1\text{-loop}}$ is negative, M decreases as the universe expands and is thus forever climbing its potential [17]. Notice that this behaviour contradicts the naive expectation that M should run away to infinity and lead to large, negative and *a priori* non-negligible potential energy. We also point out that the above perturbative properties are expected to be robust when higher order loop corrections are taken into account.[3] Finally, we summarize our results and outlooks in Sect. 7.

2. The setup

In this section, we consider a simplified heterotic string no-scale model in dimension $d \geq 3$, in the sense that the dynamics of only a restricted number of light degrees of freedom is taken into account. Our goal is to derive the 1-loop low energy effective action and associated field equations of motion to be solved in the following sections.

At the classical level, the background is compactified on $n \geq 1$ circles of radii R_i, times a torus,

[2] A particular case in dimension 4 is already presented in Ref. [19], and describes the cosmological evolution of a universe at finite temperature T, when $T \ll M$.

[3] This supposes the implementation of a regularization scheme to get rid off infrared divergences arising at genus g, when massless propagators and non-vanishing tadpoles at genus $g-1$ exist. This may be done by introducing a small mass gap by curving spacetime [20].

$$\prod_{i=d}^{d+n-1} S^1(R_i) \times T^{10-d-n} \,. \tag{2.1}$$

The volume moduli of T^{10-d-n} are supposed to be small enough for the lightest Kaluza–Klein (KK) mass scale $cM_{\rm s}$ associated with this torus to be very large, $c \lesssim 1$. On the contrary, the n circles are supposed to be large, $R_i \gg 1$, and are used to implement a coordinate-dependent compactification responsible for the total spontaneous breaking of supersymmetry [4,5]. In σ-model frame, we define the resulting low supersymmetry breaking scale to be

$$M_{(\sigma)} \equiv \frac{M_{\rm s}}{\left(\prod_{i=d}^{d+n-1} R_i\right)^{\frac{1}{n}}} \ll cM_{\rm s} \,. \tag{2.2}$$

At the quantum level, assuming a perturbative regime, an effective potential is generated at 1-loop [10,11,21],

$$\begin{aligned} \mathcal{V}^{(\sigma)}_{\text{1-loop}} &\equiv -\frac{M_{\rm s}^d}{(2\pi)^d} \int_{\mathcal{F}} \frac{d^2\tau}{2\tau_2^2} \, Z \\ &= (n_{\rm F} - n_{\rm B}) \, v_{d,n} \, M^d_{(\sigma)} + \mathcal{O}\left((cM_{\rm s} M_{(\sigma)})^{\frac{d}{2}} \, e^{-cM_{\rm s}/M_{(\sigma)}} \right), \end{aligned} \tag{2.3}$$

where Z is the genus-1 partition function and $\mathcal{F}$ is the fundamental domain of $SL(2,\mathbb{Z})$, parameterized by $\tau \equiv \tau_1 + i\tau_2$. In the second expression, $n_{\rm F}, n_{\rm B}$ count the numbers of massless fermionic and bosonic degrees of freedom, while $v_{d,n} > 0$ depends (when $n \geq 2$) on the $n-1$ complex structure moduli, R_i/R_d, $i = d+1, \ldots, d+n-1$. The origins of the different contributions are the following:

– The $n_{\rm B} + n_{\rm F}$ towers of pure KK modes associated with the massless states and arising from the n large directions yield the term proportional to $M^d_{(\sigma)}$.

– On the contrary, the pure KK towers based on the states at higher string oscillator level lead to the exponentially suppressed contribution.

– Finally, all states with non-trivial winding numbers along the n large directions, as well as the unphysical *i.e.* non-level matched states yield even more suppressed corrections, $\mathcal{O}\left(e^{-M_{\rm s}^2/M^2_{(\sigma)}}\right)$.

Since we restrict in the present paper to the regime where $M_{(\sigma)} \ll cM_{\rm s}$, we will neglect from now on the exponentially suppressed terms. Splitting the dilaton field into a constant background and a fluctuation, $\phi_{\rm dil} \equiv \langle \phi_{\rm dil} \rangle + \phi$, the 1-loop low energy effective action restricted to the graviton, ϕ and the radii R_i's takes the following form in Einstein frame[4]:

$$S = \frac{1}{\kappa^2} \int d^d x \, \sqrt{-g} \left[\frac{\mathcal{R}}{2} - \frac{2}{d-2} (\partial\phi)^2 - \frac{1}{2} \sum_{i=d}^{d+n-1} \left(\frac{\partial R_i}{R_i} \right)^2 - \kappa^2 \mathcal{V}_{\text{1-loop}} \right]. \tag{2.4}$$

[4] The 1-loop effective potential induces a backreaction implying a motion of the classical background. Adding the 1-loop correction to the kinetic terms is then unnecessary since it would introduce a correction to the cosmological evolution effectively at second order in string coupling $g_{\rm s}$.

In this expression, $\mathcal{R}$ is the Ricci curvature, $\kappa^2 = e^{2\langle\phi_{\rm dil}\rangle}/M_{\rm s}^{d-2}$ is the Einstein constant, and the potential is dressed with the dilaton fluctuation,

$$\mathcal{V}_{\text{1-loop}} \equiv e^{\frac{2d}{d-2}\phi}\,\mathcal{V}^{(\sigma)}_{\text{1-loop}} \simeq (n_{\rm F} - n_{\rm B})\, v_{d,n}\, M^d\,, \tag{2.5}$$

where M is the supersymmetry breaking scale measured in Einstein frame,

$$M \equiv e^{\frac{2}{d-2}\phi}\, M_{(\sigma)}\,. \tag{2.6}$$

Note that the classical limit of the theory is recovered by taking $\kappa^2 \to 0$.

In order to write the equations of motion, it may be convenient to perform field redefinitions. The kinetic term of the scalar field M being non-canonical, we define the so-called "no-scale modulus" Φ as

$$M \equiv e^{\alpha\Phi} M_{\rm s} \qquad i.e. \qquad \alpha\Phi = \frac{2}{d-2}\,\phi - \frac{1}{n}\sum_{i=d}^{d+n-1} \ln R_i\,, \tag{2.7}$$

where α is an appropriate normalization factor,

$$\alpha = \sqrt{\frac{1}{d-2} + \frac{1}{n}}\,. \tag{2.8}$$

Moreover, the effective potential being by construction independent on the orthogonal combination

$$\phi_\perp = \frac{1}{\sqrt{d-2+n}}\Big(2\phi + \sum_{i=d}^{d+n-1} \ln R_i\Big), \tag{2.9}$$

the latter is a canonical free field. By also redefining the complex structure deformations as

$$\varphi_k = \frac{1}{\sqrt{k(k+1)}}\Big(k \ln R_{d+k} - \sum_{i=d}^{d+k-1} \ln R_i\Big), \qquad k = 1, \ldots, n-1\,, \tag{2.10}$$

the action takes the final form

$$S = \frac{1}{\kappa^2}\int d^dx\,\sqrt{-g}\left[\frac{\mathcal{R}}{2} - \frac{1}{2}(\partial\Phi)^2 - \frac{1}{2}(\partial\phi_\perp)^2 - \frac{1}{2}\sum_{k=1}^{n-1}(\partial\varphi_k)^2 - \kappa^2\mathcal{V}_{\text{1-loop}}\right], \tag{2.11}$$

where the 1-loop effective potential is

$$\mathcal{V}_{\text{1-loop}} = (n_{\rm F} - n_{\rm B})\, v_{d,n}(\varphi_1, \ldots, \varphi_{n-1})\, e^{d\alpha\Phi}\, M_{\rm s}^d\,. \tag{2.12}$$

To keep the toy model as simple as possible, we treat the complex structures as constants, $\varphi_k \equiv$ cst., $k = 1, \ldots, n-1$, and ignore as well the remaining internal moduli (other than the volume $\prod_{i=d}^{d+n-1} R_i$ appearing in the definitions of Φ and $\phi_\perp$). Looking for homogeneous and isotropic cosmological evolutions in flat space, we consider the metric and scalar field anzats[5]

$$ds^2 = -N(x^0)^2(dx^0)^2 + a(x^0)^2\Big((dx^1)^2 + \cdots + (dx^{d-1})^2\Big), \quad \Phi(x^0), \quad \phi_\perp(x^0)\,. \tag{2.13}$$

[5] When $d = 4$, we also take the axion field dual to the spacetime antisymmetric tensor to be constant.

The equations of motion for the lapse function N, scale factor a, no-scale modulus Φ and $\phi_\perp$ take the following forms, in the gauge $N \equiv 1$ which defines cosmic time $x^0 \equiv t$,

$$\frac{1}{2}(d-1)(d-2)\,H^2 = \mathcal{K} + \kappa^2 \mathcal{V}_{\text{1-loop}}\,, \qquad \mathcal{K} = \frac{1}{2}\dot{\Phi}^2 + \frac{1}{2}\dot{\phi}_\perp^2\,, \tag{2.14}$$

$$(d-2)\,\dot{H} + \frac{1}{2}(d-1)(d-2)\,H^2 = -\mathcal{K} + \kappa^2 \mathcal{V}_{\text{1-loop}}\,, \tag{2.15}$$

$$\ddot{\Phi} + (d-1)\,H\,\dot{\Phi} = -d\alpha\kappa^2 \mathcal{V}_{\text{1-loop}}\,, \tag{2.16}$$

$$\ddot{\phi}_\perp + (d-1)\,H\,\dot{\phi}_\perp = 0\,, \tag{2.17}$$

where $H \equiv \dot{a}/a$. In order to solve the above differential system, we consider a linear combination of the three first equations that eliminates both $\mathcal{K}$ and $\mathcal{V}_{\text{1-loop}}$,

$$\Big(\alpha\dot{\Phi} + \frac{\alpha^2}{2}\,d(d-2)\,H\Big)^{\cdot} + (d-1)\,H\Big(\alpha\dot{\Phi} + \frac{\alpha^2}{2}\,d(d-2)\,H\Big) = 0\,, \tag{2.18}$$

which is a free field equation identical to that of $\phi_\perp$. Integrating, we have

$$\dot{\phi}_\perp = \sqrt{2}\,\frac{c_\perp}{a^{d-1}}\,, \qquad \alpha\dot{\Phi} + \frac{\alpha^2}{2}\,d(d-2)\,H = \frac{c_\Phi}{a^{d-1}}\,, \tag{2.19}$$

where $c_\perp, c_\Phi$ are arbitrary constants. Note that under time-reversal, the constants $c_\Phi, c_\perp$ change to $-c_\Phi, -c_\perp$. To proceed, it is useful to eliminate the effective potential between Eqs. (2.14) and (2.15),

$$\frac{1}{2}(d-2)\,\dot{H} = -\mathcal{K}\,. \tag{2.20}$$

The above equation is however a consequence of the others, as can be shown by taking the time derivative of Eq. (2.14) and using the scalar equations (2.16), (2.17). Therefore, we can solve it and insert the solution in Friedmann equation (2.14) in order to find, when $n_{\text{F}} - n_{\text{B}} \neq 0$, the fully integrated expression of the no-scale modulus or M.

To reach this goal, we first use Eqs. (2.19) to express the scalar kinetic energy $\mathcal{K}$ as a function of the scale factor and H, so that Eq. (2.20) becomes a second order differential equation in a only. Second, when $c_\Phi \neq 0$, we introduce a new (dimensionless) time variable τ, in terms of which this equation becomes

$$\tau\,d\tau = -A\,\mathcal{P}(\tau)\,\frac{da}{a}\,, \qquad \mathcal{P}(\tau) = \tau^2 - 2\tau + \omega\Big[1 + 2\alpha^2\Big(\frac{c_\perp}{c_\Phi}\Big)^2\Big]\,, \tag{2.21}$$

where we have defined

$$\tau \equiv \frac{2A}{d c_\Phi}\,\dot{a}\,a^{d-2}\,, \qquad A = \frac{\omega}{4}\,d^2(d-2)\alpha^2\,, \qquad \omega = 1 - \frac{4(d-1)}{d^2(d-2)\alpha^2}\,. \tag{2.22}$$

Note that using the definition of α in Eq. (2.8), we have $0 < \omega < 1$, for arbitrary $d \geq 3$ and $n \geq 1$. Finally, using again Eqs. (2.19), Friedmann equation (2.14) takes an algebraic form, once expressed in terms of time τ,

$$(n_{\text{F}} - n_{\text{B}})\,v_{d,n}\,\kappa^2 M^d = -\frac{c_\Phi^2}{2\alpha^2\omega}\,\frac{\mathcal{P}(\tau)}{a^{2(d-1)}}\,. \tag{2.23}$$

We will see that the forms of the solutions for the scale factor a and the supersymmetry breaking scale M depend drastically on the number of real roots allowed by the quadratic polynomial

$\mathcal{P}(\tau)$. Moreover, in order to find the restrictions for string perturbation theory to be valid, we will need to display the dilaton field evolution. Using the definitions of the scalars Φ and $\phi_\perp$, we have

$$e^{2d\alpha^2\phi} = e^{d\alpha\Phi}\, e^{\frac{d}{n}\sqrt{d-2+n}\,\phi_\perp}\,, \tag{2.24}$$

where $\phi_\perp$ is determined by its cosmic time derivative, or

$$\frac{d\phi_\perp}{d\tau}\,\mathcal{P}(\tau) = -\frac{2\sqrt{2}}{d}\,\frac{c_\perp}{c_\Phi}\,. \tag{2.25}$$

To derive the above relation, we have used the definition of τ and Eq. (2.21) to relate the time variables t and τ,

$$\frac{d\tau}{dt} = -\frac{d}{2}\,\frac{c_\Phi}{a^{d-1}}\,\mathcal{P}(\tau)\,. \tag{2.26}$$

In the following sections, we describe the cosmological evolution obtained for arbitrary $c_\perp/c_\Phi$, which admits a critical value

$$\gamma_c = \sqrt{\frac{1-\omega}{2\alpha^2\omega}}\,, \tag{2.27}$$

corresponding to a null discriminant for $\mathcal{P}(\tau)$.

3. Supercritical case

When $c_\perp$ and $c_\Phi \neq 0$ satisfy the supercritical condition

$$\left|\frac{c_\perp}{c_\Phi}\right| > \gamma_c\,, \tag{3.1}$$

$\mathcal{P}(\tau)$ has no real root. Due to Friedmann equation (2.23), the no-scale model must satisfy $n_\mathrm{F} - n_\mathrm{B} < 0$. Moreover, the classical limit $\kappa^2 \to 0$ is not allowed (!) This very fact means that in the case under consideration, the cosmological evolution of the universe is intrinsically driven by quantum effects. In particular, the time-trajectory cannot allow any regime where the 1-loop effective potential may be neglected.

To be specific, integrating Eq. (2.21), we find

$$a = a_0\,\frac{e^{-\frac{1}{As}\arctan(\frac{\tau-1}{s})}}{\mathcal{P}(\tau)^{\frac{1}{2A}}}\,, \qquad \text{where} \qquad s = \sqrt{1-\omega}\,\sqrt{\left(\frac{c_\perp}{\gamma_c c_\Phi}\right)^2 - 1} \tag{3.2}$$

and a_0 is an integration constant, while combining this result with Eq. (2.23) yields

$$M^d = -\frac{c_\Phi^2}{2\alpha^2\omega\kappa^2}\,\frac{a_0^{2A}}{(n_\mathrm{F}-n_\mathrm{B})\,v_{d,n}}\,\frac{e^{-\frac{2}{s}\arctan(\frac{\tau-1}{s})}}{a^{2(A+d-1)}}\,. \tag{3.3}$$

Fig. 1(*i*) shows the qualitative shape of the scale factor as a function of τ. The arrow shows the direction of the evolution for increasing cosmic time t, when $c_\Phi > 0$. The opposite direction is realized by time-reversal, *i.e.* by choosing $c_\Phi < 0$. We see that all solutions describe an initially growing universe that reaches a maximal size before contracting.

In the limits $\tau \to \epsilon\infty$, $\epsilon = \pm 1$, the expression $a(\tau)$ together with the definition of τ yield

$$a(t) \sim \left[\frac{d(A+d-1)}{2A}\,a_0^A\, e^{-\frac{\epsilon\pi}{2s}}\,\epsilon c_\Phi (t-t_\epsilon)\right]^{\frac{1}{A+d-1}}\,, \tag{3.4}$$

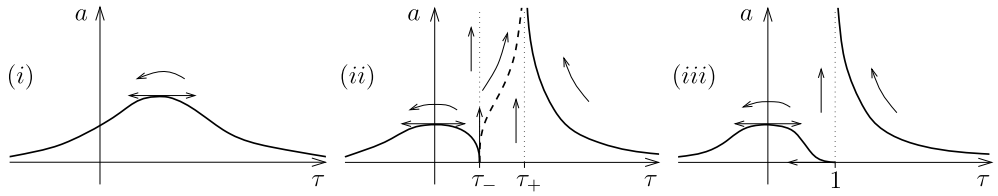

Fig. 1. Qualitative behaviours of the allowed branches of the scale factor a as a function of time τ: (i) In the supercritical, (ii) subcritical and (iii) critical cases. The directions of the evolutions for increasing cosmic time t are indicated for $c_\Phi > 0$. Solid curves correspond to no-scale models with $n_F - n_B < 0$. The dashed curve corresponds to no-scale models with $n_F - n_B > 0$. Dotted lines correspond to super no-scale models, $n_F - n_B = 0$.

where t_ϵ is an integration constant. For $\epsilon c_\Phi > 0$, this describes a Big Bang at $t \gtrsim t_\epsilon$, while $\epsilon c_\Phi < 0$ corresponds to a Big Crunch at $t \lesssim t_\epsilon$. Since $A > 0$, we have in these regimes

$$H^2 \sim \# \dot{\Phi}^2 \sim \# \kappa^2 \mathcal{V}_{1\text{-loop}} \sim \# \frac{a_0^{2A} c_\Phi^2}{a^{2(A+d-1)}} \gg \frac{1}{2} \dot{\phi}_\perp^2 = \frac{c_\perp^2}{a^{2(d-1)}} , \tag{3.5}$$

which shows that the evolution of the universe at the Big Bang and Big Crunch is dominated by the no-scale modulus kinetic energy, partially compensated by the negative potential energy. As announced at the beginning of this section, the quantum effective potential plays also a fundamental role at the bounce, since

$$H = 0 \quad \Longrightarrow \quad \frac{1}{2} (d-2) \frac{\ddot{a}}{a} = -\mathcal{K} = \kappa^2 \mathcal{V}_{1\text{-loop}} < 0 . \tag{3.6}$$

To study the domain of validity of perturbation theory during the cosmological evolution, it is enough to focus on the dilaton in the above $\tau \to \epsilon\infty$ limits. Eq. (2.25) shows that asymptotically, $\phi_\perp$ converges to an integration constant, so that Eq. (2.24) leads to

$$e^{2d\alpha^2\phi} \sim \# |\tau|^{\frac{2}{\omega}} \to +\infty . \tag{3.7}$$

Thus, the consistency of the 1-loop analysis is guaranteed late enough after the Big Bang and early enough before the Big Crunch. Moreover, the scale factor is assumed to be large enough, for the kinetic energies in Eq. (3.5) to be small compared to the string scale. This is required not to have to take into account higher derivative terms in the effective action or, possibly, the dynamics of the whole string spectrum. For the above two reasons, the cosmological evolution can only be trusted far enough from its formal initial Big Bang ($t \gtrsim t_{\text{sign}\, c_\Phi}$) and final Big Crunch ($t \lesssim t_{-\text{sign}\, c_\Phi}$).

To summarize, the supercritical case realizes a quantum universe whose existence is only allowed for a finite lapse of cosmic time (unless string theory resolves the Big Crunch and allows a never-ending evolution). Since the quantum corrections to the off-shell classical action allow new cosmological evolutions which describe the birth of a world sentenced to death, we may interpret this finite history as that of an "unstable flat FLRW universe" arising by quantum effects. It is however not excluded that the expanding phase of the solution (3.2), (3.3), (2.25) may be related in some way to some cosmological era of the real world.

4. Subcritical case and quantum no-scale regimes

When the integration constants $c_\perp$ and $c_\Phi \neq 0$ satisfy the subcritical condition

$$\left| \frac{c_\perp}{c_\Phi} \right| < \gamma_c , \tag{4.1}$$

$\mathcal{P}(\tau)$ admits two distinct real roots,

$$\tau_\pm = 1 \pm r\,, \qquad \text{where} \qquad r = \sqrt{1-\omega}\sqrt{1-\left(\frac{c_\perp}{\gamma_c c_\Phi}\right)^2}\,. \tag{4.2}$$

Important remarks follow from Friedmann equation (2.23). First, the bosonic or fermionic nature of the massless spectrum determines the allowed ranges of variation of τ,

$$\begin{aligned} n_{\rm F} - n_{\rm B} < 0 \quad &\Longrightarrow \quad \tau < \tau_- \quad \text{or} \quad \tau > \tau_+ \\ n_{\rm F} - n_{\rm B} = 0 \quad &\Longrightarrow \quad \tau \equiv \tau_- \quad \text{or} \quad \tau \equiv \tau_+ \\ n_{\rm F} - n_{\rm B} > 0 \quad &\Longrightarrow \quad \tau_- < \tau < \tau_+\,. \end{aligned} \tag{4.3}$$

Second, taking the classical limit $\kappa^2 \to 0$ is allowed, and yields evolutions $\tau(t) \equiv \tau_-$ or $\tau(t) \equiv \tau_+$. Therefore, the classical trajectories are identical to those obtained for quantum super no-scale models, *i.e.* when $n_{\rm F} - n_{\rm B} = 0$. In the following, we start by describing the cosmological solutions in the super no-scale case, and then show that the quantum evolutions for generic no-scale models ($n_{\rm F} - n_{\rm B} \neq 0$) admit quantum no-scale regimes, *i.e.* behave the same way.

4.1. Case $n_{\rm F} - n_{\rm B} = 0$

When $\tau \equiv \tau_\pm$,[6] Eqs. (2.21) and (2.23) being trivial, we use the definition of τ given in Eq. (2.22) to derive the scale factor as a function of cosmic time t,

$$a = \left[\frac{d(d-1)}{2A}\,(1 \pm r)\,c_\Phi (t - t_\pm)\right]^{\frac{1}{d-1}}, \tag{4.4}$$

where $t_\pm$ is an integration constant. For $c_\Phi > 0$, this describes a never-ending era $t > t_\pm$ of expansion, initiated by a Big Bang occurring at $t = t_\pm$. Of course, the solution obtained by time-reversal satisfies $c_\Phi < 0$ and describes an era $t < t_\pm$ of contraction that ends at the Big Crunch occurring at $t_\pm$. Integrating the no-scale modulus equation in (2.19), we find

$$M^d = \frac{e^{d\alpha\Phi_\pm}}{a^{2(d-1)+K_\pm}}\,M_{\rm s}^d\,, \tag{4.5}$$

where $\Phi_\pm$ is an integration constant and

$$K_\pm = \pm\frac{2Ar}{1 \pm r}\,. \tag{4.6}$$

In total, when the 1-loop effective potential vanishes (up to exponentially suppressed terms), the cosmological evolution is driven by the kinetic energies of the free scalar fields,

$$H^2 \propto \dot\phi_\perp^2 \propto \dot\Phi^2 \propto \frac{c_\Phi^2}{a^{2(d-1)}}\,. \tag{4.7}$$

The dilaton evolution is found using Eq. (2.24),

$$e^{2d\alpha^2\phi} = \frac{e^{d\alpha\Phi_\pm}\,e^{\frac{d}{n}\sqrt{d-2+n}\,\phi_{\perp\pm}}}{a^{P_\pm}}\,, \tag{4.8}$$

[6] One may think that the space of solutions in the super no-scale case is divided in two parts, corresponding to either $\tau \equiv \tau_+$ or $\tau \equiv \tau_-$. This is however not true. Including the critical case of Sect.5.1, all the evolutions are actually of the form $\tau \equiv \tau_i$, where $1 - \sqrt{1-\omega} \leq \tau_i \leq 1 + \sqrt{1-\omega}$.

where $\phi_{\perp\pm}$ is an integration constant and

$$P_\pm = \frac{K_\pm}{\omega r}\Big(r \pm \big(1-\omega-\frac{\omega}{n}\sqrt{2(d-2+n)}\,\frac{c_\perp}{c_\Phi}\big)\Big)\,. \tag{4.9}$$

Unless $P_\pm$ vanishes, in which case the dilaton is constant, the string coupling $g_s = e^\phi$ varies monotonically between perturbative and non-perturbative regimes. For instance, the solution $\tau \equiv \tau_+$ is perturbative in the large scale factor limit, $c_\Phi(t-t_+) \to +\infty$, when $P_+ > 0$. In order to translate this condition into a range for $c_\perp/c_\Phi$, we introduce

$$\gamma_\pm = \frac{(1-\omega)\sqrt{\frac{2(d-2)}{n}} \pm \alpha\sqrt{2(1-\omega)(d-2)}}{2\alpha(\omega\frac{d-2}{n}+1)}\,, \tag{4.10}$$

which satisfy $0 < \pm\gamma_\pm < \gamma_c$, and find $P_+ > 0$ if and only if

$$-\gamma_c < \frac{c_\perp}{c_\Phi} < \gamma_+ \quad \text{when} \quad n < \frac{d^2(d-2)}{4(d-1)}\,, \qquad -\gamma_c < \frac{c_\perp}{c_\Phi} < \gamma_c \quad \text{when} \quad n > \frac{d^2(d-2)}{4(d-1)}\,. \tag{4.11}$$

In a similar way, the solution $\tau \equiv \tau_-$ is perturbative in the small scale factor limit, $c_\Phi(t-t_-) \to 0_+$, when $P_- < 0$ *i.e.*

$$\gamma_- < \frac{c_\perp}{c_\Phi} < \gamma_c \quad \text{when} \quad n < \frac{d^2(d-2)}{4(d-1)}\,, \qquad \gamma_- < \frac{c_\perp}{c_\Phi} < \gamma_+ \quad \text{when} \quad n > \frac{d^2(d-2)}{4(d-1)}\,. \tag{4.12}$$

As already mentioned in the supercritical case, beside the conditions for the g_s-expansion to be valid, the above solutions suppose the scale factor to be large enough, for the higher derivative terms (α'-corrections) to be small. Because of this constraint, the Big Bang ($t \gtrsim t_\pm$) and Big Crunch ($t \lesssim t_\pm$) behaviours are only formal.

4.2. *Case* $n_F - n_B \neq 0$

Let us turn to the analysis of a generic no-scale model, thus characterized by $n_F - n_B \neq 0$. In this case, τ can actually be treated as a time variable and, integrating Eq. (2.21), we find

$$a = \frac{a_0}{|\tau-\tau_-|^{\frac{1}{K_-}}\,|\tau-\tau_+|^{\frac{1}{K_+}}}\,, \tag{4.13}$$

where $a_0 > 0$ is an integration constant. Using this result with Friedmann equation (2.23) yields M^d, which can be written in two different suggestive ways,

$$M^d = \frac{M_+^d}{a^{2(d-1)+K_+}}\left|\frac{\tau-\tau_-}{\tau_+-\tau_-}\right|^{\frac{2}{\tau_+}} = \frac{M_-^d}{a^{2(d-1)+K_-}}\left|\frac{\tau_+-\tau}{\tau_+-\tau_-}\right|^{\frac{2}{\tau_-}}\,, \tag{4.14}$$

where we have defined

$$M_\pm^d = \frac{c_\Phi^2}{2\alpha^2\omega\kappa^2}\,\frac{a_0^{K_\pm}}{|n_F-n_B|\,v_{d,n}}\,|\tau_+-\tau_-|^{\frac{2}{\tau_\pm}}\,. \tag{4.15}$$

Fig. 1(*ii*) shows schematically the scale factor a as a function of τ. As expected from Eq. (4.3), two branches (in solid lines) exist when $n_F - n_B < 0$. Thus, depending on the choice of initial

condition $\tau_i \equiv \tau(t_i)$, the scale factor evolves along one or the other. When $n_F - n_B > 0$, a single branch (in dashed line) can be followed by the universe. For completeness, the constant $\tau \equiv \tau_\pm$ trajectories found in the previous subsection for the super no-scale case $n_F - n_B = 0$ are also displayed (in dotted lines). The arrows indicate the directions of the evolutions for increasing cosmic time t, when $c_\Phi > 0$. The opposite directions are realized by time-reversal, with $c_\Phi < 0$. We see that all branches start and/or end with a vanishing scale factor, when $\tau \to \pm\infty$ or $\tau \to \tau_-$.[7] In all cases, whether $da/d\tau$ vanishes, is infinite or is finite when $a(\tau) \to 0$, we will see that da/dt diverges at a finite cosmic time, thus describing a formal Big Bang or Big Crunch.

Note that when $n_F - n_B \neq 0$, all branches allow τ to approach τ_+ and/or τ_-. When this is the case, the behaviour $\tau(t) \to \tau_\pm$ yields, using the definition of τ given in Eq. (2.22),

$$a \sim \left[\frac{d(d-1)}{2A}\,(1 \pm r)\, c_\Phi (t - t_\pm)\right]^{\frac{1}{d-1}}, \qquad M^d \sim \frac{M_\pm^d}{a^{2(d-1)+K_\pm}}, \tag{4.16}$$

for some integration constant $t_\pm$. This shows that the cosmological evolution of the universe as well as that of the scalars Φ and $\phi_\perp$ approach those found in the super no-scale case $n_F - n_B = 0$, *i.e.* for vanishing 1-loop effective potential (up to exponentially suppressed terms). For this reason, *we define the limits $\tau \to \tau_\pm$ of the generic no-scale models as "quantum no-scale regimes"*. These are characterized by phases of the universe dominated by the scalar kinetic energies,

$$H^2 \sim \#\,\dot\phi_\perp^2 \sim \#\,\dot\Phi^2 \sim \#\,\frac{c_\Phi^2}{a^{2(d-1)}} \gg \kappa^2 |\mathcal{V}_{\text{1-loop}}| \sim \#\,\frac{a_0^{K_\pm} c_\Phi^2}{a^{2(d-1)+K_\pm}}\,. \tag{4.17}$$

In fact, when $\tau \to \tau_+$, the divergence of the scale factor, $a(\tau) \to +\infty$, and the fact that $K_+ > 0$ imply that the quantum potential is effectively dominated. Moreover, Eq. (4.16) shows that this regime lasts for an indefinitely long cosmic time, $c_\Phi t \to +\infty$. In a similar way, when $\tau \to \tau_-$, since $a(\tau) \to 0$ and $K_- < 0$, the effective potential is again dominated, and this process is realized when cosmic time approaches t_-, $c_\Phi(t - t_-) \to 0_+$. To summarize, when $\tau \to \tau_\pm$, assuming a perturbative regime, the quantum cosmological evolution of the no-scale model is attracted to that of a classical background ($\kappa^2 = 0$), where the no-scale structure is exact. In particular, the temporal evolution of the no-scale modulus Φ approaches that of a free field, so that the no-scale structure tends to withstand perturbative corrections. Note however that the cosmological solutions found for no-scale models satisfying $n_F - n_B < 0$ can also admit other regimes. As in the supercritical case, the latter correspond to limits $\tau \to \epsilon\infty$, $\epsilon = \pm 1$, describing a formal Big Bang or Big Crunch,

$$a(t) \sim \left[\frac{d(A+d-1)}{2A}\, a_0^A\, \epsilon c_\Phi (t - t_\epsilon)\right]^{\frac{1}{A+d-1}}, \tag{4.18}$$

where t_ϵ is an integration constant. In these circonstances, the universe is dominated by the kinetic energy and negative potential of the no-scale modulus, as summarized in Eq. (3.5).

[7] The trajectories allowing τ to approach τ_- are shown in Fig. 1(ii) in the case $da/d\tau \to \pm\infty$, when $\tau \to \tau_-$. This occurs when $|c_\perp/c_\Phi| < \gamma_M$, where $\gamma_M = [(\frac{1}{\omega}(1 - \frac{1}{(1+2A)^2}) - 1)\frac{1}{2\alpha^2}]^{\frac{1}{2}}$. On the contrary, when $\gamma_M < |c_\perp/c_\Phi| < \gamma_c$, one has $da/d\tau = 0$ at $\tau = \tau_-$. Finally, $|c_\perp/c_\Phi| = \gamma_M$ implies $|da/d\tau|$ to be finite and non-vanishing at $\tau = \tau_-$. However, these different behaviours do not play any important role in the sequel.

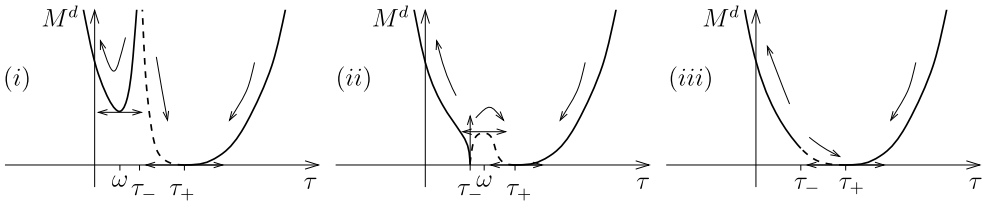

Fig. 2. Qualitative behaviours of the allowed branches of M^d as a function of τ, in the subcritical case: (i) When $\sqrt{\omega}\gamma_c < |c_\perp/c_\Phi| < \gamma_c$, (ii) when $|c_\perp/c_\Phi| < \sqrt{\omega}\gamma_c$, (iii) or when $|c_\perp/c_\Phi| = \sqrt{\omega}\gamma_c$. The directions of the evolutions for increasing cosmic time t are indicated for $c_\Phi > 0$. Solid curves refer to no-scale models with $n_{\rm F} - n_{\rm B} < 0$, while the dashed ones refer to no-scales models with $n_{\rm F} - n_{\rm B} > 0$.

To determine the domain of validity of perturbation theory, we integrate Eq. (2.25), which introduces an arbitrary constant mode $\phi_{\perp 0}$, and use Eq. (2.24) to derive the time dependance of the dilaton,

$$e^{2d\alpha^2\phi} = \frac{c_\Phi^2}{2\alpha^2\omega\kappa^2 M_{\rm s}^d}\,\frac{1}{|n_{\rm F}-n_{\rm B}|\,v_{d,n}}\,\frac{e^{\frac{d}{n}\sqrt{d-2+n}\,\phi_{\perp 0}}}{a_0^{2(d-1)}}\,|\tau-\tau_+|^{L_+}\,|\tau-\tau_-|^{L_-}, \qquad L_\pm = \frac{P_\pm}{K_\pm}, \tag{4.19}$$

where $P_\pm$ is defined in Eq. (4.9). Therefore, the conditions $L_\pm > 0$ for perturbative consistency of the attractions to the quantum no-scale regimes $\tau \to \tau_\pm$ are those found in the super no-scale case: For $\tau \to \tau_+$, $c_\perp/c_\Phi$ must satisfy Eq. (4.11), while for $\tau \to \tau_-$, $c_\perp/c_\Phi$ must respect Eq. (4.12). In particular, when $n_{\rm F} - n_{\rm B} > 0$, the cosmological evolution between τ_- and τ_+ is all the way perturbative if $\gamma_- < c_\perp/c_\Phi < \gamma_+$. In this case, the quantum potential is negligible, $\mathcal{V}_{\text{1-loop}} \ll \mathcal{K}$, throughout the evolution, except in the vicinity of $\tau = 1$, where it induces the transition from one no-scale regime to the other. On the contrary, the regimes $\tau \to \epsilon\infty$, which can be reached when $n_{\rm F} - n_{\rm B} < 0$, can be trusted up to the times the evolutions become non-perturbative, as follows from Eq. (3.7), which is valid for arbitrary $c_\perp/c_\phi \in \mathbb{R}$.

For $n_{\rm F} - n_{\rm B} \neq 0$, the subcritical case can also give rise to non-trivial dynamics of the no-scale modulus, which can be summarized as follows, for instance in the case $c_\Phi > 0$:

(i) When $\sqrt{\omega}\gamma_c < |c_\perp/c_\Phi| < \gamma_c$, even if the effective potential is dominated in the no-scale regime $\tau \to \tau_-$, M^d turns out to diverge, as can be seen in Fig. 2(i), which shows the three branches M^d can follow as a function of τ. The directions of the evolutions for increasing cosmic time t are again indicated for $c_\Phi > 0$. Along the trajectories satisfying $\tau > \tau_+$, the universe expands and is attracted to the no-scale regime $\tau \to \tau_+$, while $M(t)$ decreases. Thus, even if this is counterintuitive, the supersymmetry breaking scale forever climbs its negative effective potential $(n_{\rm F} - n_{\rm B})v_{d,n}M^d$ [17]. This fact contradicts the expectation that M should increase and yield a large, negative potential energy. On the contrary, the situation is more natural in the other branches. For the solutions satisfying $\tau < \tau_-$, if $M(t)$ also starts climbing its negative potential, it is afterwards attracted back to large values, with the turning point sitting at $\tau = \omega$. Finally, along the branch $\tau_- < \tau < \tau_+$, the universe expands and is attracted to the no-scale regime $\tau \to \tau_+$, while $M(t)$ drops along its positive potential $(n_{\rm F} - n_{\rm B})v_{d,n}M^d$.

(ii) When $|c_\perp/c_\Phi| < \sqrt{\omega}\gamma_c$, as shown in Fig. 2$(ii)$, M^d vanishes when $\tau \to \tau_-$. Along the branch $\tau > \tau_+$, $M(t)$ climbs as before its negative potential [17], while for $\tau < \tau_-$, it drops. The branch $\tau_- < \tau < \tau_+$ is the most interesting one: While the scale factor increases, $M(t)$ first climbs the positive potential $(n_{\rm F} - n_{\rm B})v_{d,n}M^d$, and then descends. At the turning point located at $\tau = \omega$, we have $\dot\Phi = 0$ and $\mathcal{V}_{\text{1-loop}} > 0$, which is enough to show that for small enough $|c_\perp|$, the

scale factor accelerates for a lapse of cosmic time [16–18]. However, the resulting e-fold number being of order 1, this acceleration of the universe does not yield any efficient inflationary effect.[8]

(iii) Finally, Fig. 2(iii) plots $M^d(\tau)$ in the limit case $|c_\perp/c_\Phi| = \sqrt{\omega}\gamma_c$.

To conclude on the subcritical case, let us stress again that the dynamics arising from initial conditions such that

$$c_\Phi > 0 \text{ when } n_F - n_B \geq 0\,, \qquad \text{or} \qquad c_\Phi > 0 \text{ and } \tau_i > \tau_+ \text{ when } n_F - n_B < 0\,, \quad (4.20)$$

and satisfying Eq. (4.11) to insure validity of perturbation theory, forces the universe to enter the no-scale regime $\tau(t) \to \tau_+$.[9] After the Big Bang, the solutions describe flat, ever-expanding FLRW universes that are not destabilized by quantum effects. Instead of generating a cosmological constant, quantum corrections induce a time-dependent effective potential proportional to M^d and asymptotically negligible, from a cosmological point of view. Note however that M plays a fundamental role in the effective d-dimensional renormalizable theory in rigid Minkowski space, which is found by keeping only the relevant operators present in supergravity. In fact, M determines the order of magnitude of all soft breaking terms in the resulting MSSM-like theory of particles [1].

5. Critical case

In the critical case, which corresponds to

$$\left|\frac{c_\perp}{c_\Phi}\right| = \gamma_c\,, \quad (5.1)$$

the polynomial $\mathcal{P}(\tau)$ has a double root $\tau_+ = \tau_- = 1$, and the no-scale model must satisfy $n_F - n_B \leq 0$, as follows from Eq. (2.23). In the sequel, we show that the qualitative behaviour of the associated cosmological evolutions are similar to those found in the subcritical case.

5.1. Case $n_F - n_B = 0$

The solutions in the super no-scale case are actually those found in the subcritical case for $c_\perp/c_\Phi = \eta\gamma_c$, $\eta = \pm 1$, *i.e.* for $r = 0$:

$$a = \left[\frac{d(d-1)}{2A}\, c_\Phi (t - t_0)\right]^{\frac{1}{d-1}}, \qquad M^d = \frac{e^{d\alpha\Phi_0}}{a^{2(d-1)}}\, M_s^d, \qquad e^{2d\alpha^2\phi} = \frac{e^{d\alpha\Phi_0}\, e^{\frac{d}{n}\sqrt{d-2+n}\,\phi_{\perp 0}}}{a^{P_0}}, \quad (5.2)$$

where t_0, Φ_0, $\phi_{\perp 0}$ are integration constants and

$$P_0 = 2(d-1)\left(1 - \eta\sqrt{\frac{d-2}{n}\,\frac{\omega}{1-\omega}}\right). \quad (5.3)$$

The above evolutions are perturbative in the large scale factor regime, $c_\Phi(t - t_0) \to +\infty$, when $P_0 > 0$. This is the case for $c_\perp/c_\Phi = -\gamma_c$, as well as for $c_\perp/c_\Phi = \gamma_c$ if $n > \frac{d^2(d-2)}{4(d-1)}$.

---

[8] We warmly thank Lucien Heurtier to have analyzed the magnitude of the e-fold number.

[9] At 1-loop, the super no-scale models, $n_F - n_B = 0$, also admit the expanding solution $c_\phi > 0$, $\tau(t) \equiv \tau_-$, which is perturbative if $|c_\perp/c_\Phi| < \gamma_c$ satisfies the condition complementary to that given in Eq. (4.12). However, we expect this statement to be invalidated when higher order corrections in g_s are taken into account and the effective potential is no more vanishing (up to exponentially suppressed terms).

5.2. Case $n_{\rm F} - n_{\rm B} < 0$

For the no-scale models with negative 1-loop effective potentials, Eqs. (2.21) and (2.23) yield

$$a = a_0 \, \frac{e^{\frac{1}{A(\tau-1)}}}{|\tau-1|^{\frac{1}{A}}} \,, \qquad M^d = \frac{c_\Phi^2}{2\alpha^2\omega\kappa^2} \, \frac{-1}{(n_{\rm F}-n_{\rm B})\, v_{d,n}} \, \frac{(\tau-1)^2}{a^{2(d-1)}} \,, \tag{5.4}$$

where $a_0 > 0$ is an integration constant. Fig. 1(iii) shows in solid lines the two branches $\tau > 1$ and $\tau < 1$ the scale factor $a(\tau)$ can follow, while the dotted line $\tau \equiv 1$ corresponds to the critical super no-scale case. The trajectories admit one of the two limits $\tau \to 1_+$ or $\tau \to 1_-$, which lead in terms of cosmic time to

$$a \sim \left[\frac{d(d-1)}{2A} \, c_\Phi (t - t_\pm) \right]^{\frac{1}{d-1}} \,, \tag{5.5}$$

where $t_\pm$ is an integration constant. The behaviour $\tau \to 1_+$ describes an expanding or contracting flat FLRW solution, $c_\Phi(t-t_+) \to +\infty$, while $\tau \to 1_-$ corresponds to a Big Bang or Big Crunch, $c_\Phi(t-t_-) \to 0_+$. Note that even if $K_\pm$ in Eq. (4.6) vanishes for $r = 0$, the effective potential is still dominated by the moduli kinetic energies,

$$H^2 \sim \#\, \dot\phi_\perp^2 \sim \#\, \dot\Phi^2 \sim \#\, \frac{c_\Phi^2}{a^{2(d-1)}} \gg \kappa^2 |\mathcal{V}_{\text{1-loop}}| \sim \#\, c_\Phi^2 \, \frac{(\tau-1)^2}{a^{2(d-1)}} \,, \tag{5.6}$$

which proves that the limits $\tau \to 1_\pm$ describe quantum no-scale regimes. On the contrary, the limits $\tau \to \epsilon\infty$, $\epsilon = \pm 1$, yield Big Bang/Big Crunch behaviours, as shown in Eqs. (4.18) and (3.5).

Finally, for $c_\perp / c_\Phi = \eta\gamma_c$, $\eta = \pm 1$, the dilaton trajectory is given by

$$e^{2d\alpha^2\phi} = \frac{c_\Phi^2}{2\alpha^2\omega\kappa^2 M_{\rm s}^d} \, \frac{-1}{(n_{\rm F}-n_{\rm B})\, v_{d,n}} \, \frac{e^{\frac{d}{n}\sqrt{d-2+n}\,\phi_{\perp 0}}}{a_0^{2(d-1)}} \, (\tau-1)^{\frac{2}{\omega}} \, e^{-\frac{P_0}{A(\tau-1)}} \,, \tag{5.7}$$

where P_0 is defined in Eq. (5.3) and $\phi_{\perp 0}$ is the arbitrary constant mode of $\phi_\perp$. Thus,[10] the no-scale regime $\tau \to 1_+$ is perturbative for $c_\perp / c_\Phi = -\gamma_c$, as well as for $c_\perp / c_\Phi = \gamma_c$ if $n > \frac{d^2(d-2)}{4(d-1)}$. On the contrary, the regime $\tau \to 1_-$ is perturbative only for $c_\perp / c_\Phi = \gamma_c$, if $n < \frac{d^2(d-2)}{4(d-1)}$. In the limits $\tau \to \epsilon\infty$, $\epsilon = \pm 1$, the models are non-perturbative (see Eq. (3.7)).

6. Case $c_\Phi = 0$

What remains to be presented is the cosmological evolution for $c_\Phi = 0$. The supersymmetry breaking scale can be found by integrating the no-scale modulus equation in (2.19), which gives

$$M^d = \frac{e^{d\alpha\Phi_0}}{a^{2(A+d-1)}} \, M_{\rm s}^d \,, \tag{6.1}$$

where Φ_0 is a constant. This result can be used to write Friedmann equation (2.14) as

$$\frac{A}{2}\,(d-2)\,H^2 = -\frac{c_\perp^2}{a^{2(d-1)}} - (n_{\rm F}-n_{\rm B})\, v_{d,n} \, \frac{e^{d\alpha\Phi_0}}{a^{2(A+d-1)}} \, \kappa^2 M_{\rm s}^d \,, \tag{6.2}$$

which for $c_\perp \neq 0$ requires the no-scale model to satisfy $n_{\rm F} - n_{\rm B} < 0$. Note that this is not surprising since this case is somehow "infinitely supercritical". As a result, no-scale regimes are not

[10] These remarks can be recovered from Eqs. (4.11) and (4.12) by taking $c_\perp / c_\Phi \to \eta\gamma_c$.

expected to exist. To be specific, when $c_\perp \neq 0$, the above differential equation can be used to determine the cosmic time as a function of the scale factor,

$$t = t_* - \epsilon\, \frac{a_{\max}^{A+d-1}}{c_v} \int_{a/a_{\max}}^{1} \frac{x^{A+d-2}\, dx}{\sqrt{1-x^{2A}}}\,, \qquad \text{where} \qquad \epsilon = \pm 1\,,$$

$$a_{\max}^{2A} = \frac{|n_{\rm F} - n_{\rm B}|\, v_{d,n}\, e^{d\alpha\Phi_0}}{c_\perp^2}\, \kappa^2 M_{\rm s}^d\,, \qquad c_v^2 = \frac{2}{d-2}\, \frac{|n_{\rm F} - n_{\rm B}|\, v_{d,n}\, e^{d\alpha\Phi_0}}{A}\, \kappa^2 M_{\rm s}^d\,, \tag{6.3}$$

and t_* is an integration constant. Defining

$$t_\epsilon = t_* - \epsilon t_0\,, \qquad t_0 = \frac{a_{\max}^{A+d-1}}{c_v} \int_0^1 \frac{x^{A+d-2}\, dx}{\sqrt{1-x^{2A}}}\,, \tag{6.4}$$

the time variable t varies from t_+ to t_-. At $t = t_+$, a Big Bang initiates an era of expansion that stops when the scale factor reaches its maximum $a_{\max}$ at $t = t_*$. Then, the universe contracts until a Big Crunch occurs at $t = t_-$. Close to the initial and final times $t_\pm$, the scale factor behaves as

$$a(t) \sim \big(c_v\, (A+d-1)\, \epsilon (t - t_\epsilon)\big)^{\frac{1}{A+d-1}}\,, \tag{6.5}$$

which leads to scalings similar to those given in Eq. (3.5), namely

$$H^2 \sim \#\, \dot\Phi^2 \sim \#\, \kappa^2 \mathcal{V}_{\text{1-loop}} \sim \#\, \frac{c_v^2}{a^{2(A+d-1)}} \gg \frac{1}{2}\, \dot\phi_\perp^2 = \frac{c_\perp^2}{a^{2(d-1)}}\,. \tag{6.6}$$

However, the scalar $\phi_\perp$ converges in this case to a constant, so that Eq. (2.24) yields

$$e^{2d\alpha^2\phi} \sim \frac{\#}{c_v^2 (t - t_\epsilon)^2} \to +\infty\,. \tag{6.7}$$

As a result of Eqs. (6.6) and (6.7), the cosmological solution we have found can only be trusted far enough from the formal Big Bang and Big Crunch, not to have to take into account α'- and $g_{\rm s}$-corrections.

Finally, when $c_\perp = 0$ and $n_{\rm F} - n_{\rm B} < 0$, the maximum scale factor $a_{\max}$ is formally infinite, so that no turning point exists anymore. In fact, relations (6.5) and (6.7) become equalities: The evolution for $\epsilon = +1$ describes a never-ending era $t > t_+$ of expansion, while the trajectory for $\epsilon = -1$ describes an era $t < t_-$ of contraction. For super no-scale models, *i.e.* when $n_{\rm F} - n_{\rm B} = 0$, the case $c_\perp = 0$ yields the trivial solution where all fields a, Φ, $\phi_\perp$ are static.

7. Summary and conclusion

We have considered the low energy effective action of heterotic no-scale models compactified on tori down to d dimensions. At 1-loop, the effective potential backreacts on the classical background, which is therefore time-dependent. Interested in homogeneous and isotropic cosmological evolutions, we have restricted our analysis to the dynamics of the scale factor $a(t)$, the no-scale modulus $\Phi(t)$ and a free scalar $\phi_\perp(t)$, which is a combination of the dilaton and the volume involved in the stringy Scherk–Schwarz supersymmetry breaking [4,5]. The space of solutions can be parameterized by $(c_\perp/c_\Phi, \tau_i)$, where $c_\perp$, c_Φ are integration constants and τ_i is the initial value of $\tau(t) = \frac{2A}{dc_\Phi}\, \dot a\, a^{d-2}$ (see Eq. (2.22)). Fig. 3 shows the partition of the $\mathbb{R}^2$-plane of cosmological solutions: The interior of the ellipse is realized by models where $n_{\rm F} - n_{\rm B} > 0$, and

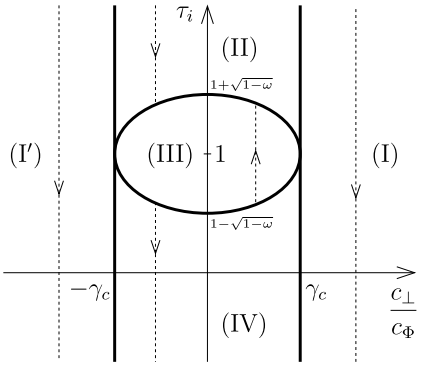

Fig. 3. Partition of the $\mathbb{R}^2$-plane $(c_\perp/c_\Phi, \tau_i)$ of cosmological solutions. The supercritical regions satisfy $|c_\perp/c_\Phi| > \gamma_c$ and $n_\mathrm{F} - n_\mathrm{B} < 0$. The subcritical region, $|c_\perp/c_\Phi| < \gamma_c$, contains an ellipse $\tau_- < \tau_i < \tau_+$, the interior (exterior) of it corresponding to models satisfying $n_\mathrm{F} - n_\mathrm{B} > 0$ (< 0). The trajectories $\tau(t)$ for increasing cosmic time t are represented by dashed lines, for $c_\Phi > 0$.

yields trajectories $\tau(t)$ which follow dashed vertical lines, from bottom to up when $c_\Phi > 0$. Similarly, the exterior of the ellipse corresponds to models having $n_\mathrm{F} - n_\mathrm{B} < 0$, with $\tau(t)$ following vertical lines from up to bottom when $c_\Phi > 0$.

The trajectories in the supercritical regions (I) and (I′), which have no classical counterparts, are characterized by a bounded scale factor. The evolution starts and ends with a Big Bang and a Big Crunch, where the universe is dominated by the kinetic energy and quantum potential of the no-scale modulus. Translated in terms of a perfect fluid of energy density ρ and pressure P, we have

$$\rho \sim \frac{1}{2}\,\dot{\Phi}^2 + \kappa^2 \mathcal{V}_{\text{1-loop}}\,, \quad P \sim \frac{1}{2}\,\dot{\Phi}^2 - \kappa^2 \mathcal{V}_{\text{1-loop}}\,, \quad P \sim \left(\frac{2A}{d-1} + 1\right)\rho\,. \tag{7.1}$$

However, the above regime $\tau \to \pm\infty$ of low scale factor can only be trusted until higher order corrections in g_s and α' become important.

On the contrary, the solutions in the subcritical regions (II) and (III) are attracted to the quantum no-scale regime $\tau \to \tau_+$, which restores the no-scale structure [2] as the universe expands, and is easily (if not always, see Eq. (4.11)) perturbative in g_s. As a result, the evolution is asymptotically dominated by the classical kinetic energies of Φ and $\phi_\perp$. The endless expansion and flatness of the universe are compatible with quantum corrections, which justifies that rigid Minkowski spacetime may be postulated in quantum field theory. Moreover, the evolutions in the subcritical regions (III) and (IV) admit the second quantum no-scale regime $\tau \to \tau_-$, which is realized as the scale factor tends (formally) to 0. In total, the trajectories in region (III) connect two regimes where

$$P \sim \rho \sim \frac{1}{2}\,\dot{\Phi}^2 + \frac{1}{2}\,\dot{\phi}_\perp^2\,, \tag{7.2}$$

with possibly an intermediate period of accelerated cosmology, however too short to account for inflation. In regions (II) and (IV), the state equation of the fluid evolves between $P \sim \rho$ and $P \sim \left(\frac{2A}{d-1} + 1\right)\rho$.

On the one hand, the drop in $M(t)$, which takes place in the quantum no-scale regime $\tau \to \tau_+$ and is independent of the sign of the potential, forbids the existence of any cosmological constant *i.e.* fluid satisfying $P \sim -\rho$. On the other hand, neglecting the time-evolution (which makes sense at a cosmological scale) of the scale factor and scalar fields to end up with a theory in rigid Minkowski spacetime valid today, the energy density M^d is effectively constant but not coupled

to gravity. Thus, from either of these points of view, the words "cosmological" and "constant" exclude somehow each other. Note that this is also the case in other frameworks. For instance, compactifying a string theory on a compact hyperbolic space, flat FLRW solutions can be found, where the volume of the internal space is time-dependent and plays formally the role of $M(t)$ in the present work. Its associated canonical field, which is similar to Φ, admits an exponential and positive potential, however arising at tree level [16–18]. This setup can be realized by considering S-brane backgrounds or non-trivial fluxes. In all these cases, it is important to study the constraints arising from variations of couplings and masses at cosmological time scales, as well as present violations of the equivalence principle [15].

The simple model we have analyzed in details in the present work can be upgraded in various ways. First of all, the full dependence of the 1-loop effective potential on the internal metric, internal antisymmetric tensor and Wilson lines can be computed [11]. New effects then occur, due to the non-trivial metric of the moduli space and the existence of enhanced symmetry points [22]. Another direction of study consists in switching on finite temperature T [5,23,19,24,25]. To see that the qualitative behaviour of the evolutions may be modified, let us assume $T \ll M$ and an expanding universe in quantum no-scale regime $\tau \to \tau_+$. In this case, we have [19]

$$M^d = \frac{M_+^d}{a^{2(d-1)+K_+}}\,, \qquad T^d \sim \frac{\#}{a^d}\,, \tag{7.3}$$

so that M/T decreases and the screening of thermal effects by quantum corrections eventually stops. In fact, new attractor mechanisms exist [19,24]. For instance, when $n_{\rm F} - n_{\rm B} > 0$, quantum and thermodynamic corrections balance so that the free energy, which is nothing but the effective potential at finite temperature, yields a stabilization of $M(t)/T(t)$. At late times, the evolutions satisfy

$$\frac{1}{a(t)} \sim \# M(t) \sim \# T(t) \sim \# e^{2\alpha^2\phi(t)} \sim \frac{\#}{t^{\frac{2}{d}}}\,, \tag{7.4}$$

and are said "radiation-like". This is justified since the *total* energy density and pressure satisfy $\rho_{\rm tot} \sim (d-1)P_{\rm tot}$, where $\rho_{\rm tot}, P_{\rm tot}$ take into account the thermal energy density and pressure derived from the free energy, as well as the kinetic energy of the no-scale modulus Φ [23,19,24].

Acknowledgements

We are grateful to Steve Abel, Carlo Angelantonj, Keith Dienes, Emilian Dudas, Sergio Ferrara, Lucien Heurtier, Alexandros Kahagias and Costas Kounnas for fruitful discussions. The work of H.P. is partially supported by the Royal Society International Cost Share Award. H.P. would like to thank the C.E.R.N. Theoretical Physics Department, the Simons Center for Geometry and Physics, and the IPPP in Durham University for hospitality.

References

[1] R. Barbieri, S. Ferrara, C.A. Savoy, Gauge models with spontaneously broken local supersymmetry, Phys. Lett. B 119 (1982) 343;
E. Cremmer, P. Fayet, L. Girardello, Gravity induced supersymmetry breaking and low-energy mass spectrum, Phys. Lett. B 122 (1983) 41.

[2] E. Cremmer, S. Ferrara, C. Kounnas, D.V. Nanopoulos, Naturally vanishing cosmological constant in $\mathcal{N} = 1$ supergravity, Phys. Lett. B 133 (1983) 61;
J.R. Ellis, C. Kounnas, D.V. Nanopoulos, Phenomenological $SU(1,1)$ supergravity, Nucl. Phys. B 241 (1984) 406;

J.R. Ellis, A.B. Lahanas, D.V. Nanopoulos, K. Tamvakis, No-scale supersymmetric standard model, Phys. Lett. B 134 (1984) 429;
J.R. Ellis, C. Kounnas, D.V. Nanopoulos, No scale supersymmetric GUTs, Nucl. Phys. B 247 (1984) 373.

[3] S. Weinberg, The cosmological constant problem, Rev. Mod. Phys. 61 (1989) 1.

[4] R. Rohm, Spontaneous supersymmetry breaking in supersymmetric string theories, Nucl. Phys. B 237 (1984) 553;
C. Kounnas, M. Porrati, Spontaneous supersymmetry breaking in string theory, Nucl. Phys. B 310 (1988) 355;
S. Ferrara, C. Kounnas, M. Porrati, Superstring solutions with spontaneously broken four-dimensional supersymmetry, Nucl. Phys. B 304 (1988) 500;
S. Ferrara, C. Kounnas, M. Porrati, F. Zwirner, Superstrings with spontaneously broken supersymmetry and their effective theories, Nucl. Phys. B 318 (1989) 75.

[5] C. Kounnas, B. Rostand, Coordinate-dependent compactifications and discrete symmetries, Nucl. Phys. B 341 (1990) 641.

[6] J. Scherk, J.H. Schwarz, Spontaneous breaking of supersymmetry through dimensional reduction, Phys. Lett. B 82 (1979) 60.

[7] S. Kachru, J. Kumar, E. Silverstein, Vacuum energy cancellation in a non-supersymmetric string, Phys. Rev. D 59 (1999) 106004, arXiv:hep-th/9807076;
G. Shiu, S.H.H. Tye, Bose–Fermi degeneracy and duality in non-supersymmetric strings, Nucl. Phys. B 542 (1999) 45, arXiv:hep-th/9808095;
Y. Satoh, Y. Sugawara, T. Wada, Non-supersymmetric asymmetric orbifolds with vanishing cosmological constant, J. High Energy Phys. 1602 (2016) 184, arXiv:1512.05155 [hep-th];
Y. Sugawara, T. Wada, More on non-supersymmetric asymmetric orbifolds with vanishing cosmological constant, J. High Energy Phys. 1608 (2016) 028, arXiv:1605.07021 [hep-th].

[8] R. Blumenhagen, L. Gorlich, Orientifolds of non-supersymmetric asymmetric orbifolds, Nucl. Phys. B 551 (1999) 601, arXiv:hep-th/9812158;
C. Angelantonj, I. Antoniadis, K. Forger, Non-supersymmetric type I strings with zero vacuum energy, Nucl. Phys. B 555 (1999) 116, arXiv:hep-th/9904092.

[9] S. Groot Nibbelink, O. Loukas, A. Mütter, E. Parr, P.K.S. Vaudrevange, Tension between a vanishing cosmological constant and non-supersymmetric heterotic orbifolds, arXiv:1710.09237 [hep-th].

[10] H. Itoyama, T.R. Taylor, Supersymmetry restoration in the compactified $O(16) \times O(16)'$ heterotic string theory, Phys. Lett. B 186 (1987) 129;
S. Abel, K.R. Dienes, E. Mavroudi, Towards a non-supersymmetric string phenomenology, Phys. Rev. D 91 (2015) 126014, arXiv:1502.03087 [hep-th].

[11] C. Kounnas, H. Partouche, Super no-scale models in string theory, Nucl. Phys. B 913 (2016) 593, arXiv:1607.01767 [hep-th];
C. Kounnas, H. Partouche, $\mathcal{N} = 2 \to 0$ super no-scale models and moduli quantum stability, Nucl. Phys. B 919 (2017) 41, arXiv:1701.00545 [hep-th].

[12] I. Florakis, J. Rizos, Chiral heterotic strings with positive cosmological constant, Nucl. Phys. B 913 (2016) 495, arXiv:1608.04582 [hep-th].

[13] J.A. Harvey, String duality and non-supersymmetric strings, Phys. Rev. D 59 (1999) 026002, arXiv:hep-th/9807213.

[14] K. Aoki, E. D'Hoker, D.H. Phong, Two-loop superstrings on orbifold compactifications, Nucl. Phys. B 688 (2004) 3, arXiv:hep-th/0312181;
R. Iengo, C.J. Zhu, Evidence for nonvanishing cosmological constant in nonSUSY superstring models, J. High Energy Phys. 0004 (2000) 028, arXiv:hep-th/9912074;
S. Abel, R.J. Stewart, On exponential suppression of the cosmological constant in non-SUSY strings at two loops and beyond, Phys. Rev. D 96 (2017) 106013, arXiv:1701.06629 [hep-th].

[15] T. Damour, F. Piazza, G. Veneziano, Violations of the equivalence principle in a dilaton runaway scenario, Phys. Rev. D 66 (2002) 046007, arXiv:hep-th/0205111;
T. Damour, F. Piazza, G. Veneziano, Runaway dilaton and equivalence principle violations, Phys. Rev. Lett. 89 (2002) 081601, arXiv:gr-qc/0204094;
T. Damour, J.F. Donoghue, Equivalence principle violations and couplings of a light dilaton, Phys. Rev. D 82 (2010) 084033, arXiv:1007.2792 [gr-qc];
T. Damour, J.F. Donoghue, Phenomenology of the equivalence principle with light scalars, Class. Quantum Gravity 27 (2010) 202001, arXiv:1007.2790 [gr-qc].

[16] J.J. Halliwell, Scalar fields in cosmology with an exponential potential, Phys. Lett. B 185 (1987) 341;
A.B. Burd, J.D. Barrow, Inflationary models with exponential potentials, Nucl. Phys. B 308 (1988) 929, Nucl. Phys. B 324 (1989) 276 (Erratum);

L.P. Chimento, General solution to two-scalar field cosmologies with exponential potentials, Class. Quantum Gravity 15 (1998) 965;
I.P.C. Heard, D. Wands, Cosmology with positive and negative exponential potentials, Class. Quantum Gravity 19 (2002) 5435, arXiv:gr-qc/0206085;
Z.K. Guo, Y.S. Piao, Y.Z. Zhang, Cosmological scaling solutions and multiple exponential potentials, Phys. Lett. B 568 (2003) 1, arXiv:hep-th/0304048;
P.K. Townsend, Cosmic acceleration and M-theory, arXiv:hep-th/0308149;
I.P. Neupane, Accelerating cosmologies from exponential potentials, Class. Quantum Gravity 21 (2004) 4383, arXiv:hep-th/0311071;
P. Vieira, Late-time cosmic dynamics from M-theory, Class. Quantum Gravity 21 (2004) 2421, arXiv:hep-th/0311173;
E. Bergshoeff, A. Collinucci, U. Gran, M. Nielsen, D. Roest, Transient quintessence from group manifold reductions or how all roads lead to Rome, Class. Quantum Gravity 21 (2004) 1947, arXiv:hep-th/0312102;
J.G. Russo, Exact solution of scalar tensor cosmology with exponential potentials and transient acceleration, Phys. Lett. B 600 (2004) 185, arXiv:hep-th/0403010;
L. Jarv, T. Mohaupt, F. Saueressig, Quintessence cosmologies with a double exponential potential, J. Cosmol. Astropart. Phys. 0408 (2004) 016, arXiv:hep-th/0403063;
P.K. Townsend, M.N.R. Wohlfarth, Cosmology as geodesic motion, Class. Quantum Gravity 21 (2004) 5375, arXiv:hep-th/0404241;
A. Collinucci, M. Nielsen, T. Van Riet, Scalar cosmology with multi-exponential potentials, Class. Quantum Gravity 22 (2005) 1269, arXiv:hep-th/0407047.

[17] E. Dudas, N. Kitazawa, A. Sagnotti, On climbing scalars in string theory, Phys. Lett. B 694 (2011) 80, arXiv:1009.0874 [hep-th].

[18] P.K. Townsend, M.N.R. Wohlfarth, Accelerating cosmologies from compactification, Phys. Rev. Lett. 91 (2003) 061302, arXiv:hep-th/0303097;
N. Ohta, Accelerating cosmologies from S-branes, Phys. Rev. Lett. 91 (2003) 061303, arXiv:hep-th/0303238;
S. Roy, Accelerating cosmologies from M/string theory compactifications, Phys. Lett. B 567 (2003) 322, arXiv:hep-th/0304084;
M.N.R. Wohlfarth, Accelerating cosmologies and a phase transition in M-theory, Phys. Lett. B 563 (2003) 1, arXiv:hep-th/0304089;
R. Emparan, J. Garriga, A Note on accelerating cosmologies from compactifications and S-branes, J. High Energy Phys. 0305 (2003) 028, arXiv:hep-th/0304124;
N. Ohta, A Study of accelerating cosmologies from superstring/M theories, Prog. Theor. Phys. 110 (2003) 269, arXiv:hep-th/0304172;
C.M. Chen, P.M. Ho, I.P. Neupane, J.E. Wang, A Note on acceleration from product space compactification, J. High Energy Phys. 0307 (2003) 017, arXiv:hep-th/0304177;
C.M. Chen, P.M. Ho, I.P. Neupane, N. Ohta, J.E. Wang, Hyperbolic space cosmologies, J. High Energy Phys. 0310 (2003) 058, arXiv:hep-th/0306291;
M.N.R. Wohlfarth, Inflationary cosmologies from compactification?, Phys. Rev. D 69 (2004) 066002, arXiv:hep-th/0307179.

[19] F. Bourliot, C. Kounnas, H. Partouche, Attraction to a radiation-like era in early superstring cosmologies, Nucl. Phys. B 816 (2009) 227, arXiv:0902.1892 [hep-th].

[20] E. Kiritsis, C. Kounnas, Infrared regularization of superstring theory and the one-loop calculation of coupling constants, Nucl. Phys. B 442 (1995) 472, arXiv:hep-th/9501020.

[21] A.E. Faraggi, C. Kounnas, H. Partouche, Large volume susy breaking with a solution to the decompactification problem, Nucl. Phys. B 899 (2015) 328, arXiv:1410.6147 [hep-th].

[22] T. Coudarchet, H. Partouche, work in progress.

[23] T. Catelin-Jullien, C. Kounnas, H. Partouche, N. Toumbas, Thermal/quantum effects and induced superstring cosmologies, Nucl. Phys. B 797 (2008) 137, arXiv:0710.3895 [hep-th];
T. Catelin-Jullien, C. Kounnas, H. Partouche, N. Toumbas, Induced superstring cosmologies and moduli stabilization, Nucl. Phys. B 820 (2009) 290, arXiv:0901.0259 [hep-th].

[24] F. Bourliot, J. Estes, C. Kounnas, H. Partouche, Cosmological phases of the string thermal effective potential, Nucl. Phys. B 830 (2010) 330, arXiv:0908.1881 [hep-th];
J. Estes, C. Kounnas, H. Partouche, Superstring cosmology for $\mathcal{N}_4 = 1 \to 0$ superstring vacua, Fortschr. Phys. 59 (2011) 861, arXiv:1003.0471 [hep-th].

[25] J. Estes, L. Liu, H. Partouche, Massless D-strings and moduli stabilization in type I cosmology, J. High Energy Phys. 1106 (2011) 060, arXiv:1102.5001 [hep-th];
L. Liu, H. Partouche, Moduli stabilization in type II Calabi–Yau compactifications at finite temperature, J. High Energy Phys. 1211 (2012) 079, arXiv:1111.7307 [hep-th].

Available online at www.sciencedirect.com

ScienceDirect

Nuclear Physics B 933 (2018) 134–184

NUCLEAR PHYSICS B

www.elsevier.com/locate/nuclphysb

Quantum no-scale regimes and moduli dynamics

Thibaut Coudarchet, Hervé Partouche *

Centre de Physique Théorique, Ecole Polytechnique, CNRS [1]*, Université Paris-Saclay, Route de Saclay, 91128 Palaiseau, France*

Received 12 April 2018; accepted 14 June 2018
Available online 18 June 2018
Editor: Stephan Stieberger

Abstract

We analyze quantum no-scale regimes (QNSR) in perturbative heterotic string compactified on tori, with total spontaneous breaking of supersymmetry. We show that for marginal deformations initially at any point in moduli space, the dynamics of a flat, homogeneous and isotropic universe can always be attracted to a QNSR. This happens independently of the characteristics of the 1-loop effective potential $\mathcal{V}_{1\text{-loop}}$, which can be initially positive, negative or vanishing, and maximal, minimal or at a saddle point. In all cases, the classical no-scale structure is restored at the quantum level, during the cosmological evolution. This is shown analytically by considering moduli evolutions entirely in the vicinity of their initial values. Global attractor mechanisms are analyzed numerically and depend drastically on the sign of $\mathcal{V}_{1\text{-loop}}$. We find that all initially expanding cosmological evolutions along which $\mathcal{V}_{1\text{-loop}}$ is positive are attracted to the QNSR describing a flat, ever-expanding universe. On the contrary, when $\mathcal{V}_{1\text{-loop}}$ can reach negative values, the expansion comes to a halt and the universe eventually collapses into a Big Crunch, unless the initial conditions are tuned in a tiny region of the phase space. This suggests that flat, ever-expanding universes with positive potentials are way more natural than their counterparts with negative potentials.

* Corresponding author.
E-mail addresses: thibaut.coudarchet@ens-lyon.fr (T. Coudarchet), herve.partouche@polytechnique.edu (H. Partouche).
[1] Unité mixte du CNRS et de l'Ecole Polytechnique, UMR 7644.

https://doi.org/10.1016/j.nuclphysb.2018.06.009

1. Introduction

To account for an extremely small cosmological constant, a natural starting point in supergravity is the class of no-scale models [1]. The latter describe the spontaneous breaking of local supersymmetry at a scale M that parameterizes a flat direction of a positive semi-definite potential. In perturbative string theory in d dimensions, this setup can be realized at tree level by coordinate-dependent compactification [2,3], which implements the Scherk–Schwarz mechanism [4]. The magnitude of the supersymmetry breaking scale measured in σ-model frame, $M_{(\sigma)}$, can be restricted to be lower than the string scale $M_{\rm s}$, for Hagedorn-like instabilities [3,5] to be avoided. However, quantum effects lift in general the classical flat directions. At 1-loop, supposing for simplicity that there is no non-trivial mass scale lower than M, a contribution of order $(n_{\rm F}-n_{\rm B})M^d$ to the effective potential is generated, where $n_{\rm F}$ and $n_{\rm B}$ are the numbers of massless fermionic and bosonic degrees of freedom. In this case, a mechanism responsible for the stabilization of M would generically yield a large cosmological constant. For this reason, the theories satisfying $n_{\rm F}=n_{\rm B}$, which are sometimes referred as "super no-scale models", have attracted attention [6–8], since their 1-loop effective potentials turn out to be exponentially suppressed. In some models, the potentials can even vanish exactly at 1-loop, at specific points in moduli space [9]. However, even in these instances, the smallness of the potential happens to be invalidated once Higgs masses lower than M are introduced [7,8], and/or generic higher order loop corrections are taken into account [10].

Alternatively, one may not assume the stabilization of the supersymmetry breaking scale. In this case, the motion of M induced by the effective potential may be analyzed in a cosmological framework [11,12], and eventually at finite temperature [12–15]. One of the main motivations of [11] was to find conditions (which we extend in the present paper) for flat, homogeneous and isotropic expanding universes to be allowed by the dynamics. In this reference, the analysis is done by taking into account a reduced set of fields, namely the volume vol of the torus involved in the Scherk–Schwarz supersymmetry breaking, the dilaton ϕ and the scale factor a of the universe. For convenience, the degrees of freedom associated with $\ln(vol)$ and ϕ are implemented by two canonical fields Φ and $\phi_\perp$. They are orthogonal linear combinations, where Φ is the "no-scale modulus" which satisfies $M\equiv e^{\alpha\Phi}M_{\rm s}$, with α a normalization factor. The history of the universe described by a flat Friedmann–Lemaître–Robertson–Walker (FLRW) metric proves to depend drastically on the sign of the 1-loop effective potential[2]:

• For $n_{\rm F}\geq n_{\rm B}$, up to time reversal, the evolution is ever-expanding. At initial and late times, it is driven by the kinetic energies of Φ and $\phi_\perp$, which dominate over the quantum effective potential. As a result, the cosmological solution converges in both limits to classical ones, which are characterized by exact no-scale structures with free scalars Φ and $\phi_\perp$.[3] For this reason, the universe is said to be at early and late times in "quantum no-scale regime" (QNSR). It is only during an intermediate era that connects both QNSRs that the effective potential is relevant. The latter may even induce a transient period of acceleration.

• For $n_{\rm F}<n_{\rm B}$, up to time reversal, three different histories can be encountered. In two of them, the universe starts with a Big Bang dominated by the total energy (kinetic plus potential) of Φ. Then, it may forever expand by entering in QNSR, or it may reach a maximum size, before

[2] Technically, similar analyzes involving scalar fields with exponential potentials can be found in Ref. [16]. They can be realized at tree level in string theory, with backgrounds involving compact hyperbolic internal spaces, S-branes or non-trivial fluxes [17].

[3] These limit solutions become exact trajectories in the super no-scale models *i.e.* when $n_{\rm F}-n_{\rm B}=0$.

collapsing into a Big Crunch again dominated by the total energy of the no-scale modulus. In the third kind of trajectories, the universe starts with a Big Bang in QNSR, reaches a maximal size and then collapses as before in a Big Crunch dominated by the total energy of Φ.

The goal of the present work is to improve the analysis of Ref. [11] by taking into account the dynamics of other moduli fields. To be specific, we consider the heterotic string compactified on a torus, where the Scherk–Schwarz spontaneous breaking of all supersymmetries involves a single internal direction X^d. The latter is large, for $M_{(\sigma)}$ to be lower than $M_{\rm s}$. Due to the underlying maximally supersymmetric structure of the setup, all classical marginal deformations can be interpreted as Wilson lines $y_{I\Upsilon}$, $I \in \{d, \dots, 9\}$, $\Upsilon \in \{d, \dots, 25\}$. In Sect. 2, we first present the generic expression of the 1-loop effective potential obtained by switching on small deformations of any background (that has initially no non-trivial mass scale below M). The Wilson lines associated with each gauge group factor can be massive, massless or tachyonic. Then, we focus on a specific configuration to be analyzed in great details, where the moduli of the internal directions X^d and X^{d+1} are allowed to vary, while all other deformations are frozen at extrema of the effective potential.

Sect. 3 is devoted to the derivation of exact results in the framework of the above simple model. Beside Φ, the effective potential depends on $\phi_\perp$, which is no longer a free field, and on three Wilson lines $y_{d,d+1}$, $y_{d+1,d}$ and $y_{d+1,d+1}$. Physically, $y_{d+1,d+1}$ parameterizes a Coulomb branch, and $|y_{d+1,d+1}|M_{\rm s}$ is a contribution to the σ-model frame mass of the component fields belonging to supermultiplets charged under the gauge group. When $|y_{d+1,d+1}|M_{\rm s} \ll M_{(\sigma)}$, supermultiplets are light and their Kaluza–Klein (KK) towers of states along the large direction X^d contribute effectively to the 1-loop potential. In this case, $y_{d,d+1}$ (or a combination of all three Wilson lines when $y_{d+1,d+1}$ is not exactly vanishing) plays the role of a phase, which determines whether it is the fermions or the bosons within these charged supermultiplets that acquire a mass by the supersymmetry breaking mechanism. The exact kinetic terms of the model are also presented.

QNSRs compatible with weak string coupling are described in this setup in Sect. 4. They involve the scale factor a, the scalars Φ, $\phi_\perp$, and the Wilson lines $y_{d,d+1}$, $y_{d+1,d}$, $y_{d+1,d+1}$ which at this stage are restricted to be small perturbations of the initial background. Both types of regimes are considered, namely expanding eras $t \to +\infty$ or Big Bangs $t \underset{>}{\to} t_{\rm BB}$, where t is cosmic time and $t_{\rm BB}$ a constant. Their existence is shown, regardless of the sign of $n_{\rm F} - n_{\rm B}$ and whether the small Wilson lines are massive, massless or tachyonic at 1-loop. Compared to Ref. [11], a novelty is that the moduli space metric is curved, which implies non-canonical kinetic terms. We find that this fact imposes a new condition for the universe to be in QNSR: The scale $M_{(\sigma)}$ of supersymmetry breaking measured in sigma-model frame must increase as $t \to +\infty$ or $t \underset{>}{\to} t_{\rm BB}$. As a result, the regimes are valid until $M_{(\sigma)}$ reaches $M_{\rm s}$, when new stringy effects are expected to arise. Moreover, the new constraint reduces drastically the phase space where the system in QNSR can evolve. For instance, it reduces it by a factor of about 170 for $d = 4$. However, this does not mean that the initial conditions that yield such regimes must be tuned within very narrow ranges, due to possible global attraction mechanisms.

In Sect. 5, all results valid for small Wilson lines are checked by numerical simulations, in the case of the QNSR $t \to +\infty$. Moreover, it turns out that the quadratic kinetic terms are exact for arbitrary $y_{d,d+1}$ and $y_{d+1,d}$, as long as $y_{d+1,d+1}$ is restricted to vanish. In Sect. 6, we use this fact to simulate large deformations of the initial background parameterized by the Wilson lines $y_{d,d+1}$, $y_{d+1,d}$. When the effective potential is positive, we find that for arbitrary initial conditions (up to time reversal), the universe expands and is attracted to the QNSR $t \to +\infty$. On

the contrary, when the potential is negative, for the universe to be in QNSR $t \to +\infty$, its initial conditions must sit in the tiny phase space associated with this regime. Otherwise, the initially growing scale factor reaches a maximal size before collapsing. Altogether, these remarks suggest that in order to describe expanding universes in the framework we have considered, naturalness favors models having more fermions than bosons in their light spectra, $n_{\rm F} - n_{\rm B} \geq 0$.

Our concluding remarks are given in Sect. 7, while technical derivations can be found in a long but self-content Appendix. The latter describes the implementation of continuous and discrete Wilson lines in an heterotic toroidal partition function, the spontaneous breaking of supersymmetry, and generic formulas for the effective potential.

2. 1-Loop effective potential

The notion of QNSR in string theory was introduced in Ref. [11], in the context of the heterotic string compactified on tori, where the total spontaneous breaking of supersymmetry is implemented by a stringy Scherk–Schwarz mechanism. However, beside the scale factor of the universe, only the dynamics of the dilaton and that of the internal volume involved in the breaking of supersymmetry were taken into account. In order to remedy this fact, we consider in this section features about the dependence of the 1-loop effective potential on all moduli fields. We restrict our analysis to the case where the breaking of supersymmetry is induced along a single internal direction.

Marginal deformations

To be specific, we consider a Minkowskian heterotic background in dimension $d \geq 3$,[4] with internal space T^{10-d},

$$\mathbb{R}^{0,d-1} \times T^{10-d}\,, \tag{2.1}$$

where the total spontaneous breaking of supersymmetry is induced by a coordinate-dependent compactification along the direction X^d. The gauge symmetry group arising in this no-scale model from the Kac–Moody algebra realized on the right-moving bosonic side of the string is $\mathcal{G}_{26-d}$, where gauge groups of rank r will in general be denoted $\mathcal{G}_r$. At this stage, the background sits at a specific point of the Narain lattice moduli space [18]

$$\frac{SO(10-d,26-d)}{SO(10-d)\times SO(26-d)}\,, \tag{2.2}$$

whose real dimension is $(10-d)\times(26-d)$. This manifold can be parameterized by the internal metric G_{IJ}, the antisymmetric tensor B_{IJ}, $I,J \in \{d,\dots,9\}$, and the Wilson lines $Y_{I\mathcal{J}}$, $\mathcal{J} \in \{10,\dots,25\}$. However, all of these $(10-d)\times(26-d)$ moduli fields can be interpreted from a KK point of view as the components along T^{10-d} of 10-dimensional vector bosons in the Cartan subalgebra of $\mathcal{G}_{26-d}$. Thus, they can be viewed as Wilson lines, and it is natural to split the associated degrees of freedom into initial background values $(G+B)^{(0)}_{IJ}$, $Y^{(0)}_{I\mathcal{J}}$ and arbitrary Wilson line deformations[5]

[4] The equations of motion and solutions we will derive in Sect. 4 are formally valid for arbitrary real dimension $d > 2$. Cosmological evolutions in 2 dimensions could be found by taking the limit $d \to 2_+$.

[5] Notations used in the core of the paper are slightly different from those used in the Appendix. The antisymmetric tensor B stands for $B + \Delta B$ in Appendices A.4–A.6. Moreover, in Eq. (A.25), $Y^{(0)}_{d\mathcal{J}}$ is denoted $\eta^R_{\mathcal{J}}$, the arbitrary origin of the fields $Y_{i\mathcal{J}}$ is chosen so that $Y^{(0)}_{i\mathcal{J}} = 0$, and the continuous Wilson lines are denoted with upper indices "R".

$$(G+B)_{IJ} = \begin{pmatrix} (G+B)_{dd} & (G^{(0)}+B^{(0)})_{dj} + \sqrt{2}\, y_{dj} \\ (G^{(0)}+B^{(0)})_{id} + \sqrt{2}\, y_{id} & (G^{(0)}+B^{(0)})_{ij} + \sqrt{2}\, y_{ij} \end{pmatrix},$$
$$Y_{d\mathcal{J}} = Y^{(0)}_{d\mathcal{J}} + y_{d\mathcal{J}}\,, \quad Y_{i\mathcal{J}} = Y^{(0)}_{i\mathcal{J}} + y_{i\mathcal{J}}\,, \qquad i,j \in \{d+1,\dots,9\},\ \mathcal{J} \in \{10,\dots,25\}. \tag{2.3}$$

In our conventions, $y_{I\Upsilon}$, $I \in \{d,\dots,9\}$, $\Upsilon \in \{d,\dots,25\}$, is the Wilson line along X^I of the $U(1)$ Cartan generator arising from the right-moving bosonic coordinate Υ. In particular, factors $\sqrt{2}$ are introduced in components of the matrix $(G+B)$ to account for the conventional length $\sqrt{2}$ of the roots of the simply laced Lie groups. In this setup, the scale of supersymmetry breaking measured in σ-model frame can be defined as the KK mass

$$M_{(\sigma)} = \sqrt{G^{dd}}\, M_{\rm s}\,, \tag{2.4}$$

where $G^{IJ} \equiv (G^{-1})_{IJ}$. As long as G_{dd} is at least slightly larger than 1, in which case $M_{(\sigma)} \simeq M_{\rm s}/\sqrt{G_{dd}}$, no scalar field can be tachyonic at tree level, *i.e.* there is no possibility for a Hagedorn-like instability to take place [5]. Moreover, the gauge symmetry $\mathcal{G}_{26-d}$ is spontaneously broken to $U(1) \times \mathcal{G}_{25-d}$.

Higgs instabilities may however occur at the quantum level. In fact, if the classical no-scale structure guaranties $M_{(\sigma)}$ and all other marginal deformations y's to be flat directions of a positive semi-definite tree-level potential [1], this is no longer the case when perturbative corrections are taken into account. As described extensively in the Appendix, a non-trivial effective potential $\mathcal{V}^{(\sigma)}_{\text{1-loop}}$ is already generated at 1-loop. Assuming that $M_{(\sigma)}$ is lower than the string scale $M_{\rm s}$, and that the spectrum in the initial background has no mass scale below $M_{(\sigma)}$,[6] the generic form of $\mathcal{V}_{\text{1-loop}}$ for small Wilson line deformations is [7,8]

$$\begin{aligned} \mathcal{V}^{(\sigma)}_{\text{1-loop}} &= (n_{\rm F} - n_{\rm B})\, v_d\, M^d_{(\sigma)} \\ &\quad + M^d_{(\sigma)}\, \frac{v_{d-2}}{2\pi} \sum_{\Upsilon=d+1}^{25} c_\Upsilon \Big[(d-1) y^2_{d\Upsilon} + \frac{1}{G^{dd}} \sum_{i=d+1}^{9} y^2_{i\Upsilon} \Big] + \cdots \\ &\quad + \mathcal{O}\big((c M_{\rm s} M_{(\sigma)})^{\frac{d}{2}}\, e^{-2\pi c M_{\rm s}/M_{(\sigma)}} \big)\,, \end{aligned} \tag{2.5}$$

where the ellipses stand for higher order interactions in y's. In this expression, $n_{\rm B}$ and $n_{\rm F}$ are the numbers of massless bosonic and fermionic degrees of freedom in the undeformed background, while v_d is a dressing coefficient that accounts for the towers of associated KK modes arising from the large supersymmetry breaking compact direction X^d,

$$v_d = \frac{\Gamma(\frac{d+1}{2})\, \zeta(d+1)}{2^{d-1}\, \pi^{\frac{3d+1}{2}}} \Big(1 - \frac{1}{2^{d+1}} \Big)\,. \tag{2.6}$$

In the last line, $cM_{\rm s}$ is the lowest mass scale above $M_{(\sigma)}$. When the former is much larger than the latter, all states that are not in the above mentioned KK towers yield exponentially suppressed contributions. We see that the scalars y_{id}, $i \in \{d+1,\dots,9\}$, are massless. Moreover, for all Cartan generator $\Upsilon \in \{d+1,\dots,25\}$, the coefficient c_Υ determines whether the Wilson lines

[6] Relaxing this hypothesis amounts to shifting Wilson lines by small constant backgrounds, thus inducing tadpoles in Eq. (2.5).

$y_{I\Upsilon}$, $I \in \{d, \dots, 9\}$, are massive, massless or tachyonic at 1-loop.[7] Actually, decomposing $\mathcal{G}_{25-d}$ into simple Lie groups and $U(1)$ factors as follows,

$$\mathcal{G}_{25-d} = \prod_\lambda \mathcal{G}_{r_\lambda}^{(\lambda)} \qquad \text{where} \qquad \sum_\lambda r_\lambda = 25 - d\,, \tag{2.7}$$

the Wilson lines $y_{I\Upsilon}$, $I \in \{d, \dots, 9\}$, where Υ takes values corresponding to the Cartan generators of $\mathcal{G}_{r_\lambda}^{(\lambda)}$, share a common coefficient $c_\Upsilon \equiv c_{\mathcal{G}_{r_\lambda}^{(\lambda)}}$. The latter is related to the quadratic charges of the representations $\mathcal{R}_{\rm B}^{(\lambda)}$ and $\mathcal{R}_{\rm F}^{(\lambda)}$ of the massless bosons and fermions charged under $\mathcal{G}_{r_\lambda}^{(\lambda)}$ in the initial background (see Eq. (A.78)),

$$c_{\mathcal{G}_{r_\lambda}^{(\lambda)}} = 8\big(C_{\mathcal{R}_{\rm B}^{(\lambda)}} - C_{\mathcal{R}_{\rm F}^{(\lambda)}}\big)\,. \tag{2.8}$$

By switching on small y-deformations of the background we started with, some charged and initially massless states acquire Higgs masses lower than $M_{(\sigma)}$. This reduces the dimension (but not the rank) of the gauge symmetry, which enters a Coulomb branch.

Example 1. To illustrate the above generalities, let us consider the supersymmetric $E_8 \times E_8'$ heterotic string compactified on T^{10-d}. Taking $G_{dd} \gg 1$, the gauge symmetry arising from the right-moving sector is $\mathcal{G}_{26-d} = U(1) \times \mathcal{G}_{9-d} \times E_8 \times E_8'$. When we sit at a point in moduli space where $\mathcal{G}_{9-d}$ is maximally enhanced *i.e.* contains no $U(1)$ factor, the model presents only two scales, namely the KK mass $M_{(\sigma)}$ and the much greater string scale $M_{\rm s}$. As reviewed in Appendices A.1–A.3, denoting $a \in \mathbb{Z}_2$ the fermionic number, the simplest choice of implementation of the Scherk–Schwarz breaking of supersymmetry along the large compact direction X^d induces KK masses[8] $\frac{1}{2}aM_{(\sigma)}$ to all initially massless degrees of freedom. As a result, the no-scale model has no massless fermions, $n_{\rm F} = 0$, and its mass coefficients are positive, $c_{\mathcal{G}_{r_\lambda}^{(\lambda)}} = 8C_{\mathcal{R}_{\rm B}^{(\lambda)}}$. For instance, one obtains for $\mathcal{G}_{9-d} = SU(2)^{9-d}$

$$\begin{aligned} &n_{\rm B} = 8\big[d - 2 + \dim\big(U(1) \times SU(2)^{9-d} \times E_8 \times E_8'\big)\big] = 8\,(522 - 2d)\,,\\ &c_{SU(2)} = 8 \times C_{[3]_{SU(2)}} = 8 \times 2 = 16 \qquad \text{for the } 9-d \ SU(2) \text{ factors}\,,\\ &c_{E_8} \quad = 8 \times C_{[248]_{E_8}} = 8 \times 30 = 240 \quad \text{for } E_8 \text{ and } E_8'\,. \end{aligned} \tag{2.9}$$

This yields a negative effective potential and no Higgs instabilities for the y-fields at the quantum level.

Example 2. For massless fermions to be present in the no-scale model, a more sophisticated choice of supersymmetry breaking must be considered.[9] For instance, one can define a charge $\gamma \in \mathbb{Z}_2$ in terms of which the affine character of E_8 can be divided into $SO(16)$ ones,

$$\frac{1}{2}\sum_{\gamma,\delta\in\mathbb{Z}_2}\left(\frac{\bar\theta[^\gamma_\delta]}{\bar\eta}\right)^8 = \bar O_{16} + \bar S_{16}\,. \tag{2.10}$$

[7] Strictly speaking, the notion of "mass" here is a misnomer when $M_{(\sigma)}$ is treated as a dynamical field, in which case all terms in Eq. (2.5) are interactions.

[8] The representative of $a \in \mathbb{Z}_2$ in $\{0, 1\}$ is understood.

[9] In the notations of Appendix A.6, this can be done by switching on discrete Wilson lines, as in Eq. (A.54), (A.55).

In this relation, $\gamma = 0$ leads to the unit character $\bar{O}_{16}$, while $\gamma = 1$ corresponds to the spinorial one $\bar{S}_{16}$. At the massless level, this amounts to splitting the adjoint representation of E_8 into adjoint and spinorial representations of $SO(16)$, $[248]_{E_8} = [120]_{SO(16)} \oplus [128]_{SO(16)}$. As seen in Appendix A.4, it is possible to implement a Scherk–Schwarz supersymmetry breaking that induces KK masses[10] $\frac{1}{2}(a + \gamma + \gamma')M_{(\sigma)}$ to all initially massless degrees of freedom, where $\gamma' \in \mathbb{Z}_2$ is the charge similar to γ but associated with E_8'. As in Example 1, the fermions acquire masses if they belong to supermultiplets with $\gamma + \gamma'$ even. The situation is however reversed when $\gamma + \gamma'$ is odd, since it is the bosons which become massive. As a result, the mechanism breaks spontaneously all supersymmetries as well as the gauge symmetry $E_8 \times E_8' \to SO(16) \times SO(16)'$. The gauge group $\mathcal{G}_{9-d}$ can be chosen as before to be $SU(2)^{9-d}$. However, it is instructive to also consider Coulomb branches $\mathcal{G}_{9-d} = SU(2)^{9-d-s} \times U(1)^s$, $s \in \{0, \dots, 9-d\}$, when the masses of the non-Cartan gauge bosons are greater than $M_{(\sigma)}$, for Eq. (2.5) to be valid. In this case, we obtain

$$
\begin{aligned}
&n_{\rm B} = 8\left[d - 2 + \dim\left(U(1) \times SU(2)^{9-d-s} \times U(1)^s\right) + 120 + 120\right] = 8\,(266 - 2d - 2s)\,,\\
&n_{\rm F} = 8\,(128 + 128) = 8 \times 256\,,\\
&c_{SU(2)} = 8 \times C_{[3]_{SU(2)}} = 8 \times 2 = 16 \qquad \text{for the } 9-d-s \ SU(2) \text{ factors}\,,\\
&c_{U(1)} \ = 0 \qquad\qquad\qquad\qquad\quad \text{for the } s \ U(1) \text{ factors of } \mathcal{G}_{9-d}\,,\\
&c_{SO(16)} = 8 \times (C_{[120]_{SO(16)}} - C_{[128]_{SO(16)}}) = 8\,(14 - 16) = -16 \ \text{ for } SO(16) \text{ and } SO(16)'\,.
\end{aligned}
\tag{2.11}
$$

We see that $n_{\rm F} - n_{\rm B} = 8(2d + 2s - 10)$, which is greater or equal to 0 for $d \geq 5$ and can be positive, negative or null for $d = 3$ and 4. However, the Wilson lines of $SO(16) \times SO(16)'$ are all tachyonic at 1-loop and Higgs instabilities may arise.

Example 3. We are naturally invited to reconsider Example 2 after Higgs transition, in the Coulomb branch where $SO(16) \times SO(16)' \to U(1)^{16}$. Again, we assume the masses of the 2×112 non-Cartan gauge bosons to be greater than $M_{(\sigma)}$, for Eq. (2.5) to be applicable. Since all states in the spinorial representations $[128]_{SO(16)}$ and $[128]_{SO(16)'}$ are also massive, we automatically obtain vanishing mass coefficients $c_{U(1)}$'s for the 16 Cartan $U(1)$'s. Moreover, we are back to a configuration where $n_{\rm F} = 0$, and the effective potential is necessarily negative. In fact, we could have reached the same point in moduli space by considering the Coulomb branch in Example 1, where $E_8 \times E_8' \to U(1)^{16}$.

The above 3 simple examples illustrate the fact that at the quantum level, local stability (eventually marginal) of the Wilson lines ($C_{\mathcal{R}_{\rm B}^{(\lambda)}} \geq C_{\mathcal{R}_{\rm F}^{(\lambda)}}$, for all λ) and non-negativity of the effective potential ($n_{\rm F} \geq n_{\rm B}$) are conditions that are easily in contradiction. Actually, it would be interesting to clarify whether they may be compatible. However, insofar as in the present paper we are interested in flat FLRW cosmological evolutions where the effective potential is dominated by the kinetic energies of moduli fields, it happens that the sign of $n_{\rm F} - n_{\rm B}$ as well as those of the mass coefficients $c_{\mathcal{G}_{r_\lambda}^{(\lambda)}}$'s do not play significant roles in the existence of QNSRs. Before showing this in Sect. 4 in an heterotic context we will now describe, we signal that global attractor mechanisms are nonetheless sensitive to the signs, as will be seen in the numerical simulations of Sect. 6.

[10] The representative of $a + \gamma + \gamma' \in \mathbb{Z}_2$ in $\{0, 1\}$ is understood.

A specific setup

Before y-deformation, we consider from now on a background to be studied in great details,

$$\mathbb{R}^{0,d-1} \times S^1_{\rm SS}(R_d) \times S^1(R_{d+1}=1) \times T^{8-d}\,, \tag{2.12}$$

where the index SS signals a supersymmetry breaking coordinate-dependent compactification along the circle of radius $R_d \equiv \sqrt{G_{dd}} \gg 1$. Note that the block-diagonal form of the internal space metric does not say anything about the antisymmetric tensor, so that we may choose

$$2B^{(0)}_{d,d+1} = \eta^R_{d+1} \in \mathbb{Z}\,, \quad G^{(0)}_{d,d+1} = 0\,, \quad G^{(0)}_{d+1,d+1} = 1\,. \tag{2.13}$$

Altogether, these data imply the gauge symmetry group generated by the right-moving sector to be factorized as $\mathcal{G}_{26-d} = U(1) \times \mathcal{G}_1 \times \mathcal{G}_{8-d} \times \mathcal{G}_{16}$.[11] In the decompactification limit $R_d \to +\infty$, where supersymmetry is restored, our choice of radius $R_{d+1} \equiv \sqrt{G^{(0)}_{d+1,d+1}} = 1$ for the second circle implies an $SU(2)$ enhancement of the gauge symmetry (in 5 dimensions). However, as explained at the end of Appendix A.4, two cases can arise at finite R_d, depending on the parity of the "discrete Wilson line" $\eta^R_{d+1} \equiv 2(G^{(0)} + B^{(0)})_{d,d+1} \in \mathbb{Z}$ (see Eq. (A.36)). When η^R_{d+1} is even, all fermionic degrees of freedom of the supermultiplets in the adjoint representation of $SU(2)$ acquire a mass $\frac{1}{2}M_{(\sigma)}$. In this case, the enhancement of the gauge symmetry is preserved, and $\mathcal{G}_1 = SU(2)$. On the contrary, when η^R_{d+1} is odd, the spontaneous breaking operates simultaneously on supersymmetry and on the $SU(2)$ gauge symmetry. In practice, the bosonic degrees of freedom of the $SU(2)$ non-Cartan supermultiplets acquire a mass $\frac{1}{2}M_{(\sigma)}$. As a result, only the Cartan gauge symmetry is preserved, $\mathcal{G}_1 = U(1)$, and the latter is coupled to the massless fermions belonging to the non-Cartan supermultiplets of charges $\pm\sqrt{2}$. In all instances, the mass coefficients are given by

$$\begin{aligned} &\eta^R_{d+1} = 0 \text{ even} \quad \Longrightarrow \quad \mathcal{G}_1 = SU(2)\,, \;\; c_{\mathcal{G}_1} = 8 \times C_{[3]_{SU(2)}} = 8 \times 2 = 16\,, \\ &\eta^R_{d+1} = 0 \text{ odd} \quad \Longrightarrow \quad \mathcal{G}_1 = U(1)\,, \quad c_{\mathcal{G}_1} = -8 \times C_{\pm\sqrt{2}} = -8 \times 2 = -16\,. \end{aligned} \tag{2.14}$$

Our goal being to switch on moduli fields in order to study their dynamics later on, we will make further assumptions for the sake of simplicity. We suppose that the undeformed background (2.12) does not introduce mass scales below $M_{(\sigma)}$. As already mentioned in Footnote 6, this ensures that the 1-loop potential does not induce tadpoles for the y-fields. This can be realized by considering maximally enhanced gauge groups $\mathcal{G}_{8-d} \times \mathcal{G}_{16}$ or points in their Coulomb branches where the non-Cartan generators have masses above $M_{(\sigma)}$. Under these conditions, it is consistent to freeze to 0 the Wilson lines of $\mathcal{G}_{8-d} \times \mathcal{G}_{16}$ along $S^1_{\rm SS}(R_d) \times S^1(R_{d+1}=1) \times T^{8-d}$, as well as those of $U(1) \times \mathcal{G}_1$ along T^{8-d}. In fact, the configuration

$$y_{I,d+2} \equiv \cdots \equiv y_{I,25} \equiv 0\,,\; I \in \{d, \ldots, 9\}\,, \qquad y_{id} \equiv y_{i,d+1} \equiv 0\,,\; i \in \{d+2, \ldots, 9\}\,, \tag{2.15}$$

solves trivially the equations of motion of the associated degrees of freedom, even when the 1-loop potential is included in the effective supergravity. Given these restrictions, we are left with non-trivial Wilson lines $y_{d,d+1}$, $y_{d+1,d}$, $y_{d+1,d+1}$, which are those of $U(1) \times \mathcal{G}_1$ along the compact directions X^d and X^{d+1}. For small deformations, the effective potential then becomes:

[11] This is clear for $B^{(0)}_{d,d+1} = 0$ mod 2 but remains true for arbitrary real $B^{(0)}_{d,d+1}$, as will be described in details in Sect. 3.

$$\mathcal{V}^{(\sigma)}_{\text{1-loop}} = (n_{\rm F} - n_{\rm B})\, v_d\, M^d_{(\sigma)} + M^d_{(\sigma)}\, \frac{v_{d-2}}{2\pi}\, c_{\mathcal{G}_1}\Big[(d-1)y^2_{d,d+1} + \frac{y^2_{d+1,d+1}}{G^{dd}}\Big] + \cdots + \mathcal{O}\big((cM_{\rm s}M_{(\sigma)})^{\frac{d}{2}} e^{-2\pi c M_{\rm s}/M_{(\sigma)}}\big)\,. \tag{2.16}$$

Of course, if $M_{(\sigma)}$ acquired a vacuum expectation value, it would be very artificial to impose Eq. (2.15) and expand $\mathcal{V}^{(\sigma)}_{\text{1-loop}}$ at $y_{d,d+1} = y_{d+1,d} = y_{d+1,d+1} = 0$, when $c_{\mathcal{G}^{(\lambda)}_{r_\lambda}} < 0$ for some λ's. However, as already announced, the situation happens to be drastically different in a QNSR. Before observing this fact for $c_{\mathcal{G}_1} = -16$ in Sect. 4, we find instructive to make explicit the ellipses in Eq. (2.16), by presenting the exact expression of $\mathcal{V}^{(\sigma)}_{\text{1-loop}}$ valid for arbitrary Wilson lines $y_{d,d+1}$, $y_{d+1,d}$, $y_{d+1,d+1}$.

3. Exact formulas

In this section, we would like to have a better idea of the global structure of the "reduced" moduli space parameterized by the continuous Wilson lines $y_{d,d+1}$, $y_{d+1,d}$, $y_{d+1,d+1}$. In particular, we will describe periodicity properties of the effective potential, as well as the exact kinetic terms.

Effective potential

For arbitrary deformations, the expression of the 1-loop effective potential $\mathcal{V}^{(\sigma)}_{\text{1-loop}}$ is obtained by applying the generic formula Eq. (A.52), derived in Appendix A.5. Up to the $\mathcal{O}\big((cM_{\rm s}M_{(\sigma)})^{\frac{d}{2}} e^{-2\pi c M_{\rm s}/M_{(\sigma)}}\big)$ exponentially suppressed terms, $\mathcal{V}^{(\sigma)}_{\text{1-loop}}$ can be written as a sum over a finite number of KK towers of states associated with the large compact direction X^d (along which they have vanishing winding numbers, $n_d = 0$). These KK towers are those characterized by mass scales denoted $\mathcal{M}'_{L0}$ that are lower than the KK *i.e.* supersymmetry breaking scale $M_{(\sigma)}$. They always appear in groups of 8, due to the degeneracy arising from the left-moving supersymmetric side of the string. For the initial background satisfying Eqs (2.12), (2.13), they can be listed as follows:

(i) The 8 KK towers at right-moving oscillator level $\ell_R = 0$, whose right-moving quantum numbers are a given root of $SU(2)$, and that are neutral under $\mathcal{G}_{8-d} \times \mathcal{G}_{16}$. For each root $\epsilon\sqrt{2}$, $\epsilon \in \{-1, 1\}$, the momentum and winding numbers along T^{8-d} are

$$m_{d+1} = -n_{d+1} = -\epsilon\,, \qquad m_i = n_i = 0\,, \quad i \in \{d+2, \ldots, 9\}\,. \tag{3.1}$$

These towers arise in the Neveu–Schwarz sector of the 32 extra right-moving worldsheet fermions, $\vec{a}^{\,R} = \vec{0}$.

(ii) The 8 KK towers at oscillator level $\ell_R = 0$, whose right-moving quantum numbers are a given root or weight[12] vector (of length equal to $\sqrt{2}$) of a representation of $\mathcal{G}_{8-d}$, and that are neutral under $\mathcal{G}_1 \times \mathcal{G}_{16}$. They have non-trivial momentum and winding numbers along T^{8-d} and arise in sector $\vec{a}^{\,R} = \vec{0}$.

[12] In the notations of Eq. (A.36), non-adjoint representations of $\mathcal{G}_{8-d}$ exist when some of the discrete Wilson lines $\eta^R_j \in \mathbb{Z}$, $j \in \{d+2, \ldots, 9\}$, are odd. In this case, $\mathcal{G}_{8-d}$ may contain $U(1)$ factors coupled to fermions, with non-trivial charges we still refer as weight vectors' components.

(iii) The 8 KK towers at oscillator level $\ell_R = 0$, whose right-moving quantum numbers are a given root or weight vector (of length equal to $\sqrt{2}$) of a representation of $\mathcal{G}_{16}$, and that are neutral under $\mathcal{G}_1 \times \mathcal{G}_{8-d}$. They have trivial momentum and winding numbers along T^{8-d} and arise in any sector $\vec{a}^R$.

(iv) The 8×24 KK towers at oscillator level $\ell_R = 1$ that are neutral under $\mathcal{G}_1 \times \mathcal{G}_{8-d} \times \mathcal{G}_{16}$. They have trivial momentum and winding numbers along T^{8-d} and arise in sector $\vec{a}^R = \vec{0}$.

Due to our restriction on the allowed non-trivial Wilson line deformations, Eq. (2.15), all KK towers (ii)–(iv) have characteristic masses $\mathcal{M}'_{L0} = 0$ (see Eq. (A.50)) and "phases" $\zeta^d = 0$. Defined in Eq. (A.48), ζ^d actually determines the relative weights of the bosonic and fermionic modes within a given KK tower. The non-trivial Wilson lines $y_{d,d+1}$, $y_{d+1,d}$, $y_{d+1,d+1}$ however impact the characteristic masses and phases of the 8×2 KK towers (i). In total, the 1-loop effective potential given in Eq. (A.52) takes the specific form

$$\begin{aligned}\mathcal{V}^{(\sigma)}_{\text{1-loop}} = &\big(n_{\rm F} - n_{\rm B} + (-1)^{\eta^R_{d+1}}\, 8\times 2\big)\, v_d\, M^d_{(\sigma)} \\ &- (-1)^{\eta^R_{d+1}}\, 8\times 2\, \frac{2M^d_{(\sigma)}}{(2\pi)^{\frac{3d+1}{2}}} \sum_{\tilde m_d} \frac{\cos\big(2\pi(2\tilde m_d+1)z\big)}{|2\tilde m_d+1|^{d+1}}\, F\Big(2\pi|2\tilde m_d+1|\frac{\mathcal{M}}{M_{(\sigma)}}\Big) \\ &+ \mathcal{O}\big((cM_{\rm s}M_{(\sigma)})^{\frac{d}{2}} e^{-2\pi c M_{\rm s}/M_{(\sigma)}}\big)\,. \end{aligned} \tag{3.2}$$

In this formula, the definition of the function F can be found in Eq. (A.51), we have introduced z instead of ζ^d for notational convenience, and the non-trivial characteristic mass is denoted $\mathcal{M}$,

$$z = \sqrt{2}\left(y_{d,d+1} - \frac{y_{d,d+1}+y_{d+1,d}}{\sqrt{2}\left(1+\sqrt{2}\,y_{d+1,d+1}\right)}\, y_{d+1,d+1}\right), \qquad \mathcal{M} = \frac{\sqrt{2}\,|y_{d+1,d+1}|}{\sqrt{1+\sqrt{2}\,y_{d+1,d+1}}}\,. \tag{3.3}$$

If it is physically natural to use $M_{(\sigma)}$ and $y_{d,d+1}$, $y_{d+1,d}$, $y_{d+1,d+1}$ to parameterize the classical moduli space, it is however a matter of convention. Another choice may be to consider the "volume" G_{dd} as the remaining degree of freedom independent of $y_{d,d+1}$, $y_{d+1,d}$, $y_{d+1,d+1}$, in terms of which the supersymmetry breaking scale satisfies

$$M^2_{(\sigma)} \equiv G^{dd} M^2_{\rm s} = \frac{M^2_{\rm s}}{G_{dd}\left(1 - \dfrac{(y_{d,d+1}+y_{d+1,d})^2}{2G_{dd}\,(1+\sqrt{2}\,y_{d+1,d+1})}\right)}\,. \tag{3.4}$$

Some remarks about Eq. (3.2) are in order:

• The dependence in Wilson lines of $\mathcal{V}^{(\sigma)}_{\text{1-loop}}$ involves only two combinations of fields, z and $\mathcal{M}$. Thus, a flat direction exists at 1-loop.

• The expansions of the cosine and function F for small arguments contain exclusively even powers. However, depending on d, only a finite number of monomials can be summed term by term. At order z^2 and $\mathcal{M}^2$, summing over $\tilde m_d$ and restricting to the quadratic terms in Wilson lines, one obtains the approximate result (2.16).

• Due to the factor $|2\tilde m_d + 1|^{d+1}$ in the denominator, as well as the exponential suppression of the function F for large argument, the discrete sum in Eq. (3.2) is numerically very close to that restricted to $\tilde m_d = 0$ and -1. The error introduced this way in the sum is about 1% or (much) less.

• The potential is 1-periodic in z. A half-period shift $z \to z + \frac{1}{2}$ flips the sign of the second line in Eq. (3.2).

• The mass $\mathcal{M}$, which characterizes as a whole each KK tower (i), depends only on $y_{d+1,d+1}$, due to an exact cancellation of the contributions of $y_{d,d+1}$ and $y_{d+1,d}$ in the general expression (A.50). This is remarkable, since the mass of each KK mode (see Eq. (A.46)) does depend on the three Wilson lines.

• For instance in the case η^R_{d+1} even, when $\mathcal{M} = 0$ *i.e.* $y_{d+1,d+1} = 0$, the lightest KK masses and z (for example in the range $[-\frac{1}{2}, \frac{1}{2}]$) satisfy

$$m^2 = \Big(\frac{a}{2} - |z|\Big)^2 M^2_{(\sigma)}\,, \qquad z = \sqrt{2}\, y_{d,d+1}\,. \tag{3.5}$$

For $z = 0$, the associated states are the massless $SU(2)$ non-Cartan gauge and scalar bosons ($a = 0$) and their fermionic superpartners ($a = 1$) of masses $\frac{1}{2}M_{(\sigma)}$. As a result, the second line of Eq (3.2) cancels the contribution 8×2 in the first line. The situation is reversed for $z = \pm\frac{1}{2}$, for which the fermions are massless and the bosons massive, so that the role of the second line of Eq (3.2) is to shift $n_{\rm F} \to n_{\rm F} + 8 \times 2$ in the first line. When z varies between these two extreme cases, the KK towers do not contain massless states. Their absolute contributions are lower and actually vanish for $z = \pm\frac{1}{4}$. In fact, when $|z| \in (0, \frac{1}{2}]$, the gauge symmetry is in the Coulomb branch, $SU(2) \to U(1)$. On the contrary, when η^R_{d+1} is odd, a is replaced with $1 - a$ in the mass formula of Eq. (3.5) and the roles of bosons and fermions are reversed. In particular, for $z = \pm\frac{1}{2}$, the second line of Eq (3.2) simply shifts $n_{\rm B} \to n_{\rm B} + 8 \times 2$.

• When $y_{d+1,d+1}$ is switched on, the dependence of z and thus $\mathcal{V}_{1\text{-loop}}$ on $y_{d+1,d}$ becomes non-trivial. For instance, in the neighborhood of the undeformed background, $y_{d+1,d}$ appears at lowest order in Eq. (3.2) in the interaction term

$$-M^d_{(\sigma)}\, \frac{v_{d-2}}{2\pi}\, c_{\mathcal{G}_1}\, (d-1)\, \sqrt{2}\, y_{d+1,d}\, y_{d,d+1}\, y_{d+1,d+1}\,. \tag{3.6}$$

Thus, even if it is still massless, it is not identified anymore with the flat direction of the 1-loop potential.

• The function F is even, positive, shaped like a bell centered at the origin, and exponentially suppressed for large a argument. As a result, when $\mathcal{M}$ is non-vanishing but still smaller than $M_{(\sigma)}$, the magnitude (at fixed phase z) of the contributions of the 8×2 KK towers (i) is lowered. In fact, $y_{d+1,d+1}$ induces a small Higgs mass, so that the towers do not contain massless modes, even for $z = 0$ or $\frac{1}{2}$ mod 1, and the gauge theory always sits in the Coulomb branch $SU(2) \to U(1)$. When $\mathcal{M}$ is greater than $M_{(\sigma)}$, the Higgsing is large and we are free to omit the second line of Eq. (3.2).[13] In this case, the Wilson lines $y_{d,d+1}$, $y_{d+1,d}$, $y_{d+1,d+1}$ are flat directions, up to exponentially suppressed terms.

Kinetic terms

At tree level, imposing the restriction (2.15), the massless degrees of freedom allowed to have non-trivial homogeneous and isotropic backgrounds[14] are the graviton, the dilaton and the complex moduli

[13] At the transition, *i.e.* when $\mathcal{M}$ is slightly greater than $M_{(\sigma)}$, omitting the second line should be accompanied by fixing $c = \mathcal{M}$ in the last one.

[14] In dimension $d = 4$, we also impose the axion field dual to the spacetime antisymmetric tensor to be constant.

$$\mathcal{T} = B_{d,d+1} + i\sqrt{G_{dd}G_{d+1,d+1} - G_{d,d+1}^2}\,, \quad \mathcal{U} = \frac{G_{d+1,d} + i\sqrt{G_{dd}G_{d+1,d+1} - G_{d,d+1}^2}}{G_{dd}}\,. \tag{3.7}$$

Splitting the dilaton into a constant plus a dynamical field, $\phi_{\rm dil} \equiv \langle\phi_{\rm dil}\rangle + \phi$, the Einstein frame metric is defined as $g_{\mu\nu} = e^{-\frac{4}{d-2}\phi} G_{\mu\nu}$ and the classical effective action of the above degrees of freedom reduces to their kinetic terms,

$$S_{\rm tree} = \frac{1}{\kappa^2}\int d^d x\,\sqrt{-g}\,g^{\mu\nu}\left[\frac{\mathcal{R}_{\mu\nu}}{2} - \frac{2}{d-2}\,\partial_\mu\phi\partial_\nu\phi + \frac{\partial_\mu\mathcal{T}\partial_\nu\bar{\mathcal{T}}}{(\mathcal{T}-\bar{\mathcal{T}})^2} + \frac{\partial_\mu\mathcal{U}\partial_\nu\bar{\mathcal{U}}}{(\mathcal{U}-\bar{\mathcal{U}})^2}\right]. \tag{3.8}$$

In our conventions, the signature of the metric is $(-,+,\cdots,+)$, $\mathcal{R}_{\mu\nu}$ is the Ricci tensor and $\kappa^2 = e^{2\langle\phi_{\rm dil}\rangle}/M_{\rm s}^{d-2}$ is Einstein's constant. To make contact with the arbitrary Wilson lines $y_{d,d+1}$, $y_{d+1,d}$, $y_{d+1,d+1}$, the following dictionary can be used,

$$\begin{aligned} G_{d+1,d+1} &= 1 + \sqrt{2}\,y_{d+1,d+1}\,,\\ G_{d,d+1} &= \frac{1}{\sqrt{2}}\,(y_{d,d+1} + y_{d+1,d}) \equiv h_{d,d+1}\,,\\ B_{d,d+1} &= \frac{\eta^R_{d+1}}{2} + \frac{1}{\sqrt{2}}\,(y_{d,d+1} - y_{d+1,d})\,. \end{aligned} \tag{3.9}$$

Moreover, the supersymmetry breaking scale measured in Einstein frame is dressed with a dilaton factor and can be redefined in terms of the so-called "no-scale modulus" Φ,

$$M \equiv e^{\frac{2}{d-2}\phi}\,M_{(\sigma)} \equiv e^{\alpha\Phi} M_{\rm s}\,, \quad \text{where} \quad \alpha\Phi = \frac{2}{d-2}\,\phi + \ln\sqrt{G^{dd}}\,, \quad \alpha = \sqrt{\frac{d-1}{d-2}}\,. \tag{3.10}$$

Noticing that the kinetic terms of T and U yield, among other things, a contribution $-\frac{1}{2}\times(\partial\ln\sqrt{G_{dd}})^2$, it is natural to relate the latter to $-\frac{1}{2}(\partial\ln\sqrt{G^{dd}})^2$ by using the identity

$$G^{dd}G_{dd} = \frac{1+\sqrt{2}\,y_{d+1,d+1}}{1+f}\,, \quad \text{where} \quad f = \sqrt{2}\,y_{d+1,d+1} - \frac{h^2_{d,d+1}}{G_{dd}}\,. \tag{3.11}$$

In this way, the kinetic terms of ϕ and $\ln\sqrt{G^{dd}}$ can be combined into those of Φ and an "orthogonal" combination $\phi_\perp$,

$$\sqrt{d-1}\,\phi_\perp = 2\phi - \ln\sqrt{G^{dd}}\,. \tag{3.12}$$

In total, we ultimately find

$$\begin{aligned} S_{\rm tree} = \frac{1}{\kappa^2}\int d^d x\,\sqrt{-g}\Big[&\frac{\mathcal{R}}{2} - \frac{1}{2}(\partial\Phi)^2 - \frac{1}{2}(\partial\phi_\perp)^2\\ &- \frac{\Omega_1}{4}\,G^{dd}\Big((\partial y_{d,d+1})^2 + (\partial y_{d+1,d})^2\Big) - \frac{\Omega_2}{4}\,(\partial y_{d+1,d+1})^2 + \Omega_3\Big], \end{aligned} \tag{3.13}$$

where we have defined

$$\Omega_1 = \frac{1}{1+\sqrt{2}\,y_{d+1,d+1}}\,, \qquad \Omega_2 = \frac{1-\frac{h^4_{d,d+1}}{G^2_{dd}}}{(1+f)^2}\,,$$
$$\Omega_3 = \frac{\partial y_{d+1,d+1}}{2\sqrt{2}}\left(\partial\Big(\frac{h^2_{d,d+1}}{G_{dd}}\Big)\frac{1-\frac{h^2_{d,d+1}}{G_{dd}}}{(1+f)^2} + \frac{\partial G_{dd}}{G_{dd}}\,\frac{h^2_{d,d+1}}{G_{dd}}\,\frac{1}{(1+\sqrt{2}\,y_{d+1,d+1})(1+f)}\right). \tag{3.14}$$

Local marginal deformations

With exact formulas for the potential and kinetic terms at hand, we can make precise the notion of "small Wilson lines deformations" used in Sect. 2, for the backgrounds satisfying Eqs (2.12), (2.13) and (2.15):

$$|y_{d+1,d+1}| \ll \sqrt{G^{dd}} \ll 1\,, \quad |y_{d,d+1}| \ll 1\,, \quad |y_{d+1,d}| \ll 1\,. \tag{3.15}$$

Our goal being to study the dynamics of moduli fields, the restriction on $y_{d+1,d+1}$ implies $\mathcal{M} \ll M_{(\sigma)}$ so that the three Wilson lines are not flat directions. The conditions on $y_{d,d+1}$ and $y_{d+1,d}$ imply $|h_{d,d+1}| \ll 1$. Noticing that

$$\Omega_3 = \frac{G^{dd}}{2\sqrt{2}}\,\partial y_{d+1,d+1}\,\partial h^2_{d,d+1} + \cdots\,, \tag{3.16}$$

where the ellipses stand for at least quartic terms in Wilson lines, it is then consistent at leading order to set $(\Omega_1, \Omega_2, \Omega_3) = (1, 1, 0)$ in the kinetic terms. Moreover, the cubic interaction (3.6) and higher order ones in the potential can also be neglected, compared to the quadratic mass terms in Eq. (2.16).

4. Quantum no-scale regimes

Our goal in this section is to show that QNSRs do exist when the dynamics of marginal deformations of the internal space are taken into account. Indeed, we will find conditions under which such regimes can be reached in the setup described at the end of Sect. 2.

When the assumptions (3.15) are fulfilled, the 1-loop effective action in Einstein frame can be written as

$$S_{\text{1-loop}} = \frac{1}{\kappa^2}\int d^dx\,\sqrt{-g}\,\Big[\frac{\mathcal{R}}{2} - \frac{1}{2}(\partial\Phi)^2 - \frac{1}{2}(\partial\phi_\perp)^2 - \frac{G^{dd}}{4}(\partial y_{d,d+1})^2 - \frac{G^{dd}}{4}(\partial y_{d+1,d})^2 - \frac{1}{4}(\partial y_{d+1,d+1})^2 + \cdots - \kappa^2\mathcal{V}_{\text{1-loop}}\Big]\,, \tag{4.1}$$

where the potential is given by,

$$\mathcal{V}_{\text{1-loop}} = e^{d\alpha\Phi}M_{\text{s}}^d\Big[(n_{\text{F}}-n_{\text{B}})\,v_d + \frac{v_{d-2}}{2\pi}\,c_{\mathcal{G}_1}\Big((d-1)y^2_{d,d+1} + \frac{y^2_{d+1,d+1}}{G^{dd}}\Big)\Big] + \cdots\,. \tag{4.2}$$

In the kinetic terms, the ellipses correspond to 2-derivatives, cubic and higher order terms in Wilson lines $y_{d,d+1}$, $y_{d+1,d}$, $y_{d+1,d+1}$, while in $\mathcal{V}_{\text{1-loop}}$ they stand for cubic and higher order interactions, or exponentially suppressed corrections when $c/\sqrt{G^{dd}} \gg 1$. In the following, we will neglect all of these subdominant contributions.

Equation for a

Focusing on homogeneous and isotropic cosmological evolutions in flat space, we consider a metric and scalar field ansatz

$$ds^2 = -N(x^0)^2(dx^0)^2 + a(x^0)^2\Big((dx^1)^2 + \cdots + (dx^{d-1})^2\Big)\,,$$
$$\Phi(x^0)\,,\ \phi_\perp(x^0)\,,\ y_{d,d+1}(x^0)\,,\ y_{d+1,d}(x^0)\,,\ y_{d+1,d+1}(x^0)\,. \tag{4.3}$$

The equations of motion for the lapse function N and scale factor a take the following forms, in the gauge $N \equiv 1$ which defines cosmic time $x^0 \equiv t$,

$$\frac{1}{2}(d-1)(d-2)H^2 = \mathcal{K} + \kappa^2 \mathcal{V}_{\text{1-loop}}\,, \tag{4.4}$$
$$(d-2)\dot{H} + \frac{1}{2}(d-1)(d-2)H^2 = -\mathcal{K} + \kappa^2 \mathcal{V}_{\text{1-loop}}\,, \tag{4.5}$$

where $H \equiv \dot{a}/a$ and the kinetic terms are

$$\mathcal{K} = \frac{1}{2}\dot{\Phi}^2 + \frac{1}{2}\dot{\phi}_\perp^2 + \frac{G^{dd}}{4}\dot{y}_{d,d+1}^2 + \frac{G^{dd}}{4}\dot{y}_{d+1,d}^2 + \frac{1}{4}\dot{y}_{d+1,d+1}^2\,. \tag{4.6}$$

Interested in QNSRs, we eliminate $\mathcal{K}$ between Eqs (4.4) and (4.5),

$$\frac{1}{d-1}\frac{(a^{d-1})^{\cdot\cdot}}{a^{d-1}} \equiv \dot{H} + (d-1)H^2 = \frac{2}{d-2}\kappa^2 \mathcal{V}_{\text{1-loop}}\,, \tag{4.7}$$

and look for cosmological evolutions satisfying either

$$a(t) \underset{t-t_+\to+\infty}{\longrightarrow} +\infty \qquad \text{or} \qquad a(t) \underset{t-t_-\to 0_+}{\longrightarrow} 0\,, \tag{4.8}$$

for some constants $t_\pm$, with the effective potential dominated by H^2. To be specific, we assume the solutions to satisfy

$$\kappa^2 M_{\rm s}^d\, e^{d\alpha\Phi} = \mathcal{O}\left(\frac{H^2}{a^{K_\pm}}\right) \tag{4.9}$$

in the above limits, where $\pm K_\pm > 0$ are constants to be determined. The $t - t_+ \to +\infty$ asymptotic regime describes an ever-expanding universe, while $t - t_- \to 0_+$ corresponds to a Big Bang arising at $t = t_-$. Of course, contracting evolutions in QNSR may also be found by time reversal. Under these hypotheses, and supposing a power law behavior of the scale factor, Eq. (4.7) can be integrated once,

$$C_\pm - \frac{1}{H} = -(d-1)(t-t_\pm)\left(1 + \mathcal{O}\left(\frac{1}{a^{K_\pm}}\right)\right). \tag{4.10}$$

Without loss of generality, the constant C_+ can be absorbed in a redefinition of t_+, while C_- has to vanish for $a(t)$ to vanish at t_-. Integrating a second time, one obtains

$$a = \mathscr{A}(t-t_\pm)^{\frac{1}{d-1}}\left(1 + \mathcal{O}\left(\frac{1}{a^{K_\pm}}\right)\right), \tag{4.11}$$

where $\mathscr{A} > 0$ is a not yet specified constant. Up to the subdominant term $\mathcal{O}(1/a^{K_\pm})$, the time-dependence of the scale factor is by no way surprising since a negligible potential energy implies the evolution of the universe to be driven by the moduli kinetic energies, *i.e.* a cosmic fluid of energy density ρ and pressure P satisfying $\rho \sim P$.

Equation for $y_{d+1,d}$

At quadratic order in Wilson line deformations, $y_{d+1,d}$ has a vanishing potential but a non-canonical kinetic term. Thus, its equation of motion is that of a free field, with non-conventional friction term,

$$\ddot{y}_{d+1,d} + \left[(d-1)H + (\ln G^{dd})^{\cdot}\right]\dot{y}_{d+1,d} = 0\,, \tag{4.12}$$

which yields

$$\dot{y}_{d+1,d} = \frac{2\,c_{d+1,d}}{a^{d-1}G^{dd}}\,, \tag{4.13}$$

where $c_{d+1,d}$ is an integration constant. A consequence of Eq. (4.11) is that the l.h.s. of Friedmann equation (4.4) is

$$\frac{1}{2}(d-1)(d-2)H^2 = \frac{d-2}{2(d-1)}\,\frac{\mathscr{A}^{2(d-1)}}{a^{2(d-1)}}\left(1+\mathcal{O}\left(\frac{1}{a^{K_\pm}}\right)\right), \tag{4.14}$$

while the kinetic and potential terms in the r.h.s. satisfy

$$\mathcal{K} \geq \frac{c_{d+1,d}^2}{a^{2(d-1)}G^{dd}}\,, \qquad |\kappa^2\mathcal{V}_{\text{1-loop}}| \ll H^2\,. \tag{4.15}$$

For these facts to be consistent, we proceed by assuming a power law behavior

$$G^{dd} \sim \mathscr{G}(t-t_\pm)^{J_\pm}\,, \tag{4.16}$$

for some coefficient $\pm J_\pm > 0$ to be determined, and a constant $\mathscr{G} > 0$. In this case, the kinetic term of $y_{d+1,d}$ is subdominant in $\mathcal{K}$,

$$H^2\mathcal{O}_1 \equiv \mathcal{O}\left(G^{dd}\dot{y}_{d+1,d}^2\right) = \mathcal{O}\left(\frac{c_{d+1,d}^2}{\mathscr{A}^{2(d-1)}}\,\frac{H^2}{G^{dd}}\right) \ll \mathcal{K} = \mathcal{O}(H^2)\,. \tag{4.17}$$

In the end, we obtain

$$y_{d+1,d} \simeq y_{d+1,d}^{(0)} - \frac{\mathscr{C}_{d+1,d}}{J_\pm(t-t_\pm)^{J_\pm}}\,, \quad \text{where} \quad \mathscr{C}_{d+1,d} = \frac{2\,c_{d+1,d}}{\mathscr{A}^{d-1}\mathcal{G}}\,, \tag{4.18}$$

and the second integration constant satisfies $|y_{d+1,d}^{(0)}| \ll 1$.

Notice that in the QNSR $t - t_+ \to +\infty$, the initial hypothesis (4.9) implies M to drop. This is also the case for the QNSR $t - t_- \to 0_+$, if $\frac{|K_-|}{d-1} > 2$. On the contrary, Eq. (4.16) implies the supersymmetry breaking scale measured in σ-model frame, $M_{(\sigma)}$, to rise and formally tend to infinity, when $t - t_+ \to +\infty$ (or $t - t_- \to 0_+$). This means that in the QNSRs, t should not exceed some maximal value $t_{\rm f}$ (or reach values below $t_{\rm f}$) such that $G^{dd}(t_{\rm f}) = c^2$. After (or before) $t_{\rm f}$, the exponential terms in the effective potential (2.16) are no more suppressed.[15]

Equation for $y_{d+1,d+1}$

In order to determine $y_{d+1,d+1}$ in the QNSRs, one can insert in its equation of motion,

$$\ddot{y}_{d+1,d+1} + (d-1)H\dot{y}_{d+1,d+1} + \frac{2v_{d-2}}{\pi}\,c_{\mathcal{G}_1}\kappa^2 M_{\rm s}^d\,\frac{e^{d\alpha\Phi}}{G^{dd}}\,y_{d+1,d+1} = 0\,, \tag{4.19}$$

[15] When $c = \mathcal{O}(1)$, Hagedorn-like transitions may even occur when $G^{dd} = \mathcal{O}(1)$.

the behaviors of $(d-1)H \sim 1/(t-t_\pm)$, $G^{dd} \sim \mathscr{G}(t-t_\pm)^{J_\pm}$ and $e^{d\alpha\Phi} \sim \#H^2/a^{K_\pm}$. For $c_{\mathcal{G}_1} > 0$, the generic solution of the differential equation can be expressed in terms of Bessel functions of the first kind, J_0, and second kind, Y_0,

$$y_{d+1,d+1} = C\, J_0\left(\frac{L}{(t-t_\pm)^{\frac{1}{2}(J_\pm+\frac{K_\pm}{d-1})}}\right) + C'\, Y_0\left(\frac{L}{(t-t_\pm)^{\frac{1}{2}(J_\pm+\frac{K_\pm}{d-1})}}\right), \tag{4.20}$$

where $L > 0$ and the arbitrary C, C' are constants. For $c_{\mathcal{G}_1} < 0$, the Bessel functions are "modified" into I_0 and K_0. In both cases, the value of L is irrelevant when taking the limit $t - t_+ \to +\infty$ or $t - t_- \to 0_+$, and we obtain

$$y_{d+1,d+1} \simeq \mathscr{C}_{d+1,d+1} \ln \frac{t-t_\pm}{t_0 - t_\pm}\,, \tag{4.21}$$

where $\mathscr{C}_{d+1,d+1}$ and t_0 are constants. Notice that this logarithmic behavior is not in contradiction with the smallness of $y_{d+1,d+1}$ we have assumed in Eq. (3.15). This follows from the fact that in a QNSR, $|y_{d+1,d+1}|/\sqrt{G^{dd}}$ decreases, due to the power-dependence of G^{dd} in time. Physically, the supersymmetry breaking scale in σ-model frame $M_{(\sigma)}$ grows faster than the Higgs mass $|y_{d+1,d+1}|M_{\rm s}$.

Before proceeding, it is instructive to use

$$\dot{y}_{d+1,d+1} \sim \frac{\mathscr{C}_{d+1,d+1}}{t-t_\pm}\,, \tag{4.22}$$

in order to evaluate the mass term,

$$\mathcal{O}\left(\kappa^2 M_{\rm s}^d\, \frac{e^{d\alpha\Phi}}{G^{dd}}\, y_{d+1,d+1}\right) = \mathcal{O}\left(H\dot{y}_{d+1,d+1}\frac{1}{a^{K_\pm}G^{dd}} \ln\frac{t-t_\pm}{t_0-t_\pm}\right) \equiv H\dot{y}_{d+1,d+1}\mathcal{O}_2\,. \tag{4.23}$$

With this result, Eq. (4.19) becomes

$$\ddot{y}_{d+1,d+1} + (d-1)H\dot{y}_{d+1,d+1}\big(1+\mathcal{O}_2\big) = 0\,, \tag{4.24}$$

which can be integrated once to yield the more accurate result

$$\dot{y}_{d+1,d+1} = \frac{2\,c_{d+1,d+1}}{a^{d-1}}\big(1+\mathcal{O}_2\big)\,, \qquad \text{where} \qquad \mathscr{C}_{d+1,d+1} = \frac{2\,c_{d+1,d+1}}{\mathscr{A}^{d-1}}\,. \tag{4.25}$$

Equation for $y_{d,d+1}$

As before, one can solve the equation of motion of $y_{d,d+1}$,

$$\ddot{y}_{d,d+1} + \big[(d-1)H + (\ln G^{dd})^{\cdot}\big]\dot{y}_{d,d+1} + \frac{2v_{d-2}}{\pi}(d-1)\,c_{\mathcal{G}_1}\kappa^2 M_{\rm s}^d\,\frac{e^{d\alpha\Phi}}{G^{dd}}\,y_{d,d+1} = 0\,, \tag{4.26}$$

after substituting H, G^{dd} and $e^{d\alpha\Phi}$ with their limit behaviors. For $c_{\mathcal{G}_1} > 0$, the generic solution turns out to be expressed in terms of Bessel functions of the first kind,

$$y_{d,d+1} = \frac{C}{(t-t_\pm)^{\frac{J_\pm}{2}}}\, J_k\left(\frac{L}{(t-t_\pm)^{\frac{1}{2}(J_\pm+\frac{K_\pm}{d-1})}}\right) + \frac{C'}{(t-t_\pm)^{\frac{J_\pm}{2}}}\, J_{-k}\left(\frac{L}{(t-t_\pm)^{\frac{1}{2}(J_\pm+\frac{K_\pm}{d-1})}}\right), \tag{4.27}$$

where $k = J_\pm/(J_\pm + \frac{K_\pm}{d-1})$. For $c_{\mathcal{G}_1} < 0$, the Bessel functions are "modified", $J_k, J_{-k} \to I_k, I_{-k}$. In the limit $t - t_+ \to +\infty$ or $t - t_- \to 0_+$ we are interested in, this leads to

$$y_{d,d+1} \simeq y^{(0)}_{d,d+1} - \frac{\mathscr{C}_{d,d+1}}{J_\pm (t-t_\pm)^{J_\pm}} \equiv y^{(0)}_{d,d+1}(1+\tilde{\mathcal{O}}_1)\,, \tag{4.28}$$

where $y^{(0)}_{d,d+1}$ and $\mathscr{C}_{d,d+1}$ are integration constants, with $|y^{(0)}_{d,d+1}| \ll 1$. Alternatively, one can write

$$\dot{y}_{d,d+1} \sim \frac{2\,c_{d,d+1}}{a^{d-1}G^{dd}}\,, \qquad \text{where} \qquad \mathscr{C}_{d,d+1} = \frac{2\,c_{d,d+1}}{\mathscr{A}^{d-1}\mathcal{G}}\,. \tag{4.29}$$

The kinetic energies of $y_{d,d+1}$ and $y_{d+1,d}$ are thus of same order,

$$H^2\mathcal{O}_1 \equiv \mathcal{O}\Big(G^{dd}\dot{y}^2_{d,d+1}\Big) = \mathcal{O}\left(\frac{c^2_{d,d+1}}{\mathscr{A}^{2(d-1)}}\frac{H^2}{G^{dd}}\right) \ll \mathcal{K} = \mathcal{O}(H^2)\,. \tag{4.30}$$

Equation for $\phi_\perp$

Once Wilson lines are taken into account, the scalar $\phi_\perp$ is no longer a free field. Due to the fact that

$$G^{dd} = e^{\frac{2}{\alpha}\Phi}\, e^{-\frac{2}{\sqrt{d-1}}\phi_\perp}\,, \tag{4.31}$$

$\phi_\perp$ couples non-trivially to kinetic and mass terms, and its equation of motion is highly non-linear,

$$\ddot{\phi}_\perp + (d-1)H\dot{\phi}_\perp = -\frac{G^{dd}}{2\sqrt{d-1}}\big(\dot{y}^2_{d,d+1} + \dot{y}^2_{d+1,d}\big) - \frac{v_{d-2}}{\pi\sqrt{d-1}}\, c_{\mathcal{G}_1}\kappa^2 M_{\rm s}^d\, \frac{e^{d\alpha\Phi}}{G^{dd}}\, y^2_{d+1,d+1}\,. \tag{4.32}$$

However, up to a numerical factor, the two terms in the r.h.s. show up respectively in $\mathcal{K}$ and $\kappa^2\mathcal{V}_{\text{1-loop}}$. We have already seen that the former is of order $H^2\mathcal{O}_1$, while the second is of order

$$H^2\mathcal{O}_3 \equiv \mathcal{O}\left(\kappa^2 M_{\rm s}^d\, \frac{e^{d\alpha\Phi}}{G^{dd}}\, y^2_{d+1,d+1}\right) = \mathcal{O}\left(\frac{H^2}{a^{K_\pm}}\frac{y^2_{d+1,d+1}}{G^{dd}}\right) \ll H^2\,. \tag{4.33}$$

For reasons that will become clearer later, it is useful to explain the term $\mathcal{O}_1$. Assuming $\dot{\phi}_\perp = \mathcal{O}(H)$, we define the constant $C_\perp$ such that

$$\frac{1}{a^{2(d-1)}} \sim C_\perp (d-1) H\dot{\phi}_\perp\,, \tag{4.34}$$

and write Eq. (4.32) in the following form,

$$\ddot{\phi}_\perp + (d-1)H\dot{\phi}_\perp\left(1 + \frac{2C_\perp}{\sqrt{d-1}}\,\frac{c^2_{d,d+1}+c^2_{d+1,d}}{G^{dd}} + \cdots + \mathcal{O}_3\right) = 0 \tag{4.35}$$

where the ellipses stand for subdominant contributions in the $\mathcal{O}_1$ term. Integrating once, we obtain

$$\dot{\phi}_\perp = \sqrt{2}\,\frac{c_\perp}{a^{d-1}}\left(1+\frac{2C_\perp}{\sqrt{d-1}}\,\frac{c_{d,d+1}^2+c_{d+1,d}^2}{J_\pm\,G^{dd}}+\cdots+\mathcal{O}_3\right), \tag{4.36}$$

where $c_\perp$ is an arbitrary constant. Using the above result, Eq. (4.34) is consistent and we can identify

$$C_\perp = \frac{1}{\sqrt{2}\,c_\perp\,\mathscr{A}^{d-1}}\,. \tag{4.37}$$

Equation for Φ

The treatment of the no-scale modulus Φ can be similar. Its equation of motion,

$$\begin{aligned}\alpha\ddot{\Phi}+(d-1)H\alpha\dot{\Phi} = &-d\alpha^2\kappa^2 M_{\rm s}^d\mathcal{V}_{\text{1-loop}}+\frac{G^{dd}}{2}\left(\dot{y}_{d,d+1}^2+\dot{y}_{d+1,d}^2\right)\\ &+\frac{v_{d-2}}{\pi}\,c_{\mathcal{G}_1}\kappa^2 M_{\rm s}^d\,\frac{e^{d\alpha\Phi}}{G^{dd}}\,y_{d+1,d+1}^2\,,\end{aligned} \tag{4.38}$$

can be linearly combined with Eq. (4.7) to eliminate the term proportional to $\mathcal{V}_{\text{1-loop}}$. One obtains

$$\begin{aligned}&\left(\alpha\dot{\Phi}+\frac{\alpha^2}{2}\,d(d-2)H\right)^{\cdot}+(d-1)\,H\left(\alpha\dot{\Phi}+\frac{\alpha^2}{2}\,d(d-2)H\right)=\\ &\qquad\frac{G^{dd}}{2}\left(\dot{y}_{d,d+1}^2+\dot{y}_{d+1,d}^2\right)+\frac{v_{d-2}}{\pi}\,c_{\mathcal{G}_1}\kappa^2 M_{\rm s}^d\,\frac{e^{d\alpha\Phi}}{G^{dd}}\,y_{d+1,d+1}^2\,,\end{aligned} \tag{4.39}$$

which is an equation whose form is identical to that of $\phi_\perp$. Thus, assuming $\dot{\Phi}=\mathcal{O}(H)$, we can proceed in a similar way to obtain

$$\alpha\dot{\Phi}+\frac{\alpha^2}{2}\,d(d-2)H=\frac{c_\Phi}{a^{d-1}}\left(1-2C_\Phi\,\frac{c_{d,d+1}^2+c_{d+1,d}^2}{J_\pm\,G^{dd}}+\cdots+\mathcal{O}_3\right), \tag{4.40}$$

where c_Φ is an arbitrary constant and

$$C_\Phi=\frac{1}{c_\Phi\,\mathscr{A}^{d-1}}\,. \tag{4.41}$$

Friedmann constraint

We started our discussion by solving Eq. (4.7) for the scale factor $a(t)$, which introduced two integration constants $\mathscr{A}$ and $t_\pm$ in the solution (4.11). However, Friedmann differential equation (4.4) being only first-order, it can be used to fix $\mathscr{A}$ in terms of the other parameters.

To reach this goal, we first collect all results found for the scalar fields to write the total kinetic energy as

$$\begin{aligned}\mathcal{K}=&\frac{1}{8}\,d^2(d-2)^2\alpha^2H^2-\frac{1}{2}\,d(d-2)H\,\frac{c_\Phi}{a^{d-1}}+\frac{\frac{c_\Phi^2}{2\alpha^2}+c_\perp^2+c_{d+1,d+1}^2}{a^{2(d-1)}}\\ &+\frac{c_{d,d+1}^2+c_{d+1,d}^2}{a^{2(d-1)}\,G^{dd}}\,(C_{\mathcal{K}}+\cdots)+H^2\mathcal{O}_3+\frac{c_{d+1,d+1}^2}{a^{2(d-1)}}\,\mathcal{O}_2\,,\end{aligned} \tag{4.42}$$

where

$$C_{\mathcal{K}} = 1 + \frac{1}{J_\pm}\left(\sqrt{\frac{2}{d-1}}\,\frac{2c_\perp}{\mathscr{A}^{d-1}} - \frac{2}{\alpha^2}\,\frac{c_\Phi}{\mathscr{A}^{d-1}} + \frac{d}{\alpha^2}\right). \tag{4.43}$$

In the expression of $\mathcal{K}$, all terms in the first line are $\mathcal{O}(H^2)$. In the second line, the contribution proportional to $1/(a^{2(d-1)}G^{dd})$ and $H^2\mathcal{O}_3$ arise from the kinetic terms of $y_{d,d+1}$ and $y_{d+1,d}$, as well as the subdominant contributions of those associated with $\phi_\perp$ and Φ. Moreover, the last term, which is the subdominant part of the kinetic energy of $y_{d+1,d+1}$, can be compared to the other contributions by noticing that

$$\frac{c^2_{d+1,d+1}}{a^{2(d-1)}}\,\mathcal{O}_2 = \mathcal{O}\big(H^2\mathscr{C}^2_{d+1,d+1}\big)\mathcal{O}_2 = \mathcal{O}\left(\frac{H^2}{a^{K_\pm}}\,\frac{y^2_{d+1,d+1}}{G^{dd}}\,\frac{1}{\ln\left(\frac{t-t_\pm}{t_0-t_\pm}\right)}\right) = H^2\frac{\mathcal{O}_3}{\ln\left(\frac{t-t_\pm}{t_0-t_\pm}\right)}\,. \tag{4.44}$$

The latter being dominated by $H^2\mathcal{O}_3$, it can be omitted in Eq. (4.42). In a similar spirit, the 1-loop effective potential can be written as

$$\mathcal{V}_{\text{1-loop}} = e^{d\alpha\Phi}M_{\rm s}^d\Big[(n_{\rm F}-n_{\rm B})\,v_d + \frac{v_{d-2}}{2\pi}\,c_{\mathcal{G}_1}(d-1)y^{(0)^2}_{d,d+1}(1+\tilde{\mathcal{O}}_1)\Big] + H^2\mathcal{O}_3\,. \tag{4.45}$$

Finally, we may follow Ref. [11] by defining

$$\tau \equiv \frac{(d^2-4)(d-1)}{2dc_\Phi}\,Ha^{d-1} = \frac{(d^2-4)}{2dc_\Phi}\,(a^{d-1})^{\cdot}\,, \tag{4.46}$$

in terms of which the l.h.s. of Friedmann equation (4.4) and the dominant terms $\mathcal{O}(H^2)$ of $\mathcal{K}$ combine into a suitable form. The result is

$$\begin{aligned}-\frac{d^2c_\Phi^2}{2(d-1)(d+2)}\,\frac{\mathcal{P}(\tau)}{a^{2(d-1)}} = \kappa^2M_{\rm s}^d\,e^{d\alpha\Phi}\Big[&(n_{\rm F}-n_{\rm B})\,v_d\\ &+\frac{v_{d-2}}{2\pi}\,c_{\mathcal{G}_1}(d-1)y^{(0)^2}_{d,d+1}(1+\tilde{\mathcal{O}}_1)\Big]\\ &+\frac{c^2_{d,d+1}+c^2_{d+1,d}}{a^{2(d-1)}G^{dd}}\,(C_{\mathcal{K}}+\cdots)+H^2\mathcal{O}_3\,,\end{aligned} \tag{4.47}$$

where $\mathcal{P}$ is a quadratic polynomial,

$$\mathcal{P}(\tau) = \tau^2 - 2\tau + \left(1-\frac{4}{d^2}\right)\left(1+2\alpha^2\,\frac{c_\perp^2+c^2_{d+1,d+1}}{c_\Phi^2}\right). \tag{4.48}$$

In the limits we are interested in, the behavior (4.11) of the scale factor implies τ to converge to a constant,

$$\tau = \tau_0\left(1+\mathcal{O}\left(\frac{1}{a^{K_\pm}}\right)\right), \qquad \text{where} \qquad \tau_0 = \frac{d^2-4}{2d}\,\frac{\mathscr{A}^{d-1}}{c_\Phi}\,, \tag{4.49}$$

and $\mathcal{P}(\tau)$ to satisfy

$$\mathcal{P}(\tau) = \mathcal{P}(\tau_0) + \mathcal{O}\left(\frac{1}{a^{K_\pm}}\right). \tag{4.50}$$

Thus, for Eq. (4.47) to be consistent, two conditions must be fulfilled:

(i) τ_0 must be a root of $\mathcal{P}$. In this instance only, instead of being $\mathcal{O}(H^2)$, the l.h.s. of Eq. (4.47) satisfies

$$-\frac{d^2 c_\Phi^2}{2(d-1)(d+2)}\,\frac{\mathcal{P}(\tau)}{a^{2(d-1)}} = \mathcal{O}\left(\frac{H^2}{a^{K_\pm}}\right). \tag{4.51}$$

(ii) We must have

$$\mathcal{O}\left(\frac{H^2}{a^{K_\pm}}\right) \gg \frac{c_{d,d+1}^2 + c_{d+1,d}^2}{a^{2(d-1)} G^{dd}}\,(C_{\mathcal{K}} + \cdots)\,, \qquad \mathcal{O}\left(\frac{H^2}{a^{K_\pm}}\right) \gg H^2 \mathcal{O}_3\,, \tag{4.52}$$

for our initial defining assumption of a QNSR to be true, Eq. (4.9).

Condition (i) requires the discriminant of $\mathcal{P}$ to be positive, which amounts to having

$$\left(\frac{c_\perp}{\gamma_{\rm c} c_\Phi}\right)^2 + \left(\frac{c_{d+1,d+1}}{\gamma_{\rm c} c_\Phi}\right)^2 \leq 1\,, \quad \text{where} \quad \gamma_{\rm c} = \sqrt{\frac{2}{(d-1)(d+2)}}\,. \tag{4.53}$$

In this case, the value of $\mathscr{A}$, which appears in the definition of τ_0, is determined up to a sign ϵ,

$$\mathscr{A} = \left[\frac{2d}{d^2-4}\,(1+\epsilon\, r)\, c_\Phi\right]^{\frac{1}{d-1}}\,, \tag{4.54}$$

where $c_\Phi > 0$ is required and r defined as

$$r = \frac{2}{d}\sqrt{1 - \left(\frac{c_\perp}{\gamma_{\rm c} c_\Phi}\right)^2 - \left(\frac{c_{d+1,d+1}}{\gamma_{\rm c} c_\Phi}\right)^2}\,. \tag{4.55}$$

In condition (ii), the inequality that involves $\mathcal{O}_3$ is always satisfied, as follows from the decrease in $|y_{d+1,d+1}|/\sqrt{G^{dd}}$, (see Eq. (4.33)). However, the other constraint may be more intriguing. If $C_{\mathcal{K}} \neq 0$, it would imply $\pm J_\pm > \pm\frac{K_\pm}{d-1}$, which would restrict the choices of integration constants characterizing the QNSRs (see the next paragraph). However, such a reduction of the set of solutions should not occur, since we have already solved all differential equations and the only remaining piece of information captured by Friedmann equation must be the value of $\mathscr{A}$. As we will now check, $C_{\mathcal{K}}$ actually does vanish. Moreover, all implicit contributions in Eq. (4.52) in the dots should respect the inequality, without imposing further constraints on the existence of QNSRs, as will be checked numerically in Sects 5 and 6.

Determination of $K_\pm$ and $J_\pm$

Using the value of $\mathscr{A}$, Eq. (4.40) yields

$$d\alpha\dot\Phi \sim -\left(2 + \epsilon\,\frac{r(d^2-4)}{2(1+\epsilon\, r)}\right)\frac{1}{t-t_\pm}\,, \tag{4.56}$$

where the overall coefficient is to be identified with $-(2+\frac{K_\pm}{d-1})$, as follows from Eq. (4.9). The fact that $\pm K_\pm > 0$ fixes $\epsilon = \pm$, and we obtain

$$e^{d\alpha\Phi} \sim \frac{e^{d\alpha\Phi_\pm}}{[M_{\rm s}(t-t_\pm)]^{2+\frac{K_\pm}{d-1}}}\,, \qquad \text{where} \qquad K_\pm = \pm\frac{r(d^2-4)}{2(1\pm r)} \tag{4.57}$$

and $\Phi_\pm$ is an integration constant.

The coefficient $J_\pm$ can be determined in a similar way by using the linear relation between $(\ln G^{dd})^{\cdot}$, $\dot\Phi$ and $\dot\phi_\perp$. The result is

$$J_\pm = \frac{d}{\alpha^2}\left(\left(1 - \alpha^2\sqrt{\frac{2}{d-1}}\,\frac{c_\perp}{c_\Phi}\right)\frac{1-\frac{4}{d^2}}{1\pm r} - 1\right), \tag{4.58}$$

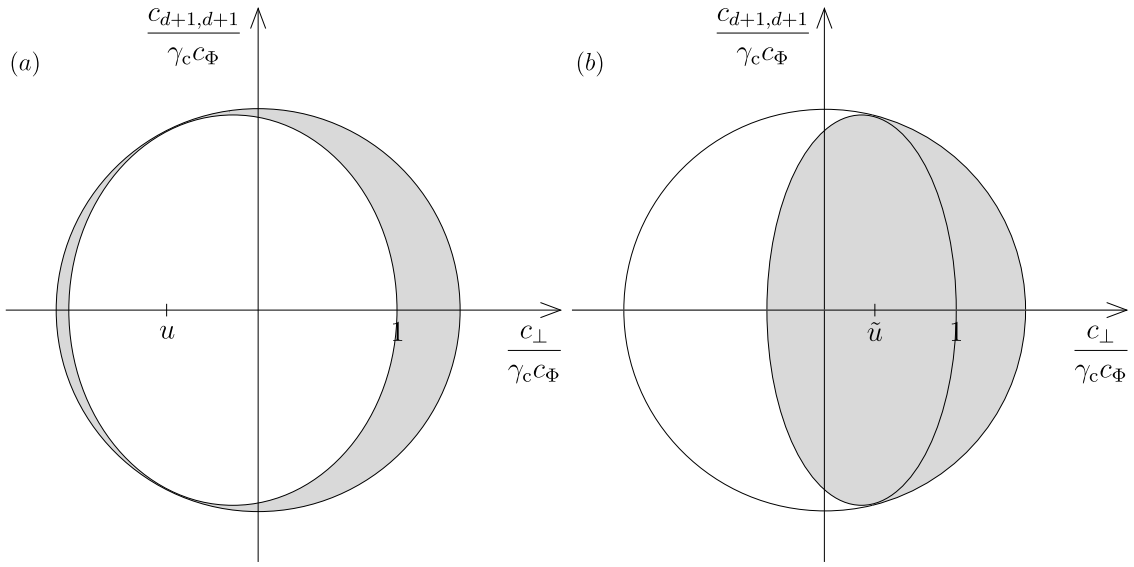

Fig. 1. The points $\left(\frac{c_\perp}{\gamma_c c_\Phi}, \frac{c_{d+1,d+1}}{\gamma_c c_\Phi}\right)$ of the disk of radius 1 that yield a QNSR $t - t_+ \to +\infty$ sit in the left crescent of figure (a). Those in the right crescent lead to a QNSR $t - t_- \to 0_+$. The former are always perturbative, while the latter are compatible with weak string coupling when $d \geq 3$ if $\left(\frac{c_\perp}{\gamma_c c_\Phi}, \frac{c_{d+1,d+1}}{\gamma_c c_\Phi}\right)$ is also located in the shaded era of figure (b).

which leads as anticipated to $C_{\mathcal{K}} = 0$. With the expression of $J_\pm$, we are ready to solve the only non-trivial consistency condition for QNSRs to exist. The points $\left(\frac{c_\perp}{\gamma_c c_\Phi}, \frac{c_{d+1,d+1}}{\gamma_c c_\Phi}\right)$ of the disk of radius 1, Eq. (4.53), compatible with the constraint

$$\pm J_\pm > 0 \tag{4.59}$$

sit outside an ellipse

$$\left(\frac{c_\perp}{\gamma_c c_\Phi} - \frac{u}{1+v}\right)^2 + \frac{v}{1+v}\left(\frac{c_{d+1,d+1}}{\gamma_c c_\Phi}\right)^2 \geq \frac{v}{(1+v)^2}(1+v-u^2)\,,$$

$$\text{where} \qquad u = -\frac{2}{\sqrt{d+2}}\,, \qquad v = \frac{d^2}{d+2}\,. \tag{4.60}$$

As shown in Fig. 1(a), for arbitrary dimension $d > 2$, this ellipse is located in the interior of the disk and is tangential to it at $\frac{c_\perp}{\gamma_c c_\Phi} = u$. The points in the left crescent $\left(\frac{c_\perp}{\gamma_c c_\Phi} \leq u\right)$ allow a QNSR $t - t_+ \to +\infty$, while those in the right crescent $\left(\frac{c_\perp}{\gamma_c c_\Phi} \geq u\right)$ yield a regime $t - t_- \to 0_+$. In reality, the left crescent is more tiny than the one shown on the qualitative Fig. 1(a). Its width at $\frac{c_{d+1,d+1}}{\gamma_c c_\Phi} = 0$ is $3\text{–}11 \cdot 10^{-3}$ for $3 \leq d \leq 9$, and actually vanishes when $d \to 2_+$. Thus, we have $r \simeq 0$ in the left crescent, so that M^d and H^2 evolve approximately at the same cosmological speed.

Finally, we can make some remark about $\mathscr{C}_{d+1,d+1}$, which is related to $c_{d+1,d+1}$ in Eq. (4.25) and must be small, as required by our assumption on $y_{d+1,d+1}$ given in Eq. (3.15). If the left and right crescents allow $\mathscr{C}_{d+1,d+1}$ to be as small as desired, its maximal value is reached for $\left(\frac{c_\perp}{\gamma_c c_\Phi}, \frac{c_{d+1,d+1}}{\gamma_c c_\Phi}\right) = (0, 1)$, which yields

$$|\mathscr{C}^{\max}_{d+1,d+1}| = \sqrt{\frac{2(d+2)}{d-1}}\,\frac{d-2}{d}\,. \tag{4.61}$$

This expression being of order 1, it is consistent as a limiting case.

Perturbative condition

At this stage, we have found time-dependent fields that extremize the 1-loop effective action in the limit $t - t_+ \to \infty$ or $t - t_- \to 0_+$. To make sense, however, this analysis requires string perturbation theory to be valid in these regimes. Expressing $\dot\phi$ as a linear combination of $\dot\Phi$ and $\dot\phi_\perp$, one obtains

$$e^{2d\alpha^2\phi} \sim \frac{e^{d\alpha\Phi_\pm}\, e^{d\sqrt{d-1}\,\phi_{\perp\pm}}}{[M_{\rm s}(t-t_\pm)]^{\frac{P_\pm}{d-1}}}\,, \tag{4.62}$$

where $\phi_{\perp\pm}$ is the constant arising by integration of Eq. (4.36) and

$$P_\pm = \frac{K_\pm}{(1-\frac{4}{d^2})\,r}\left[r \pm \Big(\frac{4}{d^2} - \big(1-\frac{4}{d^2}\big)\sqrt{2(d-1)}\,\frac{c_\perp}{c_\Phi}\Big)\right]. \tag{4.63}$$

The QNSR $t - t_+ \to +\infty$ happens to be perturbative, since $P_+ > 0$ is always satisfied when the point $\big(\frac{c_\perp}{\gamma_{\rm c} c_\Phi}, \frac{c_{d+1,d+1}}{\gamma_{\rm c} c_\Phi}\big)$ sits in the left crescent in Fig. 1(a). For the regime $t - t_- \to 0_+$, string perturbation theory is valid when $P_- < 0$. If $d \geq d_{\rm c} \simeq 2.90$, this condition is satisfied for $\frac{c_\perp}{\gamma_{\rm c} c_\Phi} \geq \tilde u$ or when $\big(\frac{c_\perp}{\gamma_{\rm c} c_\Phi}, \frac{c_{d+1,d+1}}{\gamma_{\rm c} c_\Phi}\big)$ sits in the interior of an ellipse

$$\Big(\frac{c_\perp}{\gamma_{\rm c} c_\Phi} - \frac{\tilde u}{1+\tilde v}\Big)^2 + \frac{\tilde v}{1+\tilde v}\Big(\frac{c_{d+1,d+1}}{\gamma_{\rm c} c_\Phi}\Big)^2 \leq \frac{\tilde v}{(1+\tilde v)^2}(1+\tilde v - \tilde u^2)\,,$$

$$\text{where} \qquad \tilde u = \frac{2}{(d-2)\sqrt{d+2}}\,, \qquad \tilde v = \frac{d^2}{(d-2)^2(d+2)}\,. \tag{4.64}$$

As shown in Fig. 1(b), this second ellipse is inside the disk of radius 1 and tangential to it at $\frac{c_\perp}{\gamma_{\rm c} c_\Phi} = \tilde u$. As a result, the right part of the right crescent in Fig. 1(a) yields perturbative QNSRs $t - t_- \to 0_+$. If $2 < d < d_{\rm c}$, $\tilde u$ being greater than 1, the condition $P_- < 0$ is true only inside the ellipse (4.64), which now sits entirely in the interior of the disk. However, the intersection of this perturbative domain with the right crescent of in Fig. 1(a) is always non-empty. It is only in the limit $d \to 2_+$, where the ellipse (4.64) vanishes, that the QNSRs $t - t_- \to 0_+$ are always formal because non-perturbative (unless we fine tune $\big(\frac{c_\perp}{\gamma_{\rm c} c_\Phi}, \frac{c_{d+1,d+1}}{\gamma_{\rm c} c_\Phi}\big)$ to be exactly $(0,0)$).

To summarize, the QNSRs we have found in arbitrary dimension $d > 2$ depend on 5 velocity parameters $c_\Phi > 0$, $c_\perp$, $c_{d+1,d+1}$, $c_{d,d+1}$, $c_{d+1,d}$, 5 zero modes $\Phi_\pm$, $\phi_{\perp\pm}$, t_0, $y^{(0)}_{d,d+1}$, $y^{(0)}_{d+1,d}$, and the last constant $t_\pm$ arising by integration of the scale factor. Therefore, they are limit behaviors of generic solutions, even if the left crescent in Fig. 1(a) is tiny.

5. Simulations of QNSRs at small Wilson lines

From now on, we study numerically the dynamics of the scale factor a, no-scale modulus Φ and scalar $\phi_\perp$, in the presence of the moduli fields $y_{d,d+1}$, $y_{d+1,d}$, $y_{d+1,d+1}$. Our goal in the present section is to check the validity of QNSRs described in Sect. 4, where the Wilson lines implement small deformations of the initial background. We fix in the analysis the spacetime dimension to be $d = 4$ and focus only on the expanding solutions where $t \to +\infty$ (we set $t_+ = 0$). In all simulations, we take $\langle\phi_{\rm dil}\rangle = 0$ so that $\kappa^2 = 1/M_{\rm s}^2$, thus identifying the Planck mass with the string scale. This has the advantage of matching the weak string coupling condition with the negativity of ϕ. Once the range of time compatible with perturbation theory is identified, it is always possible to restore a sensible value of the Planck mass by shifting the dilaton zero-mode.

As can be seen in Eq. (4.57), one feature of the QNSR $t \to +\infty$ is that the supersymmetry breaking scale M always drops. If this may be expected when $\mathcal{V}_{\text{1-loop}}$ is positive, it may be counterintuitive when it is negative, since M climbs the potential in this case. Moreover, the behaviors of $y_{d,d+1}$ and $y_{d+1,d+1}$ are independent of the fact that these moduli are massive or tachyonic at 1-loop. To check these striking properties, we simulate solutions of the differential equations of Sect. 4, which are valid for small Wilson lines deformations. This is done for 4 initial backgrounds characterized by different signs for $n_{\rm F}-n_{\rm B}$ and $c_{\mathcal{G}_1}$:

(i) $n_{\rm F}-n_{\rm B}>0$, $c_{\mathcal{G}_1}>0$: This case can be achieved in Example 2 of Sect. 2. For $d=4$ and $s=4$, the right-moving gauge group is $U(1)\times\mathcal{G}_1\times U(1)^4\times SO(16)\times SO(16)'$, where $\mathcal{G}_1=SU(2)$, which corresponds in the setup described below Eq. (2.12) to η_5^R even. In this model, one obtains $n_{\rm F}-n_{\rm B}=8\times 6$ and $c_{\mathcal{G}_1}=8\times 2$.

(ii) $n_{\rm F}-n_{\rm B}>0$, $c_{\mathcal{G}_1}<0$: To flip the sign of $c_{\mathcal{G}_1}$, it is enough to choose η_5^R odd in setup (i). This yields $\mathcal{G}_1=U(1)$, with $n_{\rm F}-n_{\rm B}=8\times 10$ and $c_{\mathcal{G}_1}=-8\times 2$.

(iii) $n_{\rm F}-n_{\rm B}<0$, $c_{\mathcal{G}_1}>0$: This case can be realized in Example 1 of Sect. 2. The right-moving gauge group for $d=4$ is $U(1)\times\mathcal{G}_1\times SU(2)^4\times E_8\times E_8'$, where $\mathcal{G}_1=SU(2)$, which corresponds to η_5^R even. This leads to $n_{\rm F}-n_{\rm B}=-8\times 514$ and $c_{\mathcal{G}_1}=8\times 2$.

(iv) $n_{\rm F}-n_{\rm B}<0$, $c_{\mathcal{G}_1}>0$: To flip the sign of $c_{\mathcal{G}_1}$, one can take η_5^R odd in setup (iii). This yields $\mathcal{G}_1=U(1)$, $n_{\rm F}-n_{\rm B}=-8\times 510$ and $c_{\mathcal{G}_1}=-8\times 2$.

To set initial conditions adapted to our purpose, we proceed as follows:

• We consider the case analyzed in Ref. [11], where no y-deformation is implemented. All trajectories that reach a QNSR $t\to+\infty$ are characterized by two constants $c_{\perp 0}$, $c_{\Phi 0}$ (defined as $c_\perp$ and c_Φ in the present work) such that $\left|\frac{c_{\perp 0}}{\gamma_c c_{\Phi 0}}\right|<1$. In order to allow the Wilson lines to vary, we take $c_{\perp 0}$, $c_{\Phi 0}$ for the expression of J_+ in Eq. (4.58) evaluated at $(c_\perp,c_\Phi,c_{55})=(c_{\perp 0},c_{\Phi 0},0)$ to be positive. This imposes $\approx 0.9941<\left|\frac{c_{\perp 0}}{\gamma_c c_{\Phi 0}}\right|<1$, thus reducing the allowed range of this ratio by approximately a factor of 170.

• In the presence of Wilson lines, we define dynamical quantities

$$c_\perp^{\rm dyn}=\frac{a^{d-1}}{\sqrt{2}}\,\dot\phi_\perp\,,\qquad c_\Phi^{\rm dyn}=a^{d-1}\left(\alpha\dot\Phi+\frac{\alpha^2}{2}\,d(d-2)H\right),\qquad c_{55}^{\rm dyn}=\frac{a^{d-1}}{2}\,\dot y_{55}\,,\tag{5.1}$$

which are expected to converge to the constants $c_\perp$, c_Φ and c_{55} introduced in Sect. 4.

• For the initial conditions at $t=0$, we set $a(0)$ to be of order 1 and $c_\perp^{\rm dyn}(0)=c_{\perp 0}$ to fix $\dot\phi_\perp(0)$. We also take $c_\Phi^{\rm dyn}(0)=c_{\Phi 0}$, which can be translated into $\dot\Phi(0)$ by the knowledge of $H(0)$. The latter, which we take to be positive, is determined by Friedmann equation at $t=0$, for a given choice of $\Phi(0)$ and initial conditions for the Wilson lines. To ensure that the evolution of the system starts close to the QNSR expected to arise at late times, $\Phi(0)$ is chosen for the quantity

$$\tau^{\rm dyn}\equiv\frac{(d^2-4)(d-1)}{2dc_\Phi^{\rm dyn}}\,Ha^{d-1}\,,\tag{5.2}$$

which is inspired by Eq. (4.46), to be at $t=0$ very close to the asymptotic value it would reach when no Wilson lines are introduced. To be specific, this means

$$\tau^{\rm dyn}(0)\simeq 1+r_0,\qquad\text{where}\quad r_0=\frac{2}{d}\sqrt{1-\left(\frac{c_{\perp 0}}{\gamma_c c_{\Phi 0}}\right)^2}\,,\tag{5.3}$$

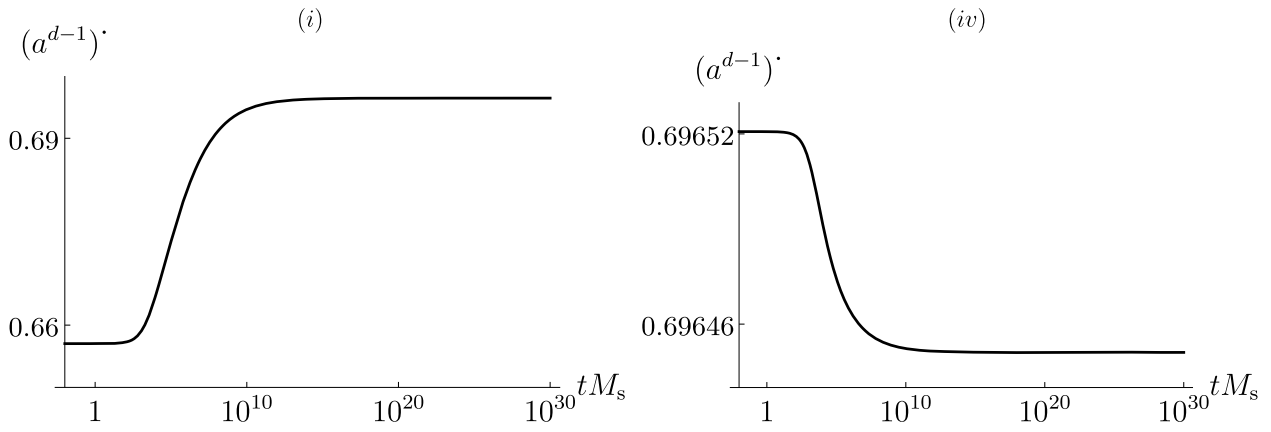

Fig. 2. Convergence of $(a^{d-1})^{\cdot}$ towards its limit $\mathscr{A}^{d-1}$, in cases (i) and (iv). The evolution is monotonically increasing or decreasing, depending on the sign of $n_F - n_B$.

as follows from Eqs (4.49) and (4.54). The choice of $\phi_\perp(0)$ is of order 1 and such that the range of cosmic time compatible with weak string coupling and $M_{(\sigma)}(t) < cM_s$ is large in the simulations.

• The remaining initial conditions are those of the Wilson lines: $y_{45}(0)$, $\dot{y}_{45}(0)$, $y_{54}(0)$, $\dot{y}_{54}(0)$ and $y_{55}(0)$, $\dot{y}_{55}(0)$. Their absolute values are chosen small enough (compared to 1 and M_s) for the trajectory of $\left(\frac{c_\perp^{\rm dyn}}{\gamma_c c_\Phi^{\rm dyn}}, \frac{c_{55}^{\rm dyn}}{\gamma_c c_\Phi^{\rm dyn}}\right)\Big|_t$ to be entirely in the left crescent in Fig. 1(a). The motion of this point is expected to converge to $\left(\frac{c_\perp}{\gamma_c c_\Phi}, \frac{c_{55}}{\gamma_c c_\Phi}\right)$, when $t \to +\infty$.

Due to Eq. (4.7), whether $(a^{d-1})^{\cdot}$ increases of decreases with time is determined in full generality by the sign of $\mathcal{V}_{1\text{-loop}}$. In order to discriminate when the universe is in QNSR, the most decisive criterion is the asymptotic behavior of the scale factor, Eq. (4.11), which must satisfy

$$(a^{d-1})^{\cdot} \longrightarrow \mathscr{A}^{d-1}\,, \qquad \text{when} \qquad t \to +\infty\,. \tag{5.4}$$

In all cases (i)–(iv), the numerical simulation confirms the above convergence to a constant, either upward or downward depending on the sign of the potential *i.e.* $n_F - n_B$. The plots in Fig. 2 show the evolutions of $(a^{d-1})^{\cdot}$ as a function of t for the backgrounds (i) and (iv). The curves in models (ii) and (iii) are qualitatively similar to those obtained respectively in cases (i) and (iv).

Solving the system of differential equations makes sense as long as the weak coupling condition is fulfilled, $\phi(t) < 0$, and the supersymmetry breaking scale measured in σ-model frame is small, $\sqrt{G^{dd}(t)} < c$. It turns out that the numerical evolutions of ϕ, $\ln(G^{dd})$ and y_{55} as functions of t present similar features when $c_{\mathcal{G}_1} > 0$ *i.e.* in models (i) and (iii), and when $c_{\mathcal{G}_1} < 0$ *i.e.* in models (ii) and (iv). The only qualitative difference may occur at early times, where y_{55} may oscillate when it is massive, $c_{\mathcal{G}_1} > 0$. The curves are shown in Fig. 3 in cases (i) and (iv), where the cosmic times above which the simulations cannot be trusted are respectively $t_f \simeq 10^{110} M_s^{-1}$ and $t_f \simeq 10^{185} M_s^{-1}$, for $c = 1$. The fact that ϕ, $\ln(G^{dd})$ and y_{55} depend asymptotically linearly on $\ln(tM_s)$ proves that the velocities $\dot{\Phi}$, $\dot{\phi}_\perp$ and $\dot{y}_{55}$ are inversely proportional to cosmic time, *i.e.* that

$$(c_\perp^{\rm dyn}, c_\Phi^{\rm dyn}, c_{55}^{\rm dyn}) \longrightarrow (c_\perp, c_\Phi, c_{55})\,, \quad \text{when} \quad t \to +\infty\,. \tag{5.5}$$

In particular, we can identify from Eq. (4.16) the limit reached by the dynamical quantity

$$J_{\rm dyn} \equiv t\,(\ln G^{dd})^{\cdot} = t\left(\frac{2}{\alpha}\,\dot{\Phi} - \frac{2}{\sqrt{d-1}}\,\dot{\phi}_\perp\right) \longrightarrow J_+ > 0\,, \quad \text{when} \quad t \to +\infty\,. \tag{5.6}$$

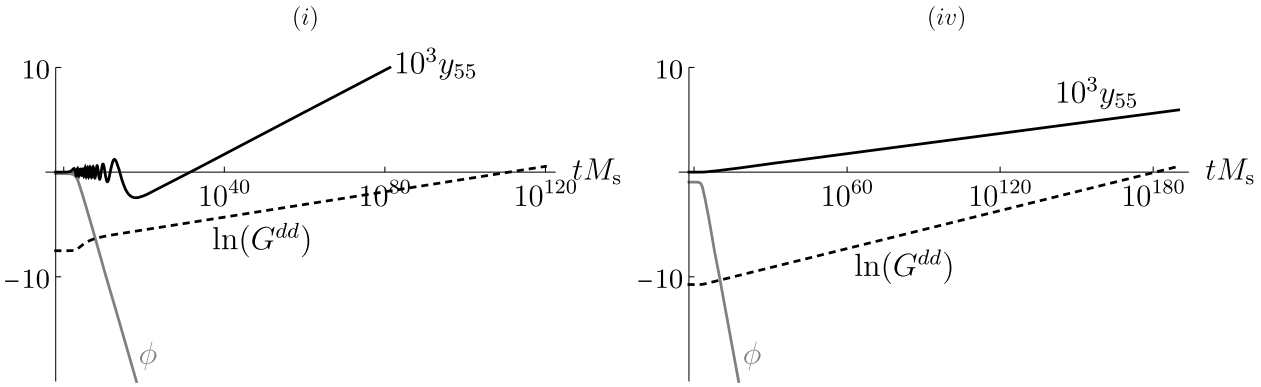

Fig. 3. The behaviors of the dilaton ϕ (gray curves), $\ln(G^{dd})$ (dotted curves) and $10^3 y_{55}$ (black curves) as functions of cosmic time (in logarithmic scale) are asymptotically linear in cases (i) and (iv). The evolutions can be trusted as long as $\phi(t) < 0$ and $\ln\big(G^{dd}(t)\big) < 0$, for $c = 1$. Oscillations of y_{55} may occur at early times when it is massive, $c_{\mathcal{G}_1} > 0$.

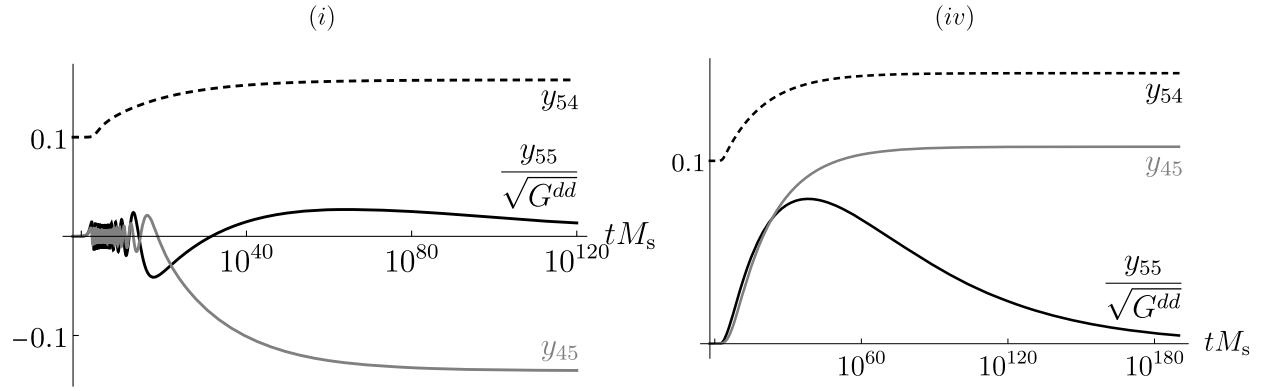

Fig. 4. Convergences of the Wilson lines y_{45} (gray curves) and y_{54} (dotted curves) to constants, and of $y_{55}/\sqrt{G^{dd}}$ to 0, in cases (i) and (iv). Oscillations of y_{45} and y_{55} may occur when they are massive, $c_{\mathcal{G}_1} > 0$.

What remains to be checked are the behaviors of y_{45} and y_{54}, as well as the smallness of all Wilson lines. Fig. 4 shows $y_{45}(t)$, $y_{54}(t)$ and $y_{55}(t)/\sqrt{G^{dd}(t)}$ simulated in model (i) (which is similar to (iii)) and in model (iv) (which is similar to (ii)). As predicted in Sect. 4 when $J_+ > 0$, all curves converge to constants,

$$y_{45} \longrightarrow y_{45}^{(0)}\,, \quad y_{54} \longrightarrow y_{54}^{(0)}\,, \quad \frac{y_{55}}{\sqrt{G^{dd}}} \longrightarrow 0\,, \quad \text{when} \quad t \to +\infty\,, \tag{5.7}$$

while their upper and lower bounds are small, in the sense of Eq. (3.15). Let us stress again that even when $c_{\mathcal{G}_1} < 0$, contrary to common sense, the tachyonic scalars y_{45} and y_{55} do not induce large destabilizations of the backgrounds, when the universe enters the QNSR regime. These remarks complete our numerical validation of the existence of the QNSR $t \to +\infty$, demonstrated in the previous section. Note however that even if the solutions can be trusted all the way until $t_{\rm f}$, the universe enters the QNSR only after a certain duration, as can be seen in all Figs. 2–4. During this transient period, the dynamics is affected by the effective potential, as shown on Figs. 3 and 4. In fact, when $c_{\mathcal{G}_1} > 0$ *i.e.* case (i) and (iii), the Wilson lines y_{45} and y_{55} are massive and oscillate around minima of $\mathcal{V}_{\text{1-loop}}$. It is only when the universe enters the QNSR that the potential is dominated by the canonical kinetic energies of Φ, $\phi_\perp$ and y_{55}, so that not only y_{54} but also y_{45} freeze at arbitrary values, while Φ, $\phi_\perp$ and y_{55} behave logarithmically with cosmic time. On the contrary, when $c_{\mathcal{G}_1} < 0$ *i.e.* case (ii) and (iv), the tachyonic Wilson lines y_{45} and y_{55} do not oscillate during the early transient regime.

Before proceeding, we would like to provide comments on the first constraint appearing in Eq. (4.52), for a QNSR to be reached. As was argued below Eq. (4.55), it is expected to be trivial, a fact that implies $C_{\mathcal{K}}$ to vanish, which we have verified analytically in Sect. 4. In fact, when a QNSR yields $\pm J_\pm > \pm\frac{K_\pm}{d-1} > 0$, the kinetic terms of $y_{d,d+1}$ and $y_{d+1,d}$, as well as all terms subdominant compared to 1 in the parentheses appearing in Eqs (4.36) and (4.40) are all individually dominated by $\mathcal{V}_{1\text{-loop}}$. However, when $\pm\frac{K_\pm}{d-1} > \pm J_\pm > 0$, it is remarkable that the leading contributions of these terms cancel one another, so that $C_{\mathcal{K}} = 0$. To check that this cancellation is actually exact, we have varied the initial conditions of our simulations of the QNSR $t \to +\infty$, for the characteristic point $\left(\frac{c_\perp}{\gamma_c c_\Phi}, \frac{c_{55}}{\gamma_c c_\Phi}\right)$ to explore all of the left crescent in Fig. 1(*a*). This means that the condition for the existence of the QNSR $t \to +\infty$ is $J_+ > 0$, and nothing more.

6. Global attractor mechanisms

The numerical validation of the QNSR $t \to +\infty$ in presence of small Wilson line deformations being established, we would like to consider possible global attractor mechanisms. Our aim is to see whether it is possible to relax, at least in come cases, the constraint of imposing the trajectories to be entirely in the tiny phase space described in the previous sections. It turns out that the kinetic terms in Eq. (3.13) become quadratic in Wilson lines, when $y_{d+1,d+1}$ is identically frozen at the origin. As a result, the action (4.1) is exact in $y_{d,d+1}$ and $y_{d+1,d}$, provided we set $y_{d+1,d+1} \equiv 0$ and use the full 1-loop effective potential,

$$\begin{aligned}\mathcal{V}_{1\text{-loop}} = &\left(n_{\rm F} - n_{\rm B} + (-1)^{\eta^R_{d+1}}\, 8\times 2\right) v_d\, M^d \\ &- (-1)^{\eta^R_{d+1}}\, 8\times 2\, \frac{2M^d}{(2\pi)^{\frac{3d+1}{2}}} \sum_{\tilde m_d} \frac{\cos\left(2\pi(2\tilde m_d+1)\sqrt{2}\, y_{d,d+1}\right)}{|2\tilde m_d+1|^{d+1}}\, F(0) + \cdots\,,\end{aligned} \tag{6.1}$$

where the ellipses stand for the exponentially suppressed contributions we neglect as before. In the following, we use this fact to simulate numerically the 1-loop dynamics of the scale factor a, no-scale modulus Φ and scalar $\phi_\perp$, in the presence of arbitrary Wilson lines deformations $y_{d,d+1}$ and $y_{d+1,d}$ of the initial background.

We will find that the sign of $\mathcal{V}_{1\text{-loop}}$ plays a critical role. Depending on the integer $n_{\rm F} - n_{\rm B}$, the latter can be fixed,

$$\begin{aligned}(-1)^{\eta^R_{d+1}}\,(n_{\rm F}-n_{\rm B}) \geq 0 \quad &\Longrightarrow \quad (-1)^{\eta^R_{d+1}}\mathcal{V}_{1\text{-loop}} \geq 0 \quad \text{for all } y_{d,d+1}\,,\\ (-1)^{\eta^R_{d+1}}\,(n_{\rm F}-n_{\rm B}) \leq -32 \quad &\Longrightarrow \quad (-1)^{\eta^R_{d+1}}\mathcal{V}_{1\text{-loop}} \leq 0 \quad \text{for all } y_{d,d+1}\,,\end{aligned} \tag{6.2}$$

or varying,

$$-31 \leq (-1)^{\eta^R_{d+1}}\,(n_{\rm F}-n_{\rm B}) \leq -1 \quad \Longrightarrow \quad \text{the sign of } \mathcal{V}_{1\text{-loop}} \text{ varies with } y_{d,d+1}\,. \tag{6.3}$$

Note that since $y_{d,d+1}$ is allowed to explore a large range of values during its evolution, there is no need to consider separately the cases η^R_{d+1} even or odd. For instance, in spacetime dimension $d = 4$ we consider from now on, a half-period shift $\sqrt{2}\, y_{45} \to \sqrt{2}\, y_{45} + \frac{1}{2}$ maps into each other backgrounds (i) and (ii) which have $\mathcal{V}_{1\text{-loop}} > 0$ for all y_{45}, or (iii) and (iv) which have $\mathcal{V}_{1\text{-loop}} < 0$ for all y_{45}.

In the simulations, we take as initial conditions $y_{45}(0)$, $y_{54}(0)$, $a(0)$ and $c_{\perp 0} \equiv c_\perp^{\rm dyn}(0)$, $c_{\Phi 0} \equiv c_\Phi^{\rm dyn}(0)$ to be of order 1. This fixes $\dot\phi_\perp(0)$ and $\dot\Phi(0)$, provided $H(0)$ (which we take to be positive)

or equivalently $\tau^{\rm dyn}(0)$ (see Eq. (5.2)) is known. The latter is related to $\Phi(0)$ *via* Friedmann equation at $t=0$, which we write in the following form

$$-\frac{d^2c_{\Phi 0}^2}{2(d-1)(d+2)}\,\frac{\mathcal{P}_0\big(\tau^{\rm dyn}(0)\big)}{a(0)^{2(d-1)}}=\frac{G^{dd}(0)}{4}\,\dot{y}_{45}(0)^2+\frac{G^{dd}(0)}{4}\,\dot{y}_{54}(0)^2 + \mathcal{V}_{\text{1-loop}}\big(\Phi(0),y_{45}(0)\big)\,, \tag{6.4}$$

where $\mathcal{P}_0$ is the degree two polynomial

$$\mathcal{P}_0(\tau)=\tau^2-2\tau+\left(1-\frac{4}{d^2}\right)\left(1+2\alpha^2\,\frac{c_{\perp 0}^2}{c_{\Phi 0}^2}\right). \tag{6.5}$$

We impose the Wilson lines' kinetic terms at $t=0$ to be of the order of $\big|\mathcal{V}_{\text{1-loop}}\big(\Phi(0),y_{45}(0)\big)\big|$. This fixes $\dot{y}_{45}(0)$ and $\dot{y}_{54}(0)$, once we make our choices for $\Phi(0)$ and $\phi_\perp(0)$. The latter is determined *a posteriori* for the numerical simulation to satisfy the conditions of weak string coupling and low supersymmetry breaking scale $M_{(\sigma)}$, for a long period of cosmic time. The last initial data $\Phi(0)$ is equivalent to choosing $\tau^{\rm dyn}(0)$:

- When $\mathcal{V}_{\text{1-loop}}\big(\Phi(0),y_{45}(0)\big)>0$, Eq. (6.4) imposes

$$\left|\frac{c_{\perp 0}}{\gamma_c c_{\Phi 0}}\right|<1 \qquad \text{and} \qquad 1-r_0<\tau^{\rm dyn}(0)<1+r_0\,, \tag{6.6}$$

where r_0 is defined in Eq. (5.3). We have already studied in Sect. 5 the case where $\tau^{\rm dyn}(0)\simeq 1+r_0$, which corresponds to a cosmological evolution starting almost in QNSR $t\to+\infty$. Thus, we will consider the two remaining qualitatively different types of initial conditions (a) and (b), defined as follows:

(a) For $\tau^{\rm dyn}(0)\simeq 1$, the cosmological evolution is generic, in the sense that the initial kinetic energies of Φ, $\phi_\perp$, y_{45} and y_{54} as well as the potential are all of the order of $H(0)^2$.

(b) For $\tau^{\rm dyn}(0)\gtrsim 1-r_0$, the potential and Wilson lines' kinetic energies are small compared to $H(0)^2$. This is clear by looking at Eq. (6.4), whose l.h.s. vanishes in the limit $\tau^{\rm dyn}(0)\underset{>}{\to}1-r_0$. As a result, the motion of the Wilson lines and the effective potential become irrelevant and the cosmological evolution is expected to approach that of the classical theory, with frozen Wilson lines, *i.e.* $(a^{d-1})^{\cdot}\equiv\frac{2dc_{\Phi 0}}{d^2-4}(1-r_0)$ [11].

- When $\mathcal{V}_{\text{1-loop}}\big(\Phi(0),y_{45}(0)\big)<0$, the r.h.s. of Eq. (6.4) can be negative or positive. In the former case, $\tau^{\rm dyn}(0)$ is arbitrary if $\left|\frac{c_{\perp 0}}{\gamma_c c_{\Phi 0}}\right|\geq 1$, while it must satisfy $\tau^{\rm dyn}(0)>1+r_0$ or $\tau^{\rm dyn}(0)<1-r_0$ if $\left|\frac{c_{\perp 0}}{\gamma_c c_{\Phi 0}}\right|<1$. When the r.h.s. of Eq. (6.4) is positive, condition (6.6) applies.

In the models where $\mathcal{V}_{\text{1-loop}}$ is negative for some/all y_{45}, which are illustrated by the backgrounds (iii) or (iv), we find that the numerical simulations yield the following scenario: The universe expands, reaches a maximal size and then collapses into a Big Crunch, unless the initial conditions are tuned so that the whole trajectory sits inside the tiny phase space that yields the ever-expanding QNSR $t\to+\infty$, as described in Sect. 5. Notice that in Ref. [11], where the dynamics of the Wilson lines is not taken into account, the initially expanding cosmological solutions arising when $\mathcal{V}_{\text{1-loop}}<0$ are also either attracted to the QNSR $t\to+\infty$, or lead in the end to a Big Crunch. However, we emphasize again that in this case, the attraction to the QNSR follows from initial conditions chosen in a much larger space, namely $\left|\frac{c_{\perp 0}}{\gamma_c c_{\Phi 0}}\right|<1$, $\tau^{\rm dyn}(0)>1+r_0$. In other words, the dynamics of internal moduli fields provides a severe source of instability for a flat, expanding universe, when the quantum potential can reach negative values.

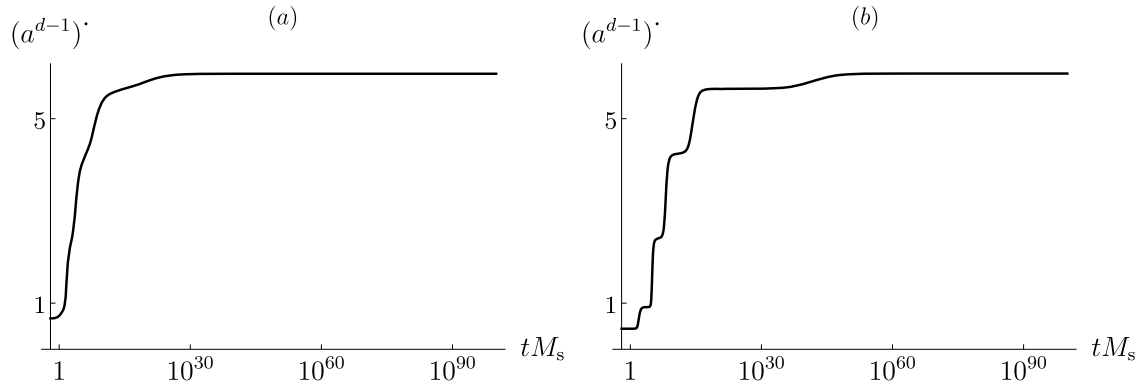

Fig. 5. Convergence of $(a^{d-1})^{\cdot}$ towards its limit $\mathscr{A}^{d-1}$ in model (ii), for initial conditions (a) or (b). Moving from case (a) to (b), a structure of plateaux appears.

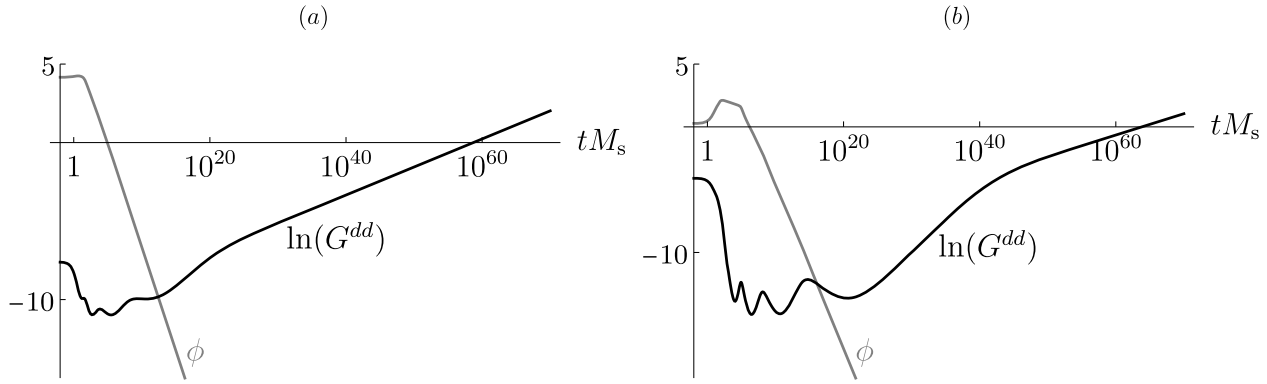

Fig. 6. The behaviors of the dilaton ϕ (gray curves), $\ln(G^{dd})$ (black curves) as functions of cosmic time (in logarithmic scale) are asymptotically linear in model (ii), for initial conditions of type (a) or (b). The evolutions can be trusted as long as $\phi(t) < 0$ and $\ln\big(G^{dd}(t)\big) < 0$, for $c = 1$.

To describe a flat, expanding universe, the numerical simulations show that the models where $\mathcal{V}_{\text{1-loop}} \geq 0$ for all y_{45} are much more appealing, due to a global attraction mechanism to the QNSR $t \to +\infty$. Fig. 5(a) presents the temporal evolution of $(a^{d-1})^{\cdot}$ obtained in Example (ii) which has η_5^R odd, for initial conditions of type (a). The potential being positive, the curve is monotonically increasing, and turns out to converge to a constant, as in Eq. (5.4). Note the existence of several inflection points, which are not numerical artefacts. Actually, by choosing initial values of type (b), a structure of plateaux appears, as shown in Fig. 5(b). The latter are longer and longer and, after a finite number of steps, the last one is endless. Comments on this peculiar dynamics will be given at the end of the section. In any case, this phenomenon is the way the trajectory evolves, in order to converge to the straight line encountered in the extreme initial condition $\tau^{\rm dyn}(0) \underset{>}{\to} 1 - r_0$.

To figure out when string perturbation theory is valid and $M_{(\sigma)} < cM_{\rm s}$, we plot in Fig. 6 the dilaton and $\ln(G^{dd})$ as functions of time. The constraints $\phi(t) < 0$ and $\ln(G^{dd}(t)) < \ln c$ determine the ranges of time $[t_{\rm i}, t_{\rm f}]$ where the simulations can be trusted. In model (ii), with $c = 1$, an example of initial conditions (a) yields $[t_{\rm i}, t_{\rm f}] = [10^5 M_{\rm s}^{-1}, 10^{59} M_{\rm s}^{-1}]$, while for initial values of type (b) we obtain $[t_{\rm i}, t_{\rm f}] = [10^6 M_{\rm s}^{-1}, 10^{65} M_{\rm s}^{-1}]$. In both simulations, the final asymptotes are reached before $t_{\rm f}$. At late times (in logarithmic scale), the linearity of the plots and the positivity of the slope of $\ln(G^{dd})$ show the convergences

$$(c_\perp^{\rm dyn}, c_\Phi^{\rm dyn}) \longrightarrow (c_\perp, c_\Phi) \quad \text{and} \quad J_{\rm dyn} \longrightarrow J_+ > 0\,, \quad \text{when} \quad t \to +\infty\,. \tag{6.7}$$

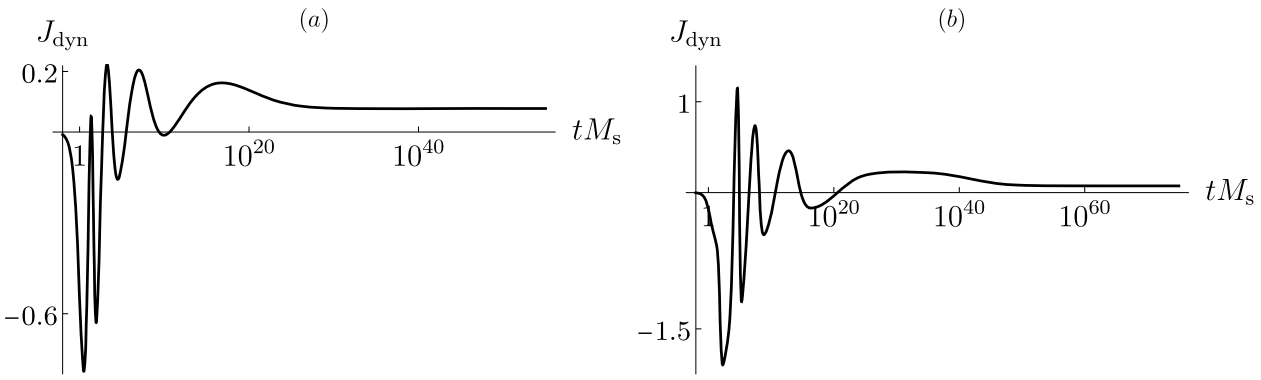

Fig. 7. Convergence of $J_{\rm dyn}$ towards a positive value J_+ in model (ii), for initial conditions of type (a) or (b).

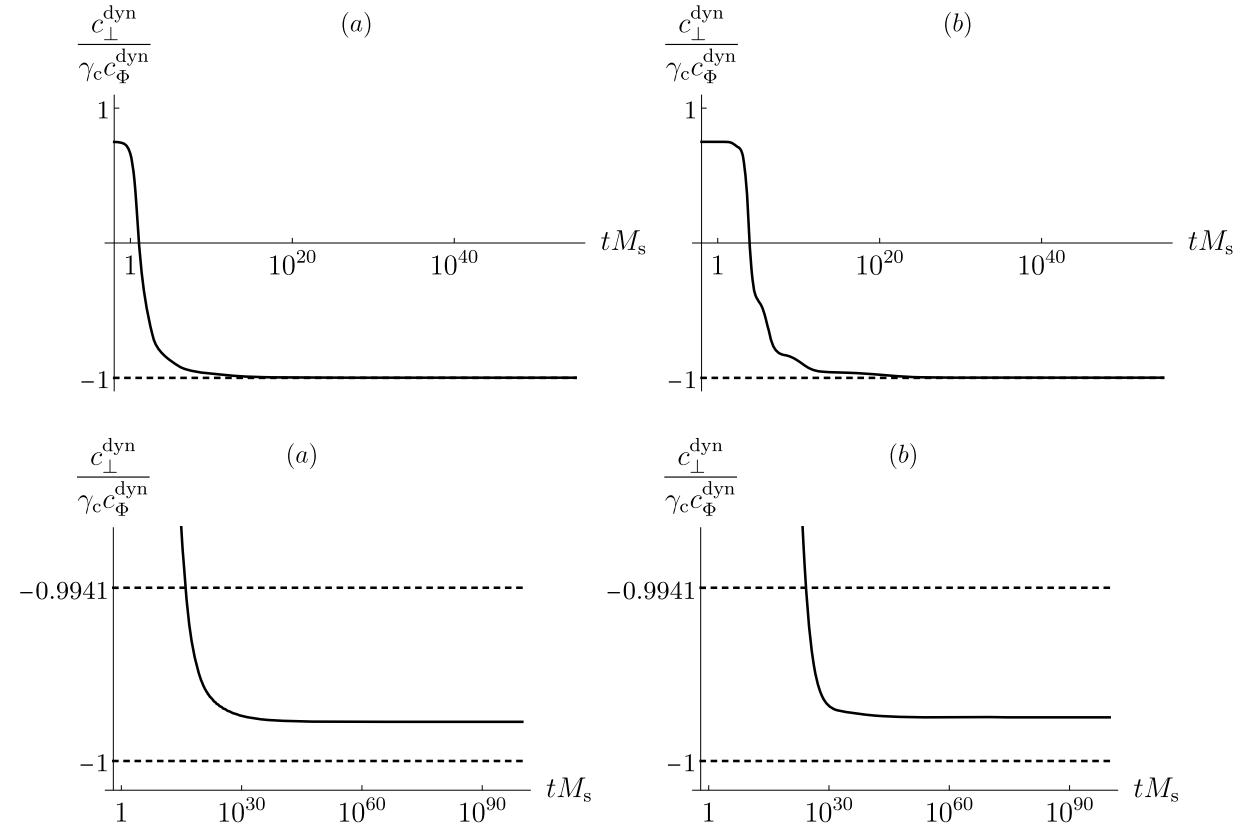

Fig. 8. Attraction of $\frac{c^{\rm dyn}}{\gamma_{\rm c} c^{\rm dyn}}$ towards the tiny range $[-1, \approx -0.9941]$ in model (ii), for initial conditions of type (a) or (b) (upper plots). The ratio stabilizes once it enters the interval (lower plots).

Fig. 7 details the evolution of $J_{\rm dyn}(t)$, which describes a transient regime of damped oscillations between positive and negative values, followed by a stabilization at a positive constant J_+. In view of our analysis in Sect. 4, the sign of J_+ suggests that the trajectory of the point $\left(\frac{c_\perp^{\rm dyn}}{\gamma_{\rm c} c_\Phi^{\rm dyn}}, 0\right)$ enters the left crescent in Fig. 1(a). This is confirmed by the upper plots in Fig. 8. Even if the initial value $\frac{c_{\perp 0}}{\gamma_{\rm c} c_{\Phi 0}}$ is far above the tiny range $[-1, \approx -0.9941]$, the ratio $\frac{c_\perp^{\rm dyn}}{\gamma_{\rm c} c_\Phi^{\rm dyn}}$ is inexorably attracted to this interval, where it stabilizes. The lower plots in Fig. 8 zoom the entrance and freezing of $\frac{c_\perp^{\rm dyn}}{\gamma_{\rm c} c_\Phi^{\rm dyn}}$ in the range.

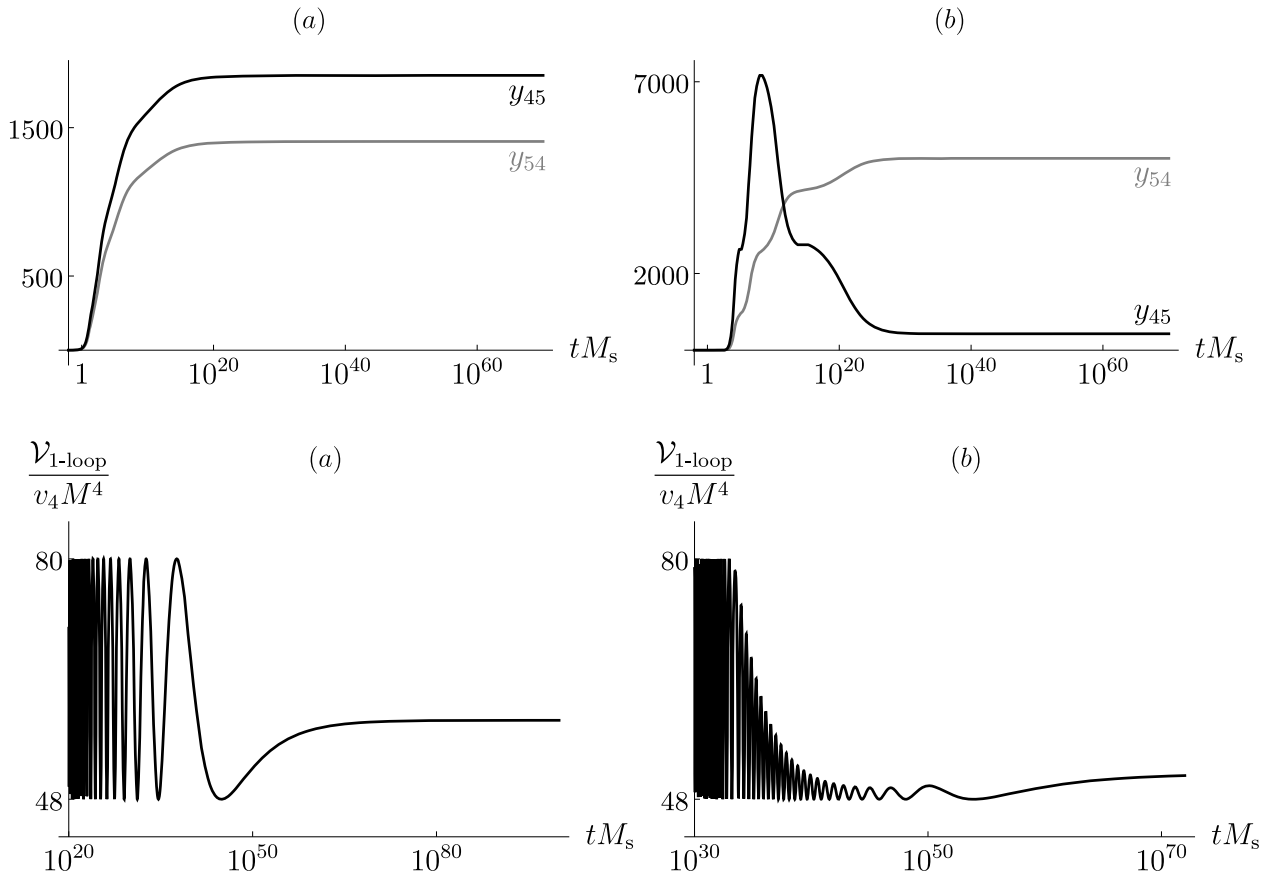

Fig. 9. Convergence of y_{45} (black curves) and y_{54} (gray curves) to their limits $y_{45}^{(0)}$ and $y_{54}^{(0)}$ in model (ii), for initial conditions of type (a) or (b) (upper plots). If the curve $y_{54}(t)$ is always monotonic, that of $y_{45}(t)$ may not be so in case (b). The final value $y_{45}^{(0)}$ is random in case (a), while it is close to a minimum of $\mathcal{V}_{1\text{-loop}}$ in case (b), due to the existence of damped oscillations (lower plots).

The remaining numerical behaviors to be described are those of the Wilson lines. The upper plots in Fig. 9 show the evolutions of $y_{45}(t)$ and $y_{54}(t)$, which converge to constants $y_{45}^{(0)}$, $y_{54}^{(0)}$. Due to Eq. (4.13), which is exact when $y_{55} \equiv 0$, the curve $y_{54}(t)$ is monotonic. This however may not be the case for $y_{45}(t)$, which is not a free field. Actually, accentuating the plateaux structure *i.e.* in case (b), the magnitudes of both velocities $\dot{y}_{45}$, $\dot{y}_{54}$ drop during the transient eras of quasi static $(a^{d-1})^{\cdot}$, and y_{45} may even stop and go backward. Notice that these effects are consistent with the fact that in the limit $\tau^{\rm dyn}(0) \to 1 - r_0$ of the initial conditions, the Wilson lines are expected to become static, $\dot{y}_{45} \equiv \dot{y}_{54} \equiv \overset{>}{0}$.

Since $\sqrt{2}\, y_{45}$ can be very large, its convergence to $\sqrt{2}\, y_{45}^{(0)}$ is more accurately accounted for by the effective potential, which is 1-periodic. As shown in the lower plots in Fig. 9, $\frac{\mathcal{V}_{1\text{-loop}}}{v_d M^d}$ oscillates over time between 80 and 48, which are the values of $n_{\rm F} - n_{\rm B}$ in backgrounds (ii) and (i), when they are not deformed. For initial conditions of type (b), we see that before $\sqrt{2}\, y_{45}$ starts freezing, its kinetic energy is larger than the potential, since $\sqrt{2}\, y_{45}$ evolves quickly, passing easily the maxima and minima. This does not last, however, and $\sqrt{2}\, y_{45}$ ends up oscillating around a minimum, until it stabilizes at a random value close to it. The last fluctuations are those described in Sect. 5, in the massive case in Fig. 4(i). As a result, $\sqrt{2}\, y_{45}^{(0)} \simeq 2k + 1$, where $k \in \mathbb{Z}$, *i.e.* the dynamics has driven spontaneously the system from the initial state (ii) to a slightly deformed background (i). Remarkably, soon after y_{45} is stabilized, we have checked that its

remnant kinetic energy starts again to dominate over the potential, and their ratio even tends to infinity (!). In the notations used at the end of the previous section, the case at hand leads to $\frac{K_+}{d-1} > J_+ > 0$, which is nevertheless compatible with the stability of the cosmological solution. Concerning the modulus y_{54}, its monotonicity and the fact that it is a flat direction of the potential when $y_{55} \equiv 0$ imply its stabilization not to be preceded by oscillations, and its limit value $y_{54}^{(0)}$ to be fully arbitrary. As described for y_{45}, the remnant kinetic energy of y_{54} is greater than $\mathcal{V}_{\text{1-loop}}$ right before and soon after its stabilization process. On the contrary, as seen in the lower plot in Fig. 9(a), the attraction of y_{45} to the neighborhood of a minimum of $\mathcal{V}_{\text{1-loop}}$ turns out to be inefficient for generic initial conditions of type (a). This is due to the fact that as soon as the Wilson line cannot pass the next maximum of the potential, it freezes.

To summarize, the simulated cosmological evolutions in model (ii) are attracted to the QNSR $t \to +\infty$, for both initial conditions (a) and (b). The asymptotic behaviors are reached in a finite number of steps, more visible in case (b), where the dynamics can be described as follows:

• The plateaux present in Fig. 5(b) are characterized by almost constant $(a^{d-1})^{\cdot}$.

• At the beginning of each plateau, the kinetic energy of y_{45} and y_{54} is lower than the effective potential. The motion of these moduli is slowing down, especially for y_{45} whose time-derivative may change sign. As a result, the universe enters an approximate QNSR (see Ref. [11] for the limit case of frozen Wilson lines, which yields a global attraction to the QNSR $t \to +\infty$).

• However, except at the last step, J_{dyn} reaches negative minimum values at the beginning of each plateau, as seen in Fig. 7(b). As a result, the domination of the potential over the Wilson lines' kinetic energies does not last. When the latter become greater than the canonical kinetic energies of Φ and $\phi_\perp$, the approximate QNSR is destabilized and $(a^{d-1})^{\cdot}$ leaves its current plateau.

• We have checked analytically that there is no power-like asymptotic solution that describes an ever-expanding flat universe, dominated by the Wilson lines' kinetic energies.[16] Thus, y_{45} and y_{54} have to release their kinetic energies to the rest of the system, so that the universe is again attracted to an approximate QNSR. In other words, $(a^{d-1})^{\cdot}$ has moved from one plateau to the next.

• This process of climbing steps ends when the system enters a plateau where J_{dyn} is positive. In this case, the Wilson lines' kinetic energies may soon dominate over the effective potential (when $\frac{K_+}{d-1} > J_+$), but never over the canonical kinetic energies of Φ and $\phi_\perp$ (because $J_+ > 0$). As a result, the universe remains in QNSR for good.

For generic initial conditions of type (a), even if the plateaux of $(a^{d-1})^{\cdot}$ and the slowdowns of the Wilson lines are less pronounced, the correspondence between the negative minima of J_{dyn} and the transient dominations of the potential over the kinetic energies of y_{45} and y_{54} remains valid.

7. Conclusion

In this work, we have shown that the notion of QNSR introduced in Ref. [11] for toy models involving only the scale factor a, the supersymmetry breaking scale $M \equiv e^{\alpha\Phi}$ and the dilaton ϕ can be extended to full string theories. This has been done at the 1-loop level in toroidally compactified heterotic string at weak coupling, where a Scherk–Schwarz mechanism involving a

[16] Power-like limit behaviors describing a Big Crunch (or Big Bang) dominated by the Wilson lines' kinetic energies however exist.

single internal direction X^d breaks spontaneously all supersymmetries. The key point is the presence of a bunch of marginal deformations: $\sqrt{G^{dd}}$ and ϕ, which are equivalent to the canonical no-scale modulus Φ and scalar $\phi_\perp$, and the Wilson lines $y_{d\Upsilon}$, y_{id}, $y_{i\Upsilon}$, for $\Upsilon \in \{d+1,\dots,25\}$, $i \in \{d+1,\dots,9\}$. If we have analyzed in great details the dynamics involving the moduli where $\Upsilon = i = d+1$, our results should be more general. In the QNSRs describing an ever-expanding universe or a Big Bang, the kinetic energies of Φ, $\phi_\perp$, $y_{i\Upsilon}$ are expected to dominate over those of $y_{d\Upsilon}$, y_{id} and the effective potential $\mathcal{V}_{1\text{-loop}}$. As a result, the classical no-scale structure is restored at the quantum level during the cosmological evolution of the flat universe.

The existence of the QNSRs is independent of the characteristics of $\mathcal{V}_{1\text{-loop}}$. Denoting the values at $t=0$ of the scale factor and moduli fields as $a(0)$ and $(\Phi(0),\phi(0),y(0))$, the initial time derivatives $(\dot\Phi(0),\dot\phi(0),\dot y(0))$ can always be set in a phase space region for the universe to be attracted to a QNSR. This turns out to be the case whether $\mathcal{V}_{1\text{-loop}}(\Phi(0),\phi(0),y(0))$ is positive, negative or null, as well as maximal, minimal or at a saddle point.

Global effects, however, depend drastically on the sign of $\mathcal{V}_{1\text{-loop}}$. We have "shown numerically" in dimension 4 that when y_{45} and y_{54} vary arbitrarily, while keeping y_{55} frozen at a point of extended light spectrum, the initially growing universes always end in the QNSR $a \to +\infty$, provided $\mathcal{V}_{1\text{-loop}} \geq 0$ for all y_{45}. Allowing all y-deformations to be dynamical, we expect this attraction to be true when the trajectory does not explore regions in moduli space where $\mathcal{V}_{1\text{-loop}} < 0$.[17] As noticed before, this sufficient condition is not necessary, when the initial conditions are tuned in tiny intervals. On the contrary, when an initially growing cosmological evolution does not converge to the QNSR $a \to +\infty$, which requires $\mathcal{V}_{1\text{-loop}}$ to reach negative values, the simulated expansion of the scale factor comes to a halt and the universe eventually collapses. In Ref. [11], such a Big Crunch can be realized in two ways: With the QNSR $a \to 0$ (by applying time reversal on the Big Bang solution), or as an evolution dominated by the no-scale modulus kinetic and potential energies. As noticed in Footnote 16, taking into account the Wilson lines' dynamics, the kinetic energies of the scalars $y_{d\Upsilon}$, y_{id} may also dominate. It would be interesting to extend the analysis of the system to derive an overview of all possible limit behaviors of the solutions and associated attractor mechanisms.

An important consequence of the above remarks is that a flat expanding universe is more naturally described by a model with positive potential, while Big Crunch solutions arise in most cases when the potential is negative. This result is in the spirit of Refs. [12–15], where hot universes are considered, *i.e.* when finite temperature T is switched on in addition to the implementation of the spontaneous breaking of supersymmetry. In this case, when the zero-temperature effective potential is positive, the trajectory of the flat universe at finite T is attracted to an expanding solution satisfying proportionality properties [12,14],

$$\frac{1}{a(t)} \sim \# \frac{M(t)}{M_{\rm s}} \sim \# \frac{T(t)}{M_{\rm s}} \sim \# e^{2\alpha^2\phi(t)} \sim \frac{\#}{(tM_{\rm s})^{\frac{2}{d}}} \,. \tag{7.1}$$

The above asymptotic evolution is said to be "radiation-like", due to the state equation $\rho_{\rm tot} \sim (d-1)P_{\rm tot}$ satisfied by the total energy density $\rho_{\rm tot}$ and pressure $P_{\rm tot}$ present in the universe. The latter take into account the thermal contributions derived from the 1-loop free energy, as well as the kinetic energy of the no-scale modulus Φ. On the contrary, when the zero-temperature 1-loop potential is negative, the universe at finite T collapses into a Big Crunch, where temperature effects tend to be screened, $T/M \to 0$.

[17] In any case, the evolutions along which $\mathcal{V}_{1\text{-loop}} \geq 0$ are ever-expanding, due to the monotonicity of $(a^{d-1})^{\cdot} > 0$ (see Eq. (4.7)), which forbids H to vanish.

Acknowledgements

We are grateful to Steve Abel, Carlo Angelantonj, Keith Dienes, Emilian Dudas, Sergio Ferrara, Claude Fleming, Lucien Heurtier, Alexandros Kahagias and Costas Kounnas for fruitful discussions. The work of H.P. is partially supported by the Royal Society International Cost Share Award. H.P. thanks the C.E.R.N. Theoretical Physics Department, the Simons Center for Geometry and Physics, and the IPPP in Durham University for hospitality.

Appendix A. Moduli dependence of the effective potential

For the present work to be self-content, let us review how discrete deformations responsible for the total spontaneous breaking of supersymmetry, as well as continuous Wilson lines, can be introduced in maximally supersymmetric heterotic string. Our final goal is to derive an expression of the effective potential valid when the supersymmetry breaking scale is low, compared to the string scale $M_{\rm s}$.

A.1. The deformations

In the 1-loop partition function, the relevant deformed conformal block to be considered turns out to be

$$\mathcal{Z}[\vec{a},\vec{b},G,B,\vec{Y}]=\frac{\sqrt{\det G}}{\tau_2^{\frac{10-d}{2}}}\sum_{\substack{\tilde m_d,\dots,\tilde m_9\\ n_d,\dots,n_9}} e^{-\frac{\pi}{\tau_2}(\tilde m_I+n_I\bar\tau)(G+B)_{IJ}(\tilde m_J+n_J\tau)}$$
$$\times\, e^{i\pi n_I\vec Y_I\cdot(\vec b-\tilde m_J\vec Y_J)}\prod_{\mathcal{A}=1}^{4}\theta\begin{bmatrix}a^L_{\mathcal{A}}-2n_IY^L_{I\mathcal{A}}\\ b^L_{\mathcal{A}}-2\tilde m_IY^L_{I\mathcal{A}}\end{bmatrix}(\tau)\prod_{\mathcal{J}=10}^{25}\bar\theta\begin{bmatrix}a^R_{\mathcal{J}}-2n_IY^R_{I\mathcal{J}}\\ b^R_{\mathcal{J}}-2\tilde m_IY^R_{I\mathcal{J}}\end{bmatrix}(\bar\tau)\,, \tag{A.1}$$

where sums over repeated indices $I,J\in\{d,\dots,9\}$ are understood. Our notations are as follows:

• The first line is the contribution of the zero modes of the $10-d$ bosonic coordinates compactified on a torus, whose metric and antisymmetric tensor are G_{IJ}, B_{IJ}, $I,J\in\{d,\dots,9\}$. Written in Lagrangian form, this expression involves a discrete sum over the integers $\tilde m_I$ and winding numbers n_I.

• In the second line, the holomorphic Jacobi θ functions arise from the partition functions θ/η of the 4 complex left-moving fermions of the superstring, where η is the Dedekind function.[18] In their brackets, $a^L_{\mathcal{A}}$ and $b^L_{\mathcal{A}}$, $\mathcal{A}\in\{1,\dots,4\}$, define their boundary conditions before deformation, along the cycles $z\to z+1$ and $z\to z+\tau$ of the genus-1 worldsheet parameterized by z and of Teichmüller parameter $\tau\equiv\tau_1+i\tau_2$. Similarly, the antiholomorphic $\bar\theta$ functions arise from the contributions $\bar\theta/\bar\eta$ associated with the 16 complex right-moving fermions of the bosonic string, with boundary conditions before deformation determined by $a^R_{\mathcal{J}}$ and $b^R_{\mathcal{J}}$, $\mathcal{J}\in\{10,\dots,25\}$. In the derivation to come, $\vec a\equiv(\vec a^{\,L},\vec a^{\,R})$ and $\vec b\equiv(\vec b^{\,L},\vec b^{\,R})$ can have arbitrary real entries. However, modular invariance of the entire model imposes constraints on the set of values they can take. For instance, in our maximally supersymmetric case of interest, we have $a^L_1=\cdots=a^L_4$ and $b^L_1=\cdots=b^L_4$. However, we will keep the 4-components of $\vec a^{\,L}$ and $\vec b^{\,L}$ independent, since this

[18] Our conventions for θ and η functions can be found in Ref. [19].

can be useful when dealing with non-maximally supersymmetric models. (See Ref. [8] for an example in 4 dimensions realizing the $\mathcal{N}=2\to 0$ spontaneous breaking.)

• Beside the torus moduli $(G+B)_{IJ}$, we introduce deformations of the left- and right-moving (super)-conformal theories,

$$Y^L_{I\mathcal{A}}\,,\ Y^R_{I\mathcal{J}}\,,\quad I\in\{d,\dots,9\}\,,\ \mathcal{A}\in\{1,\dots,4\}\,,\ \mathcal{J}\in\{10,\dots,25\}\,. \tag{A.2}$$

For the holomorphic supercurrent to be preserved, the left-moving ones are quantized [2], $Y^L_{I\mathcal{A}}\in\mathbb{Z}$. Thus, different choices of $Y^L_{I\mathcal{A}}$'s yield different models. On the contrary, the right-moving $Y^R_{I\mathcal{J}}$'s are arbitrary marginal deformations. In each given model, they are moduli fields that can be interpreted as Wilson lines along T^{10-d} of a rank 16 gauge group $\mathcal{G}_{16}$.

• In the second line of Eq. (A.1), the overall phase uses the following definition of scalar product: For two vectors $\vec v\equiv(\vec v^{\,L},\vec v^{\,R})$ and $\vec w\equiv(\vec w^{\,L},\vec w^{\,R})$ in $\mathbb{R}^{4,16}$, we write

$$\vec v\cdot\vec w=\vec v^{\,L}\cdot\vec w^{\,L}-\vec v^{\,R}\cdot\vec w^{\,R}=\sum_{\mathcal{A}=1}^{4}v^L_{\mathcal{A}}w^L_{\mathcal{A}}-\sum_{\mathcal{J}=10}^{25}v^R_{\mathcal{J}}w^R_{\mathcal{J}}\,. \tag{A.3}$$

The phase is introduced for the following modular transformations of the entire conformal block to be independent of $\vec Y_I\equiv(\vec Y^{\,L}_I,\vec Y^{\,R}_I)$:

$$\begin{aligned}
\tau\to-\frac{1}{\tau}\iff&\begin{cases}(n_I,\tilde m_I)\to(n_I,\tilde m_I)\mathcal{S}\\ (a^L_{\mathcal{A}},b^L_{\mathcal{A}})\to(a^L_{\mathcal{A}},b^L_{\mathcal{A}})\mathcal{S}\,,\ (a^R_{\mathcal{J}},b^R_{\mathcal{J}})\to(a^R_{\mathcal{J}},b^R_{\mathcal{J}})\mathcal{S}\end{cases}\\
\tau\to\tau+1\iff&\begin{cases}(n_I,\tilde m_I)\to(n_I,\tilde m_I)\mathcal{T}\\ (a^L_{\mathcal{A}},b^L_{\mathcal{A}})\to(a^L_{\mathcal{A}},b^L_{\mathcal{A}}+a^L_{\mathcal{A}}-1)\,,\ (a^R_{\mathcal{J}},b^R_{\mathcal{J}})\to(a^R_{\mathcal{J}},b^R_{\mathcal{J}}+a^R_{\mathcal{J}}-1)\end{cases}\\
&\text{where}\qquad\mathcal{S}=\begin{pmatrix}0&-1\\1&0\end{pmatrix}\,,\qquad\mathcal{T}=\begin{pmatrix}1&1\\0&1\end{pmatrix}\,.
\end{aligned} \tag{A.4}$$

Thus, any 1-loop partition function, which is modular invariant for $\vec Y_I=\vec 0$, $I\in\{d,\dots,9\}$, remains consistent when arbitrary Y-deformations are switched on.

Another way to write Eq. (A.1) clarifies the spectrum interpretation of the conformal block, at the cost of obscuring the modular transformation $\tau\to-1/\tau$. It is obtained by inserting in $\mathcal{Z}[\vec a,\vec b,G,B,\vec Y]$ the definition of the θ functions in terms of a sum over $N\in\mathbb{Z}$,

$$\theta[{}^a_b](\tau)=\sum_N q^{\frac12(N-\frac a2)^2}e^{-bi\pi(N-\frac a2)}\,,\quad\text{where}\quad q\equiv e^{2i\pi\tau}\,, \tag{A.5}$$

and applying a Poisson summation over the integers $\tilde m_d,\dots,\tilde m_9$. The result is the Hamiltonian form [20],

$$\begin{aligned}
\mathcal{Z}[\vec a,\vec b,G,B,\vec Y]=&\sum_{\substack{m_d,\dots,m_9\\ n_d,\dots,n_9}}\sum_{\vec N}e^{-i\pi\vec b\cdot\vec Q}\,q^{\frac14\left[P^L_IG^{IJ}P^L_J+2(\vec Q^{\,L}+n_I\vec Y^{\,L}_I)^2\right]}\\
&\times\bar q^{\frac14\left[P^R_IG^{IJ}P^R_J+2(\vec Q^{\,R}+n_I\vec Y^{\,R}_I)^2\right]}\,,
\end{aligned} \tag{A.6}$$

where we have defined $\vec N\equiv(\vec N^{\,L},\vec N^{\,R})$, $G^{IJ}\equiv(G^{-1})_{IJ}$ and

$$P^L_I=m_I-\vec Y\cdot\vec Q-\frac12\vec Y_I\cdot n_J\vec Y_J+(B+G)_{IJ}n_J\,,\quad I\in\{d,\dots,9\}\,,$$

$$P_I^R = m_I - \vec{Y}\cdot\vec{Q} - \frac{1}{2}\,\vec{Y}_I\cdot n_J\vec{Y}_J + (B-G)_{IJ}n_J\,,$$
$$\vec{Q} \equiv (\vec{Q}^L, \vec{Q}^R) = \vec{N} - \frac{\vec{a}}{2}\,. \tag{A.7}$$

The genus-1 partition function of a model takes the following form

$$Z[G,B,\vec{Y}] = \frac{1}{\tau_2^{\frac{d-2}{2}}}\,\frac{1}{\eta^{12}\,\bar\eta^{24}}\,\frac{1}{|\Xi|}\sum_{\vec a,\vec b\in\Xi} \mathcal{C}\big[{}^{\vec a}_{\vec b}\big]\mathcal{Z}[\vec a,\vec b,G,B,\vec Y]\,, \tag{A.8}$$

where Ξ is the set of spin structures $\vec a$ and $\vec b$ take, $|\Xi|$ is the cardinal of Ξ, and $\mathcal{C}\big[{}^{\vec a}_{\vec b}\big]$ are complex numbers of modulus 1, so that $Z[G,B,\vec{\mathbf{0}}]$ is modular invariant. Expanding

$$\frac{1}{\eta^{12}\,\bar\eta^{24}} = \frac{1}{q^{\frac12}\,\bar q}\sum_{\ell_L,\ell_R\geq 0} c^L_{\ell_L}c^R_{\ell_R}\,q^{\ell_L}\,\bar q^{\ell_R}, \tag{A.9}$$

we obtain

$$Z[G,B,\vec Y] = \frac{1}{\tau_2^{\frac{d-2}{2}}}\,\frac{1}{|\Xi|}\sum_{\vec a,\vec b\in\Xi}\sum_{\vec N}\mathcal{C}\big[{}^{\vec a}_{\vec b}\big]e^{-i\pi\vec b\cdot\vec Q}\sum_{\ell_L,\ell_R\geq 0} c^L_{\ell_L}c^R_{\ell_R}\sum_{\substack{m_d,\dots,m_9\\ n_d,\dots,n_9}} q^{\frac14 M_L^2/M_{\rm s}^2}\,\bar q^{\frac14 M_R^2/M_{\rm s}^2}, \tag{A.10}$$

in terms of left- and right-moving squared masses

$$M_L^2 = M_{\rm s}^2\Big[P_I G^{IJ}P_J + 2(\vec Q^L + n_I\vec Y_I^L)^2 + 4\ell_L - 2\Big],$$
$$M_R^2 = M_{\rm s}^2\Big[\bar P_I G^{IJ}\bar P_J + 2(\vec Q^R + n_I\vec Y_I^R)^2 + 4\ell_R - 4\Big]. \tag{A.11}$$

In Eq. (A.10), the sum over $\vec b\in\Xi$ divided by $|\Xi|$ implements the generalized GSO projection. Since

$$q^{\frac14 M_L^2/M_{\rm s}^2}\,\bar q^{\frac14 M_R^2/M_{\rm s}^2} = e^{2i\pi\tau_1\frac{M_L^2-M_R^2}{4M_{\rm s}^2}}\;e^{-\pi\tau_2\frac{M_L^2+M_R^2}{2M_{\rm s}^2}}\,, \tag{A.12}$$

invariance under $\tau_1\to\tau_1+1$ implies

$$\frac{M_L^2-M_R^2}{4M_{\rm s}^2} \equiv m_I n_I + \frac12\big(\vec Q^2+1\big) + \ell_L - \ell_R \in \mathbb{Z}, \tag{A.13}$$

for all states that survive the GSO projection. Among them, the physical ones are those which contribute to the integral over $\tau_1\in[-\frac12,\frac12]$ *i.e.* whose squared masses satisfy $M^2 = M_L^2 = M_R^2$.

A.2. The $SO(32)$ and $E_8\times E_8'$ heterotic string

As a warm up, let us recover the massless spectrum of the $SO(32)$ and $E_8\times E_8$ heterotic string compactified on T^{10-d}. In the former case, the partition function is obtained with

$$\Xi = \big\{(4,16)\text{-tuples } (a,\dots,a;\gamma,\dots,\gamma)\,,\ \text{where } a,\gamma\in\mathbb{Z}_2\big\} \implies |\Xi| = 2^2\,,$$
$$\mathcal{C}[{}^{a;\gamma}_{b\,;\delta}] = (-1)^{a+b+ab}\,,$$
$$\vec Y_I^L = \vec 0\,,\ \vec Y_I^R = \vec 0\,,\quad I\in\{d,\dots,9\}\,. \tag{A.14}$$

The lightest physical states have, on the left-moving side, $\ell_L = 0$ and $P_I^L = 0$, $I \in \{d, \dots, 9\}$. The sector $a = 0$ yields spacetime bosons, whose charges $\vec{Q}^L$ are the weights of the $\mathbf{8_v}$ vectorial representation of the $SO(8)$ affine Lie algebra, while $a = 1$ leads to fermions in the $\mathbf{8_s}$ spinorial representation. All are massless. On the right-moving side, this implies $\gamma = 0$. Moreover, at oscillator level $\ell_R = 1$, we have $P_I^R = 0$, $I \in \{d, \dots, 9\}$, and $\vec{Q}^R = \vec{0}$, corresponding to $c_1^R = 24$ modes. For $\ell_R = 0$, the charges $\vec{Q}^R$ are either the roots of $\mathcal{G}_{16} = SO(32)$ with $P_I^R = 0$, $I \in \{d, \dots, 9\}$, or $\vec{Q}^R = \vec{0}$ with $\frac{1}{2} P_I^R G^{IJ} P_J^R = 2$. In the latter case, the modes have charges equal to the roots of a gauge group $\mathcal{G}_{10-d}$ of rank $10 - d$. Writing $24 = (d-2) + (10-d) + 16$, the massless states are organized as follows,

$$(\mathbf{8_v} \oplus \mathbf{8_s}) \otimes \big([d-2] \oplus \mathrm{Adj}_{\mathcal{G}_{10-d}} \oplus \mathrm{Adj}_{\mathcal{G}_{16}}\big), \tag{A.15}$$

corresponding to a supergravity multiplet in d dimensions, coupled to a vector multiplet in the adjoint representation of $\mathcal{G}_{10-d} \times \mathcal{G}_{16}$.

The 1-loop partition function of the $E_8 \times E_8'$ heterotic strings is realized with

$$\begin{aligned}
&\Xi = \big\{(4, 8+8)\text{-tuples } (a, \dots, a; \gamma, \dots, \gamma, \gamma', \dots, \gamma')\,, \text{ where } a, \gamma, \gamma' \in \mathbb{Z}_2\big\} \Longrightarrow \\
&|\Xi| = 2^3\,, \\
&\mathcal{C}[^{a;\gamma,\gamma'}_{b\,;\delta,\,\delta'}] = (-1)^{a+b+ab}\,, \\
&\vec{Y}_I^L = \vec{0}\,,\ \vec{Y}_I^R = \vec{0}\,, \quad I \in \{d, \dots, 9\}\,.
\end{aligned} \tag{A.16}$$

The left-moving side of the lightest physical states is identical to that encountered in the $SO(32)$ case. It is massless, which implies $(\gamma, \gamma') \neq (1, 1)$ on the right-moving side. At oscillator level $\ell_R = 1$, there are again $c_1^R = 24$ modes with $P_I^R = 0$, $I \in \{d, \dots, 9\}$, and $\vec{Q}^R = \vec{0}$ (implying $(\gamma, \gamma') = (0, 0)$). For $\ell_R = 0$, the charges $\vec{Q}^R$ in the sector $(\gamma, \gamma) = (0, 0)$ are either the roots of $SO(16) \times SO(16)'$ with $P_I^R = 0$, $I \in \{d, \dots, 9\}$, or $\vec{Q}^R = \vec{0}$ with $\frac{1}{2} P_I^R G^{IJ} P_J^R = 2$, corresponding to states whose charges are the roots of a gauge group $\mathcal{G}_{10-d}$. For $(\gamma, \gamma') = (1, 0)$ or $(0, 1)$, $\vec{Q}^R$ is a weight of the spinorial representation of $SO(16)$ or $SO(16)'$ with $P_I^R = 0$, $I \in \{d, \dots, 9\}$. Noticing that the adjoint of E_8 can be decomposed into the adjoint plus spinorial representation of $SO(16)$, $[248]_{E_8} = [120]_{SO(16)} \oplus [128]_{SO(16)}$, the massless spectrum is given in Eq. (A.15), with $\mathcal{G}_{16} = E_8 \times E_8'$.

A.3. Spontaneous supersymmetry breaking and Wilson lines

The spontaneous breaking of all supersymmetries can be realized by a suitable choice of discrete left-moving deformations. For instance, for a stringy Scherk–Schwarz [2,3] mechanism implemented along a single internal direction X^d, we can take

$$Y_{I\mathcal{A}}^L = \delta_{Id}\, \delta_{\mathcal{A}1}\,,\ Y_{I\mathcal{J}}^R \text{ arbitrary}\,, \quad I \in \{d, \dots, 9\}\,,\ \mathcal{A} \in \{1, \dots, 4\}\,,\ \mathcal{J} \in \{10, \dots, 25\}\,, \tag{A.17}$$

in terms of which the conformal block in Eq. (A.1) becomes

$$\frac{\sqrt{\det G}}{\tau_2^{\frac{10-d}{2}}} \sum_{\substack{\tilde m_d,\dots,\tilde m_9\\ n_d,\dots,n_9}} e^{-\frac{\pi}{\tau_2}(\tilde m_I+n_I\bar\tau)(G+B)_{IJ}(\tilde m+n_I\tau)}\, e^{-i\pi(\tilde m_d a_1^L - n_d b_1^L+\tilde m_d n_d)}$$

$$\times\, e^{-i\pi n_I \vec Y_I^R\cdot(\vec b^R-\tilde m_J\vec Y_J^R)} \prod_{\mathcal{A}=1}^{4}\theta\begin{bmatrix}a_{\mathcal{A}}^L\\ b_{\mathcal{A}}^L\end{bmatrix}(\tau)\prod_{\mathcal{J}=10}^{25}\bar\theta\begin{bmatrix}a_{\mathcal{J}}^R-2n_I Y_{I\mathcal{J}}^R\\ b_{\mathcal{J}}^R-2\tilde m_I Y_{I\mathcal{J}}^R\end{bmatrix}(\bar\tau)\,. \qquad (A.18)$$

Compared to $\mathcal{Z}[\vec a,\vec b,G,B,(\vec{\mathbf{0}}^L,\vec Y^R)]$, a pure phase appears in the first line. Consistently, the latter is invariant under the modular transformations (A.4). The key point is that it depends on a_1^L, which determines the Neveu–Schwarz ($a_1^L=0$) or Ramond ($a_1^L=1$) boundary condition of the light cone worldsheet fermions ψ^2,ψ^3, *i.e.* the bosonic or fermionic nature of the states. By Poisson summation, the momentum along the direction X^d being shifted by $a_1^L/2$, the boson/fermion degeneracy is lifted.

To see how this works explicitly, we consider the Hamiltonian form given in Eq. (A.6). It is convenient to write the latter using redefined internal metric, antisymmetric tensor and Wilson lines,

$$(G'+B')_{IJ}=\begin{pmatrix}4(G+B)_{dd} & 2(G+B)_{dj}\\ 2(G+B)_{id} & (G+B)_{ij}\end{pmatrix},$$
$$\vec Y_d'^R=2\vec Y_d^R\,,\ \vec Y_i'^R=\vec Y_i^R\,,\ \ i,j\in\{d+1,\dots,9\}\,, \qquad (A.19)$$

as well as new momenta, winding numbers and indices N''s,

$$m_d'=2(m_d-N_1^L)+a_1^L-n_d\,,\ m_i'=m_i\,,\quad i\in\{d+1,\dots,9\}$$
$$n_d'=\frac{n_d}{2}\,,\ n_i'=n_i\,,$$
$$N_1'^L=N_1^L+n_d\,,\ N_{\mathcal{A}}'^L=N_{\mathcal{A}}^L\,,\ N_{\mathcal{J}}'^R=N_{\mathcal{J}}^R\,,\quad \mathcal{A}\in\{2,3,4\}\,,\ \mathcal{J}\in\{10,\dots,25\}\,, \qquad (A.20)$$

where $n_d'\in\mathbb{Z}\cup(\mathbb{Z}+\frac12)$. Given the above notations, we set

$$P_I'^L=m_I'+\vec Y_I'^R\cdot\vec Q'^R+\frac12\vec Y_I'^R\cdot n_J'\vec Y_J'^R+(B'+G')_{IJ}n_J'\,,\quad I\in\{d,\dots,9\}\,,$$
$$P_I'^R=m_I'+\vec Y_I'^R\cdot\vec Q'^R+\frac12\vec Y_I'^R\cdot n_J'\vec Y_J'^R+(B'-G')_{IJ}n_J'\,,$$
$$\vec Q'\equiv(\vec Q'^L,\vec Q'^R)=\vec N'-\frac{\vec a}{2}\,, \qquad (A.21)$$

in terms of which the conformal block (A.6) becomes

$$\sum_{\substack{m_d\\ n_d}} e^{2i\pi b_1^L n_d'}\sum_{\substack{m_{d+1}',\dots,m_9'\\ n_{d+1}',\dots,n_9'}}\sum_{\vec N'} e^{-i\pi\vec b\cdot\vec Q'}\, q^{\frac14\left[P_I'^L G'^{IJ}P_J'^L+2(\vec Q'^L)^2\right]}\,\bar q^{\frac14\left[P_I'^R G'^{IJ}P_J'^R+2(\vec Q'^R+n_I'\vec Y_I'^R)^2\right]}. \qquad (A.22)$$

As a result, the partition function takes the suggestive form

$$Z'[G',B',\vec{Y}'^R]=\frac{1}{\tau_2^{\frac{d-2}{2}}}\frac{1}{|\Xi|}\sum_{\vec{a},\vec{b}\in\Xi}\sum_{\vec{N}'}\mathcal{C}\left[\begin{smallmatrix}\vec{a}\\ \vec{b}\end{smallmatrix}\right]e^{-i\pi\vec{b}\cdot\vec{Q}'}\sum_{\ell_L,\ell_R\geq 0}c^L_{\ell_L}c^R_{\ell_R}$$
$$\times\sum_{n'_d\in\mathbb{Z}\cup(\mathbb{Z}+\frac{1}{2})}e^{2i\pi b^L_1 n'_d}\,\delta_{a^L_1,m'_d-2n'_d \bmod 2}\sum_{\substack{m'_d,\dots,m'_9\\ n'_{d+1},\dots,n'_9}}q^{\frac{1}{4}M'^2_L/M^2_{\rm s}}\,\bar{q}^{\frac{1}{4}M'^2_R/M^2_{\rm s}}\,, \tag{A.23}$$

where the left- and right-masses satisfy

$$M'^2_L=M^2_{\rm s}\left[P'^L_I G'^{IJ}P'^L_J+2(\vec{Q}'^L)^2+4\ell_L-2\right],$$
$$M'^2_R=M^2_{\rm s}\left[P'^R_I G'^{IJ}P'^R_J+2(\vec{Q}'^R+n'_I\vec{Y}'^R_I)^2+4\ell_R-4\right]. \tag{A.24}$$

Comparing $Z'[G',B',\vec{Y}'^R]$ with the supersymmetric partition function $Z[G,B,(\vec{\mathbf{0}}^L,\vec{Y}^R)]$, we observe three modifications:

- The exchange of the moduli fields, as shown in Eq (A.19).
- The winding number n'_d along the Scherk–Schwarz breaking direction can be integer or half-integer. In the latter case, the GSO-projection is reversed.
- The fermionic number a^L_1 is restricted to be equal to the parity of $m'_d-2n'_d$, which shows that there is no more boson/fermion degeneracy.

Note however that when the compact direction X^d is large compared to the string scale, and the right-moving Wilson lines are small compared to $\sqrt{G'^{dd}}$, the states lighter than the KK mass $M'_{(\sigma)}=M_{\rm s}\sqrt{G'^{dd}}$ have vanishing momentum and winding numbers, $m'_d=n'_d=0$. Therefore, they are bosons, $a^L_1=0$, while their superpartners, $m'_d=1$, $n'_d=0$, acquire a KK mass $M'_{(\sigma)}$ identified with the supersymmetry breaking scale. For light fermions to exist, we consider in the following more general patterns of supersymmetry breaking.

A.4. Supersymmetry breaking, discrete and continuous Wilson lines

In the setup described in the previous section, when the supersymmetry breaking scale $M'_{(\sigma)}=M_{\rm s}\sqrt{G'^{dd}}$ is low compared to the string scale $M_{\rm s}$, one way to have fermions lighter than $M'_{(\sigma)}$ is to introduce large Y-deformations. For this purpose, we consider left- and right-moving discrete Wilson lines along the direction X^d,

$$Y^L_{I\mathcal{A}}=\delta_{Id}\,\delta_{\mathcal{A}1}\,,$$
$$Y^R_{I\mathcal{J}}=\delta_{Id}\,\eta^R_{\mathcal{J}}+y^R_{I\mathcal{J}}\,,\quad I\in\{d,\dots,9\}\,,\ \mathcal{A}\in\{1,\dots,4\}\,,\ \mathcal{J}\in\{10,\dots,25\}\,,$$
$$\text{where}\quad \vec{\eta}^R\cdot a^R\in\mathbb{Z}\,,\quad y^R_{\mathcal{J}}\ \text{arbitrary}\,. \tag{A.25}$$

In the above notations, $\vec{\eta}^R$ can be interpreted as a constant background, while $\vec{y}^R$ plays the role of continuous Wilson lines. Using properties of the θ functions,[19] the conformal block (A.1) becomes

[19] We use the fact that $\vec{\eta}^R$ has integer entries. More specifically, in a consistent model, the components of $\vec{a}^R$ are of the form $a^R_{\mathcal{J}}=k/\chi_{\mathcal{J}}$, $\mathcal{J}\in\{10,\dots,25\}$, where $\chi_{\mathcal{J}}\in\mathbb{N}^*$ and k spans the set $\{0,\dots,\chi_{\mathcal{J}}-1\}$. Thus, $\eta^R_{\mathcal{J}}\in\chi_{\mathcal{J}}\mathbb{Z}$.

$$\frac{\sqrt{\det G}}{\tau_2^{\frac{10-d}{2}}} \sum_{\substack{\tilde m_d,\dots,\tilde m_9\\ n_d,\dots,n_9}} e^{-\frac{\pi}{\tau_2}(\tilde m_I+n_I\bar\tau)(G+B)_{IJ}(\tilde m+n_I\tau)}\, e^{i\pi\vec\eta^R\cdot\vec y_i^R(n_d\tilde m_i-n_i\tilde m_d)}$$
$$\times\, e^{-i\pi\left[\tilde m_d(a_1^L-\eta^R\cdot\vec a^R)-n_d(b_1^L-\eta^R\cdot\vec b^R)+\tilde m_d n_d(1-(\vec\eta^R)^2)\right]}$$
$$\times\, e^{-i\pi n_I\vec y_I^R\cdot(\vec b^R-\tilde m_J\vec y_J^R)}\prod_{\mathcal A=1}^{4}\theta\begin{bmatrix}a_{\mathcal A}^L\\ b_{\mathcal A}^L\end{bmatrix}(\tau)\prod_{\mathcal J=10}^{25}\bar\theta\begin{bmatrix}a_{\mathcal J}^R-2n_I y_{I\mathcal J}^R\\ b_{\mathcal J}^R-2\tilde m_I y_{I\mathcal J}^R\end{bmatrix}(\bar\tau)\,, \tag{A.26}$$

where sums over repeated indices $i\in\{d+1,\dots,9\}$ are understood. The phase in the second line generalizes that found in Eq. (A.18), and will be shown to yield a new pattern of spontaneous breaking of supersymmetry in the light spectrum. In the first line, another phase, which is $\vec\eta^R$-dependent, has appeared. Consistently, it is invariant under the transformations (A.4), so that the modular properties of the whole conformal block are not spoiled. Actually, since

$$e^{i\pi\vec\eta^R\cdot\vec y_i^R(n_d\tilde m_i-n_i\tilde m_d)}=e^{-\frac{\pi}{\tau_2}(\tilde m_I+n_I\bar\tau)\Delta B_{IJ}(\tilde m_J+n_J\tau)}\,, \tag{A.27}$$

where ΔB_{IJ} is antisymmetric and defined as

$$\Delta B_{dj}=\frac12\,\eta^R\cdot\vec y_j^R\,,\quad \Delta B_{ij}=0\,,\quad i,j\in\{d+1,\dots,9\}\,, \tag{A.28}$$

it is natural to write Eq. (A.26) in the following form

$$\frac{\sqrt{\det G}}{\tau_2^{\frac{10-d}{2}}} \sum_{\substack{\tilde m_d,\dots,\tilde m_9\\ n_d,\dots,n_9}} e^{-\frac{\pi}{\tau_2}(\tilde m_I+n_I\bar\tau)(G+B+\Delta B)_{IJ}(\tilde m+n_I\tau)}$$
$$\times\, e^{-i\pi\left[\tilde m_d(a_1^L-\eta^R\cdot\vec a^R)-n_d(b_1^L-\eta^R\cdot\vec b^R)+\tilde m_d n_d(1-(\vec\eta^R)^2)\right]}$$
$$\times\, e^{-i\pi n_I\vec y_I^R\cdot(\vec b^R-\tilde m_J\vec y_J^R)}\prod_{\mathcal A=1}^{4}\theta\begin{bmatrix}a_{\mathcal A}^L\\ b_{\mathcal A}^L\end{bmatrix}(\tau)\prod_{\mathcal J=10}^{25}\bar\theta\begin{bmatrix}a_{\mathcal J}^R-2n_I y_{I\mathcal J}^R\\ b_{\mathcal J}^R-2\tilde m_I y_{I\mathcal J}^R\end{bmatrix}(\bar\tau)\,. \tag{A.29}$$

The Hamiltonian form of the above result can be expressed in terms of

$$\begin{aligned}
&(G'+B')_{IJ}=\begin{pmatrix}4(G+B)_{dd} & 2(G+B)_{dj}\\ 2(G+B)_{id} & (G+B)_{ij}\end{pmatrix},\\
&\vec y_d'^R=2\vec y_d^R\,,\ \vec y_i'^R=\vec y_i^R\,,\ i,j\in\{d+1,\dots,9\}\,,\\
&\Delta B'_{IJ}\ \text{antisymmetric}\,,\quad \Delta B'_{dj}=\eta^R\cdot\vec y_j'^R\,,\quad \Delta B'_{ij}=0\,,
\end{aligned} \tag{A.30}$$

and by redefining the momenta, winding numbers and indices N''s as

$$\begin{aligned}
&m'_d=2(m_d-N_1^L+\vec\eta^R\cdot\vec N^R)+a_1^L-\vec\eta^R\cdot\vec a^R-(1-(\vec\eta^R)^2)\,n_d\,,\\
&m'_i=m_i\,,\ i\in\{d+1,\dots,9\}\,,\\
&n'_d=\frac{n_d}{2}\,,\ n'_i=n_i\,,\\
&N_1'^L=N_1^L+n_d\,,\ N'^L_{\mathcal A}\in N^L_{\mathcal A}\,,\ N'^R_{\mathcal J}=N^R_{\mathcal J}+n_d\,\eta^R_{\mathcal J}\,,\quad \mathcal A\in\{2,3,4\}\,,\ \mathcal J\in\{10,\dots,25\}\,,
\end{aligned} \tag{A.31}$$

where $n'_d\in\mathbb{Z}\cup(\mathbb{Z}+\frac12)$. With these conventions, we set

$$
\begin{aligned}
P'^L_I &= m'_I + \vec{y}'^R_I \cdot \vec{Q}'^R + \frac{1}{2}\,\vec{y}'^R_I \cdot n'_J \vec{y}'^R_J + (B' + \Delta B' + G')_{IJ} n'_J\,, \quad I \in \{d, \dots, 9\}\,,\\
P'^R_I &= m'_I + \vec{y}'^R_I \cdot \vec{Q}'^R + \frac{1}{2}\,\vec{y}'^R_I \cdot n'_J \vec{y}'^R_J + (B' + \Delta B' - G')_{IJ} n'_J\,,\\
\vec{Q}' &\equiv (\vec{Q}'^L, \vec{Q}'^R) = \vec{N}' - \frac{\vec{a}}{2}\,,
\end{aligned}
\tag{A.32}
$$

and write the conformal block (A.6) as

$$
\begin{aligned}
&\sum_{\substack{m_d\\ n_d}} e^{2i\pi(b^L_1 - \vec{\eta}^R\cdot\vec{b}^R)n'_d} \sum_{\substack{m'_{d+1},\dots,m'_9\\ n'_{d+1},\dots,n'_9}} \sum_{\vec{N}'} e^{-i\pi \vec{b}\cdot\vec{Q}'}\\
&\quad \times q^{\frac{1}{4}\left[P'^L_I G'^{IJ} P'^L_J + 2(\vec{Q}'^L)^2\right]}\, \bar{q}^{\frac{1}{4}\left[P'^R_I G'^{IJ} P'^R_J + 2(\vec{Q}'^R + n'_I \vec{y}'^R_I)^2\right]}\,.
\end{aligned}
\tag{A.33}
$$

As a result, when the condition $\vec{\eta}^R \cdot \vec{a}^R \in \mathbb{Z}$ is satisfied for all sectors $\vec{a} \in \Xi$, the partition function takes the final form

$$
\begin{aligned}
Z'[G', B', \vec{y}'^R]_{\vec{\eta}^R} = &\frac{1}{\tau_2^{\frac{d-2}{2}}} \frac{1}{|\Xi|} \sum_{\vec{a},\vec{b}\in\Xi} \sum_{\vec{N}'} \mathcal{C}\left[\begin{matrix}\vec{a}\\ \vec{b}\end{matrix}\right] e^{-i\pi\vec{b}\cdot\vec{Q}'} \sum_{\ell_L,\ell_R\geq 0} c^L_{\ell_L} c^R_{\ell_R}\\
&\times \sum_{\substack{m'_d\\ n'_d\in\mathbb{Z}\cup(\mathbb{Z}+\frac{1}{2})}} e^{2i\pi(b^L_1 - \vec{\eta}^R\cdot b^R)n'_d}\, \delta_{a^L_1, m'_d + \vec{\eta}^R\cdot a^R - (1-(\vec{\eta}^R)^2)2n'_d \bmod 2}\\
&\times \sum_{\substack{m'_{d+1},\dots,m'_9\\ n'_{d+1},\dots,n'_9}} q^{\frac{1}{4}M'^2_L/M^2_{\rm s}}\, \bar{q}^{\frac{1}{4}M'^2_R/M^2_{\rm s}}\,,
\end{aligned}
\tag{A.34}
$$

where the left- and right-masses satisfy

$$
\begin{aligned}
M'^2_L &= M^2_{\rm s}\left[P'^L_I G'^{IJ} P'^L_J + 2(\vec{Q}'^L)^2 + 4\ell_L - 2\right],\\
M'^2_R &= M^2_{\rm s}\left[P'^R_I G'^{IJ} P'^R_J + 2(\vec{Q}'^R + n'_I \vec{y}'^R_I)^2 + 4\ell_R - 4\right].
\end{aligned}
\tag{A.35}
$$

Comparing with the case $\vec{\eta}^R = \vec{0}^R$ given in Eq (A.23), there are two differences:

• There is a shift $\Delta B'_{IJ}$ of the antisymmetric tensor. In the core of the present paper, we however denote $B + \Delta B$ as B (or $B' + \Delta B'$ as B'), using a field redefinition.

• The states $m'_d = n'_d = 0$ have fermionic number a^L_1 equal to the parity of $\vec{\eta}^R \cdot a^R$, which may be even or odd. When the compact direction X^d is large compared to the string scale, and the components of the Wilson line vector $\vec{y}'^R$ are small compared to $\sqrt{G'^{dd}}$, the lightest states may therefore be bosons or fermions, while their superpartners acquire a KK mass $M'_{(\sigma)} = M_{\rm s}\sqrt{G'^{dd}}$ (see next section).

Additional discrete Wilson lines can also be switched on as follows. Without loss of generality, we can split the internal metric plus antisymmetric tensor component (d, J) into a quantized background and continuous Wilson line deformations:

$$
(G' + B' + \Delta B')_{dJ} = \eta^R_J + \sqrt{2}\, y'^R_{dJ}\,, \quad J \in \{d, \dots, 9\}\,, \quad \text{where} \quad \eta^R_J \in \mathbb{Z}\,, \quad y'^R_{dJ} \text{ arbitrary}\,.
\tag{A.36}
$$

In terms of the redefined momentum quantum number $\hat{m}'_d = m'_d + \eta^R_J n'_J$, we obtain new expressions for

$$P'^L_d = \hat{m}'_d + \vec{y}'^R_d \cdot \vec{Q}'^R + \frac{1}{2}\,\vec{y}'^R_d \cdot n'_J \vec{y}'^R_J + \sqrt{2}\, y'^R_{dJ} n'_J\,,$$
$$P'^R_d = \hat{m}'_d + \vec{y}'^R_d \cdot \vec{Q}'^R + \frac{1}{2}\,\vec{y}'^R_d \cdot n'_J \vec{y}'^R_J + (\sqrt{2}\, y'^R - 2G')_{dJ} n'_J\,, \tag{A.37}$$

and the partition function takes the alternative form

$$\begin{aligned} Z'[G', B', \vec{y}'^R]_{\eta^R_d,\dots,\eta^R_9,\vec{\eta}^R} = & \frac{1}{\tau_2^{\frac{d-2}{2}}} \frac{1}{|\Xi|} \sum_{\vec{a},\vec{b}\in\Xi} \sum_{\vec{N}'} \mathcal{C}\big[{\vec{a}\atop\vec{b}}\big] e^{-i\pi \vec{b}\cdot\vec{Q}'} \sum_{\ell_L,\ell_R\geq 0} c^L_{\ell_L} c^R_{\ell_R} \\ & \times \sum_{\substack{\hat{m}'_d \\ n'_d\in\mathbb{Z}\cup(\mathbb{Z}+\frac{1}{2})}} e^{2i\pi(b^L_1 - \vec{\eta}^R\cdot b^R) n'_d} \\ & \times \delta_{a^L_1, \hat{m}'_d - \eta^R_J n'_J + \vec{\eta}^R\cdot a^R - (1-(\vec{\eta}^R)^2) 2n'_d \bmod 2} \\ & \times \sum_{\substack{m'_{d+1},\dots,m'_9 \\ n'_{d+1},\dots,n'_9}} q^{\frac{1}{4}M'^2_L/M^2_s}\, \bar{q}^{\frac{1}{4}M'^2_R/M^2_s}\,, \end{aligned} \tag{A.38}$$

where one argument of the Kronecker symbol is shifted. To conclude, we stress that the above partition function is equivalent to the initial one in Eq. (A.8), with left-moving discrete Wilson lines given in Eq. (A.17). It is therefore independent of $\eta^R_d, \dots, \eta^R_9, \vec{\eta}^R$. However, in order to describe the light spectrum encountered in a given region of moduli space, it may be helpful to choose $\eta^R_d, \dots, \eta^R_9, \vec{\eta}^R$ suitably.

A.5. Low supersymmetry breaking scale

From now on in the Appendix, we consider the case where $\sqrt{G'_{dd}} \gg 1$, while all other components of the internal metric and antisymmetric tensor are of order 1. We find convenient to set $\eta^R_d = 0$ and use only the notation G'_{dd} (rather than y'^R_{dd}), in terms of which the supersymmetry breaking scale $M'_{(\sigma)} = M_s\sqrt{G'^{dd}} = \mathcal{O}(M_s/\sqrt{G'_{dd}})$ is low. In the following, our goal is to derive in these conditions expressions of the effective potential,

$$\mathcal{V}^{(\sigma)}_{1\text{-loop}} \equiv -\frac{M^d_s}{(2\pi)^d} \int_{\mathcal{F}} \frac{d^2\tau}{2\tau_2^2}\, Z'[G', B', \vec{y}'^R]_{0,\eta^R_{d+1},\dots,\eta^R_9,\vec{\eta}^R}\,. \tag{A.39}$$

In the Hamiltonian form of the partition function (A.38), the left- and right-moving masses satisfy

$$q^{\frac{1}{4}M'^2_L/M^2_s}\, \bar{q}^{\frac{1}{4}M'^2_R/M^2_s} = \mathcal{O}\big(e^{-\pi\tau_2(G'_{dd}n'^2_d + \mathcal{O}(1))}\big)\,, \quad \text{where} \quad \tau_2 > \frac{\sqrt{3}}{2}\,. \tag{A.40}$$

Therefore, all strings stretched non-trivially along the very large direction X^d are supermassive (even much more than oscillator states) and yield contributions to $\mathcal{V}^{(\sigma)}_{1\text{-loop}}$ that are exponentially suppressed in G'_{dd}. Thus, we proceed by focusing on the modes having trivial winding number, $n'_d = 0$.

Next, we note that in the Langrangian formulation of the conformal block (A.26), the phase responsible for the spontaneous breaking of supersymmetry is trivial when $n_d = 2n'_d$ and $\tilde{m}_d$ are even. Hence, in the sector $n_d = 2n'_d = 0$, the only non-vanishing contributions arise for $\tilde{m}_d$ odd. In this case, denoting $\tilde{m}_d = 2\tilde{k}_d + 1$, each term of the integrand in Eq. (A.39) contains a τ_2-dependent factor

$$\frac{1}{\tau_2^{2+\frac{10-d}{2}}}\, e^{-\frac{\pi}{\tau_2}[(2\tilde{k}_d+1)^2 G_{dd}+\mathcal{O}(1)]}\, e^{-\pi\tau_2\mathcal{O}(1)}\,. \tag{A.41}$$

The latter allows an extension of the integration over the fundamental domain $\mathcal{F}$ to the "upper half strip",

$$\int_{\mathcal{F}} d\tau_1 d\tau_2 \longrightarrow \int_{-\frac{1}{2}}^{\frac{1}{2}} d\tau_1 \int_0^{+\infty} d\tau_2\,, \tag{A.42}$$

at the price of introducing an error exponentially suppressed in G'_{dd}. Note that no ultraviolet divergence occurs as $\tau_2 \to 0$.

Switching back to the Hamiltonian picture, the integration over τ_1 projects out the non-level matched states. Therefore, we obtain

$$\mathcal{V}^{(\sigma)}_{\text{1-loop}} = -\frac{M_{\rm s}^d}{(2\pi)^d}\int_0^{+\infty}\frac{d\tau_2}{2\tau_2^{\frac{d+2}{2}}}\sum_s (-1)^{\hat{m}'_d-\eta^R_j n'_j+\vec{\eta}^R\cdot\vec{a}^R}\, e^{-\pi\tau_2 M'^2_L/M_{\rm s}^2} + \mathcal{O}\big(e^{-\#G'_{dd}}\big)\,, \tag{A.43}$$

where # is an order 1 positive coefficient and the discrete sum is over all physical states s having $n'_d = 0$. To be explicit, they belong to some sector labeled by $\vec{a}^R \in \Xi$ and have arbitrary quantum numbers $\hat{m}'_d, m'_{d+1}, \ldots, m'_9, n'_{d+1}, \ldots, n'_9$ and ℓ_L, ℓ_R. Notice that we have used the spin-statistics theorem as well as the Kronecker symbol appearing in the partition function (A.38) to fix the sign of the contribution of s. Since the level matching condition

$$\frac{1}{4}(M'^2_L - M'^2_R) \equiv M_{\rm s}^2\Big[(\hat{m}'_d - \eta'^R_I n'_I)n'_d + m'_i n'_i + \frac{1}{2}\big(\vec{Q}^2+1\big) + \ell_L - \ell_R\Big] \in \mathbb{Z} \tag{A.44}$$

is independent of $\hat{m}'_d$ when $n'_d = 0$, the states s are actually organized in KK towers of modes of arbitrary momentum $\hat{m}'_d$, so that we may write

$$\mathcal{V}^{(\sigma)}_{\text{1-loop}} = -\frac{M_{\rm s}^d}{(2\pi)^d}\sum_{s_0}(-1)^{\vec{\eta}^R\cdot\vec{a}^R-\eta'^R_j n'_j}\int_0^{+\infty}\frac{d\tau_2}{2\tau_2^{\frac{d+2}{2}}}\sum_{\hat{m}'_d}(-1)^{\hat{m}'_d}\, e^{-\pi\tau_2 M'^2_L/M_{\rm s}^2} + \mathcal{O}\big(e^{-\#G'_{dd}}\big)\,, \tag{A.45}$$

where the first discrete sum is over the physical states s_0 having $\hat{m}'_d = n'_d = 0$. In the above expression, M'_L is the mass of the KK mode of momentum $\hat{m}'_d$,

$$M'^2_L = M_{\rm s}^2\Big[\hat{m}'^2_d G'^{dd} + 2\hat{m}'_d\zeta^d\Big] + M'^2_{L0}\,, \tag{A.46}$$

where M'_{L0} is that of the zero-momentum state s_0,

$$M'^2_{L0} = M_{\rm s}^2\Big[\xi_d^2 G'^{dd} + 2\xi_d G'^{dj}P'^L_j + P'^L_i G'^{ij}P'^L_j + 2(\vec{Q}'^L)^2 + 4\ell_L - 2\Big]\,, \tag{A.47}$$

and ξ_d, ζ^d are introduced for notational convenience,

$$\xi_d = \vec{y}_d'^R \cdot \vec{Q}'^R + \frac{1}{2}\,\vec{y}_d'^R \cdot n'_j \vec{y}_j'^R + \sqrt{2}\, y'^R_{dj} n'_j\,, \qquad \zeta^d = G'^{dd}\xi_d + G'^{dj} P'^L_j\,. \tag{A.48}$$

By Poisson summation over $\hat{m}'_d$, one obtains a mixed Lagrangian/Hamiltonian form of the effective potential, where the order of the integral and the discrete sum can be inverted. One finds

$$\begin{aligned}\mathcal{V}^{(\sigma)}_{\text{1-loop}} = &-\frac{M_{\rm s}^d}{(2\pi)^d}\sum_{s_0}(-1)^{\vec{\eta}^R\cdot\vec{a}^R-\eta^R_j n'_j}\sum_{\tilde{m}'_d} e^{i\pi(2\tilde{m}'_d+1)\frac{\zeta^d}{G'^{dd}}}\,\frac{1}{\sqrt{G'^{dd}}}\\ &\times\int_0^{+\infty}\frac{d\tau_2}{2\tau_2^{\frac{d+3}{2}}}\,e^{-\pi\frac{(\tilde{m}'_d+\frac{1}{2})^2}{\tau_2 G'^{dd}}}\,e^{-\pi\tau_2\mathcal{M}'^2_{L0}}\\ &+\mathcal{O}\big(e^{-\#G'_{dd}}\big)\,,\end{aligned} \tag{A.49}$$

where $\mathcal{M}'_{L0}$ is a characteristic mass associated with the KK tower labeled by s_0,

$$\mathcal{M}'^2_{L0} \equiv M'^2_{L0} - \frac{(\zeta^d M_{\rm s})^2}{G'^{dd}} = M_{\rm s}^2\left[P'^L_i G'^{ij} P'^L_j - \frac{(G'^{dj}P'_j)^2}{G'^{dd}} + 2(\vec{Q}'^L)^2 + 4\ell_L - 2\right] \geq 0\,. \tag{A.50}$$

The result of the integration over τ_2 can be formulated in terms of a function

$$\begin{aligned}F(z) \equiv z^{\frac{d+1}{2}}\,K_{\frac{d+1}{2}}(z) = 2^{\frac{d-1}{2}}\Gamma\Big(\frac{d+1}{2}\Big)\left[1-\frac{z^2}{2(d-1)}+\mathcal{O}(z^4)\right], \quad &\text{when} \quad z\to 0\,,\\ \sim z^{\frac{d}{2}}\,e^{-z}\sqrt{\frac{\pi}{2}}\,, \quad &\text{when} \quad z\to+\infty\,,\end{aligned} \tag{A.51}$$

where $K_{\frac{d+1}{2}}$ is a modified Bessel function of the second kind. If F is finite at $z=0$, it happens to be exponentially suppressed for $z\gg 1$, thus implying that only a finite number of towers yields significant contributions. To be specific, let us consider the $n_{\rm B}$ (or $n_{\rm F}$) KK towers having $\mathcal{M}'_{L0}$ lower than a few times $M'_{(\sigma)}$ (say $\varrho M'_{(\sigma)}$ for some $\varrho=\mathcal{O}(1)$), and such that $\vec{\eta}^R\cdot\vec{a}^R-\eta^R_j n'_j$ is even (or odd). Defining $cM_{\rm s}$ to be the lowest mass $\mathcal{M}'_{L0}$ of the infinite number of heavier KK towers, we obtain[20]

$$\begin{aligned}\mathcal{V}^{(\sigma)}_{\text{1-loop}} = &-\frac{M'^d_{(\sigma)}}{(2\pi)^{\frac{3d+1}{2}}}\sum_{s_0=1}^{n_{\rm B}+n_{\rm F}}(-1)^{\vec{\eta}^R\cdot\vec{a}^R-\eta^R_j n'_j}\sum_{\tilde{m}'_d}\frac{\cos\left(\pi(2\tilde{m}'_d+1)\frac{\zeta^d M_{\rm s}^2}{M'^2_{(\sigma)}}\right)}{|\tilde{m}'_d+\frac{1}{2}|^{d+1}}\\ &\times F\left(\pi|2\tilde{m}'_d+1|\frac{\mathcal{M}'_{L0}}{M'_{(\sigma)}}\right)\\ &+\mathcal{O}\big((cM_{\rm s}M'_{(\sigma)})^{\frac{d}{2}}e^{-\pi cM_{\rm s}/M'_{(\sigma)}}\big)\,.\end{aligned} \tag{A.52}$$

[20] Choosing for instance $\varrho=3$, the most unfavorable configuration, which corresponds to $cM_{\rm s}=\varrho M'_{(\sigma)}$, implies the non-explicit terms in the second line of Eq. (A.52) to be about 1% of the contribution of a KK tower with vanishing characteristic mass. Of course, $M_{\rm s}\geq cM_{\rm s}>\varrho M'_{(\sigma)}$ yields much lower errors.

In fact, the KK towers with characteristic masses $\mathcal{M}'_{L0} > \varrho M'_{(\sigma)}$ are almost supersymmetric and do not contribute significantly to the effective potential. Going back to the Hamiltonian picture given in Eq. (A.45), we also have

$$\mathcal{V}^{(\sigma)}_{\text{1-loop}} = -\frac{M_{\rm s}^d}{(2\pi)^d}\sum_{s_0=1}^{n_{\rm B}+n_{\rm F}}(-1)^{\vec{\eta}^R\cdot\vec{a}^R-\eta^R_j n'_j}\int_0^{+\infty}\frac{d\tau_2}{2\tau_2^{\frac{d+2}{2}}}\sum_{\hat{m}'_d}(-1)^{\hat{m}'_d}\,e^{-\pi\tau_2 M_L'^2/M_{\rm s}^2} + \mathcal{O}\big((cM_{\rm s}M'_{(\sigma)})^{\frac{d}{2}}e^{-\pi c M_{\rm s}/M'_{(\sigma)}}\big)\,. \quad \text{(A.53)}$$

Some remarks are in order:

• The gauge symmetry arising from the $10-d+16$ internal directions and extra dimensions of the right-moving bosonic string yield an $U(1)\times\mathcal{G}_{9-d+16}$ gauge symmetry, where the rank of $\mathcal{G}_{9-d+16}$ is $9-d+16$. When $\mathcal{G}_{9-d+16}$ is "maximally enhanced", *i.e.* contains no $U(1)$ factor, we have in particular $y'^R_{dj}=0$, $j\in\{d+1,\dots,9\}$, $\vec{y}'^R_d=\vec{0}$, so that $\xi_d=0$.[21] Moreover, except the KK scale $M'_{(\sigma)}$ itself, there is no mass scale between 0 and $M_{\rm s}$. As a result, there are $n_{\rm B}+n_{\rm F}$ KK towers with exactly vanishing characteristic masses, $\mathcal{M}'_{L0}=0$, while all other towers are very heavy, $\mathcal{M}'_{L0}=\mathcal{O}(M_{\rm s})$. The former satisfy $P'^L_i=0$, $i\in\{d+1,\dots,9\}$, $(\vec{Q}'^L)^2=1$, $\ell_L=0$, so that $\zeta^d=0$. From the Hamiltonian point of view, the $n_{\rm B}+n_{\rm F}$ zero-modes s_0 are massless, $M'_{L0}=0$, their KK counterparts satisfy $M'_L\geq M'_{(\sigma)}$, and the string states belonging to other KK towers satisfy $M'_L=\mathcal{O}(M_{\rm s})$.

• The situation presents mild differences when some moduli fields are switched on and bring the model slightly away from the background where $\mathcal{G}_{9-d+16}$ is maximally enhanced. This happens when deviations of $(G'+B'+\Delta B')_{ij}$, $i,j\in\{d+1,\dots,9\}$, from the initial background are smaller (in absolute value) than $\varrho\sqrt{G'^{dd}}$, or when some non-vanishing $|y'^R_{dj}|$, $|y'^R_{d\mathcal{J}}|$, $j\in\{d+1,\dots,9\}$, $\mathcal{J}\in\{10,\dots,25\}$, are lower than 1. In both cases, new scales lower than $\varrho\sqrt{G'^{dd}}M_{\rm s}$ are introduced, whose effects are to induce small Higgs masses to some of the $n_{\rm B}+n_{\rm F}$ initially massless modes s_0. However, the KK towers they belong to remain light, in the sense that their characteristic masses still satisfy $\mathcal{M}'_{L0}<\varrho M'_{(\sigma)}$.

• When a deviation ς of some $(G'+B'+\Delta B')_{ij}$, $i,j\in\{d+1,\dots,9\}$, becomes larger (in absolute value) than $\varrho\sqrt{G'^{dd}}$, the number $n_{\rm B}+n_{\rm F}$ of KK towers such that $\mathcal{M}'_{L0}<\varrho M'_{(\sigma)}$ decreases. Physically, the gauge theory enters a Coulomb branch where the component $(G'+B'+\Delta B')_{ij}$ is a flat direction of the effective potential, up to $\mathcal{O}\big((|\varsigma|M_{\rm s}M'_{(\sigma)})^{\frac{d}{2}}e^{-\pi|\delta|M_{\rm s}/M'_{(\sigma)}}\big)$ terms.

A.6. Example with $n_{\rm F}$ greater, lower or equal to $n_{\rm B}$

In order to illustrate the results of Sects (A.4) and (A.5), we consider the $E_8\times E'_8$ heterotic string compactified on $S^1(R_d)\times T^{9-d}$, where R_d is the radius of the circle, in the presence of discrete deformations,

$$\Xi=\big\{(4,8+8)\text{-tuples }(a,\dots,a;\gamma,\dots,\gamma,\gamma',\dots,\gamma')\,,\\ \text{where } a,\gamma,\gamma'\in\mathbb{Z}_2\big\}\implies|\Xi|=2^3\,,$$

$$\mathcal{C}[^{a;\gamma,\gamma'}_{b\,;\delta,\,\delta'}]=(-1)^{a+b+ab}\,,$$

[21] An arbitrary component $(G'+B')_{id}$, $i\in\{d+1,\dots,9\}$, is however allowed.

$$
\begin{aligned}
&Y^L_{I\mathcal{A}} = \delta_{Id}\,\delta_{\mathcal{A}1}\,, \quad I \in \{d,\dots,9\}\,,\ \mathcal{A} \in \{1,\dots,4\}\,,\\
&Y^R_{I\mathcal{J}} = \delta_{Id}\eta^R_{\mathcal{J}} \quad i.e. \quad y^R_{I\mathcal{J}} = 0\,, \quad \mathcal{J} \in \{10,\dots,25\}\,,\\
&0 = (G' + B' + \Delta B')_{dJ} = \eta^R_J \quad i.e. \quad y'^R_{dJ} = 0\,, \quad J \in \{d,\dots,9\}\,.
\end{aligned}
\tag{A.54}
$$

As explained before, the left-moving discrete deformation implements a spontaneous breaking of supersymmetry *via* a stringy Scherk–Schwarz mechanism along the direction X^d. Moreover, when the supersymmetry breaking scale is low, the bosonic or fermionic nature of the lightest states is determined by $\vec{\eta}^R$, a fact that has a direct impact on the gauge symmetry. In the following, we consider in details the example where

$$
\eta^R_{\mathcal{J}} = \delta_{\mathcal{J},10} + \delta_{\mathcal{J},18}\,, \quad \mathcal{J} \in \{10,\dots,25\}\,.
\tag{A.55}
$$

We first derive the partition function of the model under the above assumptions. Then, we switch on arbitrary (but small) Wilson line deformations around such a background and derive the 1-loop effective potential at low supersymmetry breaking scale.

Using Eq. (A.29), the 1-loop partition function (A.8) can be written as

$$
\begin{aligned}
Z = \frac{1}{\tau_2^{\frac{d-2}{2}}}\,\frac{1}{\eta^{12}\,\bar\eta^{24}}\,\frac{1}{2}\sum_{a,b}(-1)^{a+b+ab}\,\theta[{}^a_b]^4\,\frac{1}{2}\sum_{\gamma,\delta}\theta[{}^\gamma_\delta]^8\,\frac{1}{2}\sum_{\gamma',\delta'}\theta[{}^{\gamma'}_{\delta'}]^8\\
\times\,\frac{R_d}{\sqrt{\tau_2}}\sum_{\tilde m_d,n_d} e^{-\frac{\pi}{\tau_2}R_d^2|\tilde m_d+n_d\tau|^2}\,\Gamma_{9-d,9-d}\,(-1)^{\tilde m_d(a-\gamma-\gamma')-n_d(b-\delta-\delta')-\tilde m_d n_d}\,,
\end{aligned}
\tag{A.56}
$$

where we have used the fact that the lattice of zero-modes associated with the internal torus is factorized, $\Gamma_{10-d,10-d} = \Gamma_{1,1}(R_d)\times\Gamma_{9-d,9-d}$. Defining $R'_d = 2R_d$ and $\tilde m_d = 2\tilde k_d + g$, $n_d = 2l_d + h$, where $g,h\in\mathbb{Z}_2$, the above formula becomes

$$
\begin{aligned}
Z = \frac{1}{\tau_2^{\frac{d-2}{2}}}\,\frac{1}{\eta^8\,\bar\eta^8}\,\Gamma_{9-d,9-d}\,\frac{1}{2}\sum_{h,g}\Gamma_{1,1}\begin{bmatrix}h\\ g\end{bmatrix}(R'_d)\\
\times\,\frac{1}{2}\sum_{a,b}(-1)^{a+b+ab}\,\frac{\theta[{}^a_b]^4}{\eta^4}\,(-1)^{ga-hb-hg}\;\frac{1}{2}\sum_{\gamma,\delta}\frac{\bar\theta[{}^\gamma_\delta]^8}{\bar\eta^8}\,(-1)^{g\gamma-h\delta}\\
\times\,\frac{1}{2}\sum_{\gamma',\delta'}\frac{\bar\theta[{}^{\gamma'}_{\delta'}]^8}{\bar\eta^8}\,(-1)^{g\gamma'-h\delta'}\,,
\end{aligned}
\tag{A.57}
$$

where we have introduced shifted lattices, which can be considered either in Langrangian or Hamiltonian forms,

$$
\begin{aligned}
\Gamma_{1,1}\begin{bmatrix}h\\ g\end{bmatrix}(R'_d) &= \frac{R'_d}{\sqrt{\tau_2}}\sum_{\tilde k_d,l_d} e^{-\frac{\pi}{\tau_2}R'^2_d\left|\tilde k_d+\frac{g}{2}+(l_d+\frac{h}{2})\tau\right|^2}\\
&= \sum_{k_d,l_d} e^{i\pi g k_d}\,q^{\frac{1}{4}\left(\frac{k_d}{R'_d}+(l_d+\frac{h}{2})R'_d\right)^2}\,\bar q^{\frac{1}{4}\left(\frac{k_d}{R'_d}-(l_d+\frac{h}{2})R'_d\right)^2}\,.
\end{aligned}
\tag{A.58}
$$

In terms of the $O(2n)$ affine characters

$$O_{2n} = \frac{\theta[^0_0]^n + \theta[^0_1]^n}{2\eta^n}\,, \qquad V_{2n} = \frac{\theta[^0_0]^n - \theta[^0_1]^n}{2\eta^n}\,,$$
$$S_{2n} = \frac{\theta[^1_0]^n + (-i)^n\theta[^1_1]^n}{2\eta^n}\,, \qquad C_{2n} = \frac{\theta[^1_0]^n - (-i)^n\theta[^1_1]^n}{2\eta^n}\,, \tag{A.59}$$

and

$$\gamma_{1,1}\left[\begin{smallmatrix}h\\g\end{smallmatrix}\right](R'_d) = \frac{1}{2}\left(\Gamma_{1,1}\left[\begin{smallmatrix}h\\0\end{smallmatrix}\right](R'_d) + (-1)^g\,\Gamma_{1,1}\left[\begin{smallmatrix}h\\1\end{smallmatrix}\right](R'_d)\right)$$
$$= \sum_{k'_d,l_d} q^{\frac{1}{4}\left(\frac{2k'_d+g}{R'_d}+(l_d+\frac{h}{2})R'_d\right)^2}\,\bar q^{\frac{1}{4}\left(\frac{2k'_d+g}{R'_d}-(l_d+\frac{h}{2})R'_d\right)^2}\,, \tag{A.60}$$

we obtain the final expression

$$Z = \frac{1}{\tau_2^{\frac{d-2}{2}}}\,\frac{1}{\eta^8\,\bar\eta^8}\,\Gamma_{9-d,9-d}\Big[\ \gamma_{1,1}[^0_0](R'_d)\Big(V_8(\bar O_{16}\bar O'_{16}+\bar S_{16}\bar S'_{16}) - S_8(\bar O_{16}\bar S'_{16}+\bar S_{16}\bar O'_{16})\Big)$$
$$+\gamma_{1,1}[^0_1](R'_d)\Big(V_8(\bar O_{16}\bar S'_{16}+\bar S_{16}\bar O'_{16}) - S_8(\bar O_{16}\bar O'_{16}+\bar S_{16}\bar S'_{16})\Big)$$
$$+\gamma_{1,1}[^1_0](R'_d)\Big(O_8(\bar V_{16}\bar C'_{16}+\bar C_{16}\bar V'_{16}) - C_8(\bar V_{16}\bar V'_{16}+\bar C_{16}\bar C'_{16})\Big)$$
$$+\gamma_{1,1}[^1_1](R'_d)\Big(O_8(\bar V_{16}\bar V'_{16}+\bar C_{16}\bar C'_{16}) - C_8(\bar V_{16}\bar C'_{16}+\bar C_{16}\bar V'_{16})\Big)\Big]. \tag{A.61}$$

To make contact with the notations of the previous subsections, we identify $R'_d = \sqrt{G'_{dd}}$, and recognize the momentum $\hat m'_d \equiv 2k'_d + g$ and winding number $n'_d = l_d + \frac{h}{2} \in \mathbb{Z}\cup(\mathbb{Z}+\frac{1}{2})$. When $R'_d \gg 1$, the states contributing in the third and fourth lines of Eq. (A.61) are super massive. The physical states s_0, which have $\hat m'_d = n'_d = 0$, are massless and arise in the first line. They are $n_{\rm B} = 8\times[(d-2)+1+\dim\mathcal{G}_{9-d}+2\times 120]$ bosonic degrees of freedom,

$$\mathbf{8_v}\otimes\big([d-2]\oplus \mathrm{Adj}_{U(1)\times\mathcal{G}_{9-d}}\oplus \mathrm{Adj}_{SO(16)\times SO(16)'}\big), \tag{A.62}$$

where $\mathcal{G}_{9-d}$ is the gauge symmetry induced by the $\Gamma_{9-d,9-d}$ lattice, and $n_{\rm F} = 8\times 2\times 128$ fermionic degrees of freedom,

$$\mathbf{8_s}\otimes\big(\mathrm{Spinorial}_{SO(16)}\oplus\mathrm{Spinorial}_{SO(16)'}\big). \tag{A.63}$$

Their superpartners, which have $\hat m'_d = 1, n'_d = 0$, show up in the second line and have masses $M_{\rm s}/R'_d$. The sign of $n_{\rm F}-n_{\rm B}$ can be arbitrary, as can be seen for example by choosing $\mathcal{G}_{9-d} = SU(2)^{9-d-s}\times U(1)^s$, which yields $n_{\rm F}-n_{\rm B} = 16(d+s-5)$. In dimension $d=4$, this is negative for $s=0$, vanishes for $s=1$ and is positive for $s=2,3,4,5$.

To see explicitly the dependence of the 1-loop effective potential on the Wilson lines, let us consider as an example in arbitrary dimension $d\geq 3$ the case of an initial background characterized by a maximally enhanced gauge group $\mathcal{G}_{9-d} = SU(2)^{9-d}$. In the notations of Eq. (A.30), the y-deformations we introduce are given by

$$(G'+B'+\Delta B')_{IJ} = \begin{pmatrix} G'_{dd} & \sqrt{2}\,y'^R_{dj} \\ \sqrt{2}\,y'^R_{id} & \delta_{ij}+\sqrt{2}\,y'^R_{ij}\end{pmatrix},\ \ \vec y_d{}'^R\,,\ \vec y_i{}'^R\,,\ \ i,j\in\{d+1,\dots,9\}\,,$$
$$\Delta B'_{IJ}\ \text{antisymmetric}\,,\quad \Delta B'_{dj} = y'^R_{j,10}+y'^R_{j,18}\,,\quad \Delta B'_{ij} = 0\,. \tag{A.64}$$

We are going to apply Eq. (A.52), which is valid when $G'_{dd} \gg 1$, in the case the continuous Wilson lines are small, namely

$$\begin{aligned} &|y'^R_{ij}|, |y'^R_{i\mathcal{J}}| \ll \varrho\sqrt{G'^{dd}}\,, \\ &|y'^R_{dj}|, |y'^R_{d\mathcal{J}}|, |y'^R_{id}| \ll 1\,, \quad i,j \in \{d+1,\dots,9\}\,,\ \mathcal{J} \in \{10,\dots,25\}\,. \end{aligned} \tag{A.65}$$

For this purpose, we list the KK towers s_0, which satisfy $(\vec{Q}'^L)^2 = 1$, $\ell_L = 0$:

• For any given $j \in \{d+1,\dots,9\}$ and $\epsilon \in \{-1,1\}$, there are 8 KK towers s_0 associated with the root $\epsilon\sqrt{2}$ of the $SU(2)$ factor, and corresponding to momentum states along the direction X^j. The quantum numbers of the KK modes are $(\gamma,\gamma') = (0,0)$, $\vec{Q}'^R = \vec{0}$, $\ell_R = 0$ and

$$\hat{m}'_d \in \mathbb{Z}\,,\ n'_d = 0\,, \qquad m'_j = -n'_j = -\epsilon\,, \qquad m'_i = n'_i = 0\,,\ i \in \{d+1,\dots,9\},\ i \neq j\,. \tag{A.66}$$

Using these data, we derive

$$\xi_d = \epsilon\sqrt{2}\big(y'^R_{dj} + \frac{1}{2\sqrt{2}}\,\vec{y}'^R_d \cdot \vec{y}'^R_j\big)\,,\ P'_i = \epsilon\sqrt{2}\big(y'^R_{ij} + \frac{1}{2\sqrt{2}}\,\vec{y}'^R_i \cdot \vec{y}'^R_j\big)\,,\ i \in \{d+1,\dots,9\}\,, \tag{A.67}$$

and find

$$\frac{\zeta^d M_{\rm s}}{M'_{(\sigma)}} = y'^R_{dj}\,\epsilon\sqrt{2} + \cdots\,, \qquad \mathcal{M}'^2_{L0} = \sum_{i=d+1}^{9} \big(y'^R_{ij}\,\epsilon\sqrt{2}\big)^2 + \cdots\,, \tag{A.68}$$

where the ellipses stand for higher order terms in Wilson line deformations. The contribution of the 8 KK towers to the effective potential is then found to be

$$\begin{aligned} \mathcal{V}^{(\sigma)j,\epsilon}_{\text{1-loop}} = 8M'^d_{(\sigma)}\Big\{ &- v_d\,2^d + \frac{v_{d-2}}{4\pi}\,2^{d-2} \\ &\times \Big[(d-1)\big(y'^R_{dj}\,\epsilon\sqrt{2}\big)^2 + \frac{1}{G'^{dd}} \sum_{i=d+1}^{9} \big(y'^R_{ij}\,\epsilon\sqrt{2}\big)^2\Big]\Big\} + \cdots\,, \end{aligned} \tag{A.69}$$

where we have defined

$$v_d = \frac{\Gamma(\frac{d+1}{2})\,\zeta(d+1)}{2^{d-1}\,\pi^{\frac{3d+1}{2}}}\Big(1 - \frac{1}{2^{d+1}}\Big). \tag{A.70}$$

• For any root $\vec{Q}^R$ of $SO(16)\times SO(16)'$, or any weight $\vec{Q}^R$ of the spinorial representation of $SO(16)$ or $SO(16)'$, there are 8 KK towers s_0. The former have $(\gamma,\gamma') = (0,0)$ and the latter $(\gamma,\gamma') = (1,0)$ or $(0,1)$. The other quantum numbers of the KK modes are $\hat{m}'_d \in \mathbb{Z}$, $n'_d = 0$, $m'_i = n'_i = 0$, $i \in \{d+1,\dots,9\}$, $\ell_R = 0$. This leads

$$\xi_d = \vec{y}'^R_d \cdot \vec{Q}^R\,, \qquad P'_i = \vec{y}'^R_i \cdot \vec{Q}^R\,, \quad i \in \{d+1,\dots,9\}\,, \tag{A.71}$$

so that

$$\frac{\zeta^d M_{\rm s}}{M'_{(\sigma)}} = \vec{y}'^R_d \cdot \vec{Q}^R + \cdots\,, \qquad \mathcal{M}'^2_{L0} = \sum_{i=d+1}^{9} \big(\vec{y}'^R_i \cdot Q^R\big)^2 + \cdots\,. \tag{A.72}$$

The contribution of the 8 KK towers of charge $\vec{Q}^R$ to the effective potential is then

$$\mathcal{V}^{(\sigma)\vec{Q}^R}_{\text{1-loop}} = (-1)^{\gamma+\gamma'}\, 8M'^d_{(\sigma)}\Big\{ - v_d\, 2^d + \frac{v_{d-2}}{4\pi}\, 2^{d-2} \times \Big[(d-1)\big(\vec{y}'^R_d\cdot\vec{Q}^R\big)^2 + \frac{1}{G'^{dd}}\sum_{i=d+1}^{9}\big(\vec{y}'^R_i\cdot\vec{Q}^R\big)^2\Big]\Big\} + \cdots . \quad \text{(A.73)}$$

• Finally, there are 8 KK towers s_0 for each of the 24 states at right-moving oscillator level $\ell_R = 1$. Being neutral with respect to $SU(2)^{9-d}\times SO(16)^2$, the quantum numbers of the KK modes are $\hat{m}'_d\in\mathbb{Z}$, $n'_d = 0$, $m'_i = n'_i = 0$, $i\in\{d+1,\dots,9\}$, $\vec{Q}^R = \vec{0}$ and $(\gamma,\gamma') = (0,0)$. Therefore, $\xi_d = 0$ and $P'_i = 0$, $i\in\{d+1,\dots,9\}$, which implies

$$\frac{\zeta^d M_{\rm s}}{M'_{(\sigma)}} = 0\,, \qquad \mathcal{M}'^2_{L0} = 0\,. \quad \text{(A.74)}$$

For each $e\in\{2,\dots,25\}$, the contribution of the 8 neutral KK towers to $\mathcal{V}^{(\sigma)}_{\text{1-loop}}$ is therefore

$$\mathcal{V}^{(\sigma)e}_{\text{1-loop}} = 8M'^d_{(\sigma)}\Big\{ - v_d\, 2^d\Big\}\,. \quad \text{(A.75)}$$

Combining the above results, the total 1-loop effective potential takes the form

$$\begin{aligned}\mathcal{V}^{(\sigma)}_{\text{1-loop}} &= (n_{\rm F}-n_{\rm B})\, v_d\, M'^d_{(\sigma)}\, 2^d \\ &\quad + M'^d_{(\sigma)}\,\frac{v_{d-2}}{2\pi}\,2^{d-2}\Big\{\sum_{j=d+1}^{9} c_{SU(2)}\Big[(d-1)(y'^R_{dj})^2 + \frac{1}{G'^{dd}}\sum_{i=d+1}^{9}(y'^R_{ij})^2\Big] \\ &\qquad + c_{SO(16)}\Big[(d-1)(\vec{y}'^R_d)^2 + \frac{1}{G'^{dd}}\sum_{i=d+1}^{9}(\vec{y}'^R_i)^2\Big]\Big\} + \cdots \\ &\quad + \mathcal{O}\big((M_{\rm s}M'_{(\sigma)})^{\frac{d}{2}} e^{-\pi M_{\rm s}/M'_{(\sigma)}}\big)\,, \end{aligned} \quad \text{(A.76)}$$

where we have defined

$$\begin{aligned} c_{SU(2)} &= 8\,C_{[3]_{SU(2)}} = 8\times 2 = 16\,, \\ c_{SO(16)} &= 8\big(C_{[120]_{SO(16)}} - C_{[128]_{SO(16)}}\big) = 8\times(14-16) = -16\,, \end{aligned} \quad \text{(A.77)}$$

in terms of coefficients $C_{\mathcal{R}}$ considered for any representation $\mathcal{R}$ of a gauge group $\mathcal{G}$,

$$\frac{1}{2}\sum_{\substack{\text{weights}\\ \text{of }\mathcal{R}}} Q \sum_{\mathcal{I}=1}^{\text{rank}\,\mathcal{G}} A_{\mathcal{I}}Q_{\mathcal{I}} \sum_{\mathcal{J}=1}^{\text{rank}\,\mathcal{G}} B_{\mathcal{J}}Q_{\mathcal{J}} = C_{\mathcal{R}}\sum_{\mathcal{I}=1}^{\text{rank}\,\mathcal{G}} A_{\mathcal{I}}B_{\mathcal{I}}\,. \quad \text{(A.78)}$$

As a result, the Wilson lines of $SU(2)^{9-d}$ along T^{10-d} are massive at 1-loop, while those of $SO(16)^2$ are tachyonic. Notice that y'^R_{id}, $i\in\{d+1,\dots,9\}$, multiplies n'_d in Eq. (A.32). Therefore, the non-exponentially suppressed contributions of $\mathcal{V}_{\text{1-loop}}$ involve them only *via* the expressions of G'^{dd}, G'^{dj}, $j\in\{d+1,\dots,9\}$. Expanding the cosine in Eq. (A.52), it happens that the y'^R_{id}'s appear in at least cubic interactions with other Wilson lines. In other words, they remain massless at 1-loop, but are no more flat directions of the effective potential.

Using the dictionary (A.30) and defining

$$(G+B+\Delta B)_{IJ} = \begin{pmatrix} G_{dd} & \sqrt{2}\,y^R_{dj} \\ \sqrt{2}\,y^R_{id} & \delta_{ij}+\sqrt{2}\,y^R_{ij}\end{pmatrix}, \quad i,j\in\{d+1,\dots,9\}\,, \quad \text{(A.79)}$$

where ΔB is given in Eq. (A.28), we obtain the final result,

$$\begin{aligned}\mathcal{V}^{(\sigma)}_{\text{1-loop}} &= (n_{\rm F}-n_{\rm B})\, v_d\, M^d_{(\sigma)} \\ &\quad + M^d_{(\sigma)}\,\frac{v_{d-2}}{2\pi}\Big\{\sum_{j=d+1}^{9} c_{SU(2)}\Big[(d-1)(y^R_{dj})^2+\frac{1}{G^{dd}}\sum_{i=d+1}^{9}(y^R_{ij})^2\Big] \\ &\qquad\qquad + c_{SO(16)}\Big[(d-1)(\vec{y}^{\,R}_d)^2+\frac{1}{G^{dd}}\sum_{i=d+1}^{9}(\vec{y}^{\,R}_i)^2\Big]\Big\}+\cdots \\ &\quad + \mathcal{O}\big((M_{\rm s}M_{(\sigma)})^{\frac{d}{2}}e^{-2\pi M_{\rm s}/M_{(\sigma)}}\big)\,, \end{aligned} \tag{A.80}$$

which is written using the redefined supersymmetry breaking scale

$$M_{(\sigma)} = M_{\rm s}\sqrt{G^{dd}}\,. \tag{A.81}$$

Eq. (A.80) is an example of the expression we use in the main text of the present work, Eq. (2.5), up to the minor change of notations consisting in omitting the upper indices "R".

References

[1] E. Cremmer, S. Ferrara, C. Kounnas, D.V. Nanopoulos, Naturally vanishing cosmological constant in $\mathcal{N}=1$ supergravity, Phys. Lett. B 133 (1983) 61;
J.R. Ellis, C. Kounnas, D.V. Nanopoulos, Phenomenological $SU(1,1)$ supergravity, Nucl. Phys. B 241 (1984) 406;
J.R. Ellis, A.B. Lahanas, D.V. Nanopoulos, K. Tamvakis, No-scale supersymmetric standard model, Phys. Lett. B 134 (1984) 429;
J.R. Ellis, C. Kounnas, D.V. Nanopoulos, No scale supersymmetric GUTs, Nucl. Phys. B 247 (1984) 373.

[2] R. Rohm, Spontaneous supersymmetry breaking in supersymmetric string theories, Nucl. Phys. B 237 (1984) 553;
C. Kounnas, M. Porrati, Spontaneous supersymmetry breaking in string theory, Nucl. Phys. B 310 (1988) 355;
S. Ferrara, C. Kounnas, M. Porrati, Superstring solutions with spontaneously broken four-dimensional supersymmetry, Nucl. Phys. B 304 (1988) 500;
S. Ferrara, C. Kounnas, M. Porrati, F. Zwirner, Superstrings with spontaneously broken supersymmetry and their effective theories, Nucl. Phys. B 318 (1989) 75.

[3] C. Kounnas, B. Rostand, Coordinate-dependent compactifications and discrete symmetries, Nucl. Phys. B 341 (1990) 641.

[4] J. Scherk, J.H. Schwarz, Spontaneous breaking of supersymmetry through dimensional reduction, Phys. Lett. B 82 (1979) 60.

[5] R. Hagedorn, Statistical thermodynamics of strong interactions at high-energies, Nuovo Cim. Suppl. 3 (1965) 147;
S. Fubini, G. Veneziano, Level structure of dual-resonance models, Nuovo Cimento A 64 (1969) 811;
K. Bardakci, S. Mandelstam, Analytic solution of the linear-trajectory bootstrap, Phys. Rev. 184 (1969) 1640;
K. Huang, S. Weinberg, Ultimate temperature and the early universe, Phys. Rev. Lett. 25 (1970) 895;
J.J. Atick, E. Witten, The Hagedorn transition and the number of degrees of freedom of string theory, Nucl. Phys. B 310 (1988) 291;
M. Axenides, S.D. Ellis, C. Kounnas, Universal behavior of D-dimensional superstring models, Phys. Rev. D 37 (1988) 2964;
D. Kutasov, N. Seiberg, Number of degrees of freedom, density of states and tachyons in string theory and CFT, Nucl. Phys. B 358 (1991) 600;
I. Antoniadis, C. Kounnas, Superstring phase transition at high temperature, Phys. Lett. B 261 (1991) 369;
I. Antoniadis, J.P. Derendinger, C. Kounnas, Nonperturbative temperature instabilities in $\mathcal{N}=4$ strings, Nucl. Phys. B 551 (1999) 41, arXiv:hep-th/9902032.

[6] H. Itoyama, T.R. Taylor, Supersymmetry restoration in the compactified $O(16)\times O(16)'$ heterotic string theory, Phys. Lett. B 186 (1987) 129;
S. Abel, K.R. Dienes, E. Mavroudi, Towards a non-supersymmetric string phenomenology, Phys. Rev. D 91 (2015) 126014, arXiv:1502.03087 [hep-th];

S. Abel, K.R. Dienes, E. Mavroudi, GUT precursors and entwined SUSY: the phenomenology of stable non-supersymmetric strings, arXiv:1712.06894 [hep-ph];
I. Florakis, J. Rizos, Chiral heterotic strings with positive cosmological constant, Nucl. Phys. B 913 (2016) 495, arXiv:1608.04582 [hep-th].

[7] C. Kounnas, H. Partouche, Super no-scale models in string theory, Nucl. Phys. B 913 (2016) 593, arXiv:1607.01767 [hep-th].

[8] C. Kounnas, H. Partouche, $\mathcal{N} = 2 \to 0$ super no-scale models and moduli quantum stability, Nucl. Phys. B 919 (2017) 41, arXiv:1701.00545 [hep-th].

[9] S. Kachru, J. Kumar, E. Silverstein, Vacuum energy cancellation in a non-supersymmetric string, Phys. Rev. D 59 (1999) 106004, arXiv:hep-th/9807076;
G. Shiu, S.H.H. Tye, Bose–Fermi degeneracy and duality in non-supersymmetric strings, Nucl. Phys. B 542 (1999) 45, arXiv:hep-th/9808095;
J.A. Harvey, String duality and non-supersymmetric strings, Phys. Rev. D 59 (1999) 026002, arXiv:hep-th/9807213;
R. Blumenhagen, L. Gorlich, Orientifolds of non-supersymmetric asymmetric orbifolds, Nucl. Phys. B 551 (1999) 601, arXiv:hep-th/9812158;
C. Angelantonj, I. Antoniadis, K. Forger, Non-supersymmetric type I strings with zero vacuum energy, Nucl. Phys. B 555 (1999) 116, arXiv:hep-th/9904092;
Y. Satoh, Y. Sugawara, T. Wada, Non-supersymmetric asymmetric orbifolds with vanishing cosmological constant, J. High Energy Phys. 1602 (2016) 184, arXiv:1512.05155 [hep-th];
Y. Sugawara, T. Wada, More on non-supersymmetric asymmetric orbifolds with vanishing cosmological constant, J. High Energy Phys. 1608 (2016) 028, arXiv:1605.07021 [hep-th];
S. Groot Nibbelink, O. Loukas, A. Mütter, E. Parr, P.K.S. Vaudrevange, Tension between a vanishing cosmological constant and non-supersymmetric heterotic orbifolds, arXiv:1710.09237 [hep-th].

[10] S. Abel, R.J. Stewart, On exponential suppression of the cosmological constant in non-SUSY strings at two loops and beyond, Phys. Rev. D 96 (2017) 106013, arXiv:1701.06629 [hep-th];
K. Aoki, E. D'Hoker, D.H. Phong, Two-loop superstrings on orbifold compactifications, Nucl. Phys. B 688 (2004) 3, arXiv:hep-th/0312181;
R. Iengo, C.J. Zhu, Evidence for nonvanishing cosmological constant in nonSUSY superstring models, J. High Energy Phys. 0004 (2000) 028, arXiv:hep-th/9912074.

[11] T. Coudarchet, C. Fleming, H. Partouche, Quantum no-scale regimes in string theory, Nucl. Phys. B 930 (2018) 235, arXiv:1711.09122 [hep-th].

[12] F. Bourliot, C. Kounnas, H. Partouche, Attraction to a radiation-like era in early superstring cosmologies, Nucl. Phys. B 816 (2009) 227, arXiv:0902.1892 [hep-th].

[13] T. Catelin-Jullien, C. Kounnas, H. Partouche, N. Toumbas, Thermal/quantum effects and induced superstring cosmologies, Nucl. Phys. B 797 (2008) 137, arXiv:0710.3895 [hep-th];
T. Catelin-Jullien, C. Kounnas, H. Partouche, N. Toumbas, Induced superstring cosmologies and moduli stabilization, Nucl. Phys. B 820 (2009) 290, arXiv:0901.0259 [hep-th].

[14] F. Bourliot, J. Estes, C. Kounnas, H. Partouche, Cosmological phases of the string thermal effective potential, Nucl. Phys. B 830 (2010) 330, arXiv:0908.1881 [hep-th];
J. Estes, C. Kounnas, H. Partouche, Superstring cosmology for $\mathcal{N}_4 = 1 \to 0$ superstring vacua, Fortschr. Phys. 59 (2011) 861, arXiv:1003.0471 [hep-th].

[15] J. Estes, L. Liu, H. Partouche, Massless D-strings and moduli stabilization in type I cosmology, J. High Energy Phys. 1106 (2011) 060, arXiv:1102.5001 [hep-th];
L. Liu, H. Partouche, Moduli stabilization in type II Calabi–Yau compactifications at finite temperature, J. High Energy Phys. 1211 (2012) 079, arXiv:1111.7307 [hep-th].

[16] J.J. Halliwell, Scalar fields in cosmology with an exponential potential, Phys. Lett. B 185 (1987) 341;
A.B. Burd, J.D. Barrow, Inflationary models with exponential potentials, Nucl. Phys. B 308 (1988) 929, Erratum: Nucl. Phys. B 324 (1989) 276;
L.P. Chimento, General solution to two-scalar field cosmologies with exponential potentials, Class. Quantum Gravity 15 (1998) 965;
I.P.C. Heard, D. Wands, Cosmology with positive and negative exponential potentials, Class. Quantum Gravity 19 (2002) 5435, arXiv:gr-qc/0206085;
Z.K. Guo, Y.S. Piao, Y.Z. Zhang, Cosmological scaling solutions and multiple exponential potentials, Phys. Lett. B 568 (2003) 1, arXiv:hep-th/0304048;
P.K. Townsend, Cosmic acceleration and M-theory, arXiv:hep-th/0308149;

I.P. Neupane, Accelerating cosmologies from exponential potentials, Class. Quantum Gravity 21 (2004) 4383, arXiv:hep-th/0311071;
P. Vieira, Late-time cosmic dynamics from M-theory, Class. Quantum Gravity 21 (2004) 2421, arXiv:hep-th/0311173;
E. Bergshoeff, A. Collinucci, U. Gran, M. Nielsen, D. Roest, Transient quintessence from group manifold reductions or how all roads lead to Rome, Class. Quantum Gravity 21 (2004) 1947, arXiv:hep-th/0312102;
J.G. Russo, Exact solution of scalar tensor cosmology with exponential potentials and transient acceleration, Phys. Lett. B 600 (2004) 185, arXiv:hep-th/0403010;
L. Jarv, T. Mohaupt, F. Saueressig, Quintessence cosmologies with a double exponential potential, J. Cosmol. Astropart. Phys. 0408 (2004) 016, arXiv:hep-th/0403063;
P.K. Townsend, M.N.R. Wohlfarth, Cosmology as geodesic motion, Class. Quantum Gravity 21 (2004) 5375, arXiv:hep-th/0404241;
A. Collinucci, M. Nielsen, T. Van Riet, Scalar cosmology with multi-exponential potentials, Class. Quantum Gravity 22 (2005) 1269, arXiv:hep-th/0407047;
E. Dudas, N. Kitazawa, A. Sagnotti, On climbing scalars in string theory, Phys. Lett. B 694 (2011) 80, arXiv:1009.0874 [hep-th].

[17] P.K. Townsend, M.N.R. Wohlfarth, Accelerating cosmologies from compactification, Phys. Rev. Lett. 91 (2003) 061302, arXiv:hep-th/0303097;
N. Ohta, Accelerating cosmologies from S-branes, Phys. Rev. Lett. 91 (2003) 061303, arXiv:hep-th/0303238;
S. Roy, Accelerating cosmologies from M/string theory compactifications, Phys. Lett. B 567 (2003) 322, arXiv:hep-th/0304084;
M.N.R. Wohlfarth, Accelerating cosmologies and a phase transition in M-theory, Phys. Lett. B 563 (2003) 1, arXiv:hep-th/0304089;
R. Emparan, J. Garriga, A note on accelerating cosmologies from compactifications and S-branes, J. High Energy Phys. 0305 (2003) 028, arXiv:hep-th/0304124;
N. Ohta, A study of accelerating cosmologies from superstring/M theories, Prog. Theor. Phys. 110 (2003) 269, arXiv:hep-th/0304172;
C.M. Chen, P.M. Ho, I.P. Neupane, J.E. Wang, A note on acceleration from product space compactification, J. High Energy Phys. 0307 (2003) 017, arXiv:hep-th/0304177;
C.M. Chen, P.M. Ho, I.P. Neupane, N. Ohta, J.E. Wang, Hyperbolic space cosmologies, J. High Energy Phys. 0310 (2003) 058, arXiv:hep-th/0306291;
M.N.R. Wohlfarth, Inflationary cosmologies from compactification?, Phys. Rev. D 69 (2004) 066002, arXiv:hep-th/0307179.

[18] K.S. Narain, New heterotic string theories in uncompactified dimensions < 10, Phys. Lett. B 169 (1986) 41;
K.S. Narain, M.H. Sarmadi, E. Witten, A note on toroidal compactification of heterotic string theory, Nucl. Phys. B 279 (1987) 369;
P.H. Ginsparg, Comment on toroidal compactification of heterotic superstrings, Phys. Rev. D 35 (1987) 648.

[19] E. Kiritsis, String Theory in a Nutshell, Princeton University Press, 2007.

[20] E. Kiritsis, C. Kounnas, Perturbative and nonperturbative partial supersymmetry breaking: $\mathcal{N} = 4 \to \mathcal{N} = 2 \to \mathcal{N} = 1$, Nucl. Phys. B 503 (1997) 117, arXiv:hep-th/9703059.

Published for SISSA by Springer

Received: *January 15, 2019*
Accepted: *March 18, 2019*
Published: *March 20, 2019*

Spontaneous dark-matter mass generation along cosmological attractors in string theory

Thibaut Coudarchet,[a] **Lucien Heurtier**[b] **and Hervé Partouche**[a]

[a] *Centre de Physique Théorique, École Polytechnique and CNRS, Palaiseau, 91128, France*
[b] *Department of Physics, University of Arizona, Tucson, AZ 85721, U.S.A.*

E-mail: thibaut.coudarchet@polytechnique.edu, heurtier@email.arizona.edu, herve.partouche@polytechnique.edu

Abstract: We propose a new scenario for generating a relic density of non-relativistic dark matter in the context of heterotic string theory. Contrary to standard thermal freeze-out scenarios, dark-matter particles are abundantly produced while still relativistic, and then decouple from the thermal bath due to the sudden increase of their mass above the universe temperature. This mass variation is sourced by the condensation of an order-parameter modulus, which is triggered when the temperature $T(t)$ drops below the supersymmetry breaking scale $M(t)$, which are both time-dependent. A cosmological attractor mechanism forces this phase transition to take place, in an explicit class of heterotic string models with spontaneously broken supersymmetry, and at finite temperature.

Keywords: Cosmology of Theories beyond the SM, Superstrings and Heterotic Strings, Supersymmetry Breaking

ArXiv ePrint: 1812.10134

https://doi.org/10.1007/JHEP03(2019)117

JHEP03(2019)117

Contents

JHEP03(2019)117

1 Introduction

As an ultraviolet complete theory unifying gravity with gauge interactions, string theory is a natural framework to study the primordial universe and describe cosmology using a top-down approach. In modern language, a possible question to be asked is whether ingredients which are used in the most common cosmological scenarios — such as models including a cosmological constant and a cold dark-matter component (ΛCDM) — can be derived from models of the string theory landscape, rather than embedded in only apparently consistent low energy field theories of the swampland [1, 2].

It is nowadays established that our universe is constituted of three crucial components, which are dark energy, dark matter and Standard-Model particles. The amount of each of these ingredients have been measured with very good accuracy in the present universe [3], indicating that a very large portion of the universe energy density is shared by dark energy and dark matter rather than baryons and radiation. Furthermore, the study of the cosmic microwave background has shown to be compatible with dark energy and non-relativistic matter playing a key role in diluting the inhomogeneities of the primordial universe at early times, throughout a phase of so-called *cosmic inflation* (see e.g. [4] for a review). If a lot of the string-cosmology literature has been focusing on finding a way to generate enough e-folds of inflation in the primordial universe (see debates on such a possibility [1, 2, 5–8]), studies trying to obtain a phase of matter domination during the late cosmological evolution of the universe are much more rare [9–18]. In practice, most of the dark-matter

models which have been proposed in the context of string theory are *string inspired*, in the sense that the particle interactions and mass spectrum are derived from string-theory models. Therefore, in such a framework, the discussion of dark-matter decoupling and non-relativistic matter production remains to be an effective, low-energy discussion, or relies on purely geometrical effects such as domain-walls or cosmic-strings decay. The interesting possibility that a whole tower of KK-states contribute collectively to the dark-matter relic density, while different species decay at different time scales, was also proposed in [19–21] under the name *dynamical dark-matter*. In these models, the relic density is typically produced in the early universe through a misalignment mechanism. The freeze-out mechanism was also considered in [22], although in such context the particle spectrum is taken to be a time-independent data set, contrary to what we will consider.

In particular, in the usual *thermal freeze-out* scenario, it is assumed that a significant amount of dark matter is produced in the early universe, before it decouples from the thermal bath when the temperature drops under the dark-matter mass. In this paper, we present an alternative mechanism in which dark matter is naturally abundantly produced while still relativistic, and then decouples from the thermal bath due to the brutal variation of its mass above the temperature. This scenario arises within a class of explicit string models in d dimensions, due to cosmological attractors that yield a phase transition responsible for the spontaneous mass generation of the dark-matter particles. Note that the possibility of a variable-mass dark-matter particle has already been proposed in [23] in a different context, but relatively unexplored from the phenomenological perspective.

In the past literature, heterotic string models compactified on tori (or orbifolds) with spontaneously broken supersymmetry [24–28] à la Scherk-Schwarz [29, 30] have been considered at finite temperature [28] and weak string coupling. It was shown that in the context of flat, homogeneous and isotropic cosmological evolutions, the universe is attracted towards a "radiation-like critical solution" [31–35], along which the supersymmetry breaking scale $M(t)$, the temperature $T(t)$ and the inverse of the scale factor $a(t)$ evolve proportionally, $M(t) \propto T(t) \propto 1/a(t)$. The denomination "radiation-like" is motivated by the fact that the *total* energy density and pressure arising from (i) the thermal bath of the infinite towers of Kaluza-Klein (KK) states along the internal Scherk-Schwarz directions and (ii) the coherent motion of $M(t)$ satisfy the same state equation as pure radiation, $\rho_{\rm tot} = (d-1)P_{\rm tot}$ [32, 33]. If helpful to understand the behavior of the early universe after reheating, when the light matter content of the universe is in thermal equilibrium, such a critical solution cannot be a low energy attractor for our universe since we know that (i) at present time the supersymmetry breaking scale is extremely large as compared to the universe temperature, and (ii) that the universe is matter dominated. Therefore, one needs to complexify the picture in order to open the possibility that part of the massless spectrum becomes massive and then decouples, while the universe evolves.

This is precisely what we do in the present work. We use the fact that at special points in moduli space, states which are generically very heavy become massless [36]. When these states contain more fermions than bosons, the free energy density $\mathcal{F}$ arising from their thermalized towers of KK modes shows very peculiar properties. First of all, at such a point in moduli space, $\mathcal{F}$ is extremal. Second, this extremum is a minimum (maximum)

JHEP03(2019)117

for large enough (low enough) temperature T, as compared to the supersymmetry breaking scale M. Assuming generic initial conditions compatible with a minimum, the destabilization of the order parameter, which is a modulus, then occurs dynamically, provided the attractor mechanism described in the above paragraph enforces $T(t)/M(t)$ to reach low enough values. As a result, while the universe expands and the temperature (as well as the supersymmetry breaking scale) drops, for the evolution dictated by the radiation-like critical solution to be approached, a phase transition takes place, where the condensation of the order-parameter modulus induces a large mass to the whole initially light KK towers. We will see that such a condensation is naturally pushed up to values which are necessarily larger than the temperature of the thermal bath, generating spontaneously an important amount of non-relativistic matter that may freeze-out later on i.e. quit equilibrium, due to the expansion of the universe.

The paper is organized as follows: in section 2, we construct the simplest heterotic models for which the free energy density presents suitable features for developing the instability required for the spontaneous dark-matter mass generation. Section 3 is devoted to the analytical description of the attractor mechanisms. In a first stage, the order-parameter modulus is attracted towards the minimum of its potential well, while the whole cosmological evolution approaches a radiation-like critical solution [34, 35]. This effect is already non-trivial, in the sense that the mechanism avoids the so-called "cosmological moduli problem" [37, 38].[1] Then, the ratio T/M being dynamically pushed to some low enough value, the phase transition suddenly takes place, inducing the dark-matter particle to become heavier than the temperature scale. In section 4, we first review how dark-matter particles decouple from a thermal bath in the context of the usual thermal freeze-out scenario. Then, we present the new mechanism which we propose in this paper to make dark matter decouple spontaneously from the thermal bath, when the phase transition happens. We finally relate the relic energy density of cold dark matter to the scale factor of the universe and the freshly acquired dark-matter mass. Our conclusions and perspectives can be found in section 5, where we summarize our results and present futur prospects.

2 Thermal effective potential

Throughout this paper, all dimensionful quantities will be expressed in string units ($\alpha' = 1$), and denoted with suffixes "(σ)" when measured in string frame i.e. σ-model frame. In this section, we consider models realizing a spontaneous breaking of supersymmetry at a scale $M_{(\sigma)}$, and derive their free energy density $\mathcal{F}_{(\sigma)}$ at finite temperature $T_{(\sigma)}$. To be more specific, we would like $\mathcal{F}_{(\sigma)}$, which is nothing but the effective potential at finite temperature, to depend on a modulus that will be massive at high temperature and tachyonic at low temperature, as compared to the supersymmetry breaking scale. As will be shown in section 3, the dynamics of the universe may then enforce the time evolutions of $T_{(\sigma)}$ and

[1] Typically encountered in inflationary scenarios, the universe at intermediate times may be dominated by the energy stored in massive scalars, which cannot stabilize. Their eventual decay into radiation can lead to an entropy excess.

JHEP03(2019)117

$M_{(\sigma)}$ to trigger a destabilization of the modulus, which is responsible for a dark-matter mass generation.

2.1 Heterotic models and free energy

Our starting point is the $E_8 \times E_8$ heterotic string compactified on the background

$$S^1_{\rm E}(R_0) \times \mathbb{R}^{d-1} \times T^2 \times T^{8-d}, \tag{2.1}$$

where time is Euclidean and compactified on a circle of radius R_0, and $\mathbb{R}^{d-1}$ stands for the spatial directions. For simplicity, we consider the internal space to be factorized in two tori. The radius of one direction in T^2, say X^d, is the modulus to be (de-)stabilized, while the second direction, which we denote by X^9, is responsible for the spontaneous breaking of supersymmetry. On the contrary, all moduli associated with T^{8-d} will play a minor role in the sequel.

Technically, both finite temperature and spontaneous breaking of supersymmetry can be implemented by a stringy version of the Scherk-Schwarz mechanism [24–28]. At 1-loop, the free energy density can be written as

$$\begin{aligned}
\mathcal{F}_{(\sigma)} = -\frac{1}{2(2\pi)^d} \int_F \frac{{\rm d}\tau_1 {\rm d}\tau_2}{\tau_2^{1+\frac{d+2}{2}}} \sum_{g_0,h_0} \sum_{\tilde{k}_0,l_0} e^{-\frac{\pi R_0^2}{\tau_2}|2\tilde{k}_0+g_0+(2l_0+h_0)\tau|^2} \\
\frac{1}{2}\sum_{g_9,h_9} \sqrt{\det G} \sum_{\substack{\tilde{k}_d,l_d \\ \tilde{k}_9,l_9}} e^{-\frac{\pi}{\tau_2}\left[\tilde{k}_i+\frac{g_i}{2}+(l_i+\frac{h_i}{2})\bar{\tau}\right](G_{ij}+B_{ij})\left[\tilde{k}_j+\frac{g_j}{2}+(l_j+\frac{h_j}{2})\tau\right]} \\
\frac{1}{2}\sum_{a,b}(-1)^{a+b+ab}\theta[{}^a_b]^4\,(-1)^{g_0 a+h_0 b+g_0 h_0}\,(-1)^{g_9 a+h_9 b+g_9 h_9} \\
\frac{1}{2}\sum_{\gamma,\delta}\bar{\theta}[{}^\gamma_\delta]^8\,(-1)^{g_9\gamma+h_9\delta+g_9 h_9}\;\frac{1}{2}\sum_{\gamma',\delta'}\bar{\theta}[{}^{\gamma'}_{\delta'}]^8\,(-1)^{g_9\gamma'+h_9\delta'+g_9 h_9} \\
\frac{\Gamma_{8-d,8-d}}{\eta^{12}\bar{\eta}^{24}},
\end{aligned} \tag{2.2}$$

where we use the following notations:

- $\tau = \tau_1 + i\tau_2$ is the Teichmüller parameter of the genus-1 Riemann surface and F the fundamental domain of the modular group. $\eta(\tau)$ and $\theta[{}^\alpha_\beta](\tau)$ are the Dedekind and Jacobi modular forms, for which conventions can be found in [39].

- The lattices of zero modes associated to the Euclidean circle and the T^2 coordinates are in the first and second lines. The numbers $\tilde{k}_0, \tilde{k}_d, \tilde{k}_9$ and l_0, l_d, l_9 are arbitrary integers, while g_0, h_0 and g_9, h_9 are parities i.e. equal to 0 or 1. For notational compactness, we have also introduced g_d, h_d but those are simply vanishing. Moreover, G_{ij} and B_{ij} are the metric and antisymmetric tensor background values on T^2, to be specified shortly.

- The worldsheet left-moving fermions contribute to the conformal block in the third line. The latter is dressed with "cocycles" i.e. phases that couple the above mentioned

JHEP03(2019)117

lattices to the spin structures $a, b \in \{0, 1\}$, thus implementing finite temperature and spontaneous breaking of supersymmetry [28]. In string frame, the temperature is the inverse of the Euclidean-time circle circumference,

$$T_{(\sigma)} = \frac{1}{2\pi R_0}. \tag{2.3}$$

- In the fourth line, the 16 extra right-moving coordinates of the bosonic string yield two E_8 lattices, where γ, δ and $\gamma', \delta' \in \{0, 1\}$. Cocycles responsible for the $E_8 \times E_8 \to \mathrm{SO}(16) \times \mathrm{SO}(16)$ spontaneous breaking are also included [40]. In total, the lattice of the direction X^9 is involved in the phase

$$(-1)^{g_9(a+\gamma+\gamma')+h_9(b+\delta+\delta')+g_9 h_9}, \tag{2.4}$$

  which shows that super-Higgs and Higgs mechanisms combine in a non-trivial way. Consider an initially massless, supersymmetric pair of bosonic ($a = 0$) and fermionic ($a = 1$) degrees of freedom: if their gauge charge $\gamma + \gamma'$ is even, then the Scherk-Schwarz mechanism along X^9 induces a non-trivial mass to the fermion, while the boson remains massless. On the contrary, when $\gamma + \gamma'$ is odd, the mass splitting is reversed, in the sense that the boson becomes massive, while the fermion remains massless [32, 33, 41, 42].

- The last line contains the lattice of zero modes associated to the internal directions $X^{d+1}, \ldots, X^8$, and worldsheet left- or right-moving oscillator contributions.

- We consider a T^2 metric and antisymmetric tensor

$$(G + B)_{ij} = \begin{pmatrix} R_d^2 & \epsilon \\ -\epsilon & 4R_9^2 \end{pmatrix}, \qquad i, j \in \{d, 9\}, \tag{2.5}$$

  where R_d and R_9 are dynamical radii, while $\epsilon \in \mathbb{Z}$ is a constant background. To motivate this choice, notice that in the absence of any cocycle responsible for finite temperature and supersymmetry breaking along X^9, we would have an $\mathrm{U}(1) \to \mathrm{SU}(2)$ enhancement of the gauge symmetry at $R_d = 1$ and arbitrary $\epsilon \in \mathbb{Z}$. In fact, a pair of non-Cartan vector multiplets would be exactly massless at such a point in moduli space. As shown in great details in [43],[2] once supersymmetry breaking is implemented along X^9, the effect of an even value of the "discrete Wilson line" ϵ is to induce a tree-level mass $1/(2R_9)$ (equal to that of the gravitini) only to the fermions of the non-Cartan vector multiplets. Conversely, an odd value of ϵ implies the fermions to remain massless, while their bosonic superpartners become massive. In both cases, we may define the scale of supersymmetry breaking in string frame to be

$$M_{(\sigma)} = \frac{1}{2\pi R_9}. \tag{2.6}$$

[2] In the appendix of [43], all marginal deformations of the heterotic theory are taken into account. However, for the sake of clarity and simplicity in the present work, we only discuss and keep dynamical the moduli relevant to the phase transition under consideration.

JHEP03(2019)117

In the remaining part of this subsection, we show how the picture is generalized in presence of both supersymmetry breaking and finite temperature.

Redefining $a = \hat{a} + h_0 + h_9$, $b = \hat{b} + g_0 + g_9$, and using the Jacobi identity to handle the sum over $\hat{a}, \hat{b}$, the free energy density becomes

$$\begin{aligned}\mathcal{F}_{(\sigma)} = & \frac{1}{2(2\pi)^d} \int_F \frac{\mathrm{d}\tau_1 \mathrm{d}\tau_2}{\tau_2^{1+\frac{d+2}{2}}} \sum_{g_0,h_0} \sum_{\tilde{k}_0,l_0} e^{-\frac{\pi R_0^2}{\tau_2}|2\tilde{k}_0+g_0+(2l_0+h_0)\tau|^2} \\ & R_d \sum_{\tilde{m}_d,n_d} e^{-\frac{\pi R_d^2}{\tau_2}|\tilde{m}_d+n_d\tau|^2} R_9 \sum_{g_9,h_9} \sum_{\tilde{k}_9,l_9} e^{-\frac{\pi R_9^2}{\tau_2}|2\tilde{k}_9+g_9+(2l_9+h_9)\tau|^2} (-1)^{\epsilon(\tilde{m}_d h_9 + n_d g_9)} \\ & \theta\big[{}^{1-h_0-h_9}_{1-g_0-g_9}\big]^4 \frac{1}{2} \sum_{\gamma,\delta} \bar{\theta}[{}^{\gamma}_{\delta}]^8 \frac{1}{2} \sum_{\gamma',\delta'} \bar{\theta}[{}^{\gamma'}_{\delta'}]^8 \frac{\Gamma_{8-d,8-d}}{\eta^{12}\bar{\eta}^{24}} (-1)^{\varphi},\end{aligned}$$

$$\text{where} \quad \varphi = g_0 + g_9 + h_0 + h_9 + g_9 h_0 + g_0 h_9 + g_9(\gamma + \gamma') + h_9(\delta + \delta'). \tag{2.7}$$

To proceed, we assume that the radii of the periodic directions X^0, X^9, are large compared to the Hagedorn radius, in order for Hagedorn-like instabilities not to occur,

$$R_0,\ R_9 \gg R_H = \frac{1+\sqrt{2}}{\sqrt{2}}. \tag{2.8}$$

This guarantees that the integrand does not develop level-matched tachyonic modes and the free energy to be well defined. By noticing that all contributions with non-vanishing winding numbers $2l_0 + h_0$ or $2l_9 + h_9$ yield contributions $\mathcal{O}(e^{-\#R_0^2})$ or $\mathcal{O}(e^{-\#R_9^2})$, where $\#$ is positive and $\mathcal{O}(1)$, we may focus on the sectors $h_0 = h_9 = 0$, with $l_0 = l_9 = 0$. Due to the $\theta\big[{}^{1}_{1-g_0-g_9}\big]^4$ factor, non-trivial contributions arise only for $(g_0, g_9) = (1, 0)$ or $(0, 1)$. As a result, we obtain

$$\begin{aligned}\mathcal{F}_{(\sigma)} = & \frac{R_9}{2(2\pi)^d} \int_F \frac{\mathrm{d}\tau_1 \mathrm{d}\tau_2}{\tau_2^{1+\frac{d+1}{2}}} \sum_{\substack{(g_0,g_9)= \\ (1,0) \text{ or } (0,1)}} \sum_{\tilde{k}_0,\tilde{k}_9} e^{-\frac{\pi}{\tau_2}\left[R_0^2(2\tilde{k}_0+1)^2 + R_9^2(2\tilde{k}_9+1)^2\right]} \sum_{m_d,n_d} q^{\frac{1}{2}p_L^2} \bar{q}^{\frac{1}{2}p_R^2} (-1)^{\epsilon n_d g_9} \\ & \frac{\theta\big[{}^{1}_{0}\big]^4}{\eta^{12}\bar{\eta}^{24}} \frac{1}{2} \sum_{\gamma,\delta} \bar{\theta}[{}^{\gamma}_{\delta}]^8 (-1)^{g_9\gamma} \frac{1}{2} \sum_{\gamma',\delta'} \bar{\theta}[{}^{\gamma'}_{\delta'}]^8 (-1)^{g_9\gamma'} \Gamma_{8-d,8-d} + \mathcal{O}(e^{-\#R_0^2}) + \mathcal{O}(e^{-\#R_9^2}),\end{aligned} \tag{2.9}$$

where $q = e^{2i\pi\tau}$. In this expression, we have written the lattice of zero modes associated to $S^1(R_d)$ in Hamiltonian form, where

$$p_L = \frac{1}{\sqrt{2}}\Big(\frac{m_d}{R_d} + n_d R_d\Big)^2, \quad p_R = \frac{1}{\sqrt{2}}\Big(\frac{m_d}{R_d} - n_d R_d\Big)^2. \tag{2.10}$$

Due to the presence of factors $e^{-\frac{\pi R_0^2}{\tau_2}(2\tilde{k}_0+1)^2}$ or $e^{-\frac{\pi R_9^2}{\tau_2}(2\tilde{k}_9+1)^2}$ in the integrand, we may extend the fundamental domain F of integration to the "upper half strip",

$$\int_F \mathrm{d}\tau_1 \mathrm{d}\tau_2 \, (\cdots) = \int_{-\frac{1}{2}}^{\frac{1}{2}} \mathrm{d}\tau_1 \int_0^{+\infty} \mathrm{d}\tau_2 \, (\cdots) + \mathcal{O}(e^{-\#R_0^2}) + \mathcal{O}(e^{-\#R_9^2}). \tag{2.11}$$

Hence, integrating over τ_1 projects on the physical i.e. level-matched spectrum.

JHEP03(2019)117

To evaluate explicitly the free energy, we expand

$$\begin{aligned}\frac{\theta_2^4}{\eta^{12}} &= 16\big(1+\mathcal{O}(q)\big),\\ \frac{1}{2}\sum_{\gamma,\delta}\bar\theta\big[{}^{\gamma}_{\delta}\big]^8(-1)^{g_9\gamma} &= 1+112\bar q+(-1)^{g_9}128\bar q+\mathcal{O}(\bar q^2),\\ \frac{1}{\bar\eta^{24}} &= \frac{1}{\bar q}\big(1+24\bar q+\mathcal{O}(\bar q^2)\big).\end{aligned} \tag{2.12}$$

Moreover, choosing the radius of the direction X^d to be "moderate",

$$\frac{1}{R_0},\frac{1}{R_9}\ll R_d\ll R_0,R_9, \tag{2.13}$$

R_d may sit in the neighborhood of 1, where the states with momenta and winding numbers $m_d=-n_d=\pm1$ become massless. We may then write

$$\sum_{m_d,n_d} q^{\frac{1}{2}p_L^2}\bar q^{\frac{1}{2}p_R^2}(-1)^{\epsilon n_d g_9}=1+2(-1)^{\epsilon g_9}\bar q\, e^{-\pi\tau_2\left(R_d-\frac{1}{R_d}\right)^2}+\cdots, \tag{2.14}$$

where the ellipses stand for all other modes, $m_dn_d\neq-1$. Note that the latter cannot yield states in the spectrum simultaneously level-matched and lighter than $T_{(\sigma)}$ and $M_{(\sigma)}$. In a similar way, we assume the size of $T^{8-d,8-d}$ to be "moderate", i.e. with metric satisfying

$$\frac{1}{R_0^2},\frac{1}{R_9^2}\ll|G_{IJ}|\ll R_0^2,R_9^2,\qquad I,J\in\{d+1,\ldots,8\}. \tag{2.15}$$

Hence, $(G+B)_{IJ}$ may sit at a point of enhanced gauge symmetry in moduli space, $\mathrm{U}(1)^{8-d}\to G_{\mathrm{en}}$, so that

$$\Gamma_{(8-d,8-d)}=1+d_{\mathrm{en}}\bar q+\cdots. \tag{2.16}$$

In the above formula, we take for simplicity $(G+B)_{IJ}$ to sit exactly at such a point, or to be outside of their neighborhoods, in which case $d_{\mathrm{en}}=0$. We are now ready to integrate physical mode by physical mode. This can be done using the identity

$$\mathcal{H}_\nu(x)\equiv\frac{1}{\Gamma(\nu)}\int_0^{+\infty}\frac{\mathrm{d}u}{u^{1+\nu}}\,e^{-\frac{1}{u}-x^2u}=\frac{2}{\Gamma(\nu)}\,x^\nu K_\nu(2x), \tag{2.17}$$

where K_ν is the modified Bessel function of the second kind. In practice, x is essentially the ratio of mass in the spectrum, to $T_{(\sigma)}$ or $M_{(\sigma)}$. As a consequence, different contributions can have different orders of magnitude, as follows from the behaviors of $\mathcal{H}_\nu(x)$ at large and small arguments,

$$\begin{aligned}\mathcal{H}_\nu(x)&\sim\frac{\sqrt{\pi}}{\Gamma(\nu)}\,x^{\nu-\frac{1}{2}}\,e^{-2x}\qquad\text{when}\quad x\gg1,\\ \mathcal{H}_\nu(x)&=1-\frac{x^2}{\nu-1}+\mathcal{O}(x^4)\quad\text{when}\quad|x|\ll1.\end{aligned} \tag{2.18}$$

The dominant contribution to $\mathcal{F}_{(\sigma)}$ arises from the (nearly) massless states, including those with $m_d=-n_d=\pm1$ when $R_d\simeq1$, together with their towers of KK modes associated

JHEP03(2019)117

to the Euclidean time and direction X^9. All other states yield exponentially suppressed contributions. They include in particular those arising from oscillator modes at the string scale, or from the states winding around the large compact directions X^0, X^9.

To write the final result, it is convenient to define

$$\zeta = \ln(R_d), \qquad \eta = \ln(R_9), \qquad z = \ln\left(\frac{R_0}{R_9}\right) = \ln\left(\frac{M_{(\sigma)}}{T_{(\sigma)}}\right), \tag{2.19}$$

in terms of which we find

$$\mathcal{F}_{(\sigma)} = T_{(\sigma)}^d f(z,\eta,\zeta) + \mathcal{O}\Big((cM_{\rm s}T_{(\sigma)})^{\frac{d}{2}} e^{-cM_{\rm s}/T_{(\sigma)}}\Big) + \mathcal{O}\Big((cM_{\rm s}M_{(\sigma)})^{\frac{d}{2}} e^{-cM_{\rm s}/M_{(\sigma)}}\Big). \tag{2.20}$$

In this expression, $cM_{\rm s} > 0$ is the lowest (Higgs-like) mass scale generated by the moduli G_{IJ}. As follows from eq. (2.15), it is heavier than $T_{(\sigma)}$ and $M_{(\sigma)}$, thus yielding exponential suppression.[3] The dominant contribution in $\mathcal{F}_{(\sigma)}$ involves

$$\begin{aligned} f(z,\eta,\zeta) = &-(n_{\rm F}+n_{\rm B}) f_{\rm T}^{(d)}(z) + (n_{\rm F}-n_{\rm B}) f_{\rm V}^{(d)}(z) \\ &-(\tilde{n}_{\rm F}+\tilde{n}_{\rm B}) \tilde{f}_{\rm T}^{(d)}(z,\eta,\zeta) + (\tilde{n}_{\rm F}-\tilde{n}_{\rm B}) \tilde{f}_{\rm V}^{(d)}(z,\eta,\zeta), \end{aligned} \tag{2.21}$$

where $n_{\rm B}$ and $n_{\rm F}$ are the numbers of bosonic and fermionic massless states for generic R_d, while $\tilde{n}_{\rm B}$ and $\tilde{n}_{\rm F}$ count those becoming massless at $R_d = 1$. The dressing functions account for the corresponding towers of KK modes along X^0, X^9 [34, 35],

$$\begin{aligned} f_{\rm T}^{(d)}(z) &= \frac{\Gamma\left(\frac{d+1}{2}\right)}{\pi^{\frac{d+1}{2}}} \sum_{\tilde{k}_0,\tilde{k}_9} \frac{e^{dz}}{\left[e^{2z}(2\tilde{k}_0+1)^2 + (2\tilde{k}_9)^2\right]^{\frac{d+1}{2}}}, \\ \tilde{f}_{\rm T}^{(d)}(z,\eta,\zeta) &= \frac{\Gamma\left(\frac{d+1}{2}\right)}{\pi^{\frac{d+1}{2}}} \sum_{\tilde{k}_0,\tilde{k}_9} \frac{e^{dz}\, \mathcal{H}_{\frac{d+1}{2}}\left(\pi|e^{\zeta}-e^{-\zeta}|e^{\eta}\sqrt{e^{2z}(2\tilde{k}_0+1)^2+(2\tilde{k}_9)^2}\right)}{\left[e^{2z}(2\tilde{k}_0+1)^2 + (2\tilde{k}_9)^2\right]^{\frac{d+1}{2}}}, \end{aligned} \tag{2.22}$$

while the last two functions can be defined by

$$f_{\rm V}^{(d)}(z) \equiv e^{(d-1)z} f_{\rm T}^{(d)}(-z), \qquad \tilde{f}_{\rm V}^{(d)}(z,\eta,\zeta) \equiv e^{(d-1)z} \tilde{f}_{\rm T}^{(d)}(-z,\eta+z,\zeta). \tag{2.23}$$

To be specific, the massless spectrum satisfies

$$\begin{aligned} n_{\rm B} &= 8\times(8+120+120+d_{\rm en}), \quad & n_{\rm F} &= 8\times(128+128), \\ \tilde{n}_{\rm B} &= 8\times 2\,(1-\epsilon), & \tilde{n}_{\rm F} &= 8\times 2\,\epsilon. \end{aligned} \tag{2.24}$$

There is a universal degeneracy factor 8 arising from the fact that at zero temperature and supersymmetry breaking scale, the theory is maximally supersymmetric i.e. with 16 supercharges ($\mathcal{N} = 4$ in 4 dimensions). In $n_{\rm B}$, the 8×8 degrees of freedom are those of the metric, antisymmetric tensor and dilaton field dimensionally reduced from 10 to d dimensions. The 120's are the dimensions of the two SO(16) gauge groups, while $d_{\rm en}$ is the number of roots of the enhanced $\mathrm{U}(1)^{8-d} \to G_{\rm en}$ gauge factor. They all satisfy

[3] For instance, if $G_{IJ} = \mathcal{O}(1)$, then so is c.

JHEP03(2019)117

$(\gamma, \gamma') = (0, 0)$. In $n_{\rm F}$, the 128's are the dimensions of the spinorial representations of the SO(16) factors, corresponding to $(\gamma, \gamma') = (1, 0)$ and $(0, 1)$. At $R_d = 1$, modes having $m_d = -n_d = \pm 1$ are massless, with charges $p_R = \pm\sqrt{2}$ under the right-moving U(1) isometry group of $S^1(R_d)$. Either $\tilde{n}_{\rm B}$ or $\tilde{n}_{\rm F}$ is non-trivial: when $\epsilon = 0$, the modes are bosons corresponding to the roots of the enhanced U(1) $\to$ SU(2) and on the contrary, $\epsilon = 1$ yields a pair of fermionic states, charged under U(1) which is not enhanced.

2.2 Properties of the free energy

From now on, we will neglect in $\mathcal{F}_{(\sigma)}$ (and omit in all formulas) the exponentially-suppressed contributions in eq. (2.20). Some remarks are in order:

- $\mathcal{F}_{(\sigma)}$ is the free energy density valid for arbitrary mass $|R_d - 1/R_d|$ of the $\tilde{n}_{\rm B}$ or $\tilde{n}_{\rm F}$ states, provided eq. (2.13) holds. Consistently, we find that when they are massless, i.e. at $R_d = 1$,

$$\begin{aligned} f(z, \eta, 0) &= -(N_{\rm F} + N_{\rm B}) f_{\rm T}^{(d)}(z) + (N_{\rm F} - N_{\rm B}) f_{\rm V}^{(d)}(z), \\ \text{where} \quad N_{\rm F} &= n_{\rm F} + \tilde{n}_{\rm F}, \quad N_{\rm B} = n_{\rm B} + \tilde{n}_{\rm B}. \end{aligned} \tag{2.25}$$

- The above split of f into two pieces is motivated by taking the limit $z \to +\infty$, where thermal effects are screened by quantum effects. In fact, we have

$$\mathcal{F}_{(\sigma)}|_{R_d=1} \underset{z\to+\infty}{\sim} M_{(\sigma)}^d \, (N_{\rm F} - N_{\rm B}) \, \xi, \quad \text{where} \quad \xi = \frac{\Gamma\left(\frac{d+1}{2}\right)}{\pi^{\frac{d+1}{2}}} \sum_m \frac{1}{|2m+1|^{d+1}}, \tag{2.26}$$

  which reproduces the expression of the 1-loop effective potential at zero temperature in a theory where supersymmetry is spontaneously broken by the Scherk-Schwarz mechanism [32, 33, 44].

- Conversely, when $z \to -\infty$, quantum corrections are screened by thermal effects. As a result, we recover

$$\mathcal{F}_{(\sigma)}|_{R_d=1} \underset{z\to-\infty}{\sim} -2\pi R_9 \, T_{(\sigma)}^{d+1} \, (N_{\rm F} + N_{\rm B}) \, \xi, \tag{2.27}$$

  which is the Stefan-Boltzmann law for radiation in $d+1$ dimensions. The overall factor $2\pi R_9$ arises consistently with the interpretation of the density in $d+1$ dimensions.

- Expanding around $\zeta = 0$, we identify the mass term of ζ,

$$\begin{aligned} f(z, \eta, \zeta) = &-(N_{\rm F}+N_{\rm B}) f_{\rm T}^{(d)}(z) + (N_{\rm F}-N_{\rm B}) f_{\rm V}^{(d)}(z) \\ &+ \frac{\zeta^2}{\pi T_{(\sigma)}^2} \Big[(\tilde{n}_{\rm F}+\tilde{n}_{\rm B}) f_{\rm T}^{(d-2)}(z) - (\tilde{n}_{\rm F}-\tilde{n}_{\rm B}) f_{\rm V}^{(d-2)}(z) \Big] + \mathcal{O}(\zeta^4), \\ \text{where} \quad \tilde{n}_{\rm F}+\tilde{n}_{\rm B} = 8\times 2, \quad &-(\tilde{n}_{\rm F}-\tilde{n}_{\rm B}) = (-1)^\epsilon 8 \times 2. \end{aligned} \tag{2.28}$$

  When the extra massless states at $R_d = 1$ are bosons (ϵ even), ζ is massive. Thus, as a function of ζ, $\mathcal{F}_{(\sigma)}$ presents a local minimum at $\zeta = 0$, as shown in the qualitative figure 1. However, the situation is more involved when the massless states

JHEP03(2019)117

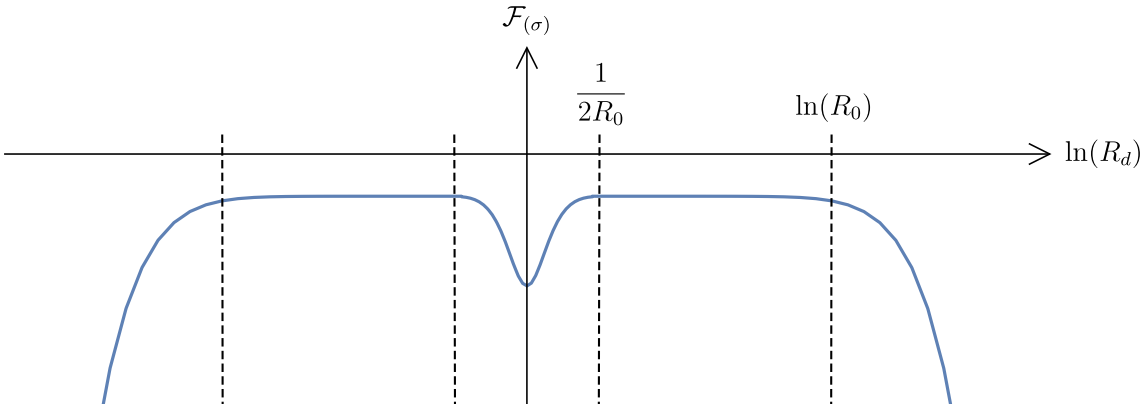

Figure 1. Qualitative shape of the free energy density $\mathcal{F}_{(\sigma)}$ as a function of $\zeta = \ln R_d$, when $\tilde{n}_{\rm F} - \tilde{n}_{\rm B} \leq 0$, or for low enough $M_{(\sigma)}/T_{(\sigma)}$ when $\tilde{n}_{\rm F} - \tilde{n}_{\rm B} > 0$. Several phases can be identified: a well of size $\max(1/R_0, 1/R_9)$. On both of its sides, plateaus extend until $\pm\min(\ln R_0, \ln R_9)$. The latter are followed/preceded by exponential falls if $n_{\rm F} - n_{\rm B} \leq 0$, or for low enough $M_{(\sigma)}/T_{(\sigma)}$ when $n_{\rm F} - n_{\rm B} > 0$. The exponential behavior is increasing for large enough $M_{(\sigma)}/T_{(\sigma)}$, when $n_{\rm F} - n_{\rm B} > 0$.

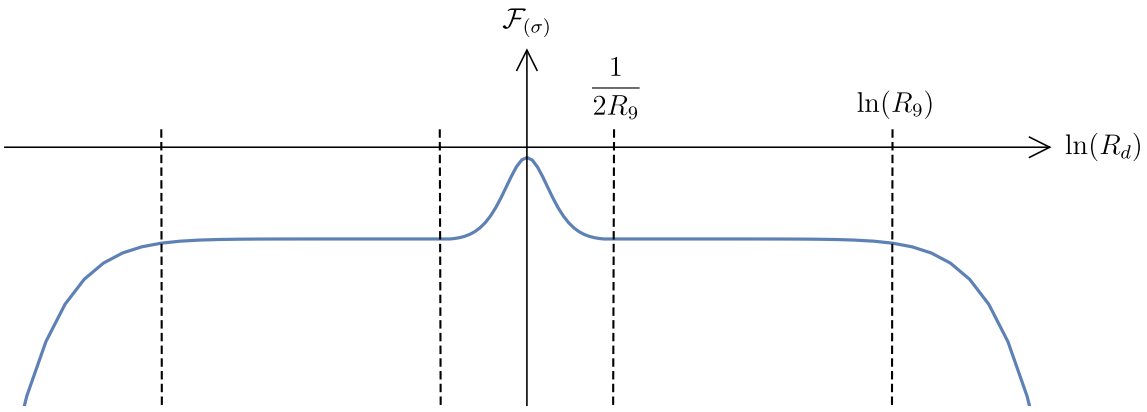

Figure 2. Qualitative shape of the free energy density $\mathcal{F}_{(\sigma)}$ as a function of $\zeta = \ln R_d$, in the case $\tilde{n}_{\rm F} - \tilde{n}_{\rm B} > 0$, when $M_{(\sigma)}/T_{(\sigma)}$ is large enough. Several phases can be identified: a bump of size $\max(1/R_0, 1/R_9)$. On both of its sides, plateaus extend until $\pm\min(\ln R_0, \ln R_9)$. The latter are followed/preceded by exponential falls if $n_{\rm F} - n_{\rm B} \leq 0$, or for low enough $M_{(\sigma)}/T_{(\sigma)}$ when $n_{\rm F} - n_{\rm B} > 0$. The exponential behavior is increasing for large enough $M_{(\sigma)}/T_{(\sigma)}$, when $n_{\rm F} - n_{\rm B} > 0$.

are fermions (ϵ odd). By noticing that the limits $z \to +\infty$ and $-\infty$ of the functions $f_{\rm T}^{(d)}(z)$ and $f_{\rm V}^{(d)}(z)$ that we took in eqs. (2.26) and (2.27) can be easily applied to the $d-2$ case, we conclude that for large enough e^z, ζ is tachyonic, while for low enough e^z, it is massive. The tachyonic case is illustrated in figure 2, where $\mathcal{F}_{(\sigma)}$ has a maximum at $\zeta = 0$. The massive case is as before, shown in figure 1. The dynamical switch from the massive case to the tachyonic case will be used in the next section to trigger the destabilization of R_d, which is responsible for the mass generation of fermionic dark matter.

JHEP03(2019)117

- For R_d sufficiently far from the self-dual point, the masses of the $\tilde{n}_{\rm B}$ or $\tilde{n}_{\rm F}$ states (depending on the parity of ϵ) exceed $T_{(\sigma)}$ and $M_{(\sigma)}$. Thus, their contributions to the free energy become exponentially suppressed and the second line of eq. (2.21), which captures all ζ- and η-dependences, can be omitted. Hence, as a function of ζ, $\mathcal{F}_{(\sigma)}$ develops a well or a bump around $\zeta = 0$, whose size is $\max(1/R_0, 1/R_9)$, and on both sides of which is a plateau (see figures 1, 2).

Large extra dimension regime. For completeness, we may ask what is the behavior of the free energy when the condition (2.13) is relaxed. When $R_d \gtrsim R_0$ or R_9, KK modes along X^d are lighter than $T_{(\sigma)}$ or $M_{(\sigma)}$ and their contributions to the free energy are no more exponentially suppressed. Similarly, the winding modes along $S^1(R_d)$ start contributing to the free energy when $R_d \lesssim 1/R_0$ or $1/R_9$. On the contrary, the $\tilde{n}_{\rm B}$ and $\tilde{n}_{\rm F}$ states being even heavier than when ζ sits on a plateau discussed above, they can be omitted in the evaluation of $\mathcal{F}_{(\sigma)}$. Under such conditions, one obtains [34]

$$\begin{aligned} f(z,\eta,\zeta) &= -(n_{\rm F}+n_{\rm B})\big[f_{\rm T}^{(d)}(z)+k_{\rm T}^{(d)}(z,\eta-|\zeta|)\big]+(n_{\rm F}-n_{\rm B})\big[f_{\rm V}^{(d)}(z)+k_{\rm V}^{(d)}(z,\eta-|\zeta|)\big] \\ &= e^{|\zeta|-\eta-z}\Big[-(n_{\rm F}+n_{\rm B})F_{\rm T}^{(d+1)}(z,\eta-|\zeta|)+(n_{\rm F}-n_{\rm B})F_{\rm V}^{(d+1)}(z,\eta-|\zeta|)\Big], \end{aligned} \tag{2.29}$$

where, in the first line, the functions $k_{\rm T}^{(d)}$ and $k_{\rm V}^{(d)}$ account for the additional corrections attributed to the KK or winding states,

$$\begin{aligned} k_{\rm T}^{(d)}(z,\eta-|\zeta|) &= \frac{\Gamma\left(\frac{d+1}{2}\right)}{\pi^{\frac{d+1}{2}}}\sum_{m_d\neq 0}\sum_{\tilde{k}_0,\tilde{k}_9}\frac{e^{dz}\,\mathcal{H}_{\frac{d+1}{2}}\left(\pi|m_d|e^{\eta-|\zeta|}\sqrt{e^{2z}(2\tilde{k}_0+1)^2+(2\tilde{k}_9)^2}\right)}{\left[e^{2z}(2\tilde{k}_0+1)^2+(2\tilde{k}_9)^2\right]^{\frac{d+1}{2}}}, \\ k_{\rm V}^{(d)}(z,\eta-|\zeta|) &= e^{(d-1)z}\;k_{\rm T}^{(d)}(-z,\eta-|\zeta|+z). \end{aligned} \tag{2.30}$$

In the second line of eq. (2.29), a Poisson summation on the momentum (or winding number) along $S^1(R_d)$ is performed, which yields

$$\begin{aligned} F_{\rm T}^{(d+1)}(z,\eta-|\zeta|) &= \frac{\Gamma\left(\frac{d+2}{2}\right)}{\pi^{\frac{d+2}{2}}}\sum_{\tilde{k}_0,\tilde{k}_9,\tilde{m}_d}\frac{e^{(d+1)z}}{\left[e^{2z}(2\tilde{k}_0+1)^2+(2\tilde{k}_9)^2+e^{-2(\eta-|\zeta|)}\tilde{m}_d^2\right]^{\frac{d+2}{2}}}, \\ F_{\rm V}^{(d+1)}(z,\eta-|\zeta|) &= e^{dz}F_{\rm T}^{(d+1)}(-z,\eta-|\zeta|+z). \end{aligned} \tag{2.31}$$

Much of the behavior of the free energy is captured in the regime $R_d \gg R_0, R_9$ (or $R_d \ll 1/R_0, 1/R_9$), which can be derived from the second expression in eq. (2.29). Defining $u = 1$ or -1 to treat both cases simultaneously, we obtain

$$\mathcal{F}_{(\sigma)} = 2\pi R_d^u T_{(\sigma)}^{d+1}\left[-(n_{\rm F}+n_{\rm B})\,f_{\rm T}^{(d+1)}(z)+(n_{\rm F}-n_{\rm B})\,f_{\rm V}^{(d+1)}(z)-\left(\frac{R_0}{R_d^u}\right)^d n_{\rm B}\xi'+\cdots\right], \tag{2.32}$$

where the ellipses stand for exponentially suppressed terms in R_d^u/R_0 and R_d^u/R_9, and

$$\xi' = \frac{\Gamma\left(\frac{d}{2}\right)}{\pi^{\frac{d}{2}}}\,\zeta(d). \tag{2.33}$$

JHEP03(2019)117

The factor $2\pi R_d^u$ of eq. (2.32) may be used to interpret the result in $d+1$ dimensions. However, from the d-dimensional point of view, this translates into an exponential behavior, $\mathcal{F}_{(\sigma)} \propto e^{|\zeta|}$ for $|\zeta| \to \infty$, which we took to be decreasing in figures 1 and 2. If this is so when $n_{\rm F} - n_{\rm B} \leq 0$, this is not always true when $n_{\rm F} - n_{\rm B} > 0$. In the latter case, we can use for $d+1$ the limits $z \to \pm\infty$ taken in eqs. (2.26) and (2.27) to conclude that the exponential behavior is decreasing for low enough e^z, and increasing for large enough e^z.

3 Dynamical stabilization / destabilization

In this section, we consider the free energy $\mathcal{F}_{(\sigma)} = T_{(\sigma)}^d f$ in generic models, namely with the function f given in eq. (2.21) (or (2.29)), for arbitrary $n_{\rm F}$, $n_{\rm B}$ and $\tilde{n}_{\rm F}$, $\tilde{n}_{\rm B}$. We want to show how the nature of the $\tilde{n}_{\rm F} + \tilde{n}_{\rm B}$ states becoming massless at $R_d = 1$ impacts the dynamics and final expectation value of R_d. After deriving the cosmological equations of motion, we review the evolution found for $\tilde{n}_{\rm F} - \tilde{n}_{\rm B} < 0$, which was considered in [34] and yields a stabilization of the modulus at the self-dual point. Then, we turn to our main case of interest, namely $\tilde{n}_{\rm F} - \tilde{n}_{\rm B} > 0$, which can trigger dynamically the destabilization of R_d from its self-dual point. During this process, the $\tilde{n}_{\rm F} + \tilde{n}_{\rm B}$ initially massless states acquire a large mass. Becoming non-relativistic, we will see in section 4 that they may realize a component of cold dark matter in our universe, given that they are stable on cosmological time scales.

3.1 Equations of motion and thermodynamics

Our starting point is the 1-loop effective action in d dimensions. Considering only the degrees of freedom relevant for the (de-)stabilization mechanism, we have

$$\mathcal{S} = \int \mathrm{d}^d x \sqrt{-g_{(\sigma)}} \left[e^{-2\phi} \left(\frac{\mathcal{R}_{(\sigma)}}{2} + 2\,\partial_\mu\phi\partial^\mu\phi - \frac{1}{2}\frac{\partial_\mu R_9 \partial^\mu R_9}{R_9^2} - \frac{1}{2}\frac{\partial_\mu R_d \partial^\mu R_d}{R_d^2} \right) - \mathcal{F}_{(\sigma)} \right], \tag{3.1}$$

where $g_{(\sigma)}$ is the string frame metric with signature $(-1,+\ldots,+)$, $\mathcal{R}_{(\sigma)}$ is the associated Ricci curvature, and ϕ is the dilaton in d dimensions. Defining the Einstein frame metric as

$$g_{\mu\nu} = e^{-\frac{4}{d-2}\phi} g_{(\sigma)\mu\nu}, \tag{3.2}$$

all dimensionful quantities acquire a dilaton dressing. In Einstein frame, the temperature, supersymmetry breaking scale and free energy density are therefore

$$T = \frac{e^{\frac{2}{d-2}\phi}}{2\pi R_0}, \qquad M = \frac{e^{\frac{2}{d-2}\phi}}{2\pi R_9} = \frac{e^{\sqrt{\frac{d-1}{d-2}}\Phi}}{2\pi}, \qquad \mathcal{F} = e^{\frac{2d}{d-2}\phi}\mathcal{F}_{(\sigma)} = T^d f(z,\eta,\zeta). \tag{3.3}$$

Note that we have introduced a new field Φ, the so-called "no-scale modulus" [45–48]. In fact, defining

$$\Phi = \sqrt{\frac{d-2}{d-1}}\left(\frac{2\phi}{d-2} - \eta\right), \qquad \Phi_\perp = \frac{1}{\sqrt{d-1}}\,(2\phi + \eta), \tag{3.4}$$

the action takes a suitable form in terms of canonical fields,

$$\mathcal{S} = \int \mathrm{d}^d x \sqrt{-g} \left[\frac{\mathcal{R}}{2} - \frac{1}{2}\partial_\mu\Phi\partial^\mu\Phi - \frac{1}{2}\partial_\mu\Phi_\perp\partial^\mu\Phi_\perp - \frac{1}{2}\partial_\mu\zeta\partial^\mu\zeta - \mathcal{F} \right]. \tag{3.5}$$

JHEP03(2019)117

Interested in flat, homogeneous and isotropic cosmological evolutions, we consider a Friedmann-Lemaître-Roberstson-Walker metric and space-independent scalar fields,

$$\mathrm{d}s^2 = -\beta(x^0)^2(\mathrm{d}x^0)^2 + a(x^0)^2\sum_{i=1}^{d-1}(\mathrm{d}x^i)^2, \quad \Phi(x^0), \quad \Phi_\perp(x^0), \quad \zeta(x^0), \tag{3.6}$$

where the lapse function β is found by analytic continuation of the Euclidean background. Hence, it is the circumference of $S^1(R_0)$ measured in Einstein frame, which is nothing but the inverse temperature,

$$\beta = e^{-\frac{2}{d-2}\phi}2\pi R_0 = \frac{1}{T}. \tag{3.7}$$

Friedmann equations can be found by varying the action with respect to β and a. They can be rewritten in terms of the more conventional cosmic time defined by $\mathrm{d}t = \beta\mathrm{d}x^0$:

$$\frac{(d-1)(d-2)}{2}H^2 = \mathcal{K} + \rho, \tag{3.8}$$

$$\frac{(d-1)(d-2)}{2}H^2 + (d-2)\dot{H} = -\mathcal{K} - P, \tag{3.9}$$

where dot-derivatives are with respect to t and $H = \dot{a}/a$. In the above equations, $\mathcal{K}$ is the kinetic energy of the scalars, while ρ and P are the energy density and pressure arising from the 1-loop contribution $\mathcal{F}$,

$$\mathcal{K} = \frac{1}{2}\left(\dot{\Phi}^2 + \dot{\Phi}_\perp^2 + \dot{\zeta}^2\right), \qquad \rho = \mathcal{F} - T\frac{\partial\mathcal{F}}{\partial T}, \qquad P = -\mathcal{F}. \tag{3.10}$$

Notice that the variational principle we have used matches perfectly with the thermodynamics laws,

$$\rho = \frac{1}{V}\left(\frac{\partial(\beta F)}{\partial\beta}\right)_V, \quad P = -\left(\frac{\partial F}{\partial V}\right)_\beta, \quad \text{where} \quad V = (2\pi a)^{d-1}, \quad F = V\mathcal{F}. \tag{3.11}$$

For convenience, we may write the thermal energy density and pressure as

$$\rho = T^d r(z,\eta,\zeta), \quad P = T^d p(z,\eta,\zeta), \quad \text{where} \quad r = f_z - (d-1)f, \quad p = -f, \tag{3.12}$$

and $f_x = \partial f/\partial x$, for $x = z, \eta, \zeta$. With these notations, the scalar-field equations of motion take the form,

$$\ddot{\Phi} + (d-1)H\dot{\Phi} = -\frac{\partial\mathcal{F}}{\partial\Phi} = -T^d\left(\sqrt{\frac{d-1}{d-2}}\,f_z - \sqrt{\frac{d-2}{d-1}}\,f_\eta\right), \tag{3.13}$$

$$\ddot{\Phi}_\perp + (d-1)H\dot{\Phi}_\perp = -\frac{\partial\mathcal{F}}{\partial\Phi_\perp} = -\frac{T^d}{\sqrt{d-1}}\,f_\eta, \tag{3.14}$$

$$\ddot{\zeta} + (d-1)H\dot{\zeta} = -\frac{\partial\mathcal{F}}{\partial\zeta} = -T^d f_\zeta. \tag{3.15}$$

Combining the equations, it can be seen that eq. (3.9) can be replaced by an equation that can be solved [34],

$$\frac{\dot{\rho}+\dot{P}}{\rho+P} + (d-1)H = \frac{\dot{T}}{T} \quad \Longrightarrow \quad (aT)^{d-1}\big(r(z,\eta,\zeta) + p(z,\eta,\zeta)\big) = S, \tag{3.16}$$

JHEP03(2019)117

where S is the integration constant. The latter can be interpreted as the entropy of the universe since the above result implies

$$U - TS = -PV \equiv F, \quad \text{where} \quad U = V\rho. \tag{3.17}$$

3.2 Radiation-like dominated solutions and stabilization

When the supplementary massless states at the self-dual point contain more bosons than fermions, $\tilde{n}_{\rm F} - \tilde{n}_{\rm B} < 0$ (recall that this means ϵ even in our example as defined in eq. (2.5)), the thermal effective potential $\mathcal{F}$ admits a local minimum at $\zeta = 0$ (see figure 1). As shown in [34], this can yield a dynamical stabilization of ζ at the origin. In this subsection, we review these results, since they will be used later on to infer the behavior of the more involved mechanism of mass generation for dark matter.

Stabilization at the bottom of the well. Let us first describe a particular cosmological solution. Clearly, $\zeta \equiv 0$ solves eq. (3.15). Since $f(z, \eta, 0)$ is independent of η, eq. (3.14) is satisfied for an arbitrary constant $\Phi_\perp \equiv \Phi_{\perp 0}$. It turns out to be convenient to replace eq. (3.13) by a differential equation for z. The latter involves a potential for z, which admits a minimum at some critical point $\tilde{z}_{\rm c}$ if and only if the massless spectrum of the model satisfies

$$0 < \frac{N_{\rm F} - N_{\rm B}}{N_{\rm F} + N_{\rm B}} < \frac{1}{2^d - 1}. \tag{3.18}$$

In that case, $z \equiv \tilde{z}_{\rm c}$ is a solution, where $\tilde{z}_{\rm c}$ is the unique root of the equation

$$\tilde{r}(\tilde{z}_{\rm c}) = d\tilde{p}(\tilde{z}_{\rm c}), \quad \text{where} \quad \tilde{r}(z) \equiv r(z, \eta, 0), \quad \tilde{p}(z) \equiv p(z, \eta, 0) > 0. \tag{3.19}$$

Note that this corresponds to the state equation of radiation in $d+1$ dimensions, $\rho = d \times P$.[4] When the model-dependent quantity $(N_{\rm F} - N_{\rm B})/(N_{\rm F} + N_{\rm B})$ varies from 0 to its upper bound, $\tilde{z}_{\rm c}$ varies from $+\infty$ to $-\infty$.[5] We are left with the Friedmann equation (3.8), which turns out to take the form $H^2 = \tilde{C}_{\rm r}/a^d$. Ultimately, we find a critical solution

$$\begin{aligned} &\zeta \equiv 0, \quad \Phi_\perp \equiv \Phi_{\perp 0}, \quad M(t) \equiv T(t) \times e^{\tilde{z}_{\rm c}} \equiv \frac{1}{a(t)} \times e^{\tilde{z}_{\rm c}} \left(\frac{S}{\tilde{r}(\tilde{z}_{\rm c}) + \tilde{p}(\tilde{z}_{\rm c})} \right)^{\frac{1}{d-1}}, \\ &\text{where} \quad a(t) = t^{\frac{2}{d}} \times \left(\frac{d}{2} \sqrt{\tilde{C}_{\rm r}} \right)^{\frac{2}{d}}, \quad \tilde{C}_{\rm r} = \frac{2(d-1)}{d(d-2)^2} \, \tilde{r}(\tilde{z}_{\rm c}) \left(\frac{S}{\tilde{r}(\tilde{z}_{\rm c}) + \tilde{p}(\tilde{z}_{\rm c})} \right)^{\frac{d}{d-1}} > 0. \end{aligned} \tag{3.20}$$

To summarize, the supersymmetry breaking scale and the temperature evolve proportionally to the inverse of the scale factor. Moreover, this solution is compatible with weak string coupling. This can be seen by using eq. (3.4) to derive the time-dependence of the dilaton,

$$e^{2\frac{d-1}{d-2}\phi(t)} = 2\pi M(t)\, e^{\sqrt{d-1}\Phi_{\perp 0}}, \tag{3.21}$$

which decreases with time.

[4] With n internal circles involved in the Scherk-Schwarz breaking of supersymmetry, this generalizes to $\rho = (d - 1 + n)P$ [33].

[5] We may include the lower bound 0 in eq. (3.18), at which we formally have $\tilde{z}_{\rm c} = +\infty$. In that case, $z(t)$ is actually running away rather than being stabilized at some finite value. The class of theories satisfying $N_{\rm F} = N_{\rm B}$ and sometimes referred to as "super no-scale models" may be of particular interest [41, 42, 44, 49–54].

JHEP03(2019)117

Note that along this very peculiar trajectory, $H^2 \propto T^d$ as if the universe was filled with pure radiation in d dimensions, which seems in contradiction with the result $\rho = d \times P$. In fact, using Friedmann equation (3.8), the puzzle is resolved by observing that the *total* energy density and pressure satisfy

$$\left.\begin{aligned} \rho_{\rm tot} &= \frac{1}{2}\dot{\Phi}^2 + \rho = \frac{(d-1)^2}{d(d-2)}\,\rho \\ P_{\rm tot} &= \frac{1}{2}\dot{\Phi}^2 + P = \frac{d-1}{d(d-2)}\,\rho \end{aligned}\right\} \quad \Longrightarrow \quad \rho_{\rm tot} = (d-1)P_{\rm tot}. \tag{3.22}$$

In other words, the classical kinetic energy of the no-scale modulus combines with the thermal free energy of the infinite towers of KK modes along X^9, to yield a "radiation-like" cosmological evolution i.e. indistinguishable with that of a universe only filled with thermalized massless states.

The local stability of this solution against small fluctuations has been shown analytically in [34] for $d \geq 4$.[6] Hence, for arbitrary initial conditions close enough to the trajectory of eq. (3.20), the generic evolution is attracted to the critical one. For this reason, we refer to these generic cosmological evolutions as "radiation-like dominated solutions". When converging to $\tilde{z}_{\rm c}$, $z(t)$ may or may not oscillate, depending on the initial conditions. Moreover, ζ always undergoes damped oscillations and eventually stabilizes at 0. Notice that this is a remarkable effect. In the literature, when such a scalar field has a constant mass and oscillates in a well, its energy does not dilute fast enough when the universe expands, the scalar does not stabilize, and the universe is not entering in a radiation-dominated era. To bypass this fact, known as the "cosmological moduli problem", the decay of the massive scalar field is invoked, which can lead to new difficulties such as an excessive entropy production [37, 38].

The cosmological moduli problem does not occur in our string theory framework because the mass m (measured in Einstein frame) of ζ is not constant. From eq. (2.28), we find

$$m^2 = \frac{2}{\pi}\, e^{\frac{4}{d-2}\phi}\, T^{d-2}, \tag{3.23}$$

which drops with time and increases the damping of the oscillations of ζ, which is not anymore solely due to the friction resulting from the expansion of the universe. Eventually, the energy stored in the modulus dilutes faster than the radiation-like density $\rho_{\rm tot}$ (or its component associated with the $N_{\rm F} + N_{\rm B}$ true species of radiation), so that ζ stabilizes.[7]

For completeness, we point out that when $(N_{\rm F} - N_{\rm B})/(N_{\rm F} + N_{\rm B}) > 1/(2^d - 1)$, the supersymmetry breaking direction X^9 spontaneously decompactifies, and the supersymmetry

[6] See also [55, 56], for supersymmetric theories at finite temperature.

[7] The generic solution for $d = 3$ turns out to be "marginally radiation-like dominated", in the following sense. As in higher dimensions, $t^{-\frac{2}{3}}a(t)$ and $a(t)T(t)$ converge to constants, while $z(t) \to z_c$ and $\zeta(t) \to 0$. However, the asymptotic behavior of $\Phi_\perp(t)$ is logarithmic rather than constant, and $\dot{\zeta}^2/H^2$ oscillates *without* damping. Altogether, we have $\#H^2 \sim \#\dot{\Phi}_\perp^2 \sim \frac{1}{2}\dot{\Phi}^2 + \frac{1}{2}\dot{\zeta}^2 + \rho$. This means that for $d = 3$, the definitions of $\rho_{\rm tot}$ and $P_{\rm tot}$ should include the kinetic energies of $\Phi_\perp$ and ζ in addition to that of Φ, to satisfy the "radiation-like" state equation $\rho_{\rm tot} \sim 2P_{\rm tot}$. If the above behavior can be checked numerically, it could also be shown as in [56], which analyzes the pure thermal case (i.e. without supersymmetry breaking). In the latter case, though, the generic solution is "marginally radiation-like dominated" for $d = 4$, rather than $d = 3$.

JHEP03(2019)117

breaking is screened by thermal effects. The generic evolution is naturally interpreted in a $(d+1)$-dimensional anisotropic universe, which is radiation dominated [35]. Our purpose being eventually to describe the destabilization of ζ arising when supersymmetry breaking effects dominate over thermal ones, this case in not interesting to us in the present work. Alternatively, when $(N_{\rm F}-N_{\rm B})/(N_{\rm F}+N_{\rm B})<0$, the initially expanding universe stops growing and then collapses, with domination of moduli kinetic energy [31]. These remarks justify why we restrict our models to satisfy eq. (3.18).

Freezing along the plateaus. The above attractor mechanism is only local, in the sense that initial conditions too far from the critical solution with $\zeta=0$ may yield a different behavior. In particular, when ζ is along one of the plateaus shown in figure 1, the $\tilde{n}_{\rm F}+\tilde{n}_{\rm B}$ states are heavier than T and M and yield exponentially suppressed contributions. Neglecting these terms, we have

$$f(z,\eta,\zeta)=-(n_{\rm F}+n_{\rm B})f_{\rm T}^{(d)}(z)+(n_{\rm F}-n_{\rm B})f_{\rm V}^{(d)}(z). \tag{3.24}$$

Let us first describe a new critical solution. Clearly, the equations of motion (3.15) and (3.14) of ζ and $\Phi_\perp$ are satisfied when these fields are arbitrary constants ζ_0 and $\Phi_{\perp 0}$. As explained in [34], one can proceed as before and find that, provided that the model satisfies

$$0<\frac{n_{\rm F}-n_{\rm B}}{n_{\rm F}+n_{\rm B}}<\frac{1}{2^d-1}, \tag{3.25}$$

a particular solution exists with constant $z\equiv z_{\rm c}$, where $z_{\rm c}$ is the unique root of the equation[8]

$$\hat{r}(z_{\rm c})=d\hat{p}(z_{\rm c}),\quad \text{where}\quad \hat{r}(z)\equiv r(z,\eta,0),\quad \hat{p}(z)\equiv p(z,\eta,0). \tag{3.26}$$

Altogether, this peculiar evolution is

$$\begin{aligned}&\zeta\equiv\zeta_0,\quad \Phi_\perp\equiv\Phi_{\perp 0},\quad M(t)\equiv T(t)\times e^{z_{\rm c}}\equiv\frac{1}{a(t)}\times e^{z_{\rm c}}\left(\frac{S}{\hat{r}(z_{\rm c})+\hat{p}(z_{\rm c})}\right)^{\frac{1}{d-1}},\\ &\text{where}\quad a(t)=t^{\frac{2}{d}}\times\left(\frac{d}{2}\sqrt{\hat{C}_{\rm r}}\right)^{\frac{2}{d}},\quad \hat{C}_{\rm r}=\frac{2(d-1)}{d(d-2)^2}\,\hat{r}(z_{\rm c})\left(\frac{S}{\hat{r}(z_{\rm c})+\hat{p}(z_{\rm c})}\right)^{\frac{d}{d-1}}>0,\end{aligned} \tag{3.27}$$

which is radiation-like. It is also stable against small fluctuations. In other words, initial conditions close enough to the trajectory (3.27) yield evolutions attracted to the critical one, and are therefore radiation-like dominated.

No eternal fall out of the plateaus. For completeness, even if we will not make use of this property in the dark-matter generation mechanism described in the following section, we mention that the attraction towards the flat regions of the thermal effective potential of ζ is even stronger than may be expected. When the exponential behavior of $\mathcal{F}_{(\sigma)}$ is decreasing, as shown in figures 1 and 2, we may worry about the possibility that $|\zeta|$ falls out of the plateaus when it rolls enough to exceed $\min(\ln R_0,\ln R_9)$. In that case, one may

[8] As in footnote 5, we may include the lower bound 0 in eq. (3.25), and have $z(t)$ running away towards $z_{\rm c}$ formally equal to $+\infty$.

JHEP03(2019)117

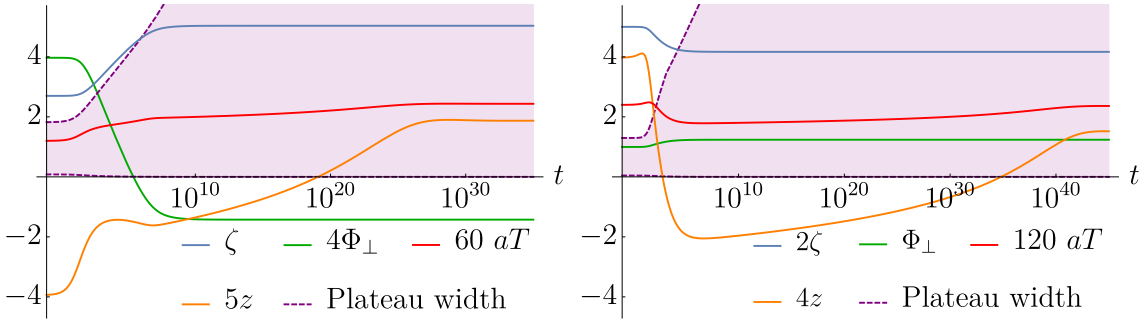

Figure 3. (a) Numerical simulation of $\zeta(t)$, $z(t)$, $\Phi_\perp(t)$ and $a(t)T(t)$, when ζ sits initially in the decreasing exponential part of its potential (see figures 1 and 2). The purple dashed curve shows the width of the plateau which increases with time. $\zeta(t)$ begins by increasing while falling along the potential until it is caught by the growing plateau. It then stabilizes while $z(t)$, $\Phi_\perp(t)$ and $a(t)T(t)$ eventually reach their asymptotic values. (b) Same simulation when the exponential region of the thermal potential increases with ζ, at initial time. $\zeta(t)$ begins by decreasing, thus approaching the plateau where it eventually freezes.

think that the internal direction X^d may spontaneously decompactify. However, analytic arguments in favor of an attraction of $|\zeta|$ back to the plateaus was raised in [34, 35]. To figure out what is going on, we can simulate numerically the system of differential equations when ζ is initially located on the waterfall part of the potential, with low enough velocity. The evolutions in 4 dimensions of $\zeta(t)$, $z(t)$, $\Phi_\perp(t)$ and the product $a(t)T(t)$ are plotted for a set of generic initial conditions in figure 3a. While it is not a surprise to see $|\zeta(t)|$ to increase, the boundary $\min(\ln R_0(t), \ln R_9(t))$ of the plateau (delimited by the shaded area) increases faster and eventually catches up $\zeta(t)$. When the latter is back to the plateau, the evolution is attracted as before towards the critical solution of eq. (3.27).

When $n_{\rm F} - n_{\rm B} > 0$ while e^z is large enough, the exponential behavior of $\mathcal{F}_{(\sigma)}$ as a function of ζ is increasing. When this is the case, the attraction back to the plateau is naturally expected to be even more efficient than in the above waterfall case. As shown in figure 3b, this expectation turns out to be confirmed by numerical simulation. As seen on the plots, $|\zeta(t)|$ starts by decreasing and then freezes once it is caught by the plateau. Notice however, that as long as $z(t) > 0$ holds, the width of the plateaus is given by $\ln R_9(t)$, while when $z(t) < 0$ it is determined by $\ln R_0(t)$. As a result, a change of the slope of the time-dependent length of the plateaus is observed when $z(t) \simeq 0$.

3.3 Dynamical phase transition and mass generation

We are now ready to describe the mechanism that triggers the phase transition responsible for generating large masses for states that will be interpreted as dark-matter constituents in the next section. The key point is to have an excess of massless fermionic modes at the self-dual point, $\tilde{n}_{\rm F} - \tilde{n}_{\rm B} > 0$ (ϵ odd in our example).

JHEP03(2019)117

Qualitative expectations and specification of the models. In order to infer what the mechanism will turn to lead to, let us remind what we learned from eq. (2.28). When T is sufficiently larger than M (i.e. e^z is small enough), ζ is massive. Assuming ζ to be initially in its potential well (see figure 1), provided that eq. (3.18) holds, we expect the generic cosmological evolution to approach the critical solution of eq. (3.20). This attraction may be definitive, if $e^{\tilde{z}_c}$ is low enough for maintaining ζ massive throughout the convergence of the evolution towards the critical one. In that case, the behavior of the universe is identical to that described for $\tilde{n}_F - \tilde{n}_B < 0$, with a stabilization of ζ at the origin.

However, in models such that $e^{\tilde{z}_c}$ is large enough for ζ to be tachyonic, the above attraction of $z(t)$ towards $\tilde{z}_c$ forces the squared mass of ζ to change sign during the evolution. The critical solution still exists, but becomes unstable at this stage. In fact, the potential well of ζ becomes the bump shown in figure 2 and a Higgs-like transition is expected to occur, responsible for the destabilization of ζ away from the origin. The latter slides along the bump until it reaches one of the plateaus. Once there, assuming that eq. (3.25) is satisfied, we have shown in the previous section that ζ gets frozen, due to the friction arising from the expansion of the universe. The final behavior of the evolution is thus attracted to the critical solution, eq. (3.27), and is therefore radiation-like dominated.

To summarize, for the mechanism to take place, the following conditions must hold:

$$\begin{aligned}
&(i) \quad \tilde{n}_F - \tilde{n}_B > 0 && \text{(more extra massless fermions than bosons at } \zeta = 0\text{)},\\
&(ii) \quad 0 < \frac{n_F - n_B}{n_F + n_B} \text{ and } \frac{N_F - N_B}{N_F + N_B} < \frac{1}{2^d - 1} && (z_c \text{ and } \tilde{z}_c \text{ exist}),\\
&(iii) \quad f_T^{(d-2)}(\tilde{z}_c) < \frac{\tilde{n}_F - \tilde{n}_B}{\tilde{n}_F + \tilde{n}_B} f_V^{(d-2)}(\tilde{z}_c) && (\zeta \text{ tachyonic at } z = \tilde{z}_c).
\end{aligned} \tag{3.28}$$

In our examples, these constraints translate into

$$(i) \ \epsilon \text{ odd}, \qquad (ii) \ 0 < 8 - d_{en} \text{ and } \frac{10 - d_{en}}{506 + d_{en}} < \frac{1}{2^d - 1}, \qquad (iii) \ \tilde{z}_c > 0, \tag{3.29}$$

which admit solutions in various dimensions:

- For $d = 3$, we can have $d_{en} = 0, 2, 4, 6$. The limit case $d_{en} = 8$ can be included if we allow $\tilde{z}_c$ to be $+\infty$. The d_{en} roots of G_{en} can be realized at SU(2) and/or SU(3) enhanced gauge symmetry points of the Narain lattice of the internal T^5.
- For $d = 4$, $d_{en} = 0, 2, 4, 6$ (and possibly 8) are allowed. The d_{en} roots can be realized at SU(2) and/or SU(3) points of the Narain lattice of T^4.
- For $d = 5$, only $d_{en} = 4, 6$ (or 8) are allowed and realized at SU(2) and/or SU(3) points of the Narain lattice of T^3.
- There is no solution for $d = 6$, 7 and 8 in our examples.

Numerical simulations. Unlike critical solutions that describe asymptotic behaviors, the phase transition is a transient regime. Thus, solving analytically the equations of motions to describe explicitly the associated solutions for generic initial conditions is difficult.

JHEP03(2019)117

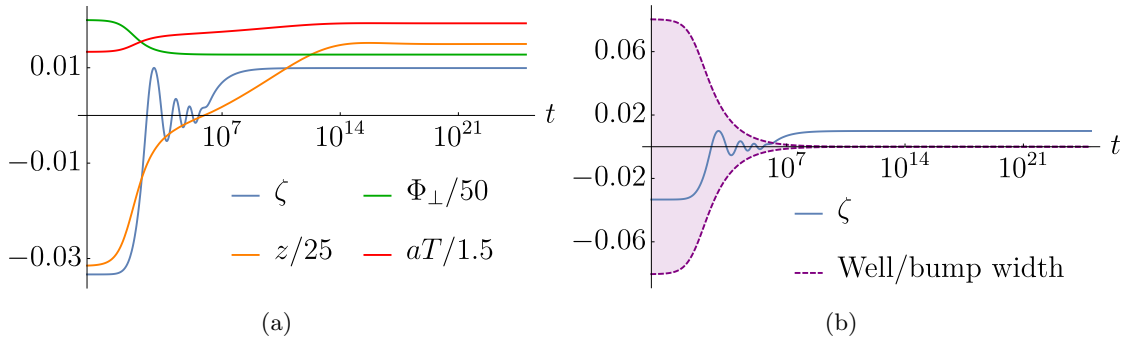

Figure 4. (a) Numerical simulation for $d = 4$ of $\zeta(t)$, $z(t)$, $\Phi_\perp(t)$ and $a(t)T(t)$, in a model that realizes the dynamical phase transition responsible for a large mass generation of initially massless states. $\zeta(t)$ oscillates with damping around 0 as long as $z(t) < 0$. When the latter become positive, $\zeta(t)$ condenses away from the origin. (b) The shaded area represents the width of the well or bump. The oscillations are within the well, while freezing takes place away from the bump, where the potential for ζ is flat.

For this reason, we have simulated numerically the system of differential equations. The results match with all the qualitative expectations described above.

Our choice of initial conditions at $t = 0$ is such that the universe expands ($\dot{a}(0) > 0$), with the temperature $T(0)$ slightly higher than the supersymmetry breaking scale $M(0)$ ($z(0) \lesssim 0$). Moreover, $\zeta(0)$ is anywhere in its well, with low enough velocity. Notice that if we assume throughout this paper the temperature (and supersymmetry breaking scale) to be lower than the Hagedorn temperature, $R_0 > R_H$, naturalness invites us to choose $R_0(0)$ equal to few units (counted in $\sqrt{\alpha'}$).[9] Note that such a radius $R_0(0)$ is enough for neglecting the exponentially suppressed contributions to the free energy, as done in section 2. Second, the well has an initial width which is not very small, say of order 1/10, and no severe fine tuning is required for $\zeta(0)$ to sit inside it.

As shown in figure 4a, letting the system evolve in $d = 4$ dimensions, $\zeta(t)$ starts oscillating with damping around the origin, while $z(t)$ is increasing (to approach $\tilde{z}_c > 0$). It is only when $z(t)$ becomes positive, so that the well turns into a bump, that ζ, which is still close to 0, acquires some potential energy and eventually starts sliding along the hill before freezing. Meanwhile, $z(t)$ and $\Phi_\perp(t)$ converge to $z_c > 0$ and some constant $\Phi_{\perp 0}$, while the product $a(t)T(t)$ also reaches a constant value. Notice that in figure 4a, because the final value of $|\zeta|$ is lower than $|\zeta(0)|$, one may think that the modulus remains stuck on the bump. However, the width of the hill decreases with time and eventually the motion of the modulus is coming to an end along a plateau. This can be seen on figure 4b, which shows the evolution of the width of the bump with time. To be specific, for the particular initial conditions we have chosen in the simulation, the final (string frame) mass $|R_d - 1/R_d| \simeq 2|\zeta|$ of the $\tilde{n}_F + \tilde{n}_B$ states is of the order of 2% of the string scale, which is

[9] This is at least the case if we imagine that the cosmological era we describe is occurring right after a Hagedorn era characterized by a temperature $T_{(\sigma)}$ comparable to the string scale. Such an intrinsically stringy epoch may describe a change of string vacuum [57–60], or bouncing cosmologies [61, 62], which are alternative to the big bang and inflationary scenarios.

JHEP03(2019)117

rapidly several orders of magnitude larger than $T_{(\sigma)}$ and $M_{(\sigma)}$ that keep on dropping. As a result, the $\tilde{n}_{\rm F} + \tilde{n}_{\rm B}$ modes yield exponentially suppressed contributions to the free energy, thus implying ζ to sit on a plateau.

Before proceeding, we would like to stress that for the sake of simplicity, we have only allowed in our analytic and numerical analyzes a minimal set of moduli fields to vary. In particular, we could have treated the 4 degrees of freedom $(G + B)_{ij}$ in eq. (2.5) as dynamical, by generalizing the results of [43] in presence of finite temperature. However, the mass generation mechanism we have presented would still take place. Moreover, it turns out that in our simple model, the SO(16) × SO(16) Wilson lines are tachyonic for large enough e^z [41–43], and it could be artificial to maintain them static.[10] However, type I string models that satisfy the constraint $n_{\rm F} - n_{\rm B} > 0$ and are tachyon free have been recently constructed [63], and the phase transition we have discussed may be implemented in their heterotic dual descriptions.

4 Relic density evolution

The ratio of the mass induced by the phase transition to the temperature being large, the Boltzmann number density of the $\tilde{n}_{\rm F} + \tilde{n}_{\rm B}$ (with $\tilde{n}_{\rm F} - \tilde{n}_{\rm B} > 0$ in generic models) initially massless degrees of freedom may drastically decrease. In the present section, we explain how the expansion of the universe may nevertheless imply a non-trivial relic density of non-relativistic matter to survive.

4.1 Dark-matter thermal freeze-out

In the well-known *thermal* scenario of cosmology, the dark-matter number density evolution throughout the universe history results from the competition between two opposite effects: on the one hand, number-depleting interactions between dark matter and the Standard Model[11] (typically, through its annihilation cross-section $\sigma_{\rm DM\leftrightarrow SM}$) give the possibility for dark-matter particles to constantly readjust their number density $n_{\rm DM}$ to its Boltzmann equilibrium value $n_{\rm DM,eq}$. The processes by which this happens are two-to-two, of the form DM + DM → SM + SM. On the other hand, the expansion of the universe tends to make interactions between dark-matter and Standard-Model particles more unlikely to happen, since it lowers their respective number densities. Hence, such a dilution renders a thermal equilibrium between dark-matter and Standard-Model particles more difficult to maintain.

Before presenting how our string theory framework provides an alternative way to generate a non-relativistic component of the universe energy density, let us first review how a non-vanishing relic density of dark matter is generated in the usual thermal scenario.

[10] To figure out whether they can be destabilized or not, the ratio M/T above which they are tachyonic should be compared with e^{z_c}.

[11] Note that number-depleting interactions within the dark sector could also maintain a thermal equilibrium in the dark sector with its own temperature. In that case, all occurrences of "Standard-Model particles" in the coming text should be replaced by "massless dark-matter particles". However, it is natural to assume gauge interactions between the dark sector and the visible sector if we deal with only one temperature.

JHEP03(2019)117

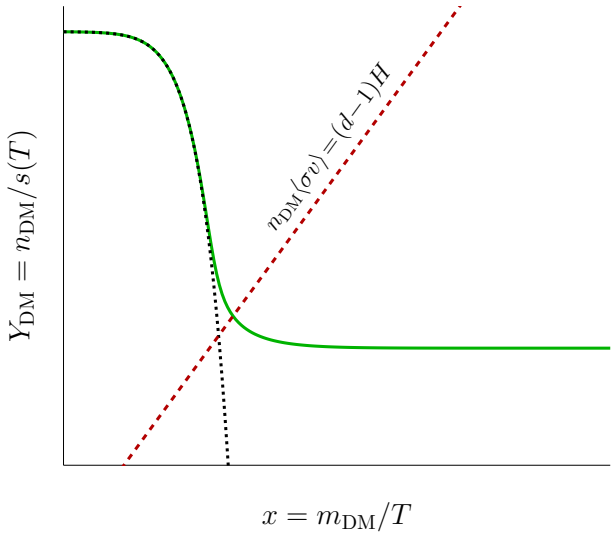

Figure 5. Evolution of the dark-matter yield $Y_{\rm DM} = n_{\rm DM}/s$ as a function of $x = m_{\rm DM}/T$ in the standard thermal scenario, in 4 dimensions (green solid line). The black-dotted line represents the value that the yield would follow if thermal equilibrium could be maintained all along the history of the universe. Freeze-out takes place when interactions with the Standard-Model particles are too weak, as compared to the expansion rate of the universe (after crossing of the red dashed line).

Cold dark matter scenario. In the standard thermal scenario,[12] a dark-matter particle has a constant mass $m_{\rm DM}$, and interacts with the Standard Model through two-to-two processes, whose annihilation cross-section is denoted $\sigma_{\rm DM\leftrightarrow SM}$. For visualizing the chronology of the dark-matter number density, we draw in figure 5 the typical evolution of the so-called yield,

$$Y_{\rm DM} = \frac{n_{\rm DM}(T)}{s(T)}, \tag{4.1}$$

where $s(T) \propto T^{d-1} \propto 1/a^{d-1}$ is the entropy density of the thermal bath. In this figure, the evolution is parametrized by $x = m_{\rm DM}/T$, and we have chosen arbitrary values of the dark-matter mass and annihilation cross-section. The thermal scenario of cold dark-matter production can be summarized as follows:

- $T \gg m_{\rm DM}$: at early times, both dark-matter and Standard-Model particles are relativistic. If their interactions are strong enough, dark matter is maintained chemically in thermal equilibrium with the Standard-Model bath so that $n_{\rm DM} = n_{\rm DM,eq} \propto T^{d-1}$. The entropy density of the universe evolving as $s \propto T^{d-1}$, the dark-matter yield $Y_{\rm DM} = n/s$ is initially constant, as can be seen on the left-hand side of figure 5. Quantitatively, the interaction is strong enough when $(d-1)H < n_{\rm DM}\langle\sigma_{\rm DM\leftrightarrow SM} v\rangle$, where v stands for the dark-matter particles relative velocities and the brackets $\langle\cdots\rangle$ denote the mean over velocity distribution.

[12] In standard cosmology, there is no dynamical dilaton field and the Einstein frame is always implicit.

JHEP03(2019)117

- $T \lesssim m_{\rm DM}$: when the temperature drops under the dark-matter mass, dark-matter particles become non-relativistic. The Boltzmann distribution becomes exponentially suppressed, $n_{\rm DM,eq} \sim e^{-m/T}$, and dark-matter particles tend to annihilate more and more into Standard-Model particles in order to maintain equilibrium, therefore lowering their number density (see figure 5, where the black-dotted and green-solid lines drop together). Standard-Model particles which have energy $\langle E \rangle \sim T$ are less and less able to produce them back. Again, such number depletion is possible as long as interactions are strong enough i.e. the condition $(d-1)H < n_{\rm DM}\langle\sigma_{\rm DM\leftrightarrow SM}v\rangle$ is still satisfied.

- $T \lesssim m_{\rm DM}$ and $(d-1)H \gtrsim n_{\rm DM}\langle\sigma_{\rm DM\leftrightarrow SM}v\rangle$: after dark-matter particles started annihilating significantly into Standard Model particles, the expansion rate of the universe can dominate over the annihilation rate, which leads to a *chemical* decoupling. In figure 5, this corresponds to the point where the red dashed curve is crossed. The universe being radiation dominated before chemical decoupling, this curve turns out to satisfy $Y_{\rm DM} \propto x^{\frac{d}{2}-1}$, which is linear for $d = 4$. At the crossing, the annihilation of dark matter stops, dark-matter particles *freeze-out*, and a relic density of dark-matter particles remains as a non-relativistic component of the universe. Thus, the number density evolves again as $n_{\rm DM} \propto 1/a^{d-1} \propto T^{d-1}$ and the yield becomes constant.

Formally speaking, such a freeze-out can be described by the Boltzmann equation, in terms of the dark-matter number density $n_{\rm DM}(t)$,

$$\frac{{\rm d}n_{\rm DM}}{{\rm d}t} + (d-1)Hn_{\rm DM} = -\langle\sigma_{\rm DM\leftrightarrow SM}v\rangle\left[n_{\rm DM}^2 - n_{\rm DM,eq}^2\right]. \tag{4.2}$$

In this formulation, Standard-Model particles are assumed to be in thermal equilibrium. Moreover, the dark-matter particles number density at equilibrium is defined as

$$n_{\rm DM,eq}(t) = \tilde{n}\int \frac{{\rm d}^{d-1}\vec{k}}{(2\pi)^{d-1}} \frac{1}{e^{\frac{\sqrt{m_{\rm DM}^2+\vec{k}^2}}{T(t)}} \pm 1}, \tag{4.3}$$

where $\tilde{n}$ is the number of dark-matter degrees of freedom, with either Bose-Einstein of Fermi-Dirac statistics and the integration runs over the momentum $\vec{k}$ of the particles. Neglecting the expansion rate $(d-1)Hn_{\rm DM}$ in eq. (4.2), an over-density (under-density) of dark-matter particles as compared to the equilibrium value would pull (push) the dark-matter density back to its equilibrium value. Therefore, as long as the expansion term can be neglected as compared to the interaction term in the right-hand side of eq. (4.2), the dark-matter density follows its equilibrium value,

$$n_{\rm DM} \simeq n_{\rm DM,eq} \qquad \text{(before freeze-out)}. \tag{4.4}$$

Conversely, when the expansion starts dominating over interactions in the equation, one can neglect the right-hand side and obtain

$$n_{\rm DM} \propto \frac{1}{a^{d-1}} \qquad \text{(after freeze-out)}. \tag{4.5}$$

JHEP03(2019)117

The neutrino case. So far, we have been discussing the case of a cold dark matter, decoupling from the thermal bath after it becomes non-relativistic. This guarantees that the dark matter is cold enough for not streaming freely on large distances after it is produced, ensuring that the large scale structures are preserved, in agreement with present cosmological measurements [64].

Nevertheless, the condition that a particle becomes non-relativistic before it decouples from the thermal bath is not necessary. In fact, as long as its interaction with Standard-Model particles becomes weak enough at a temperature larger than the dark-matter mass, dark-matter particles can still be relativistic when they freeze-out. This is exactly what happens to neutrinos, which decouple at a temperature $T \sim$ MeV from the thermal bath, far before they become non-relativistic. This mechanism will take place in some circumstances in the string theory framework we are now turning to.

Our string theory scenario. As mentioned above, experimental constraints on structure formation impose that dark matter constitutes today a large, non-relativistic component of the energy density.

Moreover, we have seen that the key point for a cold dark-matter scenario to be successful is to have at some point the temperature lower than the dark-matter mass, and to ensure that its interaction with radiation is weak enough, for a significant amount of dark-matter particles to remain frozen after they decouple. In string theory, gauge interactions between the dark and visible sectors may or may not exist. In the examples we have constructed in section 2, our main motivation was to present the simplest realization of a phase transition responsible for a mass generation of initially massless states. Being maximally supersymmetric (in a spontaneously broken version, e.g. $\mathcal{N} = 4 \to \mathcal{N} = 0$ in 4 dimensions), massless matter cannot be chiral and there is no Standard-Model to discuss in this context. However, models compatible with chirality [65–68] and realizing an $\mathcal{N} = 1 \to \mathcal{N} = 0$ spontaneous breaking of supersymmetry in four dimensions may be considered. For instance, they can be realized via orbifold compactifications or fermionic constructions. Implementing the mass generation mechanism in such models, dark and Standard-Model sectors may for instance be unified prior to the phase transition in a gauge theory based on E_6, SO(10), a Pati-Salam gauge group, etc. In such a case, a significant annihilation cross section $\sigma_{\mathrm{DM}\leftrightarrow\mathrm{SM}}$ is then natural. In the following, we assume the string theory model to be realistic enough for such a non-trivial cross-section to exist. Other possibilities may however be considered, as noticed in footnote 11.

In the standard thermal scenario, before freeze-out, when the universe is radiation dominated, as well as after dark matter decouples, the (approximate) relations $s \propto T^{d-1} \propto 1/a^{d-1}$ we have used extensively hold. Instead, the cosmological evolution derived from string theory before freeze-out is radiation-like dominated and satisfies eq. (3.16). To be specific, prior to the phase transition, ζ oscillates in the well, and the evolution approaches the critical, radiation-like solution (3.20). Similarly, if the destabilization process ends and ζ is stuck on a plateau, the evolution is attracted towards the second critical, radiation-like evolution, eq. (3.27). Hence, before freeze-out, the (approximate) relations $s \propto T^{d-1} \propto 1/a^{d-1}$ hold and the yield definition in eq. (4.1) can be used as in the standard thermal

JHEP03(2019)117

scenario. However, after dark matter decouples from the thermal bath and eventually dominates, $z(t)$ and $\Phi_\perp(t)$ have no more reason to be static, implying $S/(aT)^{d-1}$ not to be a constant. Consequently, we will use in this regime an alternative definition of the yield,

$$Y_{\rm DM} \propto n_{\rm DM}\, a^{d-1}, \tag{4.6}$$

which clearly matches with eq. (4.1) before freeze-out.

The main difference of our scenario with the usual thermal case is that the dark-matter particles masses are driven by the value of $\zeta = \ln R_d$ and suddenly increase after the phase transition described in section 3.3 takes place. Since we have shown that the transition is sufficient to render part of the spectrum spontaneously non-relativistic, such particles can freeze-out and constitute a dark component of the universe. To describe qualitatively this mechanism, we consider in the following the limit case where the condensation of ζ, i.e. the mass jump, is much faster than all other processes, such as the evolutions of the temperature and number density $n_{\rm DM}$. Hence, we assume from now on that while the temperature drops, $\tilde{n}_{\rm F}$ and $\tilde{n}_{\rm B}$ (with $\tilde{n}_{\rm F} - \tilde{n}_{\rm B} > 0$) dark-matter fermionic and bosonic degrees of freedom are massless before the phase transition, and acquire "instantaneously" a mass $m_{\rm DM}$ at a temperature $T = T_{\rm c}$ (both measured in Einstein frame)

$$m(T) = \begin{cases} 0 & \text{for } T > T_{\rm c}, \\ m_{\rm DM} & \text{for } T < T_{\rm c}. \end{cases} \tag{4.7}$$

Notice that $T_{\rm c}$ is not determined *a priori*. Our assumption of instantaneity supposes $\zeta(t)$ starts sliding from the top of the hill when $z(t) \simeq z_{\rm c}$ (its final value after the transition) but this condition fixes only the ratio M/T to its critical value $e^{z_{\rm c}} = M_{\rm c}/T_{\rm c}$ at the transition. It turns out that depending on the ratio $x_{\rm c} = m_{\rm DM}/T_{\rm c}$, two qualitatively different situations may occur, as can be seen in figure 6, which represents the evolution of the yield. For completeness, a third case is also shown on this figure. To describe them, we define the dark-matter number densities right before and right after the transition as $n^0_{\rm DM,eq}$ and $n^{m_{\rm DM}}_{\rm DM,eq}$, respectively. Moreover, we treat $\langle\sigma_{\rm DM\leftrightarrow SM} v\rangle$ as not varying at the transition.

- **Case 1.** At $T = T_{\rm c}$, $\quad n^0_{\rm DM,eq}\langle\sigma_{\rm DM\leftrightarrow SM} v\rangle > (d-1)H$ and $n^{m_{\rm DM}}_{\rm DM,eq}\langle\sigma_{\rm DM\leftrightarrow SM} v\rangle > (d-1)H$.

  In figure 6, this corresponds to the case where the black dotted curve is above the red dashed curve at $x_{\rm c} = m_{\rm DM}/T_{\rm c}$: before $x_{\rm c}$, the dark-matter constituent being thermal radiation, the yield is constant. After the dark matter acquires its mass, it can annihilate sufficiently for its number density to drop all the way down to its new equilibrium value (see the violet line in figure 6). Then, one recovers the case of a standard thermal cold dark-matter scenario. Chemical decoupling eventually occurs, the density quits equilibrium and the yield of eq. (4.6) freezes-out.

- **Case 2.** At $T = T_{\rm c}$, $\quad n^0_{\rm DM,eq}\langle\sigma_{\rm DM\leftrightarrow SM} v\rangle > (d-1)H$ and $n^{m_{\rm DM}}_{\rm DM,eq}\langle\sigma_{\rm DM\leftrightarrow SM} v\rangle < (d-1)H$.

  In figure 6, the black dotted curve is below the red dashed curve at $x_{\rm c} = m_{\rm DM}/T_{\rm c}$: in this case, the massless dark matter acquires a mass while its number density is

JHEP03(2019)117

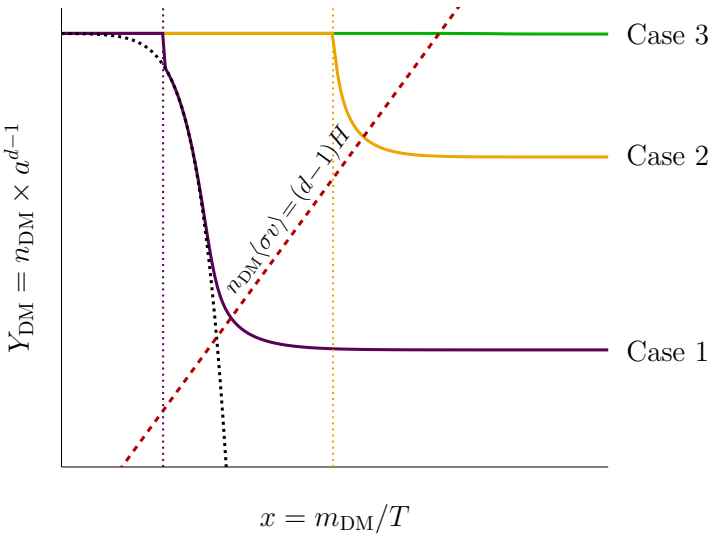

Figure 6. Evolution of the dark-matter yield $Y_{\rm DM} = n_{\rm DM} a^{d-1}$ ($\propto n_{\rm DM}/s$ before freeze-out) as a function of $x = m_{\rm DM}/T$ in the string theory scenario, in 4 dimensions. The black-dotted line represents the value that the yield would follow if the dark-matter particles always had a constant mass equal to $m_{\rm DM}$, and if thermal equilibrium could be maintained all along the history of the universe. In Cases 1 (violet line) and 2 (yellow line), two different values of the phase transition temperature $T_{\rm c}$ are considered. In Case 3 (green line), the decoupling from the thermal bath takes place while dark matter is still relativistic, and no phase transition can take place thereafter.

still sufficient for the annihilation process to be efficient for a while. However, while decreasing, the chemical decoupling limit is reached before a new thermal equilibrium can be established. Therefore, dark matter freezes-out at an intermediate relic density (see the yellow line in figure 6).

- **Case 3.** Thermal decoupling may also occur while dark-matter particles are still massless. In figure 6, the red dashed curve intersects the green horizontal line, while ζ has not been destabilized yet. Before decoupling, the number density follows the relativistic equilibrium value $n_{\rm DM,eq} \propto T^{d-1}$. Then, dark-matter decouples while still relativistic, similarly to the neutrino case. The particle number gets frozen and its density keeps evolving as $1/a^{d-1}$ due to the universe expansion. Therefore, the alternative definition of the yield, eq. (4.6), remains constant. In fact, it turns out that no mass generation can take place after decoupling, and we recover a usual hot dark-matter scenario. To reach these conclusions, let us focus on the free energy density component associated with the $\tilde{n}_{\rm F} + \tilde{n}_{\rm B}$ massless states, accompanied with their KK modes along the supersymmetry breaking direction X^9. Before freeze-out, the result (in string frame) can be extracted from eq. (2.28),

$$\begin{aligned}\mathcal{F}_{{\rm DM}(\sigma)} = T_{(\sigma)}^d \Big\{ &-(\tilde{n}_{\rm F}+\tilde{n}_{\rm B}) f_{\rm T}^{(d)}(z) + (\tilde{n}_{\rm F}-\tilde{n}_{\rm B}) f_{\rm V}^{(d)}(z) \\ &+ \frac{\zeta^2}{\pi T_{(\sigma)}^2} \Big[(\tilde{n}_{\rm F}+\tilde{n}_{\rm B}) f_{\rm T}^{(d-2)}(z) - (\tilde{n}_{\rm F}-\tilde{n}_{\rm B}) f_{\rm V}^{(d-2)}(z) \Big] + \mathcal{O}(\zeta^4) \Big\},\end{aligned} \tag{4.8}$$

JHEP03(2019)117

where $\zeta \simeq 0$ is massive. If at the decoupling from the thermal bath the dark-matter energy density $\rho^{\rm f}_{{\rm DM}(\sigma)}$ and pressure $P^{\rm f}_{{\rm DM}(\sigma)} = -\mathcal{F}^{\rm f}_{{\rm DM}(\sigma)}$ can be derived from the above formula, the corresponding expressions at later times are

$$\rho_{{\rm DM}(\sigma)} = \rho^{\rm f}_{{\rm DM}(\sigma)} \left(\frac{a^{\rm f}_{(\sigma)}}{a_{(\sigma)}}\right)^{d-1}, \quad P_{{\rm DM}(\sigma)} = P^{\rm f}_{{\rm DM}(\sigma)} \left(\frac{a^{\rm f}_{(\sigma)}}{a_{(\sigma)}}\right)^{d-1}. \tag{4.9}$$

In our notations, $a^{\rm f}_{(\sigma)}$ is the scale factor when dark matter freezes out, and the scaling rule of the energy density and pressure results from the dilution arising from the universe expansion. Therefore, Friedmann equations (3.8) and (3.9) are affected. However, more important to us is that the potential of ζ in this regime is nothing but

$$\mathcal{F}_{{\rm DM}(\sigma)} = \mathcal{F}^{\rm f}_{{\rm DM}(\sigma)} \left(\frac{a^{\rm f}_{(\sigma)}}{a_{(\sigma)}}\right)^{d-1}. \tag{4.10}$$

Up to an irrelevant overall scaling, its shape is frozen to that given at the decoupling, which we know is of a well shape around $\zeta = 0$. As a result, the possibility that any phase transition would be responsible for the mass generation of dark-matter particles is ruled out. In fact, when decoupling occurs in the massive phase of ζ, dark matter remains hot, no matter the sign of $\tilde{n}_{\rm F} - \tilde{n}_{\rm B}$ is.

Let us finally comment on the fact that, so far, we have assumed the phase transition to happen instantaneously, as compared to the time scale necessary for dark-matter particles to readjust their number density to its equilibrium value. Indeed, while the mass of dark matter varies with time, the shape of the equilibrium density as defined in eq. (4.3) also changes with time. If the mass variation is slow enough, dark-matter particles could adiabatically annihilate into Standard-Model particles (i.e. with $n_{\rm DM}$ following its mass-dependent equilibrium value), modifying the temperature at which the chemical decoupling would happen, and therefore the final value of the relic density. A careful solving of Boltzmann equation, together with a precise computation of the annihilation cross-section would be necessary to describe correctly such a situation, which will be addressed in a more complete study of the phenomenon in the future.

4.2 Dark-matter relic energy density

Our aim is now to partially compute the relic energy density after phase transition and freeze-out, in Cases 1 and 2. In the examples of section 2, the dark-particles spectrum for ϵ odd amounts to $\tilde{n}_{\rm F}$ KK towers of fermionic degrees of freedom, together with their bosonic superpartners. The former have KK momentum m_9/R_9 along the Scherk-Schwarz direction X^9, while the latter have shifted momentum $(m_9 + \frac{1}{2})/R_9$.[13]

To proceed, we need to specify the velocity distribution of each dark-matter KK species after the phase transition. Since the lowest string-frame mass $|R_d - 1/R_d|$ of the KK modes is already much higher than the temperature $T_{(\sigma)}$, we will simply assume a Dirac distribution of all velocities i.e. that all dark-matter particles are at rest. The total energy

[13] This can be seen by taking the limit $R_0 \to +\infty$ in eq. (2.2) and applying a Poisson summation over $\tilde{k}_9$.

JHEP03(2019)117

associated to the dark sector has then two origins. On the one hand, for each KK species, the mass has to be weighted by the particle number obtained when all particles have decoupled from the thermal bath (see the final constant values reached by the yield in Cases 1, 2 in figure 6). On the other hand, the vacuum energy of all degrees of freedom also contributes. The latter is the effective potential at zero-temperature associated to the KK towers of fermionic and bosonic modes. As can be seen from section 2, such an energy is exponentially suppressed in $R_9|R_d - 1/R_d| \gg 1$, since the mass of the zero-momentum mode along X^9 is much larger than the supersymmetry breaking scale $M_{(\sigma)}$.[14] To be consistent with the fact that we have neglected throughout this paper all such exponentially suppressed heavy modes contributions, we restrict to the energy arising from the relic particles at rest.

From the above considerations, the total relic dark-matter energy measured in string frame can be expressed in terms of the particle numbers and dynamical radii R_d, R_9 as follows,[15]

$$E_{(\sigma)} = \tilde{n}_{\rm F}(a^{\rm f}_{(\sigma)})^{d-1}\int {\rm d}^{d-1}\vec{k}_{(\sigma)}\sum_{m_9}\left[\mathcal{N}^{\rm f}_{{\rm B},m_9+\frac{1}{2}}\left(\vec{k}_{(\sigma)}\right)\sqrt{\left(R_d-\frac{1}{R_d}\right)^2+\left(\frac{m_9+\frac{1}{2}}{R_9}\right)^2}\right.$$
$$\left.-\mathcal{N}^{\rm f}_{{\rm F},m_9}\left(\vec{k}_{(\sigma)}\right)\sqrt{\left(R_d-\frac{1}{R_d}\right)^2+\left(\frac{m_9}{R_9}\right)^2}\right]. \tag{4.11}$$

Of course, a precise computation of the cross-section $\sigma_{\rm DM\leftrightarrow SM}$ is required to determine when decoupling takes place. This is compulsory to derive the value of the scale factor $a^{\rm f}_{(\sigma)}$ at this time. Knowledge of $\sigma_{\rm DM\leftrightarrow SM}$ is also necessary to figure out the final value of the yield (see figure 6) i.e. the distributions $\mathcal{N}^{\rm f}_{{\rm B},m_9+\frac{1}{2}}$, $\mathcal{N}^{\rm f}_{{\rm F},m_9}$. However, computing the cross section and distributions goes beyond the scope of the present paper and we leave this study for later works.

In the end, the dark-matter contribution to the action for a homogeneous and isotropic universe is

$$\mathcal{S}_{\rm DM} = -\int N_{(\sigma)}a^{d-1}_{(\sigma)}{\rm d}x^d\,\rho_{{\rm DM}(\sigma)} = -\int N a^{d-1}{\rm d}x^d\,\rho_{\rm DM}, \tag{4.12}$$

where we have expressed the result in either string or Einstein frames, with arbitrary definition of time i.e. generic lapse functions $N_{(\sigma)}$ and N, respectively. From eq. (3.2), the relic dark-matter energy densities are

$$\rho_{{\rm DM}(\sigma)} = \tilde{n}_{\rm F}\,\mathscr{E}(\eta,\zeta)\left(\frac{a^{\rm f}_{(\sigma)}}{a_{(\sigma)}}\right)^{d-1}, \qquad \rho_{\rm DM} = \tilde{n}_{\rm F}\left(a^{\rm f}_{(\sigma)}\right)^{d-1}\mathscr{E}(\eta,\zeta)\,\frac{e^{\frac{2}{d-2}\phi}}{a^{d-1}}, \tag{4.13}$$

[14] In field theory, this vacuum energy is infinite for the bosonic modes alone, infinite for the fermionic modes alone, but their sum turns out to be finite for arbitrary $|R_d - 1/R_d|$. Technically, this finiteness arises exactly as that of the free energy at finite temperature evaluated for a supersymmetric spectrum. String theory yields the same final answer, up to contributions arising from stringy heavy modes not present in field theory (see [69] for more details).

[15] If R_9 is time-dependent, $\zeta = \ln R_d$ may evolve again once the universe is matter dominated.

JHEP03(2019)117

where we have defined

$$\mathscr{E}(\eta,\zeta)=\int\frac{\mathrm{d}^{d-1}\vec{k}_{(\sigma)}}{(2\pi)^{d-1}}\sum_{m_9}\left[\mathcal{N}^{\mathrm{f}}_{\mathrm{B},m_9+\frac{1}{2}}\left(\vec{k}_{(\sigma)}\right)\sqrt{\left(R_d-\frac{1}{R_d}\right)^2+\left(\frac{m_9+\frac{1}{2}}{R_9}\right)^2}\right.$$
$$\left.-\mathcal{N}^{\mathrm{f}}_{\mathrm{F},m_9}\left(\vec{k}_{(\sigma)}\right)\sqrt{\left(R_d-\frac{1}{R_d}\right)^2+\left(\frac{m_9}{R_9}\right)^2}\right]. \tag{4.14}$$

Of course, varying $\mathcal{S}_{\mathrm{DM}}$ with respect to either of the scale factors, one derives trivial pressures for cold dark-matter,

$$P_{\mathrm{DM}(\sigma)}=0,\qquad P_{\mathrm{DM}}=0. \tag{4.15}$$

However, in string frame, the dark-matter energy density sources the equations of motion for $\zeta=\ln R_d$ and $M_{(\sigma)}=1/(2\pi R_9)$. In the Einstein frame, it affects the dynamics of ζ, the no-scale modulus Φ and $\Phi_\perp$, as follows from eq. (3.3) and the relation

$$e^{2\frac{d-1}{d-2}\phi(t)}=2\pi M(t)\,e^{\sqrt{d-1}\Phi_\perp}. \tag{4.16}$$

5 Conclusions and perspectives

The mechanism we have presented for generating non-relativistic dark matter may be relevant for describing an intermediate era of the cosmological history of the universe. At earlier times, the standard scenario assumes the existence of a period of inflation followed by reheating. While the possibility of realizing this picture in a ultraviolet complete theory is not clear so far [1, 2, 5–8], other possibilities, inherently stringy by nature, have also been considered. Among these proposals, various pre-big bang scenarios [61, 62, 70–77] have been analyzed, or Hagedorn phase transitions [57–60] may take place.

Whatever the very early eras look like, assuming that at some later time the universe is flat, homogeneous, isotropic and thermalized, we have found that the mechanism that triggers the phase transition responsible for the dark matter mass is preceded by a "Radiation-like Dominated" evolution, which is an attractor of the dynamics. This means that the motion of the supersymmetry breaking scale $M(t)$ together with the thermal energy density and pressure associated to KK towers of states conspire for the universe to evolve as if it was dominated by pure radiation. In this regime, the temperature $T(t)$ and the supersymmetry breaking scale $M(t)$ are of the same order of magnitude. However, when the dark-matter particles suddenly become massive and freeze-out, their energy density eventually dominates over radiation and a preliminary numerical analysis of the system seems to yield a rapid increase of the ratio $M(t)/T(t)$. Hence, a large hierarchy $M\gg T$ is dynamically generated, as must be the case to account for the smallness of the cosmic microwave background temperature, as compared to the very large supersymmetry breaking scale.

For the matter domination to end once dark energy takes over, the motion of $M(t)$ should come to a halt. We let for future work the proposal of a mechanism responsible

JHEP03(2019)117

for the stabilization of M. However, models yielding an extremely small (and positive) cosmological constant should be very peculiar. It could be that they satisfy conditions similar, and actually stronger, than those considered in [41, 42, 44, 49–52], which have vanishing effective potential at 1-loop.

Acknowledgments

We are grateful to Quentin Bonnefoy and Emilian Dudas for fruitful discussions. The research activities of L.H. are supported by the Department of Energy under Grant DE-FG02-13ER41976/DE-SC0009913 and by CNRS. L.H. would like to thank the CPHT of Ecole Polytechnique for hospitality. The work of H.P. is partially supported by the Royal Society International Cost Share Award.

References

[1] C. Vafa, *The string landscape and the swampland*, hep-th/0509212 [INSPIRE].

[2] H. Ooguri and C. Vafa, *On the Geometry of the String Landscape and the Swampland*, *Nucl. Phys.* **B 766** (2007) 21 [hep-th/0605264] [INSPIRE].

[3] PLANCK collaboration, *Planck 2018 results. VI. Cosmological parameters*, arXiv:1807.06209 [INSPIRE].

[4] D. Baumann, *Inflation*, in *Physics of the large and the small, TASI 09, proceedings of the Theoretical Advanced Study Institute in Elementary Particle Physics, Boulder, Colorado, U.S.A., 1–26 June 2009*, pp. 523–686, 2011, arXiv:0907.5424 [INSPIRE].

[5] G. Obied, H. Ooguri, L. Spodyneiko and C. Vafa, *de Sitter Space and the Swampland*, arXiv:1806.08362 [INSPIRE].

[6] P. Agrawal, G. Obied, P.J. Steinhardt and C. Vafa, *On the Cosmological Implications of the String Swampland*, *Phys. Lett.* **B 784** (2018) 271 [arXiv:1806.09718] [INSPIRE].

[7] S.K. Garg and C. Krishnan, *Bounds on Slow Roll and the de Sitter Swampland*, arXiv:1807.05193 [INSPIRE].

[8] H. Ooguri, E. Palti, G. Shiu and C. Vafa, *Distance and de Sitter Conjectures on the Swampland*, *Phys. Lett.* **B 788** (2019) 180 [arXiv:1810.05506] [INSPIRE].

[9] A. Dashko and R. Dick, *The shadow of dark matter as a shadow of string theory*, arXiv:1809.01089 [INSPIRE].

[10] B.S. Acharya, S.A.R. Ellis, G.L. Kane, B.D. Nelson and M. Perry, *Categorisation and Detection of Dark Matter Candidates from String/M-theory Hidden Sectors*, *JHEP* **09** (2018) 130 [arXiv:1707.04530] [INSPIRE].

[11] G. Honecker and W. Staessens, *On axionic dark matter in Type IIA string theory*, *Fortsch. Phys.* **62** (2014) 115 [arXiv:1312.4517] [INSPIRE].

JHEP03(2019)117

[12] G. Shiu, P. Soler and F. Ye, *Milli-Charged Dark Matter in Quantum Gravity and String Theory*, *Phys. Rev. Lett.* **110** (2013) 241304 [arXiv:1302.5471] [INSPIRE].

[13] A. Zanzi, *Dilaton stabilization and composite dark matter in the string frame of heterotic-M-theory*, arXiv:1210.4615 [INSPIRE].

[14] H. Kleinert, *The Purely Geometric Part of 'Dark Matter' — A Fresh Playground for 'String Theory'*, *Electron. J. Theor. Phys.* **9** (2012) 27 [arXiv:1107.2610] [INSPIRE].

[15] B.S. Acharya, G. Kane and E. Kuflik, *Bounds on scalar masses in theories of moduli stabilization*, *Int. J. Mod. Phys.* **A 29** (2014) 1450073 [arXiv:1006.3272] [INSPIRE].

[16] S.F. King and J.P. Roberts, *Natural Dark Matter from Type I String Theory*, *JHEP* **01** (2007) 024 [hep-ph/0608135] [INSPIRE].

[17] D. Bailin, G.V. Kraniotis and A. Love, *Sparticle spectrum and dark matter in type-I string theory with an intermediate scale*, *Phys. Lett.* **B 491** (2000) 161 [hep-ph/0007206] [INSPIRE].

[18] K. Benakli, J.R. Ellis and D.V. Nanopoulos, *Natural candidates for superheavy dark matter in string and M-theory*, *Phys. Rev.* **D 59** (1999) 047301 [hep-ph/9803333] [INSPIRE].

[19] K.R. Dienes and B. Thomas, *Dynamical Dark Matter: II. An Explicit Model*, *Phys. Rev.* **D 85** (2012) 083524 [arXiv:1107.0721] [INSPIRE].

[20] K.R. Dienes and B. Thomas, *Dynamical Dark Matter: I. Theoretical Overview*, *Phys. Rev.* **D 85** (2012) 083523 [arXiv:1106.4546] [INSPIRE].

[21] K.R. Dienes, F. Huang, S. Su and B. Thomas, *Dynamical Dark Matter from Strongly-Coupled Dark Sectors*, *Phys. Rev.* **D 95** (2017) 043526 [arXiv:1610.04112] [INSPIRE].

[22] K.R. Dienes, J. Fennick, J. Kumar and B. Thomas, *Dynamical Dark Matter from Thermal Freeze-Out*, *Phys. Rev.* **D 97** (2018) 063522 [arXiv:1712.09919] [INSPIRE].

[23] U. Franca and R. Rosenfeld, *Variable-mass dark matter and the age of the Universe*, in *High energy physics. Proceedings, 5th Latin American Symposium, Lima, Peru, July 12–17, 2004*, pp. 243–247, astro-ph/0412413 [INSPIRE].

[24] R. Rohm, *Spontaneous Supersymmetry Breaking in Supersymmetric String Theories*, *Nucl. Phys.* **B 237** (1984) 553 [INSPIRE].

[25] C. Kounnas and M. Porrati, *Spontaneous Supersymmetry Breaking in String Theory*, *Nucl. Phys.* **B 310** (1988) 355 [INSPIRE].

[26] S. Ferrara, C. Kounnas and M. Porrati, *Superstring Solutions With Spontaneously Broken Four-dimensional Supersymmetry*, *Nucl. Phys.* **B 304** (1988) 500 [INSPIRE].

[27] S. Ferrara, C. Kounnas, M. Porrati and F. Zwirner, *Superstrings with Spontaneously Broken Supersymmetry and their Effective Theories*, *Nucl. Phys.* **B 318** (1989) 75 [INSPIRE].

[28] C. Kounnas and B. Rostand, *Coordinate Dependent Compactifications and Discrete Symmetries*, *Nucl. Phys.* **B 341** (1990) 641 [INSPIRE].

[29] J. Scherk and J.H. Schwarz, *Spontaneous Breaking of Supersymmetry Through Dimensional Reduction*, *Phys. Lett.* **82B** (1979) 60 [INSPIRE].

[30] J. Scherk and J.H. Schwarz, *How to Get Masses from Extra Dimensions*, *Nucl. Phys.* **B 153** (1979) 61 [INSPIRE].

[31] F. Bourliot, C. Kounnas and H. Partouche, *Attraction to a radiation-like era in early superstring cosmologies*, *Nucl. Phys.* **B 816** (2009) 227 [arXiv:0902.1892] [INSPIRE].

JHEP03(2019)117

[32] T. Catelin-Jullien, C. Kounnas, H. Partouche and N. Toumbas, *Thermal/quantum effects and induced superstring cosmologies*, *Nucl. Phys.* **B 797** (2008) 137 [arXiv:0710.3895] [INSPIRE].

[33] T. Catelin-Jullien, C. Kounnas, H. Partouche and N. Toumbas, *Induced superstring cosmologies and moduli stabilization*, *Nucl. Phys.* **B 820** (2009) 290 [arXiv:0901.0259] [INSPIRE].

[34] F. Bourliot, J. Estes, C. Kounnas and H. Partouche, *Cosmological Phases of the String Thermal Effective Potential*, *Nucl. Phys.* **B 830** (2010) 330 [arXiv:0908.1881] [INSPIRE].

[35] J. Estes, C. Kounnas and H. Partouche, *Superstring Cosmology for $N_4 = 1 \to 0$ Superstring Vacua*, *Fortsch. Phys.* **59** (2011) 861 [arXiv:1003.0471] [INSPIRE].

[36] P.H. Ginsparg and C. Vafa, *Toroidal Compactification of Nonsupersymmetric Heterotic Strings*, *Nucl. Phys.* **B 289** (1987) 414 [INSPIRE].

[37] B. de Carlos, J.A. Casas, F. Quevedo and E. Roulet, *Model independent properties and cosmological implications of the dilaton and moduli sectors of 4-D strings*, *Phys. Lett.* **B 318** (1993) 447 [hep-ph/9308325] [INSPIRE].

[38] G.D. Coughlan, R. Holman, P. Ramond and G.G. Ross, *Supersymmetry and the Entropy Crisis*, *Phys. Lett.* **140B** (1984) 44 [INSPIRE].

[39] E. Kiritsis, *String theory in a nutshell*, *Princeton University Press*, (2007).

[40] L. Álvarez-Gaumé, P.H. Ginsparg, G.W. Moore and C. Vafa, *An $O(16) \times O(16)$ Heterotic String*, *Phys. Lett.* **B 171** (1986) 155 [INSPIRE].

[41] C. Kounnas and H. Partouche, *Super no-scale models in string theory*, *Nucl. Phys.* **B 913** (2016) 593 [arXiv:1607.01767] [INSPIRE].

[42] C. Kounnas and H. Partouche, *$\mathcal{N} = 2 \to 0$ super no-scale models and moduli quantum stability*, *Nucl. Phys.* **B 919** (2017) 41 [arXiv:1701.00545] [INSPIRE].

[43] T. Coudarchet and H. Partouche, *Quantum no-scale regimes and moduli dynamics*, *Nucl. Phys.* **B 933** (2018) 134 [arXiv:1804.00466] [INSPIRE].

[44] S. Abel, K.R. Dienes and E. Mavroudi, *Towards a nonsupersymmetric string phenomenology*, *Phys. Rev.* **D 91** (2015) 126014 [arXiv:1502.03087] [INSPIRE].

[45] E. Cremmer, S. Ferrara, C. Kounnas and D.V. Nanopoulos, *Naturally Vanishing Cosmological Constant in $N = 1$ Supergravity*, *Phys. Lett.* **133B** (1983) 61 [INSPIRE].

[46] J.R. Ellis, C. Kounnas and D.V. Nanopoulos, *Phenomenological* SU(1, 1) *Supergravity*, *Nucl. Phys.* **B 241** (1984) 406 [INSPIRE].

[47] J.R. Ellis, A.B. Lahanas, D.V. Nanopoulos and K. Tamvakis, *No-Scale Supersymmetric Standard Model*, *Phys. Lett.* **134B** (1984) 429 [INSPIRE].

[48] J.R. Ellis, C. Kounnas and D.V. Nanopoulos, *No Scale Supersymmetric Guts*, *Nucl. Phys.* **B 247** (1984) 373 [INSPIRE].

[49] H. Itoyama and T.R. Taylor, *Supersymmetry Restoration in the Compactified $O(16) \times O(16)$-prime Heterotic String Theory*, *Phys. Lett.* **B 186** (1987) 129 [INSPIRE].

[50] S. Abel, K.R. Dienes and E. Mavroudi, *GUT precursors and entwined SUSY: The phenomenology of stable nonsupersymmetric strings*, *Phys. Rev.* **D 97** (2018) 126017 [arXiv:1712.06894] [INSPIRE].

JHEP03(2019)117

[51] S. Abel and R.J. Stewart, *Exponential suppression of the cosmological constant in nonsupersymmetric string vacua at two loops and beyond*, *Phys. Rev.* **D 96** (2017) 106013 [arXiv:1701.06629] [INSPIRE].

[52] I. Florakis and J. Rizos, *Chiral Heterotic Strings with Positive Cosmological Constant*, *Nucl. Phys.* **B 913** (2016) 495 [arXiv:1608.04582] [INSPIRE].

[53] T. Coudarchet, C. Fleming and H. Partouche, *Quantum no-scale regimes in string theory*, *Nucl. Phys.* **B 930** (2018) 235 [arXiv:1711.09122] [INSPIRE].

[54] H. Partouche, *Quantum no-scale regimes and string moduli*, *Universe* **4** (2018) 123 [arXiv:1809.03572] [INSPIRE].

[55] L. Liu and H. Partouche, *Moduli Stabilization in Type II Calabi-Yau Compactifications at finite Temperature*, *JHEP* **11** (2012) 079 [arXiv:1111.7307] [INSPIRE].

[56] J. Estes, L. Liu and H. Partouche, *Massless D-strings and moduli stabilization in type-I cosmology*, *JHEP* **06** (2011) 060 [arXiv:1102.5001] [INSPIRE].

[57] J.J. Atick and E. Witten, *The Hagedorn Transition and the Number of Degrees of Freedom of String Theory*, *Nucl. Phys.* **B 310** (1988) 291 [INSPIRE].

[58] I. Antoniadis and C. Kounnas, *Superstring phase transition at high temperature*, *Phys. Lett.* **B 261** (1991) 369 [INSPIRE].

[59] I. Antoniadis, J.P. Derendinger and C. Kounnas, *Nonperturbative temperature instabilities in $N = 4$ strings*, *Nucl. Phys.* **B 551** (1999) 41 [hep-th/9902032] [INSPIRE].

[60] C. Angelantonj, C. Kounnas, H. Partouche and N. Toumbas, *Resolution of Hagedorn singularity in superstrings with gravito-magnetic fluxes*, *Nucl. Phys.* **B 809** (2009) 291 [arXiv:0808.1357] [INSPIRE].

[61] C. Kounnas, H. Partouche and N. Toumbas, *Thermal duality and non-singular cosmology in d-dimensional superstrings*, *Nucl. Phys.* **B 855** (2012) 280 [arXiv:1106.0946] [INSPIRE].

[62] C. Kounnas, H. Partouche and N. Toumbas, *S-brane to thermal non-singular string cosmology*, *Class. Quant. Grav.* **29** (2012) 095014 [arXiv:1111.5816] [INSPIRE].

[63] S. Abel, E. Dudas, D. Lewis and H. Partouche, *Stability and vacuum energy in open string models with broken supersymmetry*, arXiv:1812.09714 [INSPIRE].

[64] M. Viel, J. Lesgourgues, M.G. Haehnelt, S. Matarrese and A. Riotto, *Constraining warm dark matter candidates including sterile neutrinos and light gravitinos with WMAP and the Lyman-α forest*, *Phys. Rev.* **D 71** (2005) 063534 [astro-ph/0501562] [INSPIRE].

[65] A.E. Faraggi, J. Rizos and H. Sonmez, *Classification of Standard-like Heterotic-String Vacua*, *Nucl. Phys.* **B 927** (2018) 1 [arXiv:1709.08229] [INSPIRE].

[66] B. Assel, K. Christodoulides, A.E. Faraggi, C. Kounnas and J. Rizos, *Classification of Heterotic Pati-Salam Models*, *Nucl. Phys.* **B 844** (2011) 365 [arXiv:1007.2268] [INSPIRE].

[67] B. Assel, K. Christodoulides, A.E. Faraggi, C. Kounnas and J. Rizos, *Exophobic Quasi-Realistic Heterotic String Vacua*, *Phys. Lett.* **B 683** (2010) 306 [arXiv:0910.3697] [INSPIRE].

[68] A.E. Faraggi, C. Kounnas and J. Rizos, *Chiral family classification of fermionic $Z_2 \times Z_2$ heterotic orbifold models*, *Phys. Lett.* **B 648** (2007) 84 [hep-th/0606144] [INSPIRE].

[69] A. Kehagias and H. Partouche, *The Casimir effect in string theory*, arXiv:1812.10774 [INSPIRE].

JHEP03(2019)117

[70] R.H. Brandenberger and C. Vafa, *Superstrings in the Early Universe*, *Nucl. Phys.* **B 316** (1989) 391 [INSPIRE].

[71] G. Veneziano, *Scale factor duality for classical and quantum strings*, *Phys. Lett.* **B 265** (1991) 287 [INSPIRE].

[72] A.A. Tseytlin and C. Vafa, *Elements of string cosmology*, *Nucl. Phys.* **B 372** (1992) 443 [hep-th/9109048] [INSPIRE].

[73] M. Gasperini and G. Veneziano, *Pre-big bang in string cosmology*, *Astropart. Phys.* **1** (1993) 317 [hep-th/9211021] [INSPIRE].

[74] M. Gasperini, M. Maggiore and G. Veneziano, *Towards a nonsingular pre-big bang cosmology*, *Nucl. Phys.* **B 494** (1997) 315 [hep-th/9611039] [INSPIRE].

[75] M. Gasperini and G. Veneziano, *Singularity and exit problems in two-dimensional string cosmology*, *Phys. Lett.* **B 387** (1996) 715 [hep-th/9607126] [INSPIRE].

[76] R. Brustein, M. Gasperini and G. Veneziano, *Duality in cosmological perturbation theory*, *Phys. Lett.* **B 431** (1998) 277 [hep-th/9803018] [INSPIRE].

[77] M. Gasperini and G. Veneziano, *The pre-big bang scenario in string cosmology*, *Phys. Rept.* **373** (2003) 1 [hep-th/0207130] [INSPIRE].

JHEP03(2019)117

Available online at www.sciencedirect.com

ScienceDirect

Nuclear Physics B 957 (2020) 115100

NUCLEAR PHYSICS B

www.elsevier.com/locate/nuclphysb

On the stability of open-string orbifold models with broken supersymmetry

Steven Abel [a], Thibaut Coudarchet [b,*], Hervé Partouche [b]

[a] *Institute for Particle Physics Phenomenology, Durham University, and Department of Mathematical Sciences, South Road, Durham, UK*

[b] *CPHT, CNRS, Ecole Polytechnique, IP Paris, F-91128 Palaiseau, France*

Received 8 May 2020; accepted 7 June 2020
Available online 27 June 2020
Editor: Stephan Stieberger

Abstract

We consider an open-string realisation of $\mathcal{N}=2\to\mathcal{N}=0$ spontaneous breaking of supersymmetry in four-dimensional Minkowski spacetime. It is based on type IIB orientifold theory compactified on $T^2\times T^4/\mathbb{Z}_2$, with Scherk–Schwarz supersymmetry breaking implemented along T^2. We show that in the regions of moduli space where the supersymmetry breaking scale is lower than the other scales, there exist configurations with minima that have massless Bose-Fermi degeneracy and hence vanishing one-loop effective potential, up to exponentially suppressed corrections. These backgrounds describe non-Abelian gauge theories, with all open-string moduli and blowing up modes of $T^4/\mathbb{Z}_2$ stabilized, while all untwisted closed-string moduli remain flat directions. Other backgrounds with strictly positive effective potentials exist, where the only instabilities arising at one loop are associated with the supersymmetry breaking scale, which runs away. All of these backgrounds are consistent non-perturbatively.

1. Introduction

The question of how moduli come to acquire masses in the true vacuum is central in the context of string phenomenology. Indeed the working hypothesis in much of string phenomenology

* Corresponding author.
E-mail addresses: s.a.abel@durham.ac.uk (S. Abel), thibaut.coudarchet@polytechnique.edu (T. Coudarchet), herve.partouche@polytechnique.edu (H. Partouche).

https://doi.org/10.1016/j.nuclphysb.2020.115100

is that the system is initially supersymmetric, with supersymmetry being a powerful guarantor of vacuum stability. Non-perturbative effects then induce a spontaneous breaking of supersymmetry at a scale much below the string scale M_s [1–6], introducing mild instabilities in only a very limited number of moduli that lead to phenomenologically desirable effects such as the Brout-Englert-Higgs mechanism. An alternative and arguably more honest approach is to implement spontaneous supersymmetry breaking from the outset, at the classical level in flat space, and rely on perturbative calculations to derive interesting quantum physics. In this approach, loop corrections generate an effective potential for the entire system, in which one must seek local minima for the moduli. Moreover, very few of these minima would be expected to yield a cosmological constant that is close to zero.

This general route was advocated in Refs. [7–17], and the question of stability was addressed in the heterotic string in [9,10,18–22], and more recently in the type I framework in [23,24]. In all these works, supersymmetry breaking was implemented by the string versions [25–37] of the Scherk–Schwarz mechanism [38], with the effective potential being studied directly using string perturbation theory at one loop. The type I framework has the advantage of providing *via* T-dualities geometric descriptions of open-string moduli as positions of D-branes in the internal space [39]. The purpose of this paper is to demonstrate how the discussion can be extended to more phenomenologically interesting cases that also contain orbifolds.

Let us begin by making some general remarks and observations about the setup. In practice, the scale M of spontaneous supersymmetry breaking will be assumed to be lower than the other scales present, namely the string scale $M_s = 1/\sqrt{\alpha'}$, and the other scales arising from compactification. In other words the directions involved in the Scherk–Schwarz supersymmetry breaking are large compared to $\sqrt{\alpha'}$ and the other directions (or their T-duals). This restriction implies that the one-loop potential is dominated by the massless states and their Kaluza-Klein (KK) modes along the large "Scherk–Schwarz directions", and its dependence on the moduli fields becomes tractable. Moreover, any potential tree-level instabilities occurring when $M = \mathcal{O}(M_s)$ [40,41], which are related to the Hagedorn transition, are avoided. Under this assumption, in the string frame the effective potential will inevitably take the following form at an extremal point [7–16,18–24]:

$$\mathcal{V} = \xi (n_F - n_B) M^d + \mathcal{O}\left((M_s M)^{\frac{d}{2}} e^{-2\pi c \frac{M_s}{M}} \right) , \tag{1.1}$$

where d is the spacetime dimension. In this expression, n_F and n_B are the numbers of precisely massless fermionic and bosonic degrees of freedom, while $\xi > 0$ is a constant that accounts for the KK towers. Moreover, the exponentially suppressed terms arise from all other string states, where c is an $\mathcal{O}(1)$ moduli-dependent quantity, with the exponential factor corresponding to their Yukawa potential across the compact Scherk–Schwarz volume.[1]

Now let us summarise the specific results for toroidal compactification in type I found in Ref. [23], and then anticipate and review those that we will find here. Ref. [23] presented the rules for perturbatively consistent models to be tachyon free, which were based upon the fact that, when an odd number of Dp-branes is stacked on an orientifold plane (Op-plane), the position of one of the branes is rigid [42], thus enhancing the stability of the setup. Most of these configurations yield $n_F - n_B < 0$, while some others satisfy $n_F - n_B = 0$, which is an interesting

[1] Note that throughout our work, our use of the words "extremal point of the potential" is somewhat abusive, since $\mathcal{V}$ is in fact extremal with respect to all moduli except M itself, which has a tadpole unless $n_F = n_B$. In addition when we assert properties such as "tachyon free", "flat direction", and so forth, these properties are all to be understood at one loop, and when all exponentially suppressed corrections are neglected.

choice for generating a small cosmological constant. The idea being that, if the one-loop effective potential is exponentially suppressed, then it may conspire with higher loops effects to stabilise M and the dilaton, and eventually yield a cosmological term smaller than in generic models. However, after imposing all known non-perturbative consistency conditions [43–47] on configurations satisfying $n_F - n_B \geq 0$ for $d \geq 5$, it was found that there is only one survivor which has dimension $d = 5$, and $n_F - n_B = 8 \times 8$ [48]. T-dualizing the internal T^5, it corresponds to rendering all of the 32 D5-branes[2] rigid, by distributing them one by one on 32 distant O5-planes. The open-string "gauge group" denoted $SO(1)^{32}$ is trivial, where $SO(1) = \{e\}$, with e being the neutral element.

In the present work, we extend the above analysis to $d = 4$ dimensions, when $\mathcal{N} = 2$ supersymmetry is spontaneously broken to $\mathcal{N} = 0$. We show that there exist non-perturbatively consistent models that are tachyon free at one loop, with exponentially suppressed ($n_F - n_B = 0$) or positive ($n_F - n_B > 0$) potentials $\mathcal{V}$. We will construct them in the framework of the Bianchi–Sagnotti–Gimon–Polchinski (BSGP) model [49–51], with the type I theory being compactified on the partially orbifolded space $T^2 \times T^4/\mathbb{Z}_2$. We choose the Scherk–Schwarz mechanism to act along the T^2 [30–37,53,54], which implies that the entire spectrum (including the "twisted states") is sensitive to the supersymmetry breaking. As well as the usual closed strings, the model contains open strings that have Neumann (N) (or Dirichlet (D)) boundary conditions when they are attached to one of the 32 D9-branes (or 32 D5-branes) [39]. There are corresponding moduli fields of various kinds, which will be the focus of our attention. Their masses arise at the quantum level once supersymmetry is broken, and can be studied from various perspectives. Indeed one of the more general aspects of this paper is the array of tools that can be brought to bear on these questions. These will allow us to make the following conclusions about the behaviour of the zoo of moduli:

• Applying suitable T-dualities, all Wilson lines (WL's) on the worldvolumes of the D9- and D5-branes can be mapped into positions of $32 + 32$ D3-branes. The one-loop effective potential is extremal with respect to these moduli when all D3-branes sit on O3-planes. We will derive the signs and magnitudes of the quadratic mass terms at one loop using two different (but related) methods. The first, which is purely algebraic, is based on the knowledge of the massless spectrum that is charged under the Cartan $U(1)$'s associated with the WL's. The second method is to evaluate the one-loop Coleman–Weinberg effective potential with WL's switched on, and take the double-derivative at the origin of the WL moduli space. The mass matrices of these states is derived also taking into account the effect of six-dimensional anomaly-induced masses.

• In general the open-string sector also contains moduli in the ND sector, whose condensation if they are tachyonic would correspond to "recombinations of branes" [55–58]. One way to determine the masses of these states when the D3-branes sit on O3-planes is to compute the two points functions of "boundary changing vertex operators". The computation of such amplitudes in non-supersymmetric backgrounds is an interesting and delicate question, that will be presented in a companion paper [59].

• The closed strings also yield moduli, namely the internal metric and the dilaton in the Neveu–Schwarz-Neveu–Schwarz (NS-NS) sector, as well as the internal components of the Ramond-Ramond (RR) two-form. The expression of the one-loop potential $\mathcal{V}$ as a function of the metric can be derived explicitly. However, because this dependence becomes trivial when the

[2] We make the choice to call "branes" objects that live in the parent type IIB theory, *i.e.* before any orientifold (or orbifold) action is implemented. In other words, there are as many "branes" as Chan–Paton indices. In the descendant theories, these "branes" are non-dynamically independent objects.

potential is extremal with respect to the open-string WL's (see Eq. (1.1)), all degrees of freedom of the internal metric are flat directions (up to exponentially suppressed terms), except the supersymmetry breaking scale M itself when $n_F \neq n_B$. Of course, the dilaton remains a flat direction at one loop. To study the dependence of $\mathcal{V}$ on the RR moduli, we use type I/heterotic duality [60–67], which maps the RR two-form to the antisymmetric tensor. At one loop, the heterotic effective potential receives contributions from winding modes running in the virtual loop, whose masses depend on the antisymmetric tensor. Up to exponentially suppressed terms, there is no additional dependence of the potential on this tensor. Hence, because winding modes on the heterotic side are dual to non-perturbative D1-branes in type I, we will conclude that $\mathcal{V}$ does not depend on the RR moduli (up to the exponentially suppressed terms).

• Finally the moduli arising in the twisted closed-string sector belong to the quaternionic scalars of the 16 twisted hypermultiplets localized at the 16 fixed points of $T^2 \times T^4/\mathbb{Z}_2$ in the BSGP model. Thanks to the generalized Green–Schwarz mechanism taking place in six dimensions [51], between two and sixteen of these moduli acquire a large supersymmetric mass. We do not analyze the masses, which are generated at one loop by the supersymmetry breaking, of the remaining (up to fourteen) twisted quaternions.

The plan of this work is as follows. In Sect. 2, we describe the BSGP model on $T^2 \times T^4/\mathbb{Z}_2$, with the Scherk–Schwarz mechanism implemented along T^2 to break $\mathcal{N} = 2 \to \mathcal{N} = 0$. In particular, we derive the massless spectrum and the one-loop effective potential when all D3-branes (in suitable T-dual descriptions) sit on O3-planes. In Sect. 3, we determine the mass terms of the open-string WL's, the effects of the Green–Schwarz mechanism, and derive the flatness of the untwisted closed-string sector moduli. In Sect. 4, we first discuss the stability/instability of representative examples of brane configurations, which belong to distinct non-perturbatively consistent components of the open-string moduli space [51].

We then perform a full scan of the hundreds of billions of possible distributions of the D3-branes on the O3-planes, which correspond to extremal points of the one-loop effective potential.[1] We find that at the one-loop level, there are only two non-perturbatively consistent marginally stable setups with exponentially suppressed effective potential ($n_F - n_B = 0$). All open-string moduli are stabilised, together with the blowing up modes of the orbifold, while all untwisted closed-string moduli are flat directions. The anomaly free gauge symmetries are $U(1) \times SU(2) \times SU(5)^2 \times SU(7)$ and $U(1) \times SU(3) \times SU(5)^2 \times SU(6)$. There also exist four configurations that are tachyon free and have positive potential at one loop ($n_F - n_B > 0$), implying that M runs away. There are two further brane distributions that are tachyon free, but modulo possible instabilities associated with moduli existing in the ND sector: the relevant one-loop masses will be studied elsewhere [59]. One of these models has $n_F - n_B = 0$, while the other has $n_F - n_B > 0$.

Our conclusions can be found in Sect. 5. The core of the paper is accompanied by Appendices A and B, which collect those technical details required for Sects. 2 and 3, respectively.

2. $\mathcal{N} = 2 \to \mathcal{N} = 0$ open-string model

In this section, we will describe the broad features of toroidal orbifold models of type I that realize $\mathcal{N} = 2 \to \mathcal{N} = 0$ spontaneous breaking of supersymmetry in four dimensions. We will consider the partition function that takes into account arbitrary marginal deformations arising from the NN and DD sectors of the open strings, as well as from the NS-NS closed-string sector *i.e.* the internal metric. We also discuss the associated spectrum of the states that are massless at

tree level. This will prepare us for the following sections, where we consider the response of the system to the breaking of supersymmetry, in particular its one-loop stability.

2.1. The supersymmetric setup

Original BSGP model: Before implementation of the spontaneous breaking of supersymmetry, our framework is the Bianchi–Sagnotti–Gimon–Polchinski model [49–51] compactified down to four dimensions. It is obtained by applying an orientifold projection to the type IIB theory, with background

$$\mathbb{R}^{1,3} \times T^2 \times \frac{T^4}{\mathbb{Z}_2}\,, \tag{2.1}$$

where we will take Minkowski spacetime to span the directions X^0, X^1, X^2, X^3, while the T^2 torus directions are X^4, X^5. The remaining coordinates, corresponding to the T^4 torus, are twisted by the $\mathbb{Z}_2$ orbifold generator,

$$g: \quad (X^6, X^7, X^8, X^9) \longrightarrow (-X^6, -X^7, -X^8, -X^9)\,, \tag{2.2}$$

implying that the model has $\mathcal{N} = 2$ supersymmetry. The background contains orientifold planes, which are the fixed loci of the orientifold generator Ω and of the combination Ωg. Hence, an O9-plane lies along the nine spatial directions (the "fixed locus" of Ω), while an O5-plane is located at each of the 16 fixed points of $T^4/\mathbb{Z}_2$. In order to cancel their RR charges, the open-string sector comprises 32 D9-branes, as well as 32 D5-branes transverse to the $T^4/\mathbb{Z}_2$ factor. Consistency conditions require the algebra of Chan–Paton factors to correspond to unitary or symplectic gauge groups rather than orthogonal ones [50]. The simplest configuration, which has a $U(16) \times U(16)$ open-string gauge group, is obtained when no WL deformations are introduced on the worldvolumes of the D9-branes and D5-branes, and when all D5-branes are coincident on a single O5-plane. The only marginal deformations in this system would be those associated with the NS-NS internal metric $G_{\mathcal{I}\mathcal{J}}$, $\mathcal{I}, \mathcal{J} = 4, \ldots, 9$, which we can split into its T^2 components $G_{I'J'}$, $I', J' = 4, 5$, and T^4 components G_{IJ}, $I, J = 6, \ldots, 9$.

At one loop, the partition function includes contributions arising from worldsheets of closed strings and open strings, with the topologies of a torus and Klein bottle, and an annulus and Möbius strip respectively. Accordingly, the one-loop effective potential (which of course vanishes at this stage) involves four vacuum-to-vacuum amplitudes $\mathcal{T}$, $\mathcal{K}$, $\mathcal{A}$, $\mathcal{M}$, as shown in Eq. (A.2). Using the conventions for lattices and characters given in Appendix A.1, these contributions in the "undeformed" BSGP model are displayed in Appendix A.2.

Marginal deformations: The original model with $U(16) \times U(16)$ open-string gauge group can be deformed by turning on (*i.e.* giving a vev to) any of the available marginal deformations arising from the open-string or closed-string sectors. In the effective supersymmetric theory these correspond to exactly F- and D-flat directions. Let us first enumerate them and then describe them in detail:

(i) Generic positions of the D5-branes in $T^4/\mathbb{Z}_2$.
(ii) Wilson lines along T^2 for the gauge group associated with the D5-branes (in the DD sector).
(iii) WL's along all of the six internal directions for the gauge group generated by the D9-branes (in the NN sector). In fact "Wilson line" is a misnomer along $T^4/\mathbb{Z}_2$ since we will see that

non-trivial vev's of these moduli reduce the rank of the gauge group. It is only in the $\mathcal{N}=4$ parent theory, without the orbifold generated by g, that these moduli are truly WL's.

(iv) Non-trivial vev's of the moduli in the ND sector. When the latter condense, the background can be described in terms of brane recombinations or magnetized branes [55–58].

(v) Non-trivial vev's of the RR moduli, namely the 2-form components $C_{I'J'}$, $I', J' = 4, 5$, and C_{IJ}, $I, J = 6, \ldots, 9$.

(vi) Non-trivial vev's of the quaternionic scalars of the 16 twisted hypermultiplets in the closed-string sector. These are the blowing up modes of the orbifold, which are localized at the 16 fixed points of $T^4/\mathbb{Z}_2$. When they are turned on, the $T^4/\mathbb{Z}_2$ is deformed into a smooth $K3$ manifold.

In the present work, we will not consider deformations of the ND sector moduli (iv).[3] On the contrary, we will justify that the RR moduli (v) do not yield relevant effects. We will also discuss how the twisted quaternionic moduli in (vi) acquire supersymmetric masses thanks to a generalized Green–Schwarz mechanism.

Let us start the detailed discussion of actual deformations, with the moduli (i) corresponding to the positions along directions X^6, X^7, X^8, X^9 of the 32 D5-branes of the type IIB theory. These must be symmetric with respect to the generators Ω and g, hence the orientifold projection requires that if a brane is located at X^I, $I = 6, \ldots, 9$, then a distinct brane sits at $-X^I$ [39].[4] Similarly, the $\mathbb{Z}_2$ twist projection correlates the position of a brane at X^I, with that of a brane (distinct or otherwise) at $-X^I$. Broadly speaking, in the type I string theory, D5-brane positions in $T^4/\mathbb{Z}_2$ vary in 4's. For instance, if $2n$ D5-branes are sitting at a fixed point, they support a gauge symmetry $U(n)$ that can be broken to $U(n-2k) \times USp(2k)$, with rank reduced to $n-k$, if $2k$ branes move away from the fixed point together with their $2k$ "mirror branes" at the opposite coordinates. Hence the moduli space splits into disconnected components characterized by the value of $2n$ modulo 4, which can be either 0 or 2. In other words, the parity of n matters.[5]

The Wilson lines (ii) along the T^2 of the D5 gauge groups parameterise the Coulomb branch of the gauge symmetry, and therefore preserve the rank. These also have a geometric interpretation. Upon T-dualizing T^2, the D5-branes become D3-branes transverse to the six-dimensional internal space, and the WL's can then be thought of as the positions of the D3-branes along the T-dual torus $\tilde{T}^2$ of coordinates $\tilde{X}^4$, $\tilde{X}^5$. Moreover, the 16 O5-planes become 64 O3-planes sitting at the fixed loci of $\Omega I_{45} g$, where I_{45} is the inversion $(\tilde{X}^4, \tilde{X}^5) \to (-\tilde{X}^4, -\tilde{X}^5)$. Similarly to the deformations (i), the position of a D3-brane in $\tilde{X}^{I'}$, $I' = 4, 5$, is correlated with that of a distinct partner D3-brane at $-\tilde{X}^{I'}$. Hence, brane positions along $\tilde{T}^2/I_{45}$ vary in 2's. In this T-dual geometric picture, the six-dimensional internal space can be thought of as a "box", a generalization of a one-dimensional segment, with an O3-plane sitting at each of its 64 corners. This box along with the D3-branes sitting on O3-planes is depicted in Fig. 1a.

In the original type I picture, D5-branes and D9-branes are on an equal footing, in the sense that a T-duality on $T^4/\mathbb{Z}_2$ turns the former into the latter and *vice versa*. Hence, the moduli

[3] A subsequent work [59] will be entirely devoted to the delicate computation of their masses generated at one loop when supersymmetry is spontaneously broken.

[4] Before implementation of the $\mathbb{Z}_2$ orbifold action, this can be understood by T-dualizing T^4 in order to translate the D5-brane positions into D9-brane Wilson lines along the T-dual torus. These WL's are associated with orthogonal gauge groups [39].

[5] Even though configurations with an odd number of D5-branes sitting on an O5-plane are symmetric under $X^I \to -X^I$, they are not allowed due to the unitary structure of the gauge group factors.

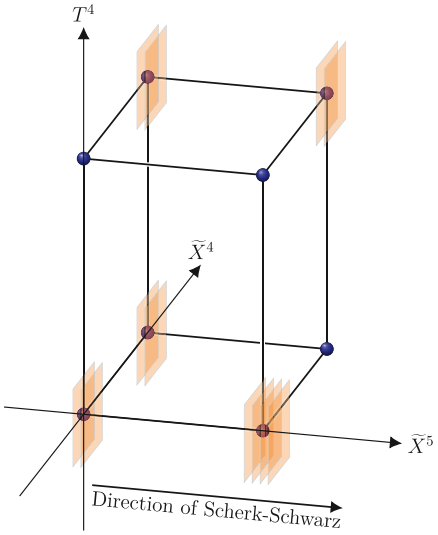

(a) A configuration of D3-branes associated with the D5-branes of the initial type I theory, once T^2 is T-dualized. In this example, the D3-branes sit on O3-planes.

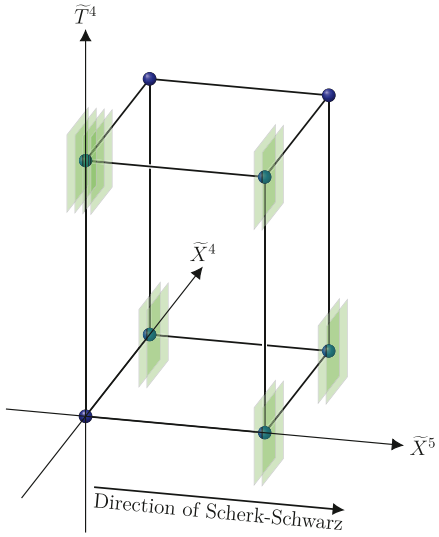

(b) A configuration of D3-branes associated with the D9-branes of the initial type I theory, once both T^2 and $T^4/\mathbb{Z}_2$ are T-dualized. In this example, the D3-branes sit on O3-planes.

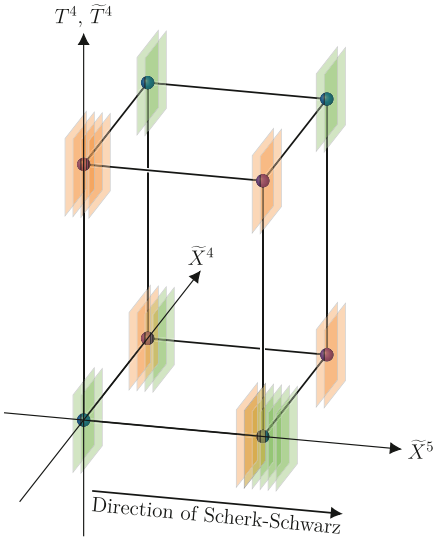

(c) Superposition of pictures (a) and (b). D3-branes associated with the D5-branes (D9-branes) of the initial type I theory are shown in orange (green).

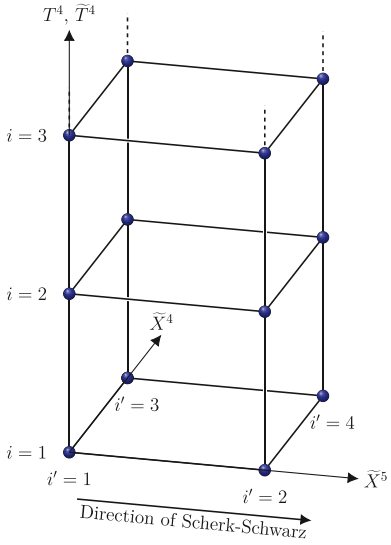

(d) Labelling of the $\tilde{T}^2/I_{45}$ fixed points $i' = 1, 2, 3, 4$, and schematic labelling of the $T^4/\mathbb{Z}_2$ or $\tilde{T}^4/\mathbb{Z}_2$ fixed points $i = 1, \ldots, 16$. Odd i' correspond to points located at $\tilde{X}^5 = 0$, while even i' are associated with points at $\tilde{X}^5 = \pi$, where $\tilde{X}^5$ is the coordinate T-dual to the direction along which the Scherk–Schwarz mechanism is implemented.

Fig. 1. Geometric T-dual description of the moduli arising from the NN and DD sectors of the orientifold theory. (For interpretation of the colours in the figure, the reader is referred to the web version of this article. This is valid for all subsequent figures in this article as they follow the same colour code.)

(*iii*) associated with the gauge group induced by the D9-branes can also be given a geometric interpretation in terms of positions of D3-branes, upon T-dualizing *all* the directions of $T^2 \times T^4/\mathbb{Z}_2$. An example of a configuration in which the resulting D3-branes sit on O3-planes is shown in Fig. 1b, where $\tilde{T}^4$ denotes the T-dual four-dimensional torus.

Despite the fact that Figs. 1a and 1b refer to T-dual theories, it is convenient to represent all the D-branes on a single picture, as shown in Fig. 1c. Although this depiction is certainly abusive, it turns out to be very useful to understand and manipulate various moduli configurations. In practice, we will refer interchangeably to "positions" and "Wilson lines" bearing in mind that they refer to the appropriate T-dual pictures.

Let us now define the Wilson lines in detail. We should repeat that the denomination "Wilson line" is only fully justified along the T^2, or in the parent type I model, when no orbifold action is implemented. In such an $\mathcal{N}=4$ theory, a Wilson line matrix living in the Cartan subgroup of the D9-brane $SO(32)$ gauge group can be associated with every direction in $T^2\times T^4$. For $\mathcal{I}=4,\dots,9$, it can be parameterised as

$$\begin{aligned}\mathcal{W}^{\rm D9}_{\mathcal{I}} &= \text{diag}\left(e^{2i\pi a^{\mathcal{I}}_{\alpha}}, \alpha=1,\dots,32\right)\\ &= \text{diag}\left(e^{2i\pi a^{\mathcal{I}}_{1}}, e^{-2i\pi a^{\mathcal{I}}_{1}}, e^{2i\pi a^{\mathcal{I}}_{2}}, e^{-2i\pi a^{\mathcal{I}}_{2}}, \dots, e^{2i\pi a^{\mathcal{I}}_{16}}, e^{-2i\pi a^{\mathcal{I}}_{16}}\right),\end{aligned} \tag{2.3}$$

where α labels the 32 D9-branes, and the corresponding D3-brane positions in $\tilde{T}^2\times\tilde{T}^4$ are $\tilde{X}^{\mathcal{I}}=2\pi a^{\mathcal{I}}_{\alpha}$. In the orbifold model, the number of degrees of freedom of the matrices associated with the $T^4/\mathbb{Z}_2$ directions is reduced, and there are nine disconnected components in the moduli space corresponding to different numbers of fixed points supporting 2 modulo 4 branes:

• The first component of moduli space contains a Higgs branch parameterised by

$$\mathcal{W}^{\rm D9}_{I} = \text{diag}\left(e^{2i\pi a^{I}_{1}}, e^{-2i\pi a^{I}_{1}}, \dots, e^{2i\pi a^{I}_{8}}, e^{-2i\pi a^{I}_{8}}, e^{-2i\pi a^{I}_{1}}, e^{2i\pi a^{I}_{1}}, \dots, e^{-2i\pi a^{I}_{8}}, e^{2i\pi a^{I}_{8}}\right), \tag{2.4}$$

where $I=6,\dots,9$. Generically this yields a gauge symmetry $USp(2)^8$ of rank 8, whose Coulomb branch is parameterised by the WL matrices $I'=4,5$,

$$\mathcal{W}^{\rm D9}_{I'} = \text{diag}\left(e^{2i\pi a^{I'}_{1}}, e^{-2i\pi a^{I'}_{1}}, \dots, e^{2i\pi a^{I'}_{8}}, e^{-2i\pi a^{I'}_{8}}, e^{2i\pi a^{I'}_{1}}, e^{-2i\pi a^{I'}_{1}}, \dots, e^{2i\pi a^{I'}_{8}}, e^{-2i\pi a^{I'}_{8}}\right), \tag{2.5}$$

and along which the gauge symmetry is reduced at generic points to $U(1)^8$. However, $USp(2)^8$ can be initially enhanced up to $U(16)$ of rank 16 at the points $a^I_1=\dots=a^I_8\in\{0,\frac{1}{2}\}$, $I=6,\dots,9$, and the Coulomb branch is then parameterised by

$$\mathcal{W}^{\rm D9}_{I'} = \text{diag}\left(e^{2i\pi a^{I'}_{1}}, e^{-2i\pi a^{I'}_{1}}, e^{2i\pi a^{I'}_{2}}, e^{-2i\pi a^{I'}_{2}}, \dots, e^{2i\pi a^{I'}_{16}}, e^{-2i\pi a^{I'}_{16}}\right) \tag{2.6}$$

for $I'=4,5$. This leads generically to an Abelian symmetry $U(1)^{16}$, with the 8 positions in $\tilde{T}^4/\mathbb{Z}_2$ stabilised.[6]

• A second component of the moduli space contains a Higgs branch that may be parameterised as

$$\begin{aligned}\mathcal{W}^{\rm D9}_{I} = \text{diag}\big(&e^{2i\pi a^{I}_{1}}, e^{-2i\pi a^{I}_{1}}, \dots, e^{2i\pi a^{I}_{7}}, e^{-2i\pi a^{I}_{7}}, \eta^I_8, \eta^I_8,\\ &e^{-2i\pi a^{I}_{1}}, e^{2i\pi a^{I}_{1}}, \dots, e^{-2i\pi a^{I}_{7}}, e^{2i\pi a^{I}_{7}}, \eta^I_{16}, \eta^I_{16}\big),\end{aligned} \tag{2.7}$$

$$\text{where}\quad \eta^I_8,\eta^I_{16}\in\{1,-1\}\,,\quad (\eta^6_8,\eta^7_8,\eta^8_8,\eta^9_8)\neq(\eta^6_{16},\eta^7_{16},\eta^8_{16},\eta^9_{16})\,.$$

[6] From the gauge theory perspective, they acquire tree level Higgs masses. From the geometric point of view, two pairs of D3-branes at a fixed point of $\tilde{T}^4/\mathbb{Z}_2$ can only move away from it if the coordinates of the pairs along $\tilde{T}^2/I_{45}$ match, in order to respect the $\mathbb{Z}_2$ symmetry in $\tilde{T}^4$. When this is the case for all 8 pairs of pairs, the Coulomb branch takes consistently the form given in Eq. (2.5).

Generically, the gauge symmetry is $USp(2)^7 \times U(1)^2$, which can again be enhanced up to $U(15) \times U(1)$. In the former case, the gauge group in the Coulomb branch is $U(1)^9$ for generic matrices $\mathcal{W}^{\rm D9}_{I'}$, while in the second case it is $U(1)^{16}$ with all positions in $\tilde{T}^4/\mathbb{Z}_2$ stabilised.

• There are seven more disconnected components of moduli space. In the ultimate one, the Higgs branch is zero-dimensional, the positions of all 32 branes in $\tilde{T}^4/\mathbb{Z}_2$ being rigid. To be specific, we have

$$\mathcal{W}^{\rm D9}_{I} = \text{diag}\left(\eta^I_1, \eta^I_1, \ldots, \eta^I_{16}, \eta^I_{16}\right) ,$$
$$\text{where} \quad \eta^I_\alpha \in \{1, -1\} \ , \ \alpha = 1, \ldots, 16 \ , \quad (\eta^6_\alpha, \eta^7_\alpha, \eta^8_\alpha, \eta^9_\alpha) \neq (\eta^6_\beta, \eta^7_\beta, \eta^8_\beta, \eta^9_\beta) \ , \ \alpha \neq \beta \ . \tag{2.8}$$

There is only a Coulomb branch with the gauge symmetry always being $U(1)^{16}$, regardless of the WL's along T^2,

$$\mathcal{W}^{\rm D9}_{I'} = \text{diag}\left(e^{2i\pi a^{I'}_1}, e^{-2i\pi a^{I'}_1}, e^{2i\pi a^{I'}_2}, e^{-2i\pi a^{I'}_2}, \ldots, e^{2i\pi a^{I'}_{16}}, e^{-2i\pi a^{I'}_{16}}\right) . \tag{2.9}$$

Similarly, the positions in $\tilde{T}^2 \times T^4/\mathbb{Z}_2$ of the D3-branes T-dual to D5-branes $\alpha = 1, \ldots, 32$ can be written as $\tilde{X}^{I'} = 2\pi b^{I'}_\alpha$, $I' = 4, 5$, $X^I = 2\pi b^I_\alpha$, $I = 6, \ldots, 9$. They span 9 disconnected components that admit various Higgs, Coulomb or mixed Higgs/Coulomb branches. The latter can be parameterised with matrices $\mathcal{W}^{\rm D5}_{\mathcal{I}}$ exactly analogous to those of the D9-branes, up to the exchange $a^{\mathcal{I}}_\alpha \to b^{\mathcal{I}}_\alpha$.

Discrete deformations: In what follows we will be mostly interested in configurations where all branes are located at the corners of the appropriate six-dimensional "boxes".[7] In order to write the corresponding one-loop amplitudes, we label the 64 corners by a pair of indices ii', where $i \in \{1, \ldots, 16\}$ refers to the $T^4/\mathbb{Z}_2$ (or its T-dual counterpart) fixed points, and $i' \in \{1, \ldots, 4\}$ specifies the $\tilde{T}^2/I_{45}$ fixed points. Fig. 1d shows schematically how the labelling works. At a given corner ii', we denote $N_{ii'}$ the number of D3-branes T-dual to D9-branes, and $D_{ii'}$ the number of D3-branes T-dual to D5-branes. In this setup, the Wilson lines/D3-brane positions $2\pi a^{\mathcal{I}}_\alpha$ and $2\pi b^{\mathcal{I}}_\alpha$, $\alpha = 1, \ldots, 32$, associated with the D9-branes and D5-branes take values equivalent to the coordinates of some corner ii', which we denote by the six-vectors $2\pi\vec{a}_{ii'}$. It is also convenient to write $\vec{a}_{ii'} \equiv (\vec{a}_{i'}, \vec{a}_i)$, where $\vec{a}_{i'}$, $\vec{a}_i$ are two- and four-vectors, whose components take values 0 or $\frac{1}{2}$. With these definitions, the amplitudes $\mathcal{A}$ and $\mathcal{M}$ arising from the open-string sector are as shown in Appendix A.3. In the closed-string sector, the amplitudes $\mathcal{T}$ and $\mathcal{K}$ are independent of the WL's/brane positions, and their expressions are simply those of the "undeformed" $U(16) \times U(16)$ BSGP model (see Appendix A.2). On the contrary, $\mathcal{A}$ and $\mathcal{M}$ involve the numbers of branes $N_{ii'}$, $D_{ii'}$, as well as their counterparts $R^{\rm N}_{ii'}$ and $R^{\rm D}_{ii'}$ under the orbifold action. These coefficients can be parameterised as

$$N_{ii'} = n_{ii'} + \bar{n}_{ii'} \ , \quad D_{ii'} = d_{ii'} + \bar{d}_{ii'} \ , \quad R^{\rm D}_{ii'} = i(n_{ii'} - \bar{n}_{ii'}) \ , \quad R^{\rm D}_{ii'} = i(d_{ii'} - \bar{d}_{ii'}) \ , \tag{2.10}$$

where $n_{ii'} = \bar{n}_{ii'}$ and $d_{ii'} = \bar{d}_{ii'}$ are positive integers. The tadpole cancellation condition then implies

[7] We will see in Sect. 3 that in the presence of spontaneous supersymmetry breaking, such configurations yield extrema of the effective potential.

$$\sum_{i,i'} n_{ii'} = 16\,, \qquad \sum_{i,i'} d_{ii'} = 16\,, \tag{2.11}$$

which leads to the open-string gauge group

$$\mathcal{G}_{\rm open} = \prod_{ii'/n_{ii'}\neq 0} U(n_{ii'}) \times \prod_{jj'/d_{jj'}\neq 0} U(d_{jj'})\,. \tag{2.12}$$

Non-perturbative consistency: Although consistent at the perturbative level, the models constructed so far must satisfy additional requirements to remain valid at the non-perturbative level [51]. To state these additional constraints, let us first consider the BSGP model in six dimensions. We have seen that the moduli space of the positions of the D5-branes in $T^4/\mathbb{Z}_2$ splits into 9 disconnected pieces. These are characterized by the even number $\mathcal{R} = 0, 2, \ldots, 16$ of pairs of D5-branes mirror to each other with respect to Ω that have rigid positions at distinct fixed points of $T^4/\mathbb{Z}_2$. To be consistent non-perturbatively, a model must have $\mathcal{R} = 0$, 8 or 16. When $\mathcal{R} = 8$, the mirror pairs must sit on the 8 corners of one of the hyperplanes $X^I = 0$ or π, $I = 6, \ldots, 9$. Similarly, the number of mirror pairs of D5-branes T-dual to the D9-branes with rigid positions in $\tilde{T}^4/\mathbb{Z}_2$ must be $\tilde{\mathcal{R}} = 0$, 8 or 16. Hence, there are only 3×3 fully consistent components in the moduli space, which can be further reduced to 6 by T-duality[8]:

$$(\mathcal{R}, \tilde{\mathcal{R}}) = (0,0)\,,\ \ (0,8)\,,\ \ \ (0,16)\,,\ \ (8,8)\,,\ \ (8,16)\,,\ \ (16,16)\,. \tag{2.13}$$

Compactifying down to four dimensions and T-dualizing T^2, there are no additional constraints on the distribution of D3-branes. The latter, including the $2\mathcal{R} + 2\tilde{\mathcal{R}}$ ones with rigid positions in $T^4/\mathbb{Z}_2$ or $\tilde{T}^4/\mathbb{Z}_2$, can move in pairs along the directions of $\tilde{T}^2/I_{45}$.

2.2. *Spontaneous breaking of supersymmetry*

What remains to be implemented is the spontaneous breaking of $\mathcal{N} = 2$ supersymmetry. This can be done *via* a stringy version [30–37] of the Scherk–Schwarz mechanism [38]. To this end, we consider an additional $\mathbb{Z}_2$ orbifold shift on the fifth direction, $X^5 \to X^5 + \pi$, coupled to $(-1)^F$, where F is the spacetime fermion number. Denoting the integer momenta along T^2 in the "undeformed" supersymmetric BSGP model by $\vec{m}' \equiv (m_4, m_5)$, the combined effects of the continuous deformations considered so far plus the extra freely acting orbifold action amounts to the following shifts:

$$\begin{aligned}
\vec{m}' &\longrightarrow \vec{m}' + F\,\vec{a}'_S && \text{in the closed-string sector}\,,\\
\vec{m}' &\longrightarrow \vec{m}' + F\,\vec{a}'_S + \vec{a}'_\alpha - \vec{a}'_\beta && \text{in the NN sector}\,,\\
\vec{m}' &\longrightarrow \vec{m}' + F\,\vec{a}'_S + \vec{b}'_\alpha - \vec{b}'_\beta && \text{in the DD sector}\,,\\
\vec{m}' &\longrightarrow \vec{m}' + F\,\vec{a}'_S + \vec{a}'_\alpha - \vec{b}'_\beta && \text{in the ND sector}\,.
\end{aligned} \tag{2.14}$$

In the above, we have defined

$$\vec{a}'_{\rm S} = \left(0, \frac{1}{2}\right)\,, \tag{2.15}$$

while $\vec{a}'_\alpha \equiv (a^4_\alpha, a^5_\alpha)$ and $\vec{b}'_\alpha \equiv (b^4_\alpha, b^5_\alpha)$, $\alpha = 1, \ldots, 32$, denote the WL's along T^2. Equivalently, in the D3-brane picture where $2\pi\vec{a}'_\alpha$ (or $2\pi\vec{b}'_\alpha$) and $2\pi\vec{a}'_\beta$ (or $2\pi\vec{b}'_\beta$) are the positions of the two

[8] They can be connected to each other by deforming $T^4/\mathbb{Z}_2$ into smooth $K3$ manifolds [51].

ends of the open strings in $\tilde{T}^2$, the components of $\vec{m}'$ are winding numbers. The key point is of course that the gravitini have acquired masses

$$M = \frac{\sqrt{G^{55}}}{2} M_{\rm s} \,, \tag{2.16}$$

showing that the breaking of $\mathcal{N}=2 \to \mathcal{N}=0$ supersymmetry is spontaneous. Moreover, M itself is one of the marginal deformations, provided it is less than the critical value of order of the string scale $M_{\rm s}$, at which a tree-level tachyonic instability arises [40,41]. In the language of supergravity, the background is then a "no-scale model" [68], which means that the tree-level potential is positive, semi-definite, and admits a flat direction parameterised by M.

As described above, when the WL deformations are discrete (the D3-branes sit on the O3-planes of the six-dimensional boxes), the vectors $\vec{a}'_\alpha$ and $\vec{b}'_\alpha$ take values equal to the appropriate $\vec{a}_{i'}$, $i'=1,\ldots,4$. This has an important consequence for the light spectrum, because KK modes in the open-string sector are massless if

$$\vec{m}' + F\,\vec{a}'_S + \vec{a}_{i'} - \vec{a}_{j'} = \vec{0} \,. \tag{2.17}$$

This equation admits solutions for both bosons ($F=0$) and fermions ($F=1$) depending on the relative displacements. This will be detailed in the next paragraph.

The potential and tree-level massless spectrum: The one-loop effective potential in the non-supersymmetric case no longer vanishes. For discrete WL deformations, the amplitudes $\mathcal{T}$, $\mathcal{K}$, $\mathcal{A}$ and $\mathcal{M}$ take the form displayed in Appendix A.4. They are expressed in terms of partition functions, from which we can derive the massless bosonic and fermionic spectra. To this end, it is useful to specify the labelling of the $\tilde{T}^2/I_{45}$ fixed points as follows: we will denote by $i'=1,3$ those located at the origin of the T-dual Scherk–Schwarz direction, $\tilde{X}^5=0$, and by $i'=2,4$ those at $\tilde{X}^5=\pi$ (see Fig. 1d). From Eqs. (A.23)–(A.26), we can then read off the massless spectrum of the $\mathcal{N}=2\to\mathcal{N}=0$ model when the WL's take discrete values as described above. Knowledge of the massless-state representations will be important to derive conditions for the stability of the one-loop potential using a simple algebraic method in Sect. 3.1.

In the open-string sector, the massless states arise from characters appearing in $\mathcal{A}$ and $\mathcal{M}$ at the origin of the T^2 and T^4 lattices. Eq. (2.17), which defines the origin of the T^2 lattice, implies that massless bosons require the ends of the strings (in the D3-brane picture) to be located on fixed points of coordinates $\vec{a}_{ii'} \equiv (\vec{a}_{i'}, \vec{a}_i)$ and $\vec{a}_{jj'} \equiv (\vec{a}_{j'}, \vec{a}_j)$ satisfying

$$\textit{massless bosons:} \quad \vec{a}_{i'} - \vec{a}_{j'} = \vec{0} \iff i' = j' \,. \tag{2.18}$$

On the contrary, massless fermions require

$$\textit{massless fermions:} \quad \vec{a}_{i'} - \vec{a}_{j'} = \mp \vec{a}'_{\rm S} \iff \begin{cases} i' = 2i''-1 \,, \;\; j' = 2i'' \\ \text{or} \\ i' = 2i'' \,, \;\; j' = 2i''-1 \end{cases} , \quad i'' = 1,2 \,, \tag{2.19}$$

implying that in the $\tilde{T}^2/I_{45}$, the string is stretched along the T-dual Scherk–Schwarz direction $\tilde{X}^5$. For such states the contributions to the mass induced by the spontaneous breaking of supersymmetry and by the WL's cancel exactly, *i.e.* the Superhiggs and the Higgs mechanisms offset each other. In the NN and DD sectors, whose contributions to the partition functions involve respectively T^4 momentum and T^4 winding number lattices (in the D9- and D5-brane picture), massless states must also satisfy

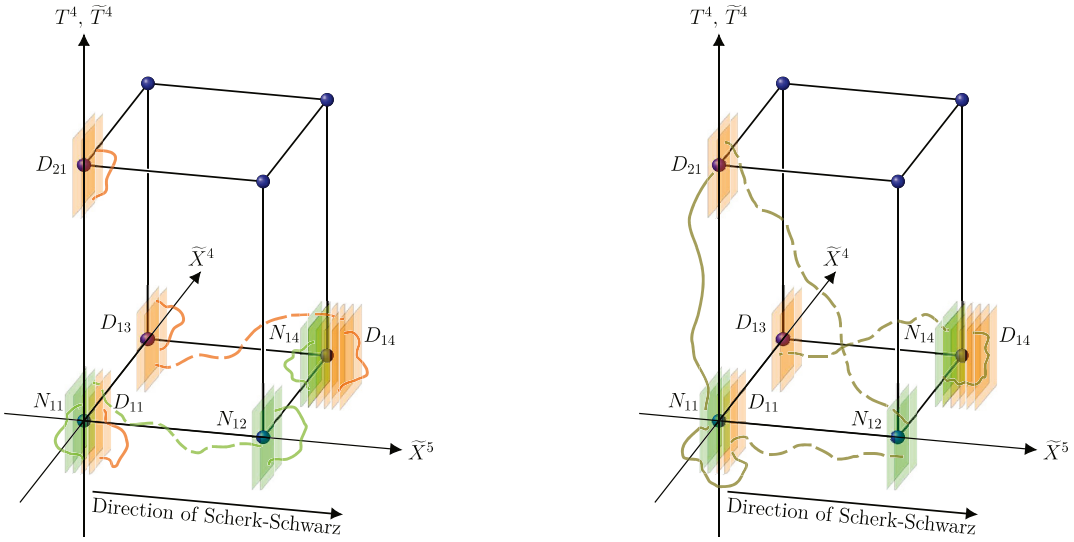

(a) Bosonic NN and DD states (solid strings) are massless when they correspond in the D3-brane picture to strings with both ends attached to the same stack of branes. By contrast fermionic NN and DD states (dashed strings) are massless when they correspond to strings stretched between corners of the six-dimensional box that are adjacent along the T-dual Scherk–Schwarz direction.

(b) ND states correspond to strings stretched between a stack of D3-branes T-dual to D9-branes and a stack of D3-branes T-dual to D5-branes. Bosonic ND states (solid strings) are massless when the stacks are located on corners with common coordinates in $\tilde{T}^2/I_{45}$. Fermionic ND states (dashed strings) are massless when the corners have common coordinate $\tilde{X}^4$ and distinct coordinate $\tilde{X}^5$.

Fig. 2. Open-string massless modes.

$$\textit{massless NN or DD states:} \quad \vec{a}_i - \vec{a}_j = \vec{0} \iff i = j \ . \tag{2.20}$$

Finally, because the ND sector does not involve T^4 lattices, i and j need not be correlated to yield massless states, hence

$$\textit{massless ND states:} \quad i, j \ \text{ arbitrary} \ . \tag{2.21}$$

To illustrate the above considerations, Fig. 2a displays massless states arising in the NN sector (green) and DD sector (orange) that are bosonic (solid strings) or fermionic (dashed strings). Similarly, Fig. 2b shows massless strings in the ND sector (khaki) which are bosonic (solid strings) or fermionic (dashed strings).

At the origin of the lattices appearing in the amplitude $\mathcal{A} + \mathcal{M}$, the massless states arise from the constant terms in the combinations of characters O_4/η^4, V_4/η^4, S_4/η^4, C_4/η^4 (see Eqs. (A.25), (A.26)) (*i.e.* the terms q^0 in the notations of Appendix A, where $q = e^{-\pi\tau_2}$ and τ_2 is the Schwinger parameter).[9] These combinations are dressed with coefficients which can be expressed using the unitary parameterisation (2.10). For the bosons and fermions, the relevant characters are respectively

$$\textbf{Bosons:} \ \frac{1}{\eta^8} \sum_{i,i'} \Big\{ V_4 O_4 \left[n_{ii'} \bar{n}_{ii'} + d_{ii'} \bar{d}_{ii'} \right]$$

[9] O_4, V_4, S_4, C_4 are $SO(4)$ affine characters arising from the breaking of the ten-dimensional little group $SO(8) \to SO(4) \times SO(4)$ imposed by the $\mathbb{Z}_2$-orbifold action.

$$
\begin{aligned}
&+ O_4 V_4 \left[\frac{n_{ii'}(n_{ii'}-1)}{2} + \frac{\bar{n}_{ii'}(\bar{n}_{ii'}-1)}{2} + \frac{d_{ii'}(d_{ii'}-1)}{2} + \frac{\bar{d}_{ii'}(\bar{d}_{ii'}-1)}{2} \right] \\
&+ O_4 C_4 \sum_j \left[\frac{1-e^{4i\pi \vec{a}_i\cdot\vec{a}_j}}{2} \left(n_{ii'} d_{ji'} + \bar{n}_{ii'} \bar{d}_{ji'} \right) + \frac{1+e^{4i\pi \vec{a}_i\cdot\vec{a}_j}}{2} \left(n_{ii'} \bar{d}_{ji'} + \bar{n}_{ii'} d_{ji'} \right) \right] \Bigg\} ,
\end{aligned}
$$

$$
\begin{aligned}
\textbf{Fermions: } & \frac{1}{\eta^8} \sum_{i,i''} \Big\{ C_4 C_4 \left[n_{i,2i''-1} \bar{n}_{i,2i''} + \bar{n}_{i,2i''-1} n_{i,2i''} + d_{i,2i''-1} \bar{d}_{i,2i''} + \bar{d}_{i,2i''-1} d_{i,2i''} \right] \\
&+ S_4 S_4 \left[n_{i,2i''-1} n_{i,2i''} + \bar{n}_{i,2i''-1} \bar{n}_{i,2i''} + d_{i,2i''-1} d_{i,2i''} + \bar{d}_{i,2i''-1} \bar{d}_{i,2i''} \right] \qquad (2.22) \\
&+ S_4 O_4 \sum_j \left[\frac{1-e^{4i\pi \vec{a}_i\cdot\vec{a}_j}}{2} \left(n_{i,2i''-1} d_{j,2i''} + \bar{n}_{i,2i''-1} \bar{d}_{j,2i''} + n_{i,2i''} d_{j,2i''-1} + \bar{n}_{i,2i''} \bar{d}_{j,2i''-1} \right) \right. \\
&\qquad \left. + \frac{1+e^{4i\pi \vec{a}_i\cdot\vec{a}_j}}{2} \left(n_{i,2i''-1} \bar{d}_{j,2i''} + \bar{n}_{i,2i''-1} d_{j,2i''} + n_{i,2i''} \bar{d}_{j,2i''-1} + \bar{n}_{i,2i''} d_{j,2i''-1} \right) \right] \Big\} .
\end{aligned}
$$

We can immediately read off from these formulae the numbers of massless bosonic and fermionic open-string degrees of freedom:

$$
\begin{aligned}
n_{\mathrm{B}}^{\mathrm{open}} &= 4 \left[2 \sum_{ii'} \left(n_{ii'}^2 + d_{ii'}^2 \right) + \sum_{i,i',j} n_{ii'} d_{ji'} - 32 \right] , \\
n_{\mathrm{F}}^{\mathrm{open}} &= 4 \left[4 \sum_{i,i''} \left(n_{i,2i''-1} n_{i,2i''} + d_{i,2i''-1} d_{i,2i''} \right) + \sum_{i,i'',j} \left(n_{i,2i''-1} d_{j,2i''} + n_{i,2i''} d_{j,2i''-1} \right) \right] .
\end{aligned} \qquad (2.23)
$$

We can also deduce the representations in which these massless modes are organized. For the bosons, the first line in Eq. (2.22) corresponds to the bosonic content of $\mathcal{N}=2$ vector multiplets in the adjoint representations of the $U(n_{ii'})$ and $U(d_{ii'})$ gauge groups. The second line is associated with the scalars of $\mathcal{N}=2$ hypermultiplets in the antisymmetric $\oplus$ antisymmetric representations of $U(n_{ii'})$ and $U(d_{ii'})$. Finally, the last line corresponds to the scalars of hypermultiplets in the ND sector, which are in bifundamental representations of $U(n_{ii'}) \times U(d_{ji'})$. To be more precise, they are in tensor products of fundamental $\otimes$ fundamental or fundamental representations, depending on the parity of $4\vec{a}_i \cdot \vec{a}_j \in \mathbb{Z}$. The massless fermions in the NN, DD and ND sectors are those of hypermultiplets, all in various bifundamental representations of unitary gauge groups supported on stacks of D3-branes separated along the T-dual Scherk–Schwarz direction (and possibly for the ND states also along T^4 or $\tilde{T}^4$).

For later use in Sect. 3.1, it is relevant to perform a precise counting of the representations of each individual unitary gauge group factor. In Table 1 we gather the massless states charged under $U(n_{i,2i''-1})$ and $U(n_{i,2i''})$ for given $i = 1, \ldots, 16$ and $i'' = 1, 2$, which are found from Eq. (2.22). The counting for the gauge groups $U(d_{i,2i''-1})$ and $U(d_{i,2i''})$, which are generated by the D5-branes, is of course identical, up to the exchange of all coefficients $n_{kk'} \leftrightarrow d_{kk'}$.

In the closed-string sector, all the initially massless fermions in the BSGP model acquire a mass M after implementation of the Scherk–Schwarz mechanism. The massless spectrum thus reduces to the bosonic one encountered in the BSGP model, and is more easily described from a six-dimensional point of view. In the untwisted sector, we have the components of $(G+C)_{\hat{\mu}\hat{\nu}}$, $\hat{\mu}, \hat{\nu} = 2, \ldots, 5$, and the internal components $(G+C)_{IJ}$, $I, J = 6, \ldots, 9$, which yield in light-cone gauge $(6-2) \times (6-2) + 4 \times 4$ degrees of freedom. Moreover, there are also the scalars of the 16 twisted hypermultiplets. Hence, we obtain a total of

Table 1
Representations of $U(n_{i,2i''-1})$ and $U(n_{i,2i''})$ into which the massless degrees of freedom are organized.

Massless representations of $U(n_{i,2i''-1})$	
Bosonic degrees of freedom:	Fermionic degrees of freedom:
• 4 adjoint	• $8n_{i,2i''}$ (fundamental $\oplus$ $\overline{\text{fundamental}}$)
• 4 (antisymmetric $\oplus$ $\overline{\text{antisymmetric}}$)	• $2\sum_j d_{j,2i''}$ (fundamental $\oplus$ $\overline{\text{fundamental}}$)
• $2\sum_j d_{j,2i''-1}$ (fundamental $\oplus$ $\overline{\text{fundamental}}$)	
Massless representations of $U(n_{i,2i''})$	
Bosonic degrees of freedom:	Fermionic degrees of freedom:
• 4 adjoint	• $8n_{i,2i''-1}$ (fundamental $\oplus$ $\overline{\text{fundamental}}$)
• 4 (antisymmetric $\oplus$ $\overline{\text{antisymmetric}}$)	• $2\sum_j d_{j,2i''-1}$ (fundamental $\oplus$ $\overline{\text{fundamental}}$)
• $2\sum_j d_{j,2i''}$ (fundamental $\oplus$ $\overline{\text{fundamental}}$)	

$$n_{\rm B}^{\rm closed} = 4\times(4+4+16)\,, \qquad n_{\rm F}^{\rm closed} = 0 \tag{2.24}$$

bosonic and fermionic degrees of freedom. In terms of six dimensional $\mathcal{N}=1$ supermultiplets, the $n_{\rm B}^{\rm closed}$ states comprise the bosonic components of the gravity multiplet $(g_{\hat\mu\hat\nu}, C^+_{\hat\mu\hat\nu})$, where $g_{\hat\mu\hat\nu}$ is the traceless graviton and $C^+_{\hat\mu\hat\nu}$ is a self-dual 2-form, a tensor multiplet $(C^-_{\hat\mu\hat\nu}, \phi)$, where $C^-_{\hat\mu\hat\nu}$ is an anti self-dual 2-form and ϕ is the dilaton, and $4+16$ hypermultiplets.

Taking into account both the closed-string and open-string sectors, the numbers $n_{\rm F}$ and $n_{\rm B}$ of massless fermionic and bosonic degrees of freedom in the $\mathcal{N}=2\to\mathcal{N}=0$ model that includes discrete WL deformations satisfy

$$\begin{aligned} n_{\rm F}-n_{\rm B} = 4\Big[8 &- 2\sum_{i,i''}\left(n_{i,2i''-1}-n_{i,2i''}\right)^2 - 2\sum_{i,i''}\left(d_{i,2i''-1}-d_{i,2i''}\right)^2 \\ &- \sum_{i,i'',j}\left(n_{i,2i''-1}-n_{i,2i''}\right)\left(d_{j,2i''-1}-d_{j,2i''}\right)\Big]\,. \end{aligned} \tag{2.25}$$

3. Stability conditions

Let us now consider the model described in the previous section at those points in moduli space where the WL's take discrete values. In this section we will show that, at such points, the one-loop effective potential is extremal with respect to the WL's,[10] and we will derive the masses of these moduli at the quantum level. We will also determine the masses of (some of) the 16 twisted quaternionic moduli acquired by a generalized Green–Schwarz mechanism in six dimensions. For the WL's, we use an algebraic method based on our knowledge of the representations of the massless spectrum, as well as a direct derivation from the one-loop effective potential. We will see that the final answer for the WL masses is obtained by combining these results with a detailed analysis of the one-loop anomaly cancellation mechanism that involves couplings of anomalous $U(1)$ gauge bosons to twisted Stueckelberg fields.

[10] It is also extremal with respect to the scalars in the ND sector [59].

3.1. Signs of the Wilson line masses

In this and the following subsection, we consider the WL mass terms arising from the one-loop Coleman–Weinberg effective potential. However, we will see in Sect. 3.3 that additional large contributions (still proportional to the open-string coupling) arise from a generalized Green–Schwarz mechanism that takes place in six dimensions. This effect implies that tachyonic instabilities at the one-loop level can only arise in submanifolds of the WL moduli space described in Sect. 2.1. Therefore, negative signs of the WL mass terms derived in the present subsection do not necessarily imply tachyonic instabilities, as will be seen in Sect. 4.

In Refs. [9,10,21], an expression for the one-loop effective potential $\mathcal{V}$ was derived for heterotic string compactified on a torus, when supersymmetry is broken by the Scherk–Schwarz mechanism acting along one compact coordinate, say X^5. It applies in the local neighbourhood of points in moduli space where extra massless states arise, and is valid provided the size of X^5 is greater than the string length as well as all the other compactification length scales (or their T-dual counterparts). In four dimensions, denoting the WL of the r-th Cartan $U(1)$ of the gauge group $\mathcal{G}$ along the internal direction $X^{\mathcal{I}}$ by $y_r^{\mathcal{I}}$, we can develop the potential to second order around a point of enhanced massless spectrum as follows:

$$\mathcal{V} = M^4(n_{\rm F}-n_{\rm B})\xi + M^4\Big(\sum_{\text{weights } Q\in\mathcal{R}_{\rm B}} - \sum_{\text{weights } Q\in\mathcal{R}_{\rm F}}\Big)\xi' Q_r Q_s\Big(\sum_{\substack{\mathcal{I}=4\\ \neq 5}}^{9}\frac{y_r^{\mathcal{I}}y_s^{\mathcal{I}}}{3G^{55}} + y_r^5 y_s^5\Big) + \cdots , \tag{3.1}$$

where $\xi, \xi' > 0$, the supersymmetry breaking scale is M, and where $n_{\rm F}$, $n_{\rm B}$ denote the numbers of massless fermionic and bosonic degrees of freedom at $y_r^{\mathcal{I}} = 0$, living respectively in reducible representations $\mathcal{R}_{\rm F}$, $\mathcal{R}_{\rm B}$ of $\mathcal{G}$. Note that there is no WL tadpole. This follows from the fact that linear terms in WL's are also linear in Cartan charges Q_r and that the latter can be paired for particles and antiparticles. Writing the gauge group as $\mathcal{G} \equiv \prod_\kappa \mathcal{G}_\kappa$, the sums over the weights of $\mathcal{R}_{\rm F}$, $\mathcal{R}_{\rm B}$ can be expressed in terms of Dynkin indices $T_{\mathcal{R}_u^{(\kappa)}}$ of irreducible representations $\mathcal{R}_u^{(\kappa)}$ of the gauge group factors $\mathcal{G}_\kappa$, using the relation

$$T_{\mathcal{R}_u^{(\kappa)}}\delta_{rs} = \frac{1}{2}\sum_{\text{weights } Q\in\mathcal{R}_u^{(\kappa)}} Q_r Q_s \ , \qquad r,s = 1,\ldots,\text{rank}\,\mathcal{G}_\kappa \ . \tag{3.2}$$

Indeed, we may write (with no sum over r and $\mathcal{I}$)

$$\frac{\partial^2\mathcal{V}}{(\partial y_r^{\mathcal{I}})^2}\bigg|_{y=0} \propto \sum_u T_{\mathcal{R}_{{\rm B}u}^{(\kappa)}} - \sum_u T_{\mathcal{R}_{{\rm F}u}^{(\kappa)}} \ , \quad r = 1,\ldots,\text{rank}\,\mathcal{G}_\kappa \ , \quad \mathcal{I} = 4,\ldots,9 \ , \tag{3.3}$$

where $\mathcal{R}_{{\rm B}u}^{(\kappa)}$ and $\mathcal{R}_{{\rm F}u}^{(\kappa)}$ are the bosonic and fermionic massless representations of $\mathcal{G}_\kappa$.

Note that in Eq. (3.1) the coefficients ξ, ξ' capture the contributions of the KK modes propagating along the large extra dimension X^5, while all corrections arising from the other massive states (level-matched or not) are exponentially suppressed. Therefore, the resulting expression holds in more general contexts, such as the type I string theory compactified on tori studied in Ref. [23], or in the orbifold model considered in the present work, for the WL's along T^2. In particular, the signs of the one-loop contributions to their squared masses can be found by subtracting the Dynkin indices of the fermionic representations from those of the bosonic ones. From

Table 2
Dimensions and Dynkin indices of representations of special orthogonal and unitary groups. The Dynkin indices of the fundamental representations are normalized to 1 by convention.

Gauge factor $\mathcal{G}_\kappa$	Representation $\mathcal{R}_u^{(\kappa)}$	$\dim \mathcal{R}_u^{(\kappa)}$	$T_{\mathcal{R}_u}^{(\kappa)}$
$SO(p)$, $p \geq 2$	fundamental	p	1
	adjoint	$\frac{p(p-1)}{2}$	$p-2$
$SU(q)$, $q \geq 2$	fundamental	q	1
	$\overline{\text{fundamental}}$	q	1
	adjoint	q^2-1	$2q$
	antisymmetric	$\frac{q(q-1)}{2}$	$q-2$
	$\overline{\text{antisymmetric}}$	$\frac{q(q-1)}{2}$	$q-2$

Table 1, which lists the relevant representations of $SU(q)$, and Table 2 which gives the associated Dynkin indices, we find that the one-loop contributions to the squared masses of the WL's along T^2, of the special unitary groups supported by the stacks of D9-branes and D5-branes are proportional (up to positive dressing factors) to[11]

$$
\begin{aligned}
&4(n_{i,2i''-1} - n_{i,2i''} - 1) + \sum_{j=1}^{16}(d_{j,2i''-1} - d_{j,2i''}) \qquad \text{for} \qquad U(n_{i,2i''-1})\ , \\
&4(n_{i,2i''} - n_{i,2i''-1} - 1) + \sum_{j=1}^{16}(d_{j,2i''} - d_{j,2i''-1}) \qquad \text{for} \qquad U(n_{i,2i''})\ , \\
&4(d_{i,2i''-1} - d_{i,2i''} - 1) + \sum_{j=1}^{16}(n_{j,2i''-1} - n_{j,2i''}) \qquad \text{for} \qquad U(d_{i,2i''-1})\ , \\
&4(d_{i,2i''} - d_{i,2i''-1} - 1) + \sum_{j=1}^{16}(n_{j,2i''} - n_{j,2i''-1}) \qquad \text{for} \qquad U(d_{i,2i''})\ .
\end{aligned}
\tag{3.4}
$$

Note that at this stage, these mass-term coefficients have been derived assuming $n_{ii'} \geq 2$ and $d_{ii'} \geq 2$. To extend them to the case where $n_{ii'} = 1$ or $d_{ii'} = 1$, one may consider Eq. (3.3) where the adjoint representations have vanishing charges and the antisymmetric representations are zero-dimensional, so that only "fundamental" or "$\overline{\text{fundamental}}$" representations contribute. Then Eq. (3.3) is still applicable but the corresponding coefficients $T_{\mathcal{R}_{\text{B}u}^{(\kappa)}}$ and $T_{\mathcal{R}_{\text{F}u}^{(\kappa)}}$ are no longer strictly speaking Dynkin indices. As the associated $U(1)$ charges are universal Chan–Paton factors, one finds that the conditions (3.4) remain valid.

On the contrary, because WL is a misnomer for the moduli describing the positions of the D3-branes along $\tilde{T}^4/\mathbb{Z}_2$ (or $T^4/\mathbb{Z}_2$), the signs of their squared masses cannot be determined by applying Eq. (3.3) for unitary groups. However, inspecting the amplitude $\mathcal{A} + \mathcal{M}$ in Eqs. (A.25), (A.26), we see that small (continuous) deformations of these positions appear only

[11] The effect of a generalised Green–Schwarz mechanism must be taken into account to determine if the WL's along T^2 are stable or not (see Sect. 3.3).

in the NN sector (or DD sector), when the $\mathbb{Z}_2$-orbifold generator g does not act.[12] Consequently, up to an overall factor of $\frac{1}{2}$, the NN sector contribution is simply that of the open-string sector in the parent $\mathcal{N}=4 \to \mathcal{N}=0$ model studied in [23], which has orthogonal gauge groups. The signs of the moduli masses arising at one loop can therefore be found using Dynkin indices of representations of special orthogonal groups, which are shown in Table 2. In the parent $\mathcal{N}=4 \to \mathcal{N}=0$ model, a pair of stacks of $N_{i,2i''-1}$ and $N_{i,2i''}$ D3-branes T-dual to D9-branes produces an $SO(N_{i,2i''-1}) \times SO(N_{i,2i''})$ gauge factor. The states charged under $SO(N_{i,2i''-1})$ are 8 bosons in the adjoint representation, and $8N_{i,2i''}$ fermions in the fundamental arising from bifundamentals of $SO(N_{i,2i''-1}) \times SO(N_{i,2i''})$. The representations of the degrees of freedom charged under $SO(N_{i,2i''})$ are identical, up to the exchange $N_{i,2i''-1} \leftrightarrow N_{i,2i''}$. The end result is that the masses of the WL's along T^4 of the special orthogonal groups are non-negative when

$$\begin{aligned} &N_{i,2i''-1} - N_{i,2i''} - 2 \;\geq\; 0 \qquad \text{for} \qquad SO(N_{i,2i''-1})\,, \\ &N_{i,2i''} - N_{i,2i''-1} - 2 \;\geq\; 0 \qquad \text{for} \qquad SO(N_{i,2i''})\,. \end{aligned} \tag{3.5}$$

In the $\mathcal{N}=2 \to \mathcal{N}=0$ orbifold model, this result implies that the masses of the position moduli of the D3-branes in $\tilde{T}^4/\mathbb{Z}_2$ (or $T^4/\mathbb{Z}_2$) are non-negative when

$$\begin{aligned} &n_{i,2i''-1} - n_{i,2i''} \;\geq\; 1 \qquad \text{for} \qquad U(n_{i,2i''-1})\,, \quad n_{i,2i''-1} \geq 2\,, \\ &n_{i,2i''} - n_{i,2i''-1} \;\geq\; 1 \qquad \text{for} \qquad U(n_{i,2i''})\,, \quad n_{i,2i''} \geq 2\,, \\ &d_{i,2i''-1} - d_{i,2i''} \;\geq\; 1 \qquad \text{for} \qquad U(d_{i,2i''-1})\,, \quad d_{i,2i''-1} \geq 2\,, \\ &d_{i,2i''} - d_{i,2i''-1} \;\geq\; 1 \qquad \text{for} \qquad U(d_{i,2i''})\,, \quad d_{i,2i''} \geq 2\,. \end{aligned} \tag{3.6}$$

In the above, the conditions for the D5-brane locations are deduced by T-dualizing $T^4/\mathbb{Z}_2$, which amounts to changing all coefficients $n_{kk'} \to d_{kk'}$. Finally we recall the special cases: namely that when $n_{i,2i'-1}$, $n_{i,2i'}$, $d_{i,2i'-1}$ or $d_{i,2i'} = 1$, the antisymmetric and antisymmetric representations are zero-dimensional, so the positions of the D3-branes in $\tilde{T}^4/\mathbb{Z}_2$ or $T^4/\mathbb{Z}_2$ are no longer moduli fields.[13] Notice that the conditions (3.6) are valid even when there are fewer than 8 dynamical positions in $\tilde{T}^4/\mathbb{Z}_2$ or $T^4/\mathbb{Z}_2$ (see Sect. 2.1), *i.e.* when there are $U(k)$ gauge group factors with odd k's. This follows from the fact that the remaining dynamical positions of the branes generating the $U(k)$'s must not be tachyonic.

Notice that the two first (last) inequalities in (3.6) are incompatible. Hence, one of them must be absent, which means that either $n_{i,2i''-1}$ or $n_{i,2i''}$ ($d_{i,2i''-1}$ or $d_{i,2i''}$) must be 0 or 1. In other words, the WL positions along $\tilde{T}^4/\mathbb{Z}_2$ and $T^4/\mathbb{Z}_2$ are non-tachyonic if and only if the configuration satisfies

$$\forall\, i\,, i'' :\; (n_{i,2i''-1}, n_{i,2i''})\,,\; (d_{i,2i''-1}, d_{i,2i''}) \in \big\{(0,p),\,(p,0),\,(1,p),\,(p,1) \text{ where } p \in \mathbb{N}\big\}\,. \tag{3.7}$$

3.2. *Wilson line masses and effective potential*

Prior to taking into account the effect of the Green–Schwarz mechanism in the next subsection, let us also discuss how the signs and absolute values of the open-string WL masses may

[12] Explicit expressions are actually given in Eqs. (B.2) and (B.3).

[13] As explained in Sect. 2.1, the cause of the rigidity of the position in $\tilde{T}^4/\mathbb{Z}_2$ or $T^4/\mathbb{Z}_2$ of a pair of coincident D3-branes can be six-dimensional (in all components of the moduli space with $(\mathcal{R}, \tilde{\mathcal{R}}) \neq (0,0)$). Or it can be four-dimensional, by splitting two pairs of pairs of D3-branes at fixed points ii' and ij', where $i' \neq j'$.

be inferred from the one-loop Coleman-Weinberg effective potential $\mathcal{V}$. This is a check on the above stability conditions. To this end, the potential may be evaluated for arbitrary (continuous) D3-brane positions $2\pi a_\alpha^{\mathcal{I}}$, $2\pi b_\alpha^{\mathcal{I}}$, $\alpha = 1, \ldots, 32$, and Taylor expanded at quadratic order around the backgrounds of interest corresponding to branes localized on O3-planes. Hence, we define the WL fluctuations as

$$\begin{aligned} a_\alpha^{\mathcal{I}} &= \langle a_\alpha^{\mathcal{I}} \rangle + \epsilon_\alpha^{\mathcal{I}} \,, \qquad \langle a_\alpha^{\mathcal{I}} \rangle \in \left\{0, \frac{1}{2}\right\} \,, \\ b_\alpha^{\mathcal{I}} &= \langle b_\alpha^{\mathcal{I}} \rangle + \xi_\alpha^{\mathcal{I}} \,, \qquad \langle b_\alpha^{\mathcal{I}} \rangle \in \left\{0, \frac{1}{2}\right\} \,. \end{aligned} \tag{3.8}$$

As in the previous subsection, we are interested in regions of moduli space in which the KK mass scale associated with the large Scherk–Schwarz direction X^5 is lower than the string scale as well as all other mass scales induced by the compactification moduli $G_{\mathcal{I}\mathcal{J}}$. In practice, this translates to the conditions

$$G^{55} \ll G_{44}, |G_{IJ}| \ll G_{55} \,, \quad |G_{45}|, |G_{5J}| \ll \sqrt{G_{55}} \,, \quad I, J = 6, \ldots, 9 \,, \quad G_{55} \gg 1 \,. \tag{3.9}$$

The detailed computation of the open-string contribution to the one-loop potential is performed in Appendix B. For the closed-string sector, the derivation proceeds as in the $\mathcal{N} = 4$ case in four dimensions which can be found in Ref. [23]. The full result takes the form

$$\mathcal{V} = \frac{\Gamma\left(\frac{5}{2}\right)}{\pi^{\frac{13}{2}}} M^4 \sum_{l_5} \frac{\mathcal{N}_{2l_5+1}(\epsilon, \xi, G)}{|2l_5+1|^5} + \mathcal{O}\left((M_s M)^2 e^{-2\pi c \frac{M_s}{M}}\right) \,, \tag{3.10}$$

where c is a positive constant of order 1. In this expression, we have defined

$$\mathcal{N}_{2l_5+1}(\epsilon, \xi, G) = n_{\rm F}^{\rm closed} - n_{\rm B}^{\rm closed} + \mathcal{N}_{2l_5+1}^{\rm open}(\epsilon, \xi, G) \,, \tag{3.11}$$

where $\mathcal{N}_{2l_5+1}^{\rm open}(\epsilon, \xi, G)$ is given in Eq. (B.19). The above quantity captures the dominant contributions to $\mathcal{V}$, which arise from the massless states as well as their towers of KK modes propagating along the direction X^5. As compared to M, all other string modes are super heavy, yielding (together with the non level-matched states in the closed-string sector) exponentially suppressed corrections, as indicated in Eq. (3.10). Hence, $\mathcal{N}_{2l_5+1}^{\rm open}(\epsilon, \xi, G)$ is expressed as a sum over massless open strings stretched between pairs (α, β) of branes in the NN, DD or ND sectors. The dependencies on the WL fluctuations $\epsilon_\alpha^{\mathcal{I}}$, $\xi_\alpha^{\mathcal{I}}$ appear in the arguments taken by a function $\mathcal{H}_{\frac{5}{2}}$ given in Eq. (B.9), which is dressed by oscillatory cosines. Finally, the definition of $\hat{G}^{44}$ can be found in Eq. (B.11).

In order to find the effective potential contribution to the WL masses, we must expand $\mathcal{N}_{2l_5+1}(\epsilon, \xi, G)$ to quadratic order using the small argument behaviour of the function $\mathcal{H}_{\frac{5}{2}}$ shown in Eq. (B.13). As seen in Sect. 2.1, the $\epsilon_\alpha^{\mathcal{I}}$, $\xi_\alpha^{\mathcal{I}}$ are however correlated or frozen to zero. To take this fact into account, we label the independent degrees of freedom with indices r and r' as follows,

$$
\begin{aligned}
&\epsilon_r^I\ , && I=6,\dots,9, && r=1,\dots,\sum_{i,i'}\left\lfloor\frac{N_{ii'}}{4}\right\rfloor=\sum_{i,i'}\left\lfloor\frac{n_{ii'}}{2}\right\rfloor\leq 8-\frac{\tilde{\mathcal{R}}}{2}\ ,\\
&\xi_r^I\ , && I=6,\dots,9, && r=1,\dots,\sum_{i,i'}\left\lfloor\frac{D_{ii'}}{4}\right\rfloor=\sum_{i,i'}\left\lfloor\frac{d_{ii'}}{2}\right\rfloor\leq 8-\frac{\mathcal{R}}{2}\ ,\\
&\epsilon_{r'}^{I'}\ ,\ \xi_{r'}^{I'}\ , && I'=4,5, && r'=1,\dots,16\ ,
\end{aligned}
\tag{3.12}
$$

where $\tilde{\mathcal{R}}$ and $\mathcal{R}$ were defined previously as the numbers of pairs of D3-branes with rigid positions either in $\tilde{T}^4/\mathbb{Z}_2$ or $T^4/\mathbb{Z}_2$. To write the expansion in compact notations, it is convenient to introduce the following notations:

• $i(r)i'(r)$ denotes the corner of $\tilde{T}^2/I_{45}\times\tilde{T}^4/\mathbb{Z}_2$ around which $2\pi\epsilon_r^I$ fluctuates, and $i(r)\hat{i}'(r)$ denotes the adjacent corner along the Scherk–Schwarz direction $\tilde{X}^5$. Note that because ϵ_r^I is dynamical, the two pairs of D3-branes whose position it describes are at the same fixed point of $\tilde{T}/I_{45}$.

• Similarly, $j(r)j'(r)$ denotes the corner of $\tilde{T}^2/I_{45}\times T^4/\mathbb{Z}_2$ around which $2\pi\xi_r^I$ fluctuates, and $j(r)\hat{j}'(r)$ denotes the adjacent corner along the Scherk–Schwarz direction $\tilde{X}^5$.

• $i(r')i'(r')$ denotes the corner of $\tilde{T}^2/I_{45}\times\tilde{T}^4/\mathbb{Z}_2$ around which $2\pi\epsilon_{r'}^{I'}$ fluctuates, and $i(r')\hat{i}'(r')$ the adjacent corner along the Scherk–Schwarz direction $\tilde{X}^5$.

• Similarly, $j(r')j'(r')$ denotes the corner of $\tilde{T}^2/I_{45}\times T^4/\mathbb{Z}_2$ around which $2\pi\xi_{r'}^{I'}$ fluctuates, and $j(r')\hat{j}'(r')$ the adjacent corner along the Scherk–Schwarz direction $\tilde{X}^5$.

With these conventions, we obtain

$$
\begin{aligned}
\mathcal{N}_{2l_5+1}(\epsilon,\xi,G) \;=\; & n_{\mathrm{F}}-n_{\mathrm{B}}+32\pi^2(2l_5+1)^2\Bigg\{\\
&\sum_r\left(n_{i(r)i'(r)}-n_{i(r)\hat{i}'(r)}-1\right)\epsilon_r^I\,\Delta^{IJ}\epsilon_r^J\\
&+\sum_r\left(d_{j(r)j'(r)}-d_{j(r)\hat{j}'(r)}-1\right)\xi_r^I\,\Delta_{IJ}\xi_r^J\\
&+\sum_{r'}\left(n_{i(r')i'(r')}-n_{i(r')\hat{i}'(r')}-1+\frac{1}{4}\sum_i\left(d_{ii'(r')}-d_{i\hat{i}'(r')}\right)\right)\epsilon_{r'}^{I'}\,\Delta^{I'J'}\epsilon_{r'}^{J'}\\
&+\sum_{r'}\left(d_{j(r')j'(r')}-d_{j(r')\hat{j}'(r')}-1+\frac{1}{4}\sum_j\left(n_{jj'(r')}-n_{j\hat{j}'(r')}\right)\right)\xi_{r'}^{I'}\,\Delta^{I'J'}\xi_{r'}^{J'}\\
&+\mathcal{O}\left(\epsilon^4,\xi^4\right)\Bigg\}\ ,
\end{aligned}
\tag{3.13}
$$

where we have defined

$$
\Delta^{I'J'}=\frac{1}{3}\left(\frac{G^{I'J'}}{G^{55}}+2\,\frac{G^{5I'}}{G^{55}}\,\frac{G^{5J'}}{G^{55}}\right),\qquad \Delta^{IJ}=\frac{2}{3}\,\frac{G^{IJ}}{G^{55}}\ ,\qquad \Delta_{IJ}=\frac{2}{3}\,\frac{G_{IJ}}{G^{55}}\ .
\tag{3.14}
$$

Because the above tensors have positive eigenvalues, the signs of the WL masses reproduce exactly the results displayed in Eqs. (3.6) and (3.4).

3.3. *Mass generation* **via** *generalized Green–Schwarz mechanism*

In this subsection, we discuss how Abelian vector bosons in six dimensions become massive thanks to a generalized Green–Schwarz mechanism [51]. As a result, their WL's along T^2 are automatically heavy, improving the overall stability of the models.

Since all $\mathcal{N}=1$ supersymmetric theories are chiral, anomaly cancellations in the BSGP type IIB orientifold model proceed in a non-trivial way. For any values of the WL's along $T^4/\mathbb{Z}_2$ for the D9-brane gauge group, and arbitrary positions of the D5-branes in $T^4/\mathbb{Z}_2$, the fermionic spectrum ensures the cancellation of the irreducible gauge and gravitational anomalies. However, there are residual reducible anomalies, which are described by an anomaly polynomial I_8 explicitly written down in Ref. [51]. When the WL's and positions take discrete values $\vec{a}_i$, the gauge symmetry generated by the D9-branes and D5-branes is a product of unitary groups,

$$\prod_{i/n_i\neq 0} U(n_i) \times \prod_{j/d_j\neq 0} U(d_j)\ , \quad \text{where} \quad \sum_i n_i = \sum_i d_i = 16\ , \tag{3.15}$$

and where the rank is 32. As usual in six dimensions, the anomaly polynomial I_8 does not factorise, reflecting the fact that massless forms transform nonlinearly under gauge transformations and diffeomorphisms. In the case at hand, these forms are RR fields belonging to the closed-string spectrum: there is the 2-form C in the untwisted sector, as well as sixteen 4-forms C_4^i in the twisted sector. By Hodge duality ($\mathrm{d}C_4^i = *\mathrm{d}C_0^i$), the magnetic 4-form degrees of freedom are equivalent to electric pseudoscalars C_0^i. Each of them combines with 3 NS-NS scalars of the twisted sector, thus realizing the bosonic part of the massless twisted hypermultiplet localized at the fixed point i of $T^4/\mathbb{Z}_2$.

Anomaly cancellation requires the effective action to contain tree-level couplings proportional to

$$\int C\wedge X_4 \qquad \text{or} \qquad \sum_{i,a} c_{ia}\int C_0^i\wedge F_a^3 + \sum_{i,a} c_{ia}\int C_4^i\wedge F_a\ , \tag{3.16}$$

where F_a, $a=1,\dots,16$, are the field strengths of the Cartan $U(1)$ generators of $\prod_{i/d_i\neq 0} U(d_i)$, while F_a, $a=17,\dots,32$, are those of $\prod_{i/n_i\neq 0} U(n_i)$. Similar couplings involving $\mathrm{tr}\,R^2$ also exist. In the above expressions, the coefficients are

$$\begin{aligned} c_{ia} &= 4\delta_{a\in i}\ , && \text{for } a=1,\dots,16\ ,\\ c_{ia} &= -e^{4i\pi\vec{a}_i\cdot\vec{a}_{j(a)}}\ , && \text{for } a=17,\dots,32\ , \end{aligned} \tag{3.17}$$

where $\delta_{a\in i}=1$ when the a-th $U(1)$ belongs to the Cartan subalgebra of $U(d_i)$, and $\delta_{a\in i}=0$ otherwise. Moreover, we denote by $2\pi\vec{a}_{j(a)}$ the coordinate vector of the corner of $\tilde{T}^4/\mathbb{Z}_2$ which supports the Cartan $U(1)$ labelled by a of $\prod_{j/n_j\neq 0} U(n_j)$ (in a T-dual description). The Lagrangian can be cast into a local form by dualizing the last term in Eq. (3.16), which becomes

$$\sum_i \int \big(C_0^i + \sum_a c_{ia}A_a\big)\wedge *\big(C_0^i + \sum_b c_{ib}A_b\big)\ , \tag{3.18}$$

where the A_a's denote the Abelian vector potentials, $F_a = \mathrm{d}A_a$. As a result, the latter admit a tree-level mass term

$$\frac{1}{2}\sum_{a,b} A_a\mathcal{M}^2_{ab}A_b\ , \quad \text{where} \quad \mathcal{M}^2_{ab} = \sum_i c_{ia}c_{ib}\ . \tag{3.19}$$

The mass matrix $\mathcal{M}^2$ can be diagonalized by an orthogonal transformation, $A_a = \mathcal{P}_{ab}\hat{A}_b$. Denoting the eigenvalues by $\hat{\mathcal{M}}_a^2$, the nonzero ones (which are actually positive) are in one-to-one correspondence with the Stueckelberg fields C_0^i which are eaten by the $\hat{A}_a$'s that gain a mass. One can see that if there are 16 or fewer unitary factors in Eq. (3.15), all of them are broken to SU groups, while if there are more than 16 unitary factors, exactly 16 are broken to SU groups [51]. By supersymmetry, all twisted hypermultiplets initially containing the C_0^i's which are eaten also become massive. They combine with Abelian vector multiplets to become long massive vector multiplets. As a result, there are between 2 and 16 twisted quaternionic scalars for which stability is automatically guaranteed.

Compactifying down to four dimensions, we may define the WL's along T^2 as $\hat{A}_a^{I'} = \hat{\xi}_a^{I'}$, and write their total mass terms by adding the tree-level contributions to the one-loop effective potential corrections,

$$\hat{\xi}_a^{I'}\left[\hat{\mathcal{M}}_a^2\,\delta_{ab}\,\delta_{I'J'} + \mathcal{P}_{ca}\,\frac{\partial V}{\partial\xi_c^{I'}\partial\xi_d^{J'}}\,\mathcal{P}_{db}\right]\hat{\xi}_b^{J'}\,, \tag{3.20}$$

where $(\xi_1^{I'},\ldots,\xi_{32}^{I'}) \equiv (\xi_1^{I'},\ldots,\xi_{16}^{I'},\epsilon_1^{I'},\ldots,\epsilon_{16}^{I'})$. In the above formula, both contributions are proportional to the open-string coupling. However, while the first one is a supersymmetric mass term proportional to $M_{\rm s}^2$, the second one scales like $(M^2/M_{\rm s})^2$, which is always subdominant in the regime $M < M_{\rm s}$. Hence, all WL's of massive $\hat{A}_a$'s are super heavy and can be safely set to zero in a study of moduli stability,

$$\hat{\xi}_a^{I'} \equiv 0\,, \quad \text{when } \hat{\mathcal{M}}_a^2 > 0\,. \tag{3.21}$$

For the remaining WL's denoted $\hat{\xi}_u^{I'}$ to be non-tachyonic at one loop, one needs to find brane configurations such that the mass matrix

$$\mathcal{P}_{cu}\,\frac{\partial V}{\partial\xi_c^{I'}\partial\xi_d^{J'}}\,\mathcal{P}_{dv}\,, \quad \text{for } u, v \text{ such that } \hat{\mathcal{M}}_u^2, \hat{\mathcal{M}}_v^2 = 0\,, \tag{3.22}$$

has non-negative eigenvalues.

3.4. Untwisted closed-string moduli

So far, we have mainly discussed the generation of masses for the open-string moduli, as well as for those arising in the closed-string twisted sector. We continue the discussion by considering the dependencies of the effective potential on the closed-string untwisted moduli.

We see from Eqs. (3.10) and (3.13) that when the vev's of the WL's vanish, the one-loop effective potential reduces to

$$\mathcal{V} = \xi(n_{\rm F} - n_{\rm B})M^4 + \mathcal{O}\left((M_{\rm s}M)^2 e^{-2\pi c\frac{M_{\rm s}}{M}}\right)\,, \quad \text{where} \quad \xi = \frac{\Gamma\left(\frac{5}{2}\right)}{\pi^{\frac{13}{2}}}\sum_{l_5}\frac{1}{|2l_5+1|^5}\,. \tag{3.23}$$

Up to the exponentially suppressed corrections, the dependence on the NS-NS internal metric $G_{\mathcal{I}\mathcal{J}}$ has disappeared, except *via* the supersymmetry breaking scale M. Therefore, when the D3-branes sit on O3-planes, all components of the (inverse) metric except G^{55} are flat directions. Moreover, unless the potential vanishes *i.e.* $n_{\rm F} = n_{\rm B}$, $G^{55} = 4M^2$ has a tadpole and must run away. In the NS-NS sector, the remaining untwisted modulus is the dilaton. However, since the one-loop potential is independent of it, that remains a flat direction at this order.

The components $C_{I'J'}$ of the RR two-form along T^2 can be interpreted as Wilson lines of Abelian vector bosons $C_{\hat{\mu}J'}$ in six dimensions. Therefore the algebraic method presented in Sect. 3.1 can be applied to determine their masses at the quantum level. Using the fact that the perturbative type I spectrum does not admit charged states under the RR gauge fields, we can conclude that the moduli $C_{I'J'}$ remain massless at one loop. It is however possible to draw much stronger statements using heterotic/type I duality as follows. For the case at hand, we have been careful to consider type I models that are expected to be well defined at the non-perturbative level, so that heterotic duals should exist. In four dimensions, the above equivalence of the two theories compactified on $T^2 \times T^4/\mathbb{Z}_2$ turns out to be a weak coupling/weak coupling duality [64–67]. Using the adiabatic argument [69], the equivalence remains valid once the Scherk–Schwarz breaking of supersymmetry is implemented along the large periodic direction X^5.

Let us consider first the case when the $\mathbb{Z}_2$ action generated by g is not implemented yet. The duality maps the type I variables $(G+C)_{\mathcal{I}\mathcal{J}}$ into $(G+B)_{\mathcal{I}\mathcal{J}}$ on the heterotic side, where $B_{\mathcal{I}\mathcal{J}}$ is the internal antisymmetric tensor. The moduli deformations of the Narain lattice $\Gamma_{6,6+16}$ can be parameterised by $(G+B)_{\mathcal{I}\mathcal{J}} \equiv Y_{\mathcal{I}\mathcal{J}}$, $\mathcal{I},\mathcal{J} = 6,\ldots,9$, as well as the WL's of $SO(32)$ along T^6 denoted as $Y_{\mathcal{I}\mathcal{J}}$, $\mathcal{J} = 10,\ldots,25$. Actually, all of these $6\times(6+16)$ moduli are the WL's of $SO(44)$ along T^6. At a generic point in moduli space (the Coulomb branch), the gauge symmetry is reduced to $U(1)^6 \times U(1)^{16}$. Conversely, non-Abelian gauge symmetries are restored at enhanced gauge symmetry points. In particular, non-Cartan states charged under $U(1)^6$, which are generically massive, become massless at special values of $(G+B)_{\mathcal{I}\mathcal{J}} \equiv Y_{\mathcal{I}\mathcal{J}}$. Their Cartan charges are the winding numbers $n_{\mathcal{I}}$, $\mathcal{I} = 4,\ldots,9$. Because the Coleman–Weinberg effective potential is expressed in terms of the tree-level mass spectrum, its dependence on $(G+B)_{\mathcal{I}\mathcal{J}} \equiv Y_{\mathcal{I}\mathcal{J}}$ can arise only from the aforementioned non-Cartan states running in the loop.[14] Turning back to the type I picture, these windings states are D1-branes, which belong to the non-perturbative spectrum. As a result, when $M < M_s$, the one-loop effective potential *does not depend on* $C_{\mathcal{I}\mathcal{J}}$, $I,J = 6,\ldots,9$, up to exponentially suppressed corrections.

Notice however that even though the masses of these D1-branes scale like the inverse string coupling, there is a moduli-dependent dressing that can vanish, implying such states to be in principle observable in low energy experiments. In the spirit of the seminal works of Seiberg and Witten [70] or Strominger [71], their effects in virtual loops are also captured by the heterotic effective potential [72,73]. In that case, some of the scalars $(G+C)_{\mathcal{I}\mathcal{J}}$, or rather $(G+B)_{\mathcal{I}\mathcal{J}}$, can be stabilised at the enhanced gauge symmetry points described above [74]. As shown in Ref. [21], all components $(G+B)_{\mathcal{I}\mathcal{J}}$, $\mathcal{I}\neq 5$, $\mathcal{J}\neq 5$ can be stabilised. Moreover, the potential is periodic in all $(G+B)_{\mathcal{I}5}$ and the latter can also be stabilised. Finally, the moduli $(G+B)_{5\mathcal{J}}$ remain flat directions.[15]

Re-introducing the $\mathbb{Z}_2$-orbifold action generated by g, none of the states arising from the twisted sector in heterotic string can induce an enhancement of the gauge symmetry.[16] They can however have non-trivial winding numbers along T^2 and thus introduce extra dependencies of the Coleman–Weinberg effective potential on the WL's $(G+B)_{I'J'}$, $I',J' = 4,5$. However, due to their high masses, their contributions are exponentially suppressed. The type I counterparts of these states are "twisted D1-branes", which would not be taken into account in perturbation theory.

[14] We always assume that $M < M_s$, which implies the contributions of the non-level matched states to be suppressed.

[15] We stress that this assumes M to be lower than the string scale *i.e.* the direction X^5 to be large.

[16] This follows from the fact that the zero-point energy of the twisted vacuum is higher than that of the untwisted sector.

One might question the extensive use of heterotic/type I duality, because the open-string side contains a D5-brane sector, which is mapped to a non-perturbative NS5-brane sector on the heterotic side. However, the states that are potentially responsible for the non-perturbative stabilisation of type I moduli $(G+C)_{I'J'}$, $I', J' = 4, 5$ and $(G+C)_{IJ}$, $I, J = 6, \ldots, 9$, are D1-branes. The latter are electrically charged under the two-form C, and magnetically neutral (they are not dyonic D1-D5 bound states). As a result, the stabilisation mechanism is independent of the existence of a D5-brane sector.

4. Stability analysis of the models

Let us now turn to the analysis of the one-loop stability of the moduli (or at least a sub-set of them) encountered when all D3-branes are located at corners of the six-dimensional box depicted schematically in Fig. 1d. We will restrict the discussion to the configurations satisfying the non-perturbative constraints presented at the end of Sect. 2.1. The mass terms of the WL's can be read from Eq. (3.13), but a projection on the submanifold of the moduli not acquiring a six-dimensional supersymmetric mass from the Green–Schwarz mechanism must simultaneously be applied. In our study, stability of the twisted quaternionic moduli is only guaranteed when they become massive due to this mechanism. We will not determine their stability at one loop when they remain massless in six dimension. Finally, a sufficient condition for instabilities not to arise from the ND sector of the theory is simply the absence of ND moduli, which is ensured if none of the D3-branes T-dual to the D9-branes and none of the D3-branes T-dual to the D5-branes share the same position in $\tilde{T}^2/I_{45}$,

$$\textit{no ND-sector moduli:} \quad n_{ii'}d_{ji'} = 0 \quad \text{for all } i, j, i' \text{ (no sum on } i') \,. \tag{4.1}$$

If this condition is not satisfied, then the radiatively induced masses-squared of the moduli in the ND sector must be computed. This can be done by considering the two-point functions of "boundary changing vertex operators". This is an interesting problem in its own right, which will be studied in a companion paper [59].

In what follows, we will first present simple examples lying in the $(\mathcal{R}, \tilde{\mathcal{R}}) = (0, 0)$ and $(\mathcal{R}, \tilde{\mathcal{R}}) = (16, 16)$ components of the moduli space to get familiar with the implementation of the generalized Green–Schwarz mechanism. Thanks to a numerical exploration of all brane configurations, we then list all setups that yield a vanishing or positive one-loop potential and that are tachyon free (up to exponentially suppressed terms).

4.1. Simple configurations in the component $(\mathcal{R}, \tilde{\mathcal{R}}) = (0, 0)$

At tree level in the branch $(\mathcal{R}, \tilde{\mathcal{R}}) = (0, 0)$ of the WL moduli space, all $32 + 32$ D3-branes are free to move in 4's in $T^4/\mathbb{Z}_2$ or $\tilde{T}^4/\mathbb{Z}_2$. Let us consider the simplest configuration where all D3-branes T-dual to the D5-branes have the same positions $2\pi\vec{a}_{i_0}$ in $T^4/\mathbb{Z}_2$, while those T-dual to the D9-branes have common positions $2\pi\vec{a}_{j_0}$ in $\tilde{T}^4/\mathbb{Z}_2$. In six dimensions, the open-string gauge group before taking into account the Green–Schwarz mechanism is thus $U(16) \times U(16)$. To determine the anomalous $U(1)$'s that become massive, we need to write the mass matrix squared $\mathcal{M}^2_{ab}$ of the 32 Abelian vector potentials A_a in six dimensions. To this end, it is convenient to refine our labelling as follows:

$$\begin{aligned} a \equiv r' = 1, \ldots, 16 \quad &: \text{ Cartan generators of the } U(16) \text{ arising from the D5-branes,} \\ a \equiv \tilde{r}' + 16 = 17, \ldots, 32 \quad &: \text{ Cartan generators of the } U(16) \text{ arising from the D9-branes.} \end{aligned}$$

With this notation the mass matrix squared is

$$\mathcal{M}^2 = \left(\begin{array}{c|c} \mathcal{M}^2_{r's'} & \mathcal{M}^2_{r'\tilde{s}'} \\ \hline \mathcal{M}^2_{\tilde{r}'s'} & \mathcal{M}^2_{\tilde{r}'\tilde{s}'} \end{array}\right) , \tag{4.2}$$

where the 16×16 blocks are given by

$$\begin{aligned} &\mathcal{M}^2_{r's'} = 16 \,, && \mathcal{M}^2_{r'\tilde{s}'} = -4\, e^{4i\pi \vec{a}_{i_0}\cdot\vec{a}_{j_0}} \,, \\ &\mathcal{M}^2_{\tilde{r}'s'} = -4\, e^{4i\pi \vec{a}_{j_0}\cdot\vec{a}_{i_0}} \,, && \mathcal{M}^2_{\tilde{r}'\tilde{s}'} = 16 \,. \end{aligned} \tag{4.3}$$

Among the 32 eigenvalues, 2 are positive while the others vanish. Setting to zero the vev's of the massive eigenvectors yields the conditions

$$-\sum_{r'} A_{r'} + \sum_{\tilde{r}'} A_{\tilde{r}'} = 0 \qquad \text{and} \qquad \sum_{r'} A_{r'} + \sum_{\tilde{r}'} A_{\tilde{r}'} = 0 \,, \tag{4.4}$$

implying that $U(16) \times U(16)$ is actually reduced to $SU(16) \times SU(16)$, as expected.

To proceed, let us consider the examples where all D3-branes T-dual to the D5-branes are coincident at $2\pi\vec{a}_{i'_0}$ in $\tilde{T}^2/I_{45}$, and similarly those T-dual to the D9-branes are stacked at $2\pi\vec{a}_{j'_0}$. The gauge symmetry in four dimensions is therefore still $SU(16) \times SU(16)$. The mass terms of the moduli/positions ξ^I_r along $T^4/\mathbb{Z}_2$ and ϵ^I_r along $\tilde{T}^4/\mathbb{Z}_2$ (see Eq. (3.12)), $I = 6, \ldots, 9$, $r = 1, \ldots, 8$, can be read from Eq. (3.13). Omitting all dressing factors, they are given by $n_{ii'}$- and $d_{jj'}$-dependent coefficients equal to $(16-0-1) = 15$, which is positive. Hence, the positions of the D3-branes along the internal directions $I = 6, \ldots, 9$ are stabilised.

As seen in Eq. (3.13), the mass terms of the T^2 WL's $\xi^{I'}_{r'}$ and $\epsilon^{I'}_{\tilde{r}'}$ arising from the one-loop effective potential depend on the precise locations of the stacks in $\tilde{T}^2/I_{45}$. Omitting irrelevant dressings as earlier, they are given by coefficients $(16 - 0 - 1 + \frac{\delta}{4}\, 16) = 15 + 4\delta$, where

(a) $\delta = +1$ if $i'_0 = j'_0$,
(b) $\delta = -1$ if the corners i'_0 and j'_0 of $\tilde{T}^2/I_{45}$ are facing each other along the Scherk–Schwarz direction $\tilde{X}^5$,
(c) $\delta = 0$ if the corners i'_0 and j'_0 of $\tilde{T}^2/I_{45}$ have distinct positions along $\tilde{X}^4$.

The three possibilities are depicted in Fig. 3. Note that $\delta = +1$ ($\delta = -1$) in Case (a) (Case (b)) thanks to the existence at tree level of massless scalars (fermions) in the ND sector. Because these mass terms are positive, we can immediately conclude that all positions in $\tilde{T}^2/I_{45}$ are stabilised. However, it is instructive to also take into account the effect of the generalized Green–Schwarz mechanism, which makes the components $I' = 4, 5$ of the linear combinations of six-dimensional vector bosons of Eq. (4.4) even more massive. Indeed, this can be used to eliminate say $\xi^{I'}_1$ and $\epsilon^{I'}_1$,

$$\xi^{I'}_1 = -\sum_{r' \neq 1} \xi^{I'}_{r'} \,, \qquad \epsilon^{I'}_1 = -\sum_{\tilde{r}' \neq 1} \epsilon^{I'}_{\tilde{r}'} \,, \tag{4.5}$$

in the mass terms of Eq. (3.13). This results in a new 30×30 mass matrix squared for the remaining moduli $\xi^{I'}_{r'}, \epsilon^{I'}_{\tilde{r}'}$, which of course has only strictly positive eigenvalues.[17]

[17] 14 are equal and the last one is 16 times larger.

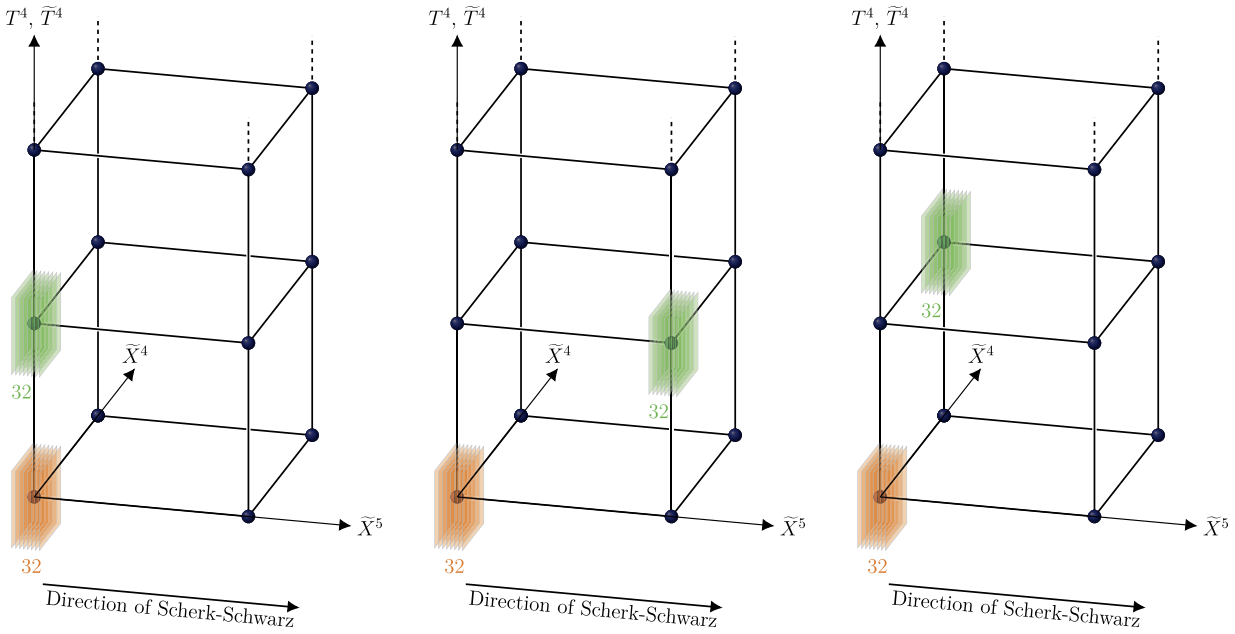

(a) The two stacks of 32 D3-branes T-dual to the D5- or D9-branes have common positions in $\tilde{T}^2/I_{45}$.

(b) The two stacks have the same coordinates along $\tilde{X}^4$ and distinct coordinates along $\tilde{X}^5$.

(c) The two stacks have distinct coordinates along $\tilde{X}^4$.

Fig. 3. D3-brane configurations in component $(\mathcal{R}, \tilde{\mathcal{R}}) = (0, 0)$ of the WL moduli space.

To conclude on the above examples, the masses of the moduli we have not analyzed are those of the 14 remaining hypermultiplets in the twisted closed-string sector, as well as those of the hypermultiplet in the single bifundamental of $SU(16) \times SU(16)$ arising from the open-string ND sector in Case (a). Using Eq. (2.25), we have $n_{\rm F} - n_{\rm B} = -4064 - 1024\,\delta < 0$, which implies that the supersymmetry breaking scale (*i.e.* gravitino mass) M runs away, while all other components of the NS-NS metric $G_{\mathcal{I}\mathcal{J}}$ and the dilaton as well as the RR two-form $C_{\mathcal{I}\mathcal{J}}$ are flat directions.

4.2. *Simple configurations in the component* $(\mathcal{R}, \tilde{\mathcal{R}}) = (16, 16)$

In this case, all D3-branes positions in $T^4/\mathbb{Z}_2$ or $\tilde{T}^4/\mathbb{Z}_2$ are rigid. Indeed, there is a mirror pair (with respect to the orientifold projection) of D3-branes T-dual to the D5-branes at each of the 16 fixed point of $T^4/\mathbb{Z}_2$, and similarly a mirror pair of D3-branes T-dual to the D9-branes at each fixed point of $\tilde{T}^4/\mathbb{Z}_2$. Before taking into account the effect of the Green–Schwarz mechanism, the gauge symmetry is $U(1)^{16} \times U(1)^{16}$. Hence, all antisymmetric representations are zero dimensional (see Eq. (2.22) or Table 1) and there is indeed no position modulus among them to consider. In this component of the moduli space, the only freedom is in the coordinates of the mirror pairs in $\tilde{T}^2/I_{45}$, which in our case of interest coincide with the positions of the four fixed points.

To study the masses of the moduli/positions along $\tilde{T}^2/I_{45}$, as well as those of the twisted quaternionic scalars in the closed-string sector, our starting point is the mass matrix squared $\mathcal{M}^2_{ab}$ of the 32 Abelian vector potentials present in the six-dimensional theory. Its components are given by

$$\begin{aligned} \mathcal{M}^2_{r's'} &= 16\,\delta_{r's'}\ , & \mathcal{M}^2_{r'\tilde{s}'} &= -4\,e^{4i\pi\vec{a}_{i(r')}\cdot\vec{a}_{i(\tilde{s}')}}\ , \\ \mathcal{M}^2_{\tilde{r}'s'} &= -4\,e^{4i\pi\vec{a}_{i(\tilde{r}')}\cdot\vec{a}_{i(s')}}\ , & \mathcal{M}_{\tilde{r}'\tilde{s}'} &= 16\,\delta_{\tilde{r}'\tilde{s}'}\ . \end{aligned} \tag{4.6}$$

Because the gauge group contains more than 16 unitary factors, the matrix has 16 positive eigenvalues and 16 vanishing ones. This implies that the gauge symmetry $U(1)^{32}$ is actually reduced to $U(1)^{16}$, and that all of the 16 twisted quaternionic scalars are massive, ensuring that $T^4/\mathbb{Z}_2$ will not undergo deformation into a smooth K3 manifold. Setting to zero all massive linear combinations of vector potentials, we obtain for their components along $\tilde{T}^2/I_{45}$ the relations

$$4\epsilon^{I'}_{\tilde{r}'} = -\sum_{s'} e^{4i\pi\vec{a}_{i(\tilde{r}')}\cdot\vec{a}_{i(s')}}\xi^{I'}_{s'}\ , \tag{4.7}$$

showing that all $\epsilon^{I'}_{\tilde{r}'}$ can be eliminated in terms of the $\xi^{I'}_{r'}$'s. Let us now consider various D3-brane configurations and explore their stability along $\tilde{T}^2/I_{45}$.

Example 1: The simplest setup amounts to having all D3-branes T-dual to the D5-branes at the same position $2\pi\vec{a}_{i'_0}$ of $\tilde{T}^2/I_{45}$, and similarly all D3-branes T-dual to the D9-branes at some common position $2\pi\vec{a}_{j'_0}$. Three cases (a), (b), (c) can be distinguished however, since all mass-term coefficients of the $\xi^{I'}_{r'}$ and $\epsilon^{I'}_{\tilde{r}'}$ read from Eq. (3.13) are $(1-0-1+\frac{\delta}{4}16) = 4\delta$, where δ is defined as explained below Eq. (4.4). Fig. 4 shows the three possibilities for distributing the pairs of branes. Therefore, we can conclude even before taking into account the Green–Schwarz mechanism that the positions of all the D3-branes are stabilised in Case (a), are unstable in Case (b), and are massless in Case (c). However, eliminating the $\epsilon^{I'}_{\tilde{r}'}$ thanks to the relations (4.7), it turns out that the mass terms of the remaining degrees of freedom $\xi^{I'}_{r'}$ are simply multiplied by a factor of 2. Moreover, $n_{\rm F} - n_{\rm B} = -224 - 1024\,\delta$, implying that M has a tadpole and runs away. In detail the behaviour of the configurations are as follows:

• In Case (a), the potential is negative, and there are 16^2 massless quaternionic scalars charged under $U(1)^{16}$ arising from the ND sector. Their masses must be determined to make a conclusion about the stability/instability of the configuration, which we discuss in [59]. Note however that in component $(\mathcal{R}, \tilde{\mathcal{R}}) = (16, 16)$ of the moduli space, Case (a) yields the most negative value of $n_{\rm F} - n_{\rm B}$. Hence, we do not expect the moduli of the ND sector to be tachyonic at one loop, and expect the configuration to be stable, except for the supersymmetry breaking scale M, and for the remaining closed-string moduli $G_{\mathcal{I}\mathcal{J}}$, $C_{\mathcal{I}\mathcal{J}}$ and ϕ which are flat directions. The possibility that the model leads to brane recombination *via* condensation of the ND-sector moduli remains a possibility that is discussed further in [59].

• In Case (b), the potential is positive but the D3-brane positions are unstable, so the distribution will evolve in $\tilde{T}^2/I_{45}$.

• In Case (c), the potential is negative and the WL's are massless. It turns out that (up to exponentially suppressed terms) the one-loop effective potential does not depend on these moduli, which are therefore flat directions.[18] Hence, the configuration is marginally stable.

Example 2: Thus far, conclusions about the stability/instability of the WL positions in $\tilde{T}^2/I_{45}$ could be drawn without taking into account the effect of the Green–Schwarz mechanism. In fact, this is possible only for particularly simple choices of brane setups, when all mass terms of the $\xi^{I'}_{r'}, \epsilon^{I'}_{\tilde{r}'}$ in Eq. (3.13) have the same sign. To construct a more generic brane configuration,

[18] The one-loop potential dependencies on $U(1)$ WL's are identical to those of $SO(2)$ factors treated in Ref. [23], which turn out to be trivial.

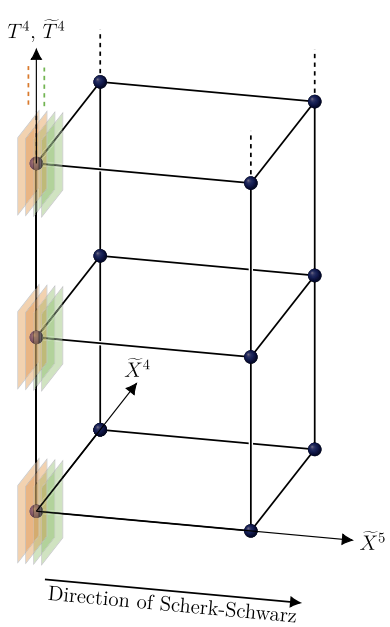

(a) The 16 + 16 pairs of D3-branes T-dual to the D5- or D9-branes have common positions in $\tilde{T}^2/\mathcal{I}_{45}$.

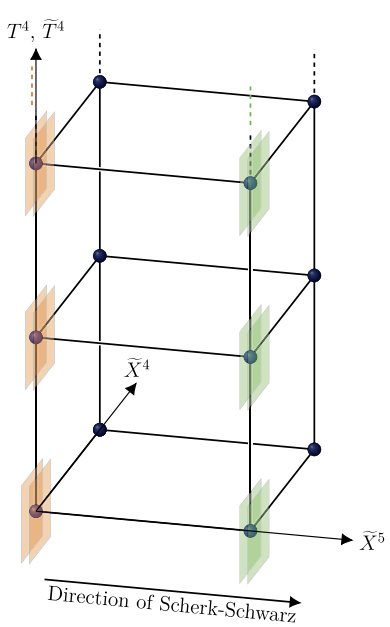

(b) Compared to Case (a), all D3-branes T-dual to the D9-branes are displaced along the Scherk–Schwarz direction $\tilde{X}^5$.

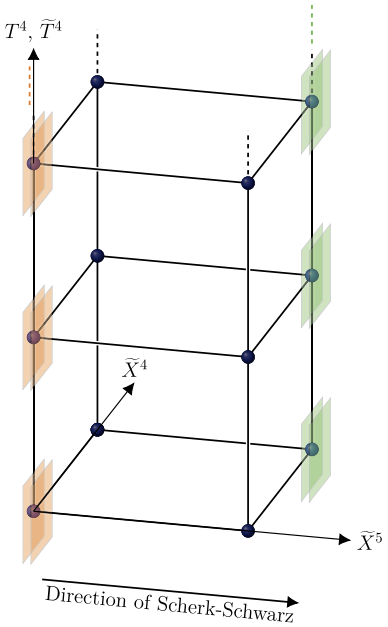

(c) Compared to either Case (a) or (b), all D3-branes T-dual to the D9-branes are displaced along $\tilde{X}^4$.

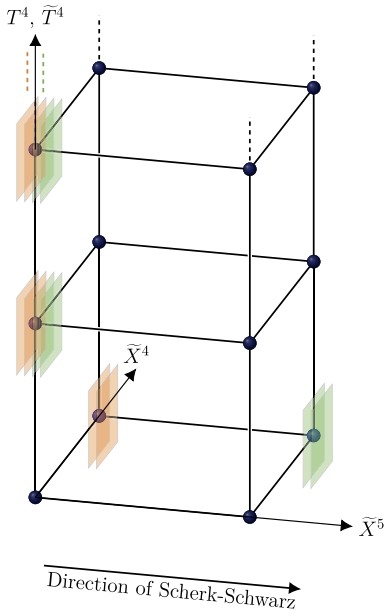

(d) Compared to Case (a), one pair of D3-branes T-dual to D5-branes is displaced along $\tilde{X}^4$, while its initially coincident pair of D3-branes T-dual to D9-branes is moved along both $\tilde{X}^4$ and $\tilde{X}^5$.

Fig. 4. D3-brane configurations in component $(\mathcal{R}, \tilde{\mathcal{R}}) = (16, 16)$ of the WL moduli space.

consider Case (a) of Example 1, and move along $\tilde{X}^4$ one pair of D3-branes T-dual to D5-branes, and move along $\tilde{X}^4$ and $\tilde{X}^5$ its initially coincident pair of D3-branes T-dual to D9-branes. The new configuration, denoted (d), is shown in Fig. 4d. The mass coefficients of fifteen $\xi^{I'}_{r'}$ and

fifteen $\epsilon^{I'}_{\tilde{r}'}$ are $\frac{15}{4}$, while those of the last two positions are $-\frac{1}{4}$. Hence, *a priori* the configuration seems unstable. However, eliminating in Eq. (3.13) all $\epsilon^{I'}_{\tilde{r}'}$'s by using Eq. (4.7) yields a new 16×16 mass-squared matrix for the $\xi^{I'}_{r'}$'s which has only positive eigenvalues. As a result, the brane configuration turns out to actually be stable, provided the 15^2 quaternionic moduli of the ND sector do not introduce instabilities, as already mentioned in Case (a) of Example 1. In the present Case (d), $n_{\rm F} - n_{\rm B} = -1120$ is higher than in Case (a), but it remains negative.

4.3. Full scan of the six components of the moduli space

Among the configurations that have been presented so far, none of them is tachyon free with a positive or exponentially suppressed potential at one loop. In fact, setups with these properties are expected to be rare. For instance, in the case of a compactification on T^6 realising $\mathcal{N} = 4 \to \mathcal{N} = 0$ breaking, this fact can be understood qualitatively by inspecting Eq. (3.1), where the massless fermions contribute positively to the potential and negatively to the WL squared masses, and *vice versa* for the massless bosons. Hence, the more positive the potential is, the more tachyonic instabilities are likely to arise. For instance, for toroidal compactifications in dimension $d \geq 5$, it was shown in Refs. [23,48] that there exists only one orientifold model[19] which is non-perturbatively consistent, tachyon-free at one loop and which has non-negative potential. It is defined in five dimensions, has a trivial open-string gauge group[20] $SO(1)^{32}$, and satisfies $n_{\rm F} - n_{\rm B} = 8 \times 8$.

To determine if tachyon free brane configurations with zero or positive one-loop potentials exist in the $\mathbb{Z}_2$-orbifold case, we have performed a computer scan of all brane configurations as follows:

- (i) In each of the six non-perturbatively consistent components of the moduli space, we loop over all distributions of mirror pairs (with respect to the orientifold action) of D3-branes in $T^4/\mathbb{Z}_2$ and $\tilde{T}^4/\mathbb{Z}_2$.
- (ii) For each configuration, we derive the squared-mass matrix $\mathcal{M}^2$ of the 32 Cartan $U(1)$'s.
- (iii) We then loop over all possible distributions of the pairs along $\tilde{T}^2/I_{45}$. We restrict to the configurations that respect the condition (3.7) for the positions in $T^4/\mathbb{Z}_2$ and $\tilde{T}^4/\mathbb{Z}_2$ not to be tachyonic, and eliminate those for which $n_{\rm F} - n_{\rm B} < 0$.
- (iv) For each distribution satisfying the above constraints, we then compute the one-loop contributions to the mass terms of the brane positions in $\tilde{T}^2/I_{45}$ (see Eq. (3.13)), and project out those combinations of moduli that become massive *via* the Green–Schwarz mechanism. We obtain the true squared-mass matrix of the remaining dynamical positions in $\tilde{T}^2/I_{45}$ and eliminate all configurations for which this matrix admits at least one strictly negative eigenvalue.

Among the hundreds of billions of initial possibilities,[21] only eight emerge from the scan: six of them are tachyon free, and two are tachyon free up to possible instabilities that may arise from

[19] The assumptions are that (i) the Scherk–Schwarz mechanism is implemented along a single direction, (ii) there are no exotic orientifold planes, and (iii) there is no discrete background for the internal NS-NS antisymmetric tensor.

[20] $SO(1)$ denotes the group containing only the neutral element.

[21] When moving a stack of branes from one fixed point to another the massless spectrum is invariant, so we count only one of these configurations. However, since the spectra whose masses are of the order of the string scale will in general differ, our counting of the inequivalent configurations is actually greatly underestimated.

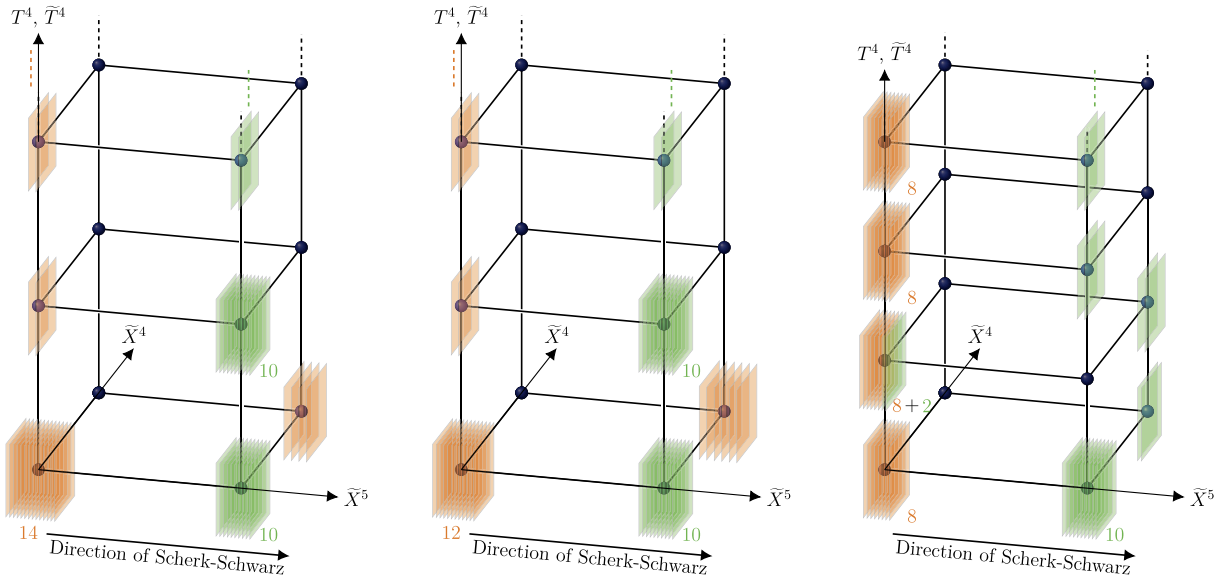

(a) Configuration tachyon free at one loop, with $n_F - n_B = 0$.

(b) Configuration tachyon free at one loop, with $n_F - n_B = 0$.

(c) Configuration with $n_F - n_B = 0$ but admitting moduli in the ND sector.

Fig. 5. Two brane configurations (a) and (b) in component $(\mathcal{R}, \tilde{\mathcal{R}}) = (8, 8)$ of the moduli space, and one configuration (c) in component $(\mathcal{R}, \tilde{\mathcal{R}}) = (0, 8)$.

ND-sector moduli. Most interestingly, two out of the six, and one out of the two configurations have vanishing one-loop potential ($n_F - n_B = 0$), up to exponentially suppressed terms. Let us summarise them:

Exponentially suppressed one-loop potentials:

• In the component $(\mathcal{R}, \tilde{\mathcal{R}}) = (8, 8)$ the scan finds two configurations referred to as Case (a) and (b), which are free of tachyons and satisfy $n_F - n_B = 0$. The gauge groups generated by the D5-branes and D9-branes are

$$\begin{aligned} &\text{Case (a)}: \quad \left[U(1)^7 \times U(2) \times U(7)\right]_{DD} \times \left[U(1)^6 \times U(5)^2\right]_{NN}, \\ &\text{Case (b)}: \quad \left[U(1)^7 \times U(3) \times U(6)\right]_{DD} \times \left[U(1)^6 \times U(5)^2\right]_{NN}. \end{aligned} \tag{4.8}$$

The D3-brane configurations are depicted in Figs. 5a and 5b, respectively. In the first case, the D3-branes T-dual to the D5-branes are distributed in $T^4/\mathbb{Z}_2$ as 7 pairs and one stack of 18 D3-branes, which is split in $\tilde{T}^2/I_{45}$ into $14 + 4$ branes. The D3-branes T-dual to the D9-branes are distributed as 6 pairs and two stacks of 10. The second configuration is identical to the previous one, up to the splitting of the 18 D3-branes now into $12 + 6$.

In both cases, all dynamical brane positions in $T^4/\mathbb{Z}_2$ or $\tilde{T}^4/\mathbb{Z}_2$ are stabilised. They are associated with the stacks of $2n$ branes with $n \geq 2$, and their masses read from Eq. (3.6) are proportional to $n - 1 > 0$. All other pairs of branes have rigid positions in $T^4/\mathbb{Z}_2$ or $\tilde{T}^4/\mathbb{Z}_2$ from the outset. Because there are initially 17 unitary gauge group factors, there are 16 anomalous $U(1)$'s becoming massive thanks to the Green–Schwarz mechanism, together with the 16 blowing-up modes arising from the twisted closed-string sector. The true gauge symmetries are therefore

$$\begin{aligned} &\text{Case (a)}: \quad U(1) \times SU(2) \times SU(7) \times SU(5)^2, \\ &\text{Case (b)}: \quad U(1) \times SU(3) \times SU(6) \times SU(5)^2. \end{aligned} \tag{4.9}$$

Along $\tilde{T}^2/I_{45}$, all D3-brane positions are also stabilised, after freezing the super heavy combinations associated with the anomalous $U(1)$'s. The ND sector does not contain moduli fields since condition (4.1) is satisfied. Thus, in Cases (a) and (b) and at the one-loop level, no tachyons are present and the potential admits flat directions parameterised by the internal metric (including G^{55} *i.e.* M, as justified in the next paragraph), the dilaton, and the RR two-form moduli. Notice that these configurations exist in four dimensions but not in five.

The massless spectrum of these two models contains the bosonic parts of $\mathcal{N}=2$ vector multiplets transforming under the adjoint representations of the groups given in Eq. (4.9), along with the scalars of $\mathcal{N}=2$ hypermultiplets in antisymmetric $\oplus$ antisymmetric representations of each non-Abelian factors. In terms of degrees of freedom, this yields $n_{\rm B}^{\rm open}=800$ in Case (a), and $n_{\rm B}^{\rm open}=736$ in Case (b). To this, one must add the 96 degrees of freedom coming from the closed-string sector yielding $n_{\rm B}=896$ in Case (a), and $n_{\rm B}=832$ in Case (b). Finally, the massless spectrum contains the fermionic degrees of freedom of hypermultiplets in the ND sector. They transform under bifundamental representations of all pairs of gauge group factors supported by stacks of D3-branes (T-dual to D5-branes) and stacks of D3-branes (T-dual to D9-branes) facing each other along the T-dual Scherk–Schwarz direction $\tilde{X}^5$. This leads to $n_{\rm F}=4\times 14\times 16=896$ in Case (a), and $n_{\rm F}=4\times 13\times 16=832$ in Case (b), which exactly equals the numbers of bosonic degrees of freedom.

• The scan also selects a third configuration with $n_{\rm F}-n_{\rm B}=0$, in component $(\mathcal{R},\tilde{\mathcal{R}})=(0,8)$ of the moduli space, which we will refer to as Case (c). The gauge symmetry (including anomalous $U(1)$'s) is

$$\text{Case (c)}: \quad \Big[U(4)^4\Big]_{\rm DD}\times\Big[U(1)^{11}\times U(5)\Big]_{\rm NN}\ , \tag{4.10}$$

and the configuration of branes is shown in Fig. 5c. The D3-branes T-dual to the D5-branes are distributed in $T^4/\mathbb{Z}_2$ as 4 stacks of 8. The D3-branes T-dual to the D9-branes are distributed as 8 pairs (with rigid positions in $\tilde{T}^4/\mathbb{Z}_2$), one stack of 4 split in $\tilde{T}^2/I_{45}$ into $2+2$, and one stack of 12 split in $\tilde{T}^2/I_{45}$ into $10+2$.

All positions along $T^4/\mathbb{Z}_2$ and $\tilde{T}^4/\mathbb{Z}_2$ are rigid or massive. Because there are 16 unitary factors in Eq. (4.10), there are 16 anomalous $U(1)$'s which are actually massive, together with the 16 twisted moduli in the closed-string sector. The true gauge symmetry is thus

$$\text{Case (c)}: \quad SU(4)^4\times SU(5)\ . \tag{4.11}$$

Taking into account the Green–Schwarz mechanism, the remaining positions along $\tilde{T}^2/I_{45}$ are all massless at one loop, except one which is massive. The internal metric and RR two-form, as well as the dilaton are flat directions of the one-loop potential (up to exponentially suppressed terms). However, we cannot determine if this configuration is fully marginally stable without also considering the masses of the ND sector moduli which are also present in this case: this is left for future work.

The massless bosonic degrees of freedom include those of an $\mathcal{N}=2$ vector multiplet in the adjoint representation of the group (4.10), along with the scalars of $\mathcal{N}=2$ hypermultiplets in antisymmetric $\oplus$ antisymmetric representations for each non-Abelian factor. There are also bosonic degrees of freedom transforming under four bifundamental representations of $U(4)_{\rm DD}\times U(1)_{\rm NN}$. Taking into account the closed-string degrees of freedom, we obtain $n_{\rm B}=832$. The massless fermionic degrees of freedom are in the bifundamental representations of all pairs of gauge group factors supported by stacks of D3-branes (T-dual to D5-branes) and stacks of D3- branes (T-dual to D9-branes) facing each other along the T-dual Scherk–Schwarz direction $\tilde{X}^5$. Their number is given by $n_{\rm F}=4\times 16\times 13=832$, again equating to $n_{\rm B}$.

Positive potentials: There also exist five configurations with strictly positive potential. They all lie in component $(\mathcal{R}, \tilde{\mathcal{R}}) = (8, 8)$ and have an identical open-string (anomalous) gauge group

$$\left[U(1)^6 \times U(5)^2\right]_{\rm DD} \times \left[U(1)^6 \times U(5)^2\right]_{\rm NN} \ . \tag{4.12}$$

The configurations are depicted in Figs. 6a-6e. All position moduli along $T^4/\mathbb{Z}_2$ and $\tilde{T}^4/\mathbb{Z}_2$ are massive. Taking into account the Green–Schwarz mechanism, the gauge symmetry is reduced to

$$SU(5)^4 \ , \tag{4.13}$$

all twisted closed-string moduli are massive, and the positions along $\tilde{T}^2/I_{45}$ are either massive or massless, depending on the case at hand.

The configuration in Fig. 6a yields $n_{\rm F} - n_{\rm B} = 40$. Notice that it may be considered in five dimensions by decompactifying the direction X^4. In the case shown in Fig. 6b, the direction $\tilde{X}^4$ is used to isolate one pair of D3-branes, which leads to $n_{\rm F} - n_{\rm B} = 24$. By displacing a second pair of the same kind as shown in Fig. 6c, one obtains $n_{\rm F} - n_{\rm B} = 8$. Starting from the distribution in Fig. 6c and displacing a pair of D3-branes of the other kind as shown in Fig. 6d, one obtains $n_{\rm F} - n_{\rm B} = 10$. Finally, the configuration in Fig. 6e yields $n_{\rm F} - n_{\rm B} = 8$, but contains moduli fields in the ND sector whose masses need to be analysed at one loop in order to make a conclusion about its stability/instability.

5. Conclusions

In this work, we have studied from various perspectives the generation at the quantum level of moduli masses in type I string theory compactified on $T^2 \times T^4/\mathbb{Z}_2$, when $\mathcal{N} = 2 \to \mathcal{N} = 0$ supersymmetry is spontaneously broken by the Scherk–Schwarz mechanism implemented along T^2. Our analysis is perturbative, restricted to the one-loop level, and our conclusions are valid when the supersymmetry breaking scale M is the lowest mass scale of the background. We have considered gauge-field backgrounds on the worldvolumes of the 32 D9-branes and 32 D5-branes, as well as positions of the D5-branes in $T^4/\mathbb{Z}_2$, that can be described from T-dual points of view as positions of $32 + 32$ D3-branes distributed on 64 O3-planes. At such points in moduli space, the effective potential is extremal, except with respect to M which runs away when $n_{\rm F} \neq n_{\rm B}$.

We find that the D3-brane positions/moduli that are not already heavy thanks to a generalized Green–Schwarz mechanism in six dimensions can be stabilised at one loop. However, up to exponentially suppressed corrections, all degrees of freedom of the internal metric $G_{\mathcal{I}\mathcal{J}}$ (except M when $n_{\rm F} \neq n_{\rm B}$), of the two-form $C_{\mathcal{I}\mathcal{J}}$ and of the dilaton remain flat directions. From heterotic/type I duality, it is however possible to infer that some of the moduli $(G + C)_{\mathcal{I}\mathcal{J}}$ can be stabilised non-perturbatively at points where D1-branes become massless [21,48]. When moduli occur in the ND sector of the (non T-dualized) theory, their quantum masses can be derived by computing two-point functions. This will be presented elsewhere [59]. Finally, the models contain blowing-up modes, which belong to quaternionic scalars arising in the twisted closed-string sector. While those involved in the Green–Schwarz mechanism are very heavy, we have not studied the masses generated for the remaining ones (if any).

Among the plethora of allowed distributions of D3-branes on O3-planes, only two are tachyon free at one loop, with an exponentially suppressed effective potential, *i.e.* with $n_{\rm F} = n_{\rm B}$. Recall that such set-ups may be interesting candidates for generating, after stabilisation of M and the dilaton, a cosmological constant which is orders of magnitude smaller than in generic models. Four more brane configurations lead to positive potentials, *i.e.* $n_{\rm F} > n_{\rm B}$, where the only instabilities are associated with the run away of the supersymmetry-breaking no-scale modulus M.

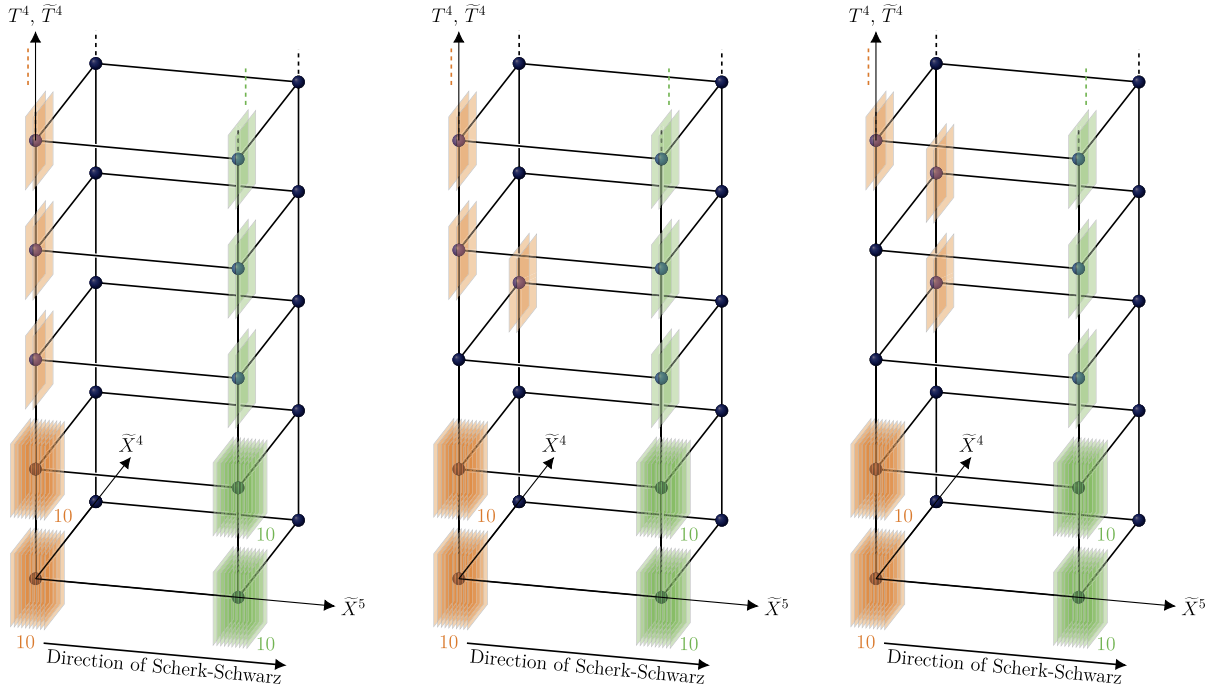

(a) Configuration tachyon free at one loop, with $n_F - n_B = 40$.

(b) Configuration tachyon free at one loop, with $n_F - n_B = 24$.

(c) Configuration tachyon free at one loop, with $n_F - n_B = 8$.

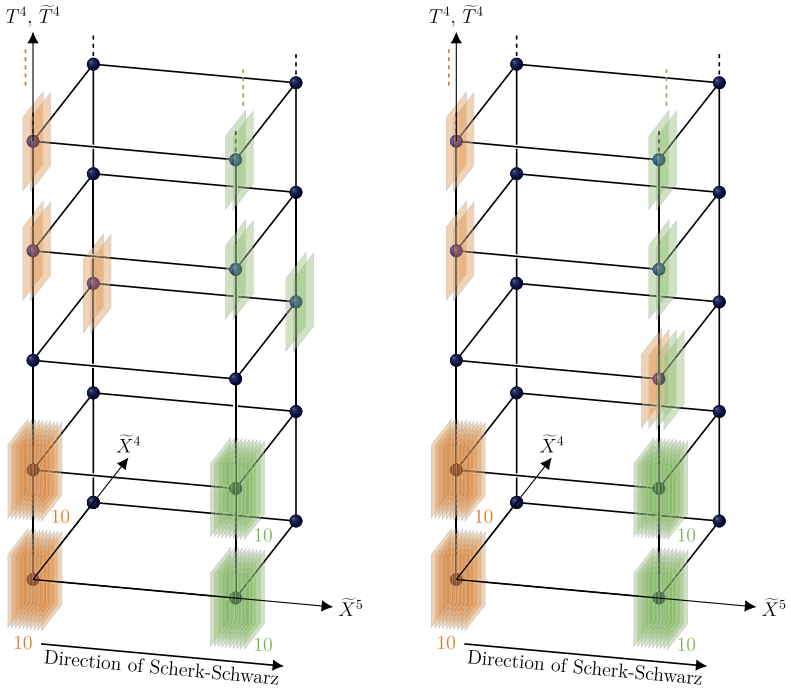

(d) Brane configuration tachyon free with $n_F - n_B = 10$.

(e) Brane configuration with $n_F - n_B = 8$ and moduli in the ND sector.

Fig. 6. Brane configurations in component $(\mathcal{R}, \tilde{\mathcal{R}}) = (8, 8)$ of the moduli space.

Finally, two brane distributions with similar properties contain moduli in the ND sector, whose one-loop masses remain to be analysed. It is worth mentioning that in a phenomenological setup, these moduli would naturally contain the Standard-Model Higgs field, so it is not *a priori* obvi-

ous that one needs to banish tachyonic masses from these states entirely. All of the above models are interesting in the sense that they describe non-Abelian gauge theories, with fermions that are massless at tree level transforming in bifundamental representations. It would be interesting to derive the masses acquired at one loop by this fermionic matter.

To explore further possibilities, it would also be interesting to relax some of the assumptions we have made. For instance, one may seek type I vacua that include "exotic" orientifold planes, often referred to as O_+-planes, which can support even or odd numbers of branes [43]. O_+-planes have RR charges and tensions opposite to those of the O_--planes we have used in the present work. Alternatively, when moduli in the ND sector are tachyonic and condense, branes recombine and the theory admits new vacua. Another possibility is to switch on discrete backgrounds for the internal components of the NSNS antisymmetric tensor (whose degrees of freedom are projected out by the orientifold action). Finally, one may analyze the theory when $T^4/\mathbb{Z}_2$ is deformed to a smooth K3 manifold.

Declaration of competing interest

The authors declare that they have no known competing financial interests or personal relationships that could have appeared to influence the work reported in this paper.

Acknowledgements

The authors would like to thank Carlo Angelantonj, Daniel Lewis and especially Emilian Dudas for discussion and useful input during the realization of this work. This work was funded by the Royal-Society/CNRS International Cost Share grant IE160590, and mutual hospitality from Durham University and the École Polytechnique is acknowledged.

Appendix A. One-loop effective potential

In this appendix, our goal is to present in some details the expression of the one-loop effective potential arising in a four-dimensional orientifold model of type IIB that realizes the $\mathcal{N}=2\to\mathcal{N}=0$ spontaneous breaking of supersymmetry. The background is

$$\mathbb{R}^{1,3}\times T^2\times\frac{T^4}{\mathbb{Z}_2}\,, \tag{A.1}$$

where a Scherk–Schwarz mechanism is implemented along one of the internal T^2 directions.

In an orientifold theory (see Refs. [52,75–80] for original papers and Refs. [39,53,54] for reviews), the one-loop effective potential may be divided into the contributions arising from the torus, Klein bottle, annulus and Möbius strip partition functions,

$$\mathcal{V}=-\frac{M_s^4}{2(2\pi)^4}\left(\mathcal{T}+\mathcal{K}+\mathcal{A}+\mathcal{M}\right), \qquad \text{where}$$

$$\mathcal{T}=\frac{1}{2}\int_{\mathcal{F}}\frac{d\tau_1 d\tau_2}{\tau_2^3}\,\mathrm{Str}\,\frac{1+g}{2}q^{L_0-\frac{1}{2}}\bar{q}^{\tilde{L}_0-\frac{1}{2}}\,, \qquad \mathcal{K}=\frac{1}{2}\int_0^{+\infty}\frac{d\tau_2}{\tau_2^3}\,\mathrm{Str}\,\Omega\frac{1+g}{2}q^{L_0-\frac{1}{2}}\bar{q}^{\tilde{L}_0-\frac{1}{2}}\,,$$

$$\mathcal{A} = \frac{1}{2}\int_0^{+\infty} \frac{\mathrm{d}\tau_2}{\tau_2^3}\,\mathrm{Str}\,\frac{1+g}{2} q^{\frac{1}{2}(L_0-1)}\ , \qquad \mathcal{M} = \frac{1}{2}\int_0^{+\infty} \frac{\mathrm{d}\tau_2}{\tau_2^3}\,\mathrm{Str}\,\Omega\frac{1+g}{2} q^{\frac{1}{2}(L_0-1)}\ . \tag{A.2}$$

In the above formula, τ_1, τ_2 are the real and imaginary parts of the Teichmüller parameter τ, $q = e^{2i\pi\tau}$, $\mathcal{F}$ is the fundamental domain of $SL(2,\mathbb{Z})$, $L_0, \tilde{L}_0$ are the zero frequency Virasoro operators, Ω is the orientifold generator and g is the twist generator acting on the T^4 coordinates as $(X^6, X^7, X^8, X^9) \to (-X^6, -X^7, -X^8, -X^9)$. The factors $\frac{1}{2}$ are due to the orientifold projection. In the following, we first introduce our notations and present the amplitudes in the supersymmetric BSGP model compactified down to four dimensions. Then, we implement discrete deformations as well as the spontaneous breaking of $\mathcal{N} = 2$ supersymmetry, and display the associated amplitudes.

A.1. Summary of conventions and notations

It is useful for reference to summarise the notation for the lattices of zero modes and for the characters that account for the oscillator excitations, that we use to write the one-loop amplitudes:

Indices: The metric of $T^2 \times T^4$ is defined as $G_{\mathcal{I}\mathcal{J}}$, $\mathcal{I}, \mathcal{J} = 4, \ldots 9$. However, due to the factorization of the internal space, it is convenient to introduce non-calligraphic indices that refer either to the T^2 or T^4 directions only. Hence, we will also use $G_{I'J'}$, $I', J' = 4, 5$ and G_{IJ}, $I, J = 6, \ldots, 9$.

Internal momentum and winding numbers along $T^2 \times T^4$ are organized in six-vectors, $\vec{M}$ and $\vec{N}$, respectively. They can be split according to the tori factorization in the following way: $\vec{M} = (\vec{m}', \vec{m})$ and $\vec{N} = (\vec{n}', \vec{n})$, where primed vectors components are two-vectors and the not primed ones are four-vectors.

Lattices: For the genus-1 Riemann surface, the expression of the amplitude $\mathcal{T}$ involves

$$\begin{aligned} &\Lambda^{(6,6)}_{\vec{M},\vec{N}}(\tau) = q^{\frac{1}{4}P^L_{\mathcal{I}} G^{\mathcal{I}\mathcal{J}} P^L_{\mathcal{J}}}\, \bar{q}^{\frac{1}{4}P^R_{\mathcal{I}} G^{\mathcal{I}\mathcal{J}} P^R_{\mathcal{J}}}\ , \\ &P^L_{\mathcal{I}} = m_{\mathcal{I}} + G_{\mathcal{I}\mathcal{J}} n_{\mathcal{J}}\ , \quad P^R_{\mathcal{I}} = m_{\mathcal{I}} - G_{\mathcal{I}\mathcal{J}} n_{\mathcal{J}}\ , \quad \mathcal{I} = 4, \ldots, 9\ , \end{aligned} \tag{A.3}$$

where $G^{\mathcal{I}\mathcal{J}} = G^{-1}_{\mathcal{I}\mathcal{J}}$. Due to the orientifold projection, the NS-NS antisymmetric tensor $B_{\mathcal{I}\mathcal{J}}$ present in the type IIB string vanishes. The $(6,6)$ lattice can again be divided into $(2,2)$ and $(4,4)$ lattices of zero modes associated with T^2 and T^4, as follows:

$$\Lambda^{(6,6)}_{\vec{M},\vec{N}}(\tau) = \Lambda^{(2,2)}_{\vec{m}',\vec{n}'}(\tau)\Lambda^{(4,4)}_{\vec{m},\vec{n}}(\tau) = q^{\frac{1}{4}P^L_{I'} G^{I'J'} P^L_{J'}}\, \bar{q}^{\frac{1}{4}P^R_{I'} G^{I'J'} P^R_{J'}} \times q^{\frac{1}{4}P^L_{I} G^{IJ} P^L_{J}}\, \bar{q}^{\frac{1}{4}P^R_{I} G^{IJ} P^R_{J}}\ . \tag{A.4}$$

By contrast, the states that are running in the Klein bottle, annulus or Möbius strip amplitudes have a vanishing momentum or winding number along each internal direction, so the relevant lattices can be defined as

$$\begin{aligned} P^{(6)}_{\vec{M}}(i\tau_2) &= \Lambda^{(6,6)}_{\vec{M},\vec{0}}(\tau) = e^{-\pi\tau_2 m_{\mathcal{I}} G^{\mathcal{I}\mathcal{J}} m_{\mathcal{J}}}\ , \\ W^{(4)}_{\vec{n}}(i\tau_2) &= \Lambda^{(4,4)}_{\vec{0},\vec{n}}(\tau) = e^{-\pi\tau_2 n_I G_{IJ} n_J}\ . \end{aligned} \tag{A.5}$$

As before, the momentum lattice can be factorized as

$$P^{(6)}_{\vec{M}}(i\tau_2) = P^{(2)}_{\vec{m}'}(i\tau_2) P^{(4)}_{\vec{m}}(i\tau_2) = e^{-\pi\tau_2 m_{I'} G^{I'J'} m_{J'}} \times e^{-\pi\tau_2 m_I G^{IJ} m_J} \ . \tag{A.6}$$

Throughout this work, the implicit arguments of the lattices are as indicated in the above definitions.

Characters: Our definitions of the Jacobi modular forms and Dedekind function are

$$\vartheta\left[\begin{smallmatrix}\alpha\\ \beta\end{smallmatrix}\right](z|\tau) = \sum_m q^{\frac{1}{2}(m+\alpha)^2} e^{2i\pi(z+\beta)(m+\alpha)} \ , \qquad \eta(\tau) = q^{\frac{1}{24}} \prod_{n=1}^{+\infty}(1-q^n) \ . \tag{A.7}$$

It is standard to denote

$$\begin{aligned} &\vartheta\left[\begin{smallmatrix}0\\ 0\end{smallmatrix}\right](z|\tau) = \vartheta_3(z|\tau) \ , \quad \vartheta\left[\begin{smallmatrix}0\\ \frac{1}{2}\end{smallmatrix}\right](z|\tau) = \vartheta_4(z|\tau) \ , \\ &\vartheta\left[\begin{smallmatrix}\frac{1}{2}\\ 0\end{smallmatrix}\right](z|\tau) = \vartheta_2(z|\tau) \ , \quad \vartheta\left[\begin{smallmatrix}\frac{1}{2}\\ \frac{1}{2}\end{smallmatrix}\right](z|\tau) = \vartheta_1(z|\tau) \ , \end{aligned} \tag{A.8}$$

and to keep implicit both arguments when $z = 0$. In these notations, the $SO(2n)$ affine characters can be written as

$$O_{2n} = \frac{\vartheta_3^n + \vartheta_4^n}{2\eta^n} \ , \qquad V_{2n} = \frac{\vartheta_3^n - \vartheta_4^n}{2\eta^n} \ , \qquad S_{2n} = \frac{\vartheta_2^n + i^{-n}\vartheta_1^n}{2\eta^n} \ , \qquad C_{2n} = \frac{\vartheta_2^n - i^{-n}\vartheta_1^n}{2\eta^n} \ . \tag{A.9}$$

They satisfy the following modular properties:

$$\begin{aligned} &\begin{pmatrix} O_{2n}\\ V_{2n}\\ S_{2n}\\ C_{2n}\end{pmatrix}(\tau+1) = e^{-in\pi/12}\mathrm{diag}\left(1,-1,e^{in\pi/4},e^{in\pi/4}\right)\begin{pmatrix} O_{2n}\\ V_{2n}\\ S_{2n}\\ C_{2n}\end{pmatrix}(\tau) \ , \\ &\begin{pmatrix} O_{2n}\\ V_{2n}\\ S_{2n}\\ C_{2n}\end{pmatrix}\left(-\frac{1}{\tau}\right) = \frac{1}{2}\begin{pmatrix} 1 & 1 & 1 & 1\\ 1 & 1 & -1 & -1\\ 1 & -1 & i^{-n} & -i^{-n}\\ 1 & -1 & -i^{-n} & i^{-n}\end{pmatrix}\begin{pmatrix} O_{2n}\\ V_{2n}\\ S_{2n}\\ C_{2n}\end{pmatrix}(\tau) \ , \end{aligned} \tag{A.10}$$

which are relevant for the amplitudes $\mathcal{T}$, $\mathcal{K}$ and $\mathcal{A}$. For the Möbius strip, it is convenient to switch from the characters χ to the real "hatted" characters $\hat{\chi}$ defined by [53,54]

$$\hat{\chi}\left(\frac{1}{2}+i\tau_2\right) = e^{-i\pi(h-\frac{c}{24})}\,\chi\left(\frac{1}{2}+i\tau_2\right) , \tag{A.11}$$

where h is the weight of the associated primary state and c is the central charge. The so-called P-transformation then takes the form

$$\begin{aligned} &\begin{pmatrix} \hat{O}_{2n}\\ \hat{V}_{2n}\\ \hat{S}_{2n}\\ \hat{C}_{2n}\end{pmatrix}\left(\frac{1}{2}+\frac{i}{2\tau_2}\right) = \begin{pmatrix} c & s & 0 & 0\\ s & -c & 0 & 0\\ 0 & 0 & \zeta c & i\zeta s\\ 0 & 0 & i\zeta s & \zeta c\end{pmatrix}\begin{pmatrix} \hat{O}_{2n}\\ \hat{V}_{2n}\\ \hat{S}_{2n}\\ C_{2n}\end{pmatrix}\left(\frac{1}{2}+i\frac{\tau_2}{2}\right) , \\ &\hat{\eta}\left(\frac{1}{2}+\frac{i}{2\tau_2}\right) = \sqrt{\tau_2}\,\hat{\eta}\left(\frac{1}{2}+i\frac{\tau_2}{2}\right) , \end{aligned} \tag{A.12}$$

where $c = \cos(n\pi/4)$, $s = \sin(n\pi/4)$ and $\zeta = e^{-in\pi/4}$. Throughout this work, the implicit arguments of the characters are τ, $2i\tau_2$, $i\tau_2/2$ and $(1+i\tau_2)/2$ for the torus, Klein bottle, annulus and Möbius strip amplitudes respectively.

A.2. Bianchi–Sagnotti–Gimon–Polchinski model

Let us first consider the amplitudes arising in the simplest version of the BSGP model [49–51] compactified on T^2. The background is as given in Eq. (A.1), with at this stage no Wilson lines switched on in the worldvolumes of the D9- and D5-branes, all D5-branes coincident on a single O5-plane, and as yet no implementation of the Scherk–Schwarz mechanism. Of course, in the absence of any breaking of supersymmetry, ultimately the total effective potential vanishes.

To write the one-loop vacuum amplitudes, we decompose the worldsheet fermion $SO(8)$ affine characters into characters of $SO(4) \times SO(4)$, where the first factor is the little group in six dimensions and the second is associated with the internal directions $6, 7, 8, 9$:

$$\begin{aligned} O_8 &= O_4 O_4 + V_4 V_4 \,, & V_8 &= V_4 O_4 + O_4 V_4 \,, \\ S_8 &= S_4 S_4 + C_4 C_4 \,, & C_8 &= S_4 C_4 + C_4 S_4 \,. \end{aligned} \tag{A.13}$$

It is convenient to define characters that mix NS and R sectors but which diagonalize the action of the $\mathbb{Z}_2$ orbifold generator g. The transformations of the $T_4/\mathbb{Z}_2$ characters under g is

$$g \cdot \begin{pmatrix} O_4 \\ V_4 \\ S_4 \\ C_4 \end{pmatrix} = \begin{pmatrix} O_4 \\ -V_4 \\ -S_4 \\ C_4 \end{pmatrix} , \tag{A.14}$$

so that defining

$$\begin{aligned} Q_{\mathrm{O}} &= V_4 O_4 - C_4 C_4 \,, & Q_{\mathrm{V}} &= O_4 V_4 - S_4 S_4 \,, \\ Q_{\mathrm{S}} &= O_4 C_4 - S_4 O_4 \,, & Q_{\mathrm{C}} &= V_4 S_4 - C_4 V_4 \,, \end{aligned} \tag{A.15}$$

the states belonging to the characters $Q_{\mathrm{O}}, Q_{\mathrm{S}}$ on the one hand, and $Q_{\mathrm{V}}, Q_{\mathrm{C}}$ on the other, have $\mathbb{Z}_2$ eigenvalues $+1$ and -1 respectively.

With these definitions and the conventions of Appendix A.1, the torus and Klein bottle amplitudes read

$$\begin{aligned} \mathcal{T} = \frac{1}{4} \int_{\mathcal{F}} \frac{\mathrm{d}^2\tau}{\tau_2^3} \Bigg\{ & |Q_{\mathrm{O}} + Q_{\mathrm{V}}|^2 \sum_{\vec{m},\vec{n}} \frac{\Lambda^{(4,4)}_{\vec{m},\vec{n}}}{|\eta^4|^2} + |Q_{\mathrm{O}} - Q_{\mathrm{V}}|^2 \left| \frac{2\eta}{\vartheta_2} \right|^4 + 16\, |Q_{\mathrm{S}} + Q_{\mathrm{C}}|^2 \left| \frac{\eta}{\vartheta_4} \right|^4 \\ & + 16\, |Q_{\mathrm{S}} - Q_{\mathrm{C}}|^2 \left| \frac{\eta}{\vartheta_3} \right|^4 \Bigg\} \sum_{\vec{m}',\vec{n}'} \frac{\Lambda^{(2,2)}_{\vec{m}',\vec{n}'}}{|\eta^4|^2} \,, \end{aligned} \tag{A.16}$$

$$\mathcal{K} = \frac{1}{4} \int_0^{+\infty} \frac{\mathrm{d}\tau_2}{\tau_2^3} \left\{ (Q_{\mathrm{O}} + Q_{\mathrm{V}}) \left(\sum_{\vec{m}} \frac{P^{(4)}_{\vec{m}}}{\eta^4} + \sum_{\vec{n}} \frac{W^{(4)}_{\vec{n}}}{\eta^4} \right) + 32\, (Q_{\mathrm{S}} + Q_{\mathrm{C}}) \left(\frac{\eta}{\vartheta_4} \right)^2 \right\} \sum_{\vec{m}'} \frac{P^{(2)}_{\vec{m}'}}{\eta^4} .$$

In the torus expression, the first term in the braces is the usual $|V_8 - S_8|^2$ contribution occurring in type IIB. The second term is obtained by acting with the orbifold generator g, which imposes to be at the origin of the T^4 lattice. The last two terms correspond to the twisted sector and are also at the origin of the T^4 lattice.

The model contains D9-branes and D5-branes in order to cancel the RR charges of an O9-plane and 32 O5-planes that are respectively the fixed point loci of Ω and Ωg. Denoting by N and D the numbers of D9-branes and D5-branes, and by R_N and R_D their counterparts under the action of g on the associated Chan–Paton charges [52–54], the amplitudes are

$$\mathcal{A} = \frac{1}{4}\int_0^{+\infty}\frac{\mathrm{d}\tau_2}{\tau_2^3}\left\{(Q_{\rm O}+Q_{\rm V})\left(N^2\sum_{\vec{m}}\frac{P^{(4)}_{\vec{m}}}{\eta^4}+D^2\sum_{\vec{n}}\frac{W^{(4)}_{\vec{n}}}{\eta^4}\right)+2ND\,(Q_{\rm S}+Q_{\rm C})\left(\frac{\eta}{\vartheta_4}\right)^2\right.$$
$$\left.+\,(R_{\rm N}^2+R_{\rm D}^2)\,(Q_{\rm O}-Q_{\rm V})\left(\frac{2\eta}{\vartheta_2}\right)^2+2R_{\rm N}R_{\rm D}\,(Q_{\rm S}-Q_{\rm C})\left(\frac{\eta}{\vartheta_3}\right)^2\right\}\sum_{\vec{m}'}\frac{P^{(2)}_{\vec{m}'}}{\eta^4},$$

$$\mathcal{M} = -\frac{1}{4}\int_0^{+\infty}\frac{\mathrm{d}\tau_2}{\tau_2^3}\left\{\left(\hat{Q}_{\rm O}+\hat{Q}_{\rm V}\right)\left(N\sum_{\vec{m}}\frac{P^{(4)}_{\vec{m}}}{\hat{\eta}^4}+D\sum_{\vec{n}}\frac{W^{(4)}_{\vec{n}}}{\hat{\eta}^4}\right)\right. \tag{A.17}$$
$$\left.-\,(N+D)\left(\hat{Q}_{\rm O}-\hat{Q}_{\rm V}\right)\left(\frac{2\hat{\eta}}{\hat{\vartheta}_2}\right)^2\right\}\sum_{\vec{m}'}\frac{P^{(2)}_{\vec{m}'}}{\hat{\eta}^4}\,.$$

The first line in the amplitude $\mathcal{A}$ ($\mathcal{M}$) contains the contributions of the NN, DD and ND sectors (N and D sectors), while the second line arises by acting with the orbifold generator g on these sectors.

The RR tadpole cancellation condition fixes the number of D9- and D5-branes to be $N = D = 32$. Moreover, the structure of the open-string partition functions prevents orthogonal gauge groups. Unitary gauge group parameterisation of the Chan–Paton multiplicities is the only possibility, with

$$N = n+\bar{n}\,,\qquad D = d+\bar{d}\,,\qquad R_{\rm N} = i(n-\bar{n})\,,\qquad R_{\rm D} = i(d-\bar{d})\,, \tag{A.18}$$

which gives $n = \bar{n} = d = \bar{d} = 16$. In this undeformed model, the open-string gauge group is $U(16)\times U(16)$.

A.3. Deformations of the BSGP model

The previous model can be deformed in various ways. In particular, the D5-branes can be displaced in $T^4/\mathbb{Z}_2$, Wilson lines along T^2 can be turned on for the gauge group associated with the D5-branes, and "Wilson lines" along all of the six internal directions can be switched on for the gauge group generated by the D9-branes. All these deformations spontaneously break the original gauge group. As described in Sect. 2.1 we are using a T-dual language in which all brane positions and WL's are understood as D3-brane positions, with the understanding that this is merely a convenience, and that there is no common physical prescription where this is actually the case.

We are mostly interested in the case where the deformations take discrete values corresponding to all $32+32$ D3-branes (T-dual to the D9- and D5-branes) sitting on the corners of a six-dimensional box (T-dual to $T^2\times T^4/\mathbb{Z}_2$). The WL's are equal to the components of $\vec{a}_{ii'}\equiv(\vec{a}_{i'},\vec{a}_i)$ which are 0 or $\frac{1}{2}$, where the corners of the box are labelled by a double index ii', in the notation of Sect. 2.1. The annulus amplitude in this case becomes

$$\mathcal{A} = \frac{1}{4}\int_0^{+\infty}\frac{\mathrm{d}\tau_2}{\tau_2^3}\sum_{\substack{i,i'\\ j,j'}}\Bigg\{(Q_{\rm O}+Q_{\rm V})\left(N_{ii'}N_{jj'}\sum_{\vec{m}}\frac{P^{(4)}_{\vec{m}+\vec{a}_i-\vec{a}_j}}{\eta^4}+D_{ii'}D_{jj'}\sum_{\vec{n}}\frac{W^{(4)}_{\vec{n}+\vec{a}_i-\vec{a}_j}}{\eta^4}\right)$$
$$+2N_{ii'}D_{jj'}\,(Q_{\rm S}+Q_{\rm C})\left(\frac{\eta}{\vartheta_4}\right)^2+\delta_{ij}\left(R^{\rm N}_{ii'}R^{\rm N}_{jj'}+R^{\rm D}_{ii'}R^{\rm D}_{jj'}\right)(Q_{\rm O}-Q_{\rm V})\left(\frac{2\eta}{\vartheta_2}\right)^2$$
$$+2e^{4i\pi\vec{a}_i\cdot\vec{a}_j}R^{\rm N}_{ii'}R^{\rm D}_{jj'}\,(Q_{\rm S}-Q_{\rm C})\left(\frac{\eta}{\vartheta_3}\right)^2\Bigg\}\sum_{\vec{m}'}\frac{P^{(2)}_{\vec{m}'+\vec{a}_{i'}-\vec{a}_{j'}}}{\eta^4}\,, \tag{A.19}$$

and the Möbius amplitude reads

$$\mathcal{M} = -\frac{1}{4}\int_0^{+\infty}\frac{\mathrm{d}\tau_2}{\tau_2^3}\sum_{i,i'}\Bigg\{\left(\hat{Q}_{\rm O}+\hat{Q}_{\rm V}\right)\left(N_{ii'}\sum_{\vec{m}}\frac{P^{(4)}_{\vec{m}}}{\hat{\eta}^4}+D_{ii'}\sum_{\vec{n}}\frac{W^{(4)}_{\vec{n}}}{\hat{\eta}^4}\right)$$
$$-(N_{ii'}+D_{ii'})\left(\hat{Q}_{\rm O}-\hat{Q}_{\rm V}\right)\left(\frac{2\hat{\eta}}{\hat{\vartheta}_2}\right)^2\Bigg\}\sum_{\vec{m}'}\frac{P^{(2)}_{\vec{m}'}}{\hat{\eta}^4}\,. \tag{A.20}$$

By contrast, the amplitudes $\mathcal{T}$ and $\mathcal{K}$ in the closed-string sector are independent of the deformations (discrete or otherwise) that we have introduced, and are the same as the expressions given in Eq. (A.16).

There are two subtleties in the annulus amplitude of Eq. (A.19): first, in the term that corresponds to the action of the generator g on the NN and DD sectors (the last term on the second line), the orbifold action enforces being at the origin of the T^4 or $\tilde{T}^4$ lattice. This explains the presence of a Krönecker symbol δ_{ij}. Second, the last contribution, which arises from the action of g on the ND sector, is dressed by signs $e^{4i\pi\vec{a}_i\cdot\vec{a}_j}$ which are necessary in the presence of discrete D9-brane WL's [51].

This leads to the following open-string gauge symmetry in the presence of discrete deformations:

$$\mathcal{G}_{\rm open} = \prod_{ii'/n_{ii'}\neq 0}U(n_{ii'})\times\prod_{jj'/d_{jj'}\neq 0}U(d_{jj'})\,,\quad \text{where}\quad n_{ii'}=\frac{N_{ii'}}{2}\,,\quad d_{jj'}=\frac{D_{jj'}}{2}\,. \tag{A.21}$$

A.4. Supersymmetry breaking

As anticipated in Sect. 2.2, the $\mathcal{N}=2\to\mathcal{N}=0$ spontaneous breaking of supersymmetry is induced by the Scherk–Schwarz mechanism [30–37]. Implementing the associated shifts in Eq. (2.14), the T^2 lattices of zero modes in presence of discrete WL's are modified as follows:

$$\begin{aligned}\Lambda^{(2,2)}_{\vec{m}',(n_4,2n_5+h)} &\longrightarrow \Lambda^{(2,2)}_{\vec{m}'+F\vec{a}'_{\rm S},(n_4,2n_5+h)}\,,\quad h=0,1\,,\\ P^{(2)}_{\vec{m}'+\vec{a}_{i'}-\vec{a}_{j'}} &\longrightarrow P^{(2)}_{\vec{m}'+F\vec{a}'_{\rm S}+\vec{a}_{i'}-\vec{a}_{j'}}\,.\end{aligned} \tag{A.22}$$

As a result, the mass of the gravitino, which we may take as defining the scale of spontaneous supersymmetry breaking, is $M = M_{\rm s}\sqrt{G^{55}}/2$.

To write the amplitudes, we work in the so called "Scherk–Schwarz basis" [53] and change $(G_{54}, G_{55}, G_{5I}) \to (G_{54}/2, G_{55}/4, G_{5I}/2)$, $I = 6, \ldots, 9$. Moreover, for the massless spectrum to be easily readable, we split the result into the contributions of the bosonic and fermionic degrees of freedom running in the loops. The torus amplitude is lengthy, being given by

$$
\begin{aligned}
\mathcal{T} = \frac{1}{4}\int_{\mathcal{F}} \frac{\mathrm{d}^2\tau}{\tau_2^3} \Bigg\{ \Bigg[& \Big(|V_4O_4 + O_4V_4|^2 + |S_4S_4 + C_4C_4|^2\Big) \sum_{\vec{m},\vec{n}} \frac{\Lambda^{(4,4)}_{\vec{m},\vec{n}}}{\left|\eta^4\right|^2} \\
& + \Big(|V_4O_4 - O_4V_4|^2 + |S_4S_4 - C_4C_4|^2\Big) \left|\frac{2\eta}{\vartheta_2}\right|^4 \\
& + 16\Big(|O_4C_4 + V_4S_4|^2 + |S_4O_4 + C_4V_4|^2\Big) \left|\frac{\eta}{\vartheta_4}\right|^4 \\
& + 16\Big(|O_4C_4 - V_4S_4|^2 + |S_4O_4 - C_4V_4|^2\Big) \left|\frac{\eta}{\vartheta_3}\right|^4 \Bigg] \sum_{\vec{m}',\vec{n}'} \frac{\Lambda^{(2,2)}_{\vec{m}',(n_4,2n_5)}}{\left|\eta^4\right|^2} \\
& - \Bigg[\Big((V_4O_4 + O_4V_4)(\bar{S}_4\bar{S}_4 + \bar{C}_4\bar{C}_4) + (S_4S_4 + C_4C_4)(\bar{V}_4\bar{O}_4 + \bar{O}_4\bar{V}_4)\Big) \sum_{\vec{m},\vec{n}} \frac{\Lambda^{(4,4)}_{\vec{m},\vec{n}}}{\left|\eta^4\right|^2} \\
& + \Big((V_4O_4 - O_4V_4)(\bar{S}_4\bar{S}_4 - \bar{C}_4\bar{C}_4) + (S_4S_4 - C_4C_4)(\bar{V}_4\bar{O}_4 - \bar{O}_4\bar{V}_4)\Big) \left|\frac{2\eta}{\vartheta_2}\right|^4 \\
& + 16\Big((O_4C_4 + V_4S_4)(\bar{S}_4\bar{O}_4 + \bar{C}_4\bar{V}_4) + (S_4O_4 + C_4V_4)(\bar{O}_4\bar{C}_4 + \bar{V}_4\bar{S}_4)\Big) \left|\frac{\eta}{\vartheta_4}\right|^4 \\
& + 16\Big((O_4C_4 - V_4S_4)(\bar{S}_4\bar{O}_4 - \bar{C}_4\bar{V}_4) + (S_4O_4 - C_4V_4)(\bar{O}_4\bar{C}_4 - \bar{V}_4\bar{S}_4)\Big) \left|\frac{\eta}{\vartheta_3}\right|^4 \Bigg] \\
& \times \sum_{\vec{m}',\vec{n}'} \frac{\Lambda^{(2,2)}_{\vec{m}'+\vec{a}'_{\rm S},(n_4,2n_5)}}{\left|\eta^4\right|^2} \\
& + \Bigg[\Big(|O_4O_4 + V_4V_4|^2 + |C_4S_4 + S_4C_4|^2\Big) \sum_{\vec{m},\vec{n}} \frac{\Lambda^{(4,4)}_{\vec{m},\vec{n}}}{\left|\eta^4\right|^2} \\
& + \Big(|O_4O_4 - V_4V_4|^2 + |S_4C_4 - C_4S_4|^2\Big) \left|\frac{2\eta}{\vartheta_2}\right|^4 \\
& + 16\Big(|O_4S_4 + V_4C_4|^2 + |S_4V_4 + C_4O_4|^2\Big) \left|\frac{\eta}{\vartheta_4}\right|^4 \\
& + 16\Big(|O_4S_4 - V_4C_4|^2 + |S_4V_4 - C_4O_4|^2\Big) \left|\frac{\eta}{\vartheta_3}\right|^4 \Bigg] \sum_{\vec{m}',\vec{n}'} \frac{\Lambda^{(2,2)}_{\vec{m}',(n_4,2n_5+1)}}{\left|\eta^4\right|^2} \\
& - \Bigg[\Big((O_4O_4 + V_4V_4)(\bar{C}_4\bar{S}_4 + \bar{S}_4\bar{C}_4) + (C_4S_4 + S_4C_4)(\bar{O}_4\bar{O}_4 + \bar{V}_4\bar{V}_4)\Big) \sum_{\vec{m},\vec{n}} \frac{\Lambda^{(4,4)}_{\vec{m},\vec{n}}}{\left|\eta^4\right|^2}
\end{aligned}
\tag{A.23}
$$

$$
\begin{aligned}
&+\left((O_4O_4-V_4V_4)(\bar{S}_4\bar{C}_4-\bar{C}_4\bar{S}_4)+(S_4C_4-C_4S_4)(\bar{O}_4\bar{O}_4-\bar{V}_4\bar{V}_4)\right)\left|\frac{2\eta}{\vartheta_2}\right|^4\\
&+16\left((O_4S_4+V_4C_4)(\bar{S}_4\bar{V}_4+\bar{C}_4\bar{O}_4)+(S_4V_4+C_4O_4)(\bar{O}_4\bar{S}_4+\bar{V}_4\bar{C}_4)\right)\left|\frac{\eta}{\vartheta_4}\right|^4\\
&+16\left((O_4S_4-V_4C_4)(\bar{S}_4\bar{V}_4-\bar{C}_4\bar{O}_4)+(S_4V_4-C_4O_4)(\bar{O}_4\bar{S}_4-\bar{V}_4\bar{C}_4)\right)\left|\frac{\eta}{\vartheta_3}\right|^4\Bigg]\\
&\times\sum_{\vec{m}',\vec{n}'}\frac{\Lambda^{(2,2)}_{\vec{m}'+\vec{a}'_{\rm S},(n_4,2n_5+1)}}{\left|\eta^4\right|^2}\Bigg\}.
\end{aligned}
$$

The proliferation of terms is due to the presence of an untwisted sector along with three twisted sectors, either twisted by g, the Scherk–Schwarz generator, or the combination of the two. The only states flowing in the Klein bottle are left/right-symmetric, leading to the simpler contribution

$$
\begin{aligned}
\mathcal{K}=\frac{1}{4}\int_0^{+\infty}\frac{\mathrm{d}\tau_2}{\tau_2^3}\Bigg\{&(V_4O_4+O_4V_4)\left(\sum_{\vec{m}}\frac{P^{(4)}_{\vec{m}}}{\eta^4}+\sum_{\vec{n}}\frac{W^{(4)}_{\vec{n}}}{\eta^4}\right)+32\,(O_4C_4+V_4S_4)\left(\frac{\eta}{\vartheta_4}\right)^2\\
&-(S_4S_4+C_4C_4)\left(\sum_{\vec{m}}\frac{P^{(4)}_{\vec{m}}}{\eta^4}+\sum_{\vec{n}}\frac{W^{(4)}_{\vec{n}}}{\eta^4}\right)-32\,(S_4O_4+C_4V_4)\left(\frac{\eta}{\vartheta_4}\right)^2\Bigg\}\sum_{\vec{m}'}\frac{P^{(2)}_{\vec{m}'}}{\eta^4}\,.
\end{aligned}
\tag{A.24}
$$

Finally, the open-string amplitudes are

$$
\begin{aligned}
\mathcal{A}=\frac{1}{4}\int_0^{+\infty}\frac{\mathrm{d}\tau_2}{\tau_2^3}\sum_{\substack{i,i'\\j,j'}}\Bigg\{\Bigg[&(V_4O_4+O_4V_4)\left(N_{ii'}N_{jj'}\sum_{\vec{m}}\frac{P^{(4)}_{\vec{m}+\vec{a}_i-\vec{a}_j}}{\eta^4}+D_{ii'}D_{jj'}\sum_{\vec{n}}\frac{W^{(4)}_{\vec{n}+\vec{a}_i-\vec{a}_j}}{\eta^4}\right)\\
&+(V_4O_4-O_4V_4)\delta_{ij}\left(R^{\rm N}_{ii'}R^{\rm N}_{jj'}+R^{\rm D}_{ii'}R^{\rm D}_{jj'}\right)\left(\frac{2\eta}{\vartheta_2}\right)^2\\
&+2N_{ii'}D_{jj'}(O_4C_4+V_4S_4)\left(\frac{\eta}{\vartheta_4}\right)^2\\
&+2e^{4i\pi\vec{a}_i\cdot\vec{a}_j}R^{\rm N}_{ii'}R^{\rm D}_{jj'}(O_4C_4-V_4S_4)\left(\frac{\eta}{\vartheta_3}\right)^2\Bigg]\sum_{\vec{m}'}\frac{P^{(2)}_{\vec{m}'+\vec{a}_{i'}-\vec{a}_{j'}}}{\eta^4}\\
-\Bigg[&(S_4S_4+C_4C_4)\left(N_{ii'}N_{jj'}\sum_{\vec{m}}\frac{P^{(4)}_{\vec{m}+\vec{a}_i-\vec{a}_j}}{\eta^4}+D_{ii'}D_{jj'}\sum_{\vec{n}}\frac{W^{(4)}_{\vec{n}+\vec{a}_i-\vec{a}_j}}{\eta^4}\right)\\
&+(C_4C_4-S_4S_4)\delta_{ij}\left(R^{\rm N}_{ii'}R^{\rm N}_{jj'}+R^{\rm D}_{ii'}R^{\rm D}_{jj'}\right)\left(\frac{2\eta}{\vartheta_2}\right)^2\\
&+2N_{ii'}D_{jj'}(S_4O_4+C_4V_4)\left(\frac{\eta}{\vartheta_4}\right)^2\\
&+2e^{4i\pi\vec{a}_i\cdot\vec{a}_j}R^{\rm N}_{ii'}R^{\rm D}_{jj'}(S_4O_4-C_4V_4)\left(\frac{\eta}{\vartheta_3}\right)^2\Bigg]\sum_{\vec{m}'}\frac{P^{(2)}_{\vec{m}'+\vec{a}'_{\rm S}+\vec{a}_{i'}-\vec{a}_{j'}}}{\eta^4}\Bigg\}\,,
\end{aligned}
\tag{A.25}
$$

$$
\begin{aligned}
\mathcal{M} = -\frac{1}{4}\int_0^{+\infty}\frac{\mathrm{d}\tau_2}{\tau_2^3}\sum_{i,i'}\Bigg\{\Bigg[&(\hat{V}_4\hat{O}_4+\hat{O}_4\hat{V}_4)\Bigg(N_{ii'}\sum_{\vec{m}}\frac{P^{(4)}_{\vec{m}}}{\hat{\eta}^4}+D_{ii'}\sum_{\vec{n}}\frac{W^{(4)}_{\vec{n}}}{\hat{\eta}^4}\Bigg)\\
&-(N_{ii'}+D_{ii'})(\hat{V}_4\hat{O}_4-\hat{O}_4\hat{V}_4)\left(\frac{2\hat{\eta}}{\hat{\vartheta}_2}\right)^2\Bigg]\sum_{\vec{m}'}\frac{P^{(2)}_{\vec{m}'}}{\hat{\eta}^4}\\
&-\Bigg[(\hat{C}_4\hat{C}_4+\hat{S}_4\hat{S}_4)\Bigg(N_{ii'}\sum_{\vec{m}}\frac{P^{(4)}_{\vec{m}}}{\hat{\eta}^4}+D_{ii'}\sum_{\vec{n}}\frac{W^{(4)}_{\vec{n}}}{\hat{\eta}^4}\Bigg)\\
&-(N_{ii'}+D_{ii'})(\hat{C}_4\hat{C}_4-\hat{S}_4\hat{S}_4)\left(\frac{2\hat{\eta}}{\hat{\vartheta}_2}\right)^2\Bigg]\sum_{\vec{m}'}\frac{P^{(2)}_{\vec{m}'+\vec{a}'_{\mathrm{S}}}}{\hat{\eta}^4}\Bigg\}\,.
\end{aligned}
\tag{A.26}
$$

Appendix B. Potential and continuous Wilson lines

In this appendix, we derive the effective potential of the model realizing the $\mathcal{N}=2\to\mathcal{N}=0$ spontaneous breaking of supersymmetry, when continuous open-string WL's are switched on. Our aim is to obtain expressions suitable for the derivation in Sect. 3.2 of the WL mass terms by taking two derivatives with respect to these moduli at points in moduli space where all D3-branes are coincident with O3-planes.

When generalizing the open-string amplitudes $\mathcal{A}$ and $\mathcal{M}$ given in Eqs. (A.25) and (A.26) to arbitrary positions of the D3-branes, the lattice deformations cannot be defined anymore by the positions $2\pi\vec{a}_{ii'}\equiv(\vec{a}_{i'},\vec{a}_i)$ of the fixed points ii'. Instead, the deformations must be parameterised by the locations $2\pi a^{\mathcal{I}}_\alpha$ and $2\pi b^{\mathcal{I}}_\alpha$, $\alpha=1,\ldots,32$, of the D3-branes in their appropriate six-dimensional boxes. However, as described in Sect. 2.1, the moduli space of WL's admits disconnected components, themselves admitting various Higgs, Coulomb and mixed Higgs–Coulomb branches. The number of moduli fields at tree level is thus highly dependent on the branch under interest. To capture the information needed to Taylor expand the potential at any point in moduli space where all D3-branes are stacked on O3-planes, we denote

$$
\begin{aligned}
&\vec{a}'_\alpha\equiv(a^4_\alpha,a^5_\alpha)\,, \qquad \vec{a}_\alpha\equiv(a^6_\alpha,a^7_\alpha,a^8_\alpha,a^9_\alpha)\,,\\
&\vec{b}'_\alpha\equiv(b^4_\alpha,b^5_\alpha)\,, \qquad \vec{b}_\alpha\equiv(b^6_\alpha,b^7_\alpha,b^8_\alpha,b^9_\alpha)\,,
\end{aligned}
\tag{B.1}
$$

and write the annulus amplitude as follows,

$$
\begin{aligned}
\mathcal{A} = \frac{1}{4}\int_0^{+\infty}\frac{\mathrm{d}\tau_2}{\tau_2^3}\sum_{\alpha,\beta}\sum_{\vec{m}'}\Bigg\{&\frac{(V_4O_4+O_4V_4)}{\eta^8}\Bigg(\sum_{\vec{m}}P^{(4)}_{\vec{m}+\vec{a}_\alpha-\vec{a}_\beta}P^{(2)}_{\vec{m}'+\vec{a}'_\alpha-\vec{a}'_\beta}\\
&+\sum_{\vec{n}}W^{(4)}_{\vec{n}+\vec{b}_\alpha-\vec{b}_\beta}P^{(2)}_{\vec{m}'+\vec{b}'_\alpha-\vec{b}'_\beta}\Bigg)\\
&+2(O_4C_4+V_4S_4)\left(\frac{\eta}{\vartheta_4}\right)^2\frac{P^{(2)}_{\vec{m}'+\vec{a}'_\alpha-\vec{b}'_\beta}}{\eta^4}\\
&-\Bigg[\frac{(S_4S_4+C_4C_4)}{\eta^8}\Bigg(\sum_{\vec{m}}P^{(4)}_{\vec{m}+\vec{a}_\alpha-\vec{a}_\beta}P^{(2)}_{\vec{m}'+\vec{a}'_{\mathrm{S}}+\vec{a}'_\alpha-\vec{a}'_\beta}+\sum_{\vec{n}}W^{(4)}_{\vec{n}+\vec{b}_\alpha-\vec{b}_\beta}P^{(2)}_{\vec{m}'+\vec{a}'_{\mathrm{S}}+\vec{b}'_\alpha-\vec{b}'_\beta}\Bigg)
\end{aligned}
\tag{B.2}
$$

$$+ 2(S_4 O_4 + C_4 V_4) \left(\frac{\eta}{\vartheta_4}\right)^2 \frac{P^{(2)}_{\vec{m}'+\vec{a}'_{\rm S}+\vec{a}'_\alpha-\vec{b}'_\beta}}{\eta^4}\Bigg]\Bigg\} .$$

Some remarks are in order:

- In this expression, even if all components $a^{\mathcal{I}}_\alpha$, $b^{\mathcal{I}}_\alpha$ appear formally as independent variables, it is understood that they are correlated 4 by 4 or 2 by 2, or identically equal to 0 or $\frac{1}{2}$, according to the point in moduli space around which fluctuations are considered.
- All terms appearing in the braces are continuous deformations of the contributions proportional to $N_{ii'}$ or $D_{ii'}$ coefficients in Eq. (A.25).
- When continuous WL's are switched on only along T^2, the model sits in a Coulomb branch where the unitary nature of all gauge group factors persists. Hence, all terms proportional to coefficients $R^{\rm N}_{ii'}$ or $R^{\rm D}_{ii'}$ in Eq. (A.25) yield after deformation contributions vanishing identically.[22]
- When continuous WL's are switched on only along $T^4/\mathbb{Z}_2$ or $\tilde{T}^4\mathbb{Z}_2$, the model sits in a Higgs branch where unitary and symplectic gauge group factors cohabit. In that case, the coefficients $R^{\rm N}_{ii'}$ and $R^{\rm D}_{ii'}$ need to be re-evaluated with the numbers of D3-branes that remain localized on the O3-planes. Therefore, all terms proportional to coefficients $R^{\rm N}_{ii'}$ or $R^{\rm D}_{ii'}$ in Eq. (A.25) yield after deformation contributions vanishing identically.[22]

Similarly, the Möbius strip amplitude (A.26) reads in presence of continuous deformations

$$\begin{aligned}\mathcal{M} = -\frac{1}{4}\int_0^{+\infty}\frac{{\rm d}\tau_2}{\tau_2^3}\sum_\alpha\sum_{\vec{m}'}\Bigg\{&\frac{(\hat{V}_4\hat{O}_4+\hat{O}_4\hat{V}_4)}{\hat{\eta}^8}\left(\sum_{\vec{m}} P^{(4)}_{\vec{m}+2\vec{a}_\alpha} P^{(2)}_{\vec{m}'+2\vec{a}'_\alpha} + \sum_{\vec{n}} W^{(4)}_{\vec{n}+2\vec{b}_\alpha} P^{(2)}_{\vec{m}'+2\vec{b}'_\alpha}\right)\\ &- \frac{(\hat{C}_4\hat{C}_4+\hat{S}_4\hat{S}_4)}{\hat{\eta}^8}\left(\sum_{\vec{m}} P^{(4)}_{\vec{m}+2\vec{a}_\alpha} P^{(2)}_{\vec{m}'+\vec{a}'_{\rm S}+2\vec{a}'_\alpha} + \sum_{\vec{n}} W^{(4)}_{\vec{n}+2\vec{b}_\alpha} P^{(2)}_{\vec{m}'+\vec{a}'_{\rm S}+2\vec{b}'_\alpha}\right)\Bigg\} ,\end{aligned} \tag{B.3}$$

where all $a^{\mathcal{I}}_\alpha$, $b^{\mathcal{I}}_\alpha$ are again formally treated as free variables. In this expression, the terms proportional to the combinations of $SO(4)\times SO(4)$ characters $\hat{V}_4\hat{O}_4 - \hat{O}_4\hat{V}_4$ or $\hat{C}_4\hat{C}_4 - \hat{S}_4\hat{S}_4$ are omitted, since they vanish identically.[22]

Next, we may expand the characters as follows,

$$\begin{aligned}&\frac{V_4O_4+O_4V_4}{\eta^8} = \frac{C_4C_4+S_4S_4}{\eta^8} = 8\sum_{k\geq 0} c_k e^{-\pi k\tau_2} ,\\ &\frac{\hat{V}_4\hat{O}_4+\hat{O}_4\hat{V}_4}{\hat{\eta}^8} = \frac{\hat{C}_4\hat{C}_4+\hat{S}_4\hat{S}_4}{\hat{\eta}^8} = 8\sum_{k\geq 0}(-1)^k c_k e^{-\pi k\tau_2} ,\\ &2(O_4C_4+V_4S_4)\left(\frac{\eta}{\vartheta_4}\right)^2\frac{1}{\eta^4} = 2(S_4O_4+C_4V_4)\left(\frac{\eta}{\vartheta_4}\right)^2\frac{1}{\eta^4} = 4\sum_{k\geq 0} d_k e^{-\frac{\pi}{2}k\tau_2} ,\end{aligned} \tag{B.4}$$

where $c_0 = d_0 = 1$, to obtain

[22] This cancellation is only numerical, thanks to the pairing of degenerate modes of eigenvalues ± 1 under the orbifold generator g.

$$\mathcal{A} = 2\int_0^{+\infty} \frac{\mathrm{d}\tau_2}{\tau_2^3} \sum_{k\geq 0} \sum_{\alpha,\beta} \sum_{\vec{m}'} \Bigg\{ c_k e^{-\pi k \tau_2} \Bigg[\sum_{\vec{m}} P^{(4)}_{\vec{m}+\vec{a}_\alpha-\vec{a}_\beta} \left(P^{(2)}_{\vec{m}'+\vec{a}'_\alpha-\vec{a}'_\beta} - P^{(2)}_{\vec{m}'+\vec{a}'_S+\vec{a}'_\alpha-\vec{a}'_\beta} \right) + \sum_{\vec{n}} W^{(4)}_{\vec{n}+\vec{b}_\alpha-\vec{b}_\beta} \left(P^{(2)}_{\vec{m}'+\vec{b}'_\alpha-\vec{b}'_\beta} - P^{(2)}_{\vec{m}'+\vec{a}'_S+\vec{b}'_\alpha-\vec{b}'_\beta} \right) \Bigg] + d_k e^{-\frac{\pi}{2} k \tau_2} \left(P^{(2)}_{\vec{m}'+\vec{a}'_\alpha-\vec{b}'_\beta} - P^{(2)}_{\vec{m}'+\vec{a}'_S+\vec{a}'_\alpha-\vec{b}'_\beta} \right) \Bigg\} , \tag{B.5}$$

and

$$\mathcal{M} = -2\int_0^{+\infty} \frac{\mathrm{d}\tau_2}{\tau_2^3} \sum_{k\geq 0} \sum_{\alpha} \sum_{\vec{m}'} \Bigg\{ (-1)^k c_k \Bigg[\sum_{\vec{m}} P^{(4)}_{\vec{m}+2\vec{a}_\alpha} \left(P^{(2)}_{\vec{m}'+2\vec{a}'_\alpha} - P^{(2)}_{\vec{m}'+\vec{a}'_S+2\vec{a}'_\alpha} \right) + \sum_{\vec{n}} W^{(4)}_{\vec{n}+2\vec{b}_\alpha} \left(P^{(2)}_{\vec{m}'+2\vec{b}'_\alpha} - P^{(2)}_{\vec{m}'+\vec{a}'_S+2\vec{b}'_\alpha} \right) \Bigg] \Bigg\} . \tag{B.6}$$

The moduli space region in which we are interested to find the WL masses is where the lightest non-vanishing scale of the model is the supersymmetry breaking scale $M = M_s\sqrt{G^{55}}/2$. In terms of internal metric components, this means that

$$G^{55} \ll G_{44}, |G_{IJ}| \ll G_{55} , \quad |G_{45}|, |G_{5J}| \ll \sqrt{G_{55}} , \quad I, J \in \{6, \ldots, 9\} , \quad G_{55} \gg 1 . \tag{B.7}$$

The Scherk–Schwarz compact direction X^5 being large, it is convenient to Poisson sum over the momentum m_5 (the new sum index is denoted l_5). The annulus amplitude becomes

$$\begin{aligned} \mathcal{A} = {} & \left(G^{55}\right)^2 \frac{\Gamma\left(\frac{5}{2}\right)}{\pi^{\frac{5}{2}}} 4 \sum_{k\geq 0} \sum_{\alpha,\beta} \sum_{m_4} \sum_{l_5} \frac{1}{|2l_5+1|^5} \\ & \Bigg\{ \sum_{\vec{m}} c_k \cos\left[2\pi |2l_5+1| \left(a^5_\alpha - a^5_\beta + \frac{G^{54}}{G^{55}} (m_4 + a^4_\alpha - a^4_\beta) \right) \right] \mathcal{H}_{\frac{5}{2}} \left(\pi |2l_5+1| \frac{\mathcal{M}_{\mathcal{A}_1}}{\sqrt{G^{55}}} \right) \\ & + \sum_{\vec{n}} c_k \cos\left[2\pi |2l_5+1| \left(b^5_\alpha - b^5_\beta + \frac{G^{54}}{G^{55}} (m_4 + b^4_\alpha - b^4_\beta) \right) \right] \mathcal{H}_{\frac{5}{2}} \left(\pi |2l_5+1| \frac{\mathcal{M}_{\mathcal{A}_2}}{\sqrt{G^{55}}} \right) \\ & + \frac{d_k}{2} \cos\left[2\pi |2l_5+1| \left(a^5_\alpha - b^5_\beta + \frac{G^{54}}{G^{55}} (m_4 + a^4_\alpha - b^4_\beta) \right) \right] \mathcal{H}_{\frac{5}{2}} \left(\pi |2l_5+1| \frac{\mathcal{M}_{\mathcal{A}_3}}{\sqrt{G^{55}}} \right) \Bigg\} , \end{aligned} \tag{B.8}$$

where the function $\mathcal{H}_\nu$ can be expressed in terms of K_ν, a modified Bessel function of the second kind,

$$\mathcal{H}_\nu(z) = \frac{1}{\Gamma(\nu)} \int_0^{+\infty} \frac{dx}{x^{1+\nu}} e^{-\frac{1}{x} - z^2 x} = \frac{2}{\Gamma(\nu)} z^\nu K_\nu(2z) . \tag{B.9}$$

In Eq. (B.8), $\mathcal{M}_{\mathcal{A}_1}$, $\mathcal{M}_{\mathcal{A}_2}$ and $\mathcal{M}_{\mathcal{A}_3}$ define three characteristic mass scales (in string units) satisfying

$$\begin{aligned}
\mathcal{M}^2_{\mathcal{A}_1} &= (m_I + a^I_\alpha - a^I_\beta) G^{IJ} (m_J + a^J_\alpha - a^J_\beta) + (m_4 + a^4_\alpha - a^4_\beta)^2 \hat{G}^{44} + k \ , \\
\mathcal{M}^2_{\mathcal{A}_2} &= (n_I + b^I_\alpha - b^I_\beta) G_{IJ} (n_J + b^J_\alpha - b^J_\beta) + (m_4 + b^4_\alpha - b^4_\beta)^2 \hat{G}^{44} + k \ , \\
\mathcal{M}^2_{\mathcal{A}_3} &= (m_4 + a^4_\alpha - b^4_\beta)^2 \hat{G}^{44} + \frac{k}{2} \ ,
\end{aligned} \tag{B.10}$$

where

$$\hat{G}^{44} = G^{44} - \frac{G^{45}}{G^{55}} G^{55} \frac{G^{54}}{G^{55}} \ . \tag{B.11}$$

Because we are interested in motions of D3-brane around O3-planes, we split the WL moduli into background values and fluctuations,

$$\begin{aligned}
a^{\mathcal{I}}_\alpha &= \langle a^{\mathcal{I}}_\alpha \rangle + \epsilon^{\mathcal{I}}_\alpha \ , \qquad \langle a^{\mathcal{I}}_\alpha \rangle \in \left\{ 0, \frac{1}{2} \right\} \ , \\
b^{\mathcal{I}}_\alpha &= \langle b^{\mathcal{I}}_\alpha \rangle + \xi^{\mathcal{I}}_\alpha \ , \qquad \langle b^{\mathcal{I}}_\alpha \rangle \in \left\{ 0, \frac{1}{2} \right\} \ ,
\end{aligned} \tag{B.12}$$

which allow us to determine when the masses (B.10) are large or small compared to M. This is relevant since $\mathcal{H}_\nu$ is finite for small argument and exponentially suppressed for large argument:

$$\mathcal{H}_\nu(z) = 1 - \frac{z^2}{\nu - 1} + \mathcal{O}(z^4) \quad \text{as} \quad |z| \ll 1 \ , \qquad \mathcal{H}_\nu(z) \sim \frac{\sqrt{\pi}}{\Gamma(\nu)} z^{\nu - \frac{1}{2}} e^{-2z} \quad \text{as} \quad z \gg 1 \ . \tag{B.13}$$

For $\mathcal{M}_{\mathcal{A}_1}/\sqrt{G^{55}}$ not to yield exponentially suppressed contributions to $\mathcal{A}$, we need $k = 0$, $m_I + \langle a^I_\alpha \rangle - \langle a^I_\beta \rangle = 0$ and $m_4 + \langle a^4_\alpha \rangle - \langle a^4_\beta \rangle = 0$. This amounts to having $\vec{m} = \vec{0}$, $m_4 = 0$ and (α, β) in the set $L_{\rm NN}$ such that the D3-branes α, β T-dual to D9-branes

- belong to the same stack of $N_{ii'}$ branes, $i = 1, \ldots, 16$, $i' = 1, \ldots, 4$,
- or belong respectively to stacks of $N_{i,2i''-1}$ and $N_{i,2i''}$ branes, $i = 1, \ldots, 16$, $i'' = 1, 2$,
- or belong respectively to stacks of $N_{i,2i''}$ and $N_{i,2i''-1}$ branes, $i = 1, \ldots, 16$, $i'' = 1, 2$.

Similarly, for $\mathcal{M}_{\mathcal{A}_2}/\sqrt{G^{55}}$ not to yield exponentially suppressed terms in $\mathcal{A}$, we need $k = 0$, $\vec{n} = \vec{0}$, $m_4 = 0$ and (α, β) in the set $L_{\rm DD}$ such that the D3-branes α, β T-dual to D5-branes

- belong to the same stack of $D_{ii'}$ branes, $i = 1, \ldots, 16$, $i' = 1, \ldots, 4$,
- or belong respectively to stacks of $D_{i,2i''-1}$ and $D_{i,2i''}$ branes, $i = 1, \ldots, 16$, $i'' = 1, 2$,
- or belong respectively to stacks of $D_{i,2i''}$ and $D_{i,2i''-1}$ branes, $i = 1, \ldots, 16$, $i'' = 1, 2$.

Finally, terms involving $\mathcal{M}_{\mathcal{A}_3}/\sqrt{G^{55}}$ are relevant when $k = 0$ and $m_4 + \langle a^4_\alpha \rangle - \langle b^4_\beta \rangle = 0$. This is achieved if $m_4 = 0$ and (α, β) is in the set $L_{\rm ND}$ such that the D3-branes α, β T-dual to a D9-brane and a D5-brane

- belong respectively to stacks of $N_{ii'}$ and $D_{ji'}$ branes, $i, j = 1, \ldots, 16$, $i' = 1, \ldots, 4$,
- or belong respectively to stacks of $N_{i,2i''-1}$ and $D_{j,2i''}$ branes, $i, j = 1, \ldots, 16$, $i'' = 1, 2$,
- or belong respectively to stacks of $N_{j,2i''}$ and $D_{i,2i''-1}$ branes, $i, j = 1, \ldots, 16$, $i'' = 1, 2$.

Up to exponentially suppressed terms, we thus obtain

$$\begin{aligned}
\mathcal{A} = & \left(G^{55}\right)^2 \frac{\Gamma\left(\frac{5}{2}\right)}{\pi^{\frac{5}{2}}} \\
& \times \sum_{l_5} \frac{4}{|2l_5+1|^5} \Bigg\{ \sum_{(\alpha,\beta)\in L_{\rm NN}} (-)^{2(\langle a^5_\alpha\rangle - \langle a^5_\beta\rangle)} \cos\left[2\pi|2l_5+1|\left(\epsilon^5_\alpha - \epsilon^5_\beta + \frac{G^{54}}{G^{55}}(\epsilon^4_\alpha - \epsilon^4_\beta)\right)\right] \\
& \qquad \times \mathcal{H}_{\frac{5}{2}}\left(\pi|2l_5+1|\frac{\left[(\epsilon^I_\alpha - \epsilon^I_\beta)G^{IJ}(\epsilon^J_\alpha - \epsilon^J_\beta) + (\epsilon^4_\alpha - \epsilon^4_\beta)^2\hat{G}^{44}\right]^{\frac{1}{2}}}{\sqrt{G^{55}}}\right) \\
& + \sum_{(\alpha,\beta)\in L_{\rm DD}} (-)^{2(\langle b^5_\alpha\rangle - \langle b^5_\beta\rangle)} \cos\left[2\pi|2l_5+1|\left(\xi^5_\alpha - \xi^5_\beta + \frac{G^{54}}{G^{55}}(\xi^4_\alpha - \xi^4_\beta)\right)\right] \\
& \qquad \times \mathcal{H}_{\frac{5}{2}}\left(\pi|2l_5+1|\frac{\left[(\xi^I_\alpha - \xi^I_\beta)G_{IJ}(\xi^J_\alpha - \xi^J_\beta) + (\xi^4_\alpha - \xi^4_\beta)^2\hat{G}^{44}\right]^{\frac{1}{2}}}{\sqrt{G^{55}}}\right) \\
& + \frac{1}{2}\sum_{(\alpha,\beta)\in L_{\rm ND}} (-)^{2(\langle a^5_\alpha\rangle - \langle b^5_\beta\rangle)} \cos\left[2\pi|2l_5+1|\left(\epsilon^5_\alpha - \xi^5_\beta + \frac{G^{54}}{G^{55}}(\epsilon^4_\alpha - \xi^4_\beta)\right)\right] \\
& \qquad \times \mathcal{H}_{\frac{5}{2}}\left(\pi|2l_5+1|\frac{\left[(\epsilon^4_\alpha - \xi^4_\beta)^2\hat{G}^{44}\right]^{\frac{1}{2}}}{\sqrt{G^{55}}}\right)\Bigg\} + \mathcal{O}\left(G^{55}e^{-\frac{2\pi c}{\sqrt{G^{55}}}}\right),
\end{aligned} \tag{B.14}$$

where c is positive of order one.

Proceeding in a similar way with the Möbius amplitude, we may write

$$\begin{aligned}
\mathcal{M} = & -\left(G^{55}\right)^2 \frac{\Gamma\left(\frac{5}{2}\right)}{\pi^{\frac{5}{2}}} 4\sum_{k\geq 0}(-1)^k c_k \sum_\alpha \sum_{m_4}\sum_{l_5} \frac{1}{|2l_5+1|^5} \\
& \Bigg\{ \sum_{\vec{m}} \cos\left[2\pi|2l_5+1|\left(2a^5_\alpha + \frac{G^{54}}{G^{55}}(m_4+2a^4_\alpha)\right)\right] \mathcal{H}_{\frac{5}{2}}\left(\pi|2l_5+1|\frac{\mathcal{M}_{\mathcal{M}_1}}{\sqrt{G^{55}}}\right) \\
& + \sum_{\vec{n}} \cos\left[2\pi|2l_5+1|\left(2b^5_\alpha + \frac{G^{54}}{G^{55}}(m_4+2b^4_\alpha)\right)\right] \mathcal{H}_{\frac{5}{2}}\left(\pi|2l_5+1|\frac{\mathcal{M}_{\mathcal{M}_2}}{\sqrt{G^{55}}}\right)\Bigg\},
\end{aligned} \tag{B.15}$$

which involves characteristic mass scales

$$\begin{aligned}
\mathcal{M}^2_{\mathcal{M}_1} &= (m_I + 2a^I_\alpha)G^{IJ}(m_J + 2a^J_\alpha) + (m_4 + 2a^4_\alpha)^2\hat{G}^{44} + k\,, \\
\mathcal{M}^2_{\mathcal{M}_2} &= (n_I + 2b^I_\alpha)G_{IJ}(n_J + 2b^J_\alpha) + (m_4 + 2b^4_\alpha)^2\hat{G}^{44} + k\,.
\end{aligned} \tag{B.16}$$

The functions $\mathcal{H}_{\frac{5}{2}}$ are exponentially suppressed unless their arguments satisfy $k = 0$ and $m_I = -2\langle a^I_\alpha\rangle$, $m_4 = -2\langle a^4_\alpha\rangle$, or $n_I = -2\langle b^I_\alpha\rangle$, $m_4 = -2\langle b^4_\alpha\rangle$. As a result, the amplitude takes the following form

$$\mathcal{M} = -\left(G^{55}\right)^2 \frac{\Gamma\left(\frac{5}{2}\right)}{\pi^{\frac{5}{2}}} \sum_{\alpha} \sum_{l_5} \frac{4}{|2l_5+1|^5} \left\{ \cos\left[4\pi |2l_5+1| \left(\epsilon_\alpha^5 + \frac{G^{54}}{G^{55}} \epsilon_\alpha^4 \right) \right] \right.$$
$$\times \mathcal{H}_{\frac{5}{2}} \left(2\pi |2l_5+1| \frac{\left[\epsilon_\alpha^I G^{IJ} \epsilon_\alpha^J + \left(\epsilon_\alpha^4\right)^2 \hat{G}^{44} \right]^{\frac{1}{2}}}{\sqrt{G^{55}}} \right)$$
$$+ \cos\left[4\pi |2l_5+1| \left(\xi_\alpha^5 + \frac{G^{54}}{G^{55}} \xi_\alpha^4 \right) \right] \tag{B.17}$$
$$\left. \times \mathcal{H}_{\frac{5}{2}} \left(2\pi |2l_5+1| \frac{\left[\xi_\alpha^I G_{IJ} \xi_\alpha^J + \left(\xi_\alpha^4\right)^2 \hat{G}^{44} \right]^{\frac{1}{2}}}{\sqrt{G^{55}}} \right) \right\}$$
$$+ \mathcal{O}\left(G^{55} e^{-\frac{2\pi c}{\sqrt{G^{55}}}} \right).$$

Adding the annulus and Möbius strip amplitudes, the contribution of the open-string sector to the one-loop effective potential can be written as

$$-\frac{M_s^4}{2(2\pi)^4} (\mathcal{A}+\mathcal{M}) = \frac{\Gamma\left(\frac{5}{2}\right)}{\pi^{\frac{13}{2}}} M^4 \sum_{l_5} \frac{\mathcal{N}^{\text{open}}_{2l_5+1}(\epsilon,\xi,G)}{|2l_5+1|^5} + \mathcal{O}\left((M_s M)^2 e^{-2\pi c \frac{M_s}{M}} \right), \tag{B.18}$$

where $\mathcal{N}^{\text{open}}_{2l_5+1}(\epsilon,\xi,G)$ is given by

$$\mathcal{N}^{\text{open}}_{2l_5+1}(\epsilon,\xi,G) = 2 \left\{ - \sum_{(\alpha,\beta)\in L_{\text{NN}}} (-)^F \cos\left[2\pi |2l_5+1| \frac{G^{5I'}}{G^{55}} \left(\epsilon_\alpha^{I'} - \epsilon_\beta^{I'} \right) \right] \right.$$
$$\times \mathcal{H}_{\frac{5}{2}} \left(\pi |2l_5+1| \frac{\left[(\epsilon_\alpha^I - \epsilon_\beta^I) G^{IJ} (\epsilon_\alpha^J - \epsilon_\beta^J) + (\epsilon_\alpha^4 - \epsilon_\beta^4)^2 \hat{G}^{44} \right]^{\frac{1}{2}}}{\sqrt{G^{55}}} \right)$$
$$- \sum_{(\alpha,\beta)\in L_{\text{DD}}} (-)^F \cos\left[2\pi |2l_5+1| \frac{G^{5I'}}{G^{55}} \left(\xi_\alpha^{I'} - \xi_\beta^{I'} \right) \right]$$
$$\times \mathcal{H}_{\frac{5}{2}} \left(\pi |2l_5+1| \frac{\left[(\xi_\alpha^I - \xi_\beta^I) G_{IJ} (\xi_\alpha^J - \xi_\beta^J) + (\xi_\alpha^4 - \xi_\beta^4)^2 \hat{G}^{44} \right]^{\frac{1}{2}}}{\sqrt{G^{55}}} \right) \tag{B.19}$$
$$- \frac{1}{2} \sum_{(\alpha,\beta)\in L_{\text{ND}}} (-)^F \cos\left[2\pi |2l_5+1| \frac{G^{5I'}}{G^{55}} \left(\epsilon_\alpha^{I'} - \xi_\beta^{I'} \right) \right]$$
$$\left. \times \mathcal{H}_{\frac{5}{2}} \left(\pi |2l_5+1| \frac{\left[(\epsilon_\alpha^4 - \xi_\beta^4)^2 \hat{G}^{44} \right]^{\frac{1}{2}}}{\sqrt{G^{55}}} \right) \right\}$$

$$+\sum_{\alpha}\cos\left[4\pi|2l_5+1|\frac{G^{5I'}}{G^{55}}\epsilon_\alpha^{I'}\right]$$
$$\times\mathcal{H}_{\frac{5}{2}}\left(2\pi|2l_5+1|\frac{\left[\epsilon_\alpha^I G^{IJ}\epsilon_\alpha^J+\left(\epsilon_\alpha^4\right)^2\hat{G}^{44}\right]^{\frac{1}{2}}}{\sqrt{G^{55}}}\right)$$
$$+\sum_{\alpha}\cos\left[4\pi|2l_5+1|\frac{G^{5I'}}{G^{55}}\xi_\alpha^{I'}\right]$$
$$\times\mathcal{H}_{\frac{5}{2}}\left(2\pi|2l_5+1|\frac{\left[\xi_\alpha^I G_{IJ}\xi_\alpha^J+\left(\xi_\alpha^4\right)^2\hat{G}^{44}\right]^{\frac{1}{2}}}{\sqrt{G^{55}}}\right)\Bigg\}.$$

In this expression, F is the fermionic number of the string $(\alpha,\beta)\in L_{\rm NN}\cup L_{\rm DD}\cup L_{\rm ND}$.

References

[1] H.P. Nilles, Dynamically broken supergravity and the hierarchy problem, Phys. Lett. B 115 (1982) 193.
[2] H.P. Nilles, Supergravity generates hierarchies, Nucl. Phys. B 217 (1983) 366.
[3] S. Ferrara, L. Girardello, H.P. Nilles, Breakdown of local supersymmetry through gauge fermion condensates, Phys. Lett. B 125 (1983) 457.
[4] J.P. Derendinger, L.E. Ibanez, H.P. Nilles, On the low-energy $d=4$, $\mathcal{N}=1$ supergravity theory extracted from the $d=10$, $\mathcal{N}=1$ superstring, Phys. Lett. B 155 (1985) 65.
[5] M. Dine, R. Rohm, N. Seiberg, E. Witten, Gluino condensation in superstring models, Phys. Lett. B 156 (1985) 55.
[6] C. Kounnas, M. Porrati, Duality and gaugino condensation in superstring models, Phys. Lett. B 191 (1987) 91.
[7] H. Itoyama, T.R. Taylor, Supersymmetry restoration in the compactified $O(16)\times O(16)'$ heterotic string theory, Phys. Lett. B 186 (1987) 129.
[8] S. Abel, K.R. Dienes, E. Mavroudi, Towards a non-supersymmetric string phenomenology, Phys. Rev. D 91 (2015) 126014, arXiv:1502.03087 [hep-th].
[9] C. Kounnas, H. Partouche, Super no-scale models in string theory, Nucl. Phys. B 913 (2016) 593, arXiv:1607.01767 [hep-th].
[10] C. Kounnas, H. Partouche, $\mathcal{N}=2\to 0$ super no-scale models and moduli quantum stability, Nucl. Phys. B 919 (2017) 41, arXiv:1701.00545 [hep-th].
[11] I. Florakis, J. Rizos, Chiral heterotic strings with positive cosmological constant, Nucl. Phys. B 913 (2016) 495, arXiv:1608.04582 [hep-th].
[12] S. Abel, R.J. Stewart, On exponential suppression of the cosmological constant in non-SUSY strings at two loops and beyond, Phys. Rev. D 96 (2017) 106013, arXiv:1701.06629 [hep-th].
[13] S. Abel, K.R. Dienes, E. Mavroudi, GUT precursors and entwined SUSY: the phenomenology of stable nonsupersymmetric strings, Phys. Rev. D 97 (12) (2018) 126017, arXiv:1712.06894 [hep-ph].
[14] T. Catelin-Jullien, C. Kounnas, H. Partouche, N. Toumbas, Thermal/quantum effects and induced superstring cosmologies, Nucl. Phys. B 797 (2008) 137, arXiv:0710.3895 [hep-th].
[15] F. Bourliot, C. Kounnas, H. Partouche, Attraction to a radiation-like era in early superstring cosmologies, Nucl. Phys. B 816 (2009) 227, arXiv:0902.1892 [hep-th].
[16] T. Coudarchet, C. Fleming, H. Partouche, Quantum no-scale regimes in string theory, Nucl. Phys. B 930 (2018) 235, arXiv:1711.09122 [hep-th].
[17] M. Borunda, M. Serone, M. Trapletti, On the quantum stability of IIB orbifolds and orientifolds with Scherk–Schwarz SUSY breaking, Nucl. Phys. B 653 (2003) 85, arXiv:hep-th/0210075.
[18] T. Catelin-Jullien, C. Kounnas, H. Partouche, N. Toumbas, Induced superstring cosmologies and moduli stabilization, Nucl. Phys. B 820 (2009) 290, arXiv:0901.0259 [hep-th].
[19] F. Bourliot, J. Estes, C. Kounnas, H. Partouche, Cosmological phases of the string thermal effective potential, Nucl. Phys. B 830 (2010) 330, arXiv:0908.1881 [hep-th].
[20] J. Estes, C. Kounnas, H. Partouche, Superstring cosmology for $\mathcal{N}_4=1\to 0$ superstring vacua, Fortschr. Phys. 59 (2011) 861, arXiv:1003.0471 [hep-th].

[21] T. Coudarchet, H. Partouche, Quantum no-scale regimes and moduli dynamics, Nucl. Phys. B 933 (2018) 134, arXiv:1804.00466 [hep-th].
[22] H. Itoyama, S. Nakajima, Stability, enhanced gauge symmetry and suppressed cosmological constant in 9D heterotic interpolating models, arXiv:2003.11217 [hep-th].
[23] S. Abel, E. Dudas, D. Lewis, H. Partouche, Stability and vacuum energy in open string models with broken supersymmetry, J. High Energy Phys. 1910 (2019) 226, arXiv:1812.09714 [hep-th].
[24] H. Partouche, Quantum stability in open string theory with broken supersymmetry, arXiv:1901.02428 [hep-th].
[25] R. Rohm, Spontaneous supersymmetry breaking in supersymmetric string theories, Nucl. Phys. B 237 (1984) 553.
[26] C. Kounnas, M. Porrati, Spontaneous supersymmetry breaking in string theory, Nucl. Phys. B 310 (1988) 355.
[27] S. Ferrara, C. Kounnas, M. Porrati, Superstring solutions with spontaneously broken four-dimensional supersymmetry, Nucl. Phys. B 304 (1988) 500.
[28] S. Ferrara, C. Kounnas, M. Porrati, F. Zwirner, Superstrings with spontaneously broken supersymmetry and their effective theories, Nucl. Phys. B 318 (1989) 75.
[29] C. Kounnas, B. Rostand, Coordinate-dependent compactifications and discrete symmetries, Nucl. Phys. B 341 (1990) 641.
[30] J.D. Blum, K.R. Dienes, Duality without supersymmetry: the case of the $SO(16) \times SO(16)$ string, Phys. Lett. B 414 (1997) 260, arXiv:hep-th/9707148.
[31] J.D. Blum, K.R. Dienes, Strong/weak coupling duality relations for nonsupersymmetric string theories, Nucl. Phys. B 516 (1998) 83, arXiv:hep-th/9707160.
[32] I. Antoniadis, E. Dudas, A. Sagnotti, Supersymmetry breaking, open strings and M-theory, Nucl. Phys. B 544 (1999) 469, arXiv:hep-th/9807011.
[33] I. Antoniadis, G. D'Appollonio, E. Dudas, A. Sagnotti, Partial breaking of supersymmetry, open strings and M-theory, Nucl. Phys. B 553 (1999) 133, arXiv:hep-th/9812118.
[34] I. Antoniadis, G. D'Appollonio, E. Dudas, A. Sagnotti, Open descendants of $\mathbb{Z}_2 \times \mathbb{Z}_2$ freely acting orbifolds, Nucl. Phys. B 565 (2000) 123, arXiv:hep-th/9907184.
[35] A.L. Cotrone, A $\mathbb{Z}_2 \times \mathbb{Z}_2$ orientifold with spontaneously broken supersymmetry, Mod. Phys. Lett. A 14 (1999) 2487, arXiv:hep-th/9909116.
[36] C.A. Scrucca, M. Serone, On string models with Scherk–Schwarz supersymmetry breaking, J. High Energy Phys. 0110 (2001) 017, arXiv:hep-th/0107159.
[37] C. Angelantonj, M. Cardella, N. Irges, Scherk–Schwarz breaking and intersecting branes, Nucl. Phys. B 725 (2005) 115, arXiv:hep-th/0503179.
[38] J. Scherk, J.H. Schwarz, Spontaneous breaking of supersymmetry through dimensional reduction, Phys. Lett. B 82 (1979) 60.
[39] J. Polchinski, TASI lectures on D-branes, arXiv:hep-th/9611050.
[40] H. Partouche, B. de Vaulchier, Hagedorn-like transition at high supersymmetry breaking scale, J. High Energy Phys. 1908 (2019) 155, arXiv:1903.09116 [hep-th].
[41] H. Partouche, B. de Vaulchier, Phase transition at high supersymmetry breaking scale in string theory, arXiv:1911.06558 [hep-th].
[42] J.H. Schwarz, Some properties of type I' string theory, in: M.A. Shifman (Ed.), The Many Faces of the Superworld, 2000, pp. 388–397, arXiv:hep-th/9907061.
[43] J. de Boer, R. Dijkgraaf, K. Hori, A. Keurentjes, J. Morgan, D.R. Morrison, S. Sethi, Triples, fluxes, and strings, Adv. Theor. Math. Phys. 4 (2002) 995, arXiv:hep-th/0103170.
[44] E. Witten, D-branes and K-theory, J. High Energy Phys. 9812 (1998) 019, arXiv:hep-th/9810188.
[45] R. Minasian, G.W. Moore, K-theory and Ramond-Ramond charge, J. High Energy Phys. 9711 (1997) 002, arXiv:hep-th/9710230.
[46] A.M. Uranga, D-brane probes, RR tadpole cancellation and K-theory charge, Nucl. Phys. B 598 (2001) 225, arXiv:hep-th/0011048.
[47] E. Witten, An $SU(2)$ anomaly, Phys. Lett. B 117 (1982) 324.
[48] C. Angelantonj, H. Partouche, G. Pradisi, Heterotic-type I dual pairs, rigid branes and broken SUSY, Nucl. Phys. B 954 (2020) 114976, arXiv:1912.12062 [hep-th].
[49] M. Bianchi, A. Sagnotti, Twist symmetry and open string Wilson lines, Nucl. Phys. B 361 (1991) 519.
[50] E.G. Gimon, J. Polchinski, Consistency conditions for orientifolds and D-manifolds, Phys. Rev. D 54 (1996) 1667, arXiv:hep-th/9601038.
[51] M. Berkooz, R.G. Leigh, J. Polchinski, J.H. Schwarz, N. Seiberg, E. Witten, Anomalies, dualities, and topology of $D = 6$ $\mathcal{N} = 1$ superstring vacua, Nucl. Phys. B 475 (1996) 115, arXiv:hep-th/9605184.
[52] G. Pradisi, A. Sagnotti, Open string orbifolds, Phys. Lett. B 216 (1989) 59.

[53] C. Angelantonj, A. Sagnotti, Open strings, Phys. Rep. 371 (2002) 1, Phys. Rep. 376 (2003) 339 (Erratum), arXiv:hep-th/0204089.
[54] E. Dudas, Theory and phenomenology of type I strings and M-theory, Class. Quantum Gravity 17 (2000) R41, arXiv:hep-ph/0006190.
[55] D. Cremades, L.E. Ibanez, F. Marchesano, Intersecting brane models of particle physics and the Higgs mechanism, J. High Energy Phys. 0207 (2002) 022, arXiv:hep-th/0203160.
[56] D. Cremades, L.E. Ibanez, F. Marchesano, Yukawa couplings in intersecting D-brane models, J. High Energy Phys. 0307 (2003) 038, arXiv:hep-th/0302105.
[57] B. Kors, P. Nath, Effective action and soft supersymmetry breaking for intersecting D-brane models, Nucl. Phys. B 681 (2004) 77, arXiv:hep-th/0309167.
[58] D. Cremades, L.E. Ibanez, F. Marchesano, Computing Yukawa couplings from magnetized extra dimensions, J. High Energy Phys. 0405 (2004) 079, arXiv:hep-th/0404229.
[59] Work in progress.
[60] J. Polchinski, E. Witten, Evidence for heterotic - type I string duality, Nucl. Phys. B 460 (1996) 525, arXiv:hep-th/9510169.
[61] E. Witten, String theory dynamics in various dimensions, Nucl. Phys. B 443 (1995) 85, arXiv:hep-th/9503124.
[62] C.M. Hull, String-string duality in ten-dimensions, Phys. Lett. B 357 (1995) 545, arXiv:hep-th/9506194.
[63] A. Dabholkar, Ten-dimensional heterotic string as a soliton, Phys. Lett. B 357 (1995) 307, arXiv:hep-th/9506160.
[64] C. Angelantonj, M. Bianchi, G. Pradisi, A. Sagnotti, Y.S. Stanev, Comments on Gepner models and type I vacua in string theory, Phys. Lett. B 387 (1996) 743, arXiv:hep-th/9607229.
[65] I. Antoniadis, C. Bachas, C. Fabre, H. Partouche, T.R. Taylor, Aspects of type I - type II - heterotic triality in four dimensions, Nucl. Phys. B 489 (1997) 160, arXiv:hep-th/9608012.
[66] I. Antoniadis, H. Partouche, T.R. Taylor, Duality of $\mathcal{N} = 2$ heterotic type I compactifications in four dimensions, Nucl. Phys. B 499 (1997) 29, arXiv:hep-th/9703076.
[67] I. Antoniadis, H. Partouche, T.R. Taylor, Lectures on heterotic type I duality, Nucl. Phys. B, Proc. Suppl. 61A (1998) 58, Nucl. Phys. B, Proc. Suppl. 67 (1998) 3, NATO Sci. Ser. C 520 (1999) 179, arXiv:hep-th/9706211.
[68] E. Cremmer, S. Ferrara, C. Kounnas, D.V. Nanopoulos, Naturally vanishing cosmological constant in $\mathcal{N} = 1$ supergravity, Phys. Lett. B 133 (1983) 61.
[69] C. Vafa, E. Witten, Dual string pairs with $\mathcal{N} = 1$ and $\mathcal{N} = 2$ supersymmetry in four-dimensions, Nucl. Phys. B, Proc. Suppl. 46 (1996) 225, arXiv:hep-th/9507050.
[70] N. Seiberg, E. Witten, Electric - magnetic duality, monopole condensation, and confinement in $\mathcal{N} = 2$ supersymmetric Yang-Mills theory, Nucl. Phys. B 426 (1994) 19, Nucl. Phys. B 430 (1994) 485 (Erratum), arXiv:hep-th/9407087.
[71] A. Strominger, Massless black holes and conifolds in string theory, Nucl. Phys. B 451 (1995) 96, arXiv:hep-th/9504090.
[72] J. Estes, L. Liu, H. Partouche, Massless D-strings and moduli stabilization in type I cosmology, J. High Energy Phys. 1106 (2011) 060, arXiv:1102.5001 [hep-th].
[73] L. Liu, H. Partouche, Moduli stabilization in type II Calabi-Yau compactifications at finite temperature, J. High Energy Phys. 1211 (2012) 079, arXiv:1111.7307 [hep-th].
[74] P.H. Ginsparg, C. Vafa, Toroidal compactification of nonsupersymmetric heterotic strings, Nucl. Phys. B 289 (1987) 414.
[75] A. Sagnotti, Open strings and their symmetry groups, in: G. Mack, et al. (Eds.), Non-perturbative Quantum Field Theory, Cargese '87, Pergamon Press, 1988, p. 521, arXiv:hep-th/0208020.
[76] P. Horava, Strings on world sheet orbifolds, Nucl. Phys. B 327 (1989) 461.
[77] P. Horava, Background duality of open string models, Phys. Lett. B 231 (1989) 251.
[78] M. Bianchi, A. Sagnotti, On the systematics of open string theories, Phys. Lett. B 247 (1990) 517.
[79] A. Sagnotti, A note on the Green–Schwarz mechanism in open string theories, Phys. Lett. B 294 (1992) 196, arXiv:hep-th/9210127.
[80] M. Bianchi, G. Pradisi, A. Sagnotti, Toroidal compactification and symmetry breaking in open string theories, Nucl. Phys. B 376 (1992) 365.

CPHT-RR090.112020, November 2020

One-loop masses of Neumann–Dirichlet open strings and boundary-changing vertex operators

Thibaut Coudarchet and Hervé Partouche

CPHT, CNRS, Ecole Polytechnique, IP Paris,
F-91128 Palaiseau, France

thibaut.coudarchet@polytechnique.edu
herve.partouche@polytechnique.edu

Abstract

We derive the masses acquired at one loop by massless scalars in the Neumann–Dirichlet sector of open strings, when supersymmetry is spontaneously broken. It is done by computing two-point functions of "boundary-changing vertex operators" inserted on the boundaries of the annulus and Möbius strip. This requires the evaluation of correlators of "excited boundary-changing fields," which are analogous to excited twist fields for closed strings. We work in the type IIB orientifold theory compactified on $T^2 \times T^4/\mathbb{Z}_2$, where $\mathcal{N} = 2$ supersymmetry is broken to $\mathcal{N} = 0$ by the Scherk–Schwarz mechanism implemented along T^2. Even though the full expression of the squared masses is complicated, it reduces to a very simple form when the lowest scale of the background is the supersymmetry breaking scale $M_{3/2}$. We apply our results to analyze in this regime the stability at the quantum level of the moduli fields arising in the Neumann–Dirichlet sector. This completes the study of Ref. [32], where the quantum masses of all other types of moduli arising in the open- or closed-string sectors are derived. Ultimately, we identify all brane configurations that produce backgrounds without tachyons at one loop and yield an effective potential exponentially suppressed, or strictly positive with runaway behavior of $M_{3/2}$.

1 Introduction

Superstring-theory models based on two-dimensional conformal field theories of free fields have the advantage of allowing, at least in principle, string amplitudes to be computed exactly in string tension α' by including all worldsheet instantons. Backgrounds whose internal spaces are $\mathbb{Z}_N$-twist orbifolds of tori are of particular interest since their numbers of spacetime supersymmetries are reduced in a "hard way" compared to the case of toroidal compactifications. In this framework, twisted states in the closed-string Hilbert space are mandatory for modular invariance to hold, which implies "twist fields" to exist in the conformal field theory to create them [1]. String amplitudes involving external states in the twisted sectors are based on correlation functions of twist fields, which are notoriously difficult to handle. Indeed, the seminal work of Ref. [2] presents results only for the case of twist fields creating ground states in the closed-string sector.

In open-string theory, the consistency of orbifold models also implies the presence of distinct D-brane sectors. For instance, in the type IIB orientifold on $T^4/\mathbb{Z}_2$ [3–5], open strings have either Neumann (N) or Dirichlet (D) boundary conditions in the orbifold directions, and are thus attached to D9- or D5-branes. In particular, strings with Neumann boundary conditions at one end and Dirichlet conditions at the other end populate the ND sector. In string amplitudes involving external states of this type, a conformal transformation maps the legs of the diagram to vertex operators localized along the worldsheet boundary. The key point is that the nature of an ND-sector state implies that the worldsheet boundary condition changes from Neumann on one side of the vertex to Dirichlet on the other side. Hence, vertex operators creating states in the ND sector involve "boundary-changing fields" [6] dressed by other objects encoding the quantum numbers.

It turns out that twist fields and boundary-changing fields have identical OPE's [2,6], up to the fact that the former are inserted in the bulk of the worldsheet and the latter on the boundary. Combining this with the method of images which defines surfaces with boundaries as Rienmann surfaces modded by involutions [7,8], correlation functions of boundary-changing fields can be related to those of twist fields. In the literature, this point of view was applied for computing amplitudes with external states of ND sectors in supersymmetric theories at tree level [9–12] and one loop [13–18], while other approaches were followed in Refs. [19–21].

In the present work, we consider the type IIB orientifold model of Refs. [3–5] compactified on $T^2 \times T^4/\mathbb{Z}_2$, when $\mathcal{N} = 2$ supersymmetry is spontaneously broken to $\mathcal{N} = 0$. The implementation of the breaking consists of a string version [22–29] of the Scherk–Schwarz mechanism [30, 31] along one direction of T^2. In this case, the supersymmetry breaking scale, $M_{3/2}$, is a modulus inversely proportional to the size of the compact direction involved in the mechanism. Moreover, the free nature of the bosonic and fermionic fields defining the worldsheet conformal field theory is preserved and the results of Ref. [2] apply. An effective potential which depends on all moduli fields is generated by quantum corrections and the question of their stability must be addressed. Assuming the string coupling to be in perturbative regime, loci in moduli space where the one-loop effective potential is extremal with respect to all moduli fields except $M_{3/2}$ have been determined in Ref. [32], up to exponentially suppressed terms. At these points, the potential reads

$$\mathcal{V}_{\text{1-loop}} = \upsilon(n_{\text{F}} - n_{\text{B}})M_{3/2}^4 + \mathcal{O}\Big((M_{\text{s}}M_{3/2})^2\, e^{-\pi\frac{cM_{\text{s}}}{M_{3/2}}}\Big)\,, \tag{1.1}$$

where n_{F} and n_{B} are the numbers of massless fermionic and bosonic degrees of freedom present at genus-0. Moreover, $\upsilon > 0$ is a constant, $M_{\text{s}} \equiv 1/\sqrt{\alpha'}$ is the string scale, and cM_{s} is the lowest non-vanishing mass scale other than $M_{3/2}$, $0 < c \leq 1$. Hence, Eq. (1.1) is of interest in all regions in moduli space where cM_{s}, which is a compactification scale, is greater than $M_{3/2}$. When this is the case and the exponential contributions are neglected, $M_{3/2}$ runs away, except when the background satisfies a Bose/Fermi degeneracy at genus-0, $n_{\text{F}} - n_{\text{B}} = 0$, implying $M_{3/2}$ to be a flat direction (for other theories, see Refs. [33–43]). For arbitrary $n_{\text{F}} - n_{\text{B}}$, though, stability of all remaining moduli fields can be analyzed from different points of view.

In Ref. [32], the mass terms of all moduli fields in the NN and DD open-string sectors were derived by direct computation of the potential for arbitrary backgrounds of these scalars. The untwisted closed-string sector contains three types of moduli fields: Firstly, since the internal metric components do not show up in the dominant term of Eq. (1.1) (except the combination $M_{3/2}$), they parametrize flat directions up to the suppressed terms. Secondly, heterotic/type I duality was used to show that the Ramond-Ramond (RR) two-form moduli are also flat directions. Finally, the same conclusion definitely applies to the dilaton at one loop. The twisted closed-string sector contains 16 blowing-up modes of $T^4/\mathbb{Z}_2$ among which 2 to 16 are absorbed by anomalous $U(1)$'s, which become massive vector fields thanks to

a generalized Green–Schwarz mechanism. In this regard, the present work can be seen as a companion paper of Ref. [32], as it provides a derivation of the mass terms generated at one loop by the remaining moduli fields, namely those belonging to the ND+DN open-string sector. This will be done by computing two-point functions of boundary-changing vertex operators of massless scalars in the ND+DN sector, on the annulus and Möbius strip.

In Sect. 2, we review the description of the type IIB orientifold model with broken $\mathcal{N} = 2$ supersymmetry, which involves D9- and D5-branes. Alternative T-dual pictures are also introduced for describing the NN- and DD-sector moduli as positions of D3-branes in the internal space. Sect. 3 defines the string amplitudes we are interested in. Sect. 4 presents all correlators needed to calculate these amplitudes on the double-cover tori of the annulus and Möbius strip. In particular, we review the derivation of Ref. [2] of the correlation function of twist fields that create ground states in the twisted sectors of closed strings. Following the method introduced in Refs. [13–17], we extend the result to the case of "excited twist fields" *i.e.* operators appearing as higher order terms in the OPE of ordinary twist fields.

In Sect. 5 we compute the two-point functions of interest. While the formulas can be used to extract the one-loop corrections to the Kähler metric and masses of the classically massless scalars of the ND+DN sector, they turn out to be rather cumbersome and obscure. For this reason, we derive in Sect. 6 a simplified expression of the squared masses at one loop that is valid when $M_{3/2}$ is lower than all other non-vanishing mass scales present in the background, precisely in the spirit of Eq. (1.1) which holds in this regime.

In Sect. 7, we apply this result to the last two models highlighted in Ref. [32], which presented all brane configurations that are tachyon free (or potentially tachyon free) at one loop[1] and satisfy $n_{\rm F} - n_{\rm B} \geq 0$. The outcome of the two papers is that among the $\mathcal{O}(10^{11})$ non-perturbatively consistent brane configurations, there exist 2 tachyon free setups with $n_{\rm F} - n_{\rm B} = 0$, and 5 with $n_{\rm F} - n_{\rm B} > 0$. A third configuration with $n_{\rm F} - n_{\rm B} = 0$ and ND+DN-sector moduli is tachyon free at one loop, up to 2 blowing-up modes of $T^4/\mathbb{Z}_2$ for which we have not computed the quantum mass terms.

Finally, our conclusions can be found in Sect. 8, while technical points are reported in three appendices.

[1] When the suppressed terms in Eq. (1.1) can be neglected.

2 The $\mathcal{N} = 2 \to \mathcal{N} = 0$ open-string model

In this section, we review the open-string model considered in Ref. [32, 44], which realizes at tree level the spontaneous breaking of $\mathcal{N} = 2$ supersymmetry in four-dimensional Minkowski spacetime. Our goals are to fix our notations, list the massless spectrum at genus-0, and specify the moduli fields whose masses will be computed at one loop in the sections to come.

2.1 The supersymmetric parent model

At the supersymmetric level, our starting point is the type IIB orientifold model constructed in six dimensions by Bianchi and Sagnotti [3], as well as by Gimon and Polchinski [4, 5]. Compactified down to four dimensions, the full gravitational background becomes

$$\mathbb{R}^{1,3} \times T^2 \times \frac{T^4}{\mathbb{Z}_2}\,, \tag{2.1}$$

whose coordinates will be labeled by Greek, primed Latin and unprimed Latin indices

$$\begin{aligned} &\text{spacetime:} \quad X^\mu\,, \qquad \mu \in \{0,\ldots,3\}\,, \\ &\text{two-torus:} \quad X^{I'}\,, \qquad I' \in \{4,5\}\,, \\ &\text{four-torus:} \quad X^I\,, \qquad I \in \{6,\ldots,9\}\,, \end{aligned} \tag{2.2}$$

and where the $\mathbb{Z}_2$-orbifold generator is defined as

$$g: \quad (X^6, X^7, X^8, X^9) \longrightarrow (-X^6, -X^7, -X^8, -X^9)\,. \tag{2.3}$$

The background also contains orientifold planes and D-branes. First of all, there is an O9-plane and 32 D9-branes spanned along all spatial directions. Second, there is an O5-plane localized at each of the 16 fixed points of $T^4/\mathbb{Z}_2$, and 32 D5-branes transverse to $T^4/\mathbb{Z}_2$. Open strings with one end attached to a D9-brane have Neumann boundary conditions in all spacetime coordinates, while those stuck to a D5-brane have Dirichlet boundary conditions along the directions of $T^4/\mathbb{Z}_2$ (and Neumann along $\mathbb{R}^{1,3} \times T^2$).

Moduli fields:

- On the worldvolumes of the 32 D5-branes, the gauge bosons can develop vacuum expectation values (vev's) along T^2, which are Wilson lines. T-dualizing the two-torus,

the 32 D5-branes become D3-branes whose positions along $\tilde{X}^{I'}$, the coordinates along the T-dual torus $\tilde{T}^2$ of metric $\tilde{G}_{I'J'} \equiv G^{I'J'}$, are nothing but the Wilson-line moduli of the original description [45]. Because in the T-dual picture a D3-brane at $(\tilde{X}^{I'}, X^I)$ is transformed under Ω, the orientifold generator, into an "orientifold-mirror" D3-brane located at $(-\tilde{X}^{I'}, -X^I)$ [45], there are 64 fixed points in this description, all supporting one O3-plane.[2] Moreover, at genus-0, there are only 16 independent positions along $\tilde{T}^2$, which are associated with the brane/mirror brane pairs.

- The locations of the 32 D3-branes (T-dual to the D5-branes) in $T^4/\mathbb{Z}_2$ are also allowed to vary, provided this is done consistently with the symmetries generated by g and Ω. Indeed, a D3-brane sitting at $(\tilde{X}^{I'}, X^I)$ must be paired with an image brane under g at $(\tilde{X}^{I'}, -X^I)$. Moreover, both admit "mirror branes" under Ω, which are located at $(-\tilde{X}^{I'}, -X^I)$ and $(-\tilde{X}^{I'}, X^I)$. Hence, there are at most 8 independent D3-brane positions in $T^4/\mathbb{Z}_2$. Notice that this number is lowered when there are 2 modulo 4 D3-branes sitting on one of the 64 O3-planes, since such a configuration is still symmetric under g and Ω but does not allow 2 D3-branes to move in the bulk of $T^4/\mathbb{Z}_2$. In other words, 2 D3-branes have rigid positions in $T^4/\mathbb{Z}_2$.

- Applying a T-duality on the four-torus of the background (2.1), D5-branes and D9-branes are turned into each other. Therefore, all moduli fields described for the D5-branes admit counterparts for the D9-branes. In particular, the D9-brane moduli are mapped into positions of 32 D3-branes in $\tilde{T}^2 \times \tilde{T}^4/\mathbb{Z}_2$, where $\tilde{T}^4$ is the dual four-torus with metric $\tilde{G}_{IJ} \equiv G^{IJ}$ and coordinates $\tilde{X}^I$. In this alternative T-dual picture, there are again 64 O3-planes at the fixed points of the inversion $(\tilde{X}^{I'}, \tilde{X}^I) \to (-\tilde{X}^{I'}, -\tilde{X}^I)$.[3]

- In the original picture involving D5- and D9-branes, all open-string moduli described so far correspond to modes realized in the DD and NN sectors. However, open strings stretched between one D5-brane and one D9-brane can also lead to moduli fields. The present paper is devoted to the study of these moduli. To be specific, we will derive the masses they acquire at one loop, when supersymmetry is spontaneously broken and their vev's vanish. When these moduli condense, the backgrounds can be described in terms of brane recombinations or magnetized branes [46–49].

[2] In addition, the initial D9-branes become D7-branes.

[3] The initial D5-branes also become D7-branes in this alternative T-dual picture.

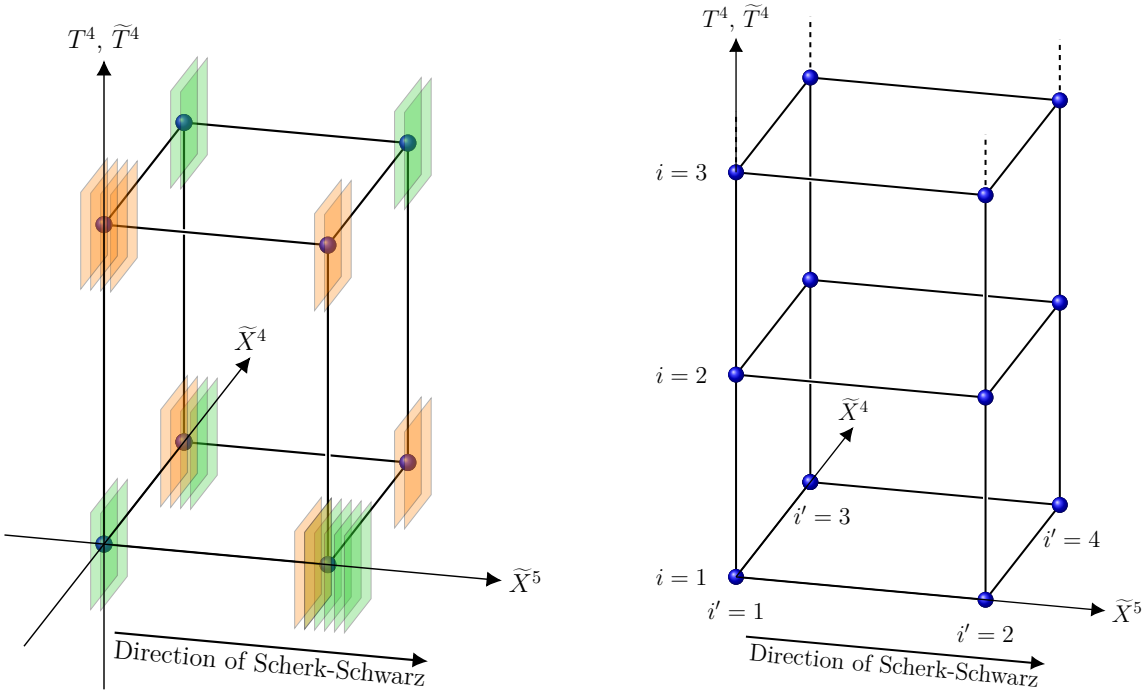

(a) Configuration of D3-branes associated with D5-branes (orange) and D9-branes (green) in T-dual pictures. In this example, all D3-branes sit on O3-planes (blue dots).

(b) Labelling of the fixed points $i' \in \{1, ..., 4\}$ along the directions of $\tilde{T}^2$, and schematic labelling of the fixed points $i \in \{1, ..., 16\}$ along the directions of T^4 or $\tilde{T}^4$. $i' = 1$ or 3 correspond to points at $\tilde{X}^5 = 0$, while $i' = 2$ or 4 correspond to points at $\tilde{X}^5 = \pi$, where $\tilde{X}^5$ is the coordinate T-dual to the direction along which the Scherk–Schwarz mechanism is implemented.

Figure 1: Description in terms of D3-brane positions of the moduli arising from the NN and DD sectors of the orientifold theory.

Geometric picture: In order to specify a particular set of vev's for the moduli arising from the DD and NN sectors, we will use a pictorial representation [32], as shown in Fig. 1a. We represent the fundamental domain of $\tilde{T}^2 \times T^4/\mathbb{Z}_2$ modded by the involution $(\tilde{X}^{I'}, X^I) \to (-\tilde{X}^{I'}, -X^I)$ by a schematic six-dimensional "box", with an O3-plane represented by a dot at each fixed point *i.e.* corner of the box. The moduli in the DD sector correspond to the positions of the 32 D3-branes (drawn in orange) T-dual to the D5-branes. Similarly, we consider a second box corresponding to the fundamental domain of $\tilde{T}^2 \times \tilde{T}^4/\mathbb{Z}_2$ modded by the involution $(\tilde{X}^{I'}, \tilde{X}^I) \to (-\tilde{X}^{I'}, -\tilde{X}^I)$, with the moduli of the NN sector given by the positions of the 32 D3-branes (drawn in green) T-dual to the D9-branes. Finally, we

superpose the two boxes, keeping in mind that the resulting picture combines information from two distinct T-dual descriptions of the same theory.

In the schematic example of Fig. 1a, all D3-branes are located on O3-planes. Indeed, it has been shown in Ref. [32] that in presence of supersymmetry breaking (to be introduced in the next subsection) these configurations are of particular interest, since they yield extrema of the one-loop effective potential with respect to the moduli arising from the NN and DD sectors (except for $M_{3/2}$ when $n_{\rm F} \neq n_{\rm B}$), up to exponentially suppressed terms (see Eq. (1.1)). Therefore, from now on, we will consider background values of the moduli in the DD and NN sectors corresponding to stacks of D3-branes all located on corners of the six-dimensional boxes. To this end, we label the 64 corners by a double index ii', where $i \in \{1, \ldots, 16\}$ refers to the fixed points of $T^4/\mathbb{Z}_2$ (or $\tilde{T}^4/\mathbb{Z}_2$), and $i' \in \{1, \ldots, 4\}$ is associated with those in the $\tilde{T}^2$ directions. Hence, the coordinates of corner ii' are captured by a two-vector $2\pi\vec{a}_{i'}$ and a four-vector $2\pi\vec{a}_i$, whose components satisfy

$$a^{I'}_{i'} \,,\; a^{I}_{i} \in \left\{0, \frac{1}{2}\right\}, \quad i' \in \{1, \ldots, 4\}\,, \quad i \in \{1, \ldots, 16\}\,. \tag{2.4}$$

Fig. 1b shows how the labelling looks like when the fixed points $i \in \{1, \ldots, 16\}$ are schematically arranged linearly along a vertical axis. In these notations, we will denote by $D_{ii'}$ and $N_{ii'}$ the numbers of D3-branes T-dual to the D5-branes and D9-branes that are located at corners ii' of the appropriate boxes.

2.2 Spontaneous supersymmetry breaking

In quantum field theory, the Scherk–Schwarz mechanism amounts to imposing fields to satisfy boundary conditions along compact directions that are compatible with global symmetries and depend on associated conserved charges [30, 31]. When charges vary between superpartners, distinct Kaluza–Klein masses arise in lower dimension and supersymmetry is spontaneously broken. The implementation of this mechanism in closed-string theory was developed in Refs. [50–54], and extended to the open-string framework in Refs. [22–29].

In the model based on the background (2.1), we make the choice to implement the Scherk–Schwarz mechanism along the periodic direction X^5 only, and to use the fermionic number F as conserved charge. In practice, $F = 0$ for the bosonic degrees of freedom and $F = 1$ for the fermionic ones. Denoting $\vec{m}'$ the two-vector whose components are the Kaluza–Klein

momenta $(m_4, m_5) \in \mathbb{Z}^2$ along T^2, the lattices of zero modes appearing in the one-loop partition function are shifted according to the rules[4]

$$\begin{aligned} &\vec{m}' + F\,\vec{a}'_{\rm S} && \text{for closed string}\,, \\ &\vec{m}' + F\,\vec{a}'_{\rm S} + \vec{a}_{i'} - \vec{a}_{j'} && \text{for open string}\,, \end{aligned} \tag{2.5}$$

where we have defined

$$\vec{a}'_{\rm S} = \left(0, \frac{1}{2}\right). \tag{2.6}$$

As a result, the two gravitino masses are

$$M_{3/2} = \frac{\sqrt{G^{55}}}{2}\, M_{\rm s}\,, \tag{2.7}$$

which is the scale of $\mathcal{N} = 2 \to \mathcal{N} = 0$ spontaneous breaking of supersymmetry. In the open-string case, the extra shift $\vec{a}_{i'} - \vec{a}_{j'}$ arises from the Wilson-line background along T^2 of the gauge fields living on the worldvolumes of the D5- and D9-branes. In the D3-brane T-dual pictures, it means that an open string is stretched between D3-branes sitting on corners ii' and jj', regardless of whether they are dual to D5- or D9-branes.[5] Because of the particular role played by the direction $\tilde{X}^5$, which is T-dual to the Scherk–Schwarz direction X^5 of the original picture, it is convenient to specify our labelling of the fixed points along the directions of $\tilde{T}^2$. We will denote by $i' = 1$ and 3 those located at $\tilde{X}^5 = 0$, and by $i' = 2$ and 4 those located at $\tilde{X}^5 = \pi$ (see Fig. 1b).

Partition function: The one-loop partition function can be divided into four contributions Z_Σ, which can be derived from path integrals on worldsheets whose topologies are those of a torus ($\mathcal{T}$), Klein bottle ($\mathcal{K}$), annulus ($\mathcal{A}$) and Möbius strip ($\mathcal{M}$). These contributions can also be expressed as supertraces over the modes belonging to the untwisted and twisted closed-string sectors, as well as over those in the NN, DD, ND and DN open-string sectors. For the closed strings, we have

$$Z_{\mathcal{T}} = \frac{1}{\tau_2^2}\,\mathrm{Str}\,\frac{1}{2}\,\frac{1+g}{2}\,q^{L_0-\frac{1}{2}}\,\bar{q}^{\tilde{L}_0-\frac{1}{2}}\,, \quad Z_{\mathcal{K}} = \frac{1}{\tau_2^2}\,\mathrm{Str}\,\frac{\Omega}{2}\,\frac{1+g}{2}\,q^{L_0-\frac{1}{2}}\,\bar{q}^{\tilde{L}_0-\frac{1}{2}}\,, \quad q = e^{2i\pi\tau}\,, \tag{2.8}$$

[4] In the closed-string sector, this is the only modification in the untwisted sector of the extra generator that implements the Scherk–Schwarz breaking in orbifold language.

[5] For the ND and DN sectors, our description in terms of "stretched strings" is somewhat abusive since the corners ii' and jj' are to be understood in distinct T-dual descriptions.

where τ is the Teichmüller parameter of the worldsheet torus with real and imaginary parts denoted τ_1 and $\tau_2 > 0$, while for the open strings we have

$$Z_{\mathcal{A}} = \frac{1}{\tau_2^2}\,\mathrm{Str}\,\frac{1}{2}\,\frac{1+g}{2}\,q^{\frac{1}{2}(L_0-1)}\,, \qquad Z_{\mathcal{M}} = \frac{1}{\tau_2^2}\,\mathrm{Str}\,\frac{\Omega}{2}\,\frac{1+g}{2}\,q^{\frac{1}{2}(L_0-1)}\,, \qquad q = e^{-2\pi\tau_2}\,. \tag{2.9}$$

In these formulas, L_0, $\tilde{L}_0$ are the zero-frequency Virasoro operators.

In order to give explicit expressions of $Z_{\mathcal{A}}$ and $Z_{\mathcal{M}}$, we first define four-vectors $\vec{m}$ and $\vec{n}$ whose components are the Kaluza–Klein momenta $m_I \in \mathbb{Z}$ and winding numbers $n_I \in \mathbb{Z}$ along the directions of T^4. The lattices of zero modes (to be shifted by Wilson lines) of the bosonic coordinates are then given by

$$\begin{aligned} \sum_{\vec{m}} P^{(4)}_{\vec{m}}(i\tau_2) &= \sum_{\vec{m}} e^{-\pi\tau_2 m_I G^{IJ} m_J} && \text{for the NN sector}\,, \\ \sum_{\vec{n}} W^{(4)}_{\vec{n}}(i\tau_2) &= \sum_{\vec{n}} e^{-\pi\tau_2 n_I G_{IJ} n_J} && \text{for the DD sector}\,, \\ 1 & && \text{for the ND and DN sectors}\,, \end{aligned} \tag{2.10}$$

while the lattice of momenta along T^2 is

$$\sum_{\vec{m}'} P^{(2)}_{\vec{m}'}(i\tau_2) = \sum_{\vec{m}'} e^{-\pi\tau_2 m_{I'} G^{I'J'} m_{J'}} \tag{2.11}$$

in all open-string sectors.

In the annulus contribution to the partition function, the actions of the neutral group element 1 and generator g on the Chan–Paton indices can be represented by matrices acting on each Neumann or Dirichlet sector ii' [4, 5],

$$\begin{aligned} \gamma^{ii'}_{\mathrm{N},1} &= I_{N_{ii'}}\,, & \gamma^{ii'}_{\mathrm{N},g} &= J_{N_{ii'}}\,, \\ \gamma^{ii'}_{\mathrm{D},1} &= I_{D_{ii'}}\,, & \gamma^{ii'}_{\mathrm{D},g} &= J_{D_{ii'}}\,, \end{aligned} \tag{2.12}$$

where I_k is the $k \times k$ identity matrix while for k even

$$J_k = \begin{pmatrix} 0 & I_{\frac{k}{2}} \\ -I_{\frac{k}{2}} & 0 \end{pmatrix}. \tag{2.13}$$

Actually, the precise dictionary between the above matrices and those defined in Refs. [4, 5] can be found in Appendix A. To be specific, by labelling the branes with Greek indices, the actions of $G = 1$ or g are represented in the NN sector as follows:

$$\forall\alpha \in \{1,\ldots,N_{ii'}\}\,, \forall\beta \in \{1,\ldots,N_{jj'}\}\,, \quad |\alpha\beta\rangle \to \sum_{\alpha'=1}^{N_{ii'}} \sum_{\beta'=1}^{N_{jj'}} (\gamma^{ii'}_{\mathrm{N},G})_{\alpha\alpha'} |\alpha'\beta'\rangle (\gamma^{jj'\,-1}_{\mathrm{N},G})_{\beta'\beta}\,. \tag{2.14}$$

Similar expressions apply to the DD sector for $G = 1$, g, as well as to the ND and DN sectors for $G = 1$. There exists only one subtlety in the ND and DN sectors for $G = g$, where one has to multiply all Neumann matrices by signs in the transformation rules,

$$\gamma^{ii'}_{\mathrm{N},g} \quad \longrightarrow \quad e^{4i\pi\vec{a}_i\cdot\vec{a}_j}\gamma^{ii'}_{\mathrm{N},g}\,, \tag{2.15}$$

where the index j refers to the fixed point of $T^4/\mathbb{Z}_2$ where the stack of D5-branes sits. This is explained in Ref. [5] and translated into the notations of our paper in Appendix A. Moreover, the worldsheet fermions associated with the directions $X^2, \ldots, X^5$ on the one-hand, and those associated with the directions $X^6, \ldots, X^9$ on the other hand, yield contributions expressed as characters of the $SO(4)$ affine algebra. The latter are associated with a singlet (O), vectorial (V) and two spinorial (S and C) conjugacy classes [55–57]. For the annulus partition function, these characters denoted O_4, V_4, S_4, C_4 are defined in Eq. (B.4) and evaluated at argument $i\tau_2/2$. Altogether, one obtains

$$\begin{aligned}
Z_{\mathcal{A}} = \frac{1}{4}\,\frac{1}{\tau_2^2}\sum_{\substack{i,i'\\ j,j'}}
&\Bigg\{\Bigg[(V_4O_4+O_4V_4)\Bigg(\mathrm{tr}(\gamma^{ii'}_{\mathrm{N},1})\mathrm{tr}(\gamma^{jj'\,-1}_{\mathrm{N},1})\sum_{\vec{m}}\frac{P^{(4)}_{\vec{m}+\vec{a}_i-\vec{a}_j}}{\eta^4}+\mathrm{tr}(\gamma^{ii'}_{\mathrm{D},1})\mathrm{tr}(\gamma^{jj'\,-1}_{\mathrm{D},1})\sum_{\vec{n}}\frac{W^{(4)}_{\vec{n}+\vec{a}_i-\vec{a}_j}}{\eta^4}\Bigg)\\
&-(V_4O_4-O_4V_4)\,\delta_{ij}\Big(\mathrm{tr}(\gamma^{ii'}_{\mathrm{N},g})\mathrm{tr}(\gamma^{jj'\,-1}_{\mathrm{N},g})+\mathrm{tr}(\gamma^{ii'}_{\mathrm{D},g})\mathrm{tr}(\gamma^{jj'\,-1}_{\mathrm{D},g})\Big)\left(\frac{2\eta}{\vartheta_2}\right)^2\\
&+(O_4C_4+V_4S_4)\Big(\mathrm{tr}(\gamma^{ii'}_{\mathrm{N},1})\mathrm{tr}(\gamma^{jj'\,-1}_{\mathrm{D},1})+\mathrm{tr}(\gamma^{ii'}_{\mathrm{D},1})\mathrm{tr}(\gamma^{jj'\,-1}_{\mathrm{N},1})\Big)\left(\frac{\eta}{\vartheta_4}\right)^2\\
&-(O_4C_4-V_4S_4)\,e^{4i\pi\vec{a}_i\cdot\vec{a}_j}\Big(\mathrm{tr}(\gamma^{ii'}_{\mathrm{N},g})\mathrm{tr}(\gamma^{jj'\,-1}_{\mathrm{D},g})+\mathrm{tr}(\gamma^{ii'}_{\mathrm{D},g})\mathrm{tr}(\gamma^{jj'\,-1}_{\mathrm{N},g})\Big)\left(\frac{\eta}{\vartheta_3}\right)^2\Bigg]\sum_{\vec{m}'}\frac{P^{(2)}_{\vec{m}'+\vec{a}_{i'}-\vec{a}_{j'}}}{\eta^4}\\
&-\Bigg[(S_4S_4+C_4C_4)\Bigg(\mathrm{tr}(\gamma^{ii'}_{\mathrm{N},1})\mathrm{tr}(\gamma^{jj'\,-1}_{\mathrm{N},1})\sum_{\vec{m}}\frac{P^{(4)}_{\vec{m}+\vec{a}_i-\vec{a}_j}}{\eta^4}+\mathrm{tr}(\gamma^{ii'}_{\mathrm{D},1})\mathrm{tr}(\gamma^{jj'\,-1}_{\mathrm{D},1})\sum_{\vec{n}}\frac{W^{(4)}_{\vec{n}+\vec{a}_i-\vec{a}_j}}{\eta^4}\Bigg)\\
&-(C_4C_4-S_4S_4)\,\delta_{ij}\Big(\mathrm{tr}(\gamma^{ii'}_{\mathrm{N},g})\mathrm{tr}(\gamma^{jj'\,-1}_{\mathrm{N},g})+\mathrm{tr}(\gamma^{ii'}_{\mathrm{D},g})\mathrm{tr}(\gamma^{jj'\,-1}_{\mathrm{D},g})\Big)\left(\frac{2\eta}{\vartheta_2}\right)^2\\
&+(S_4O_4+C_4V_4)\Big(\mathrm{tr}(\gamma^{ii'}_{\mathrm{N},1})\mathrm{tr}(\gamma^{jj'\,-1}_{\mathrm{D},1})+\mathrm{tr}(\gamma^{ii'}_{\mathrm{D},1})\mathrm{tr}(\gamma^{jj'\,-1}_{\mathrm{N},1})\Big)\left(\frac{\eta}{\vartheta_4}\right)^2\\
&-(S_4O_4-C_4V_4)\,e^{4i\pi\vec{a}_i\cdot\vec{a}_j}\Big(\mathrm{tr}(\gamma^{ii'}_{\mathrm{N},g})\mathrm{tr}(\gamma^{jj'\,-1}_{\mathrm{D},g})+\mathrm{tr}(\gamma^{ii'}_{\mathrm{D},g})\mathrm{tr}(\gamma^{jj'\,-1}_{\mathrm{N},g})\Big)\left(\frac{\eta}{\vartheta_3}\right)^2\Bigg]\sum_{\vec{m}'}\frac{P^{(2)}_{\vec{m}'+\vec{a}'_{\mathrm{S}}+\vec{a}_{i'}-\vec{a}_{j'}}}{\eta^4}\Bigg\}\,.
\end{aligned} \tag{2.16}$$

In the the Möbius-strip contribution to the partition function, the actions of Ω and Ωg on the Chan–Paton indices can be represented by matrices associated with each Neumann

or Dirichlet sector ii',

$$\begin{aligned} \gamma^{ii'}_{\mathrm{N},\Omega} &= I_{N_{ii'}}\,, \qquad & \gamma^{ii'}_{\mathrm{N},\Omega g} &= J_{N_{ii'}}\,, \\ \gamma^{ii'}_{\mathrm{D},\Omega g} &= I_{D_{ii'}}\,, \qquad & \gamma^{ii'}_{\mathrm{D},\Omega} &= J_{D_{ii'}}\,. \end{aligned} \tag{2.17}$$

Notice the inverted roles of Ω and Ωg in the Neumann and Dirichlet sectors. The precise actions of ΩG for $G = 1$ or g on the NN sector are [4]

$$\forall\alpha \in \{1,\dots,N_{ii'}\}\,, \forall\beta \in \{1,\dots,N_{jj'}\}\,, \quad |\alpha\beta\rangle \to \sum_{\alpha'=1}^{N_{ii'}} \sum_{\beta'=1}^{N_{jj'}} (\gamma^{ii'}_{\mathrm{N},\Omega G})_{\alpha\alpha'} |\beta'\alpha'\rangle (\gamma^{jj'\,-1}_{\mathrm{N},\Omega G})_{\beta'\beta}\,, \tag{2.18}$$

and similarly for the DD sector. As compared to Eq. (2.14), note the reversal $\alpha'\beta' \to \beta'\alpha'$ in the transformation rule. As a result, the ND and DN sectors automatically yield vanishing contributions in the defining trace of $Z_{\mathcal{M}}$. Moreover, all characters denoted generically as $\hat{\chi}$ appearing in the Möbius strip partition function can be defined in terms of their counterparts χ in the annulus amplitude by the relation [58, 59]

$$\hat{\chi}\Big(\frac{1}{2} + i\frac{\tau_2}{2}\Big) = e^{-i\pi(h-\frac{c}{24})}\,\chi\Big(\frac{1}{2} + i\frac{\tau_2}{2}\Big)\,, \tag{2.19}$$

where h is the weight of the associated primary state and c the central charge of the Verma module. With these notations, one obtains

$$\begin{aligned} Z_{\mathcal{M}} = &-\frac{1}{4}\sum_{i,i'}\Bigg\{\Bigg[(\hat{V}_4\hat{O}_4 + \hat{O}_4\hat{V}_4)\Big(\mathrm{tr}(\gamma^{ii'\,\mathrm{T}}_{\mathrm{N},\Omega}\gamma^{ii'\,-1}_{\mathrm{N},\Omega})\sum_{\vec{m}}\frac{P^{(4)}_{\vec{m}}}{\hat{\eta}^4} + \mathrm{tr}(\gamma^{ii'\,\mathrm{T}}_{\mathrm{D},\Omega g}\gamma^{ii'\,-1}_{\mathrm{D},\Omega g})\sum_{\vec{n}}\frac{W^{(4)}_{\vec{n}}}{\hat{\eta}^4}\Big) \\ &- (\hat{V}_4\hat{O}_4 - \hat{O}_4\hat{V}_4)\Big(\mathrm{tr}(\gamma^{ii'\,\mathrm{T}}_{\mathrm{N},\Omega g}\gamma^{ii'\,-1}_{\mathrm{N},\Omega g}) + \mathrm{tr}(\gamma^{ii'\,\mathrm{T}}_{\mathrm{D},\Omega}\gamma^{ii'\,-1}_{\mathrm{D},\Omega})\Big)\left(\frac{2\hat{\eta}}{\hat{\vartheta}_2}\right)^2\Bigg]\sum_{\vec{m}'}\frac{P^{(2)}_{\vec{m}'}}{\hat{\eta}^4} \\ &-\Bigg[(\hat{C}_4\hat{C}_4 + \hat{S}_4\hat{S}_4)\Big(\mathrm{tr}(\gamma^{ii'\,\mathrm{T}}_{\mathrm{N},\Omega}\gamma^{ii'\,-1}_{\mathrm{N},\Omega})\sum_{\vec{m}}\frac{P^{(4)}_{\vec{m}}}{\hat{\eta}^4} + \mathrm{tr}(\gamma^{ii'\,\mathrm{T}}_{\mathrm{D},\Omega g}\gamma^{ii'\,-1}_{\mathrm{D},\Omega g})\sum_{\vec{n}}\frac{W^{(4)}_{\vec{n}}}{\hat{\eta}^4}\Big) \\ &- (\hat{C}_4\hat{C}_4 - \hat{S}_4\hat{S}_4)\Big(\mathrm{tr}(\gamma^{ii'\,\mathrm{T}}_{\mathrm{N},\Omega g}\gamma^{ii'\,-1}_{\mathrm{N},\Omega g}) + \mathrm{tr}(\gamma^{ii'\,\mathrm{T}}_{\mathrm{D},\Omega}\gamma^{ii'\,-1}_{\mathrm{D},\Omega})\Big)\left(\frac{2\hat{\eta}}{\hat{\vartheta}_2}\right)^2\Bigg]\sum_{\vec{m}'}\frac{P^{(2)}_{\vec{m}'+\vec{a}'_{\mathrm{S}}}}{\hat{\eta}^4}\Bigg\}\,, \end{aligned} \tag{2.20}$$

where the arguments of all hatted characters are $(1 + i\tau_2)/2$, and the superscript T stands for the transposition of the matrix to which it applies.

For completeness, the closed-string sector contributions to the partition function $Z_{\mathcal{T}}$ and $Z_{\mathcal{K}}$ are displayed in Appendix B.

Spectrum: The classical massless spectrum can be read from the partition function. To this end, it is useful to evaluate the traces over the Chan–Paton indices in the open string

sector, which yields

$$\begin{aligned}
N_{ii'} \equiv n_{ii'} + \bar{n}_{ii'} \qquad &= \mathrm{tr}\gamma_{\mathrm{N},1}^{ii'} = \mathrm{tr}\gamma_{\mathrm{N},1}^{ii'\,-1} = \mathrm{tr}(\gamma_{\mathrm{N},\Omega}^{ii'\,T}\gamma_{\mathrm{N},\Omega}^{ii'\,-1}) = \mathrm{tr}(\gamma_{\mathrm{N},\Omega g}^{ii'\,T}\gamma_{\mathrm{N},\Omega g}^{ii'\,-1})\,, \\
0 \equiv i(n_{ii'} - \bar{n}_{ii'}) \quad &= \mathrm{tr}\gamma_{\mathrm{N},g}^{ii'} = -\mathrm{tr}\gamma_{\mathrm{N},g}^{ii'\,-1}\,, \\
D_{ii'} \equiv d_{ii'} + \bar{d}_{ii'} \qquad &= \mathrm{tr}\gamma_{\mathrm{D},1}^{ii'} = \mathrm{tr}\gamma_{\mathrm{D},1}^{ii'\,-1} = \mathrm{tr}(\gamma_{\mathrm{D},\Omega g}^{ii'\,T}\gamma_{\mathrm{D},\Omega g}^{ii'\,-1}) = \mathrm{tr}(\gamma_{\mathrm{D},\Omega}^{ii'\,T}\gamma_{\mathrm{D},\Omega}^{ii'\,-1})\,, \\
0 \equiv i(d_{ii'} - \bar{d}_{ii'}) \quad &= \mathrm{tr}\gamma_{\mathrm{D},g}^{ii'} = -\mathrm{tr}\gamma_{\mathrm{D},g}^{ii'\,-1}\,,
\end{aligned} \tag{2.21}$$

where we use the fact that the matrix J_k for k even has equal number of eigenvalues i and $-i$.

From $Z_{\mathcal{A}} + Z_{\mathcal{M}}$, one finds that the massless bosonic degrees of freedom are the low-lying modes of the combinations of characters

$$\begin{aligned}
&\frac{1}{\eta^8}\sum_{i,i'}\Bigg\{V_4O_4\left[n_{ii'}\bar{n}_{ii'} + d_{ii'}\bar{d}_{ii'}\right] \\
&+ O_4V_4\left[\frac{n_{ii'}(n_{ii'}-1)}{2} + \frac{\bar{n}_{ii'}(\bar{n}_{ii'}-1)}{2} + \frac{d_{ii'}(d_{ii'}-1)}{2} + \frac{\bar{d}_{ii'}(\bar{d}_{ii'}-1)}{2}\right] \\
&+ O_4C_4\sum_j\left[\frac{1-e^{4i\pi\vec{a}_i\cdot\vec{a}_j}}{2}\left(n_{ii'}d_{ji'} + \bar{n}_{ii'}\bar{d}_{ji'}\right) + \frac{1+e^{4i\pi\vec{a}_i\cdot\vec{a}_j}}{2}\left(n_{ii'}\bar{d}_{ji'} + \bar{n}_{ii'}d_{ji'}\right)\right]\Bigg\}.
\end{aligned} \tag{2.22}$$

In the products of $SO(4)$ characters, the first is telling us whether the states belong to vectorial or singlet representations of the six-dimensional Lorentz group. Hence, the first line corresponds to the bosonic parts of an $\mathcal{N} = 2$ vector multiplet in the adjoint representation of the open-string gauge group

$$\prod_{ii'/n_{ii'}\neq 0} U(n_{ii'}) \quad \times \prod_{jj'/d_{jj'}\neq 0} U(d_{jj'})\,, \quad \text{where} \quad \sum_{ii'} n_{ii'} = \sum_{ii'} d_{ii'} = 16\,, \tag{2.23}$$

while the second line corresponds to the bosonic parts of one hypermultiplet in the antisymmetric $\oplus$ $\overline{\text{antisymmetric}}$ representation of each unitary factor. All of these states, which arise in the NN and DD sectors, are visualized in Fig. 2a as strings drawn in green (NN) or orange (DD) solid lines with both ends attached to the same stacks of D3-branes. On the contrary, the third line in (2.22), which is associated with the ND + DN sector, corresponds to the bosonic part of one hypermultiplet in the fundamental $\otimes$ fundamental representation of each $U(n_{ii'}) \times U(d_{ji'})$ if $e^{4i\pi\vec{a}_i\cdot\vec{a}_j} = -1$, and in the fundamental $\otimes$ $\overline{\text{fundamental}}$ of this group product if $e^{4i\pi\vec{a}_i\cdot\vec{a}_j} = 1$.[6] They are depicted in Fig. 2b as khaki strings drawn in solid lines stretched between corners ii' and ji', *i.e.* fixed points with identical positions in $\tilde{T}^2$. As

[6]Each product of characters O_4C_4 yields 2 massless degrees of freedom which can be combined into complex scalars.

already mentioned in Footnote 5, even if convenient, the visualization in terms of stretched strings is abusive in this case since corners ii' and ji' are understood in distinct T-dual descriptions. Notice that the moduli whose masses we want to calculate in the present work are among these scalars.

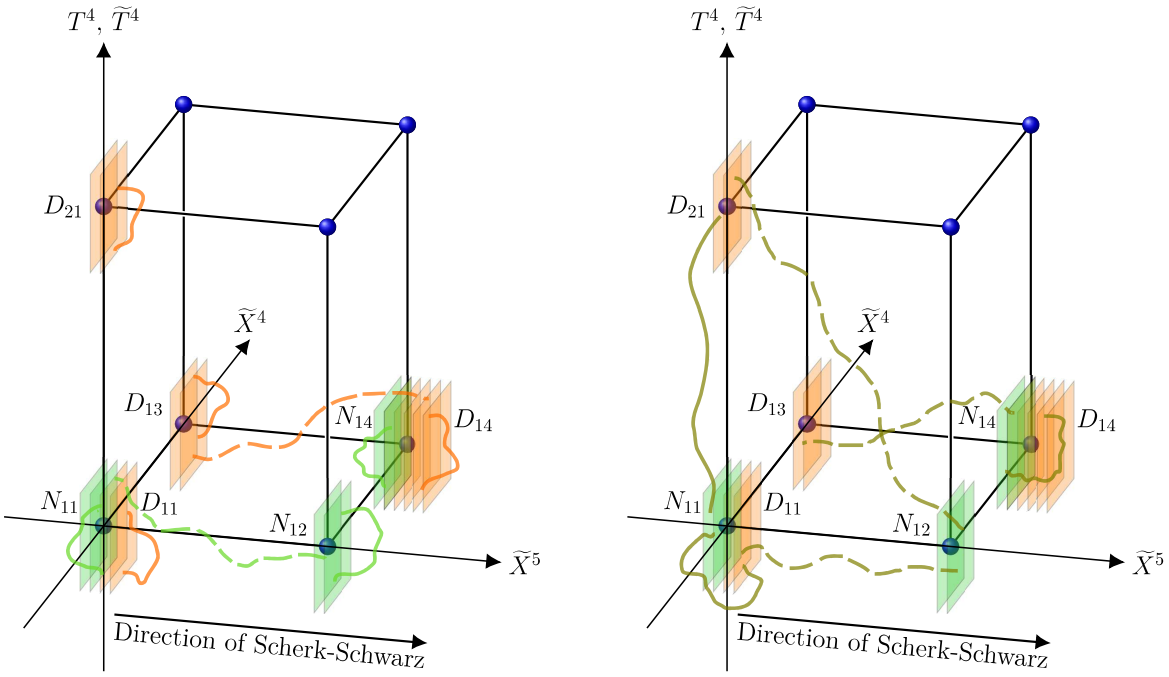

(a) Bosonic states in the NN and DD sectors are massless when their ends are attached to the same stack of branes. By contrast, fermionic states in the NN and DD sectors are massless when they are realized as strings stretched between corners of the six-dimensional boxes that are facing each other along the T-dual Scherk–Schwarz direction.

(b) Massless bosonic states in the ND+DN sector are symbolized as strings attached to stacks of D3-branes T-dual to D9-branes and D5-branes that are located at corners having the same coordinates $\tilde{X}^4$ and $\tilde{X}^5$. For the massless fermionic states in the ND+DN sector, the corners have same coordinate $\tilde{X}^4$ and distinct coordinate $\tilde{X}^5$.

Figure 2: Visualization of the massless open-string states in the D3-brane pictures. The scalars are depicted as solid lines and the fermions as dashed lines.

To proceed the same way for the fermions, it is convenient to define a new double-primed index $i'' \in \{1, 2\}$ and write $i' = 2i''$ or $2i'' - 1$. The massless fermionic degrees of freedom extracted from $Z_{\mathcal{A}}+Z_{\mathcal{M}}$ are then identified as the low-lying modes of the following characters,

$$
\begin{aligned}
&\frac{1}{\eta^8}\sum_{i,i''}\Big\{C_4C_4\left[n_{i,2i''-1}\bar{n}_{i,2i''}+\bar{n}_{i,2i''-1}n_{i,2i''}+d_{i,2i''-1}\bar{d}_{i,2i''}+\bar{d}_{i,2i''-1}d_{i,2i''}\right]\\
&+S_4S_4\left[n_{i,2i''-1}n_{i,2i''}+\bar{n}_{i,2i''-1}\bar{n}_{i,2i''}+d_{i,2i''-1}d_{i,2i''}+\bar{d}_{i,2i''-1}\bar{d}_{i,2i''}\right]\\
&+S_4O_4\sum_j\left[\frac{1-e^{4i\pi\vec{a}_i\cdot\vec{a}_j}}{2}\left(n_{i,2i''-1}d_{j,2i''}+\bar{n}_{i,2i''-1}\bar{d}_{j,2i''}+n_{i,2i''}d_{j,2i''-1}+\bar{n}_{i,2i''}\bar{d}_{j,2i''-1}\right)\right.\\
&\qquad\left.+\frac{1+e^{4i\pi\vec{a}_i\cdot\vec{a}_j}}{2}\left(n_{i,2i''-1}\bar{d}_{j,2i''}+\bar{n}_{i,2i''-1}d_{j,2i''}+n_{i,2i''}\bar{d}_{j,2i''-1}+\bar{n}_{i,2i''}d_{j,2i''-1}\right)\right]\Big\}.
\end{aligned}
\tag{2.24}
$$

They all correspond to fermionic parts of hypermultiplets in fundamental $\otimes$ fundamental or fundamental $\otimes$ $\overline{\text{fundamental}}$ representations of pairs of unitary groups supported by stacks of D3-branes (in the T-dual pictures) located at corners with distinct coordinates along the Scherk–Schwarz direction $\tilde{X}^5$ (and possibly distinct positions in $T^4/\mathbb{Z}_2$ or $\tilde{T}^4/\mathbb{Z}_2$ in the ND+DN sector). They appear as strings drawn in dashed lines in Fig. 2: Green and orange for the NN and DD sectors in Fig. 2a, and khaki for the ND+DN sector in Fig. 2b. Actually, massless fermions are realized as string stretched along the $\tilde{X}^5$ direction, translating the fact that the shifts of m_5' arising from the Wilson lines and the Scherk–Schwarz mechanism compensate each other (see Eq. (2.5)).

Because the closed-string spectrum is neutral with respect to the gauge group generated by the open strings, it is independent of the deformations $\vec{a}_i$ and $\vec{a}_{i'}$. As a result, all fermions initially massless in the parent supersymmetric model of Sect. 2.1 acquire tree-level masses equal to $M_{3/2}$ thanks to the Scherk–Schwarz mechanism. At the massless level, we are left with bosons, which are easily listed from a six-dimensional point of view. The untwisted sector contains the components $(G+C)_{\hat{\mu}\hat{\nu}}$, $\hat{\mu},\hat{\nu}\in\{2,\ldots,5\}$, and the internal components $(G+C)_{IJ}$, which yield $(6-2)\times(6-2)+4\times4$ degrees of freedom. Moreover, there are 4×16 real scalars arising from the twisted hypermultiplets.

3 Two-point functions of massless ND and DN states

In Ref. [32] the masses at one loop of the open-string moduli arising from the NN and DD sectors were derived by using the background field method. However, in the case of the moduli in the ND+DN sector, the partition function for arbitrary vev's of these scalars is not known and this approach cannot be applied. Therefore, we will derive in Sects. 5 and 6

the one-loop masses of all classically massless scalars in the bifundamental representations of unitary groups supported by D9- and D5-branes by computing two-point correlation functions with external states in the massless ND and DN bosonic sectors. This will be done by applying techniques first introduced in classical open-string theories in Refs. [9–11], and at one loop in Refs. [13–17]. For now, we define the relevant vertex operators and open-string amplitudes.

3.1 Vertex operators and amplitudes

In the T-dual pictures, let us consider two corners $i_0 i'_0$ and $j_0 i'_0$ on which are located $N_{i_0 i'_0} \geq 2$ and $D_{j_0 i'_0} \geq 2$ D3-branes T-dual to D9-branes and D5-branes, respectively. As seen in the third line of Eq. (2.22), the open strings "stretched" between these stacks give rise to $2n_{i_0 i'_0} d_{j_0 j'_0}$ massless complex scalars (depicted as solid strings in Fig. 2b). In the initial description in terms of D9- and D5-branes, we are interested in correlation functions of vertex operators in ghost pictures p and $-p$ of the form

$$\sum_{\alpha_0=1}^{N_{i_0 i'_0}} \sum_{\beta_0=1}^{D_{j_0 i'_0}} \left\langle V_p^{\alpha_0\beta_0}(z_1, k, \epsilon) V_{-p}^{\beta_0\alpha_0}(z_2, -k, -\epsilon) \right\rangle^{\Sigma} , \tag{3.1}$$

where z_1, z_2 are insertion points on the boundary of a worldsheet whose topology is either that of the annulus or Möbius strip, $\Sigma \in \{\mathcal{A}, \mathcal{M}\}$, and

$$\begin{aligned} V_{-1}^{\alpha_0\beta_0}(z_1, k, \epsilon) &= \lambda_{\alpha_0\beta_0}\, e^{-\phi}\, e^{ik\cdot X}\, e^{\epsilon \frac{i}{2}(H_3 - H_4)}\, \sigma^3\sigma^4(z_1)\,, \\ V_{-1}^{\beta_0\alpha_0}(z_2, -k, -\epsilon) &= \lambda^{\mathrm{T}}_{\beta_0\alpha_0}\, e^{-\phi}\, e^{-ik\cdot X}\, e^{-\epsilon \frac{i}{2}(H_3 - H_4)}\, \sigma^3\sigma^4(z_2)\,. \end{aligned} \tag{3.2}$$

In the above definitions, we use the following notations:

- k^μ is the external momentum satisfying on-shell the condition $k^\mu k_\mu = 0$.
- $\phi(z)$ is the ghost field encountered in the bosonization of the superconformal ghosts [60].
- λ is the matrix

  $$\lambda = \begin{pmatrix} \Lambda_1 & \Lambda_2 \\ -\Lambda_2 & \Lambda_1 \end{pmatrix}, \tag{3.3}$$

  where Λ_1, Λ_2 are arbitrary $n_{i_0 i'_0} \times d_{j_0 i'_0}$ real matrices [4]. It labels the states that transform as the $(\boldsymbol{n_{i_0 i'_0}}, \boldsymbol{d_{j_0 i'_0}}) \oplus (\boldsymbol{\bar{n}_{i_0 i'_0}}, \boldsymbol{\bar{d}_{j_0 i'_0}})$ or $(\boldsymbol{n_{i_0 i'_0}}, \boldsymbol{\bar{d}_{j_0 i'_0}}) \oplus (\boldsymbol{\bar{n}_{i_0 i'_0}}, \boldsymbol{d_{j_0 i'_0}})$ bifundamental representation of $U(n_{i_0 i'_0}) \times U(d_{j_0 i'_0})$.

- From now until Sect. 6, we restrict our analysis to the case where the internal metric is diagonal,
$$G_{I'J'} \equiv \delta_{I'J'}\,\frac{R_{I'}^2}{\alpha'}\,, \qquad G_{IJ} \equiv \delta_{IJ}\,\frac{R_I^2}{\alpha'}\,, \tag{3.4}$$
for some radii $R_{I'}$, R_I. In this case, the formalism of Ref. [2] applies without having to generalize it. Denoting $\psi^\mu(z)$, $\psi^{I'}(z)$, $\psi^I(z)$ the Grassmann fields superpartners of the bosonic-coordinate fields $X^\mu(z)$, $X^{I'}(z)$, $X^I(z)$, we define a new basis of degrees of freedom
$$\begin{aligned} Z^u &\equiv \frac{X^{2u} + iX^{2u+1}}{\sqrt{2}}\,, & \overline{Z}^u &\equiv \frac{X^{2u} - iX^{2u+1}}{\sqrt{2}}\,, \\ \Psi^u &\equiv \frac{\psi^{2u} + i\psi^{2u+1}}{\sqrt{2}} \equiv e^{iH_u}\,, & \overline{\Psi}^u &\equiv \frac{\psi^{2u} - i\psi^{2u+1}}{\sqrt{2}} \equiv e^{-iH_u}\,, \quad u \in \{0,\dots,4\}\,, \end{aligned} \tag{3.5}$$
where H_u are scalars introduced to bosonize the fermionic fields.[7]

- The characters O_4C_4 tell us that the scalars we are interested in are organized as singlet from a six-dimensional point of view, and spinors of the $T^4/\mathbb{Z}_2$ orbifold space. The operators $e^{\pm\epsilon i(H_3-H_4)}$ are therefore spin fields, which means that the coefficients of H_3, H_4 in the exponentials are the weights of the dimension-two spinorial representation of negative chirality of $SO(4)$, which are $\epsilon(\frac{1}{2},-\frac{1}{2})$, $\epsilon \in \{-1,+1\}$.[8]

- σ^u, $u \in \{3,4\}$, are so-called "boundary-changing fields" associated with the complex directions Z^u [6].

To understand the meaning and necessity of introducing operators σ^u, the open-string diagrams we want to compute are displayed in Fig. 3 for some given $\alpha_0 \in \{1,\dots,N_{i_0 i'_0}\}$ and $\beta_0 \in \{1,\dots,D_{j_0 i'_0}\}$. The left panel shows two annuli and one Möbius strip amplitudes. Because the external legs bring quantum numbers $(\lambda_{\alpha_0\beta_0},\epsilon)$ and $(\lambda^{\mathrm{T}}_{\beta_0\alpha_0},-\epsilon)$ of the ND and DN sectors, they must be attached to the *same* boundary of the annulus. Therefore, the second boundary is sticked to another brane labelled γ, which can be any of the 32 D9-branes (in green) or 32 D5-branes (in orange). On the center and right panels, the same three diagrams are displayed, with the open-string worldsheets seen as fundamental domains of the involution
$$z \longrightarrow \mathcal{I}(z) \equiv 1 - \bar{z} \tag{3.6}$$

[7] These definitions apply to a Euclidean spacetime. In the Lorentzian case, replace $(X^0,\psi^0) \to i(X^0,\psi^0)$.

[8] Characters O_4S_4 would yield states in the spinorial representation of positive chirality of $SO(4)$, whose weights are $\epsilon(\frac{1}{2},\frac{1}{2})$.

acting on double-cover tori of Teichmüller parameters [7, 8, 58, 61]

$$\tau^{\rm dc} = i\frac{\tau_2}{2} \quad \text{for the annulus} \qquad \text{and} \qquad \tau^{\rm dc} = \frac{1}{2} + i\frac{\tau_2}{2} \quad \text{for the Möbius strip}\,. \tag{3.7}$$

In this description, the external legs are conformally mapped to points z_1, z_2, where vertex operators change the boundary conditions of the worldsheet fields $X^I(z)$ (*i.e.* $Z^3(z)$, $Z^4(z)$)

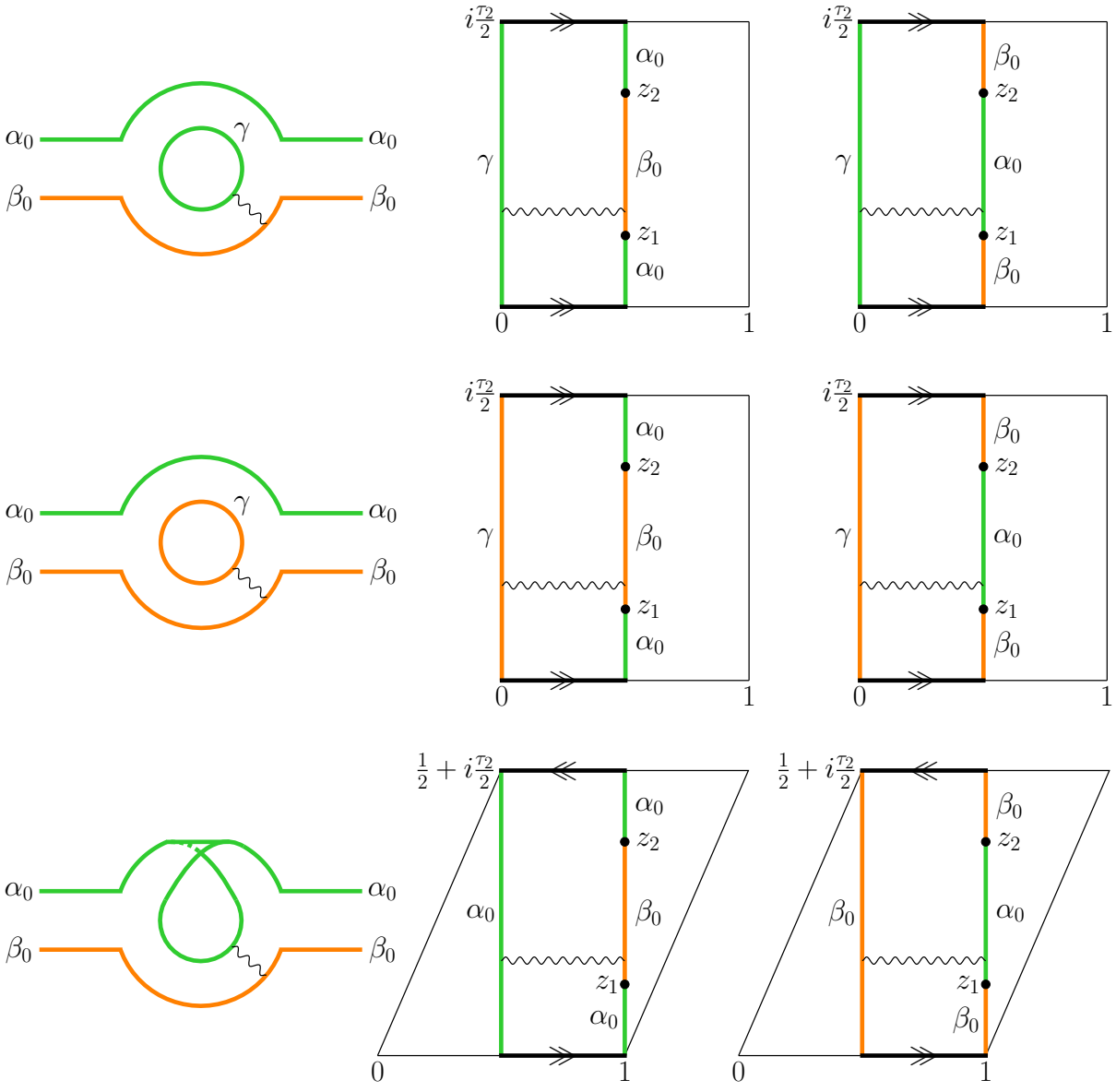

Figure 3: Open-string diagrams with two external legs in the ND and DN sectors (left panel). On the double-cover tori (center and right panels), the external legs are mapped to boundary-changing vertex operators at z_1, z_2. One switches from center to right panel by transporting z_2 along the entire edge it belongs to.

at one end of the intermediate open string running in the loop, from Neumann to Dirichlet or *vice versa*. The diagrams in the center and right panels are obtained from one another by transporting continuously z_2 along its entire boundary: $z_2 \to z_2 + i\,\mathrm{Im}\,\tau^{\mathrm{dc}}$ for the annulus and $z_2 \to z_2 + 2i\,\mathrm{Im}\,\tau^{\mathrm{dc}}$ for the Möbius strip, modulo 1 and τ^{dc}.

To conclude this subsection, notice that for consistency of the diagrams, the numbers of boundary-changing vertex operators must be even on each connected component of an open-string surface. Hence, all one-point functions *i.e.* tadpoles of states in the ND or DN sectors vanish, which shows that the backgrounds we consider, *i.e.* where no brane recombination is taking place [46–49], imply the effective potential to be extremal with respect to the scalars in the ND+DN sector.

3.2 OPE's and ghost-picture changing

In order to treat symmetrically both vertex operators when computing the correlation functions (3.1), we switch to the ghost picture $p = 0$. This is done by applying the formula

$$\begin{aligned} V_0^{\alpha_0\beta_0}(z,k,\epsilon) &= \lim_{w\to z} e^{\phi}\,T_{\mathrm{F}}(w)\,V_{-1}^{\alpha_0\beta_0}(z,k,\epsilon)\,, \\ V_0^{\beta_0\alpha_0}(z,-k,-\epsilon) &= \lim_{w\to z} e^{\phi}\,T_{\mathrm{F}}(w)\,V_{-1}^{\beta_0\alpha_0}(z,-k,-\epsilon)\,, \end{aligned} \tag{3.8}$$

where T_{F} is the supercurrent given by

$$T_{\mathrm{F}}(z) = \frac{1}{\sqrt{\alpha'}}\,\partial X^{\mu}\psi_{\mu}(z) = \frac{1}{\sqrt{\alpha'}}\Big(\partial\overline{Z}^{u}\Psi^{u}(z) + \partial Z^{u}\overline{\Psi}^{u}(z)\Big)\,. \tag{3.9}$$

To this end, we display all necessary operator product expansions (OPE's). First of all, for the "ground-state boundary-changing fields", we have

$$\begin{aligned} \partial Z^{u}(z)\sigma^{u}(w) &\underset{z\to w}{\sim} (z-w)^{-\frac{1}{2}}\,\tau^{u}(w) + \text{finite}\,, \\ \partial\overline{Z}^{u}(z)\sigma^{u}(w) &\underset{z\to w}{\sim} (z-w)^{-\frac{1}{2}}\,\tau'^{u}(w) + \text{finite}\,, \end{aligned} \tag{3.10}$$

which introduces "excited boundary-changing fields" τ^{u}, τ'^{u}. Moreover, the other fields satisfy [13, 14][9]

$$\begin{aligned} e^{a\phi}(z)e^{b\phi}(w) &\underset{z\to w}{\sim} (z-w)^{-ab}\,e^{(a+b)\phi}(w) + \text{finite}\,, \\ e^{iaH_u}(z)e^{ibH_u}(w) &\underset{z\to w}{\sim} (z-w)^{ab}\,e^{i(a+b)H_u}(w) + \text{finite}\,, \quad u\in\{3,4\}\,, \end{aligned} \tag{3.11}$$

[9]The definitions of K^0, $\overline{K}^0$ apply to a Euclidean spacetime. In the Lorentzian case, replace $k^0 \to ik^0$.

$$\partial Z^u(z)\, e^{ik\cdot X}(w) \underset{z\to w}{\sim} \frac{iK^u}{z-w}\, e^{ik\cdot X}(w) + \text{finite}\,, \quad \text{where} \quad K^u = \frac{k^{2u} + ik^{2u+1}}{\sqrt{2}}\,,$$
$$\partial \overline{Z}^u(z)\, e^{ik\cdot X}(w) \underset{z\to w}{\sim} \frac{i\overline{K}^u}{z-w}\, e^{ik\cdot X}(w) + \text{finite}\,, \quad \text{where} \quad \overline{K}^u = \frac{k^{2u} - ik^{2u+1}}{\sqrt{2}}\,, \quad u \in \{0,1,2\}\,.$$

Using these relations, we obtain for $\epsilon = +1$

$$\begin{aligned} V_0^{\alpha_0\beta_0}(z_1,k,+1) &= V_{0,\text{ext}}^{\alpha_0\beta_0}(z_1,k,+1) + V_{0,\text{int}}^{\alpha_0\beta_0}(z_1,k,+1)\,, \\ V_0^{\beta_0\alpha_0}(z_2,-k,-1) &= V_{0,\text{ext}}^{\beta_0\alpha_0}(z_1,-k,-1) + V_{0,\text{int}}^{\beta_0\alpha_0}(z_1,-k,-1)\,, \end{aligned} \tag{3.12}$$

where we have defined

$$\begin{aligned} V_{0,\text{ext}}^{\alpha_0\beta_0}(z_1,k,+1) &= \sqrt{\alpha'}\,\lambda_{\alpha_0\beta_0}\, e^{ik\cdot X}\, i\sum_{u=0}^{1}(K^u\overline{\Psi}^u + \bar{K}^u\Psi^u)\, e^{\frac{i}{2}(H_3-H_4)}\,\sigma^3\sigma^4(z_1)\,, \\ V_{0,\text{int}}^{\alpha_0\beta_0}(z_1,k,+1) &= \frac{\lambda_{\alpha_0\beta_0}}{\sqrt{\alpha'}}\, e^{ik\cdot X}\Big(e^{-\frac{i}{2}(H_3+H_4)}\,\tau^3\sigma^4(z_1) + e^{\frac{i}{2}(H_3+H_4)}\,\sigma^3\tau'^4(z_1)\Big)\,, \\ V_{0,\text{ext}}^{\beta_0\alpha_0}(z_2,-k,-1) &= \sqrt{\alpha'}\,\lambda^{\text{T}}_{\beta_0\alpha_0}\, e^{-ik\cdot X}\,(-i)\sum_{u=0}^{1}(K^u\overline{\Psi}^u + \bar{K}^u\Psi^u)\, e^{-\frac{i}{2}(H_3-H_4)}\,\sigma^3\sigma^4(z_2)\,, \\ V_{0,\text{int}}^{\beta_0\alpha_0}(z_2,-k,-1) &= \frac{\lambda^{\text{T}}_{\beta_0\alpha_0}}{\sqrt{\alpha'}}\, e^{-ik\cdot X}\Big(e^{-\frac{i}{2}(H_3+H_4)}\,\sigma^3\tau^4(z_2) + e^{\frac{i}{2}(H_3+H_4)}\,\tau'^3\sigma^4(z_2)\Big)\,, \end{aligned} \tag{3.13}$$

while the expressions for $\epsilon = -1$ are obtained by exchanging all subscripts and superscripts 3 and 4. Because we are interested in states massless at tree level, the Kaluza–Klein momentum in the T^2 complex direction $u = 2$ is set to 0 in the "external" parts of the vertex operators. In the "internal" parts, notice the appearance of "excited boundary-changing operators" $\tau^3, \tau'^3, \tau^4, \tau'^4$.

Given the above definitions, the correlation functions (3.1) split accordingly into external and internal pieces. The former,

$$\begin{aligned} A_{\text{ext}\Sigma}^{\alpha_0\beta_0} &\equiv \Big\langle V_{0,\text{ext}}^{\alpha_0\beta_0}(z_1,k,+1) V_{0,\text{ext}}^{\beta_0\alpha_0}(z_2,-k,-1)\Big\rangle^{\Sigma} \\ &= \alpha'\,\lambda_{\alpha_0\beta_0}\lambda^{\text{T}}_{\beta_0\alpha_0}\,\langle e^{ik\cdot X}(z_1)e^{-ik\cdot X}(z_2)\rangle\,\langle e^{\frac{i}{2}H_3}(z_1)e^{-\frac{i}{2}H_3}(z_2)\rangle\,\langle e^{-\frac{i}{2}H_4}(z_1)e^{\frac{i}{2}H_4}(z_2)\rangle\,\times \\ &\langle\sigma^3(z_1)\sigma^3(z_2)\rangle\,\langle\sigma^4(z_1)\sigma^4(z_2)\rangle\sum_{u=0}^{1}K^u\overline{K}^u\Big[\langle e^{iH_u}(z_1)e^{-iH_u}(z_2)\rangle + \langle e^{-iH_u}(z_1)e^{iH_u}(z_2)\rangle\Big]\,, \end{aligned} \tag{3.14}$$

are useful to derive the one-loop corrections to the Kähler potential of the ND+DN sector massless scalars. Note that in order to bypass the issue that on shell $\sum_{u=0}^{1}|K^u|^2 \equiv k^2/2 = 0$, we may have kept the Kaluza–Klein momenta along T^2 arbitrary. On the contrary, the

internal parts,

$$
\begin{aligned}
A^{\alpha_0\beta_0}_{\text{int}\Sigma} &\equiv \left\langle V^{\alpha_0\beta_0}_{0,\text{int}}(z_1,k,+1)V^{\beta_0\alpha_0}_{0,\text{int}}(z_2,-k,-1)\right\rangle^{\Sigma} \\
&= \frac{1}{\alpha'}\,\lambda_{\alpha_0\beta_0}\lambda^{\text{T}}_{\beta_0\alpha_0}\,\langle e^{ik\cdot X}(z_1)e^{-ik\cdot X}(z_2)\rangle \\
&\quad\times\Big[\langle e^{-\frac{i}{2}H_3}(z_1)e^{\frac{i}{2}H_3}(z_2)\rangle\,\langle e^{-\frac{i}{2}H_4}(z_1)e^{\frac{i}{2}H_4}(z_2)\rangle\,\langle \tau^3(z_1)\tau'^3(z_2)\rangle\,\langle \sigma^4(z_1)\sigma^4(z_2)\rangle \\
&\qquad+\langle e^{\frac{i}{2}H_3}(z_1)e^{-\frac{i}{2}H_3}(z_2)\rangle\,\langle e^{\frac{i}{2}H_4}(z_1)e^{-\frac{i}{2}H_4}(z_2)\rangle\,\langle \sigma^3(z_1)\sigma^3(z_2)\rangle\,\langle \tau'^4(z_1)\tau^4(z_2)\rangle\Big]\,,
\end{aligned}
\tag{3.15}
$$

capture the mass corrections we are interested in. The amplitudes for $\epsilon=-1$ are obtained by exchanging all subscripts 3 and 4 in Eq. (3.14) and all superscripts 3 and 4 in Eq. (3.15). For $\Sigma=\mathcal{A}$, an implicit sum over a second boundary condition γ is understood. Likewise, for $\Sigma=\mathcal{A}$, $\mathcal{M}$, sums over the spin structures of the fermions Ψ^0, Ψ^1, Ψ^2 on the one hand, and Ψ^3, Ψ^4 on the other hand are implicit.

4 Genus-1 twist-field correlation functions

The main difficulty in computing the two-point functions in Eqs. (3.14) and (3.15) is to evaluate the correlators of the boundary changing operators. However, it turns out that the OPE's of ∂Z^u, $\partial\overline{Z}^u$ on these operators are identical to those found for the holomorphic part of "$\mathbb{Z}_2$-twist fields" inserted on a closed-string worldsheet, *i.e.* for operators creating closed strings in the twisted sector of a $T^4/\mathbb{Z}_2$ orbifold. As a result, we may apply techniques relevant for the computation of correlation functions of twist fields in closed-string theory to our open-string case. In the present section, we review the relevant ingredients for computing correlators of twist fields at genus-1 in closed-string theory, or in the closed-string sector of an open-string theory, compactified on toroidal $\mathbb{Z}_N$ orbifolds, following the original works of Refs. [1, 2].

4.1 Instanton decomposition of correlators

In closed-string theory compactified on $T^2\times T^4/\mathbb{Z}_N$ where $N\in\mathbb{N}^*$, the complex fields defined in Eq. (3.5) depend on holomorphic and antiholomorphic worldsheet coordinates, $Z^u(z,\bar{z})$. Moreover, upon parallel transport, the internal Z^u undergo some $\mathbb{Z}_N$ rotations and

translations,

$$\begin{aligned} Z^2 &\longrightarrow Z^2 + v^2\,, \\ Z^u &\longrightarrow e^{2i\pi\kappa/N} Z^u + v^u\,, \quad u \in \{3,4\}\,, \quad \kappa \in \{0,\dots,N-1\}\,, \end{aligned} \tag{4.1}$$

where the shifts v^u and v^2 implement the T^4 and T^2 periodicities.

The twist fields create the states in the twisted sectors of the closed-string Hilbert space. For some given $\kappa \in \{1,\dots,N-1\}$ and $u \in \{3,4\}$, let us denote by $\sigma^u(z,\bar{z})$ the one that creates the ground state in the κ-th twisted sector. The requirement that positive frequency modes in the expansions of ∂Z^u and $\partial\overline{Z}^u$ annihilate the twisted ground state determines the OPE of $\partial Z^u(z)$ and $\partial\overline{Z}^u(z)$ acting on $\sigma^u(w,\bar{w})$ as z approaches w,

$$\begin{aligned} \partial Z^u(z)\sigma^u(w,\bar{w}) &\underset{z\to w}{\sim} (z-w)^{-(1-\kappa/N)}\,\tau^u(w,\bar{w}) + \text{finite}\,, \\ \partial\overline{Z}^u(z)\sigma^u(w,\bar{w}) &\underset{z\to w}{\sim} (z-w)^{-\kappa/N}\,\tau'^u(w,\bar{w}) \qquad + \text{finite}\,, \\ \bar{\partial} Z^u(\bar{z})\sigma^u(w,\bar{w}) &\underset{\bar{z}\to\bar{w}}{\sim} (\bar{z}-\bar{w})^{-\kappa/N}\,\tilde{\tau}^u(w,\bar{w}) \qquad + \text{finite}\,, \\ \bar{\partial}\overline{Z}^u(\bar{z})\sigma^u(w,\bar{w}) &\underset{\bar{z}\to\bar{w}}{\sim} (\bar{z}-\bar{w})^{-(1-\kappa/N)}\,\tilde{\tau}'^u(w,\bar{w}) + \text{finite}\,. \end{aligned} \tag{4.2}$$

In the right-hand sides, τ^u, τ'^u, $\tilde{\tau}^u$, $\tilde{\tau}'^u$ create excited states in the κ-th twisted sector. The OPE's capture the local behavior corresponding to the rotations of the coordinates Z^u but do not carry information about the global translations v^u. This data is recovered by imposing *global monodromy conditions* which describe how $Z^u(z,\bar{z})$ and $\overline{Z}^u(z,\bar{z})$ change when they are carried around a set of twist fields with vanishing total twist. Splitting the coordinates of T^2 and T^4 into background values and quantum fluctuations,

$$Z^u(z,\bar{z}) = Z^u_{\rm cl}(z,\bar{z}) + Z^u_{\rm qu}(z,\bar{z})\,, \quad u \in \{2,3,4\}\,, \tag{4.3}$$

the whole global displacements arise from the classical parts $Z^u_{\rm cl}(z,\bar{z})$.

With this decomposition, the correlators of interest on a Riemann surface Σ of genus $g \geq 0$ involve, for each complex direction $u \in \{3,4\}$, $L \geq 2$ ground-state twist fields σ^u_A of the κ_A-th twisted sector,

$$\sum_{Z_{\rm cl}} e^{-S^\Sigma_{\rm cl}} \prod_{u=3}^{4} \left\langle \prod_{A=1}^{L} \sigma^u_A(z_A,\bar{z}_A) \right\rangle_{\rm qu}\,, \tag{4.4}$$

where the total twist is trivial, $\sum_A \kappa_A = 0$ modulo N, for the result not to vanish [1]. In this expression, the sum is over instantons with worldsheet actions

$$S^\Sigma_{\rm cl} = \frac{i}{2\pi\alpha'} \int_\Sigma {\rm d}z \wedge {\rm d}\bar{z} \sum_{u=2}^{4} \left(\partial Z^u_{\rm cl}\,\bar{\partial}\overline{Z}^u_{\rm cl} + \partial\overline{Z}^u_{\rm cl}\,\bar{\partial} Z^u_{\rm cl} \right). \tag{4.5}$$

In the following, we first compute the "quantum parts" of the correlation functions and then derive the classical actions.

4.2 Stress-tensor method

To determine for a given $u \in \{3,4\}$ the quantum part $\left\langle \prod_{A=1}^{L} \sigma_A^u(z_A,\bar{z}_A)\right\rangle_{\rm qu}$ of the correlator (4.4), Ref. [2] uses the *stress-tensor method*. It consists in exploiting the OPE's between the stress tensor $T^u(z)$ and the primary fields $\sigma_A^u(z_A,\bar{z}_A)$ of conformal weights $h_A = \frac{1}{2}(\kappa_A/N)(1-\kappa_A/N)$, namely

$$T^u(z)\sigma_A^u(z_A,\bar{z}_A) \underset{z\to z_A}{\sim} \frac{h_A}{(z-z_A)^2}\,\sigma_A^u(z_A,\bar{z}_A) + \frac{1}{z-z_A}\,\partial_A\sigma_A^u(z_A,\bar{z}_A) + \text{finite}\,. \tag{4.6}$$

To this end, one considers the quantity

$$\langle\langle T^u(z)\rangle\rangle \equiv \frac{\langle T^u(z)\prod_A \sigma_A^u(z_A,\bar{z}_A)\rangle_{\rm qu}}{\langle\prod_A \sigma_A^u(z_A,\bar{z}_A)\rangle_{\rm qu}}\,, \tag{4.7}$$

in terms of which we may write

$$\partial_B \ln\Big\langle\prod_A \sigma_A^u(z_A,\bar{z}_A)\Big\rangle_{\rm qu} = \lim_{z\to z_B}\left[(z-z_B)\,\langle\langle T^u(z)\rangle\rangle - \frac{h_B}{(z-z_B)}\right], \tag{4.8}$$

upon using Eq. (4.6). To evaluate $\langle\langle T^u(z)\rangle\rangle$, one considers the *Green's function in the presence of twist fields*,[10]

$$g(z,w) \equiv \frac{\langle -\partial Z_{\rm qu}^u(z)\,\partial\overline{Z}_{\rm qu}^u(w)\prod_A \sigma_A^u(z_A,\bar{z}_A)\rangle_{\rm qu}}{\alpha'\,\langle\prod_A \sigma_A^u(z_A,\bar{z}_A)\rangle_{\rm qu}}\,, \tag{4.9}$$

and exploits the OPE

$$-\frac{1}{\alpha'}\,\partial Z_{\rm qu}^u(z)\,\partial\overline{Z}_{\rm qu}^u(w) \underset{z\to w}{\sim} \frac{1}{(z-w)^2} + T^u(w) + \mathcal{O}(z-w) \tag{4.10}$$

to obtain

$$\langle\langle T^u(z)\rangle\rangle = \lim_{w\to z}\left[g(z,w) - \frac{1}{(z-w)^2}\right]. \tag{4.11}$$

To summarise, the stress-tensor method amounts to determining the Green's function $g(z,w)$, then deduce $\langle\langle T^u(z)\rangle\rangle$, and finally integrate the differential equations (4.8).

[10] Because the integers κ_A and insertion points z_A are independent of $u \in \{3,4\}$, the Green's functions derived for $u = 3$ and 4 are equal and do not need to be distinguished by an index u.

4.3 Ground-state twist field quantum correlators on the torus

Let us specialize to the case where Σ is a genus-1 surface. We will denote its Teichmüller parameter as $\tau^{\rm dc}$ for future use, when we see the genus-1 Riemann surface as the double cover of open-string surfaces.[11]

In order to derive the quantum part of the correlator (4.4) for a given $u \in \{3,4\}$, $\left\langle \prod_{A=1}^{L} \sigma_A^u(z_A,\bar{z}_A)\right\rangle_{\rm qu}$, the starting point is to write the most general ansätze for $g(z,w)$ and the companion Green's function

$$h(\bar{z},w) \equiv \frac{\langle -\bar{\partial} Z^u_{\rm qu}(\bar{z})\, \partial \overline{Z}^u_{\rm qu}(w) \prod_A \sigma_A^u(z_A,\bar{z}_A)\rangle_{\rm qu}}{\alpha' \langle \prod_A \sigma_A^u(z_A,\bar{z}_A)\rangle_{\rm qu}}\,, \tag{4.12}$$

satisfying the following properties:

- Double periodicity $z \to z+1$, $z \to z+\tau^{\rm dc}$ and $w \to w+1$, $w \to w+\tau^{\rm dc}$ (and similarly for $\bar{z}$ in h).
- Local monodromies consistent with the OPE's given in Eq. (4.2). For instance, when z is transported along a tiny closed loop encircling some z_A, g must transform as $e^{-2i\pi(1-\kappa_A/N)}g$.
- A double pole for $g(z,w)$ as $z \to w$ dictated by Eq. (4.10), and finiteness of $h(\bar{z},w)$ as $\bar{z} \to w$ thanks to the OPE $\bar{\partial} Z^u_{\rm qu}(\bar{z}) \partial \overline{Z}^u_{\rm qu}(w) \underset{\bar{z}\to w}{\sim}$ finite.

This can be done by defining *cut differentials* [2] which form a basis of holomorphic one-forms on the torus that possess suitable monodromy behaviors as their arguments approach each of the insertion points z_A. Denoting

$$M = \sum_{A=1}^{L} \frac{\kappa_A}{N}\,, \tag{4.13}$$

which takes some value in the set $\{1,\ldots,L-1\}$, and following the notations of Ref. [2], such a basis is given by

$$\begin{aligned} \omega^{\alpha_A}_{N-\kappa}(z) &= \gamma_{N-\kappa}(z)\, \vartheta_1(z - z_{\alpha_A} - y_{N-\kappa}) \prod_{B\neq A}^{L-M} \vartheta_1(z - z_{\alpha_B})\,, \quad A \in \{1,\ldots,L-M\}\,, \\ \omega^{\beta_A}_{\kappa}(z) &= \gamma_{\kappa}(z)\, \vartheta_1(z - z_{\beta_A} - y_{\kappa}) \prod_{B\neq A}^{M} \vartheta_1(z - z_{\beta_B})\,, \qquad\quad A \in \{1,\ldots,M\}\,, \end{aligned} \tag{4.14}$$

[11] Throughout Sect. 4, the real part of $\tau^{\rm dc}$ is arbitrary.

where the second argument at $\tau^{\rm dc}$ in the modular forms is implicit. In these formulas, we have defined the functions

$$\gamma_{N-\kappa}(z) = \prod_{A=1}^{L} \vartheta_1(z-z_A)^{-(1-\kappa_A/N)}\,, \qquad \gamma_{\kappa}(z) = \prod_{A=1}^{L} \vartheta_1(z-z_A)^{-\kappa_A/N}\,, \tag{4.15}$$

and denoted

$$y_{N-\kappa} = \sum_{A=1}^{L}\left(1-\frac{k_A}{N}\right) z_A - \sum_{B=1}^{L-M} z_{\alpha_B}\,, \qquad y_{\kappa} = \sum_{A=1}^{L}\frac{\kappa_A}{N} z_A - \sum_{B=1}^{M} z_{\beta_B}\,, \tag{4.16}$$

while $\{z_{\alpha_1},\ldots,z_{\alpha_{L-M}}\}$ and $\{z_{\beta_1},\ldots,z_{\beta_M}\}$ are subsets of twist insertion points chosen arbitrarily.[12] The functions $\gamma_{N-\kappa}$ and γ_κ implement the monodromies around the z_A's, while the extra ϑ_1 modular forms in the definitions (4.14) lead to the double periodicity with respect to the variable z.[13] Given these notations, the Green's functions may be expressed as

$$\begin{aligned} g(z,w) &= g_s(z,w) + \sum_{A=1}^{L-M}\sum_{B=1}^{M} C_{AB}\,\omega_{N-\kappa}^{\alpha_A}(z)\,\omega_{\kappa}^{\beta_B}(w)\,, \\ h(\bar z,w) &= \sum_{A=1}^{M}\sum_{B=1}^{M} B_{AB}\,\bar\omega_{\kappa}^{\beta_A}(\bar z)\,\omega_{\kappa}^{\beta_B}(w)\,, \end{aligned} \tag{4.17}$$

where C_{AB} and B_{AB} are "constant coefficients."[14] The function $g_s(z,w)$ is doubly periodic in z and w and handles the double-pole structure of $g(z,w)$ as z approaches w. It can be expressed as [2]

$$g_s(z,w) = \gamma_{N-\kappa}(z)\,\gamma_\kappa(w)\left(\frac{\vartheta_1'(0)}{\vartheta_1(z-w)}\right)^2 P(z,w)\,, \tag{4.18}$$

where explicit knowledge of the function $P(z,w)$ is not required in the computation of correlation functions of ground-state twist fields. However, it does matter for correlators of excited twist fields, as will be seen in Sect. 4.5. We will come back to this issue at that stage.

The next step is to implement the global monodromy conditions, which by definition are "trivial" for the quantum fluctuations $Z^u_{\rm qu}(z,\bar z)$ (see below Eq. (4.3)). In practice, this implies that

$$0 = \oint_{\gamma_a} {\rm d}z\, g(z,w) + \oint_{\gamma_a} {\rm d}\bar z\, h(\bar z,w)\,, \quad a\in\{1,\ldots,L\}\,, \tag{4.19}$$

[12] The subscripts "$N-\kappa$" and "κ" are "names". They do not refer to varying indices. Moreover, the indices $\alpha_1,\ldots,\alpha_{L-M}$ and $\beta_1,\ldots,\beta_M$ here should not be confused with labels of branes also denoted by Greek letters elsewhere in our work.

[13] Note that no periodicity condition is imposed for the individual variables z_A (which are kept implicit in the cut differentials). However, double periodicity in z implies double periodicity of the whole set of points z_A, when they are moved together.

[14] They depend only on the insertion points and $\tau^{\rm dc}$.

where $\{\gamma_a,\ a = 1, \ldots, L\}$ is a basis of the homology group of the genus-1 surface with L punctures.[15] To solve these equations, it is convenient to define an $L \times L$ *cut-period matrix* ${W_a}^A$ as follows,

$$\begin{aligned} {W_a}^A &= \oint_{\gamma_a} \mathrm{d}z\, \omega_{N-\kappa}^{\alpha_A}(z)\,, \quad A \in \{1, \ldots, L-M\}\,, \\ {W_a}^{L-M+A} &= \oint_{\gamma_a} \mathrm{d}\bar{z}\, \bar{\omega}_{\kappa}^{\beta_A}(\bar{z})\,, \qquad A \in \{1, \ldots, M\}\,. \end{aligned} \tag{4.20}$$

Indeed, it is easily checked that the expressions

$$\begin{aligned} g(z,w) &= g_s(z,w) - \sum_{A=1}^{L-M} \omega_{N-\kappa}^{\alpha_A}(z) \sum_{a=1}^{L} (W^{-1})_A{}^a \oint_{\gamma_a} \mathrm{d}\zeta\, g_s(\zeta, w)\,, \\ h(\bar{z},w) &= -\sum_{A=1}^{M} \omega_{\kappa}^{\beta_A}(\bar{z}) \sum_{a=1}^{L} (W^{-1})_{L-M+A}{}^a \oint_{\gamma_a} \mathrm{d}\zeta\, g_s(\zeta, w)\,, \end{aligned} \tag{4.21}$$

satisfy the global monodromy conditions.

Finally, the correlator can be found by applying the stress-tensor method to find the holomorphic dependence on the z_A's, and then a second time using the Green's functions $\bar{g}(\bar{z}, \bar{w})$ and $\bar{h}(z, \bar{w})$ to determine the antiholomorphic part. The result is for $u \in \{3, 4\}$

$$\begin{aligned} \left\langle \prod_{A=1}^{L} \sigma_A^u(z_A, \bar{z}_A) \right\rangle_{\mathrm{qu}} &= f(\tau^{\mathrm{dc}}; \kappa_1, \ldots, \kappa_L)\, \frac{1}{\det W}\, \vartheta_1(y_{N-\kappa})^{L-M-1}\, \overline{\vartheta_1(y_\kappa)}^{M-1} \\ &\quad \times \prod_{\substack{A,B=1 \\ A<B}}^{L-M} \vartheta_1(z_{\alpha_A} - z_{\alpha_B}) \prod_{\substack{A,B=1 \\ A<B}}^{M} \overline{\vartheta_1(z_{\beta_A} - z_{\beta_B})} \\ &\quad \times \prod_{\substack{A,B=1 \\ A<B}}^{L} \vartheta_1(z_A - z_B)^{-(1-\kappa_A/N)(1-\kappa_B/N)}\, \overline{\vartheta_1(z_A - z_B)}^{-(\kappa_A/N)(\kappa_B/N)}\,, \end{aligned} \tag{4.22}$$

where $f(\tau^{\mathrm{dc}}, \kappa_1, \ldots, \kappa_L)$ is a function arising as an "integration constant". The latter can be determined by coalescing all insertion points, since the left-hand side reduces in this case to $\langle 1 \rangle$, which is the partition function.

4.4 Instanton actions

In the OPE's (4.2), the actions of the background parts $\partial Z_{\mathrm{cl}}^u(z)$ and $\partial \overline{Z}_{\mathrm{cl}}^u(z)$ on $\sigma^u(w, \bar{w})$ for $u \in \{3, 4\}$ are trivial multiplications. Hence, for the monodomy properties to be satisfied as

[15] For a genus g surface with L punctures, the basis has dimension $L + 2g - 2$ [2].

z is transported along a tiny closed loop encircling any z_A, the doubly-periodic $\partial Z^u_{\rm cl}(z)$ and $\partial\overline{Z}^u_{\rm cl}(z)$ must be linear sums of cut differentials. To determine the coefficients, one imposes the global monodromy conditions

$$\oint_{\gamma_a} \mathrm{d}z\, \partial Z^u_{\rm cl} + \oint_{\gamma_a} \mathrm{d}\bar{z}\, \bar{\partial} Z^u_{\rm cl} = v^u_a\,, \quad a \in \{1,\ldots,L\}\,, \tag{4.23}$$

where the v^u_a's are displacement vectors. The solution of these equations can be expressed in terms of the inverse cut-period matrix,

$$\partial Z^u_{\rm cl}(z) = \omega_{A'}(z)\,(W^{-1})_{A'}{}^a\, v^u_a\,, \qquad \bar{\partial} Z^u_{\rm cl}(\bar{z}) = \bar{\omega}_{A''}(\bar{z})\,(W^{-1})_{A''}{}^a\, v^u_a\,, \tag{4.24}$$

where in the present context the index A' is summed over $1,\ldots,L-M$, and A'' is summed over $L-M+1,\ldots,L$. Moreover, we have redefined in the above formulas

$$\begin{aligned} \omega_A(z) &\equiv \omega^{\alpha_A}_{N-\kappa}(z)\,, \quad A \in \{1,\ldots,L-M\}\,, \\ \omega_{L-M+A}(z) &\equiv \omega^{\beta_A}_{\kappa}(z)\,, \qquad A \in \{1,\ldots,M\}\,. \end{aligned} \tag{4.25}$$

With the definition of the Hermitian product

$$(\omega_i,\omega_j) \equiv i\int_\Sigma \mathrm{d}z \wedge \mathrm{d}\bar{z}\,\omega_i(z)\,\bar{\omega}_j(\bar{z}) \tag{4.26}$$

of one-forms on the torus, the classical action for a single complex coordinate $u \in \{3,4\}$ reads

$$S^\Sigma_{\rm cl}\Big|^u = \frac{v^u_a \bar{v}^u_b}{2\pi\alpha'}\Big[(W^{-1})_{A'}{}^a\,(W^{-1})_{B'}{}^b\,(\omega_{A'},\omega_{B'}) + (W^{-1})_{A''}{}^a\,(W^{-1})_{B''}{}^b\,(\omega_{A''},\omega_{B''})\Big]\,. \tag{4.27}$$

4.5 Useful correlators on the torus

In this subsection, we consider all correlators involved in the open-string amplitudes of Eqs. (3.14) and (3.15), but display their values computed on a genus-1 surface. In this case, they have holomorphic and antiholomorphic dependencies.

Correlator $\langle\boldsymbol{\sigma^u(z_1,\bar{z}_1)\sigma^u(z_2,\bar{z}_2)}\rangle_{\mathbf{qu}}$: For the OPE's of the twist fields to match those of the boundary-changing fields we are interested in, we now consider the case where

$$N = 2\,, \qquad L = 2\,, \qquad \frac{\kappa_1}{N} = \frac{\kappa_2}{N} = \frac{1}{2}\,, \qquad M = 1\,. \tag{4.28}$$

Because $\kappa_1 = \kappa_2$, we can omit from now on the subscripts A of the twist fields. Using Eq. (4.22), we obtain for $u = 3, 4$

$$\langle \sigma^u(z_1, \bar{z}_1)\sigma^u(z_2, \bar{z}_2)\rangle_{\rm qu} = f(\tau^{\rm dc}; \tfrac{1}{2}, \tfrac{1}{2})\,(\det W)^{-1}\,\vartheta_1(z_1 - z_2)^{-\frac{1}{4}}\,\overline{\vartheta_1(z_1 - z_2)}^{-\frac{1}{4}}\,. \tag{4.29}$$

The 2×2 cut-period matrix $W_a{}^i$ defined in Eq (4.20) involves only one cut differential,

$$\omega(z) = \vartheta_1(z - z_1)^{-\frac{1}{2}}\,\vartheta_1(z - z_2)^{-\frac{1}{2}}\,\vartheta_1\Big(z - \frac{z_1 + z_2}{2}\Big)\,, \tag{4.30}$$

to be integrated on the cycles of the genus-1 surface Σ, $\gamma_1 :\ z \to z + 1$ and $\gamma_2 :\ z \to z + \tau^{\rm dc}$, which yields

$$W = \begin{pmatrix} W_1 & \overline{W}_1 \\ W_2 & \overline{W}_2 \end{pmatrix}, \quad \text{where} \quad W_a = \oint_{\gamma_a} {\rm d}z\,\omega\,, \quad a \in \{1, 2\}\,. \tag{4.31}$$

In these notations, the background action written in Eq. (4.27) reads for $u =\in \{3, 4\}$

$$S_{\rm cl}^{\Sigma}\Big|^u = \frac{1}{4\pi\alpha'\,{\rm Im}(\overline{W}_1 W_2)}\left(\left|\overline{W}_2 v_1^u - \overline{W}_1 v_2^u\right|^2 + \left|W_2 v_1^u - W_1 v_2^u\right|^2\right), \tag{4.32}$$

where v_a^u, $a \in \{1, 2\}$, are the displacements introduced in Eq. (4.23). In our case of interest, given an instanton solution, the real-coordinate background $X_{\rm cl}^I(z, \bar{z})$, $I \in \{6, \ldots, 9\}$, winds n_I times and l_I times the circle $S^1(R_I)$ as z is transported along γ_1 and γ_2, so that

$$v_1^u = \frac{2\pi R_{2u} n_{2u} + 2i\pi R_{2u+1} n_{2u+1}}{\sqrt{2}}\,, \qquad v_2^u = \frac{2\pi R_{2u} l_{2u} + 2i\pi R_{2u+1} l_{2u+1}}{\sqrt{2}}\,. \tag{4.33}$$

For the T^2 coordinate $u = 2$, which is not twisted, the above formula apply with cut differentials that induce trivial local monodromies. In other words, replacing $\omega(z)$ by 1, the relevant cut-period matrix becomes

$$\begin{pmatrix} 1 & 1 \\ \tau^{\rm dc} & \bar{\tau}^{\rm dc} \end{pmatrix}. \tag{4.34}$$

Defining displacements v_a^u for $u = 2$ exactly as those given in Eq. (4.33), one obtains

$$S_{\rm cl}^{\Sigma}\Big|^2 = \frac{\pi}{\alpha'\,{\rm Im}\,\tau^{\rm dc}}\Big(R_4^2|n_4\tau^{\rm dc} - l_4|^2 + R_5^2|n_5\tau^{\rm dc} - l_5|^2\Big)\,, \tag{4.35}$$

which is the well know result for the instanton action on a two-torus [62]. The sum over instantons appearing in Eq. (4.4) translates therefore into a sum over winding numbers $n_{I'}$, n_I, and wrapping numbers $l_{I'}$, l_I, where $I' \in \{4, 5\}$ and $I \in \{6, \ldots, 9\}$.

Correlator $\langle \tau^u(z_1,\bar{z}_1)\tau'^u(z_2,\bar{z}_2)\rangle_{\rm qu}$: To derive the correlator of excited twist fields, we will follow the technique described in Refs. [13, 15–17]. Thanks to the OPE's between $\partial Z^u, \partial\overline{Z}^u$ and the ground-state twist fields given in Eq. (4.2), and using the splitting defined Eq. (4.3), we may divide accordingly this correlation function for $u \in \{3,4\}$ into two pieces,

$$\langle \tau^u(z_1,\bar{z}_1)\tau'^u(z_2,\bar{z}_2)\rangle_{\rm qu} = \langle \tau^u(z_1,\bar{z}_1)\tau'^u(z_2,\bar{z}_2)\rangle^{(1)}_{\rm qu} + \langle \tau^u(z_1,\bar{z}_1)\tau'^u(z_2,\bar{z}_2)\rangle^{(2)}_{\rm qu}\,, \tag{4.36}$$

where we have defined

$$\begin{aligned}
\langle \tau^u(z_1,\bar{z}_1)\tau'^u(z_2,\bar{z}_2)\rangle^{(1)}_{\rm qu} &= \langle \sigma^u(z_1,\bar{z}_1)\sigma^u(z_2,\bar{z}_2)\rangle_{\rm qu} \lim_{\substack{z\to z_1\\ w\to z_2}} \Big[(z-z_1)^{\frac{1}{2}}(w-z_2)^{\frac{1}{2}}\,\partial Z^u_{\rm cl}(z)\partial\overline{Z}^u_{\rm cl}(w)\Big]\,,\\
\langle \tau^u(z_1,\bar{z}_1)\tau'^u(z_2,\bar{z}_2)\,\rangle^{(2)}_{\rm qu} &= \lim_{\substack{z\to z_1\\ w\to z_2}} \Big[(z-z_1)^{\frac{1}{2}}(w-z_2)^{\frac{1}{2}}\langle \partial Z^u_{\rm qu}(z)\partial\overline{Z}^u_{\rm qu}(w)\sigma^u(z_1,\bar{z}_1)\sigma^u(z_2,\bar{z}_2)\rangle_{\rm qu}\Big]\,.
\end{aligned} \tag{4.37}$$

To derive part (1) of the correlator, we use Eq. (4.24) which becomes

$$\partial Z^u_{\rm cl}(z) = \omega(z)\,c^u_1\,, \quad \bar\partial Z^u_{\rm cl}(\bar z) = \bar\omega(\bar z)\,c^u_2\,, \quad \text{where} \quad c^u_A = (W^{-1})_A{}^a\, v^u_a\,. \tag{4.38}$$

Remember that due to their local monodromy behaviors, these expressions diverge at the insertion points. Hence, the limits defined in Eq. (4.37) contribute a finite result which is

$$\langle \tau^u(z_1,\bar{z}_1)\tau'^u(z_2,\bar{z}_2)\rangle^{(1)}_{\rm qu} = s\,i\,c^u_1\bar{c}^u_2\,\frac{\vartheta_1(\frac{z_1-z_2}{2})^2}{\vartheta_1'(0)\,\vartheta_1(z_1-z_2)}\,\langle \sigma^u(z_1,\bar{z}_1)\sigma^u(z_2,\bar{z}_2)\rangle_{\rm qu}\,, \tag{4.39}$$

where we denote

$$s\,i \;\equiv\; \left(\frac{z_2-z_1}{z_1-z_2}\right)^{\frac{1}{2}}. \tag{4.40}$$

Using the Green's function $g(z,w)$ defined in Eq. (4.9), part (2) of the correlator can be expressed as

$$\langle \tau^u(z_1,\bar{z}_1)\tau'^u(z_2,\bar{z}_2)\,\rangle^{(2)}_{\rm qu} = -\alpha'\,\langle \sigma^u(z_1,\bar{z}_1)\sigma^u(z_2,\bar{z}_2)\rangle_{\rm qu} \lim_{\substack{z\to z_1\\ w\to z_2}} \Big[(z-z_1)^{\frac{1}{2}}(w-z_2)^{\frac{1}{2}}\,g(z,w)\Big]\,. \tag{4.41}$$

In the present case, Eqs. (4.17) and (4.21) become

$$\begin{aligned}
g(z,w) &= g_s(z,w) + C\,\omega(z)\,\omega(w)\\
&= g_s(z,w) - \omega(z)(W^{-1})_1{}^a \oint_{\gamma_a} {\rm d}\zeta\, g_s(\zeta,w)\,,
\end{aligned} \tag{4.42}$$

where $g_s(z,w)$ is defined in Eq. (4.18). The latter involves a function $P(z,w)$ derived in Ref. [2], and whose expression is given by

$$\begin{aligned}
g_s(z,w) = \gamma(z)\gamma(w)\left(\frac{\vartheta_1'(0)}{\vartheta_1(z-w)}\right)^2 \frac{1}{2}\Big[&F_1(z,w)\vartheta_1(w-z_1)\vartheta_1(z-z_2)\\
&+F_2(z,w)\vartheta_1(w-z_2)\vartheta_1(z-z_1)\Big]\,.
\end{aligned} \tag{4.43}$$

The right-hand side is written in terms of a unique function γ (see Eq. (4.15))

$$\gamma(z) = \vartheta_1(z-z_1)^{-\frac{1}{2}}\,\vartheta_1(z-z_2)^{-\frac{1}{2}}\,, \tag{4.44}$$

as well as

$$\begin{aligned} &F_A(z,w) = \frac{\vartheta_1(z-w+U_A)}{\vartheta_1(U_A)}\,\frac{\vartheta_1(z-w+Y_A-U_A)}{\vartheta_1(Y_A-U_A)}\,, \quad A\in\{1,2\}\,,\\ &\text{where}\quad Y_A = \frac{z_1+z_2}{2} - z_A \quad\text{and}\quad U_A \text{ is such that } \partial_z F_A(z,w)\Big|_{z=w} = 0\,. \end{aligned} \tag{4.45}$$

Notice that in the above formula, we adopt the notations of Ref. [2] but it turns out that $F_1(z,w) \equiv F_2(w,z)$. Computing the limits in Eq. (4.41), we find

$$\begin{aligned} \langle \tau^u(z_1,\bar z_1)\tau'^u(z_2,\bar z_2)\,\rangle^{(2)}_{\rm qu} =& -\,\alpha' s\, i\,\langle \sigma^u(z_1,\bar z_1)\sigma^u(z_2,\bar z_2)\rangle_{\rm qu}\\ &\times\left[\frac{\vartheta_1'(0)\,F_1(z_1,z_2)}{2\,\vartheta_1(z_1-z_2)} + C\,\frac{\vartheta_1(\frac{z_1-z_2}{2})^2}{\vartheta_1'(0)\,\vartheta_1(z_1-z_2)}\right]. \end{aligned} \tag{4.46}$$

Moreover, using in the derivation the second expression in Eq. (4.42), an explicit expression for the term linear in C is obtained,

$$C\,\frac{\vartheta_1(\frac{z_1-z_2}{2})^2}{\vartheta_1'(0)\,\vartheta_1(z_1-z_2)} = -\frac{1}{2}\,\vartheta_1'(0)\,\vartheta_1\Big(\frac{z_1-z_2}{2}\Big)(W^{-1})_1{}^a \oint_{\gamma_a} {\rm d}z\,\frac{F_1(z,z_2)}{\vartheta_1(z-z_1)^{\frac{1}{2}}\,\vartheta_1(z-z_2)^{\frac{3}{2}}}\,. \tag{4.47}$$

Adding the pieces (1) and (2) of the correlator, we obtain for $u\in\{2,3\}$

$$\begin{aligned} \langle \tau^u(z_1,\bar z_1)\tau'^u(z_2,\bar z_2)\,\rangle_{\rm qu} =& -\,s\, i\,\langle \sigma^u(z_1,\bar z_1)\sigma^u(z_2,\bar z_2)\rangle_{\rm qu}\\ &\times\left[(\alpha' C - c_1^u\bar c_2^u)\,\frac{\vartheta_1(\frac{z_1-z_2}{2})^2}{\vartheta_1'(0)\,\vartheta_1(z_1-z_2)} + \alpha'\frac{\vartheta_1'(0)\,F_1(z_1,z_2)}{2\,\vartheta_1(z_1-z_2)}\right]. \end{aligned} \tag{4.48}$$

Correlator $\langle \tau'^u(z_1,\bar z_1)\tau^u(z_2,\bar z_2)\rangle_{\rm qu}$: Proceeding the same way, and using the fact that $F_2(z_2,z_1) = F_1(z_1,z_2)$, we obtain the identity

$$\langle \tau'^u(z_1,\bar z_1)\tau^u(z_2,\bar z_2)\,\rangle_{\rm qu} = \langle \tau^u(z_1,\bar z_1)\tau'^u(z_2,\bar z_2)\,\rangle_{\rm qu}\,. \tag{4.49}$$

Bosonic correlator: The propagator of the spacetime coordinates X^μ is given by

$$\langle X^\mu(z_1,\bar z_1)X_\nu(z_2,\bar z_2)\rangle = \delta^\mu_\nu\left[-\frac{\alpha'}{2}\ln\left|\frac{\vartheta_1(z_1-z_2)}{\vartheta_1'(0)}\right|^2 + \frac{\alpha'\pi\,[{\rm Im}(z_1-z_2)]^2}{{\rm Im}\,\tau}\right], \tag{4.50}$$

which leads to

$$\langle e^{ik\cdot X}(z_1,\bar z_1)e^{-ik\cdot X}(z_2,\bar z_2)\rangle = \left(\left|\frac{\vartheta_1(z_1-z_2)}{\vartheta_1'(0)}\right| e^{-\frac{\pi[{\rm Im}(z_1-z_2)]^2}{{\rm Im}\,\tau}}\right)^{-\alpha' k^2}\,. \tag{4.51}$$

Bosonized-fermion correlators: Each complex fermion Ψ^u, $u \in \{0,\dots,4\}$, has one out of four pairs of periodic/antiperiodic boundary conditions on the genus-1 surface Σ, which corresponds to a spin structure $\nu \in \{1,2,3,4\}$. In bosonized picture, for any H_u-charge q, one finds by applying the stress-tensor method that the following correlator depends accordingly on ν,

$$\langle e^{iqH_u}(z_1)e^{-iqH_u}(z_2)\rangle_\nu = K_{\nu,|q|}\,\vartheta_\nu(q(z_1-z_2))\,\vartheta_1(z_1-z_2)^{-q^2}\,, \tag{4.52}$$

where $K_{\nu,|q|}$ is a $\tau^{\rm dc}$-dependent normalization factor [13].

5 Full amplitudes of massless ND and DN states

We are now ready to use all ingredients introduced in Sects. 3 and 4 to compute the two-point functions of massless bosonic states in the ND and DN sectors. As depicted in Fig. 3, the annulus and Möbius strip can be described as tori with Teichmüller parameters given in Eq. (3.7) and modded by the involution (3.6). The boundaries of the open-string surfaces being the fixed points, we may choose the insertion points of the boundary-changing vertex operators to be

$$z_A \equiv x_A + iy_A\,, \quad \text{where} \quad \begin{cases} 0 \le y_A \le \operatorname{Im}\tau^{\rm dc}\,, & A \in \{1,2\}\,, \\ x_1 = x_2 \in \left\{0,\dfrac{1}{2}\right\} & \text{for } \ \Sigma = \mathcal{A}\,, \\ x_1, x_2 \in \left\{0,\dfrac{1}{2}\right\} & \text{for } \ \Sigma = \mathcal{M}\,. \end{cases} \tag{5.1}$$

5.1 Useful correlators on the annulus and Möbius strip

Let us first collect the correlators presented in the previous section now evaluated on the open-string surfaces $\Sigma = \mathcal{A}$ and $\mathcal{M}$, and to be used to express the amplitudes $A^{\alpha_0\beta_0}_{{\rm ext}\Sigma}$ and $A^{\alpha_0\beta_0}_{{\rm int}\Sigma}$.

Correlator $\langle \boldsymbol{\sigma}^u(\boldsymbol{z_1})\boldsymbol{\sigma}^u(\boldsymbol{z_2})\rangle_{\mathbf{qu}}$: In Ref. [13], the method of images was applied on the Green's functions of Sects. 4.2 and 4.3 to define their open-string counterparts. The latter were used to derive the correlator between two ground-state boundary-changing fields by using the stress-tensor method. The result amounts essentially to take the "square root" of

the closed-string result, *i.e.* for $u \in \{3,4\}$,

$$\langle \sigma^u(z_1)\sigma^u(z_2)\rangle_{\rm qu} = f_{\rm op}(\tau^{\rm dc};\tfrac{1}{2},\tfrac{1}{2})\,(\det W)^{-\frac{1}{2}}\,\vartheta_1(z_1-z_2)^{-\frac{1}{4}}\,, \tag{5.2}$$

where $f_{\rm op}$ is a normalization function. Notice that the product $\langle\sigma^3\sigma^3\rangle_{\rm qu}\langle\sigma^4\sigma^4\rangle_{\rm qu}$ involves $\vartheta_1(z_1-z_2)^{-\frac{1}{2}}$, which is well defined up to a sign. We will see in the next subsection how such ambiguities can be lifted.

The instanton actions can also be derived from the closed-string result given in Eqs. (4.32) and (4.35). These expressions must be divided by 2, the order of the involution $\mathcal{I}$, to account for the fact that the open-string worldsheets are halves of their genus-1 double-covers. Moreover, we have to consider instantonic worldsheets with NN, DD, ND or DN boundary conditions for $\mathcal{A}$, and N or D boundary conditions for $\mathcal{M}$. In the NN and N case, all winding numbers along $T^2\times T^4$ must vanish, $n_{I'}=n_I=0$. The DD and D case is similar, up to the T-duality transformation $R_I\to\alpha'/R_I$. Denoting the T-dual wrapping numbers with "tildes", we have $\tilde n_{I'}=\tilde n_I=0$. Finally, for worldsheets with ND or DN boundary conditions in the annulus case, non-trivial instantons wrap T^2 only, *i.e.* satisfy $n_{I'}=n_I=l_I=0$ or $\tilde n_{I'}=\tilde n_I=\tilde l_I=0$. In total, we thus have for $\Sigma=\mathcal{A}$ or $\mathcal{M}$

$$S^\Sigma_{\rm cl}=\frac{\pi[(R_4l_4)^2+(R_5l_5)^2]}{\alpha'\tau_2}+\frac{|W_1|^2}{4\pi\alpha'\,{\rm Im}(\overline{W}_1W_2)}\times\begin{cases}\displaystyle\sum_{u=3}^4|v_2^u|^2 & \text{for NN and N}\,,\\ \displaystyle\sum_{u=3}^4|\tilde v_2^u|^2 & \text{for DD and D}\,,\\ 0 & \text{for ND and DN}\,,\end{cases} \tag{5.3}$$

where the displacements and their T-dual counterparts are given by

$$v_2^u=\frac{2\pi R_{2u}l_{2u}+2i\pi R_{2u+1}l_{2u+1}}{\sqrt{2}}\,,\quad \tilde v_2^u=\frac{2\pi\frac{\alpha'}{R_{2u}}\tilde l_{2u}+2i\pi\frac{\alpha'}{R_{2u+1}}\tilde l_{2u+1}}{\sqrt{2}}\,,\quad u\in\{3,4\}\,. \tag{5.4}$$

Correlators $\langle\tau^u(z_1)\tau'^u(z_2)\rangle_{\rm qu}$ and $\langle\tau'^u(z_1)\tau^u(z_2)\rangle_{\rm qu}$: On the genus-1 surfaces, the twist fields $\tau^u(z,\bar z)$ and $\tau'^u(z,\bar z)$ are excited only on their holomorphic sides (see Eq. (4.2)). Therefore, their correlation functions take formally the same forms as those of the excited boundary-changing fields $\tau^u(z)$ and $\tau'^u(z)$ evaluated on $\mathcal{A}$ and $\mathcal{M}$. There is however a subtlety concerning part (1) of the correlator, Eq. (4.39).

When considering the *full* amplitudes *i.e.* with the instanton dressings $e^{-S^\Sigma_{\rm cl}}$, the open-string actions are divided by 2 compared to the closed-string case. Hence, for the full open-string correlators to preserve their interpretations on double-cover tori, one should rescale

the displacements in parts (1) as follows, $|v_2^u|^2 \to |v_2^u|^2/2$ and $|\tilde{v}_2^u|^2 \to |\tilde{v}_2^u|^2/2$. As a result we have for $u \in \{3,4\}$

$$\langle \tau^u(z_1)\tau'^u(z_2)\rangle_{\rm qu} = \langle \tau'^u(z_1)\tau^u(z_2)\rangle_{\rm qu} = -s\, i\, \langle \sigma^u(z_1)\sigma^u(z_2)\rangle_{\rm qu} \times \left[\left(\alpha' C + \frac{\overline{W}_1^2\,|v_2^u|^2}{8[{\rm Im}\,(\overline{W}_1 W_2)]^2}\right)\frac{\vartheta_1(\frac{z_1-z_2}{2})^2}{\vartheta_1'(0)\,\vartheta_1(z_1-z_2)} + \alpha'\frac{\vartheta_1'(0)\,F_1(z_1,z_2)}{2\,\vartheta_1(z_1-z_2)}\right], \tag{5.5}$$

when the worldsheet has NN or N boundary conditions on the annulus or Möbius strip. For DD or D boundary conditions, the correlators take identical forms up to the change $v_2^u \to \tilde{v}_2^u$. Finally, for boundary conditions ND or DN on the annulus, the classical displacements vanish and only the pure quantum contributions proportional to α' survive.

Note that $\langle \tau^3\tau'^3\rangle_{\rm qu}\,\langle \sigma^4\sigma^4\rangle_{\rm qu}$ and $\langle \sigma^3\sigma^3\rangle_{\rm qu}\,\langle \tau'^4\tau^4\rangle_{\rm qu}$ contain factors $\vartheta_1(z_1-z_2)^{-\frac{1}{2}}$, which yield signs ambiguities.

Bosonic correlator: The spacetime-coordinate propagators on the annulus and Möbius strip can be expressed in terms of those on the double-cover tori by symmetrizing with respect to the involution. The result is

$$\langle X^\mu(z_1)X_\nu(z_2)\rangle = \delta^\mu_\nu\left[-\alpha'\,\ln\left|\frac{\vartheta_1\,(z_1-z_2)}{\vartheta_1'(0)}\right|^2 + \frac{\alpha' 4\pi\,[{\rm Im}(z_1-z_2)]^2}{\tau_2}\right], \tag{5.6}$$

which can be used to derive

$$\langle e^{ik\cdot X}(z_1)e^{-ik\cdot X}(z_2)\rangle = \left(\left|\frac{\vartheta_1(z_1-z_2)}{\vartheta_1'(0)}\right| e^{-\frac{2\pi[{\rm Im}(z_1-z_2)]^2}{\tau_2}}\right)^{-2\alpha' k^2}. \tag{5.7}$$

Bosonized-fermion correlators: In Ref. [13], it is shown by applying the method of images on the Green's functions used in the stress-tensor method that the correlators of bosonized-fermion on the open-string worldsheets are identical to those on the double-cover tori. They are given in Eq. (4.52). For $q = \pm\frac{1}{2}$, products of two such correlators are well defined up to signs.

5.2 Full expressions of the amplitudes

Putting everything together and defining $z_{12} = z_1 - z_2$ to lighten notations, the full expression (3.14) of the external part of the one-loop two-point function of massless bosonic states

in the ND and DN sectors is, for $\Sigma \in \{\mathcal{A}, \mathcal{M}\}$,

$$\begin{aligned} A^{\alpha_0\beta_0}_{\text{ext}\Sigma} = \alpha' k^2\, \lambda_{\alpha_0\beta_0}\lambda^{\mathrm{T}}_{\beta_0\alpha_0} \left[\left|\frac{\vartheta_1(z_{12})}{\vartheta_1'(0)}\right| e^{-\frac{2\pi}{\tau_2}[\mathrm{Im}(z_{12})]^2}\right]^{-2\alpha' k^2} \frac{1}{\det W\, \vartheta_1(z_{12})^2} \\ \times \sum_{\nu_{\text{ext}}\neq 1} K_{\nu_{\text{ext}},1}\, \vartheta_{\nu_{\text{ext}}}(z_{12}) \sum_{\nu_{\text{int}}} (-1)^{\delta_{\nu_{\text{int}},1}}\, \vartheta_{\nu_{\text{int}}}\Big(\frac{z_{12}}{2}\Big)^2 \\ \times \sum_{\vec{l}'} e^{-\frac{\pi}{\alpha'\tau_2}\sum_{I'}(R_{I'}l_{I'})^2} \left[\sum_{\vec{l}} e^{-\frac{|W_1|^2(|v_2^3|^2+|v_2^4|^2)}{4\pi\alpha' \mathrm{Im}\,(\overline{W}_1 W_2)}}\, \mathcal{C}^{\Sigma\vec{l}'\vec{l}}_{\nu_{\text{int}}} + \sum_{\vec{\tilde{l}}} e^{-\frac{|W_1|^2(|\tilde{v}_2^3|^2+|\tilde{v}_2^4|^2)}{4\pi\alpha' \mathrm{Im}\,(\overline{W}_1 W_2)}}\, \tilde{\mathcal{C}}^{\Sigma\vec{l}'\vec{\tilde{l}}}_{\nu_{\text{int}}}\right], \end{aligned} \tag{5.8}$$

which is independent of the choice of $\epsilon \in \{-1, +1\}$. In this expression, we use the following notations:

- $\vec{l}'$ stands for (l_4, l_5), and $\vec{l}$, $\vec{\tilde{l}}$ are the four-vectors whose components are l_I and $\tilde{l}_I$.
- $\nu_{\text{ext}}, \nu_{\text{int}} \in \{1, 2, 3, 4\}$ denote the spin structures of the worldsheet complex fermions: The former for Ψ^0, Ψ^1 (and Ψ^2), and the latter for Ψ^3, Ψ^4.
- The normalization factor of the external fermion correlators is given by [62]

$$K_{\nu_{\text{ext}},1} = \frac{\vartheta_1'(0)}{\vartheta_{\nu_{\text{ext}}}(0)}\,, \quad \nu_{\text{ext}} \in \{2, 3, 4\}\,, \quad \text{where} \quad \vartheta_1'(0) = -2\pi\eta^3\,. \tag{5.9}$$

- $\mathcal{C}^{\Sigma\vec{l}'\vec{l}}_{\nu_{\text{int}}}$ and $\tilde{\mathcal{C}}^{\Sigma\vec{l}'\vec{\tilde{l}}}_{\nu_{\text{int}}}$ are normalization functions to be determined. They stand for products of the form

$$K_{\nu_{\text{int}},\frac{1}{2}}(\tau^{\text{dc}})^2\, f_{\text{op}}(\tau^{\text{dc}}; \tfrac{1}{2}, \tfrac{1}{2})\, f_{\text{op}}(\tau^{\text{dc}}; \tfrac{1}{2}, \tfrac{1}{2})\,, \tag{5.10}$$

  possibly dressed by signs that may depend on the instanton numbers $\vec{l}, \vec{l}'$ or $\vec{\tilde{l}}, \vec{l}'$. Indeed, as stressed before, pairs of correlators of twist fields as well as pairs of correlators of spin fields yield signs ambiguities. Moreover, for the amplitude computed on the annulus, the normalization functions should contain sums over the free boundary condition denoted γ. Furthermore, $\mathcal{C}^{\mathcal{A}\vec{l}'\vec{0}}_{\nu_{\text{int}}}$ takes into account two contributions associated with the NN and ND worldsheet boundary conditions, while $\tilde{\mathcal{C}}^{\mathcal{A}\vec{l}'\vec{0}}_{\nu_{\text{int}}}$ describes those arising from DD and DN boundary conditions.

Similarly, the internal piece (3.15) of the amplitude is independent of ϵ and can be

expressed in terms of the same normalization functions,

$$
\begin{aligned}
A_{\mathrm{int}\Sigma}^{\alpha_0\beta_0} = &- \frac{s\,i}{\alpha'}\,\lambda_{\alpha_0\beta_0}\lambda^{\mathrm{T}}_{\beta_0\alpha_0}\left[\left|\frac{\vartheta_1(z_{12})}{\vartheta_1'(0)}\right| e^{-\frac{2\pi}{\tau_2}[\mathrm{Im}(z_{12})]^2}\right]^{-2\alpha' k^2} \quad \frac{\vartheta_1(\frac{z_{12}}{2})^2}{\det W\,\vartheta_1(z_{12})^2\,\vartheta_1'(0)} \\
&\times 4\sum_{\nu_{\mathrm{int}}}\vartheta_{\nu_{\mathrm{int}}}\Big(\frac{z_{12}}{2}\Big)^2\sum_{\vec{l}'} e^{-\frac{\pi}{\alpha'\tau_2}\sum_{I'}(R_{I'}l_{I'})^2} \\
&\times\Bigg\{\sum_{\vec{l}} e^{-\frac{|W_1|^2(|v_2^3|^2+|v_2^4|^2)}{4\pi\alpha'\mathrm{Im}\,(\overline{W}_1W_2)}}\mathcal{C}^{\Sigma\vec{l}'\vec{l}}_{\nu_{\mathrm{int}}}\left[\frac{\overline{W}_1^2\,(|v_2^3|^2+|v_2^4|^2)}{8[\mathrm{Im}\,(\overline{W}_1W_2)]^2}+2\alpha'(C+\hat{C})\right] \\
&\quad+\sum_{\vec{l}} e^{-\frac{|W_1|^2(|\tilde{v}_2^3|^2+|\tilde{v}_2^4|^2)}{4\pi\alpha'\mathrm{Im}\,(\overline{W}_1W_2)}}\tilde{\mathcal{C}}^{\Sigma\vec{l}'\vec{l}}_{\nu_{\mathrm{int}}}\left[\frac{\overline{W}_1^2\,(|\tilde{v}_2^3|^2+|\tilde{v}_2^4|^2)}{8[\mathrm{Im}\,(\overline{W}_1W_2)]^2}+2\alpha'(C+\hat{C})\right]\Bigg\}\,,
\end{aligned}
\tag{5.11}
$$

where the factor 4 accounts for the trivial sum over the external-fermion spin structure ν_{ext}, C is given in Eq. (4.47), and we have defined

$$
\hat{C}\equiv\frac{\vartheta_1'(0)^2}{2\,\vartheta_1(\frac{z_{12}}{2})^2}\,F_1(z_1,z_2)\,. \tag{5.12}
$$

In the following, we will not consider anymore in Eqs. (5.8) and (5.11) the irrelevant contributions of the external bosonic correlators, $[\cdots]^{-2\alpha' k^2}$, which are equal to 1 on shell. We stress again that we could have introduced non-trivial Kaluza–Klein momenta along T^2 to avoid ambiguities in extracting information from the amplitude $A_{\mathrm{ext}\Sigma}^{\alpha_0\beta_0}$.

Normalization functions $\mathcal{C}^{\Sigma\vec{l}'\vec{l}}_{\nu_{\mathrm{int}}}$ and $\tilde{\mathcal{C}}^{\Sigma\vec{l}'\vec{l}}_{\nu_{\mathrm{int}}}$: As said in the remark below Eq. (4.22), $\mathcal{C}^{\Sigma\vec{l}'\vec{l}}_{\nu_{\mathrm{int}}}$ and $\tilde{\mathcal{C}}^{\Sigma\vec{l}'\vec{l}}_{\nu_{\mathrm{int}}}$ may be determined by using the fact that when z_1 and z_2 coalesce, the effects of the ground-state boundary-changing operators compensate each other. Hence, the external part of the amplitude reduces, up to a multiplicative factors, to selected pieces of the open-string contributions to the partition function. To identify precisely which pieces are relevant, Fig. 4 shows what the diagrams in Fig. 3 become when $z_{12}\to 0$. In this limit, the cut differential associated with either of the complex directions $u\in\{3,4\}$ becomes trivial, $\omega(z)\to 1$, so that

$$
W_1\underset{z_{12}\to 0}{\longrightarrow}1\,,\qquad W_2\underset{z_{12}\to 0}{\longrightarrow}\tau^{\mathrm{dc}}\,. \tag{5.13}
$$

This leads to

$$
\begin{aligned}
A_{\mathrm{ext}\Sigma}^{\alpha_0\beta_0}\underset{z_{12}\to 0}{\sim}&\frac{3}{2i\pi}\,\alpha' k^2\,\lambda_{\alpha_0\beta_0}\lambda^{\mathrm{T}}_{\beta_0\alpha_0}\,\frac{1}{z_{12}^2}\,\frac{1}{\tau_2\eta^3}\sum_{\nu_{\mathrm{int}}}(-1)^{\delta_{\nu_{\mathrm{int}},1}}\,\vartheta_{\nu_{\mathrm{int}}}^2\,\times \\
&\sum_{\vec{l}'} e^{-\frac{\pi}{\alpha'\tau_2}\sum_{I'}(R_{I'}l_{I'})^2}\left[\sum_{\vec{l}} e^{-\frac{\pi}{\alpha'\tau_2}\sum_{I}(R_{I}l_{I})^2}\mathcal{C}^{\Sigma\vec{l}'\vec{l}}_{\nu_{\mathrm{int}}}+\sum_{\vec{\tilde{l}}} e^{-\frac{\pi\alpha'}{\tau_2}\sum_{I}(\tilde{l}_I/R_I)^2}\tilde{\mathcal{C}}^{\Sigma\vec{l}'\vec{\tilde{l}}}_{\nu_{\mathrm{int}}}\right],
\end{aligned}
\tag{5.14}
$$

which has to be identified with

$$\begin{aligned} &\frac{3}{2i\pi}\,\alpha' k^2\,\lambda_{\alpha_0\beta_0}\lambda^{\mathrm{T}}_{\beta_0\alpha_0}\,\frac{8\mathcal{C}}{z_{12}^2}\times\frac{1}{\tau_2^2}\sum_{\gamma=1}^{32+32}\operatorname*{Str}_{\alpha_0\gamma+\beta_0\gamma}\frac{1}{2}\,\frac{1+g}{2}\,q^{\frac{1}{2}(L_0-1)} \qquad \text{for } \mathcal{A}\,,\\ \text{and}\quad &\frac{3}{2i\pi}\,\alpha' k^2\,\lambda_{\alpha_0\beta_0}\lambda^{\mathrm{T}}_{\beta_0\alpha_0}\,\frac{8\mathcal{C}}{z_{12}^2}\times\frac{1}{\tau_2^2}\operatorname*{Str}_{\alpha_0\alpha_0+\beta_0\beta_0}\frac{\Omega}{2}\,\frac{1+g}{2}\,q^{\frac{1}{2}(L_0-1)} \qquad \text{for } \mathcal{M}\,. \end{aligned} \tag{5.15}$$

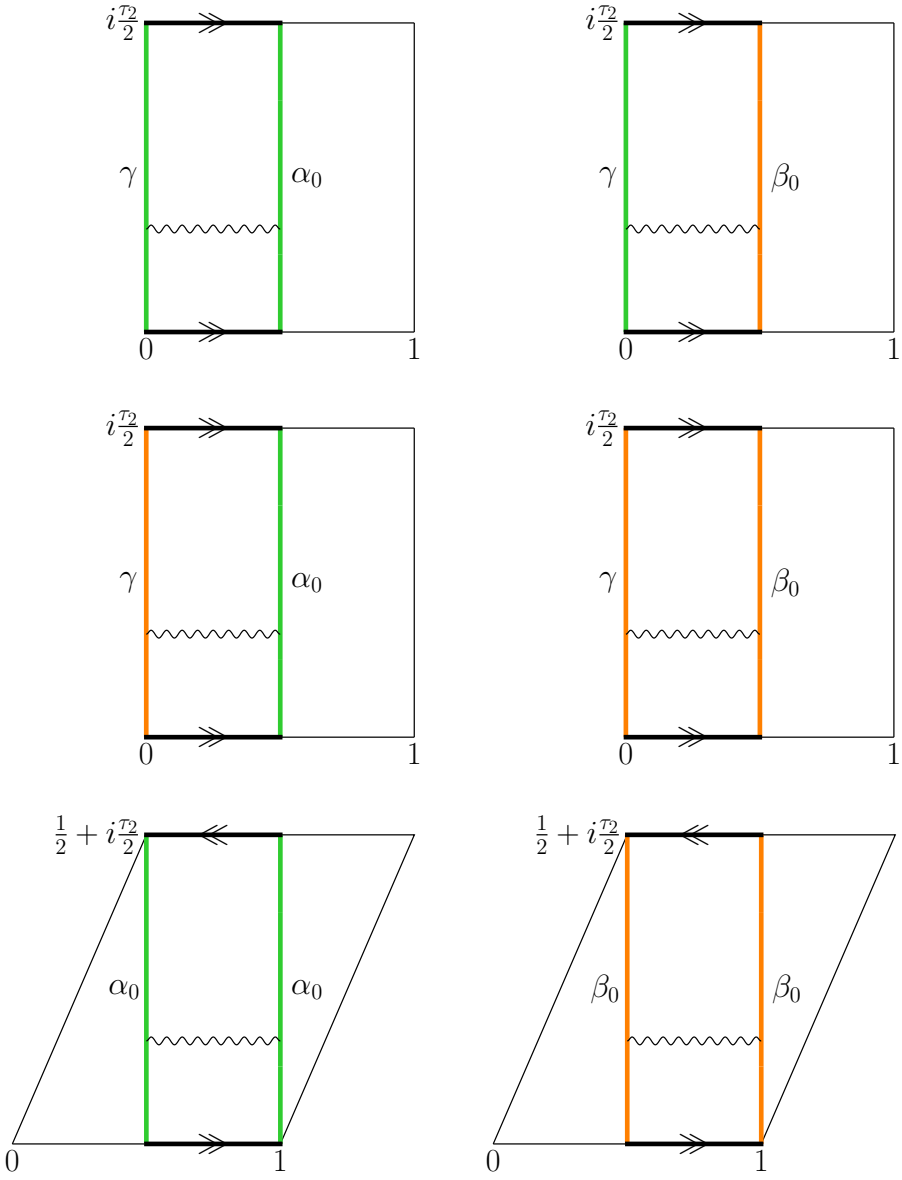

Figure 4: Open-string diagrams of Fig. 3 in the limit $z_{12}\to 0$.

In these expressions, $\mathcal{C}$ is a constant number,[16] while the supertraces are restricted to the open-string modes with ends attached to branes as shown in Fig. 4. For the identification to be possible, one has to switch the T^2, T^4 and $\tilde{T}^4$ lattices in the partition functions $Z_{\mathcal{A}}$ and $Z_{\mathcal{M}}$ from Hamiltonian to instantonic forms, which is done by Poisson summations,

$$\begin{aligned}
\sum_{\vec{m}} P^{(4)}_{\vec{m}+\vec{a}_i-\vec{a}_j} &= \frac{\mathrm{v}_4}{\alpha'^2\,\tau_2^2}\sum_{\vec{l}} e^{-\frac{\pi}{\alpha'\tau_2}\sum_I (R_I l_I)^2} e^{2i\pi\vec{l}\cdot(\vec{a}_i-\vec{a}_j)}\,,\\
\sum_{\vec{m}} W^{(4)}_{\vec{n}+\vec{a}_i-\vec{a}_j} &= \frac{\alpha'^2}{\mathrm{v}_4\,\tau_2^2}\sum_{\vec{\tilde{l}}} e^{-\frac{\pi\alpha'}{\tau_2}\sum_I (\tilde{l}_I/R_I)^2} e^{2i\pi\vec{\tilde{l}}\cdot(\vec{a}_i-\vec{a}_j)}\,,\\
\sum_{\vec{m}'} P^{(2)}_{\vec{m}'+F\vec{a}'_{\rm S}+\vec{a}_{i'}-\vec{a}_{j'}} &= \frac{\mathrm{v}_2}{\alpha'\,\tau_2}\sum_{\vec{l}'} e^{-\frac{\pi}{\alpha'\tau_2}\sum_I (R_{I'} l_{I'})^2} e^{2i\pi\vec{l}'\cdot(\vec{a}_{i'}-\vec{a}_{j'})} e^{2i\pi F\vec{l}'\cdot\vec{a}'_{\rm S}}\,,
\end{aligned} \tag{5.16}$$

where we have defined

$$\mathrm{v}_4 = R_6R_7R_8R_9\,,\qquad \mathrm{v}_2 = R_4R_5\,. \tag{5.17}$$

For the case of the annulus, using the definitions of the characters given in Eq. (B.4), we identify

$$\begin{aligned}
\mathcal{C}_1^{\mathcal{A}\vec{l}'\vec{l}} &= \rho\,\frac{\mathcal{C}}{\tau_2^2\,\eta^3}\,f^{\mathcal{A}\vec{l}'\vec{l}}_{\alpha_0\mathrm{D}}\,, & \tilde{\mathcal{C}}_1^{\mathcal{A}\vec{l}'\vec{l}} &= \rho\,\frac{\mathcal{C}}{\tau_2^2\,\eta^3}\,f^{\mathcal{A}\vec{l}'\vec{l}}_{\beta_0\mathrm{N}}\,,\\
\mathcal{C}_2^{\mathcal{A}\vec{l}'\vec{l}} &= \frac{\mathcal{C}}{\tau_2^2\,\eta^3}\,\frac{\vartheta_3^2}{\vartheta_4^2}\,f^{\mathcal{A}\vec{l}'\vec{l}}_{\alpha_0\mathrm{D}} - \frac{\mathcal{C}\,\vartheta_2^2}{\tau_2^4\,\eta^9}\,f^{\mathcal{A}\vec{l}'\vec{l}}_{\alpha_0\mathrm{N}}\,e^{2i\pi\vec{l}'\cdot\vec{a}'_{\rm S}}\,, & \tilde{\mathcal{C}}_2^{\mathcal{A}\vec{l}'\vec{l}} &= \frac{\mathcal{C}}{\tau_2^2\,\eta^3}\,\frac{\vartheta_3^2}{\vartheta_4^2}\,f^{\mathcal{A}\vec{l}'\vec{l}}_{\beta_0\mathrm{N}} - \frac{\mathcal{C}\,\vartheta_2^2}{\tau_2^4\,\eta^9}\,f^{\mathcal{A}\vec{l}'\vec{l}}_{\beta_0\mathrm{D}}\,e^{2i\pi\vec{l}'\cdot\vec{a}'_{\rm S}}\,,\\
\mathcal{C}_3^{\mathcal{A}\vec{l}'\vec{l}} &= \frac{\mathcal{C}\,\vartheta_3^2}{\tau_2^4\,\eta^9}\,f^{\mathcal{A}\vec{l}'\vec{l}}_{\alpha_0\mathrm{N}} - \frac{\mathcal{C}}{\tau_2^2\,\eta^3}\,\frac{\vartheta_2^2}{\vartheta_4^2}\,f^{\mathcal{A}\vec{l}'\vec{l}}_{\alpha_0\mathrm{D}}\,e^{2i\pi\vec{l}'\cdot\vec{a}'_{\rm S}}\,, & \tilde{\mathcal{C}}_3^{\mathcal{A}\vec{l}'\vec{l}} &= \frac{\mathcal{C}\,\vartheta_3^2}{\tau_2^4\,\eta^9}\,f^{\mathcal{A}\vec{l}'\vec{l}}_{\beta_0\mathrm{D}} - \frac{\mathcal{C}}{\tau_2^2\,\eta^3}\,\frac{\vartheta_2^2}{\vartheta_4^2}\,f^{\mathcal{A}\vec{l}'\vec{l}}_{\beta_0\mathrm{N}}\,e^{2i\pi\vec{l}'\cdot\vec{a}'_{\rm S}}\,,\\
\mathcal{C}_4^{\mathcal{A}\vec{l}'\vec{l}} &= -\frac{\mathcal{C}\,\vartheta_4^2}{\tau_2^4\,\eta^9}\,f^{\mathcal{A}\vec{l}'\vec{l}}_{\alpha_0\mathrm{N}}\,, & \tilde{\mathcal{C}}_4^{\mathcal{A}\vec{l}'\vec{l}} &= -\frac{\mathcal{C}\,\vartheta_4^2}{\tau_2^4\,\eta^9}\,f^{\mathcal{A}\vec{l}'\vec{l}}_{\beta_0\mathrm{D}}\,,
\end{aligned} \tag{5.18}$$

where we have defined

$$\begin{aligned}
f^{\mathcal{A}\vec{l}'\vec{l}}_{\alpha_0\mathrm{N}} &= \frac{\mathrm{v}_2\mathrm{v}_4}{\alpha'^3}\sum_{i,i'} N_{ii'}\,e^{2i\pi\vec{l}\cdot(\vec{a}_{i_0}-\vec{a}_i)} e^{2i\pi\vec{l}'\cdot(\vec{a}_{i'_0}-\vec{a}_{i'})}\,, & f^{\mathcal{A}\vec{l}'\vec{\tilde{l}}}_{\beta_0\mathrm{D}} &= \frac{\mathrm{v}_2\,\alpha'^2}{\alpha'\,\mathrm{v}_4}\sum_{i,i'} D_{ii'}\,e^{2i\pi\vec{\tilde{l}}\cdot(\vec{a}_{j_0}-\vec{a}_i)} e^{2i\pi\vec{l}'\cdot(\vec{a}_{i'_0}-\vec{a}_{i'})}\,,\\
f^{\mathcal{A}\vec{l}'\vec{l}}_{\alpha_0\mathrm{D}} &= \delta_{\vec{l},\vec{0}}\,\frac{\mathrm{v}_2}{\alpha'}\sum_{i,i'} D_{ii'}\,e^{2i\pi\vec{l}'\cdot(\vec{a}_{i'_0}-\vec{a}_{i'})}\,, & f^{\mathcal{A}\vec{l}'\vec{\tilde{l}}}_{\beta_0\mathrm{N}} &= \delta_{\vec{\tilde{l}},\vec{0}}\,\frac{\mathrm{v}_2}{\alpha'}\sum_{i,i'} N_{ii'}\,e^{2i\pi\vec{l}'\cdot(\vec{a}_{i'_0}-\vec{a}_{i'})}\,.
\end{aligned} \tag{5.19}$$

To better understand how the discrete sums and coefficients $N_{ii'}$ and $D_{ii'}$ arise, let us display as an example what the first product of traces in Eq. (2.16) becomes, when restricting to open strings attached (in the T-dual picture) to the D3-brane α_0, and to a D3-brane γ in

[16] It can be determined by replacing in Eq. (3.14) all correlators by their dominant poles, which can be found by the OPE's.

the Neumann sector,

$$\sum_{\substack{i,i'\\ j,j'}} \mathrm{tr}(\gamma_{\mathrm{N},1}^{ii'})\mathrm{tr}(\gamma_{\mathrm{N},1}^{jj'\,-1}) \quad \longrightarrow \quad (\gamma_{\mathrm{N},1}^{i_0 i'_0})_{\alpha_0\alpha_0} \sum_{j,j'} \sum_{\gamma=1}^{N_{jj'}} (\gamma_{\mathrm{N},1}^{jj'\,-1})_{\gamma\gamma} = \sum_{j,j'} N_{jj'}\,. \tag{5.20}$$

On the contrary, all terms associated with the group generator g vanish, due to the fact that the diagonal components of the matrices J_k are zero. In the expressions of $\mathcal{C}_1^{\mathcal{A}\vec{l}'\vec{l}}$ and $\tilde{\mathcal{C}}_1^{\mathcal{A}\vec{l}'\vec{\tilde{l}}}$, we have introduced a coefficient ρ that accounts for the ambiguity arising in their determination, since $\vartheta^2_{\nu_{\mathrm{int}}} = 0$ for $\nu_{\mathrm{int}} = 1$. This coefficient will be determined in the sequel. Finally, notice that the identification has lifted all sign ambiguities associated with the twist- and spin-field correlators. These signs depend on the instanton numbers $\vec{l}'$, $\vec{l}$, $\vec{\tilde{l}}$ and the positions of the D3-branes α_0, β_0, γ.

To perform the similar computation in the Möbius strip case, note that $Z_{\mathcal{M}}$ is expressed in terms of "hatted characters" defined in Eq. (2.19). However, in light-cone gauge, the characters associated with the worldsheet fermions multiplied by $1/\hat{\eta}^8$ arising from the bosonic coordinates yield low-lying states at the massless level. Hence, all phases $e^{-i\pi(h-c/24)}$ appearing in the definitions of the hatted characters cancel each other and we may simply remove all "hats" on the ϑ and η functions when identifying Eq. (5.15) with the amplitude (5.14). In that case, the normalization functions are found to be

$$\begin{aligned}
\mathcal{C}_1^{\mathcal{M}\vec{l}'\vec{l}} &= 0\,, & \tilde{\mathcal{C}}_1^{\mathcal{M}\vec{l}'\vec{\tilde{l}}} &= 0\,,\\
\mathcal{C}_2^{\mathcal{M}\vec{l}'\vec{l}} &= \frac{\mathcal{C}\,\vartheta_2^2}{\tau_2^4\,\eta^9}\,\frac{\mathrm{v}_2\mathrm{v}_4}{\alpha'^3}\,e^{2i\pi\vec{l}'\cdot\vec{a}'_{\mathrm{S}}}\,, & \tilde{\mathcal{C}}_2^{\mathcal{M}\vec{l}'\vec{\tilde{l}}} &= \frac{\mathcal{C}\,\vartheta_2^2}{\tau_2^4\,\eta^9}\,\frac{\mathrm{v}_2\,\alpha'^2}{\alpha'\,\mathrm{v}_4}\,e^{2i\pi\vec{l}'\cdot\vec{a}'_{\mathrm{S}}}\,,\\
\mathcal{C}_3^{\mathcal{M}\vec{l}'\vec{l}} &= -\frac{\mathcal{C}\,\vartheta_3^2}{\tau_2^4\,\eta^9}\,\frac{\mathrm{v}_2\mathrm{v}_4}{\alpha'^3}\,, & \tilde{\mathcal{C}}_3^{\mathcal{M}\vec{l}'\vec{\tilde{l}}} &= -\frac{\mathcal{C}\,\vartheta_3^2}{\tau_2^4\,\eta^9}\,\frac{\mathrm{v}_2\,\alpha'^2}{\alpha'\,\mathrm{v}_4}\,,\\
\mathcal{C}_4^{\mathcal{M}\vec{l}'\vec{l}} &= \frac{\mathcal{C}\,\vartheta_4^2}{\tau_2^4\,\eta^9}\,\frac{\mathrm{v}_2\mathrm{v}_4}{\alpha'^3}\,, & \tilde{\mathcal{C}}_4^{\mathcal{M}\vec{l}'\vec{\tilde{l}}} &= \frac{\mathcal{C}\,\vartheta_4^2}{\tau_2^4\,\eta^9}\,\frac{\mathrm{v}_2\,\alpha'^2}{\alpha'\,\mathrm{v}_4}\,.
\end{aligned} \tag{5.21}$$

For instance, when one restricts to the boundary conditions shown in Fig. 4, the first trace appearing in the expression of $Z_{\mathcal{M}}$ yields,

$$\mathrm{tr}(\gamma_{\mathrm{N},\Omega}^{ii'\,\mathrm{T}}\gamma_{\mathrm{N},\Omega}^{jj'\,-1}) \quad \longrightarrow \quad (\gamma_{\mathrm{N},\Omega}^{i_0 i'_0\,\mathrm{T}})_{\alpha_0\alpha_0}(\gamma_{\mathrm{N},\Omega}^{jj'\,-1})_{\alpha_0\alpha_0} = 1\,. \tag{5.22}$$

On the contrary, all traces in the second line of Eq. (2.20) yield vanishing contributions since the selected diagonal matrix elements are zero.

Consistency when supersymmetry is restored: All normalization functions can be injected back in Eqs. (5.8) and (5.11) to obtain the full expressions of the amplitudes $A^{\alpha_0\beta_0}_{\text{ext}\Sigma}$ and $A^{\alpha_0\beta_0}_{\text{int}\Sigma}$ for arbitrary z_1, z_2. To analyze their structures in more details, let us focus on the instantonic sums. For the internal part of the amplitude computed on the annulus, we obtain for each given $\vec{l}'$, $\vec{l}$ a contribution of the form

$$\begin{aligned}\sum_{\nu_{\text{int}}} \vartheta_{\nu_{\text{int}}}\Big(\frac{z_{12}}{2}\Big)^2 \mathcal{C}^{\mathcal{A}\vec{l}'\vec{l}}_{\nu_{\text{int}}} &= \mathcal{C}\,\frac{f^{\mathcal{A}\vec{l}'\vec{l}}_{\alpha_0\text{N}}}{\tau_2^4\,\eta^9}\left\{\vartheta_3^2\vartheta_3\Big(\frac{z_{12}}{2}\Big)^2 - \vartheta_4^2\vartheta_4\Big(\frac{z_{12}}{2}\Big)^2 - e^{2i\pi\vec{l}'\cdot\vec{a}'_{\text{S}}}\,\vartheta_2^2\vartheta_2\Big(\frac{z_{12}}{2}\Big)^2\right\}\\ &\quad + \mathcal{C}\,\frac{f^{\mathcal{A}\vec{l}'\vec{l}}_{\alpha_0\text{D}}}{\tau_2^2\,\eta^3\,\vartheta_4^2}\left\{\vartheta_3^2\vartheta_2\Big(\frac{z_{12}}{2}\Big)^2 + \rho\,\vartheta_4^2\vartheta_1\Big(\frac{z_{12}}{2}\Big)^2 - e^{2i\pi\vec{l}'\cdot\vec{a}'_{\text{S}}}\,\vartheta_2^2\vartheta_3\Big(\frac{z_{12}}{2}\Big)^2\right\}\\ &= \mathcal{C}\left(1-(-1)^{l_5}\right)\left\{\frac{f^{\mathcal{A}\vec{l}'\vec{l}}_{\alpha_0\text{N}}}{\tau_2^4\,\eta^9}\,\vartheta_2^2\vartheta_2\Big(\frac{z_{12}}{2}\Big)^2 + \frac{f^{\mathcal{A}\vec{l}'\vec{l}}_{\alpha_0\text{D}}}{\tau_2^2\,\eta^3\,\vartheta_4^2}\,\vartheta_2^2\vartheta_3\Big(\frac{z_{12}}{2}\Big)^2\right\}\\ &\quad + \mathcal{C}\,(\rho-1)\,\frac{f^{\mathcal{A}\vec{l}'\vec{l}}_{\alpha_0\text{D}}}{\tau_2^2\,\eta^3}\,\vartheta_1\Big(\frac{z_{12}}{2}\Big)^2,\end{aligned} \tag{5.23}$$

where the second equality is obtained by applying a generalized Jacobi identities [62] with non-zero first arguments, as well as the specific form of the vector $\vec{a}'_{\text{S}}$. For given $\vec{l}'$, $\vec{\tilde{l}}$, the similar sum for the coefficients $\tilde{\mathcal{C}}^{\mathcal{A}\vec{l}'\vec{\tilde{l}}}_{\nu_{\text{int}}}$ is obtained by changing $\alpha_0 \to \beta_0$ and $\text{N} \leftrightarrow \text{D}$. We are now ready to determine the constant ρ by taking the limit $R_5 \to +\infty$ in Eq. (5.11). Indeed, $l_5 = 0$ is the only contribution in the sum over l_5 that survives in this limit. Hence, $A^{\alpha_0\beta_0}_{\text{int}\mathcal{A}}$ vanishes when supersymmetry is restored if and only if $\rho = 1$, since in that case only, Eq. (5.23) projects out all even values of the wrapping number l_5. Indeed, in the supersymmetric case, the effective potential cannot be corrected perturbatively, which implies ρ to be such that the one-loop corrections to the masses we are computing vanish.

We can proceed the same way for the internal part of the amplitude computed on the Möbius strip. For fixed $\vec{l}'$, $\vec{l}$, we have

$$\begin{aligned}\sum_{\nu_{\text{int}}} \vartheta_{\nu_{\text{int}}}\Big(\frac{z_{12}}{2}\Big)^2 \mathcal{C}^{\mathcal{M}\vec{l}'\vec{l}}_{\nu_{\text{int}}} &= \frac{\mathcal{C}\,\text{v}_2\text{v}_4}{\alpha'^3\,\tau_2^4\,\eta^9}\left\{e^{2i\pi\vec{l}'\cdot\vec{a}'_{\text{S}}}\,\vartheta_2^2\vartheta_2\Big(\frac{z_{12}}{2}\Big)^2 - \vartheta_3^2\vartheta_3\Big(\frac{z_{12}}{2}\Big)^2 + \vartheta_4^2\vartheta_4\Big(\frac{z_{12}}{2}\Big)^2\right\}\\ &= -\frac{\mathcal{C}\,\text{v}_2\text{v}_4}{\alpha'^3\,\tau_2^4\,\eta^9}\left(1-(-1)^{l_5}\right)\vartheta_2^2\vartheta_2\Big(\frac{z_{12}}{2}\Big)^2,\end{aligned} \tag{5.24}$$

while for given $\vec{l}'$, $\vec{\tilde{l}}$, the analogous sum for $\tilde{\mathcal{C}}^{\mathcal{M}\vec{l}'\vec{l}}_{\nu_{\text{int}}}$ is obtained by changing $\text{v}_4/\alpha'^2 \to \alpha'^2/\text{v}_4$. In the limit $R_5 \to +\infty$ where supersymmetry is restored, the amplitude $A^{\alpha_0\beta_0}_{\text{int}\mathcal{M}}$ vanishes consistently.

As can be seen from Eqs. (5.8) and (5.11), the sums over the spin structure ν_{int} in the external and internal parts of the amplitudes are identical, up to the insertion of the sign

$(-1)^{\delta_{\nu_{\rm int},1}}$ for $A^{\alpha_0\beta_0}_{{\rm ext}\Sigma}$. Of course, this does not make any difference in the case of the Möbius strip since the normalization functions for $\nu_{\rm int} = 1$ vanish. On the contrary, for $\Sigma = \mathcal{A}$, the extra sign amounts to changing $\rho \to -\rho$ in Eq. (5.23). As a result, the external part of the amplitude, $A^{\alpha_0\beta_0}_{{\rm ext}\mathcal{A}}$, does not vanish in the decompactification limit, and yields a one-loop correction to the Kähler potential of the massless scalars in the ND+DN sector, even in the supersymmetric case.

Integration over the moduli and vertex positions: What remains to be done is to integrate the amplitudes over the moduli of the open-string surfaces and vertex operator positions modulo the conformal Killing group [63]. The moduli of $\mathcal{A}$ and $\mathcal{M}$ are the imaginary parts of the Teichmüller parameters of the double-cover tori, $\mathrm{Im}\,\tau^{\rm dc}$. Moreover, instead of integrating over the locations of both insertion points and dividing by the volume of the conformal Killing group, we may simply fix to an arbitrary value the position of one vertex operator, say $z_2 \equiv \frac{1}{2}$, and integrate over the location of the other.

In the case of the annulus, both vertices must be located on the same boundary, so that $z_1 \equiv \frac{1}{2} + iy_1$. As a result, denoting the integrated amplitudes by calligraphic letters, the internal part reads

$$\mathcal{A}^{\alpha_0\beta_0}_{{\rm int}\mathcal{A}} = \int_0^{+\infty} \mathrm{d}\,\mathrm{Im}\,\tau^{\rm dc} \int_0^{\mathrm{Im}\,\tau^{\rm dc}} \mathrm{d}y_1\; A^{\alpha_0\beta_0}_{{\rm int}\mathcal{A}}\Big|_{\frac{1}{2}+iy_1,\frac{1}{2}}\,, \tag{5.25}$$

and likewise for the external amplitude. Similarly, for the two-point function computed on the Möbius strip, z_1 must follow the entire boundary. However, the latter being twice longer than the one considered on the annulus, z_1 can actually be parametrized as $z_1 = x_1 + iy_1$, where $x_1 \in \{0, \frac{1}{2}\}$. As a result, the internal part of the integrated amplitude is

$$\mathcal{A}^{\alpha_0\beta_0}_{{\rm int}\mathcal{M}} = \int_0^{+\infty} \mathrm{d}\,\mathrm{Im}\,\tau^{\rm dc} \int_0^{\mathrm{Im}\,\tau^{\rm dc}} \mathrm{d}y_1 \left(A^{\alpha_0\beta_0}_{{\rm int}\mathcal{M}}\Big|_{\frac{1}{2}+iy_1,\frac{1}{2}} + A^{\alpha_0\beta_0}_{{\rm int}\mathcal{M}}\Big|_{iy_1,\frac{1}{2}} \right), \tag{5.26}$$

and similarly for the external part.

In these forms, the full two-point functions are not particularly illuminating, while performing explicitly the integrals is certainly a hard task. Hence, our goal in the next section is to extract simpler answers valid in the case where the scale of supersymmetry breaking is low.

6 Limit of low supersymmetry breaking scale

The analysis of Ref. [32] is valid in regions of moduli space where the supersymmetry breaking scale $M_{3/2}$ is lower than all other non-vanishing scales present in the model. The reason of this restriction is that extrema of the one-loop effective potential are then easily found, and correspond in the open-string sector to distributing all D3-branes (in the T-dual pictures) on O3-planes. In such a case, the squared masses acquired at one loop by the moduli fields arising from the NN and DD sectors take particularly simple forms, up to exponentially suppressed corrections of order $e^{-\pi \frac{cM_{\rm s}}{M_{3/2}}}$, in the notations of Eq. (1.1). In practice, the fact that $M_{3/2}$ is lower than the string scale as well as all other scales generated by compactification means that, effectively, the dominant contributions of the effective potential and masses derived in Ref. [32] match those found in a Kaluza–Klein field theory in $4+1$ dimensions.

In the present section, we would like to find similar results for the masses of the moduli fields present in the ND+DN sector of the theory. This will be done by imposing all mass scales other than $M_{3/2}$ to be proportional to $M_{\rm s} = 1/\sqrt{\alpha'}$ and then taking the small α' limit.

6.1 Limit of super heavy oscillator states

In order to treat all massive string-oscillator states as super heavy in the Hamiltonian forms of the partition functions, let us rescale the Teichmüller parameters of the open-string surfaces as follows[17]

$$\mathrm{Im}\,\tau^{\rm dc} \equiv \frac{\tau_2}{2} \equiv \frac{t}{2\pi\alpha'} \gg 1\,, \quad \text{where} \quad t \in (0,+\infty)\,. \tag{6.1}$$

Physically, this amounts to stretching the surfaces along their proper times in order to look like field-theory worldlines with topology of a circle. The main practical consequence of the rescaling is the approximation

$$\begin{aligned} \vartheta_1(z) &\equiv -2\, q_{\rm dc}^{\frac{1}{8}} \sin(\pi z) \prod_{n\geq 1} \left[(1-q_{\rm dc}^n)(1-q_{\rm dc}^n z^{-2i\pi z})(1-q_{\rm dc}^n z^{2i\pi z})\right], \quad q_{\rm dc} \equiv e^{2i\pi\tau^{\rm dc}}\,, \\ &= -2\, q_{\rm dc}^{\frac{1}{8}} \sin(\pi z)(1+\cdots)\,, \quad \text{when} \quad |\mathrm{Im}\, z| < \mathrm{Im}\,\tau^{\rm dc}\,, \end{aligned} \tag{6.2}$$

where from now on, ellipses stand for terms exponentially suppressed when $\alpha' \to 0$, *i.e.* of order $e^{-L^2/\alpha'}$ for lengths $L > 0$. In particular, the cut differential associated with the

[17] This rescaling also implies that the imaginary parts of τ and $2i\tau_2$, the Teichmüller parameters of the torus and Klein bottle, are large. Hence, the massive oscillator states are super heavy also in the closed-string sector.

complex directions $u \in \{3,4\}$ becomes

$$\omega(z) = \frac{\sin\Big(\pi(z-\frac{z_1+z_2}{2})\Big)}{\sin\Big(\pi(z-z_1)\Big)^{\frac{1}{2}}\,\sin\Big(\pi(z-z_2)\Big)^{\frac{1}{2}}} + \cdots\,, \quad \text{when} \quad |\mathrm{Im}\, z|,\, y_1,\, y_2 < \mathrm{Im}\,\tau^{\mathrm{dc}}\,. \tag{6.3}$$

Periodicity $z \to z+1$ remains explicit, while periodicity $z \to z+\tau^{\mathrm{dc}}$ is hidden in the ellipsis. Notice that compared to Eq. (5.1), we impose y_1, y_2 to be strictly lower than $\mathrm{Im}\,\tau^{\mathrm{dc}}$ for the above formula to always be valid. More generally, throughout the derivations to come, we will write formulas in their generic forms. Indeed, because in the end all quantities will have to be integrated, taking into account extra contributions arising only at special values of the integration variables results in subdominant corrections for small α'. We will come back to this issue at the end of this section.

Keeping this in mind, we redefine

$$y_A \equiv u_A\,\mathrm{Im}\,\tau^{\mathrm{dc}} = \frac{t\,u_A}{2\pi\alpha'} \gg 1\,, \quad u_A \in (0,1)\,, \quad A \in \{1,2\}\,, \qquad \text{and} \qquad u \equiv |u_1-u_2|\,, \tag{6.4}$$

in terms of which the components of the cut-period matrix can be expressed like

$$\begin{aligned} &W_1 = 1 + \cdots\,,\\ &W_2 = \tau^{\mathrm{dc}} - \xi(z_1-z_2) + \frac{i}{\pi}\ln 4 + \cdots\,, \quad \text{where} \quad \xi \equiv \mathrm{sign}\,(y_1-y_2)\,. \end{aligned} \tag{6.5}$$

The first expression is easily found by integrating over z finite along γ_1 and replacing all sines in Eq. (6.3) by their dominant exponentials when $\mathrm{Im}\,\tau^{\mathrm{dc}}$ is large. By contrast, W_2 can be derived by integrating z between x_0 and $x_0+\tau^{\mathrm{dc}}$, $x_0 \in \mathbb{R}$, using a primitive of ω in its form given in Eq. (6.3). As a result, we obtain that

$$\mathrm{Im}\,(\overline{W}_1 W_2) = \frac{t(1-u)}{2\pi\alpha'} + \frac{\ln 4}{\pi} + \cdots\,. \tag{6.6}$$

When taking the limit of small α' in Eq. (5.23), it turns out that the terms proportional to $f_{\alpha_0\mathrm{D}}^{\mathcal{A}\vec{l}'\vec{l}}$ (and $f_{\beta_0\mathrm{N}}^{\mathcal{A}\vec{l}'\vec{\bar{l}}}$ for the formula involving $\tilde{\mathcal{C}}_{\nu_{\mathrm{int}}}^{\mathcal{A}\vec{l}'\vec{\bar{l}}}$) are exponentially suppressed. Notice that they arise from the ND and DN sectors of the partition function $Z_{\mathcal{A}}$, which therefore cease to contribute to the amplitudes in this limit. In the case of the annulus, we then arrive at the expression

$$A_{\mathrm{int}\,\mathcal{A}}^{\alpha_0\beta_0} = -\,4\mathcal{C}s\,\lambda_{\alpha_0\beta_0}\lambda^{\mathrm{T}}_{\beta_0\alpha_0}\sum_{\vec{l}'} e^{-\frac{\pi^2}{t}\sum_{I'}(R_{I'}l_{I'})^2}\sum_{\vec{l}} e^{-\frac{\pi^2}{t(1-u)+\alpha'(2\ln 4+\cdots)}\sum_I (R_I l_I)^2}\,\times$$

$$\Big(1-(-1)^{l_5}\Big)\,2\pi^3\,\frac{\alpha'^4}{t^4}\,\frac{\mathrm{v}_2\mathrm{v}_4}{\alpha'^3}\,\sum_{ii'}N_{ii'}\,e^{2i\pi\vec{l}\cdot(\vec{a}_{i_0}-\vec{a}_i)}e^{2i\pi\vec{l}'\cdot(\vec{a}_{i'_0}-\vec{a}_{i'})}\times \tag{6.7}$$
$$\frac{\pi}{t(1-u)+\alpha'(2\ln 4+\cdots)}\left[\frac{\pi^4\,\alpha'^2}{[t(1-u)+\alpha'(2\ln 4+\cdots)]^2}\sum_J(R_Jl_J)^2+2\alpha'(C+\hat{C})\right]$$
$$+\,(\vec{l},i_0,N_{ii'},R_I)\to(\vec{\tilde{l}},j_0,D_{ii'},\alpha'/R_I)+\cdots\,,$$

while for the Möbius strip we obtain

$$A^{\alpha_0\beta_0}_{\mathrm{int}\mathcal{M}}=4\mathcal{C}s\,\lambda_{\alpha_0\beta_0}\lambda^{\mathrm{T}}_{\beta_0\alpha_0}\,\sum_{\vec{l}'}e^{-\frac{\pi^2}{t}\sum_{I'}(R_{I'}l_{I'})^2}\,\sum_{\vec{l}}e^{-\frac{\pi^2}{t(1-u)+\alpha'(2\ln 4+\cdots)}\sum_I(R_Il_I)^2}\times$$
$$\Big(1-(-1)^{l_5}\Big)\,2\pi^3\,\frac{\alpha'^4}{t^4}\,\frac{\mathrm{v}_2\mathrm{v}_4}{\alpha'^3}\times \tag{6.8}$$
$$\frac{\pi}{t(1-u)+\alpha'(2\ln 4+\cdots)}\left[\frac{\pi^4\,\alpha'^2}{[t(1-u)+\alpha'(2\ln 4+\cdots)]^2}\sum_J(R_Jl_J)^2+2\alpha'(C+\hat{C})\right]$$
$$+\,(\vec{l},R_I)\to(\vec{\tilde{l}},\alpha'/R_I)+\cdots\,.$$

In the above formulas, the limit of small α' in C and $\hat{C}$ will be derived in Sects. 6.3 and 6.4.

6.2 Limits of large compactification scales

We would like now to have all compactification mass scales other than $M_{3/2}$ very large. In practice, this amounts to taking small radii R_4, R_I and dual radii α'/R_I limits. In order to avoid having to consider very large instanton numbers in such a regime, it is convenient to apply Poisson summations over l_4, $\vec{l}$ and $\vec{\tilde{l}}$ [62], which lead for $\Sigma=\mathcal{A}$ to

$$\begin{aligned}A^{\alpha_0\beta_0}_{\mathrm{int}\mathcal{A}}=&-16\mathcal{C}s\sqrt{\pi}\,\lambda_{\alpha_0\beta_0}\lambda^{\mathrm{T}}_{\beta_0\alpha_0}\,\frac{\alpha'^3R_5}{t^{\frac{7}{2}}}\,\sum_{l_5}e^{-\frac{\pi^2}{t}R_5^2(2l_5+1)^2}\,\sum_{ii'}N_{ii'}\,e^{2i\pi(a^5_{i_0}-a^5_{i'})}\\
&\times\sum_{m_4}e^{-t\left(\frac{m_4+a^4_{i'_0}-a^4_{i'}}{R_4}\right)^2}\,\sum_{\vec{m}}e^{-[t(1-u)+\alpha'(2\ln 4+\cdots)]\sum_I\left(\frac{m_I+a^I_{i_0}-a^I_i}{R_I}\right)^2}\\
&\times\left\{\pi^3\left[2-[t(1-u)+\alpha'(2\ln 4+\cdots)]\sum_J\left(\frac{m_J+a^J_{i_0}-a^J_i}{R_J}\right)^2\right]\right.\\
&\left.+\,2\pi\left[\frac{t(1-u)}{\alpha'}+2\ln 4+\cdots\right](C+\hat{C})\right\}\\
&+\,(\vec{m},i_0,N_{ii'},R_I)\to(\vec{n},j_0,D_{ii'},\alpha'/R_I)+\cdots\,,\end{aligned} \tag{6.9}$$

and for $\Sigma = \mathcal{M}$

$$\begin{aligned} A^{\alpha_0\beta_0}_{\text{int}\mathcal{M}} = & 16\mathcal{C}s\sqrt{\pi}\,\lambda_{\alpha_0\beta_0}\lambda^{\mathrm{T}}_{\beta_0\alpha_0}\,\frac{\alpha'^3 R_5}{t^{\frac{7}{2}}}\,\sum_{l_5} e^{-\frac{\pi^2}{t}R_5^2(2l_5+1)^2} \\ & \times \sum_{m_4} e^{-t(\frac{m_4}{R_4})^2}\,\sum_{\vec{m}} e^{-[t(1-u)+\alpha'(2\ln 4+\cdots)]\sum_I(\frac{m_I}{R_I})^2} \\ & \times \Bigg\{\pi^3\Bigg[2-[t(1-u)+\alpha'(2\ln 4+\cdots)]\sum_J\left(\frac{m_J}{R_J}\right)^2\Bigg] \\ & \quad + 2\pi\left[\frac{t(1-u)}{\alpha'}+2\ln 4+\cdots\right](C+\hat{C})\Bigg\} \\ & + (\vec{m},R_I)\to(\vec{n},\alpha'/R_I)+\cdots\,. \end{aligned} \tag{6.10}$$

One may think that considering T^4 to be small would imply having the T-dual torus $\tilde{T}^4$ large. This is not true, as can be seen by redefining the radii as follows,

$$R_4 = r_4\sqrt{\alpha'}\,, \qquad R_I = r_I\sqrt{\alpha'}\,, \qquad \frac{\alpha'}{R_I} = \frac{\sqrt{\alpha'}}{r_I}\,, \tag{6.11}$$

where r_4, r_I are fixed and dimensionless. Indeed, all radii and dual radii vanish as $\alpha' \to 0$. As a consequence, the limit of small R_4 implies that we may restrict the dominant term in $A^{\alpha_0\beta_0}_{\text{int}\mathcal{A}}$ to $m_4 = 0$ and $i' \in \{i'_0, \hat{\imath}'_0\}$, where

$$\hat{\imath}'_0 \text{ is the fixed point in } \tilde{T}^2 \text{ that faces } i'_0 \text{ along the direction } \tilde{X}^5 \tag{6.12}$$

in the T-dual pictures. Similarly, the limits of small R_I and α'/R_I force $\vec{m} = 0$, $i = i_0$ on the one hand, and $\vec{n} = 0$, $i = j_0$ on the other hand. All other contributions can be absorbed in the ellipsis. In total, we obtain for the amplitude computed on the annulus

$$\begin{aligned} A^{\alpha_0\beta_0}_{\text{int}\mathcal{A}} = & -16\mathcal{C}s\sqrt{\pi}\,\lambda_{\alpha_0\beta_0}\lambda^{\mathrm{T}}_{\beta_0\alpha_0}\,\frac{\alpha'^3 R_5}{t^{\frac{7}{2}}}\,\sum_{l_5} e^{-\frac{\pi^2}{t}R_5^2(2l_5+1)^2}\left(N_{i_0 i'_0} - N_{i_0\hat{\imath}'_0} + D_{j_0 i'_0} - D_{j_0\hat{\imath}'_0}\right) \\ & \times\left\{2\pi^3 + 2\pi\left[\frac{t(1-u)}{\alpha'}+2\ln 4+\cdots\right](C+\hat{C})\right\}+\cdots\,, \end{aligned} \tag{6.13}$$

while on the Möbius strip we have similarly

$$\begin{aligned} A^{\alpha_0\beta_0}_{\text{int}\mathcal{M}} = & 16\mathcal{C}s\sqrt{\pi}\,\lambda_{\alpha_0\beta_0}\lambda^{\mathrm{T}}_{\beta_0\alpha_0}\,\frac{\alpha'^3 R_5}{t^{\frac{7}{2}}}\,\sum_{l_5} e^{-\frac{\pi^2}{t}R_5^2(2l_5+1)^2}\,(1+1) \\ & \times\left\{2\pi^3 + 2\pi\left[\frac{t(1-u)}{\alpha'}+2\ln 4+\cdots\right](C+\hat{C})\right\}+\cdots\,. \end{aligned} \tag{6.14}$$

6.3 Limit $\alpha' \to 0$ of U_1 and $F_1(z, z_2)$

In this subsection and the following, our aim is to derive the limits of C and $\hat{C}$ for small α', *i.e.* the contributions arising from parts (2) of the correlators $\langle \tau^u \tau'^u \rangle_{\rm qu} = \langle \tau'^u \tau^u \rangle_{\rm qu}$. Because the results can be obtained with no more effort for any Teichmüller parameter, we will keep the real part of $\tau^{\rm dc}$ arbitrary, and z_1, z_2 will be chosen anywhere in the torus represented by $\mathcal{P}$ in the complex plane, where

$$\mathcal{P} \text{ is the parallelogram with corners at 0, 1 and } \tau^{\rm dc}\,. \tag{6.15}$$

The important thing, though, is that Eqs. (6.1) and (6.4) hold. Hence, our computations of parts (2) are valid for excited twist fields (for closed strings) and excited boundary-changing fields (for open strings). Let us start by deriving the limits of U_1 and $F_1(z, z_2)$, which will be used in the next subsection to derive those of C and $\hat{C}$.

U_1 when $\alpha' \to 0$: The function $F_1(z, w)$ defined in Eq. (4.45) involves U_1 which is a root of

$$\Omega(U) \equiv \partial_z F_1(z, w)|_{z=w} = \frac{\vartheta_1'}{\vartheta_1}(U) + \frac{\vartheta_1'}{\vartheta_1}(Y_1 - U)\,, \quad \text{where} \quad Y_1 = -\frac{z_{12}}{2}\,. \tag{6.16}$$

To see that this definition makes sense, notice that the meromorphic function $\Omega(U)$ is doubly periodic on the genus-1 Riemann surface Σ, with two simple poles at $U = 0$ and $U = Y_1$. Therefore, it has two simple zeros. Denoting one of them U_1, the second is $Y_1 - U_1$.[18]

When considering the limit $\alpha' \to 0$ in the equation $\Omega(U_1) = 0$, a difficulty we have to face is the following: If we look for U_1 such that $0 < \operatorname{Im} U_1 < \operatorname{Im} \tau^{\rm dc}$, using the fact that $|\operatorname{Im} Y_1| < \frac{1}{2} \operatorname{Im} \tau^{\rm dc}$ we obtain that

$$-\frac{3}{2} \operatorname{Im} \tau^{\rm dc} < \operatorname{Im} (Y_1 - U_1) < \frac{1}{2} \operatorname{Im} \tau^{\rm dc}\,. \tag{6.17}$$

Hence, it is not clear when we can apply Eq. (6.2) or not. For this reason, let us consider two cases:

- When $0 < \operatorname{Im} Y_1 < \frac{1}{2} \operatorname{Im} \tau^{\rm dc}$, we obtain that $|\operatorname{Im} (Y_1 - U_1)| < \frac{1}{2} \operatorname{Im} \tau^{\rm dc}$ which allows to write

$$\begin{aligned} 0 = \Omega(U_1) &= \pi \Big(\cot(\pi U_1) + \cot[\pi(Y_1 - U_1)] \Big) + \cdots \\ &= \pi \, \frac{\sin(\pi Y_1)}{\sin(\pi U_1) \sin[\pi(Y_1 - U_1)]} + \cdots\,. \end{aligned} \tag{6.18}$$

[18] It is understood that poles and zeros are defined modulo 1 and $\tau^{\rm dc}$.

For the right-hand side to vanish when $\alpha' \to 0$, we see that U_1 must satisfy $\mathrm{Im}\, U_1 \to +\infty$ and $\mathrm{Im}\,(Y_1 - U_1) < 0$. To determine U_1 more precisely, let us keep the first subdominant term in the ellipsis of Eq. (6.18), which is $2i\pi\, q_{\mathrm{dc}}\, e^{-2i\pi U_1}$.[19] In that case, the equation becomes

$$i \sin(\pi Y_1) = 2 \sin(\pi U_1) \sin[\pi(Y_1 - U_1)]\, q_{\mathrm{dc}}\, e^{-2i\pi U_1}(1 + \cdots)\,, \tag{6.19}$$

which implies the asymptotic equivalence

$$-e^{-i\pi Y_1} \underset{\alpha' \to 0}{\sim} e^{-i\pi U_1}\, e^{i\pi(Y_1 - U_1)}\, q_{\mathrm{dc}}\, e^{-2i\pi U_1}\,. \tag{6.20}$$

Redefining

$$U_1 \equiv \frac{\tau^{\mathrm{dc}} + Y_1}{2} + \frac{1}{4} + \frac{m}{2} + \varepsilon \quad \text{for some } m \in \mathbb{Z}\,, \quad \text{with} \quad |\mathrm{Re}\,\varepsilon| < \frac{1}{2}\,, \tag{6.21}$$

Eq. (6.20) shows that $\varepsilon \to 0$ when $\alpha' \to 0$.

- When $-\frac{1}{2}\,\mathrm{Im}\,\tau^{\mathrm{dc}} < \mathrm{Im}\, Y_1 < 0$, we can apply the change of variable (6.21) which yields

$$-\frac{3}{4}\,\mathrm{Im}\,\tau^{\mathrm{dc}} - \mathrm{Im}\,\varepsilon < \mathrm{Im}\,(Y_1 - U_1) < -\frac{1}{2}\,\mathrm{Im}\,\tau^{\mathrm{dc}} - \mathrm{Im}\,\varepsilon\,. \tag{6.22}$$

Hence, assuming that ε is bounded when $\alpha' \to 0$, Eq. (6.18) is legitimate for small enough α'. However, the first dominant term in the ellipsis is now $-2i\pi\, q_{\mathrm{dc}}\, e^{2i\pi(Y_1 - U_1)}$,[19] and the equation becomes

$$i \sin(\pi Y_1) = -2 \sin(\pi U_1) \sin[\pi(Y_1 - U_1)]\, q_{\mathrm{dc}}\, e^{2i\pi(Y_1 - U_1)}(1 + \cdots)\,. \tag{6.23}$$

Hence, we obtain that

$$e^{i\pi Y_1} \underset{\alpha' \to 0}{\sim} -e^{-i\pi U_1}\, e^{i\pi(Y_1 - U_1)}\, q_{\mathrm{dc}}\, e^{2i\pi(Y_1 - U_1)}\,, \tag{6.24}$$

which is equivalent to Eq. (6.20) and leads to $\varepsilon \to 0$ when $\alpha' \to 0$. The assumption on the boundedness of ε being consistent, we have also found solutions in the present case.

In both instances, ε can be expressed in terms of exponentially suppressed contributions subdominant to those we have taken into account explicitly. Its leading behavior is derived in Appendix C.

[19] It can be found from Eq. (C.2) where the function H is defined in Eq. (C.1).

By imposing U_1 to be located in $\mathcal{P}$, we find the two roots of $\Omega(U)$,

$$U_1 = \frac{\tau^{\rm dc}+Y_1}{2} + \frac{1}{4} + \cdots \quad \text{or} \quad \frac{\tau^{\rm dc}+Y_1}{2} + \frac{3}{4} + \cdots . \tag{6.25}$$

Since we know that there cannot be other solutions modulo 1 and $\tau^{\rm dc}$, a cross-check of this result is to observe that $Y_1 - U_1$ satisfies consistently

$$Y_1 - U_1 + 1 + \tau^{\rm dc} = \frac{\tau^{\rm dc}+Y_1}{2} + \frac{3}{4} + \cdots \quad \text{or} \quad \frac{\tau^{\rm dc}+Y_1}{2} + \frac{1}{4} + \cdots . \tag{6.26}$$

$F_1(z, z_2)$ when $\alpha' \to 0$: Both possible choices of U_1 yield the same function $F_1(z,w)$. What we need to analyze in order to derive the limits of C and $\hat{C}$ is its expression for $w = z_2$,

$$F_1(z,z_2) = \frac{\vartheta_1\Big(z + \frac{\tau^{\rm dc}}{2} - \frac{1}{4}\,z_1 - \frac{3}{4}\,z_2 + \frac{1}{4} + \cdots\Big)\,\vartheta_1\Big(z - \frac{\tau^{\rm dc}}{2} - \frac{1}{4}\,z_1 - \frac{3}{4}\,z_2 - \frac{1}{4} + \cdots\Big)}{\vartheta_1\Big(\frac{\tau^{\rm dc}}{2} - \frac{z_{12}}{4} + \frac{1}{4} + \cdots\Big)\,\vartheta_1\Big(-\frac{\tau^{\rm dc}}{2} - \frac{z_{12}}{4} - \frac{1}{4} + \cdots\Big)}\,, \tag{6.27}$$

where $z \equiv x + iy \in \mathcal{P}$, and $x,\ y \in \mathbb{R}$. Notice that Eq. (6.2) can be applied to both ϑ_1 functions appearing in the denominator (for small enough α').

For $0 < \frac{1}{2}\,y_1 + \frac{3}{2}\,y_2 < \operatorname{Im}\tau^{\rm dc}$, the second ϑ_1 function in the numerator fulfils the hypothesis of Eq. (6.2), while the first one requires more scrutiny:

- When $0 < y < \frac{1}{2}\operatorname{Im}\tau^{\rm dc} + \frac{1}{4}\,y_1 + \frac{3}{4}\,y_2$, Eq. (6.2) applies to the first ϑ_1.
- When $\frac{1}{2}\operatorname{Im}\tau^{\rm dc} + \frac{1}{4}\,y_1 + \frac{3}{4}\,y_2 < y < \operatorname{Im}\tau^{\rm dc}$, we have (for small enough α')

  $$\operatorname{Im}\tau^{\rm dc} < \operatorname{Im}\left(z + \frac{\tau^{\rm dc}}{2} - \frac{1}{4}\,z_1 - \frac{3}{4}\,z_2 + \frac{1}{4} + \cdots\right) < \frac{3}{2}\operatorname{Im}\tau^{\rm dc}\,, \tag{6.28}$$

  which shows that we have to multiply the second line of Eq. (6.2) by an extra factor $-q_{\rm dc}e^{-2i\pi z}$ to apply it to the first ϑ_1 function in the numerator of Eq. (6.27).

In the end, we obtain that

$$\begin{aligned} &\text{when} \quad 0 < \tfrac{1}{2}\,y_1 + \tfrac{3}{2}\,y_2 < \operatorname{Im}\tau^{\rm dc}\,, \quad \text{then} \\ &F_1(z,z_2) = \begin{cases} 1 + \cdots & \text{if} \ \ 0 < y < \frac{1}{2}\operatorname{Im}\tau^{\rm dc} + \frac{1}{4}\,y_1 + \frac{3}{4}\,y_2\,, \\ e^{-4i\pi(z - \frac{\tau^{\rm dc}}{2} - \frac{1}{4}z_1 - \frac{3}{4}z_2)}\,(1 + \cdots) & \text{if} \ \ \frac{1}{2}\operatorname{Im}\tau^{\rm dc} + \frac{1}{4}\,y_1 + \frac{3}{4}\,y_2 < y < \operatorname{Im}\tau^{\rm dc}\,. \end{cases} \end{aligned} \tag{6.29}$$

Conversely, for $\operatorname{Im}\tau^{\rm dc} < \frac{1}{2}\,y_1 + \frac{3}{2}\,y_2 < 2\operatorname{Im}\tau^{\rm dc}$, it is the first ϑ_1 function in the numerator that satisfies the condition of validity of Eq. (6.2), while for the second one we have to consider two possibilities:

- When $\frac{1}{4}\,y_1 + \frac{3}{4}\,y_2 - \frac{1}{2}\,\mathrm{Im}\,\tau^{\mathrm{dc}} < y < \mathrm{Im}\,\tau^{\mathrm{dc}}$, Eq. (6.2) applies to this ϑ_1 function.
- When $0 < y < \frac{1}{4}\,y_1 + \frac{3}{4}\,y_2 - \frac{1}{2}\,\mathrm{Im}\,\tau^{\mathrm{dc}}$, we have (for small enough α')

$$-\frac{3}{2}\,\mathrm{Im}\,\tau^{\mathrm{dc}} < \mathrm{Im}\left(z - \frac{\tau^{\mathrm{dc}}}{2} - \frac{1}{4}\,z_1 - \frac{3}{4}\,z_2 - \frac{1}{4} + \cdots\right) < -\frac{1}{2}\,\mathrm{Im}\,\tau^{\mathrm{dc}}\,. \tag{6.30}$$

  Hence, the second line of Eq. (6.2) must contain an extra factor $-q_{\mathrm{dc}}e^{2i\pi z}$ to apply it to the second ϑ_1 function in the numerator of $F_1(z, z_2)$.

All in all,

$$\begin{aligned}&\text{when}\quad \mathrm{Im}\,\tau^{\mathrm{dc}} < \tfrac{1}{2}\,y_1 + \tfrac{3}{2}\,y_2 < 2\,\mathrm{Im}\,\tau^{\mathrm{dc}}\,,\quad \text{then}\\ &F_1(z, z_2) = \begin{cases} e^{4i\pi(z - \frac{1}{4}z_1 - \frac{3}{4}z_2 + \frac{\tau^{\mathrm{dc}}}{2})}\,(1 + \cdots) & \text{if}\ \ 0 < y < \frac{1}{4}\,y_1 + \frac{3}{4}\,y_2 - \frac{1}{2}\,\mathrm{Im}\,\tau^{\mathrm{dc}}\,, \\ 1 + \cdots & \text{if}\ \ \frac{1}{4}\,y_1 + \frac{3}{4}\,y_2 - \frac{1}{2}\,\mathrm{Im}\,\tau^{\mathrm{dc}} < y < \mathrm{Im}\,\tau^{\mathrm{dc}}\,. \end{cases}\end{aligned} \tag{6.31}$$

6.4 Limit $\alpha' \to 0$ of C and $\hat{C}$

We are now ready to evaluate the limits of C and $\hat{C}$ for small α'.

$\hat{C}$ when $\alpha' \to 0$: The expression of $\hat{C}$ given in Eq. (5.12) involves $F_1(z_1, z_2)$. If this quantity can certainly be obtained by taking $z = z_1$ in the results we have just derived, it can also be computed from scratch by reasoning in the same way, which turns out to be easier. The result is

$$F_1(z_1, z_2) = \begin{cases} e^{2i\pi(\tau^{\mathrm{dc}} - \frac{3}{2}z_{12})}(1 + \cdots) & \text{if} \quad \frac{2}{3}\,\mathrm{Im}\,\tau^{\mathrm{dc}} < \mathrm{Im}\,z_{12} < \mathrm{Im}\,\tau^{\mathrm{dc}}\,, \\ (1 + \cdots) & \text{if} \quad -\frac{2}{3}\,\mathrm{Im}\,\tau^{\mathrm{dc}} < \mathrm{Im}\,z_{12} < \frac{2}{3}\,\mathrm{Im}\,\tau^{\mathrm{dc}}\,, \\ e^{2i\pi(\tau^{\mathrm{dc}} + \frac{3}{2}z_{12})}(1 + \cdots) & \text{if} \quad -\mathrm{Im}\,\tau^{\mathrm{dc}} < \mathrm{Im}\,z_{12} < -\frac{2}{3}\,\mathrm{Im}\,\tau^{\mathrm{dc}}\,. \end{cases} \tag{6.32}$$

As a result, the contributions proportional to $\hat{C}$ in Eqs. (6.13) and (6.14) are of the form

$$\begin{aligned}2\pi\left[\frac{t(1-u)}{\alpha'} + 2\ln 4 + \cdots\right]\hat{C} = -4\pi^3\left[\frac{t(1-u)}{\alpha'} + 2\ln 4 + \cdots\right]\times \\ \begin{cases} e^{2i\pi(\tau^{\mathrm{dc}} - z_{12})}(1 + \cdots) & \text{if} \quad \frac{2}{3}\,\mathrm{Im}\,\tau^{\mathrm{dc}} < \mathrm{Im}\,z_{12} < \mathrm{Im}\,\tau^{\mathrm{dc}}\,, \\ e^{i\pi z_{12}}(1 + \cdots) & \text{if} \quad 0 < \mathrm{Im}\,z_{12} < \frac{2}{3}\,\mathrm{Im}\,\tau^{\mathrm{dc}}\,, \\ e^{-i\pi z_{12}}(1 + \cdots) & \text{if} \quad -\frac{2}{3}\,\mathrm{Im}\,\tau^{\mathrm{dc}} < \mathrm{Im}\,z_{12} < 0\,, \\ e^{2i\pi(\tau^{\mathrm{dc}} + z_{12})}(1 + \cdots) & \text{if} \quad -\mathrm{Im}\,\tau^{\mathrm{dc}} < \mathrm{Im}\,z_{12} < -\frac{2}{3}\,\mathrm{Im}\,\tau^{\mathrm{dc}}\,, \end{cases} \\ = \cdots\,,\end{aligned} \tag{6.33}$$

which is exponentially suppressed. Note however that this statement is valid when the intervals of $\operatorname{Im} z_{12}$ are open.

C when $\alpha' \to 0$: Using the relation given in Eq. (4.47), the term linear in C in Eqs. (6.13) and (6.14) can be written as

$$\begin{aligned} &2\pi\biggl[\frac{t(1-u)}{\alpha'} + 2\ln 4 + \cdots\biggr] C = -2i\pi^4 \cos\Bigl(\frac{\pi}{2}\, z_{12}\Bigr)\bigl[\overline{W}_2\, \mathcal{F}_1 - \mathcal{F}_2\bigr]\,, \\ &\text{where}\quad \mathcal{F}_a = \oint_{\gamma_a} \mathrm{d}z\, \frac{F_1(z,z_2)\,(1+\cdots)}{\sin[\pi(z-z_1)]^{\frac{1}{2}} \sin[\pi(z-z_2)]^{\frac{3}{2}}}\,, \quad a \in \{1,2\}\,, \end{aligned} \tag{6.34}$$

and W_2 is given in Eq. (6.5). We are going to show that $\mathcal{F}_1$ contributes exponentially suppressed terms while $\mathcal{F}_2$ yields a finite result.

In order to evaluate $\mathcal{F}_1$, we impose the points z of the representative path of the cycle γ_1 to satisfy $\operatorname{Im} z \equiv \frac{1}{2}\operatorname{Im}\tau^{\mathrm{dc}}$. The advantage of this choice is that $F_1(z,z_2)$ can be replaced by $1+\cdots$ all along the path,

$$\mathcal{F}_1 = \int_0^1 \mathrm{d}x\, \frac{1+\cdots}{\sin[\pi(x+\frac{\tau^{\mathrm{dc}}}{2}-z_1)]^{\frac{1}{2}} \sin[\pi(x+\frac{\tau^{\mathrm{dc}}}{2}-z_2)]^{\frac{3}{2}}}\,. \tag{6.35}$$

Omitting the ellipsis, an explicit integration using a primitive of the integrand yields an exactly vanishing result. However, the exponentially suppressed terms in the numerator may be large once multiplied by $\cos(\pi z_{12}/2)$. To take them into account, one can find upper bounds valid for given signs of $\frac{1}{2}\operatorname{Im}\tau^{\mathrm{dc}} - y_1$, $\frac{1}{2}\operatorname{Im}\tau^{\mathrm{dc}} - y_2$ and $y_1 - y_2$. As an example, when $(\frac{1}{2}\operatorname{Im}\tau^{\mathrm{dc}} - y_1)(\frac{1}{2}\operatorname{Im}\tau^{\mathrm{dc}} - y_2) < 0$ we obtain

$$\Bigl|\cos\Bigl(\frac{\pi}{2}\, z_{12}\Bigr)\, \mathcal{F}_1\Bigr| \le \int_0^1 \mathrm{d}x\, 4\, e^{-\pi|\frac{1}{2}\operatorname{Im}\tau^{\mathrm{dc}} - y_2|}\, K = \cdots\,, \tag{6.36}$$

where the constant K is any majorant of $|1+\cdots|$ for small enough α'. It turns out that in all instances the contributions proportional to $\mathcal{F}_1$ are suppressed.

To compute $\mathcal{F}_2$, we have to consider two cases. When $0 < \frac{1}{2}\, y_1 + \frac{3}{2}\, y_2 < \operatorname{Im}\tau^{\mathrm{dc}}$, Eq. (6.29) allows us to decompose the integral into two pieces,

$$\begin{aligned} &\mathcal{F}_2 = \mathcal{F}_2^{(1)} + \mathcal{F}_2^{(2)}\,, \\ &\text{where}\quad \mathcal{F}_2^{(1)} = \int_0^{\frac{\tau^{\mathrm{dc}}}{2}+\frac{1}{4}z_1+\frac{3}{4}z_2} \mathrm{d}z\, \frac{1+\cdots}{\sin[\pi(z-z_1)]^{\frac{1}{2}} \sin[\pi(z-z_2)]^{\frac{3}{2}}}\,, \\ &\qquad\quad \mathcal{F}_2^{(2)} = \int_{\frac{\tau^{\mathrm{dc}}}{2}+\frac{1}{4}z_1+\frac{3}{4}z_2}^{\tau^{\mathrm{dc}}} \mathrm{d}z\, \frac{e^{-4i\pi(z-\frac{\tau^{\mathrm{dc}}}{2}-\frac{1}{4}z_1-\frac{3}{4}z_2)}\,(1+\cdots)}{\sin[\pi(z-z_1)]^{\frac{1}{2}} \sin[\pi(z-z_2)]^{\frac{3}{2}}}\,. \end{aligned} \tag{6.37}$$

A primitive of the leading term of the integrand of $\mathcal{F}_2^{(1)}$ can be found and the limit of small α' taken after integration. This second step requires considering two cases, namely

$$(a):\ y_1-y_2<\frac{2}{3}\,\mathrm{Im}\,\tau^{\mathrm{dc}}\qquad\text{and}\qquad(b):\ y_1-y_2>\frac{2}{3}\,\mathrm{Im}\,\tau^{\mathrm{dc}}\,, \tag{6.38}$$

which turn out to yield identical finite results,

$$\cos\Big(\frac{\pi}{2}\,z_{12}\Big)\int_0^{\frac{\tau^{\mathrm{dc}}}{2}+\frac{1}{4}z_1+\frac{3}{4}z_2}\mathrm{d}z\,\frac{1}{\sin[\pi(z-z_1)]^{\frac{1}{2}}\sin[\pi(z-z_2)]^{\frac{3}{2}}}=\frac{2i}{\pi}+\cdots\,. \tag{6.39}$$

The extra contribution arising from the ellipsis in the integrand of $\mathcal{F}_2^{(1)}$ turns out to be exponentially suppressed. However, this is not totally obvious since the dominant implicit term in the numerator is of the form $e^{4i\pi(\frac{\tau^{\mathrm{dc}}}{2}+\frac{1}{4}z_1+\frac{3}{4}z_2-z)}$, which is 1 at the upper bound of the integral. Hence, keeping only the ellipsis in the numerator, we divide the domain of integration from 0 to some z_0 and from z_0 to $\frac{\tau^{\mathrm{dc}}}{2}+\frac{1}{4}z_1+\frac{3}{4}z_2$. The value of z_0 is chosen such that the first domain yields an integral multiplied by $\cos(\pi z_{12}/2)$ admitting a trivial exponentially suppressed majorant, and also such that in the second domain it is legitimate to replace the two sines in the denominator by a single large exponential allowing an easy integration. In both cases (a) and (b), we obtain that

$$\cos\Big(\frac{\pi}{2}\,z_{12}\Big)\mathcal{F}_2^{(1)}=\frac{2i}{\pi}+\cdots\,. \tag{6.40}$$

In the integrand of $\mathcal{F}_2^{(2)}$, $\sin[\pi(z-z_2)]$ can always be replaced by a large exponential thanks to the fact that $\mathrm{Im}\,(z-z_2)\neq 0$ throughout the integration domain. While the same is true for $\sin[\pi(z-z_1)]$ in case (a), it turns out that $\mathrm{Im}\,(z-z_1)$ vanishes for some z in case (b). In the first instance (a), it is therefore valid to write

$$\begin{aligned}|\mathcal{F}_2^{(2)}|&=\Big|\int_{\frac{\tau^{\mathrm{dc}}}{2}+\frac{1}{4}z_1+\frac{3}{4}z_2}^{\tau^{\mathrm{dc}}}\mathrm{d}z\,4\,e^{-i\pi(2z-2\tau^{\mathrm{dc}}-\frac{1}{2}z_1-\frac{3}{2}z_2)}\,(1+\cdots)\Big|\\&<\int_{\frac{1}{2}\mathrm{Im}\,\tau^{\mathrm{dc}}+\frac{1}{4}y_1+\frac{3}{4}y_2}^{\mathrm{Im}\,\tau^{\mathrm{dc}}}\mathrm{d}y\,\frac{4K}{\sin\phi}\,e^{-\pi(\frac{1}{2}z_1-\frac{3}{2}z_2)}\,e^{2\pi(y-\mathrm{Im}\,\tau^{\mathrm{dc}})}\,,\end{aligned} \tag{6.41}$$

where we have chosen the path of integration for z to be the straight segment in the complex plane, which forms an angle $\phi\in(0,\pi)$ with the horizontal axis. Integrating the majorant, one obtains

$$\begin{aligned}\Big|\cos\Big(\frac{\pi}{2}\,z_{12}\Big)\,\mathcal{F}_2^{(2)}\Big|&<\frac{K}{\pi\sin\phi}\times\begin{cases}e^{-2\pi y_2} & \text{if}\ \ y_1-y_2>0\,,\\ e^{-\pi(y_1+y_2)} & \text{if}\ \ y_1-y_2<0\,,\end{cases}\\&=\cdots\,,\end{aligned} \tag{6.42}$$

where in the last line we use the fact that $\sin\phi \to 1$ when $\alpha' \to 0$. On the contrary, in case (b), only $\sin[\pi(z-z_2)]$ can be replaced by a single large exponential. However, it is possible to integrate the dominant term of the integrand, and show as we did for $\mathcal{F}_2^{(1)}$ that the result dominates the integral arising from the ellipsis. Combining both pieces, we find that the conclusion of Eq. (6.42) holds again.

Let us move on to the second case, namely $\mathrm{Im}\,\tau^{\rm dc} < \frac{1}{2}\,y_1 + \frac{3}{2}\,y_2 < 2\mathrm{Im}\,\tau^{\rm dc}$, which can be treated by following the same steps as before. The starting point is Eq. (6.31) which leads to the decomposition

$$\begin{aligned} &\mathcal{F}_2 = \mathcal{F}_2^{(1)} + \mathcal{F}_2^{(2)}\,, \\ \text{where}\quad &\mathcal{F}_2^{(1)} = \int_{\frac{1}{4}z_1+\frac{3}{4}z_2-\frac{\tau^{\rm dc}}{2}}^{\tau^{\rm dc}} \mathrm{d}z\,\frac{1+\cdots}{\sin[\pi(z-z_1)]^{\frac{1}{2}}\sin[\pi(z-z_2)]^{\frac{3}{2}}}\,, \\ &\mathcal{F}_2^{(2)} = \int_0^{\frac{1}{4}z_1+\frac{3}{4}z_2-\frac{\tau^{\rm dc}}{2}} \mathrm{d}z\,\frac{e^{4i\pi(z-\frac{1}{4}z_1-\frac{3}{4}z_2+\frac{\tau^{\rm dc}}{2})}\,(1+\cdots)}{\sin[\pi(z-z_1)]^{\frac{1}{2}}\sin[\pi(z-z_2)]^{\frac{3}{2}}}\,. \end{aligned} \tag{6.43}$$

Omitting the ellipsis in the integrand of $\mathcal{F}_1^{(1)}$, a direct integration yields for

$$(c):\ y_1-y_2 > -\frac{2}{3}\,\mathrm{Im}\,\tau^{\rm dc} \qquad \text{and} \qquad (d):\ y_1-y_2 < -\frac{2}{3}\,\mathrm{Im}\,\tau^{\rm dc}\,, \tag{6.44}$$

the same finite result we found in the previous case

$$\cos\Big(\frac{\pi}{2}\,z_{12}\Big)\int_{\frac{1}{4}z_1+\frac{3}{4}z_2-\frac{\tau^{\rm dc}}{2}}^{\tau^{\rm dc}} \mathrm{d}z\,\frac{1}{\sin[\pi(z-z_1)]^{\frac{1}{2}}\sin[\pi(z-z_2)]^{\frac{3}{2}}} = \frac{2i}{\pi}+\cdots\,. \tag{6.45}$$

Moreover, even if the ellipsis in the integrand of $\mathcal{F}_2^{(1)}$ equals 1 at the lower bound of the integral, it can be shown as before that it yields an extra exponentially suppressed contribution after integration. Therefore, Eq. (6.40) remains valid.

In the integrand of $\mathcal{F}_2^{(2)}$, it is always safe to replace $\sin[\pi(z-z_2)]$ by a large exponential. This is also the case for $\sin[\pi(z-z_1)]$ in case (c), for which we can write

$$\begin{aligned} |\mathcal{F}_2^{(2)}| &= \left|\int_0^{\frac{1}{4}z_1+\frac{3}{4}z_2-\frac{\tau^{\rm dc}}{2}} \mathrm{d}z\,4\,e^{i\pi(2z+2\tau^{\rm dc}-\frac{1}{2}z_1-\frac{3}{2}z_2)}\,(1+\cdots)\right| \\ &< \int_0^{\frac{1}{4}y_1+\frac{3}{4}y_2-\frac{1}{2}\mathrm{Im}\,\tau^{\rm dc}} \mathrm{d}y\,\frac{4K}{\sin\phi}\,e^{-\pi(2\mathrm{Im}\,\tau^{\rm dc}-\frac{1}{2}z_1-\frac{3}{2}z_2)}\,e^{-2\pi y}\,. \end{aligned} \tag{6.46}$$

In the first line, the path of integration for z is the segment that forms an angle $\phi \in (0,\pi)$ with the horizontal axis. Integrating the upper bound, we conclude that

$$\begin{aligned} \left|\cos\Big(\frac{\pi}{2}\,z_{12}\Big)\,\mathcal{F}_2^{(2)}\right| &< \frac{K}{\pi\sin\phi} \times \begin{cases} e^{-\pi(2\mathrm{Im}\,\tau^{\rm dc}-y_1-y_2)} & \text{if}\ \ y_1-y_2>0\,, \\ e^{-2\pi(\mathrm{Im}\,\tau^{\rm dc}-y_2)} & \text{if}\ \ y_1-y_2<0\,, \end{cases} \\ &= \cdots\,. \end{aligned} \tag{6.47}$$

In case (d), only $\sin[\pi(z-z_2)]$ can be replaced by a large exponential. The integration using a primitive as before shows that the conclusion of Eq. (6.47) is again true.

Taking into account all of the above results for the integrals $\mathcal{F}_a$, and using the fact that W_2 does not grow exponentially fast as $\alpha' \to 0$, Eq. (6.34) leads to the contribution

$$2\pi\left[\frac{t(1-u)}{\alpha'} + 2\ln 4 + \cdots\right] C = -4\pi^3 + \cdots . \tag{6.48}$$

6.5 Integration over τ_2, z_1, z_2 and final result

Collecting the contributions of parts (1) and (2) (involving C and $\hat{C}$) of the correlators $\langle \tau^u \tau'^u \rangle_{\rm qu} = \langle \tau'^u \tau^u \rangle_{\rm qu}$, the braces in the amplitudes (6.13) and (6.14) reduce to

$$\{2\pi^3 - 4\pi^3 + \cdots\} = -2\pi^3 + \cdots . \tag{6.49}$$

Because all the dependence in z_1 and z_2 of the amplitudes is now hidden in ellipses, the integrations in Eqs. (5.25) and (5.26) can be performed easily. Using the identity

$$\int_0^{+\infty} \mathrm{d}\,\mathrm{Im}\,\tau^{\rm dc} \int_0^{\mathrm{Im}\,\tau^{\rm dc}} \mathrm{d}y_1 \equiv \frac{1}{(2\pi\alpha')^2} \int_0^{+\infty} t\,\mathrm{d}t \int_0^1 du_1 \,, \tag{6.50}$$

and the fact that the integration over u_1 of the dominant contributions of the two-point functions are trivial, we obtain

$$\begin{aligned} \mathcal{A}_{\mathrm{int}\mathcal{A}}^{\alpha_0\beta_0} + \mathcal{A}_{\mathrm{int}\mathcal{M}}^{\alpha_0\beta_0} = \frac{4}{\pi}\,\mathcal{C}s\,\lambda_{\alpha_0\beta_0}\lambda^{\rm T}_{\beta_0\alpha_0} \sum_{l_5} \frac{1}{|2l_5+1|^3} \\ \times \frac{\alpha'}{R_5^2}\Big(N_{i_0 i'_0} - N_{i_0 \hat{i}'_0} - 2 + D_{j_0 i'_0} - D_{j_0 \hat{i}'_0} - 2\Big) + \mathcal{O}\left(\frac{\alpha'^2}{R_5^4}\right). \end{aligned} \tag{6.51}$$

The origin of the terms of order α'^2/R_5^4 will be explained at the end of this section.

We are now ready to display the main result of our work. Implementing the correct dimension, the mass squared acquired at one loop by the classically massless state (λ, ϵ) belonging to the ND+DN bosonic sector realized by strings "stretched" between the stack of $N_{i_0 i'_0} \geq 2$ D3-branes (T-dual to D9-branes) and the stack of $D_{j_0 i'_0} \geq 2$ D3-branes (T-dual to D5-branes) is given by

$$M^2 = \frac{1}{\alpha'} \sum_{\alpha_0=1}^{N_{i_0 i'_0}} \sum_{\beta_0=1}^{D_{j_0 i'_0}} \left(\mathcal{A}^{\alpha_0\beta_0}_{\text{int}\mathcal{A}} + \mathcal{A}^{\alpha_0\beta_0}_{\text{int}\mathcal{M}} \right) \tag{6.52}$$
$$= \frac{32}{\pi} \mathcal{C}s \sum_{l_5} \frac{1}{|2l_5+1|^3} \, \text{tr}(\lambda\lambda^{\text{T}}) \, M_{3/2}^2 \left(n_{i_0 i'_0} - n_{i_0 \hat{\imath}'_0} - 1 + d_{j_0 i'_0} - d_{j_0 \hat{\imath}'_0} - 1 \right) + \mathcal{O}\left(\frac{\alpha'}{R_5^4} \right),$$

where the supersymmetry breaking scale (2.7) reduces to

$$M_{3/2} = \frac{1}{2R_5} \, . \tag{6.53}$$

From a field theory point of view, it can be seen that the bosonic (fermionic) degrees of freedom charged under $U(n_{i_0 i'_0})$ or $U(d_{j_0 i'_0})$ which are running in the loop contribute positively (negatively) to the mass-squared term. Because $\text{tr}(\lambda\lambda^{\text{T}}) > 0$,[20] this implies that $\mathcal{C}s > 0$.

To conclude this section, notice that Eq. (6.52) guaranties or rules out the stability of moduli fields in the ND+DN sector only when the coefficient in parenthesis is not zero. When the latter vanishes, one has to compute four-point functions to conclude.

Subdominant contributions: As announced below Eq. (6.3), all our derivations have been presented at generic insertion points z_1, z_2. However, for special values of these variables, contributions we included in ellipses are actually no more exponentially suppressed when $\alpha' \to 0$.

When the limit is taken up to $\alpha' = 0$, all ellipses are identically zero, except at these particular values of z_1, z_2 which are loci of zero measure in the final integrals. Hence, the existence of such points does not affect the end result, which in this case is Eq. (6.52) with no subdominant term at all. One may expect this expression to match exactly the outcome of the computation of the masses in a pure Kaluza–Klein field theory in $4+1$ dimensions, with the field-theory Scherk–Schwarz mechanism implemented along the circle of radius R_5. The field content should include the Kaluza–Klein towers of modes (propagating along $S^1(R_5)$) present in the string model and associated with the massless states or their superpartners charged under $U(n_{i_0 i'_0}) \times U(d_{j_0 i'_0})$. However, this is not quite the case. Indeed, we already noticed above Eq. (6.7) that the ND and DN sectors do not run in the loop when $\alpha' = 0$.

[20] Since $\lambda\lambda^{\text{T}}$ is a real symmetric $n_{i_0 i'_0} \times n_{i_0 i'_0}$ matrix, it is diagonalizable and its eigenvalues are real. Moreover, since for any real $n_{i_0 i'_0}$-vector V we have $V^{\text{T}}(\lambda^T\lambda)V = (\lambda V)^{\text{T}}(\lambda V) = ||\lambda V||^2 \geq 0$, we conclude that all eigenvalues are nonnegative.

Indeed, this has to be the case since otherwise they would contribute extra terms proportional to $\delta_{\vec{l},\vec{0}}$ or $\delta_{\vec{\tilde{l}},\vec{0}}$ in Eq. (6.7). Because of the first factor $\pi/[t(1-u_1)]$ (for $\alpha'=0$ and $y_2=0$) in the third line, such contributions would yield a divergence when integrating over u_1. On the contrary, the Poisson summations over the $\vec{l}$- or $\vec{\tilde{l}}$-dependent contributions cancel the factor $\pi/[t(1-u_1)]$ and yield a finite result interpreted as the contributions of states in the NN and DD sectors running in the loop. Hence, from the point of view of a Kaluza–Klein field theory in 4+1 dimensions, the states in the ND+DN sector are treated semi-classically *i.e.* as classical backgrounds (with vanishing vev's) in interaction with quantum matter in the NN and DD sectors. Moreover, notice that the presence of infinite towers of Kaluza–Klein states associated with the Scherk–Schwarz circle and running in the Feynman diagrams prevents all ultraviolet divergences from occurring, in exactly the same way as it happens in the string computation or in a supersymmetric quantum field theory at finite temperature.

By contrast, when α' is not strictly zero, the neighborhoods of the special points in which some ellipses are not exponentially small are no longer of measure zero. For instance, the term given in Eq. (6.33) is finite for all α' at the particular values $y_1=\mathrm{Im}\,\tau^{\mathrm{dc}}$, $y_2=0$, *i.e.* $u=1$. However, integrating it over $y_1\in[\frac{2}{3}\,\mathrm{Im}\,\tau^{\mathrm{dc}},\mathrm{Im}\,\tau^{\mathrm{dc}}]$, one obtains a contribution $\mathcal{O}(\alpha'/t)$ which after insertion in the full amplitude and integration over t leads to a contribution $\mathcal{O}(\alpha'/R_5^2)$ smaller than the dominant one shown in Eq. (6.51). Another example is given by the contributions to the amplitudes arising from the *massive* Kaluza–Klein modes propagating along $T^4/\mathbb{Z}_2$ or $\tilde{T}^4/\mathbb{Z}_2$. As seen in Eqs. (6.9) and (6.10), they involve in the former case factors

$$e^{-\left[\frac{t(1-u)}{\alpha'}+2\ln 4+\cdots\right]\sum_I\left(\frac{m_I+a^I_{i0}-a^I_i}{r_I}\right)^2}\,, \tag{6.54}$$

where the discrete sum is non-zero. However, at the particular values $y_1=\mathrm{Im}\,\tau^{\mathrm{dc}}$, $y_2=0$, *i.e.* $u=1$, this factor is finite for all α'. Implementing the integrals shown in Eq. (6.50), one obtains again corrections $\mathcal{O}(\alpha'^2/R_5^4)$ in Eq. (6.51). However, throughout the computation of the amplitudes, terms similar to the above examples are numerous and we have not dealt with them in full detail.

7 Stability analysis at one loop

As seen in Ref. [32], most of the brane configurations implying the one-loop effective potential to be extremal and tachyon free[21] yield a run away behavior of $M_{3/2}$ with $n_{\rm F} - n_{\rm B} < 0$. However, setups that lead to exponentially suppressed or positive values of $\mathcal{V}_{\text{1-loop}}$ may be of particular interest. Indeed, for $n_{\rm F} - n_{\rm B} = 0$, it is conceivable that the suppressed terms at one loop combine with higher loop corrections to stabilize the dilaton and $M_{3/2}$ in a perturbative regime. In that case, the resulting cosmological constant should be small, and the issue raised in Ref. [64] avoided. Moreover, cases where $n_{\rm F} - n_{\rm B} > 0$ may shed light on the existence or non-existence of de Sitter vacua after stabilization of the string coupling and supersymmetry breaking scale.

To be specific, the existence of 2 brane configurations without tachyons at one loop[21] and satisfying classically a Bose/Fermi degeneracy at the massless level were shown to exist in Ref. [32]. Moreover, 4 more tachyon free setups with $n_{\rm F} - n_{\rm B} > 0$ were also found. In all these instances, reaching these conclusions was possible thanks to the absence of moduli in the ND+DN sectors, and thanks to anomaly-induced supersymmetric masses for all blowing-up modes of $T^4/\mathbb{Z}_2$. Furthermore, 2 extra brane configurations were presented [32], one with $n_{\rm F} - n_{\rm B} = 0$ and the other with $n_{\rm F} - n_{\rm B} > 0$, which we analyze further in the present section. Indeed, it was established that they both yield nonnegative squared masses at one loop for all moduli in the NN, DD and untwisted closed-string sectors, and that they possess moduli fields in the ND+DN sectors. Given the result of the previous section, we are going to see that the latter are non-tachyonic.

7.1 NN, DD and closed-string sector moduli masses at one loop

Before describing the two brane configurations of interest, let us review the stability conditions established in Ref. [32] for all moduli fields that are not in the ND+DN sector.

Moduli in the* NN *and* DD *open-string sectors: The number of these scalars and their masses can be determined in two steps. To start with, we can count the number of positions in $\tilde{T}^2 \times T^4/\mathbb{Z}_2$ of the D3-branes T-dual to the D5-branes that are allowed at genus-0

[21] Up to exponentially suppressed terms as shown in Eq. (1.1).

to vary consistently with the orbifold and orientifold symmetries. In $\tilde{T}^2$, we have explained in Sect. 2.1 that there are 16 independent locations,[22] which are associated with the pairs of brane/mirror brane under Ω. Moreover, we have seen that when 2 modulo 4 D3-branes sit on one of the 64 corners of the six-dimensional box in Fig. 1, 2 D3-branes have rigid coordinates in $T^4/\mathbb{Z}_2$, which reduces the maximum number of 8 independent dynamical positions in this orbifold space. Hence, for the D3-branes T-dual to the D5-branes and similarly for those T-dual to the D9-branes, the numbers of moduli fields describing the positions in $T^4/\mathbb{Z}_2$ and $\tilde{T}^4/\mathbb{Z}_2$ are given by

$$\sum_{i,i'} \left\lfloor \frac{d_{ii'}}{2} \right\rfloor \quad \text{and} \quad \sum_{i,i'} \left\lfloor \frac{n_{ii'}}{2} \right\rfloor . \tag{7.1}$$

If perturbatively all choices of coefficients $d_{ii'}$ and $n_{ii'}$ are allowed, it turns out that they must satisfy constraints, whose origin is six-dimensional, in order to guaranty the consistency of the model at the non-perturbative level [5]. Before stating these conditions, we need to define few quantities. Let us denote by $D_i \equiv \sum_{i'} D_{ii'}$ the number of D5-branes (in the initial picture) sitting at the fixed point i of $T^4/\mathbb{Z}_2$. Defining $\mathcal{R}$ the number of coefficients D_i, $i \in \{1, \ldots, 16\}$, that are equal to 2 modulo 4, a little thought allows to conclude that $\mathcal{R}$ is even, *i.e.* $\mathcal{R} \in \{0, 2, \ldots, 16\}$. Moreover, there are at most $8 - \mathcal{R}/2$ independent dynamical locations in $T^4/\mathbb{Z}_2$.[23] Hence, denoting $\tilde{\mathcal{R}}$ the counterpart of $\mathcal{R}$ for the D9-branes, the following inequalities hold,

$$\sum_{i,i'} \left\lfloor \frac{d_{ii'}}{2} \right\rfloor \leq \sum_{i} \left\lfloor \frac{\sum_{i'} d_{ii'}}{2} \right\rfloor \equiv 8 - \frac{\mathcal{R}}{2} , \qquad \sum_{i,i'} \left\lfloor \frac{n_{ii'}}{2} \right\rfloor \leq \sum_{i} \left\lfloor \frac{\sum_{i'} n_{ii'}}{2} \right\rfloor \equiv 8 - \frac{\tilde{\mathcal{R}}}{2} . \tag{7.2}$$

Notice that $(\mathcal{R}, \tilde{\mathcal{R}})$ characterizes disconnected components of the moduli space. Indeed, when the model is decompactified to six dimensions, $\mathcal{R}$ is the number of rigid pairs of D5-branes in $T^4/\mathbb{Z}_2$, while $\tilde{\mathcal{R}}$ counts the pairs of D5-branes T-dual to the D9-branes that are rigid in $\tilde{T}^4/\mathbb{Z}_2$. There is no gauge-theory phase transition in six dimensions that can describe a variation of $(\mathcal{R}, \tilde{\mathcal{R}})$. The components that are fully consistent non-perturbatively have $\mathcal{R}$ and $\tilde{\mathcal{R}}$ equal to 0, 8 or 16 [5].[24] Moreover, when $\mathcal{R}$ (or $\tilde{\mathcal{R}}$) is 8, the rigid pairs of D5-branes (D5-branes T-dual to the D9-branes) must be located on the 8 fixed points of one

[22] We will see in a second step that some of the $16+16$ positions in $\tilde{T}^2$ of the D3-branes T-dual to the D5- or D9-branes have a tree-level mass proportional to the open-string coupling.

[23] This number is not reached when the Wilson-line backgrounds on the worldvolumes of the D5-branes lead to some $D_i = 0$ modulo 4 with some $D_{ii'} = 2$ modulo 4. Physically, this corresponds to "eating" moduli fields when the gauge group is Higgsed in its Coulomb branch.

[24] In four dimensions, this results in constraints on $\sum_{i'} d_{ii'}$ and $\sum_{i'} n_{ii'}$.

of the hyperplanes $X^I = 0$ or π, $I \in \{6, \ldots, 9\}$, ($\tilde{X}^I = 0$ or π). Up to T-duality, there are therefore six inequivalent consistent classes of brane configurations in six dimensions, which are characterized by

$$(\mathcal{R}, \tilde{\mathcal{R}}) \in \Big\{(0,0), (0,8), (0,16), (8,8), (8,16), (16,16)\Big\}\,. \tag{7.3}$$

In the language of D3-branes, the mass-squared terms of the positions around the fixed points ii' have been derived in [32] by computing the effective potential at one loop and extracting the quadratic contributions in moduli fields. Up to irrelevant positive numerical factors, they are equal to $M_{3/2}^2$ multiplied by coefficients listed below. For the locations in $\tilde{T}^2$, they are given by

$$\begin{aligned} &d_{ii'} - d_{i\hat{i}'} - 1 + \frac{1}{4}\sum_{j=1}^{16}(n_{ji'} - n_{j\hat{i}'}) \quad \text{for the D3's T-dual to the D5's,} \quad \text{when } d_{ii'} \geq 1\,, \\ &n_{ii'} - n_{i\hat{i}'} - 1 + \frac{1}{4}\sum_{j=1}^{16}(d_{ji'} - d_{j\hat{i}'}) \quad \text{for the D3's T-dual to the D9's,} \quad \text{when } n_{ii'} \geq 1\,, \end{aligned} \tag{7.4}$$

while for the positions in $T^4/\mathbb{Z}_2$ and $\tilde{T}^4/\mathbb{Z}_2$, they are

$$\begin{aligned} &d_{ii'} - d_{i\hat{i}'} - 1 \quad \text{for the D3's T-dual to the D5's,} \quad \text{when } d_{ii'} \geq 2\,, \\ &n_{ii'} - n_{i\hat{i}'} - 1 \quad \text{for the D3's T-dual to the D9's,} \quad \text{when } n_{ii'} \geq 2\,. \end{aligned} \tag{7.5}$$

In order to avoid tachyons, all mass-term coefficients of the locations in $T^4/\mathbb{Z}_2$ and $\tilde{T}^4/\mathbb{Z}_2$ should be nonnegative. However, for the positions in $\tilde{T}^2$, this is not necessarily the case. As announced before, this follows from the fact that the true number of positions free to move classically in $\tilde{T}^2$ is less than $16+16$ for the D3-branes T-dual to D5-branes or D9-branes. In fact, the product of unitary open-string gauge-group factors present in six dimensions (when all D5-branes and D5-branes T-dual to D9-branes sit on fixed points) contains anomalous $U(1)$'s. To cancel the anomalies, a generalized Green–Schwarz mechanism takes place, which implies the existence of large tree-level masses proportional to the open-string coupling for the associated vector bosons [5, 32]. The net result is that if there are 16 or fewer unitary factors in six dimensions, they are all broken to SU groups, while if there are more than 16 unitary factors, exactly 16 of them are broken to SU groups. Compatifying down to four dimensions, no Wilson-line backgrounds on T^2 can be switched on for the massive vector bosons. Hence, at least 2 and at most 16 linear combinations of the $16 + 16$ D3-brane positions in $\tilde{T}^2$ are identically vanishing. Imposing these relations in the mass terms derived

from the effective potential, one obtains the true mass matrix for the remaining degrees of freedom associated with the Wilson lines along T^2. For the configuration to be potentially tachyon free at one loop, it is only this matrix that should have non-negative eigenvalues.

Moduli in the twisted closed-string sector: The anomalous $U(1)$'s in six dimensions become massive by "eating" Stueckelberg fields, which turn out to be blowing-up modes of $T^4/\mathbb{Z}_2$. Hence, there are classically between 0 and 14 surviving moduli fields in the twisted closed-string sector. When such modes exist, one may derive their squared masses at one loop by computing two-point functions of massless twisted scalars, which can be done using the results of Ref. [2] and/or our Sects. 4 and 6.

Moduli in the untwisted closed-string sector: The expression of the one-loop effective potential in the orientifold model with background (2.1) was computed in Ref. [32], for vanishing vev's of the RR two-form moduli. As can be seen in Eq. (1.1), when all D3-branes sit on O3-planes (in the T-dual languages), all dependency on the metric components $G_{I'J'}$ and G_{IJ} disappears up to exponentially small contributions, except for $G^{55} \equiv 4M_{3/2}^2/M_{\rm s}^2$. Hence, up to neglected corrections, these moduli remain flat directions at one loop, along with the dilaton at this order in string coupling. Moreover, in configurations showing a Bose-Fermi degeneracy at the massless level, the tadpole of $M_{3/2}$ vanishes and the latter is an extra flat direction. In supergravity language, the spontaneous supersymmetry breaking scale is known as the "no-scale modulus," which parametrizes a flat direction of the classical potential in Minkowski space [65]. Hence, in the particular string setups satisfying $n_{\rm F} - n_{\rm B} = 0$, the no-scale structures valid in the classical backgrounds are preserved at one loop, up to exponentially suppressed terms. For this reason, they are designated as "super no-scale models" [36, 37, 39].

As explained in Ref. [32], the heterotic/type I duality can be used to show that the dependency of the one-loop effective potential on the RR two-form components $C_{I'J'}$ and C_{IJ} appears only in the exponentially suppressed terms (even when the D3-branes are located in the bulk of the internal space). Hence, the expression (1.1) of critical points of $\mathcal{V}_{\text{1-loop}}$ remains valid when $C_{I'J'}$ and C_{IJ} are switched on. In other words, these moduli parametrize flat directions (up to the suppressed terms).

7.2 Configurations with non-tachyonic ND+DN-sector moduli

A complete computer scan of the $32+32$ D3-brane distributions on O3-planes allowed in the non-perturbatively consistent components of the moduli space was performed in Ref. [32]. Six tachyon-free configurations with $n_{\rm F}-n_{\rm B}\geq 0$ were found, while two more deserved further investigation due to the existence of moduli fields in their ND+DN sectors. Let us analyze them.

Exponentially suppressed one-loop potential: The first of these D3-brane distributions satisfies Bose/Fermi degeneracy at the massless level and genus-0, $n_{\rm F}-n_{\rm B}=0$. It lies in the moduli-space component $(\mathcal{R},\tilde{\mathcal{R}})=(0,8)$ and is shown in Fig. 5a.[25]

The D3-branes T-dual to the D5-branes are distributed in $T^4/\mathbb{Z}_2$ as 4 stacks of 8. The D3-branes T-dual to the D9-branes are distributed as 8 pairs (with rigid positions in $\tilde{T}^4/\mathbb{Z}_2$), one stack of 4 divided into $2+2$ in $\tilde{T}^2$, and one stack of 12 divided into $10+2$ in $\tilde{T}^2$. All precise locations in $\tilde{T}^2$ can be read from Fig. 5a.

The open-string gauge group including anomalous $U(1)$'s is

$$\Big[U(4)^4\Big]_{\rm DD}\times\Big[U(1)^8\times U(1)^2\times\Big(U(1)\times U(5)\Big)\Big]_{\rm NN}\,. \tag{7.6}$$

It descends from the gauge symmetry $[U(4)^4]_{\rm DD}\times[U(1)^8\times U(2)\times U(6)]_{\rm NN}$ present in six dimensions, which contains 14 unitary factors. As a result, there are 14 anomalous $U(1)$'s becoming massive by "eating" 14 twisted moduli in the closed-string sector. Moreover, the mass acquired at one loop by the last 2 blowing-up modes of $T^4/\mathbb{Z}_2$ should be computed in order to conclude whether the internal space is stabilized at the orbifold point or not. The anomaly-free gauge symmetry in six dimensions may be written as $[SU(4)^4]_{\rm DD}\times[U(2)/U(1)_{\rm diag}\times U(6)/U(1)_{\rm diag}]_{\rm NN}$, where $U(2)$ and $U(6)$ are spontaneously broken to $U(1)\times U(1)\equiv U(1)_{\rm diag}\times U(1)_\perp$ and $U(1)\times U(5)\equiv U(1)_{\rm diag}\times U(1)_\perp\times SU(5)$ when the Wilson-line background on T^2 is switched on. The anomaly-free gauge group in four dimensions is thus

$$\Big[SU(4)^4\Big]_{\rm DD}\times\Big[U(1)_\perp\times\Big(U(1)_\perp\times SU(5)\Big)\Big]_{\rm NN}\,. \tag{7.7}$$

[25] It corresponds to Fig. 5c of Ref. [32].

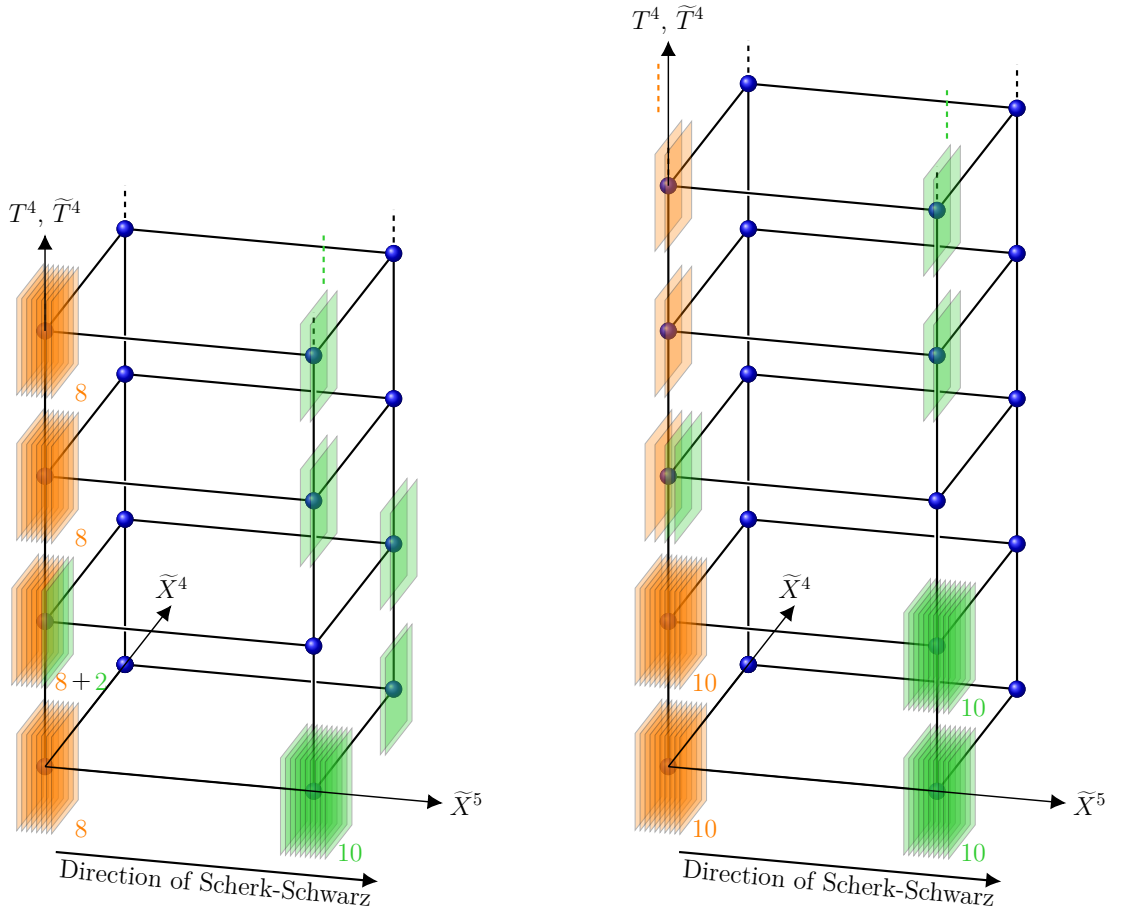

(a) Configuration in the component $(\mathcal{R}, \tilde{\mathcal{R}}) = (0, 8)$ of the moduli space, with $n_{\rm F} - n_{\rm B} = 0$. The masses at one loop of two blowing-up moduli in the twisted closed-string sector of $T^4/\mathbb{Z}_2$ deserve further study.

(b) Configuration in the component $(\mathcal{R}, \tilde{\mathcal{R}}) = (8, 8)$ of the moduli space, with $n_{\rm F} - n_{\rm B} = 32$. All twisted-sector moduli are massive.

Figure 5: D3-brane configurations without tachyons at one loop in the NN, DD and ND+DN open-string sectors, as well as in the untwisted closed string sector.

As follows from the mass-term coefficients (7.5), all D3-brane postions along $T^4/\mathbb{Z}_2$ and $\tilde{T}^4/\mathbb{Z}_2$ turn out to be rigid or massive. By taking into account the Green–Schwarz mechanism which stabilizes automatically 14 linear combinations of continuous locations along $\tilde{T}^2$, the mass-matrix of the 18 remaining positions can be found and leads to the conclusion that they are all massless except one which is massive. As explained in the previous subsection, all untwisted closed-string moduli are flat directions, including $M_{3/2}$ thanks to the vanishing of $n_{\rm F} - n_{\rm B}$. The moduli in the ND+DN sectors are realized as strings "stretched" between

the stack of 2 D3-branes T-dual to D9-branes located on the left side of Fig. 5a and any of the four stacks of 8 D3-branes T-dual to D5-branes. Indeed, they share the same coordinates in $\tilde{T}^2$. In all four cases, we have in the notations of Eqs. (6.51) and (6.52,

$$\begin{aligned} & N_{i_0 i'_0} = 2\,, \quad N_{i_0 \hat{i}'_0} = 0\,, \quad D_{j_0 i'_0} = 8\,, \quad D_{j_0 \hat{i}'_0} = 0\,, \\ \Longrightarrow \quad & n_{i_0 i'_0} - n_{i_0 \hat{i}'_0} - 1 + d_{j_0 i'_0} - d_{j_0 \hat{i}'_0} - 1 = 3 > 0\,, \end{aligned} \tag{7.8}$$

which shows that all moduli fields in the ND+DN sector are massive.

For completeness, let us review the counting of $n_{\rm B}$ and $n_{\rm F}$. In the NN and DD sectors, the bosonic degrees of freedom include those of an $\mathcal{N} = 2$ vector multiplet in the adjoint representation of the group (7.6), along with those of hypermultiplets in antisymmetric $\oplus$ $\overline{\text{antisymmetric}}$ representations of all non-Abelian factors. In the ND+DN sector, we have the bosonic degrees of freedom of 4 hypermultiplets, all transforming under a "bifundamental" representation of a $U(1)_{\rm NN} \times U(4)_{\rm DD}$ group. Adding the 96 degrees of freedom arising from the closed-string sector, we obtain a total of $n_{\rm B} = 832$. On the contrary, $n_{\rm F}$ contains only contributions from the ND+DN sector. The latter correspond to the fermionic degrees of freedom of hypermultiplets in the bifundamental representations of each pair of unitary group factors supported by stacks of D3-branes T-dual to D5-branes and stacks of D3- branes T-dual to D9-branes, provided they have distinct coordinates along $\tilde{X}^5$ but not $\tilde{X}^4$. Their total number is given by $n_{\rm F} = 4 \times 16 \times 13 = 832$, which equals $n_{\rm B}$ as claimed before.

Positive one-loop potential: The second configuration we are interested in lies in the component $(\mathcal{R}, \tilde{\mathcal{R}}) = (8, 8)$ of the moduli space. It yields a positive potential satisfying $n_{\rm F} - n_{\rm B} = 32$ and is depicted in Fig. 5b.[26] The D3-branes T-dual to the D5-branes are distributed in $T^4/\mathbb{Z}_2$ as 6 pairs and 2 stacks of 10. Similarly, the D3-branes T-dual to the D9-branes are located in $\tilde{T}^4/\mathbb{Z}_2$ as 6 pairs and 2 stacks of 10. Because the precise positions in $\tilde{T}^2$ shown in Fig. 5b do not involve the direction $\tilde{X}^4$, the configuration could be considered in five dimensions.

Including the anomalous $U(1)$'s, the open-string gauge group is

$$\Big[U(1)^6 \times U(5)^2\Big]_{\rm DD} \times \Big[U(1)^6 \times U(5)^2\Big]_{\rm NN}\,, \tag{7.9}$$

[26] It corresponds to the configuration shown in Fig. 6(e) of Ref. [32], after a T-duality on $T^4/\mathbb{Z}_2$ *i.e.* an interchange D5 $\leftrightarrow$ D9.

both in four and six dimensions. It contains 16 unitary factors, which implies that all twisted sector moduli are massive, *i.e.* that $T^4/\mathbb{Z}_2$ cannot be desingularized. Moreover, the anomaly-free gauge symmetry is reduced to

$$\Big[SU(5)^2\Big]_{\rm DD} \times \Big[SU(5)^2\Big]_{\rm NN} \,. \tag{7.10}$$

All D3-brane positions in $T^4/\mathbb{Z}_2$ or $\tilde{T}^4/\mathbb{Z}_2$ turn out to be rigid of massive at one loop, while the Green-Schwarz mechanism leaves 8 massive and 8 massless moduli associated with the locations in $\tilde{T}^2$. Moreover, all untwisted closed-string moduli are flat directions except the supersymmetry breaking scale $M_{3/2}$ which undergoes a runaway along a positive potential. There are moduli in the ND+DN sector arising from strings "stretched" between any stack of D3-branes T-dual to D5-branes and the pair of D3-branes T-dual to D9-branes located on the same edged of the box. They include 2 copies of scalars in "bifundamental" representations of $U(1)_{\rm NN} \times U(5)_{\rm DD}$ groups, and 6 copies in "bifundamental" representations of $U(1)_{\rm NN} \times U(1)_{\rm DD}$ groups. In the former case the moduli are stabilized since we have

$$\begin{aligned} & N_{i_0 i'_0} = 2\,, \quad N_{i_0 \hat{i}'_0} = 0\,, \quad D_{j_0 i'_0} = 10\,, \quad D_{j_0 \hat{i}'_0} = 0\,, \\ \Longrightarrow \quad & n_{i_0 i'_0} - n_{i_0 \hat{i}'_0} - 1 + d_{j_0 i'_0} - d_{j_0 \hat{i}'_0} - 1 = 4 > 0\,, \end{aligned} \tag{7.11}$$

while in the latter case they remain massless since

$$\begin{aligned} & N_{i_0 i'_0} = 2\,, \quad N_{i_0 \hat{i}'_0} = 0\,, \quad D_{j_0 i'_0} = 2\,, \quad D_{j_0 \hat{i}'_0} = 0\,, \\ \Longrightarrow \quad & n_{i_0 i'_0} - n_{i_0 \hat{i}'_0} - 1 + d_{j_0 i'_0} - d_{j_0 \hat{i}'_0} - 1 = 0\,. \end{aligned} \tag{7.12}$$

Finally, the counting of the classically massless degrees of freedom can be done as in the brane configuration of Fig. 5a and leads to $n_{\rm F} - n_{\rm B} = 32$.

8 Conclusions

In this work, we have calculated the quadratic mass terms of the moduli fields arising in the ND+DN sector of the type IIB orientifold model compactified on $T^2 \times T^4/\mathbb{Z}_2$, when $\mathcal{N} = 2$ supersymmetry is spontaneously broken *via* the Scherk–Schwarz mechanism implemented along one direction of T^2. Assuming the string coupling is weak, this is done at one loop by computing the two-point functions of "boundary-changing vertex operators" inserted on the boundaries of the annulus and Möbius strip. The main difficulties of the derivation to which we have paid particular attention are the following:

- Using the stress-tensor method, the correlators of ground-state boundary-changing fields and spin fields are found up to "integration constants," which are functions of the Teichmüller parameters of the double-cover tori. This leads to an ambiguity in the full amplitude of interest, which is lifted by taking the limit where the insertion points of the vertices coalesce. Indeed, the expression reduces in this case to contributions of the partition function that arise from states with specific Chan–Paton indices only. This very fact makes this step of the computation more involved than its counterpart for closed-string amplitudes of twisted-sector states for which this identification is made with the entire partition function.

- The two-point function can be split into two parts referred to as "external" and "internal." The former, which is dressed by a kinematic factor, can be used to derive the one-loop correction to the Kähler metric and involves only correlation functions of "ground-state boundary-changing fields." By contrast, the internal part which captures the mass correction also requires correlators of "excited boundary-changing fields". These extra ingredients contain two contributions:[27] One arises from periodicity properties of the orbifold-background coordinates, and the other from pure local monodromy effects. Although the latter have often been neglected in favor of the former in the literature, both turn out to be of equal order of magnitude, as we have shown explicitly.

The squared masses of all moduli fields have been derived at one loop and up to contributions that are suppressed[28] when $M_{3/2}$ is lower than the other scales of the background. When the results are strictly positive, the corresponding scalars can be stabilized dynamically during the cosmological evolution of the universe [38, 66–71] in the regions in moduli space compatible with weak coupling and the assumption on $M_{3/2}$. However the potentially dominant contributions to the mass terms of moduli in the NN, DD or ND+DN open-string sectors can accidentally vanish for certain brane configurations. In such cases, the issue of quartic interactions potentially inducing instabilities of the backgrounds arises. The fact that the untwisted closed-string moduli $(G+C)_{I'J'}$ and $(G+C)_{IJ}$ are flat directions (up to exponentially suppressed corrections) seems to be a more severe difficulty. However, heterotic/type I duality can be used to show that non-perturbative contributions of D1-branes,

[27] Denoted as (1) and (2) in the correlators $\langle \tau^u \tau'^u \rangle_{\rm qu} = \langle \tau'^u \tau^u \rangle_{\rm qu}$.

[28] They can be exponentially or power-like suppressed.

which are captured by a one-loop computation of the effective potential on the heterotic side, can stabilize some of these moduli [38, 72–74].[29] However, for large Scherk–Schwarz direction *i.e.* small $M_{3/2} \equiv M_{\rm s}\sqrt{G^{55}}/2$ compared to $M_{\rm s}$, this mechanism is ineffective for the components $(G+C)_{5J}$ and $(G+C)_{5J'}$ (which include the degree of freedom of $M_{3/2}$ itself) for which extra physics should be invoked to yield their stabilization.

Acknowledgements

The authors would like to thank Ignatios Antoniadis and especially Emilian Dudas for useful inputs during the realization of this work. Steven Abel should also be warmly thanked for fruitful discussions and his participation to advanced stages of the project.

Appendix A: Conventions of matrix actions on Chan–Paton indices

In Ref. [5], the actions of the group elements $G \in \{1, g, \Omega, \Omega g\}$ on the Dirichlet or Neumann Chan–Paton indices $\alpha \in \{1, \ldots, 32\}$ are always represented by 32×32 matrices. If needed, they define traces with an index I (that would be denoted i in our notations) labelling a fixed point of $T^4/\mathbb{Z}_2$ to indicate when they restrict to the matrix entries associated with the fixed point I (see their Eq. (2.22)). In our conventions, we work directly with smaller matrices, one for each fixed point ii' of $\tilde{T}^2 \times T^4/\mathbb{Z}_2$ or $\tilde{T}^2 \times \tilde{T}^4/\mathbb{Z}_2$, which are submatrices of those used in Ref. [5]. In this appendix, we would like to give a detailed correspondance between their notations and ours for the traces appearing in the open-string contributions to the partition function.

Let us focus on the matrices acting on the Neumann Chan–Paton factors. In order to avoid any ambiguity, we first define the sets of indices $\mathcal{H}_{ii'}$ associated with the fixed points ii' that are used to generate the submatrices from the big ones. To this end, we label the fixed points in lexicographical order, $(11, 12, 13, 14, 21, \ldots)$, and introduce a function $p(i, i')$

[29] See also Ref. [75] for a stabilization of the Kähler and complex structure moduli of Calabi–Yau manifolds in type IIB (type IIA) thanks to D3-branes (D4- and D6-branes) contributions to the free energy, when $\mathcal{N} = 2$ supersymmetry is effectively broken by thermal effects.

that gives the predecessor in this list,

$$p(i,i') = \begin{cases} i, i'-1 & \text{if } i' \in \{2,3,4\} \\ i-1, 4 & \text{if } i' = 1 \end{cases} . \tag{A.1}$$

The sets are then

$$\mathcal{H}_{11} = \begin{cases} \varnothing & \text{if } N_{11} = 0 \\ \left\{1, \ldots, \frac{N_{11}}{2}\right\} \cup \left\{17, \ldots, 16 + \frac{N_{11}}{2}\right\} & \text{if } N_{11} \neq 0 \end{cases} , \tag{A.2}$$

and for $ii' \neq 11$,

$$\mathcal{H}_{ii'} = \begin{cases} \varnothing & \text{if } N_{ii'} = 0 \\ \left\{\frac{N_{p(i,i')}}{2} + 1, \ldots, \frac{N_{p(i,i')}}{2} + \frac{N_{ii'}}{2}\right\} \cup \left\{\frac{N_{p(i,i')}}{2} + 17, \ldots, 16 + \frac{N_{p(i,i')}}{2} + \frac{N_{ii'}}{2}\right\} & \text{if } N_{ii'} \neq 0 \end{cases} . \tag{A.3}$$

Our $N_{ii'} \times N_{ii'}$ matrices $\gamma_{\mathrm{N},G}^{ii'}$ are formed from 32×32 matrices $\gamma_{\mathrm{N},G}$ as follows,

$$\gamma_{\mathrm{N},G}^{ii'} = \gamma_{\mathrm{N},G}\big|_{\mathcal{H}_{ii'}} , \tag{A.4}$$

where the notation in the right-hand side means that we form submatrices by keeping the rows and columns $\alpha \in \mathcal{H}_{ii'}$. The traces of 32×32 matrices can then be expressed as

$$\begin{aligned} \mathrm{tr}(\gamma_{\mathrm{N},G}) &= \sum_{\alpha=1}^{32} (\gamma_{\mathrm{N},G})_{\alpha\alpha} = \sum_{i,i'} \sum_{\alpha \in \mathcal{H}_{ii'}} (\gamma_{\mathrm{N},G})_{\alpha\alpha} = \sum_{i,i'} \mathrm{tr}(\gamma_{\mathrm{N},G}\big|_{\mathcal{H}_{ii'}}) \\ &= \sum_{i,i'} \mathrm{tr}(\gamma_{\mathrm{N},G}^{ii'}) , \end{aligned} \tag{A.5}$$

and similarly for the matrices associated with the Dirichlet sector.

Moreover, in order to justify the replacement (2.15), let us define in our notations the 32×32 matrix $\mathcal{W}_j$ that is denoted W_I and appears in Eq. (2.22) of Ref. [5],

$$\mathcal{W}_j = \prod_{I=6}^{9} \mathcal{W}_I^{2a_j^I} , \quad \text{where} \quad \mathcal{W}_I = I_2 \otimes \begin{pmatrix} e^{2i\pi a_1^I} I_{\frac{N_1}{2}} & & 0 \\ & \ddots & \\ 0 & & e^{2i\pi a_{16}^I} I_{\frac{N_{16}}{2}} \end{pmatrix} , \quad N_i \equiv \sum_{i'} N_{ii'} . \tag{A.6}$$

For $G = g$ we have to compute

$$\begin{aligned} \mathrm{tr}(\mathcal{W}_j \gamma_{\mathrm{N},g}) &= \sum_{\alpha=1}^{32} (\mathcal{W}_j \gamma_{\mathrm{N},g})_{\alpha\alpha} = \sum_{\alpha=1}^{32} \sum_{\beta=1}^{32} (\mathcal{W}_j)_{\alpha\beta} (\gamma_{\mathrm{N},g})_{\beta\alpha} = \sum_{\alpha=1}^{32} (\mathcal{W}_j)_{\alpha\alpha} (\gamma_{\mathrm{N},g})_{\alpha\alpha} \\ &= \sum_{i,i'} \sum_{\alpha \in \mathcal{H}_{ii'}} (\mathcal{W}_j)_{\alpha\alpha} (\gamma_{\mathrm{N},g})_{\alpha\alpha} = \sum_{i,i'} e^{4i\pi \vec{a}_i \cdot \vec{a}_j} \sum_{\alpha \in \mathcal{H}_{ii'}} (\gamma_{\mathrm{N},g})_{\alpha\alpha} \\ &= \sum_{i,i'} e^{4i\pi \vec{a}_i \cdot \vec{a}_j} \mathrm{tr}(\gamma_{\mathrm{N},g}^{ii'}) . \end{aligned} \tag{A.7}$$

In this derivation, we have used the fact that the matrix $\mathcal{W}_j$ is diagonal and that its components $\alpha\alpha$ for $\alpha \in \mathcal{H}_{ii'}$ are $e^{4i\pi \vec{a}_i \cdot \vec{a}_j}$.

Appendix B: Closed-string sector partition function

In this appendix, we display the closed-string contributions to the one-loop partition function defined in Eq. (2.8).

In order to write $Z_{\mathcal{T}}$, we introduce the lattices of zero modes of the bosonic coordinates associated with T^4 and T^2,

$$\begin{aligned}
\Lambda^{(4,4)}_{\vec{m},\vec{n}}(\tau) &= q^{\frac{1}{4}P^{\rm L}_I G^{IJ} P^{\rm L}_J}\, \bar{q}^{\frac{1}{4}P^{\rm R}_I G^{IJ} P^{\rm R}_J}\,, \qquad P^{\rm L}_I = m_I + G_{IJ} n_J\,, \qquad P^{\rm R}_I = m_I - G_{IJ} n_J\,, \\
\Lambda^{(2,2)}_{\vec{m}',\vec{n}'}(\tau) &= q^{\frac{1}{4}P^{\rm L}_{I'} G^{I'J'} P^{\rm L}_{J'}}\, \bar{q}^{\frac{1}{4}P^{\rm R}_{I'} G^{I'J'} P^{\rm R}_{J'}}\,, \quad P^{\rm L}_{I'} = m_{I'} + G_{I'J'} n_{J'}\,, \quad P^{\rm R}_{I'} = m_{I'} - G_{I'J'} n_{J'}\,,
\end{aligned} \tag{B.1}$$

where $\vec{m}$, $\vec{n}$ and $\vec{m}'$, $\vec{n}'$ are four-vectors and two-vectors whose components are integer momenta and winding numbers.

Moreover, the worldsheet fermions generate an $SO(8)$ affine symmetry broken to $SO(4)\times SO(4)$ by the $\mathbb{Z}_2$-orbifold action. As a result, their contributions to the partition function take the forms of ordered pairs of characters of $SO(4)$. The latter can be expressed in terms of Jacobi modular forms and the Dedekind function,

$$\vartheta\begin{bmatrix}\alpha\\ \beta\end{bmatrix}(z|\tau) = \sum_{k\in\mathbb{Z}} q^{\frac{1}{2}(k+\alpha)^2} e^{2i\pi(z+\beta)(k+\alpha)}\,, \qquad \eta(\tau) = q^{\frac{1}{24}}\prod_{n=1}^{+\infty}(1-q^n)\,, \qquad q = e^{2i\pi\tau}\,. \tag{B.2}$$

Denoting as usual

$$\vartheta\begin{bmatrix}0\\ 0\end{bmatrix}(z|\tau) \equiv \vartheta_3(z|\tau)\,, \quad \vartheta\begin{bmatrix}0\\ \frac{1}{2}\end{bmatrix}(z|\tau) \equiv \vartheta_4(z|\tau)\,, \quad \vartheta\begin{bmatrix}\frac{1}{2}\\ 0\end{bmatrix}(z|\tau) \equiv \vartheta_2(z|\tau)\,, \quad \vartheta\begin{bmatrix}\frac{1}{2}\\ \frac{1}{2}\end{bmatrix}(z|\tau) \equiv \vartheta_1(z|\tau)\,, \tag{B.3}$$

the characters are given by [55–57]

$$O_4 = \frac{\vartheta_3^2+\vartheta_4^2}{2\eta^2}\,, \qquad V_4 = \frac{\vartheta_3^2-\vartheta_4^2}{2\eta^2}\,, \qquad S_4 = \frac{\vartheta_2^2+i^{-2}\vartheta_1^2}{2\eta^2}\,, \qquad C_4 = \frac{\vartheta_2^2-i^{-2}\vartheta_1^2}{2\eta^2}\,, \tag{B.4}$$

where it is understood that $\vartheta_n \equiv \vartheta_n(0|\tau)$.

Given these notations, the torus contribution to the partition function takes the following form,

$$\begin{aligned}
Z_{\mathcal{T}} = \frac{1}{4}\frac{1}{\tau_2^2}\Bigg\{\Bigg[& \left(|V_4O_4+O_4V_4|^2 + |S_4S_4+C_4C_4|^2\right)\sum_{\vec{m},\vec{n}}\frac{\Lambda^{(4,4)}_{\vec{m},\vec{n}}}{|\eta^4|^2} \\
& + \left(|V_4O_4-O_4V_4|^2 + |S_4S_4-C_4C_4|^2\right)\left|\frac{2\eta}{\vartheta_2}\right|^4 \\
& + 16\left(|O_4C_4+V_4S_4|^2 + |S_4O_4+C_4V_4|^2\right)\left|\frac{\eta}{\vartheta_4}\right|^4
\end{aligned}$$

$$
\begin{aligned}
&+16\left(|O_4C_4-V_4S_4|^2+|S_4O_4-C_4V_4|^2\right)\left|\frac{\eta}{\vartheta_3}\right|^4\Big]\sum_{\vec{m}',\vec{n}'}\frac{\Lambda^{(2,2)}_{\vec{m}',(n_4,2n_5)}}{|\eta^4|^2}\\
&-\Big[\Big((V_4O_4+O_4V_4)(\bar{S}_4\bar{S}_4+\bar{C}_4\bar{C}_4)+(S_4S_4+C_4C_4)(\bar{V}_4\bar{O}_4+\bar{O}_4\bar{V}_4)\Big)\sum_{\vec{m},\vec{n}}\frac{\Lambda^{(4,4)}_{\vec{m},\vec{n}}}{|\eta^4|^2}\\
&+\Big((V_4O_4-O_4V_4)(\bar{S}_4\bar{S}_4-\bar{C}_4\bar{C}_4)+(S_4S_4-C_4C_4)(\bar{V}_4\bar{O}_4-\bar{O}_4\bar{V}_4)\Big)\left|\frac{2\eta}{\vartheta_2}\right|^4\\
&+16\left((O_4C_4+V_4S_4)(\bar{S}_4\bar{O}_4+\bar{C}_4\bar{V}_4)+(S_4O_4+C_4V_4)(\bar{O}_4\bar{C}_4+\bar{V}_4\bar{S}_4)\right)\left|\frac{\eta}{\vartheta_4}\right|^4\\
&+16\left((O_4C_4-V_4S_4)(\bar{S}_4\bar{O}_4-\bar{C}_4\bar{V}_4)+(S_4O_4-C_4V_4)(\bar{O}_4\bar{C}_4-\bar{V}_4\bar{S}_4)\right)\left|\frac{\eta}{\vartheta_3}\right|^4\Big]\sum_{\vec{m}',\vec{n}'}\frac{\Lambda^{(2,2)}_{\vec{m}'+\vec{a}'_{\rm S},(n_4,2n_5)}}{|\eta^4|^2}\\
&+\Big[\Big(|O_4O_4+V_4V_4|^2+|C_4S_4+S_4C_4|^2\Big)\sum_{\vec{m},\vec{n}}\frac{\Lambda^{(4,4)}_{\vec{m},\vec{n}}}{|\eta^4|^2}+\Big(|O_4O_4-V_4V_4|^2+|S_4C_4-C_4S_4|^2\Big)\left|\frac{2\eta}{\vartheta_2}\right|^4\\
&+16\left(|O_4S_4+V_4C_4|^2+|S_4V_4+C_4O_4|^2\right)\left|\frac{\eta}{\vartheta_4}\right|^4\\
&+16\left(|O_4S_4-V_4C_4|^2+|S_4V_4-C_4O_4|^2\right)\left|\frac{\eta}{\vartheta_3}\right|^4\Big]\sum_{\vec{m}',\vec{n}'}\frac{\Lambda^{(2,2)}_{\vec{m}',(n_4,2n_5+1)}}{|\eta^4|^2}\\
&-\Big[\Big((O_4O_4+V_4V_4)(\bar{C}_4\bar{S}_4+\bar{S}_4\bar{C}_4)+(C_4S_4+S_4C_4)(\bar{O}_4\bar{O}_4+\bar{V}_4\bar{V}_4)\Big)\sum_{\vec{m},\vec{n}}\frac{\Lambda^{(4,4)}_{\vec{m},\vec{n}}}{|\eta^4|^2}\\
&+\Big((O_4O_4-V_4V_4)(\bar{S}_4\bar{C}_4-\bar{C}_4\bar{S}_4)+(S_4C_4-C_4S_4)(\bar{O}_4\bar{O}_4-\bar{V}_4\bar{V}_4)\Big)\left|\frac{2\eta}{\vartheta_2}\right|^4\\
&+16\left((O_4S_4+V_4C_4)(\bar{S}_4\bar{V}_4+\bar{C}_4\bar{O}_4)+(S_4V_4+C_4O_4)(\bar{O}_4\bar{S}_4+\bar{V}_4\bar{C}_4)\right)\left|\frac{\eta}{\vartheta_4}\right|^4\\
&+16\left((O_4S_4-V_4C_4)(\bar{S}_4\bar{V}_4-\bar{C}_4\bar{O}_4)+(S_4V_4-C_4O_4)(\bar{O}_4\bar{S}_4-\bar{V}_4\bar{C}_4)\right)\left|\frac{\eta}{\vartheta_3}\right|^4\Big]\sum_{\vec{m}',\vec{n}'}\frac{\Lambda^{(2,2)}_{\vec{m}'+\vec{a}'_{\rm S},(n_4,2n_5+1)}}{|\eta^4|^2}\Big\},
\end{aligned}
\tag{B.5}
$$

where the momenta $\vec{m}'$ of all fermionic degrees of freedom are shifted as shown in Eq. (2.5).

The expression of the Klein-bottle contribution to the partition function involves only left-right symmetric states which are therefore bosonic. As a result it is identical to that found in the supersymmetric model of Sect. 2.1,

$$
\begin{aligned}
Z_{\mathcal{K}}=&\frac{1}{4}\,\frac{1}{\tau_2^2}\,\Bigg\{(V_4O_4+O_4V_4)\left(\sum_{\vec{m}}\frac{P^{(4)}_{\vec{m}}}{\eta^4}+\sum_{\vec{n}}\frac{W^{(4)}_{\vec{n}}}{\eta^4}\right)+32\,(O_4C_4+V_4S_4)\left(\frac{\eta}{\vartheta_4}\right)^2\\
&-(S_4S_4+C_4C_4)\left(\sum_{\vec{m}}\frac{P^{(4)}_{\vec{m}}}{\eta^4}+\sum_{\vec{n}}\frac{W^{(4)}_{\vec{n}}}{\eta^4}\right)-32\,(S_4O_4+C_4V_4)\left(\frac{\eta}{\vartheta_4}\right)^2\Bigg\}\sum_{\vec{m}'}\frac{P^{(2)}_{\vec{m}'}}{\eta^4}\,,
\end{aligned}
\tag{B.6}
$$

where all lattices are identical to those defined in the open-string sector, Eqs. (2.10) and (2.11), and the characters and modular forms are evaluated at $2i\tau_2$.

Appendix C: Leading behavior of ε when $\alpha' \to 0$

In this appendix, we reconsider the small α' limit of the roots U_1 of $\Omega(U)$ for arbitrary $|\mathrm{Im}\, Y_1| < \frac{1}{2}\,\mathrm{Im}\,\tau^{\rm dc}$, which are given in Eq. (6.21). Our goal is to find the leading behavior of ε.

Using the full expansion of $\vartheta_1(z)$ given in Eq. (6.2), one obtains

$$\frac{\vartheta_1'}{\vartheta_1}(z) = \pi\cot(\pi z) + 2i\pi \sum_{n\geq 1}\Big[H(q_{\rm dc}^n\, e^{-2i\pi z}) - H(q_{\rm dc}^n\, e^{2i\pi z})\Big]\,, \quad H(z) \equiv \frac{z}{1-z}\,, \tag{C.1}$$

which can be used to rewrite the equation $\Omega(U_1) = 0$ as follows,

$$\begin{aligned} i\sin(\pi Y_1) = 2\sin(\pi U_1)\sin[\pi(Y_1-U_1)] \sum_{n\geq 1}\Big[&H\Big(q_{\rm dc}^n\, e^{-2i\pi U_1}\Big) - H\Big(q_{\rm dc}^n\, e^{2i\pi U_1}\Big) \\ &+ H\Big(q_{\rm dc}^n\, e^{-2i\pi (Y_1-U_1)}\Big) - H\Big(q_{\rm dc}^n\, e^{2i\pi (Y_1-U_1)}\Big)\Big]\,. \end{aligned} \tag{C.2}$$

Applying the change of variable given in Eq. (6.21), the above expression becomes

$$\begin{aligned} i\sin(\pi Y_1) = \frac{1}{2}\Big(1-(-1)^m\, i\, e^{i\pi(\tau^{\rm dc}+Y_1)}\, e^{2i\pi\varepsilon}\Big)\Big(1-(-1)^m\, i\, e^{i\pi(\tau^{\rm dc}-Y_1)}\, e^{2i\pi\varepsilon}\Big)\, e^{-2i\pi\varepsilon} \\ \times\Bigg\{ -\frac{e^{-i\pi Y_1}\, e^{-2i\pi\varepsilon}}{1+(-1)^m\, i\, e^{i\pi(\tau^{\rm dc}-Y_1)}\, e^{-2i\pi\varepsilon}} \\ + 2i\sum_{n\geq 1}\frac{q_{\rm dc}^n\, e^{-i\pi Y_1}\Big(\sin(2\pi\varepsilon) + (-1)^m\, q_{\rm dc}^n\, e^{i\pi(\tau^{\rm dc}-Y_1)}\Big)}{\Big(1+(-1)^m\, i\, q_{\rm dc}^n\, e^{i\pi(\tau^{\rm dc}-Y_1)}\, e^{-2i\pi\varepsilon}\Big)\Big(1-(-1)^m\, i\, q_{\rm dc}^n\, e^{i\pi(\tau^{\rm dc}-Y_1)}\, e^{2i\pi\varepsilon}\Big)} \\ - (Y_1\to -Y_1)\Bigg\}\,, \end{aligned} \tag{C.3}$$

where the first term in the braces and its transformed under $Y_1 \to -Y_1$ arise from the contributions $n = 1$ of the first and fourth functions H in Eq. (C.2).

- If $0 < \mathrm{Im}\, Y_1 < \frac{1}{2}\,\mathrm{Im}\,\tau^{\rm dc}$, and assuming $\varepsilon \to 0$ when $\alpha' \to 0$, Eq. (C.3) reads

$$\begin{aligned} (e^{2i\pi Y_1}-1)\, e^{-i\pi Y_1} = &\Big(1-2i\pi\varepsilon-(-1)^m\, i\, e^{i\pi(\tau^{\rm dc}-Y_1)} + \text{sub dom.}\Big) \\ &\Big\{ -e^{-i\pi Y_1}\Big(1-2i\pi\varepsilon-(-1)^m\, i\, e^{i\pi(\tau^{\rm dc}-Y_1)} + \text{sub dom.}\Big) \\ &\quad + e^{i\pi Y_1}\Big(1-2i\pi\varepsilon-(-1)^m\, i\, e^{i\pi(\tau^{\rm dc}+Y_1)} + \text{sub dom.}\Big)\Big\}\,, \end{aligned} \tag{C.4}$$

  where all contributions $n \geq 1$ have been absorbed in "subdominant" contributions. Simplifying this expression, one obtains

$$0 = 4i\pi\varepsilon + 2(-1)^m\, i\, e^{i\pi(\tau^{\rm dc}-Y_1)} + \text{subdom.}\,, \tag{C.5}$$

which leads to the asymptotics

$$\varepsilon \underset{\alpha'\to 0}{\sim} -\frac{(-1)^m}{2\pi}\, e^{i\pi(\tau^{\rm dc}-Y_1)} \underset{\alpha'\to 0}{\longrightarrow} 0\,. \tag{C.6}$$

Our assumption on the convergence of ε being consistent, we have shown the existence of solutions U_1 with the above behavior.

- If $-\frac{1}{2}\,\mathrm{Im}\,\tau^{\rm dc} < \mathrm{Im}\,Y_1 < 0$, Eq. (C.3) being invariant under $Y_1 \to -Y_1$, one obtains immediately from the previous analysis that

$$\varepsilon \underset{\alpha'\to 0}{\sim} -\frac{(-1)^m}{2\pi}\, e^{i\pi(\tau^{\rm dc}+Y_1)} \underset{\alpha'\to 0}{\longrightarrow} 0\,. \tag{C.7}$$

References

[1] L. J. Dixon, D. Friedan, E. J. Martinec and S. H. Shenker, "The conformal field theory of orbifolds," Nucl. Phys. B **282** (1987) 13.

[2] J. J. Atick, L. J. Dixon, P. A. Griffin and D. Nemeschansky, "Multiloop twist field correlation functions for $\mathbb{Z}_N$ orbifolds," Nucl. Phys. B **298** (1988) 1.

[3] M. Bianchi and A. Sagnotti, "Twist symmetry and open string Wilson lines," Nucl. Phys. B **361** (1991) 519.

[4] E. G. Gimon and J. Polchinski, "Consistency conditions for orientifolds and D-manifolds," Phys. Rev. D **54** (1996) 1667 [hep-th/9601038].

[5] M. Berkooz, R. G. Leigh, J. Polchinski, J. H. Schwarz, N. Seiberg and E. Witten, "Anomalies, dualities, and topology of $D = 6\ \mathcal{N} = 1$ superstring vacua," Nucl. Phys. B **475** (1996) 115 [hep-th/9605184].

[6] A. Hashimoto, "Dynamics of Dirichlet-Neumann open strings on D-branes," Nucl. Phys. B **496** (1997), 243-258 [arXiv:hep-th/9608127 [hep-th]].

[7] C. P. Burgess and T. R. Morris, "Open and unoriented strings à la Polyakov," Nucl. Phys. B **291** (1987), 256-284.

[8] C. P. Burgess and T. R. Morris, "Open superstrings à la Polyakov," Nucl. Phys. B **291** (1987), 285-333.

[9] M. Cvetic and I. Papadimitriou, "Conformal field theory couplings for intersecting D-branes on orientifolds," Phys. Rev. D **68** (2003), 046001 [erratum: Phys. Rev. D **70** (2004), 029903] [arXiv:hep-th/0303083 [hep-th]].

[10] S. A. Abel and A. W. Owen, "Interactions in intersecting brane models," Nucl. Phys. B **663** (2003), 197-214 [arXiv:hep-th/0303124 [hep-th]].

[11] S. A. Abel and A. W. Owen, "N-point amplitudes in intersecting brane models," Nucl. Phys. B **682** (2004), 183-216 [arXiv:hep-th/0310257 [hep-th]].

[12] P. Anastasopoulos, M. D. Goodsell and R. Richter, "Three- and four-point correlators of excited bosonic twist fields," JHEP **10** (2013), 182 [arXiv:1305.7166 [hep-th]].

[13] S. A. Abel and B. W. Schofield, "One-loop Yukawas on intersecting branes," JHEP **06** (2005), 072 [arXiv:hep-th/0412206 [hep-th]].

[14] B. Schofield, "One-loop phenomenology in brane models," Durham thesis, Durham University, Ph.D. Thesis.

[15] S. A. Abel and M. D. Goodsell, "Intersecting brane worlds at one loop," JHEP **02** (2006), 049 [arXiv:hep-th/0512072 [hep-th]].

[16] S. A. Abel and M. D. Goodsell, "Realistic Yukawa couplings through instantons in intersecting brane worlds," JHEP **10** (2007), 034 [arXiv:hep-th/0612110 [hep-th]].

[17] M. D. Goodsell, "One loop phenomenology of type II string theory: intersecting d-branes and noncommutativity," Durham thesis, Durham University, Ph.D. Thesis.

[18] K. Benakli and M. D. Goodsell, "Two-point functions of chiral fields at one loop in Type II," Nucl. Phys. B **805** (2008), 72-103 [arXiv:0805.1874 [hep-th]].

[19] J. Frohlich, O. Grandjean, A. Recknagel and V. Schomerus, "Fundamental strings in Dp - Dq brane systems," Nucl. Phys. B **583** (2000), 381-410 [arXiv:hep-th/9912079 [hep-th]].

[20] P. Anastasopoulos, M. Bianchi and R. Richter, "On closed-string twist-field correlators and their open-string descendants," [arXiv:1110.5359 [hep-th]].

[21] L. Mattiello and I. Sachs, "$\mathbb{Z}_2$ boundary twist fields and the moduli space of D-branes," JHEP **07** (2018), 099 [arXiv:1803.07500 [hep-th]].

[22] J. D. Blum and K. R. Dienes, "Duality without supersymmetry: The Case of the $SO(16) \times SO(16)$ string," Phys. Lett. B **414** (1997) 260 [hep-th/9707148].

[23] J. D. Blum and K. R. Dienes, "Strong / weak coupling duality relations for nonsupersymmetric string theories," Nucl. Phys. B **516** (1998) 83 [hep-th/9707160].

[24] I. Antoniadis, E. Dudas and A. Sagnotti, "Supersymmetry breaking, open strings and M-theory," Nucl. Phys. B **544** (1999) 469 [hep-th/9807011].

[25] I. Antoniadis, G. D'Appollonio, E. Dudas and A. Sagnotti, "Partial breaking of supersymmetry, open strings and M-theory," Nucl. Phys. B **553** (1999) 133 [hep-th/9812118].

[26] I. Antoniadis, G. D'Appollonio, E. Dudas and A. Sagnotti, "Open descendants of $\mathbb{Z}_2 \times \mathbb{Z}_2$ freely acting orbifolds," Nucl. Phys. B **565** (2000) 123 [hep-th/9907184].

[27] A. L. Cotrone, "A $\mathbb{Z}_2 \times \mathbb{Z}_2$ orientifold with spontaneously broken supersymmetry," Mod. Phys. Lett. A **14** (1999) 2487 [hep-th/9909116].

[28] C. A. Scrucca and M. Serone, "On string models with Scherk–Schwarz supersymmetry breaking," JHEP **0110** (2001) 017 [hep-th/0107159].

[29] C. Angelantonj, M. Cardella and N. Irges, "Scherk–Schwarz breaking and intersecting branes," Nucl. Phys. B **725** (2005) 115 [hep-th/0503179].

[30] J. Scherk and J. H. Schwarz, "Spontaneous breaking of supersymmetry through dimensional reduction," Phys. Lett. B **82** (1979) 60.

[31] J. Scherk and J. H. Schwarz, "How to get masses from extra dimensions," Nucl. Phys. B **153** (1979), 61-88.

[32] S. Abel, T. Coudarchet and H. Partouche, "On the stability of open-string orbifold models with broken supersymmetry," Nucl. Phys. B **957** (2020), 115100 [arXiv:2003.02545 [hep-th]].

[33] S. Abel, E. Dudas, D. Lewis and H. Partouche, "Stability and vacuum energy in open string models with broken supersymmetry," JHEP **1910** (2019) 226 [arXiv:1812.09714 [hep-th]].

[34] H. Itoyama and T. R. Taylor, "Supersymmetry restoration in the compactified $O(16) \times O(16)'$ heterotic string theory," Phys. Lett. B **186** (1987) 129.

[35] S. Abel, K. R. Dienes and E. Mavroudi, "Towards a non-supersymmetric string phenomenology," Phys. Rev. D **91** (2015) 126014 [arXiv:1502.03087 [hep-th]].

[36] C. Kounnas and H. Partouche, "Super no-scale models in string theory," Nucl. Phys. B **913** (2016) 593 [arXiv:1607.01767 [hep-th]].

[37] C. Kounnas and H. Partouche, "$\mathcal{N} = 2 \to 0$ super no-scale models and moduli quantum stability," Nucl. Phys. B **919** (2017) 41 [arXiv:1701.00545 [hep-th]].

[38] T. Coudarchet and H. Partouche, "Quantum no-scale regimes and moduli dynamics," Nucl. Phys. B **933** (2018) 134 [arXiv:1804.00466 [hep-th]].

[39] I. Florakis and J. Rizos, "Chiral heterotic strings with positive cosmological constant," Nucl. Phys. B **913** (2016) 495 [arXiv:1608.04582 [hep-th]].

[40] S. Abel and R. J. Stewart, "On exponential suppression of the cosmological constant in non-SUSY strings at two loops and beyond," Phys. Rev. D **96** (2017) 106013 [arXiv:1701.06629 [hep-th]].

[41] S. Abel, K. R. Dienes and E. Mavroudi, "GUT precursors and entwined SUSY: The phenomenology of stable nonsupersymmetric strings," Phys. Rev. D **97** (2018) no.12, 126017 [arXiv:1712.06894 [hep-ph]].

[42] H. Itoyama and S. Nakajima, "Exponentially suppressed cosmological constant with enhanced gauge symmetry in heterotic interpolating models," PTEP **2019** (2019) no.12, 123B01 [arXiv:1905.10745 [hep-th]].

[43] H. Itoyama and S. Nakajima, "Stability, enhanced gauge symmetry and suppressed cosmological constant in 9D heterotic interpolating models," Nucl. Phys. B **958** (2020), 115111 [arXiv:2003.11217 [hep-th]].

[44] T. Coudarchet and H. Partouche, "Moduli stability in type I string orbifold models," PoS **CORFU2019** (2020), 164 [arXiv:2005.01764 [hep-th]].

[45] J. Polchinski, "Tasi lectures on D-branes," hep-th/9611050.

[46] D. Cremades, L. E. Ibanez and F. Marchesano, "Intersecting brane models of particle physics and the Higgs mechanism," JHEP **0207** (2002) 022 [hep-th/0203160].

[47] D. Cremades, L. E. Ibanez and F. Marchesano, "Yukawa couplings in intersecting D-brane models," JHEP **0307** (2003) 038 [hep-th/0302105].

[48] B. Kors and P. Nath, "Effective action and soft supersymmetry breaking for intersecting D-brane models," Nucl. Phys. B **681** (2004) 77 [hep-th/0309167].

[49] D. Cremades, L. E. Ibanez and F. Marchesano, "Computing Yukawa couplings from magnetized extra dimensions," JHEP **0405** (2004) 079 [hep-th/0404229].

[50] R. Rohm, "Spontaneous supersymmetry breaking in supersymmetric string theories," Nucl. Phys. B **237** (1984) 553.

[51] C. Kounnas and M. Porrati, "Spontaneous supersymmetry breaking in string theory," Nucl. Phys. B **310** (1988) 355.

[52] S. Ferrara, C. Kounnas and M. Porrati, "Superstring solutions with spontaneously broken four-dimensional supersymmetry," Nucl. Phys. B **304** (1988) 500.

[53] S. Ferrara, C. Kounnas, M. Porrati and F. Zwirner, "Superstrings with spontaneously broken supersymmetry and their effective theories," Nucl. Phys. B **318** (1989) 75.

[54] C. Kounnas and B. Rostand, "Coordinate-dependent compactifications and discrete symmetries," Nucl. Phys. B **341** (1990) 641.

[55] W. Lerche, A. N. Schellekens and N. P. Warner, "Lattices and strings," Phys. Rept. **177** (1989) 1.

[56] W. Lerche, D. Lust and A. N. Schellekens, "Chiral four-dimensional heterotic strings from selfdual lattices," Nucl. Phys. B **287** (1987) 477.

[57] R. Blumenhagen, D. Lüst and S. Theisen, "Basic concepts of string theory," Springer-Verlag, doi:10.1007/978-3-642-29497-6

[58] C. Angelantonj and A. Sagnotti, "Open strings," Phys. Rept. **371** (2002) 1 [Erratum-ibid. **376** (2003) 339] [arXiv:hep-th/0204089].

[59] E. Dudas, "Theory and phenomenology of type I strings and M-theory," Class. Quant. Grav. **17** (2000) R41 [arXiv:hep-ph/0006190].

[60] D. Friedan, E. J. Martinec and S. H. Shenker, "Conformal Invariance, Supersymmetry and String Theory," Nucl. Phys. B **271** (1986), 93-165.

[61] I. Antoniadis, C. Bachas, C. Fabre, H. Partouche and T. R. Taylor, "Aspects of type I - type II - heterotic triality in four-dimensions," Nucl. Phys. B **489** (1997) 160 [hep-th/9608012].

[62] E. Kiritsis, "String theory in a nutshell," Princeton University Press (2007) 588 p.

[63] J. Polchinski, "String theory. Vol. 1: An introduction to the bosonic string," Cambridge University Press (1998).

[64] M. Dine and N. Seiberg, "Is the superstring weakly coupled?," Phys. Lett. B **162** (1985), 299-302.

[65] E. Cremmer, S. Ferrara, C. Kounnas and D. V. Nanopoulos, "Naturally vanishing cosmological constant in $\mathcal{N} = 1$ supergravity," Phys. Lett. B **133** (1983) 61.

[66] F. Bourliot, J. Estes, C. Kounnas and H. Partouche, "Cosmological phases of the string thermal effective potential," Nucl. Phys. B **830** (2010) 330 [arXiv:0908.1881 [hep-th]].

[67] J. Estes, C. Kounnas and H. Partouche, "Superstring cosmology for $\mathcal{N}_4 = 1 \to 0$ superstring vacua," Fortsch. Phys. **59** (2011) 861 [arXiv:1003.0471 [hep-th]].

[68] T. Catelin-Jullien, C. Kounnas, H. Partouche and N. Toumbas, "Induced superstring cosmologies and moduli stabilization," Nucl. Phys. B **820** (2009) 290 [arXiv:0901.0259 [hep-th]].

[69] F. Bourliot, C. Kounnas and H. Partouche, "Attraction to a radiation-like era in early superstring cosmologies," Nucl. Phys. B **816** (2009) 227 [arXiv:0902.1892 [hep-th]].

[70] T. Catelin-Jullien, C. Kounnas, H. Partouche and N. Toumbas, "Thermal/quantum effects and induced superstring cosmologies," Nucl. Phys. B **797** (2008) 137 [arXiv:0710.3895 [hep-th]].

[71] T. Coudarchet, C. Fleming and H. Partouche, "Quantum no-scale regimes in string theory," Nucl. Phys. B **930** (2018) 235 [arXiv:1711.09122 [hep-th]].

[72] J. Estes, L. Liu and H. Partouche, "Massless D-strings and moduli stabilization in type I cosmology," JHEP **06** (2011), 060 [arXiv:1102.5001 [hep-th]].

[73] C. Angelantonj, H. Partouche and G. Pradisi, "Heterotic – type I dual pairs, rigid branes and broken SUSY," Nucl. Phys. B **954** (2020), 114976 [arXiv:1912.12062 [hep-th]].

[74] H. Partouche and B. De Vaulchier, "Heterotic orbifolds, reduced rank and $SO(2n+1)$ characters," Int. J. Mod. Phys. A **35** (2020) no.24, 2050132 [arXiv:2006.08194 [hep-th]].

[75] L. Liu and H. Partouche, "Moduli stabilization in type II Calabi–Yau compactifications at finite temperature," JHEP **11** (2012), 079 [arXiv:1111.7307 [hep-th]].

JHEP

Published for SISSA by Springer

Received: June 2, 2021
Accepted: July 2, 2021
Published: July 16, 2021

Geometry of orientifold vacua and supersymmetry breaking

Thibaut Coudarchet, Emilian Dudas and Hervé Partouche

CPHT, CNRS, Ecole Polytechnique, IP Paris,
F-91128 Palaiseau, France

E-mail: thibaut.coudarchet@polytechnique.edu,
emilian.dudas@polytechnique.edu, herve.partouche@polytechnique.edu

Abstract: Starting from a peculiar orientifold projection proposed long ago by Angelantonj and Cardella, we elaborate on a novel perturbative scenario that involves only D-branes, together with the two types of orientifold planes $O_\pm$ and anti-orientifold planes $\overline{O}_\pm$. We elucidate the microscopic ingredients of such models, connecting them to a novel realization of brane supersymmetry breaking. Depending on the position of the D-branes in the internal space, supersymmetry can be broken at the string scale on branes, or alternatively only at the massive level. The main novelty of this construction is that it features no NS-NS disk tadpoles, while avoiding open-string instabilities. The one-loop potential, which depends on the positions of the D-branes, is minimized for maximally broken, non-linearly realized supersymmetry. The orientifold projection and the effective field theory description reveal a soft breaking of supersymmetry in the closed-string sector. In such models it is possible to decouple the gravitino mass from the value of the scalar potential, while avoiding brane instabilities.

Keywords: D-branes, Superstring Vacua, Supersymmetry Breaking

ArXiv ePrint: 2105.06913

https://doi.org/10.1007/JHEP07(2021)104

JHEP07(2021)104

Contents

JHEP07(2021)104

1 Introduction

Supersymmetry breaking in string theory is notoriously difficult to achieve in a controllable manner. There are several challenging and well-known problems to overcome at the string level and at the effective field theory one.

A generic issue, both at string perturbative and effective supergravity levels, is that supersymmetry breaking generates potentials for some moduli fields that are of runaway type, which typically drive the dynamics towards zero or strong string coupling, and also lead to decompactification or compactification of the internal space [1]. The state of the art is to generate a local minimum somewhere far from the runaway regime, that is computationally reliable and such that the corresponding lifetime is beyond the age of the universe. Such a minimum is very hard to obtain in string perturbation theory, and easier

in practice to obtain at the effective field-theory level, adding extra ingredients like fluxes or nonperturbative effects.

At the string perturbative level, supersymmetry breaking generates a vacuum energy (more precisely, a scalar potential) at some order in perturbation theory. In the first models of supersymmetry breaking, so-called Scherk-Schwarz or breaking by compactification [2–7], this arises at one loop.[1] The generated scalar potential is typically of runaway type[2] and the classical vacuum used in perturbation theory is therefore not valid anymore. It is however possible, in a more refined construction, to stabilize the corresponding modulus, yielding a negative scalar potential [9]. In a subclass of models, which satisfy a classical Bose/Fermi degeneracy at the massless level, this one-loop potential turns out to be exponentially suppressed at low supersymmetry breaking scale [18–30], but not vanishing [31].

Later on, tachyon-free orientifold string models where supersymmetry is broken at the string scale in the open-string (gauge) sector, whereas the closed-string (gravity) sector is supersymmetric at lowest perturbative order were constructed [32–37]. Since in such frameworks a massless gravitino is present, supersymmetry has to be nonlinearly realized in the open sector and this was indeed shown explicitly in [38, 39]. Such models contain non-BPS tachyon-free configurations. An important application of such setups is the KKLT scenario of moduli stabilization [40], see e.g. [41–47]. There was also a recent simplification in constructing supergravity models with nonlinear supersymmetry [48–52], stimulated in part by "Brane Supersymmetry Breaking" (BSB) type models. In such settings, there is a runaway scalar potential generated at the disk level. Ignoring the true vacuum state and working naively at fixed values of moduli fields leads to so-called NS-NS tadpoles for the corresponding moduli, which ruin perturbation theory since they generate unphysical UV divergences. It is widely believed that this does not signal any inconsistency of the theory, but just the fact that naive perturbation theory is performed around a point in field space that is not an extremum. Indeed, all models of this type constructed in the literature satisfy all known consistency conditions. Mechanisms of shifting the vacuum, in analogy with field-theory examples, were proposed in the literature [53–56]. However their practical implementation is limited to toy examples or to special models with small tadpoles. Hence, whereas the BSB models are tachyon-free, the presence of NS-NS tadpoles raises the question of the validity of perturbation theory and the fate of such constructions [57–60]. Let us also mention that the coexistence of massless gravitinos and broken supersymmetry in the open sector in BSB models is shared by compactifications with internal magnetic fields that break supersymmetry [61–64].

In another class of non-supersymmetric models based on type II asymmetric orbifolds or their orientifold descendants [65–71], a classical Bose/Fermi degeneracy valid at any mass level implies that the potential arises only at two loops [72, 73]. In such frameworks, there are no tadpoles at one loop and no need to shift scalar expectation values for describing vacua at this order of perturbation theory. However, stability at one loop of the moduli fields has not been analyzed.

[1] Scherk-Schwarz compactifications also have often additional, tachyonic-like instabilities in some range of parameters. Tachyon-free examples however exist, see e.g. [8–10].

[2] The cosmological evolution of the moduli fields can be studied in a thermal [11–15] or cold [16, 17] universe.

JHEP07(2021)104

The goal of the present paper is the construction of BSB string vacua without NS-NS disk tadpoles. Recently, it was conjectured that massless gravitinos in string theory with broken supersymmetry implies a breakdown of the effective field theory [74, 75]. It is clearly of interest to check this conjecture in explicit string models, by trying to avoid NS-NS tadpoles. In this paper we identify constructions in which the supersymmetry breaking scale in the gauge (open) sector is much higher than in the closed-string sector. This was actually achieved previously in [76]. However, our construction avoids the open-string tachyonic instabilities typically present in such constructions. A runaway behaviour for internal radii is however still present. We show that the limit of vanishing gravitino mass is inconsistent. The existence of such constructions was already anticipated in the pioneering paper [77] in an algebraic construction using the tools of the Tor-Vergata school [78–86]. We provide here the correct geometric interpretation of the eight-dimensional class of models proposed in [77], which turns out to contain several types of perturbative orientifold and anti-orientifold planes. We also point out that the simultaneous presence of orientifold and antiorientifold planes suggests that the closed-string sector is not exactly supersymmetric at tree-level, but has softly broken supersymmetry. The basic mechanism goes as follows.

One starts with a supersymmetric orientifold model containing both O_- (negative tension, negative RR charge) and O_+-planes (positive tension, positive RR charge). A consistent supersymmetry-breaking deformation of the model turns one O_--O_+ pair into an $\overline{O}_-$-$\overline{O}_+$ pair, which is mutually BPS but preserves the other half of the supersymmetries compared to the $O_\pm$-planes and D-branes. Since both the initial O_--O_+ pair and its SUSY breaking avatar $\overline{O}_-$-$\overline{O}_+$ have zero total tension and charge, there will be no RR or NS-NS tadpoles generated in the non-supersymmetric case. Depending on where the background D-branes sit in the internal space, their massless spectrum can be supersymmetric (if they sit on top of O_- or O_+-planes or in the bulk) or non-supersymmetric (if they sit on top of $\overline{O}_-$ or $\overline{O}_+$-planes, in which case supersymmetry is nonlinearly realized in their world-volume). Such models also have a supersymmetric limit, when a certain radius is taken to zero.[3] For small values of this radius, the breaking can be interpreted as spontaneous, whereas for large values, supersymmetry breaking can be considered as nonlinearly realized if branes sit on top of anti-orientifold planes. Interestingly, naive energetic considerations on brane-orientifold plane interactions suggest that the branes move towards stable configurations with maximal (string scale) breaking of supersymmetry. Whereas at first sight the closed-string spectrum could be supersymmetric, we show that a detailed look at the orientifold projections leading to the geometry of O-planes and, independently, considerations from low-energy effective field theory suggest that the correct option is a specific soft supersymmetry breaking deformation in the closed-string sector. A more detailed analysis of the effective field theory of this class of models deserves however a dedicated study.

The structure of the paper is the following: in section 2, we review the 8d USp(16) supersymmetric orientifold theory and introduce the novel Brane Supersymmetry Breaking (BSB) mechanism. In particular, we discuss the consistency between the soft breaking of

[3] A similar option is available in IIB flux compactifications [87]. We thank J. Mourad and A. Sagnotti for sharing their results with us.

JHEP07(2021)104

supersymmetry in the closed-string spectrum and the supersymmetry breaking deformation in the open-string sector. The generalization of the construction to dimensions lower than 8 turns out to be rich but straightforward. We give various examples in section 3. Section 4 discusses consistency conditions coming from probe branes as well as nonperturbative constraints to be satisfied by these models. In section 5, we study the supersymmetry breaking mass scales in the closed- and open-string sectors for different positions of stacks of D7-branes in 8d. We also comment on the limit of vanishing gravitino mass and the connexion with the gravitino mass conjecture put forward recently in [74, 75], in the context of the swampland program [88–90]. Conclusions and outlooks can be found in section 6, whereas an appendix contains examples of consistent and inconsistent geometric configurations.

2 The 8d USp(16) superstring and its SUSY breaking avatar

In this section, we review the construction of the supersymmetric USp(16) orientifold model in 8 dimensions and then present its non-supersymmetric version.

2.1 The type IIB torus amplitudes

Let us start by describing alternative viewpoints for deriving the supersymmetric and non-supersymmetric torus amplitudes to be combined later on with orientifold amplitudes.

The original orientifold models described in [91, 92] make use of a non-trivial quantized background for the internal components of the antisymmetric tensor field, B_{ij}. This field is odd under worldsheet parity and therefore it is projected out by the orientifold projection Ω in type I superstring. However, this still leaves the possibility to add a quantized value $\frac{2}{\alpha'}B_{ij} \in \mathbb{Z}$, where α' is the string tension. In this case, the left and right momenta of closed-string states are given, for a torus factorized into two circles, by

$$p^8_{\rm L,R} = \frac{m_8 + n_9/2}{R_8} \pm \frac{n_8 R_8}{\alpha'}\,, \qquad p^9_{\rm L,R} = \frac{m_9 - n_8/2}{R_9} \pm \frac{n_9 R_9}{\alpha'}\,. \tag{2.1}$$

The type IIB torus amplitude is given by

$$\begin{aligned}\mathcal{T} = \int \frac{\mathrm{d}^2\tau}{\tau_2^5} \Big[&\Lambda_{m_9,2n_9}\Lambda_{m_8,2n_8} + \Lambda_{m_9+1/2,2n_9}\Lambda_{m_8,2n_8+1} \\ &+\Lambda_{m_9,2n_9+1}\Lambda_{m_8+1/2,2n_8} + \Lambda_{m_9+1/2,2n_9+1}\Lambda_{m_8+1/2,2n_8+1}\Big] \left|\frac{V_8 - S_8}{\eta^8}\right|^2\,,\end{aligned} \tag{2.2}$$

where V_8, S_8 (along with O_8, C_8) are the SO(8) affine characters and η is the Dedeking function. They all depend on the Teichmüller parameter τ of the genus-1 surface, whose imaginary part is denoted τ_2. Moreover, the lattices are expressed in terms of

$$\Lambda_{m_i,n_i} = q^{\frac{\alpha'}{4}\left(\frac{m_i}{R_i}+n_i\frac{R_i}{\alpha'}\right)^2} \bar{q}^{\frac{\alpha'}{4}\left(\frac{m_i}{R_i}-n_i\frac{R_i}{\alpha'}\right)^2}\,, \qquad q = e^{2i\pi\tau}\,, \tag{2.3}$$

where m_i, n_i are the momentum and winding numbers along direction X^i.[4] Note that this amplitude is invariant under the T-duality transformation $(R_8, R_9) \to (\frac{\alpha'}{2R_8}, \frac{\alpha'}{2R_9})$.

[4]Throughout our work, all discrete sums over integer m_i, n_i are implicit. The conventions used in partition functions are those given e.g. in the reviews [85, 86].

JHEP07(2021)104

There is another particularly useful way of constructing the torus amplitude with non-trivial discrete antisymmetric tensor uncovered by Pradisi [93]. The starting point is a freely-acting orbifold of type IIB with $B_{89}=0$ and generator $g=\delta_{w_8}\delta_{p_9}$, where δ_{w_8} stands for a winding shift along direction X^8 while δ_{p_9} denotes a momentum shift along direction X^9. The action of this generator on the lattice states is

$$g|\mathbf{m},\mathbf{n}\rangle=(-1)^{n_8+m_9}|\mathbf{m},\mathbf{n}\rangle\,. \tag{2.4}$$

The gauging of the theory with this generator implies the existence of four contributions in the torus amplitude corresponding to the untwisted and twisted sectors, both with or without insertion of the orbifold generator in the traces. One obtains

$$\mathcal{T}=\frac{1}{2}\int\frac{\mathrm{d}^2\tau}{\tau_2^5}\left[1+(-1)^{n_8+m_9}\right]\left(\Lambda_{m_8,n_8}\Lambda_{m_9,n_9}+\Lambda_{m_8+\frac{1}{2},n_8}\Lambda_{m_9,n_9+\frac{1}{2}}\right)\left|\frac{V_8-S_8}{\eta^8}\right|^2\,. \tag{2.5}$$

A rescaling of the radius $R_9\to 2R_9$ then leads to the torus amplitude with discrete anti-symmetric tensor given in eq. (2.2).

Note that another derivation can be obtained by applying the T-duality transformation $R_8\to\frac{\alpha'}{R_8}=\tilde{R}_8$ on the freely-acting orbifold of type IIB with $B_{89}=0$. In fact, the complex coordinate $Z=\frac{\tilde{X}_8+iX_9}{2\pi\tilde{R}_8}$, where $\tilde{X}_8$ is the T-dual coordinate, satisfies the identifications $Z=Z+1=Z+i\frac{R_9}{\tilde{R}_8}$. Moreover, the orbifold generator $g=\delta_{w_8}\delta_{p_9}$ is mapped to $\tilde{g}=\delta_{p_8}\delta_{p_9}$ defined as $(\tilde{X}_8,X_9)=(\tilde{X}_8+\pi\tilde{R}_8,X_9+\pi R_9)$. We have therefore three identifications, which can be encoded in the following two:

$$Z=Z+1\,,\quad Z=Z+U\,,\quad \text{where}\quad U=\frac{1}{2}+i\frac{R_9}{2\tilde{R}_8}\,. \tag{2.6}$$

Hence, by rescaling $R_9\to 2R_9$, the coordinate Z is that of a tilted torus of complex structure $U=\frac{1}{2}+i\frac{R_9}{\tilde{R}_8}$. However, it is known that the type IIA theory compactified on this tilted torus is T-dual to the type IIB theory with antisymmetric background $B_{89}=\frac{\alpha'}{2}$.

From the freely-acting orbifold perspective, it is now easy to build a non-supersymmetric deformation of the type IIB model in a Scherk-Schwarz spirit. It is obtained by replacing g with the generator $g'=(-1)^F\delta_{w_8}\delta_{p_9}$, where F denotes the spacetime fermion number. The construction of the torus amplitude is straightforward and the result is

$$\begin{aligned}\mathcal{T}=\frac{1}{2}\int\frac{\mathrm{d}^2\tau}{\tau_2^5}\Big\{&\Lambda_{m_8,n_8}\Lambda_{m_9,n_9}\left|V_8-S_8\right|^2+(-1)^{n_8+m_9}\Lambda_{m_8,n_8}\Lambda_{m_9,n_9}\left|V_8+S_8\right|^2\\&+\Lambda_{m_8+\frac{1}{2},n_8}\Lambda_{m_9,n_9+\frac{1}{2}}\left|O_8-C_8\right|^2+(-1)^{n_8+m_9}\Lambda_{m_8+\frac{1}{2},n_8}\Lambda_{m_9,n_9+\frac{1}{2}}\left|O_8+C_8\right|^2\Big\}\frac{1}{|\eta^8|^2}\,.\end{aligned} \tag{2.7}$$

The rescaling of the radius $R_9\to 2R_9$ then leads to

$$\begin{aligned}\mathcal{T}=\int\frac{\mathrm{d}^2\tau}{\tau_2^5}\Big\{&\left(\Lambda_{m_8,2n_8}\Lambda_{m_9,2n_9}+\Lambda_{m_8,2n_8+1}\Lambda_{m_9+\frac{1}{2},2n_9}\right)\left(|V_8|^2+|S_8|^2\right)\\&-\left(\Lambda_{m_8,2n_8+1}\Lambda_{m_9,2n_9}+\Lambda_{m_8,2n_8}\Lambda_{m_9+\frac{1}{2},2n_9}\right)\left(V_8\overline{S}_8+\overline{V}_8S_8\right)\\&+\left(\Lambda_{m_8+\frac{1}{2},2n_8}\Lambda_{m_9,2n_9+1}+\Lambda_{m_8+\frac{1}{2},2n_8+1}\Lambda_{m_9+\frac{1}{2},2n_9+1}\right)\left(|O_8|^2+|C_8|^2\right)\\&-\left(\Lambda_{m_8+\frac{1}{2},2n_8+1}\Lambda_{m_9,2n_9+1}+\Lambda_{m_8+\frac{1}{2},2n_8}\Lambda_{m_9+\frac{1}{2},2n_9+1}\right)\left(O_8\overline{C}_8+\overline{O}_8C_8\right)\Big\}\frac{1}{|\eta^8|^2}\,.\end{aligned} \tag{2.8}$$

JHEP07(2021)104

The type IIB gravitinos acquire masses

$$M_1 = \frac{R_8}{\alpha'} \qquad \text{or} \qquad M_2 = \frac{1}{2R_9}\,, \tag{2.9}$$

which vanish in the supersymmetric limits $R_8 \to 0$ and/or $R_9 \to \infty$. Moreover, as usual with a Scherk-Schwarz mechanism, a scalar in the twisted sector becomes tachyonic when the radii satisfy

$$\frac{1}{4R_8^2} + \frac{R_9^2}{\alpha'^2} < \frac{2}{\alpha'}\,. \tag{2.10}$$

Notice that, unlike its supersymmetric version (2.2), the torus amplitude (2.8) is not invariant under the T-duality $(R_8, R_9) \to (\frac{\alpha'}{2R_8}, \frac{\alpha'}{2R_9})$. Indeed, this transformation amounts to exchanging the lattice sums of the two directions and thus switching $X^8 \leftrightarrow X^9$, leading to the new amplitude

$$\begin{aligned}\tilde{\mathcal{T}} = \int \frac{\mathrm{d}^2\tau}{\tau_2^5}\Big\{ &\Big(\Lambda_{m_8,2n_8}\Lambda_{m_9,2n_9} + \Lambda_{m_8+\frac{1}{2},2n_8}\Lambda_{m_9,2n_9+1}\Big)\Big(|V_8|^2 + |S_8|^2\Big)\\ &- \Big(\Lambda_{m_8,2n_8}\Lambda_{m_9,2n_9+1} + \Lambda_{m_8+\frac{1}{2},2n_8}\Lambda_{m_9,2n_9}\Big)\Big(V_8\overline{S}_8 + \overline{V}_8 S_8\Big)\\ &+ \Big(\Lambda_{m_8,2n_8+1}\Lambda_{m_9+\frac{1}{2},2n_9} + \Lambda_{m_8+\frac{1}{2},2n_8+1}\Lambda_{m_9+\frac{1}{2},2n_9+1}\Big)\Big(|O_8|^2 + |C_8|^2\Big)\\ &- \Big(\Lambda_{m_8,2n_8+1}\Lambda_{m_9+\frac{1}{2},2n_9+1} + \Lambda_{m_8+\frac{1}{2},2n_8+1}\Lambda_{m_9+\frac{1}{2},2n_9}\Big)\Big(O_8\overline{C}_8 + \overline{O}_8 C_8\Big)\Big\}\frac{1}{|\eta^8|^2}\,.\end{aligned} \tag{2.11}$$

The latter can therefore be obtained by a free action generated by $g'' = (-1)^F \delta_{p_8}\delta_{w_9}$, followed by the rescaling $R_8 \to 2R_8$. In this case, the masses of the gravitinos are

$$M_1 = \frac{1}{2R_8} \qquad \text{or} \qquad M_2 = \frac{R_9}{\alpha'} \tag{2.12}$$

and supersymmetry is restored in the limits $R_8 \to \infty$ and/or $R_9 \to 0$.

2.2 The supersymmetric orientifold amplitudes

In eight dimensions, the gauge group in supersymmetric orientifold models has rank 16, 8 or 0.[5] For rank 8, the gauge group of maximal dimension, i.e. in the absence of Wilson lines, is USp(16). This 8d model was first constructed by Bianchi, Pradisi and Sagnotti in terms of D9-branes and an O9$_-$-plane [91, 92]. It also has a dual description in terms of CHL strings [94]. Moreover, it admits a geometrical T-dual picture understood later on by Witten, which we will consider hereafter [95].

In the case of the standard SO(32) type I superstring, i.e. with $B_{89} = 0$, the standard T-duality transformation $(R_8, R_9) \to (\frac{\alpha'}{R_8}, \frac{\alpha'}{R_9})$ turns the O9$_-$-plane wrapping the torus into four O7$_-$-planes located at the orientifold fixed points of the generator $\Omega' = \Omega\Pi_8\Pi_9(-1)^{F_{\rm L}}$. In our notations, Π_i is a parity operation $X^i \to -X^i$ and $F_{\rm L}$ is the left-handed fermion number. This geometry is depicted in figure 1a and the resulting model contains 16 D7-branes[6] in order to cancel the RR tadpole.

[5] We refer only to the gauge group arising from the open-string/D-brane sector.

[6] Or equivalently 32 "half-branes" of type IIB organized as 16 mirror pairs referred to as 16 "branes" in the orientifold theory.

JHEP07(2021)104

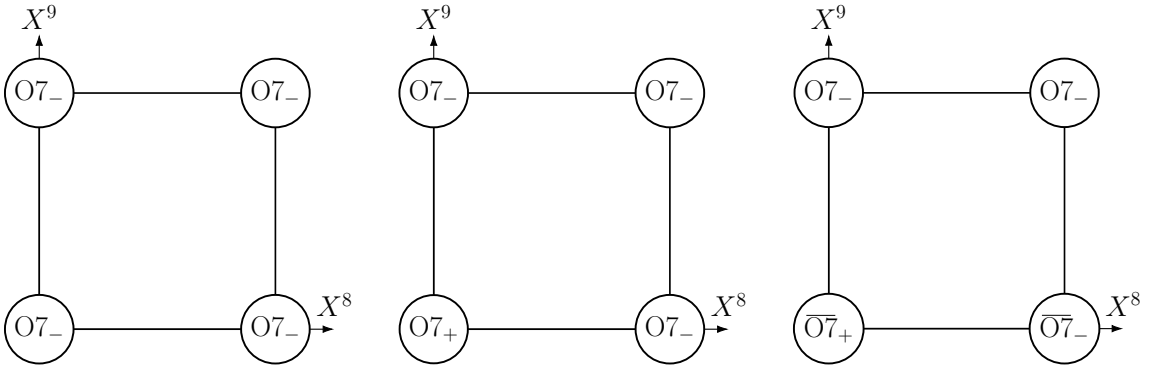

(a) Geometry of the standard SO(32) superstring. There is an O7$_-$-plane at each of the four fixed points.

(b) Geometry of the supersymmetric USp(16) model. There is 1 O7$_+$-plane at $(0,0)$ and 3 O7$_-$-planes at $(\pi R_8, 0)$, $(0, \pi R_9)$ and $(\pi R_8, \pi R_9)$.

(c) Geometry of the non-supersymmetric USp(16) model. There is 1 $\overline{\text{O7}}_+$-plane at $(0,0)$, 1 $\overline{\text{O7}}_-$-plane at $(\pi R_8, 0)$ and 2 O7$_-$-planes at $(0, \pi R_9)$ and $(\pi R_8, \pi R_9)$.

Figure 1. Eight dimensional T-dual geometries: the standard SO(32) superstring theory, the USp(16) supersymmetric theory and its non-supersymmetric version.

On the other hand, it has been shown that for the USp(16) theory, i.e. with $B_{89} = \frac{\alpha'}{2}$, the T-duality transformation $(R_8, R_9) \to (\frac{\alpha'}{2R_8}, \frac{\alpha'}{2R_9})$ turns the original O9$_-$-plane into three O7$_-$-planes and one O7$_+$-plane [95]. While an O7$_-$-plane has charge (and tension) equal to -4 in units of a regular D7-brane charge, an O7$_+$-plane has charge (and tension) equal to $+4$. The geometry is depicted in figure 1b, where R_8, R_9 now refer to the radii in the T-dual theory. The switch O7$_-$ $\to$ O7$_+$ has the overall effect of halving the RR tadpole, a fact that requires the addition of only eight D7-branes (16 half-branes). The rank of the gauge group is thus reduced to 8. Furthermore, while D7-branes on top of an O7$_-$-plane lead to an orthogonal (SO) gauge group, D7-branes on top of an O7$_+$-plane lead to a symplectic (USp) gauge factor. Therefore, the configuration with all the D7-branes sitting on top of the O7$_+$-plane yields the gauge symmetry USp(16).

From now on, the description of the USp(16) theory we choose is that of the type IIB theory with orientifold projection $\Omega' = \Omega\Pi_8\Pi_9(-1)^{F_L}$, which involves O7$_\pm$-planes and D7-branes. The spectrum is encoded in the partition functions which can be worked out using standard methods. The torus contribution is given by half that given in eq. (2.2).[7] Moreover, the Klein, cylinder and Möbius amplitudes are

$$\begin{aligned}
\mathcal{K} &= \frac{1}{2}\int_0^\infty \frac{\mathrm{d}\tau_2}{\tau_2^5}\, W_{2n_9} W_{2n_8} \frac{V_8 - S_8}{\eta^8}(2i\tau_2)\,, \\
\mathcal{A} &= \frac{N^2}{2}\int_0^\infty \frac{\mathrm{d}\tau_2}{\tau_2^5}\, W_{n_9} W_{n_8} \frac{V_8 - S_8}{\eta^8}\left(\frac{i\tau_2}{2}\right)\,, \\
\mathcal{M} &= \frac{N}{2}\int_0^\infty \frac{\mathrm{d}\tau_2}{\tau_2^5}\, W_{n_9}\left[(-1)^{n_9} W_{2n_8} - W_{2n_8+1}\right] \frac{\hat{V}_8 - \hat{S}_8}{\hat{\eta}^8}\left(\frac{i\tau_2}{2} + \frac{1}{2}\right)\,,
\end{aligned} \tag{2.13}$$

[7] Remind that the type IIB amplitude (2.2) is self-dual. Hence, it can be used in the orientifold theory obtained by modding with Ω [91, 92] or that obtained with Ω'. Being T-dual, they are physically equivalent.

JHEP07(2021)104

where N is the number of half-D7-branes and the lattices of winding modes are defined as

$$W_{n_i} = e^{-\pi\tau_2 n_i^2 \frac{R_i^2}{\alpha'}} \,. \tag{2.14}$$

The "field-theory" open-string spectrum is encoded in

$$\begin{aligned}(\mathcal{A}+\mathcal{M})|_{\rm FT} = \int_0^\infty \frac{{\rm d}\tau_2}{\tau_2^5} \Big[& \frac{N(N+1)}{2} W_{2n_9} W_{2n_8} \\ & + \frac{N(N-1)}{2} (W_{2n_9+1} W_{2n_8} + W_{n_9} W_{2n_8+1}) \Big] \, \frac{V_8 - S_8}{\eta^8}\Big|_0 \,,\end{aligned} \tag{2.15}$$

where the index 0 stands for the constant mode of the characters. It is manifestly supersymmetric and describes a USp(N) gauge symmetry. The value $N = 16$ is found by imposing the RR tadpole condition, which can be derived from the amplitudes in the tree-level channel,

$$\begin{aligned}\tilde{\mathcal{K}} &= \frac{2^5\alpha'}{8R_9R_8} \int_0^\infty {\rm d}l \, P_{m_9} P_{m_8} \frac{V_8 - S_8}{\eta^8}(il) \,, \\ \tilde{\mathcal{A}} &= \frac{2^{-5}N^2\alpha'}{2R_9R_8} \int_0^\infty {\rm d}l \, P_{m_9} P_{m_8} \frac{V_8 - S_8}{\eta^8}(il) \,, \\ \tilde{\mathcal{M}} &= \frac{N\alpha'}{2R_9R_8} \int_0^\infty {\rm d}l \, [P_{2m_9+1} - (-1)^{m_8} P_{2m_9}] P_{m_8} \frac{\hat{V}_8 - \hat{S}_8}{\hat{\eta}^8} \left(il + \frac{1}{2}\right) \,,\end{aligned} \tag{2.16}$$

where the lattices of momentum states are given by

$$P_{m_i} = e^{-\pi \frac{l}{2} m_i^2 \frac{\alpha'}{R_i^2}} \,. \tag{2.17}$$

The tree-level amplitudes encode uniquely the geometry of the D-branes and O-planes. Indeed, the geometry can in general be revealed by remembering that the tree-level channel amplitudes capture the propagation of closed strings between orientifold planes and/or D-branes. As an example, a generic Klein-bottle amplitude can be formally written as

$$\tilde{\mathcal{K}} = \sum_{a,\mathbf{m}} \sum_{A,B} (-1)^{F_{\rm L}} C_{aA} \, C_{aB} \, G_{a\mathbf{m}}(\mathbf{x}_A, \mathbf{x}_B) \,, \tag{2.18}$$

where a labels the NS-NS and RR closed-string degrees of freedom in ten dimensions and $\mathbf{m} = (m_8, m_9)$ (in 8d models as above) are the internal momenta of their Kaluza-Klein (KK) modes. Moreover, $G_{a\mathbf{m}}(\mathbf{x}_A, \mathbf{x}_B)$ is the tree-level scalar propagator transverse to the O-planes for a flat internal space, while C_{aA} captures the coupling to the O-plane A located at $\mathbf{x}_A = (x_A^8, x_A^9)$. In our examples, $C_{aA} \propto T_A$ for the NS-NS states and $C_{aA} \propto Q_A$ for the RR ones, where T_A and Q_A denote the tension and charge of the O-plane A and the proportionality constants are equal. Actually, the closed-string states $a, \mathbf{m}$ propagating in $\tilde{\mathcal{K}}$, which are bosons arising in the NS-NS and RR sector, have different Lorentz structures: for instance the dilaton is a scalar, the graviton is a tensor, etc. Hence, they have different propagators and couplings to branes and orientifolds. Contracting the couplings and the

JHEP07(2021)104

propagators, one obtains the effective couplings C_{aA} and a scalar propagator $G_{a\mathbf{m}}(\mathbf{x}_A, \mathbf{x}_B)$ for each closed-string state. Explicitly, we have

$$\begin{aligned} G_{a\mathbf{m}}(\mathbf{x}_A, \mathbf{x}_B) &= e^{i\mathbf{m}(\mathbf{x}_A - \mathbf{x}_B)} \frac{1}{p_\parallel^2 + M_a^2 + \sum_i \frac{m_i^2}{R_i^2}} \\ &= \frac{\pi\alpha'}{2} e^{i\mathbf{m}(\mathbf{x}_A - \mathbf{x}_B)} \int_0^\infty \mathrm{d}l \; e^{-\pi \frac{l}{2}\alpha' \left(M_a^2 + \sum_i \frac{m_i^2}{R_i^2} \right)} , \end{aligned} \tag{2.19}$$

where by convention the variables x_A^i take values in the range $[-\pi, \pi]$ and the internal coordinates are defined as $X^i = x^i R_i$. The closed-string channel Klein-bottle amplitude is therefore given by

$$\tilde{\mathcal{K}} = \frac{\pi\alpha'}{2} \sum_{a,\mathbf{m}} \sum_{A,B} C_{aA} C_{aB} \int_0^\infty \mathrm{d}l \; e^{i\mathbf{m}(\mathbf{x}_A - \mathbf{x}_B) - \pi \frac{l}{2}\alpha' \left(M_a^2 + \sum_i \frac{m_i^2}{R_i^2} \right)} . \tag{2.20}$$

The factors $e^{i\mathbf{m}(\mathbf{x}_A - \mathbf{x}_B)}$ capture the locations of the O-planes and display the products of the wavefunctions of a closed-string Kaluza-Klein mode $a, \mathbf{m}$ respectively located on the O-planes A and B.

In the 8d examples of this section, there are four orientifold fixed points $(0,0)$, $(0, \pi R_9)$, $(\pi R_8, 0)$, $(\pi R_8, \pi R_9)$, where the O7-planes sit. The phases $e^{i\mathbf{m}(\mathbf{x}_A - \mathbf{x}_B)}$ encoding the propagation between the four O-planes take values 1, $(-1)^{m_9}$, $(-1)^{m_8}$ or $(-1)^{m_9+m_8}$. Once dressed by the signs given by the tensions and charges, they produce projectors in the tree-level channel amplitude. In the SO(32) type IIB orientifold case, which contains 4 O7$_-$-planes, the projector in the tree-level Klein-bottle amplitude is

$$\Pi_{\tilde{\mathcal{K}}} \propto 4[1 + (-1)^{m_9}][1 + (-1)^{m_8}] , \tag{2.21}$$

which projects onto even KK states. In contrast, the corresponding one for the supersymmetric USp(16) type IIB orientifold satisfies

$$\begin{aligned} \Pi_{\tilde{\mathcal{K}}} &\propto 4 - 2(-1)^{m_9} + 2(-1)^{m_9} - 2(-1)^{m_8} + 2(-1)^{m_8} - 2(-1)^{m_9+m_8} + 2(-1)^{m_9+m_8} \\ &\propto 4 , \end{aligned} \tag{2.22}$$

leading to no projection of the KK states.

The tree-level channel cylinder and Möbius amplitudes take similar formal expressions. In the former case, the objects A and B are D-branes while in the latter case they are a D-brane and an O-plane. For instance, in the USp(16) model, the lattices in the Möbius amplitude involve all momentum states subject to the projector

$$\Pi = \frac{1 - (-1)^{m_9} - (-1)^{m_8} - (-1)^{m_9+m_8}}{2} , \tag{2.23}$$

which is consistent with the geometry of one stack of 8 (regular) D7-branes coincident with the O7$_+$-plane, whereas the three other orientifold fixed points are occupied by standard O7$_-$-planes. Moving all the D7-branes on top of one of the O7$_-$-planes lead to an SO(16) gauge group, whereas moving all of them into the bulk in one stack leads to a U(8) open-string gauge group.

JHEP07(2021)104

2.3 The non-supersymmetric orientifold amplitudes

Let us now turn to the implementation of supersymmetry breaking in the Klein, cylinder and Möbius amplitudes, *without introducing perturbative instabilities or tadpoles*. The allowed form of the corresponding torus amplitude will be determined in the next subsection.

Geometrically, the mechanism of supersymmetry breaking is the following. A pair of O7$_+$-plane and O7$_-$-plane have globally zero tension and RR charge. From a string-theory viewpoint, it is possible to replace such a pair by an $\overline{\text{O7}}_+$ and $\overline{\text{O7}}_-$ pair, which also has vanishing total tension and charge. However, the second option breaks supersymmetry in the presence of the 8 D7-branes needed to cancel the tadpoles. This geometry is depicted in figure 1c. Supersymmetry breaking is not visible in the cylinder amplitude, which describes D7-D7 amplitudes. It is less obvious but true that the orientifold configuration with 2 O7$_-$, 1 $\overline{\text{O7}}_+$, 1 $\overline{\text{O7}}_-$ and the supersymmetric one with 1 O7$_+$ and 3 O7$_-$-planes lead to identical Klein-bottle amplitudes. Indeed, in the former case we have

$$\begin{aligned}\tilde{\mathcal{K}} &\propto \Big\{[4-2(-1)^{m_8}+2(-1)^{m_8}](V_8-S_8)+\\ &\qquad [-2(-1)^{m_9}+2(-1)^{m_9}-2(-1)^{m_9+m_8}+2(-1)^{m_9+m_8}](V_8+S_8)\Big\}P_{m_8}P_{m_9}\\ &\propto 4(V_8-S_8)P_{m_8}P_{m_9}\,,\end{aligned} \tag{2.24}$$

where the character V_8-S_8 describes the tree-level propagation of closed strings between mutually BPS O7-planes (O7$_-$-O7$_-$, $\overline{\text{O7}}_\pm$-$\overline{\text{O7}}_\pm$), whereas V_8+S_8 describes the tree-level propagation of closed strings between mutually non-BPS O7-planes (O7$_-$-$\overline{\text{O7}}_\pm$, $\overline{\text{O7}}_\pm$-O7$_-$). The phases reflect the geometry of O-planes and lead to a cancellation of the non-BPS terms, leaving the unprojected supersymmetric sum over all KK states as in the supersymmetric case (see eqs. (2.16) and (2.22)).

As will be shown later, the configuration where the 8 D7-branes are coincident with the $\overline{\text{O7}}_+$-plane is the only stable configuration at one loop. Using the above given geometrical interpretation of O-planes, it is easy to check that the tree-level channel amplitudes are given by

$$\begin{aligned}\tilde{\mathcal{K}} &= \frac{2^5\alpha'}{8R_9R_8}\int_0^\infty \mathrm{d}l\, P_{m_9}P_{m_8}\frac{V_8-S_8}{\eta^8}(il)\,,\\ \tilde{\mathcal{A}} &= \frac{2^{-5}N^2\alpha'}{2R_9R_8}\int_0^\infty \mathrm{d}l\, P_{m_9}P_{m_8}\frac{V_8-S_8}{\eta^8}(il)\,,\\ \tilde{\mathcal{M}} &= \frac{N\alpha'}{2R_9R_8}\int_0^\infty \mathrm{d}l\,[P_{2m_9+1}-(-1)^{m_8}P_{2m_9}]P_{m_8}\frac{\hat{V}_8-(-1)^{m_8}\hat{S}_8}{\hat{\eta}^8}\left(il+\frac{1}{2}\right)\,.\end{aligned} \tag{2.25}$$

Notice that the only change in (2.25) compared to the supersymmetric case (2.16) is the extra phase $(-1)^{m_8}$ in the RR couplings of the closed strings propagating between the D7-branes and the O7-planes in the Möbius amplitude. The projector in the RR sector is thus transformed accordingly,

$$\begin{aligned}\Pi_{\text{NSNS}} &= \frac{+1-(-1)^{m_9}-(-1)^{m_8}-(-1)^{m_9+m_8}}{2}\\ \Pi_{\text{RR}} = (-1)^{m_8}\Pi_{\text{NSNS}} &= \frac{-1-(-1)^{m_9}+(-1)^{m_8}-(-1)^{m_9+m_8}}{2}\,,\end{aligned} \tag{2.26}$$

JHEP07(2021)104

where $\Pi_{\rm NSNS}$ is identical to that of the supersymmetric case, eq. (2.23). The above projectors encode all the information about the geometry. In fact, with all D-branes located at the origin, the change of signs of the RR couplings at $(0,0)$ and $(\pi R_8, 0)$ tells us that the orientifold planes located there preserve opposite supersymmetry as compared to the D7-branes and are therefore $\overline{\rm O7}_+$ and $\overline{\rm O7}_-$.

The loop-channel amplitudes can be worked out by the usual methods, leading to

$$\begin{aligned}
\mathcal{K} &= \frac{1}{2}\int_0^\infty \frac{{\rm d}\tau_2}{\tau_2^5}\, W_{2n_9} W_{2n_8} \frac{V_8 - S_8}{\eta^8}(2i\tau_2)\,, \\
\mathcal{A} &= \frac{N^2}{2}\int_0^\infty \frac{{\rm d}\tau_2}{\tau_2^5}\, W_{n_9} W_{n_8} \frac{V_8 - S_8}{\eta^8}\left(\frac{i\tau_2}{2}\right)\,, \\
\mathcal{M} &= \frac{N}{2}\int_0^\infty \frac{{\rm d}\tau_2}{\tau_2^5}\, W_{n_9}\left[(-1)^{n_9} W_{2n_8} - W_{2n_8+1}\right] \frac{\hat{V}_8 + (-1)^{n_9}\hat{S}_8}{\hat{\eta}^8}\left(\frac{i\tau_2}{2} + \frac{1}{2}\right)\,.
\end{aligned} \tag{2.27}$$

Comparing the Möbius amplitude with its supersymmetric counterpart (2.13) reveals a supersymmetry breaking orientifold projection

$$\Omega'' = \Omega\Pi_8\Pi_9(-1)^{F_{\rm L}}(-\delta_{w_9})^F\,, \tag{2.28}$$

where, as before, Π_i is the parity operation $X^i \to -X^i$, $F_{\rm L}$ is the left-moving fermion number, F is the spacetime fermion number and δ_{w_9} generates a winding shift in the coordinate X^9. The latter acts on the zero-modes as $|\mathbf{m},\mathbf{n}\rangle \to (-1)^{n_9}|\mathbf{m},\mathbf{n}\rangle$, as follows from a left-right asymmetric action $X^9_{\rm L} \to X^9_{\rm L} + \frac{\pi R_9}{2}$, $X^9_{\rm R} \to X^9_{\rm R} - \frac{\pi R_9}{2}$ on the left- and right-moving parts of the coordinate. Notice that since there is no fermion propagating in the Klein bottle, the supersymmetry breaking deformation $(-\delta_{w_9})^F$ has no effect in this amplitude.

The massless field-theory open-string spectrum is captured by

$$(\mathcal{A}+\mathcal{M})|_{\rm FT} = \int_0^\infty \frac{{\rm d}\tau_2}{\tau_2^5}\left[\frac{N(N+1)}{2}\,\frac{V_8}{\eta^8}\Big|_0 - \frac{N(N-1)}{2}\,\frac{S_8}{\eta^8}\Big|_0\right] \tag{2.29}$$

and displays supersymmetry breaking at the string scale, of the brane supersymmetry breaking type. The gauge group is USp(16) as before. The vector bosons are thus in the symmetric representation, but the fermions are in the antisymmetric representation, which contains in particular the gauge-singlet goldstino. This is the basic indication of the nonlinear realization of supersymmetry where the D7-branes sit. It is then easy to move D7-branes in the internal two-torus and derive the resulting spectrum. Putting all D-branes on top of the $\overline{\rm O7}_-$-plane leads to an SO(16) gauge group with massless fermions in the symmetric representation. The latter contains the singlet goldstino implying again a nonlinear supersymmetry and a supersymmetry breaking at the string scale. Putting all D7-branes on top of one of the two remaining O7$_-$-planes leads to a supersymmetric massless spectrum with SO(16) gauge group and a supersymmetry breaking at the massive level due to the far-away presence of the two $\overline{\rm O7}$-planes.

Let us stress again that despite the fact that the O7-planes are of types orientifold and anti-orientifold, the Klein bottle amplitude is exactly the same as in the supersym-

JHEP07(2021)104

metric case, due to the cancellation of the supersymmetry-breaking contributions.[8] At one loop, only the Möbius amplitude "knows" about supersymmetry breaking, without however generating NS-NS tadpoles (of course, RR tadpoles are non-negotiable and always have to cancel).

The precursor paper of Angelantonj and Cardella contains a model equivalent to the one presented above [77].[9] In our work, we provide a microscopic geometrical interpretation of the source of supersymmetry breaking in terms of the replacement of an $O7_+$-$O7_-$ pair by an $\overline{O7}_+$-$\overline{O7}_-$ pair, which leads to a novel form of brane supersymmetry breaking without tadpoles. Moreover, as argued in the next subsection, we believe that the closed-string sector is not supersymmetric at tree-level but features spontaneously broken supersymmetry.

Notice that the cancellation of the disk NS-NS tadpoles in our class of models does not imply an exact Bose/Fermi degeneracy at each mass level. Indeed, the latter is related to the cancellation of the one-loop cosmological constant, whereas the NS-NS disk tadpoles are of lower order in perturbation theory.

Let us now make considerations of energetics. The O-planes have no dynamical positions. The D7-branes, on the other hand, do have dynamical positions. To find which configuration is expected to minimize the one-loop effective potential, recall that the D7-branes are mutually BPS and have therefore no net interactions with the $O7_+$ and $O7_-$-planes. On the contrary, they are attracted by the $\overline{O7}_+$-plane and repelled by the $\overline{O7}_-$-plane. Hence, the only stable configuration is obtained by putting all D7-branes on top of the $\overline{O7}_+$-plane, leading to a USp(16) gauge group and breaking SUSY at the string scale, as explained above. At first sight, one could think that a second option would be to put some stuck (or rigid) half-D7-branes on top of $O7_-$ or $\overline{O7}_-$-planes, with no gauge group (but a $\mathbb{Z}_2$ global symmetry). As will be seen in section 4, such configurations are however inconsistent, a fact that can be checked by adding probe D3-branes.

To confirm these expectations, we write the Möbius amplitude for arbitrary brane positions along X^9 and X^8. To this end, we introduce vectors $\vec{a}_\alpha = (a^8_\alpha, a^9_\alpha)$ such that the

[8] We will discuss in the next subsection the issue of supersymmetry in the closed-string spectrum. The O-planes and anti O-planes are mutually non-BPS. The cancellation of the non-supersymmetric contributions in the Klein bottle does not mean that the closed-string sector is supersymmetric, even ignoring the supersymmetry breaking transmission from the open sector. As we will see, the most plausible possibility is that the tree-level closed-string spectrum has softly broken supersymmetry. Another possibility, which we consider however unlikely, is that the closed-string spectrum is supersymmetric but the interactions are not. Another insight about this issue is the gravitino masses: a supersymmetric closed-string spectrum would be in contradiction with the presence of orientifold and anti-orientifold planes, which impose opposite boundary conditions for the gravitinos.

[9] In the model constructed in section 3 of [77], the $\overline{O7}_+$-$\overline{O7}_-$ pair sits on the diagonal of the two-torus, which corresponds to a different choice of the projector in the Möbius, $\Pi_{\rm RR} = (-1)^{m_9+m_8}\Pi_{\rm NSNS}$. The 8 D7-branes were separated into two stacks of four branes, sitting on top of the anti-orientifolds. The attraction of the D7-branes on top of $\overline{O7}_+$ cancels the repulsion of the D7-branes on top of $\overline{O7}_-$. However, as already known by the authors of [77] and obvious from the discussion below, this configuration is unstable, since the D7-branes on top of $\overline{O7}_-$ are repelled by $\overline{O7}_-$ and attracted towards the $\overline{O7}_+$ -plane, leading to the stable configuration with one stack of eight coincident D7-branes, negative potential and USp(16) gauge group discussed above.

JHEP07(2021)104

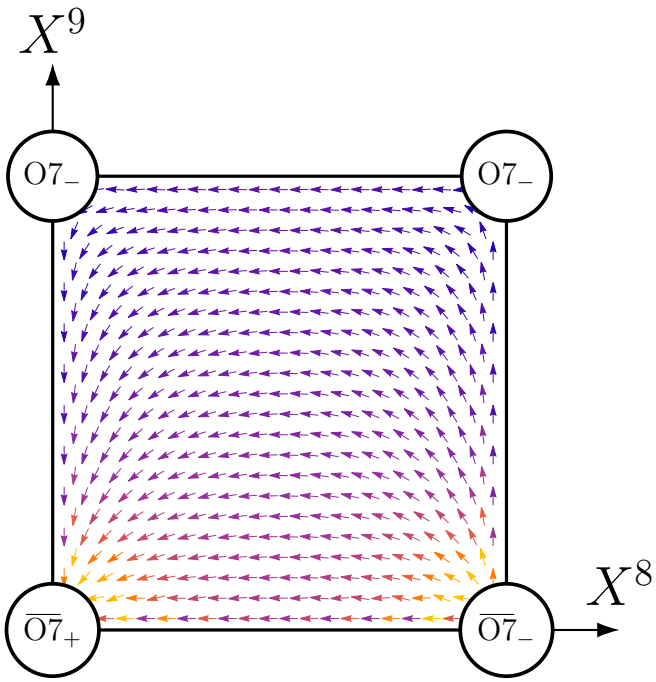

Figure 2. Example of vector field $\left(-\frac{\partial \mathcal{V}}{\partial a_r^8}, -\frac{\partial \mathcal{V}}{\partial a_r^9}\right)$ obtained numerically. The lighter the color is, the longer the vector norm is.

position of the half-brane $\alpha \in \{1, \dots, 16\}$ along direction X^i is $2\pi a_\alpha^i R_i$. In both channels, we obtain

$$\begin{aligned}
\mathcal{M} = \frac{1}{2}\sum_\alpha \int \frac{\mathrm{d}\tau_2}{\tau_2^5} \Bigg\{ & \left[(-1)^{n_9} W_{2n_8+2a_\alpha^2} - W_{2n_8+1+2a_\alpha^2}\right] \frac{\hat{V}_8}{\hat{\eta}^8} \\
& - \left[(-1)^{n_9} W_{2n_8+1+2a_\alpha^2} - W_{2n_8+2a_\alpha^2}\right] \frac{\hat{S}_8}{\hat{\eta}^8} \Bigg\} W_{n_9+2a_\alpha^1} \,, \\
\tilde{\mathcal{M}} = \frac{\alpha'}{2R_9R_8} \sum_\alpha \int \mathrm{d}l \, e^{4i\pi m_9 a_\alpha^1} e^{2i\pi m_8 a_\alpha^2} P_{m_8} \Bigg\{ & \left[e^{2i\pi a_\alpha^1} P_{2m_9+1} - (-1)^{m_8} P_{2m_9}\right] \frac{\hat{V}_8}{\hat{\eta}^8} \\
& - \left[e^{2i\pi a_\alpha^1} (-1)^{m_8} P_{2m_9+1} - P_{2m_9}\right] \frac{\hat{S}_8}{\hat{\eta}^8} \Bigg\} .
\end{aligned} \tag{2.30}$$

The dependance of the one-loop effective potential $\mathcal{V}$ on the independent positions can be derived solely from $\mathcal{M}$ and $\tilde{\mathcal{M}}$ in various regimes of the internal radii. Among the 16 vectors $\vec{a}_\alpha$, at most 8 are dynamical degrees of freedom since the half-branes move by pairs and unpaired half-branes stuck at a fixed point are not dynamical. We will label the dynamical ones by an index r. In figure 2, we display the vector field $\left(-\frac{\partial \mathcal{V}}{\partial a_r^8}, -\frac{\partial \mathcal{V}}{\partial a_r^9}\right)$ obtained numerically for a given brane r of arbitrary position. As anticipated before, the minimum of the potential is reached when the branes sit at the origin, on the $\overline{\text{O7}}_+$-plane.

JHEP07(2021)104

2.4 Consistent pairing of torus and orientifold amplitudes

At first sight, one may think that the supersymmetric torus amplitude (2.2) as well as the non-supersymmetic ones (2.8) and (2.11) are all consistent with the supersymmetric orientifold amplitudes (2.13) and their non-supersymmetric deformation (2.27). If true, this would yield six different orientifold models. There are however arguments based on the understanding of the orientifold projections as well as on the effective field theories that suggest that only two options are consistent.

Let us combine the non-supersymmetric torus amplitude (2.8) with the non-supersymmetric orientifold amplitudes (2.27). The torus amplitude can be constructed as an orbifold generated by $g' = (-1)^F \delta_{w_8} \delta_{p_9}$, while the orientifold amplitudes are obtained from the action of $\Omega'' = \Pi_8 \Pi_9 (-1)^{F_{\rm L}} (-\delta_{w_9})^F$. Hence, the (anti-)orientifold planes are located at the fixed points of Ω'' and $\Omega'' g'$. To be specific, Ω'' fixes $(0,0)$ as well as $(\pi R_8, 0)$, thanks to the $2\pi R_8$ periodicity. Moreover $\Omega'' g'$ fixes $(0, \pi R_9)$ because g' contains a factor δ_{p_9} acting as $X_9 \to X_9 + 2\pi R_9$ after rescaling of the radius $R_9 \to 2R_9$. It also fixes $(\pi R_8, \pi R_9)$ thanks to the $2\pi R_8$ periodicity. Notice that the presence of a factor $(-1)^F$ in such a group element changes the orientifolds into anti-orientifold planes, as can be seen in the Möbius amplitude where $(-1)^F$ changes the sign of the RR coupling. As a result, the fixed points of Ω'' are anti-orientifold planes, while those of $\Omega'' g'$ are orientifold planes due to the cancellation of the factors $(-1)^F$. Therefore, the nature of the O-planes derived from the non-supersymmetric amplitudes (2.27) and shown in figure 1c are in agreement with the non-supersymmetric torus amplitude (2.8).

As shown in section 2.1, the second non-supersymmetric torus amplitude (2.11) is equivalent to (2.8) under the interchange of the coordinates $X^8 \leftrightarrow X^9$. Therefore, a consistent orientifold model is obtained by applying the same operation on the non-supersymmetric orientifold amplitudes (2.27) and orientifold action (2.28). The corresponding geometry of O-planes is like in figure 1c, with the $\overline{\rm O7}_-$-plane now located at $(0, \pi R_9)$.

Finally, reasoning as above with the generators $g = \delta_{w_8} \delta_{p_9}$ and $\Omega' = \Omega \Pi_8 \Pi_9 (-1)^{F_{\rm L}}$, one concludes that the supersymmetric orientifold amplitudes (2.13) are compatible with the supersymmetric torus amplitude (2.2).

In fact, the reason why the four other combinations of torus and orientifold amplitudes are inconsistent is that the orientifold projections are not symmetries of the closed-string spectrum. For instance, the supersymmetric torus amplitude (2.2) does not seem to be compatible with the orientifold projection (2.28). Indeed, because the factor $(-\delta_{w_9})^F$ in Ω'' is equivalent to $(-1)^{n_9 F}$, fermions with even and odd winding numbers n_9 are projected differently. Due to interactions, the same conclusion should apply for bosons. However, there is no such selection rule in (2.2), as opposed to the non-supersymmetric torus amplitude (2.8), where fermions with even n_9 are gravitinos while those with odd n_9 are spin $\frac{1}{2}$ particles.

Moreover, any attempt to combine the supersymmetric torus amplitude (2.2) with the non-supersymmetric orientifold amplitudes (2.27) is unlikely to be consistent, since the former implies the existence of massless gravitinos that would be difficult to explain from the point of view of the effective field theory. Instead, there seems to be no obstruction, from the point of view of the effective supergravity, to couple the non-supersymmetric torus amplitude (2.8) with the orientifold ones (2.27), since in this case all gravitinos are massive.

JHEP07(2021)104

To understand a little better how the nature of (anti-)orientifold planes may or may not induce gravitino masses, let us consider first the orientifold projection Ω'. In this case, $O_\pm$-planes, which preserve the same supersymmetry, are located at the four fixed points of T^2. The action on the two gravitinos ψ_μ and $\tilde{\psi}_\mu$ of the 10-dimensional type IIB is given by

$$\begin{aligned}\Omega'\psi_\mu(X^8,X^9)(\Omega')^{-1} &= \psi_\mu(-X^8,-X^9) = \Gamma_8\Gamma_9\tilde{\psi}_\mu(X^8,X^9)\,,\\ \Omega'\tilde{\psi}_\mu(X^8,X^9)(\Omega')^{-1} &= \tilde{\psi}_\mu(-X^8,-X^9) = -\Gamma_8\Gamma_9\psi_\mu(X^8,X^9)\,,\end{aligned} \tag{2.31}$$

where Γ_8 and Γ_9 are 10-dimensional gamma matrices. A minus sign appears for one of the two gravitinos because of the presence of the factor $(-1)^{F_L}$ in the orientifold projection Ω'. Note that this is consistent with that fact that the action of $(\Omega')^2$ is the identity:

$$\Omega'\left(\Omega'\psi_\mu(X^8,X^9)(\Omega')^{-1}\right)(\Omega')^{-1} = -\Gamma_8\Gamma_9\Gamma_8\Gamma_9\psi_\mu(X^8,X^9) = \psi_\mu(X^8,X^9)\,. \tag{2.32}$$

As a consequence, the orientifold action (2.31) only preserves one linear combination of the two gravitinos. Let us now consider a geometry where anti-orientifold planes are located at the four fixed points. The corresponding orientifold projection denoted $\tilde{\Omega}'$ contains an additional factor $(-1)^F$ compared to Ω' which, once combined with the term $(-1)^{F_L}$, yields a factor $(-1)^{F_R}$. The action of $\tilde{\Omega}'$ then gives a minus sign to the other gravitino,

$$\begin{aligned}\tilde{\Omega}'\psi_\mu(X^8,X^9)(\tilde{\Omega}')^{-1} &= \psi_\mu(-X^8,-X^9) = -\Gamma_8\Gamma_9\tilde{\psi}_\mu(X^8,X^9)\,,\\ \tilde{\Omega}'\tilde{\psi}_\mu(X^8,X^9)(\tilde{\Omega}')^{-1} &= \tilde{\psi}_\mu(-X^8,-X^9) = \Gamma_8\Gamma_9\psi_\mu(X^8,X^9)\,,\end{aligned} \tag{2.33}$$

and thus preserves the orthogonal linear combination of gravitinos compared to Ω'. We have seen that the geometry corresponding to the non-supersymmetric orientifold amplitudes (2.27) involves both orientifold and anti-orientifold planes, as shown in figure 1c. Therefore, the boundary conditions of the gravitinos at $X^9 = 0$ are of the type (2.33), whereas at $X^9 = \pi R_9$ they are of the type (2.31). Overall, one obtains a shift in the KK spectrum of gravitinos $m_9/R_9 \to (m_9 + \frac{1}{2})/R_9$, which is precisely what features the non-supersymmetric torus amplitude (2.8) (see eq. (2.9)).

3 Lower dimensional compactifications

In this section, we extend the mechanism of supersymmetry breaking to models in even dimension $d \leq 6$.

In type IIB, a change of basis can always put an arbitrary discrete background for the antisymmetric tensor B_{ij} into a block-diagonal form, with 2×2 antisymmetric matrices,

$$B = \alpha' \begin{pmatrix} 0 & \lambda_d & & & \\ -\lambda_d & 0 & & (0) & \\ & & \ddots & & \\ & (0) & & 0 & \lambda_9 \\ & & & -\lambda_9 & 0 \end{pmatrix}, \quad \lambda_i \in \left\{0, \frac{1}{2}\right\}. \tag{3.1}$$

JHEP07(2021)104

The rank of the tensor B_{ij} is twice the number of non-zero λ_i's. Since they play no significant role in the sequel, we choose to set to zero the off-diagonal elements of the symmetric tensor G_{ij}. The internal space is thus a Cartesian product of circles of radii R_i.

In the supersymmetric case, one can switch on some λ_i's by implementing a free-orbifold action on the background where $B_{ij} = 0$. For instance, $\lambda_9 = \lambda_8 = \frac{1}{2}$ in 6d is achieved by considering the orbifold generated by $g_1 = \delta_{w_8}\delta_{p_9}$ and $g_2 = \delta_{w_6}\delta_{p_7}$. In 4d, for $\lambda_7 = \frac{1}{2}$, one simply adds an extra generator $g_3 = \delta_{w_4}\delta_{p_5}$. By considering an orientifold action involving parities in all internal directions, one obtains a model involving 2^{10-d} $\mathrm{O}(d-1)_\pm$-planes. It is then allowed to turn some $\mathrm{O}(d-1)_+$-$\mathrm{O}(d-1)_-$ pairs into $\overline{\mathrm{O}}(d-1)_+$-$\overline{\mathrm{O}}(d-1)_-$ ones in order to break supersymmetry.

In the following, we consider various configurations of orientifold planes of this type and provide the corresponding Klein, cylinder and Möbius amplitudes. In orbifold language, the corresponding type IIB backgrounds can be realized by including operators $(-1)^F$ in the definition(s) of one or several of the generators g_i.

3.1 Geometry description

The geometry of a model is given by the precise locations of the various $\mathrm{O}_\pm$ and $\overline{\mathrm{O}}_\pm$-planes. Since pictorial representations become involved when the number of internal dimensions increases, it is useful to consider another way to describe a generic geometry. If one specifies an ordering for the labelling of the fixed points, the geometry can simply be given by the list of O-plane types following this ordering. In the $10-d$ dimensional internal space, a fixed point can be represented by a $(10-d)$-vector with components 0 or 1 that indicate if it is located at the origin or at πR_i in each direction X^i, $i \in \{d, \ldots, 9\}$. For example, in 6d the fixed point located at $(X^6, X^7, X^8, X^9) = (0, \pi R_7, \pi R_8, 0)$ is represented by $(0,1,1,0)$.

In practice, let us label the fixed points by an index $A \in \{0, \ldots, 2^{(10-d)} - 1\}$. With this convention, their positions are given by A written as a binary number. For instance in 6d, the fixed points are labelled as follows,

$$\begin{aligned} &A = 0 = (0,0,0,0)\,, \qquad A = 1 = (0,0,0,1)\,, \qquad A = 2 = (0,0,1,0)\,, \\ &A = 3 = (0,0,1,1)\,, \qquad \cdots \qquad A = 15 = (1,1,1,1)\,. \end{aligned} \tag{3.2}$$

3.2 Models in six dimensions

Projectors on the momenta in the Klein-bottle and Möbius amplitude can either be factorized in the two internal T^2's, or non-factorized. However, to obtain fully consistent models, compatibility of the projectors with the RR tadpole condition turns out not to be sufficient. Indeed, we give in the appendix examples of non-factorizable projectors, where one is consistent and another one is not. In the following, we will consider only consistent factorizable projectors. Supersymmetry breaking in the orientifold amplitudes will be implemented by choosing different projectors for the NS-NS and RR closed-string states propagating between the D-branes and the O-planes in the Möbius amplitude. On the contrary, the Klein-bottle and cylinder amplitudes will take forms identical to those in the SUSY cases.

JHEP07(2021)104

In six dimensions, a non-trivial antisymmetric tensor can have rank $B = 2$ or 4.

- rank $B = 2$: 8d model compactified on T^2 (T-dualized)

  By compactifying the 8d model on an extra T^2 and T-dualizing both of its coordinates, one finds a 6d model with D5-branes and 16 O5-planes. In the supersymmetric case, one would have 12 $\mathrm{O5}_-$ and 4 $\mathrm{O5}_+$-planes. In the non-SUSY case, one obtains a configuration with 8 $\mathrm{O5}_-$ and $4 \times (\overline{\mathrm{O5}}_- + \overline{\mathrm{O5}}_+)$-planes, where the geometry is simply the 8d one duplicated along the new compact dimensions. The rank of the gauge group is 8 and, depending on the location of the stacks of D5-branes, one finds for a single stack USp(16) if the D5-branes are on top of one $\overline{\mathrm{O5}}_+$ or $\mathrm{O5}_+$-plane, SO(16) if the D5-branes are on top of one $\overline{\mathrm{O5}}_-$-plane or $\mathrm{O5}_-$-plane, or U(8) if the stack of D5-branes is in the bulk. Supersymmetry is broken at the string scale (nonlinearly realized) if the D5-branes are coincident with anti-orientifolds, and broken only at the massive level (due to the separation in the internal space from the source of supersymmetry breaking) if the D5-branes are coincident with orientifold planes.

  When the D5-branes are put at the origin, the corresponding projectors on the momentum states running in the Möbius amplitude are

$$\begin{aligned} \Pi_{\mathrm{NSNS}} &= \frac{1-(-1)^{m_9}-(-1)^{m_8}-(-1)^{m_9+m_8}}{2} \times \prod_{i=6}^{7} \frac{1+(-1)^{m_i}}{2}\,, \\ \Pi_{\mathrm{RR}} &= (-1)^{m_8}\Pi_{\mathrm{NSNS}}\,. \end{aligned} \tag{3.3}$$

  The torus amplitude can be constructed as a free-orbifold generated by $g_1' = (-1)^F \delta_{w_8}\delta_{p_9}$.

- rank $B = 4$

  Following the ordering of the fixed points given in eq. (3.2), the list of $\mathrm{O}_\pm$-planes of the SUSY model we discuss here is

$$\begin{aligned} (&\mathrm{O5}_+, \mathrm{O5}_-, \mathrm{O5}_-, \mathrm{O5}_-, \mathrm{O5}_+, \mathrm{O5}_-, \mathrm{O5}_-, \mathrm{O5}_-, \mathrm{O5}_-, \\ &\mathrm{O5}_+, \mathrm{O5}_+, \mathrm{O5}_+, \mathrm{O5}_+, \mathrm{O5}_-, \mathrm{O5}_-, \mathrm{O5}_-)\,, \end{aligned} \tag{3.4}$$

  with a total of 10 $\mathrm{O5}_-$ and 6 $\mathrm{O5}_+$-planes. There are several possible consistent SUSY breaking deformations. One example corresponds to a configuration containing 8 $\mathrm{O5}_-$ and $4 \times (\overline{\mathrm{O5}}_- + \overline{\mathrm{O5}}_+)$-planes as follows,

$$\begin{aligned} (&\overline{\mathrm{O5}}_+, \mathrm{O5}_-, \overline{\mathrm{O5}}_-, \mathrm{O5}_-, \overline{\mathrm{O5}}_+, \mathrm{O5}_-, \overline{\mathrm{O5}}_-, \mathrm{O5}_-, \overline{\mathrm{O5}}_-, \\ &\mathrm{O5}_+, \overline{\mathrm{O5}}_+, \mathrm{O5}_+, \overline{\mathrm{O5}}_+, \mathrm{O5}_-, \overline{\mathrm{O5}}_-, \mathrm{O5}_-)\,. \end{aligned} \tag{3.5}$$

  The rank of the gauge group is 4 and, depending on the location of the stacks of D5-branes, one finds for a single stack USp(8) if the D5-branes are on top of one $\overline{\mathrm{O5}}_+$ or $\mathrm{O5}_+$ -plane, SO(8) if the D5-branes are on top of one $\overline{\mathrm{O5}}_-$-plane or $\mathrm{O5}_-$-plane, and U(4) if the D5-brane stack is in the bulk. Supersymmetry breaking pattern is of course the same as in the rank $B = 2$ case discussed above.

JHEP07(2021)104

When the 4 D5-branes (8 half-D5-branes) are coincident with the $\overline{\text{O5}}_+$-plane at the origin of the internal space, the projectors on the momentum states in the tree-level channel Möbius amplitude are

$$\begin{aligned}\Pi_{\text{NSNS}} &= \frac{1-(-1)^{m_9}-(-1)^{m_8}-(-1)^{m_9+m_8}}{2}\times\frac{1+(-1)^{m_7}-(-1)^{m_6}+(-1)^{m_7+m_6}}{2}\,,\\ \Pi_{\text{RR}} &= (-1)^{m_8}\Pi_{\text{NSNS}}\,.\end{aligned}\tag{3.6}$$

In order to write the orientifold amplitudes, it is convenient to denote lattices and volume factors as folows,

$$P_{\mathbf{m}}^{(10-d)}=\prod_{i=d}^{9}P_{m_i}\,,\qquad W_{\mathbf{n}}^{(10-d)}=\prod_{i=d}^{9}W_{n_i}\,,\qquad v_{10-d}=\prod_{i=d}^{9}R_i\,.\tag{3.7}$$

In these notations, the tree-level channel amplitudes are given by

$$\begin{aligned}\tilde{\mathcal{K}} &= \frac{(\alpha')^2}{v_4}\int_0^\infty \mathrm{d}l\, P_{\mathbf{m}}^{(4)}\frac{V_8-S_8}{\eta^8}(il)\,,\\ \tilde{\mathcal{A}} &= \frac{2^{-5}N^2(\alpha')^2}{2v_4}\int_0^\infty \mathrm{d}l\, P_{\mathbf{m}}^{(4)}\frac{V_8-S_8}{\eta^8}(il)\,,\\ \tilde{\mathcal{M}} &= \frac{N(\alpha')^2}{4v_4}\int_0^\infty \mathrm{d}l\,\left[P_{2m_9+1}-(-1)^{m_8}P_{2m_9}\right]P_{m_8}\left[P_{2m_7}-(-1)^{m_6}P_{2m_7+1}\right]P_{m_6}\\ &\qquad\times\frac{\hat{V}_8-(-1)^{m_8}\hat{S}_8}{\hat{\eta}^8}\left(il+\frac{1}{2}\right)\,,\end{aligned}\tag{3.8}$$

while in the loop-channel they become

$$\begin{aligned}\mathcal{K} &= \frac{1}{2}\int_0^\infty\frac{\mathrm{d}\tau_2}{\tau_2^4}\,W_{2\mathbf{n}}^{(4)}\frac{V_8-S_8}{\eta^8}(2i\tau_2)\,,\\ \mathcal{A} &= \frac{N^2}{2}\int_0^\infty\frac{\mathrm{d}\tau_2}{\tau_2^4}\,W_{\mathbf{n}}^{(4)}\frac{V_8-S_8}{\eta^8}\left(\frac{i\tau_2}{2}\right)\,,\\ \mathcal{M} &= \frac{N}{2}\int_0^\infty\frac{\mathrm{d}\tau_2}{\tau_2^4}\,W_{n_9}\left[W_{2n_8}-(-1)^{n_9}W_{2n_8+1}\right]W_{n_7}\left[W_{2n_6}-(-1)^{n_7}W_{2n_6+1}\right]\\ &\qquad\times\frac{(-1)^{n_9}\hat{V}_8+\hat{S}_8}{\hat{\eta}^8}\left(\frac{i\tau_2}{2}+\frac{1}{2}\right)\,.\end{aligned}\tag{3.9}$$

The torus amplitude can be constructed as a free-orbifold generated by $g_1'=(-1)^F\delta_{w_8}\delta_{p_9}$ and $g_2=\delta_{w_6}\delta_{p_7}$. The presence of the factor $(-1)^F$ in g_1' can be understood from the difference between the NS-NS and RR projectors in eq. (3.6), which is the same as in 8d examples. Actually, the same will be true for all models we construct in what follows, only g_1' will contain the supersymmetry breaking deformation $(-1)^F$.

JHEP07(2021)104

3.3 Models in four dimensions

In four dimensions, a non-trivial antisymmetric tensor can have rank $B = 2$, 4 or 6.

- rank $B = 2$: 8d model compactified on T^4 (T-dualized)

  By compactifying the 8d model on T^4 and T-dualizing the four extra compact directions, one finds a 4d model with D3-branes and 64 O3-planes. In the supersymmetric case, one has 48 O3$_-$ and 16 O3$_+$-planes. In the non-SUSY case, one obtains a configuration with 32 O3$_-$ and $16 \times (\overline{\text{O3}}_- + \overline{\text{O3}}_+)$-planes. Like in the six dimensional rank $B = 2$ case, the geometry is simply the one of the 8d model duplicated along the new compact directions. Since the model is T-dual to the 8d model compactified on an extra T^4, the rank of the gauge group is 8. For a single stack of D3-branes, the gauge symmetry is USp(16) if the D3-branes are on top of one $\overline{\text{O3}}_+$ or O3$_+$-plane, SO(16) if the D3-branes are on top of one $\overline{\text{O3}}_-$-plane or O3$_-$-plane, and U(8) if the D3-brane stack is in the bulk. Supersymmetry is broken at the string scale (nonlinearly realized) if the D3-branes are coincident with anti-orientifolds, and broken only at the massive level (due to the separation in the internal space from the source of supersymmetry breaking) if the D3-branes are coincident with orientifold planes.

  When the D3-branes are put at the origin, the corresponding projectors on the momentum states running in the Möbius amplitude are

$$\begin{aligned} \Pi_{\text{NSNS}} &= \frac{1-(-1)^{m_9}-(-1)^{m_8}-(-1)^{m_9+m_8}}{2} \times \prod_{i=4}^{7} \frac{1+(-1)^{m_i}}{2}\,, \\ \Pi_{\text{RR}} &= (-1)^{m_8}\Pi_{\text{NSNS}}\,. \end{aligned} \tag{3.10}$$

- rank $B = 4$: 6d model compactified on T^2 (T-dualized)

  By compactifying the 6d model on T^2 and T-dualizing the two extra compact directions, one finds a 4d model where, in the supersymmetric case, one has 40 O3$_-$ and 24 O3$_+$-planes. In the non-SUSY case, one finds a configuration with 24 O3$_-$, 8 O3$_+$ and $16 \times (\overline{\text{O3}}_- + \overline{\text{O3}}_+)$-planes. The geometry is the one of the 6d model duplicated along the two new dimensions. Since the model is T-dual to the 6d model compactified on T^2, the rank of the gauge group is 4. For a single stack of D3-branes, the gauge symmetry is USp(8) if the D3-branes are on top of one $\overline{\text{O3}}_+$ or O3$_+$-plane, SO(8) if the D3-branes are on top of one $\overline{\text{O3}}_-$-plane or O3$_-$-plane, and U(4) if the D3-brane stack is in the bulk. The supersymmetry breaking pattern is the same as in the previous cases.

  The corresponding projectors on the momentum states in the Möbius for D3-branes put at the origin are

$$\begin{aligned} \Pi_{\text{NSNS}} &= \frac{1-(-1)^{m_9}-(-1)^{m_8}-(-1)^{m_9+m_8}}{2} \\ &\quad \times \frac{1+(-1)^{m_7}-(-1)^{m_6}+(-1)^{m_7+m_6}}{2} \times \prod_{i=4}^{5} \frac{1+(-1)^{m_i}}{2}\,, \\ \Pi_{\text{RR}} &= (-1)^{m_8}\Pi_{\text{NSNS}}\,. \end{aligned} \tag{3.11}$$

JHEP07(2021)104

- rank $B = 6$

  Following our binary ordering, the geometry of the SUSY model discussed here is

$$\begin{aligned}
&(\mathrm{O3}_+, \mathrm{O3}_-, \mathrm{O3}_-, \mathrm{O3}_-, \mathrm{O3}_-, \mathrm{O3}_+, \mathrm{O3}_+, \mathrm{O3}_+, \mathrm{O3}_-, \mathrm{O3}_+, \mathrm{O3}_+, \mathrm{O3}_+, \mathrm{O3}_-,\\
&\mathrm{O3}_+, \mathrm{O3}_+, \mathrm{O3}_+, \mathrm{O3}_-, \mathrm{O3}_+, \mathrm{O3}_+, \mathrm{O3}_+, \mathrm{O3}_+, \mathrm{O3}_-, \mathrm{O3}_-, \mathrm{O3}_-, \mathrm{O3}_+, \mathrm{O3}_-,\\
&\mathrm{O3}_-, \mathrm{O3}_-, \mathrm{O3}_+, \mathrm{O3}_-, \mathrm{O3}_-, \mathrm{O3}_-, \mathrm{O3}_-, \mathrm{O3}_+, \mathrm{O3}_+, \mathrm{O3}_+, \mathrm{O3}_+, \mathrm{O3}_-, \mathrm{O3}_-,\\
&\mathrm{O3}_-, \mathrm{O3}_+, \mathrm{O3}_-, \mathrm{O3}_-, \mathrm{O3}_-, \mathrm{O3}_+, \mathrm{O3}_-, \mathrm{O3}_-, \mathrm{O3}_-, \mathrm{O3}_-, \mathrm{O3}_+, \mathrm{O3}_+, \mathrm{O3}_+,\\
&\mathrm{O3}_+, \mathrm{O3}_-, \mathrm{O3}_-, \mathrm{O3}_-, \mathrm{O3}_+, \mathrm{O3}_-, \mathrm{O3}_-, \mathrm{O3}_-, \mathrm{O3}_+, \mathrm{O3}_-, \mathrm{O3}_-, \mathrm{O3}_-)\,, \qquad (3.12)
\end{aligned}$$

  with a total of 36 $\mathrm{O3}_-$ and 28 $\mathrm{O3}_+$-planes. Again, there are several SUSY breaking deformations that are possible. One example is a configuration with 20 $\mathrm{O3}_-$, 12 $\mathrm{O3}_+$ and 16 $\times$ ($\overline{\mathrm{O3}}_- + \overline{\mathrm{O3}}_+$)-planes as follows

$$\begin{aligned}
&(\overline{\mathrm{O3}}_+, \mathrm{O3}_-, \overline{\mathrm{O3}}_-, \mathrm{O3}_-, \overline{\mathrm{O3}}_-, \mathrm{O3}_+, \overline{\mathrm{O3}}_+, \mathrm{O3}_+, \overline{\mathrm{O3}}_-, \mathrm{O3}_+, \overline{\mathrm{O3}}_+, \mathrm{O3}_+, \overline{\mathrm{O3}}_-,\\
&\mathrm{O3}_+, \overline{\mathrm{O3}}_+, \mathrm{O3}_+, \overline{\mathrm{O3}}_-, \mathrm{O3}_+, \overline{\mathrm{O3}}_+, \mathrm{O3}_+, \overline{\mathrm{O3}}_+, \mathrm{O3}_-, \overline{\mathrm{O3}}_-, \mathrm{O3}_-, \overline{\mathrm{O3}}_+, \mathrm{O3}_-,\\
&\overline{\mathrm{O3}}_-, \mathrm{O3}_-, \overline{\mathrm{O3}}_+, \mathrm{O3}_-, \overline{\mathrm{O3}}_-, \mathrm{O3}_-, \overline{\mathrm{O3}}_-, \mathrm{O3}_+, \overline{\mathrm{O3}}_+, \mathrm{O3}_+, \overline{\mathrm{O3}}_+, \mathrm{O3}_-, \overline{\mathrm{O3}}_-,\\
&\mathrm{O3}_-, \overline{\mathrm{O3}}_+, \mathrm{O3}_-, \overline{\mathrm{O3}}_-, \mathrm{O3}_-, \overline{\mathrm{O3}}_+, \mathrm{O3}_-, \overline{\mathrm{O3}}_-, \mathrm{O3}_-, \overline{\mathrm{O3}}_-, \mathrm{O3}_+, \overline{\mathrm{O3}}_+, \mathrm{O3}_+,\\
&\overline{\mathrm{O3}}_+, \mathrm{O3}_-, \overline{\mathrm{O3}}_-, \mathrm{O3}_-, \overline{\mathrm{O3}}_+, \mathrm{O3}_-, \overline{\mathrm{O3}}_-, \mathrm{O3}_-, \overline{\mathrm{O3}}_+, \mathrm{O3}_-, \overline{\mathrm{O3}}_-, \mathrm{O3}_-)\,. \qquad (3.13)
\end{aligned}$$

  The rank of the gauge group is 2 and, depending on the location of the stacks of D3-branes, one finds for a single stack USp(4) if the D3-branes are on top of one $\overline{\mathrm{O3}}_+$ or $\mathrm{O3}_+$-plane, SO(4) if the D3-branes are on top of one $\overline{\mathrm{O3}}_-$-plane or $\mathrm{O3}_-$-plane, and U(2) if the D3-brane stack is in the bulk.

When the 2 D3-branes (4 half-D3-branes) are at the origin, the projectors on the momentum states in the Möbius amplitude are

$$\begin{aligned}
\Pi_{\mathrm{NSNS}} &= \prod_{i=2}^{4} \frac{1-(-1)^{m_{2i+1}}-(-1)^{m_{2i}}-(-1)^{m_{2i+1}+m_{2i}}}{2}\,,\\
\Pi_{\mathrm{RR}} &= (-1)^{m_8}\Pi_{\mathrm{NSNS}}\,. \qquad (3.14)
\end{aligned}$$

The tree-level amplitudes are given by

$$\begin{aligned}
\tilde{\mathcal{K}} &= \frac{(\alpha')^3}{4v_6}\int_0^\infty \mathrm{d}l\, P_{\mathbf{m}}^{(6)}\frac{V_8-S_8}{\eta^8}(il)\,,\\
\tilde{\mathcal{A}} &= \frac{2^{-5}N^2(\alpha')^3}{2v_6}\int_0^\infty \mathrm{d}l\, P_{\mathbf{m}}^{(6)}\frac{V_8-S_8}{\eta^8}(il)\,,\\
\tilde{\mathcal{M}} &= -\frac{N(\alpha')^2}{8v_4}\int_0^\infty \mathrm{d}l \prod_{i=2}^{4}\left[(-1)^{m_{2i}}P_{2m_{2i+1}}-P_{2m_{2i+1}+1}\right]P_{m_{2i}}\\
&\qquad\qquad \times \frac{\hat{V}_8-(-1)^{m_8}\hat{S}_8}{\hat{\eta}^8}\left(il+\frac{1}{2}\right)\,, \qquad (3.15)
\end{aligned}$$

JHEP07(2021)104

while in the loop-channel they become

$$\mathcal{K} = \frac{1}{2}\int_0^\infty \frac{\mathrm{d}\tau_2}{\tau_2^3} W_{2\mathbf{n}}^{(6)} \frac{V_8 - S_8}{\eta^8}(2i\tau_2)\,,$$
$$\mathcal{A} = \frac{N^2}{2}\int_0^\infty \frac{\mathrm{d}\tau_2}{\tau_2^3} W_{\mathbf{n}}^{(6)} \frac{V_8 - S_8}{\eta^8}\left(\frac{i\tau_2}{2}\right),$$
$$\mathcal{M} = \frac{N}{2}\int_0^\infty \frac{\mathrm{d}\tau_2}{\tau_2^4} \prod_{i=2}^{4} W_{n_{2i+1}}\left[(-1)^{n_{2i+1}} W_{2n_{2i}} - W_{2n_{2i}+1}\right] \frac{\hat{V}_8 + (-1)^{n_9}\hat{S}_8}{\hat{\eta}^8}\left(\frac{i\tau_2}{2} + \frac{1}{2}\right). \quad (3.16)$$

The torus amplitude can be constructed as a free-orbifold generated by $g_1' = (-1)^F \delta_{w_8}\delta_{p_9}$, $g_2 = \delta_{w_6}\delta_{p_7}$ and $g_3 = \delta_{w_4}\delta_{p_5}$.

4 Consistency conditions from probe branes

It is well-known that the standard consistency rules of open-string partition functions are not enough to define a consistent string model. There are indeed K-theory constraints [96, 97], which can also be understood in terms of the Witten SU(2) anomalies [98] on probe branes [99]. We are therefore interested in probe branes with SU(2) gauge group. Probe branes mean D-branes that are not constrained by the RR tadpole cancelation. In the type I string, background branes are D9 and the probe branes can be of D7, D5, D3 or D1 types, where the D5 and D1-branes are BPS, whereas the D7 and D3 are non-BPS. Since D1-branes lead to a 2d theory, whereas we are interested in Witten four-dimensional SU(2) anomalies, we will ignore D1-branes in what follows. D7 and D3-branes in type I support unitary gauge groups U(M), D5-branes support USp(M) gauge groups [100, 101] for $B_{ij} = 0$, whereas SO(M) is also possible on D5-branes for $B_{ij} \neq 0$. The cases of interest for us are SU(2) $\subset$ U(2) and USp(2), which will be implicitly assumed in what follows. For Witten SU(2) anomaly, only the strings stretched between the background D9-branes and the probe branes, which transform in the fundamental representation of the SU(2) probe-brane gauge group, are relevant. Since the spectrum of these bifundamental strings are given entirely by the cylinder amplitude, supersymmetry breaking by the orientifold projection is not affecting our discussion below. In the following, we will first consider the corresponding spectra in type I language and then perform T-dualities in all internal directions. After T-duality, one obtains a geometry with O$_+$, O$_-$, $\overline{\text{O}}_+$, $\overline{\text{O}}_-$-planes, but due to the argument above one can restrict to configurations with O$_\pm$-planes only. The only cases giving constraints are when background branes are located on O$_-$-planes, which is implicitly assumed in what follows.

4.1 Probe branes in eight dimensions

In the type I string compactified to eight dimensions on T^2, two T-dualities switch the description into the type IIB/Ω' orientifold framework, where Ω' contains two parity operations $(X_8, X_9) \to (-X_8, -X_9)$. One finds that: D9-D5 states contain six-dimensional Majorana-Weyl fermions in the $(M, 2)$ of the gauge group SO$(M)_9 \times$ USp$(2)_5$. After T-duality, if the D5 probe brane wraps T^2, the configuration becomes D7-D3 with four-dimensional Weyl fermions in the bifundamental representation. Placing some D7 and D3

JHEP07(2021)104

on the four O7-planes, we learn that at each orientifold fixed point, M should be even. Therefore stuck half-D7-branes i.e. without dynamical positions, and in particular SO(1) configurations, are not allowed.

Once this rule is satisfied, there are no further non-trivial constraints coming from D5 probe branes wrapped differently, or from D7 and D3 probe branes.

4.2 Probe branes in six dimensions

In type I string compactified to six-dimensions on T^4, the probe branes of interest are D5-branes (which are not points in T^4), D7-branes whose worldvolume wrap T^4 and D3-branes. The strongest constraints come from D9-D5 strings, which become D5-D5 strings after four T-dualities, with the probe D5-branes wrapping a T^2 in the compact internal space. The consistent configurations with stacks of odd numbers of background half-D5-branes on orientifold fixed points must contain even numbers of such stacks in each T^2 in T^4.

4.3 Probe branes in four dimensions

In type I string compactified to four-dimensions on T^6, the only probe branes of interest are D7-branes and D3-branes. The former give no constraint since the number of D9-D7 Weyl fermions after reduction to four dimensions is always even. Moreover, after six T-dualities, the probe D3-branes become D9-branes which wrap the entire internal space, while the background D9-branes become D3-branes. Hence, the probe D9-branes intersect all background D3-branes, leading to no constraint.

4.4 Extra non-perturbative constraint

In addition to the Witten anomaly, another constraint on the allowed configurations comes from imposing that, in any dimension, the Wilson lines (or brane positions after T-duality) belong to SO(N) (actually Spin(N)) and not O(N). This is because at a nonperturbative level, the component of O(N) disconnected from SO(N) cannot be defined [97]. This implies that all determinants of Wilson-line matrices must equal one.

In practice, when the branes are located at fixed points, the matrix of Wilson lines along a direction X^i is diagonal, with entries 1 or -1 only. The number of 1's corresponds to the number of half-branes sitting at the origin of direction X^i while the number of -1's is the number of half-branes at position $X^i = \pi R_i$ [18–30]. For the determinant to be one, we thus conclude that the allowed brane configurations are the ones for which the number of half-branes in each hyperplan $X^i = 0$ or $X^i = \pi R_i$ is even.

5 Gravitino mass versus SUSY breaking scale on D-branes

The main feature of the class of models constructed in this paper is the existence of two supersymmetry breaking mass scales: one in the closed-string sector, which is related to the compactification (KK or winding) scale, and another one in the open-string (gauge) sector, which is either the winding scale or the string scale, depending on which one is smaller. As mentioned in the introduction, this was already achieved in [76]. Our construction, which is motivated by the orientifold projection put forward in the pioneering paper [77], allows

JHEP07(2021)104

one to avoid the open-string instabilities typically present in such constructions. In the following, we discuss in some details the mass scales and the limits where supersymmetry is restored in the non-SUSY 8d model of section 2.

In the geometry of O-planes shown in figure 1c, the 8 D7-branes can be put in a single stack located in the bulk or coincident with one of the four orientifold planes. Let us consider the latter case.

- Putting the stack on top of the O7$_-$-plane closer to the $\overline{\text{O7}}_-$-plane, the Möbius contribution to the vacuum energy is positive, since the D7-branes are repelled from the $\overline{\text{O7}}_-$ plane and attracted towards the $\overline{\text{O7}}_+$-plane. The Möbius amplitude takes the form

$$\mathcal{M} = -\frac{N}{2}\int_0^\infty \frac{\mathrm{d}\tau_2}{\tau_2^5}\, W_{n_9}\left[W_{2n_8} + (-1)^{n_9} W_{2n_8+1}\right] \frac{\hat{V}_8 - (-1)^{n_9}\hat{S}_8}{\hat{\eta}^8}\left(\frac{i\tau_2}{2}+\frac{1}{2}\right), \tag{5.1}$$

while the cylinder amplitude is still given by (2.27). The "field-theory" open-string spectrum is encoded in

$$\begin{aligned}(\mathcal{A}+\mathcal{M})|_{\text{FT}} = \int_0^\infty \frac{\mathrm{d}\tau_2}{\tau_2^5}\Bigg\{&\frac{N(N-1)}{2}\left[W_{2n_9}W_{n_8}\frac{V_8-S_8}{\eta^8} + W_{2n_9+1}\left(W_{2n_8}\frac{V_8}{\eta^8} - W_{2n_8+1}\frac{S_8}{\eta^8}\right)\right]\Bigg|_0 \\ &+\frac{N(N+1)}{2}W_{2n_9+1}\left(W_{2n_8+1}\frac{V_8}{\eta^8} - W_{2n_8}\frac{S_8}{\eta^8}\right)\Bigg|_0\Bigg\},\end{aligned} \tag{5.2}$$

and is supersymmetric at the massless level. The gauge group is SO(N), where $N = 16$ is fixed by the RR tadpole condition. Since the closed-string spectrum becomes supersymmetric when $R_8 \to 0$ and/or $R_9 \to \infty$ (in particular gravitinos become massless), it is interesting to take these limits in the open (gauge) spectrum. The first limit $R_8 \to 0$ leads to a supersymmetric spectrum on the D7-branes. Indeed, the winding towers of bosons and fermions collapse to the same value. Supersymmetry is broken only at the massive winding level and for $R_8 \leq \sqrt{\alpha'}$ can therefore be considered as spontaneous at the field-theory massless level, after including quantum corrections. In the other limit $R_9 \to \infty$, the open-string states featuring supersymmetry breaking become infinitely heavy and decouple at low energy.[10]

- Putting all D7-branes on one stack coincident with the O7$_-$-plane closer to the $\overline{\text{O7}}_+$-plane, the Möbius contribution to the vacuum energy is negative. Otherwise there are no major differences.

- Let us now consider the case where all D7-branes are coincident with the $\overline{\text{O7}}_+$-plane, whose amplitudes are displayed in eqs. (2.27) and (2.25). The "field-theory" open-string spectrum is encoded in

$$\begin{aligned}(\mathcal{A}+\mathcal{M})|_{\text{FT}} = \int_0^\infty \frac{\mathrm{d}\tau_2}{\tau_2^5}\Bigg\{&\frac{N(N+1)}{2}W_{2n_9}\left(W_{2n_8}\frac{V_8}{\eta^8} - W_{2n_8+1}\frac{S_8}{\eta^8}\right)\Bigg|_0 \\ &+\frac{N(N-1)}{2}\left[W_{2n_9}\left(W_{2n_8+1}\frac{V_8}{\eta^8} - W_{2n_8}\frac{S_8}{\eta^8}\right) + W_{2n_9+1}W_{n_8}\frac{V_8-S_8}{\eta^8}\right]\Bigg|_0\Bigg\}.\end{aligned} \tag{5.3}$$

[10] However, none of the limits has a purely perturbative orientifold description. In the first case $R_8 \to 0$ the open-string spectrum does not have a 9d interpretation, whereas in the second case $R_9 \to \infty$ there are local charges and tensions that generate a strong backreaction (local tadpoles are not cancelled).

JHEP07(2021)104

The gauge group is USp(N), where $N = 16$ is fixed by the RR tadpole condition. In this case, the pattern of supersymmetry breaking depends on the value of R_8. If this radius is large (and in general when branes are coincident with anti-orientifold planes) the breaking is at the string scale, with nonlinearly realized supersymmetry. This interpretation is valid in the regime of large R_8 and $R_9 > \sqrt{\alpha'}$, when there are light gravitinos in the spectrum.

In the limit $R_8 \to 0$, the spectrum becomes however supersymmetric. In fact, when R_8 is small, supersymmetry can be interpreted as spontaneously broken, since there is a shift in the fermion masses compared to the bosons in the winding sector. Although this seems similar to the familiar Scherk-Schwarz breaking, the mechanism has also features in common with Brane Supersymmetry Breaking since the deformation does not affect the cylinder but acts in the Möbius amplitude by exchanging symmetric with antisymmetric gauge-group representations for fermions (compared to bosons) in the open-string spectrum. Throughout the paper, we have used the terminology "supersymmetry breaking at the string scale" for this situation, in order to distinguish it with the case where the D-branes are on top of $O_\pm$-planes.

When $R_9 \to \infty$ at fixed R_8, the spectrum encoded in (5.3) does not become supersymmetric, whereas the closed-string spectrum does. This is interesting since one may think that an exact Brane Supersymmetry Breaking Spectrum is realized in this limit. If true, this would also be a counter-example of the gravitino mass conjecture put forward recently in [74, 75]. However, when $R_9 \to \infty$, the local sources from D-branes and O-planes generate local tadpoles and thus large backreactions responsible for the breaking of the effective field theory description, as conjectured in [74, 75].[11] On the other hand, the model shows that the value of the gravitino mass $m_{3/2}$ can be decoupled from the size of the scalar potential V, for fixed values of the moduli. In particular, $|m_{3/2}| \ll |V|^{1/d}$ is possible. Hence, we do not see any fundamental reason in quantum gravity to necessarily have a high gravitino mass compared to the Hubble scale [102], as recently proposed in [103, 104].

- Finally, putting all D7-branes on one stack coincident with the $\overline{\text{O7}}_-$-plane, the Möbius contribution to the vacuum energy is positive and the pattern of supersymmetry breaking is similar to that found in the previous case.

Let us summarize the similarities and differences between BSB models and the ones we have constructed in this paper. In BSB models, the closed-string spectrum is supersymmetric, therefore there are massless gravitinos, whereas in the open-string spectrum supersymmetry is non-linearly realized, meaning that bosonic and fermionic degrees of freedom do not match level by level. The price to pay is the presence of a disk NS-NS

[11] Note however that these references do not claim that a limit of zero gravitino mass is not possible. There are known examples of Scherk-Schwarz type where the whole spectrum and interactions (closed and open strings in orientifolds, or only closed strings in heterotic and type II strings) become supersymmetric in the decompactification limit. The claim is that such a limit is not possible, within an effective field theory description, if there is some sector breaking supersymmetry in the limit of vanishing gravitino mass.

JHEP07(2021)104

tadpole, which could signal a breakdown of perturbation theory. In the models we discussed in this paper, supersymmetry is broken in the closed sector at the compactification scale, whereas the scale of supersymmetry breaking in the open sector can be the string scale. There are no disk NS-NS tadpoles, but generically there is a one-loop cosmological constant. There is a continuous modulus which in the limit $R_9 \to \infty$ seems to realize an exact BSB setup. However, local sources (local tadpole cancelation conditions) generate a strong backreaction and prevents this limit to be realized.

6 Conclusions and open questions

We have constructed supersymmetry-breaking orientifold models where a certain number n of O_- (negative tension, negative charge) - O_+ (positive tension, positive charge) orientifold-plane pairs are transformed into n $\overline{O}_-$ (negative tension, positive charge) - $\overline{O}_+$ (positive tension, negative charge) pairs. The anti-orientifold plane pairs preserve the other half of supersymmetries, compared to the other ingredients of the background, which are $O_\pm$-planes and D-branes. In the open-string sector, supersymmetry is only broken in the Möbius vacuum amplitude, whereas the closed-string sector has softly broken supersymmetry.

The main interest of this mechanism is that both the original O_--O_+ pairs and their SUSY breaking cousins $\overline{O}_-$-$\overline{O}_+$ have zero tension and charge, so that the total tension and charge of the models are unchanged upon replacement. Therefore there are neither NS-NS nor RR tadpoles generated in the process.

Depending on where the background D-branes sit in the internal space, their massless spectrum is supersymmetric or not. In the latter case, which corresponds to D-branes located on anti-orientifold planes, the pattern of supersymmetry breaking depends on the value of a radius. If it is large, the breaking is at the string scale, with nonlinearly realized supersymmetry. On the contrary, if the radius is small, the same configuration describes a spontaneous breaking of supersymmetry. In this regime, the winding states in the D-brane spectrum are light and supersymmetry breaking can be interpreted as a shift in the fermion masses compared to the bosons in the winding sector. This seems similar to the more familiar breaking by compactification (Scherk-Schwarz), but it differs in detail in that the brane-brane cylinder amplitude is not subject to this shift.

Constructions of this type naturally stabilize open-string moduli. Indeed, energetic considerations favor the D-branes to sit on top of $\overline{O}_+$-planes, where the scale of supersymmetry breaking on their worldvolume is maximal.

An interesting issue in such models is their effective field-theory limits. At first sight, as initially considered in [77], it seems possible that the closed-string spectrum is supersymmetric at tree level. However, we have provided arguments showing that this is not plausible, as it would be at odds with the boundary conditions of the gravitinos imposed by the simultaneous presence of orientifold and anti-orientifold planes, which suggests massive gravitinos. In fact, we have given reasons in favor of a specific soft supersymmetry-breaking deformation in the closed-string sector, rendering massive the gravitinos. Moreover, if an exact supersymmetric closed-string spectrum would be compatible with the orientifold

JHEP07(2021)104

amplitudes discussed in our paper, one would obtain new models of Brane Supersymmetry Breaking type. This would also give counter-examples of the gravitino mass conjecture [74, 75], whereas the models constructed in our paper are in agreement with it. More generally, existence of models with exact supersymmetry in the closed-string sector and broken supersymmetry in the open-string sector would contradict the conjecture in [74, 75]. Three more comments are in order here.

First of all, all known models of this type, which are of BSB type or with internal magnetic fields and broken supersymmetry, have NS-NS disk tadpoles that could plausibly trigger a breakdown of the effective field theory in the perturbative vacuum, in agreement with [74, 75]. Secondly, the exact supersymmetry in the closed-string sectors of such models is valid only at tree-level, as it is broken by quantum corrections induced by the open-string sector. It is unclear to us if the conjecture on the gravitino mass should apply to the classical theory (tree-level spectrum) or to the quantum one. Lastly, in the string models we have constructed, it is possible to decouple the gravitino mass from the size of the scalar potential. In particular, the gravitino can be much lighter than the scale determined by the magnitude of the quantum potential. This fact could play a role in inflationary models of the type studied in [102–107].

Eventually, the string models we have considered are based on toroidal compactifications and the fermionic spectrum, once reduced to four dimensions, is non-chiral. It would be of course very interesting to construct chiral four-dimensional models with supersymmetry breaking, by combining the mechanism put forward in this paper with other ingredients producing chirality, like orbifolds and/or fluxes. We hope to come back to this interesting question in the near future.

Acknowledgments

E.D. thanks Carlo Angelantonj, Jihad Mourad, Gianfranco Pradisi and Augusto Sagnotti for valuable discussions and correspondence. E.D. was supported in part by the "Agence Nationale de la Recherche" (ANR).

A Consistency of supersymmetric Möbius projectors

In the construction of models in even dimension lower than 8, we have chosen factorized Möbius projectors for simplicity. However, this is not imposed by the RR tadpole condition. In this appendix, we will confirm that non-factorized projectors can be fully consistent, but we will also see that imposing the RR tadpole condition is not enough to obtain a Möbius projector fully consistent. In the latter case, the inconsistency can only be seen in the direct Klein-bottle amplitude, while it is invisible in the open-string sector. We will study supersymmetric examples in 6d with rank $B = 4$.

A.1 A consistent non-factorized Möbius projector

In 6d, with all D-branes located at the origin, a generic Möbius projector contains 16 terms, one for each fixed point with appropriate phases. The RR tadpole condition constrains the

JHEP07(2021)104

overall charge of the O-planes and thus the number of O_- and O_+-planes. In the projector, this translates into a given number of minus and plus signs. In 6d with maximal rank for B_{ij}, there are 10 $O5_-$ and 6 $O5_+$-planes. This yields 10 terms with a minus sign and 6 terms with a plus sign in the projector. The total number of possibilities that fulfils this requirement is $\binom{16}{6} = 8008$.

Let us look at the following projector,

$$\begin{aligned}\Pi = 1 &+ (-1)^{m_9} + (-1)^{m_8} - (-1)^{m_9+m_8} + (-1)^{m_7} - (-1)^{m_9+m_7} - (-1)^{m_8+m_7} \\ &- (-1)^{m_9+m_8+m_7} + (-1)^{m_6} - (-1)^{m_9+m_6} - (-1)^{m_8+m_6} - (-1)^{m_9+m_8+m_6} \\ &- (-1)^{m_7+m_6} - (-1)^{m_9+m_7+m_6} - (-1)^{m_8+m_7+m_6} + (-1)^{m_9+m_8+m_7+m_6}\,. \end{aligned} \tag{A.1}$$

With all D-branes at the origin, we deduce the geometry of the model,

$$\begin{aligned}&(\mathrm{O5}_+, \mathrm{O5}_+, \mathrm{O5}_+, \mathrm{O5}_-, \mathrm{O5}_+, \mathrm{O5}_-, \mathrm{O5}_-, \mathrm{O5}_-, \mathrm{O5}_+, \\ &\qquad \mathrm{O5}_-, \mathrm{O5}_-, \mathrm{O5}_-, \mathrm{O5}_-, \mathrm{O5}_-, \mathrm{O5}_-, \mathrm{O5}_+)\,. \end{aligned} \tag{A.2}$$

It turns out to give no projection in the tree-level channel Klein-bottle amplitude, as was the case in eq. (3.8). This is thus consistent with the supersymmetric torus amplitude generated by g_1 and g_2. The transverse cylinder amplitude is also the one obtained in eq. (3.8), while the Möbius amplitudes, both in tree-level and loop channels, are

$$\begin{aligned}\tilde{\mathcal{M}} = &-\frac{N(\alpha')^2}{4v_4}\int_0^\infty \mathrm{d}l\,\Big[(P_{2m_9}+P_{2m_9+1}(-1)^{m_6})\,(P_{2m_8}P_{2m_7+1}+P_{2m_8+1}P_{2m_7}) \\ &+(P_{2m_9+1}-P_{2m_9}(-1)^{m_6})\,(P_{2m_8}P_{2m_7}-P_{2m_8+1}P_{2m_7+1})\Big]P_{m_6}\frac{\hat{V}_8-\hat{S}_8}{\hat{\eta}^8}\left(il+\frac{1}{2}\right) \\ \mathcal{M} = &\int_0^\infty \frac{\mathrm{d}\tau_2}{\tau_2^4}\Big[W_{n_9}\,(W_{2n_8}W_{2n_7}-W_{2n_8+1}W_{2n_7+1})\,(W_{2n_6}+W_{2n_6+1}(-1)^{n_9}) \\ &+(W_{2n_8}W_{2n_7+1}+W_{2n_8+1}W_{2n_7})\,(W_{2n_6}(-1)^{n_9}-W_{2n_6+1})\Big]\frac{\hat{V}_8-\hat{S}_8}{\hat{\eta}^8}\left(\frac{i\tau_2}{2}+\frac{1}{2}\right). \end{aligned} \tag{A.3}$$

The tree-level channel Möbius amplitude contains all momentum states, just like the tree-level Klein bottle and cylinder, so that the factorization property of the amplitudes is satisfied. The loop-channel Möbius amplitude is also consistent with the cylinder since it contains the contributions of the same states with signs. We conclude that the projector (A.1) yields a fully consistent model.

A.2 An inconsistent Möbius projector

Now consider the following projector, which has the correct number of signs to satisfy the RR tadpole condition,

$$\begin{aligned}\Pi = 1 &+ (-1)^{m_9} + (-1)^{m_8} + (-1)^{m_9+m_8} + (-1)^{m_7} + (-1)^{m_9+m_7} - (-1)^{m_8+m_7} \\ &- (-1)^{m_9+m_8+m_7} - (-1)^{m_6} - (-1)^{m_9+m_6} - (-1)^{m_8+m_6} - (-1)^{m_9+m_8+m_6} \\ &- (-1)^{m_7+m_6} - (-1)^{m_9+m_7+m_6} - (-1)^{m_8+m_7+m_6} - (-1)^{m_9+m_8+m_7+m_6}\,. \end{aligned} \tag{A.4}$$

JHEP07(2021)104

With all D-branes at the origin, the distribution of O-planes is given by

$$(\mathrm{O5}_+,\mathrm{O5}_+,\mathrm{O5}_+,\mathrm{O5}_+,\mathrm{O5}_+,\mathrm{O5}_+,\mathrm{O5}_-,\mathrm{O5}_-,\mathrm{O5}_-,\\ \mathrm{O5}_-,\mathrm{O5}_-,\mathrm{O5}_-,\mathrm{O5}_-,\mathrm{O5}_-,\mathrm{O5}_-,\mathrm{O5}_-)\,. \tag{A.5}$$

With this geometry, the tree-level channel Klein bottle is now different and not all momentum states are present. The tree-level and loop-channel Klein-bottle and Möbius amplitudes are

$$\begin{aligned}
\tilde{\mathcal{K}} &= \frac{(\alpha')^2}{v_4}\int_0^\infty \mathrm{d}l\, P_{2m_9}\left(P_{m_8}P_{m_7}P_{m_6}+8P_{2m_8}P_{2m_7}P_{2m_6+1}\right)\frac{V_8-S_8}{\eta^8}(il)\,,\\
\mathcal{K} &= \frac{1}{4}\int_0^\infty \frac{\mathrm{d}\tau_2}{\tau_2^4}\,W_{n_9}\left(W_{2n_8}W_{2n_7}W_{2n_6}+W_{n_8}W_{n_7}(-1)^{n_6}W_{n_6}\right)\frac{V_8-S_8}{\eta^8}(2i\tau_2)\,,\\
\tilde{\mathcal{M}} &= \frac{N(\alpha')^2}{4v_4}\int_0^\infty \mathrm{d}l\, P_{2m_9}\Big\{P_{2m_8}\left[P_{m_7}P_{m_6}-2P_{2m_7}\left(P_{2m_6}-P_{2m_6+1}\right)\right]\\
&\qquad + P_{2m_8+1}\left(P_{2m_7}-P_{2m_7+1}\right)P_{m_6}\Big\}\frac{\hat{V}_8-\hat{S}_8}{\hat{\eta}^8}\left(il+\frac{1}{2}\right),\\
\mathcal{M} &= \frac{N}{2}\int_0^\infty \frac{\mathrm{d}\tau_2}{\tau_2^4}\,W_{n_9}W_{n_8}\left(W_{2n_7}W_{2n_6}-W_{n_7}W_{2n_6+1}+(-1)^{n_8}W_{2n_7+1}W_{2n_6}\right)\\
&\qquad\times\frac{\hat{V}_8-\hat{S}_8}{\hat{\eta}^8}\left(\frac{i\tau_2}{2}+\frac{1}{2}\right).
\end{aligned} \tag{A.6}$$

The loop-channel Möbius amplitude contains all states present in the cylinder. Moreover, the tree-level Klein-bottle, cylinder and Möbius amplitudes respect amplitude factorization. The only inconsistency comes from the Klein bottle in the loop-channel, which contains states not present in the torus amplitude. This means that the RR tadpole condition is not enough to produce a consistent Möbius projector. The inconsistency can only be seen in the closed-string sector and comes from the geometry of the model.

References

[1] M. Dine and N. Seiberg, *Is the Superstring Weakly Coupled?*, *Phys. Lett. B* **162** (1985) 299 [INSPIRE].

[2] J. Scherk and J.H. Schwarz, *Spontaneous Breaking of Supersymmetry Through Dimensional Reduction*, *Phys. Lett. B* **82** (1979) 60 [INSPIRE].

[3] R. Rohm, *Spontaneous Supersymmetry Breaking in Supersymmetric String Theories*, *Nucl. Phys. B* **237** (1984) 553 [INSPIRE].

[4] C. Kounnas and M. Porrati, *Spontaneous Supersymmetry Breaking in String Theory*, *Nucl. Phys. B* **310** (1988) 355 [INSPIRE].

[5] S. Ferrara, C. Kounnas and M. Porrati, *Superstring Solutions With Spontaneously Broken Four-dimensional Supersymmetry*, *Nucl. Phys. B* **304** (1988) 500 [INSPIRE].

JHEP07(2021)104

[6] S. Ferrara, C. Kounnas, M. Porrati and F. Zwirner, *Superstrings with Spontaneously Broken Supersymmetry and their Effective Theories*, *Nucl. Phys. B* **318** (1989) 75 [INSPIRE].

[7] C. Kounnas and B. Rostand, *Coordinate Dependent Compactifications and Discrete Symmetries*, *Nucl. Phys. B* **341** (1990) 641 [INSPIRE].

[8] E. Dudas and C. Timirgaziu, *Nontachyonic Scherk-Schwarz compactifications, cosmology and moduli stabilization*, *JHEP* **03** (2004) 060 [hep-th/0401201] [INSPIRE].

[9] C. Angelantonj, M. Cardella and N. Irges, *An Alternative for Moduli Stabilisation*, *Phys. Lett. B* **641** (2006) 474 [hep-th/0608022] [INSPIRE].

[10] C. Angelantonj, H. Partouche and G. Pradisi, *Heterotic-type I dual pairs, rigid branes and broken SUSY*, *Nucl. Phys. B* **954** (2020) 114976 [arXiv:1912.12062] [INSPIRE].

[11] T. Catelin-Jullien, C. Kounnas, H. Partouche and N. Toumbas, *Thermal/quantum effects and induced superstring cosmologies*, *Nucl. Phys. B* **797** (2008) 137 [arXiv:0710.3895] [INSPIRE].

[12] T. Catelin-Jullien, C. Kounnas, H. Partouche and N. Toumbas, *Induced superstring cosmologies and moduli stabilization*, *Nucl. Phys. B* **820** (2009) 290 [arXiv:0901.0259] [INSPIRE].

[13] F. Bourliot, C. Kounnas and H. Partouche, *Attraction to a radiation-like era in early superstring cosmologies*, *Nucl. Phys. B* **816** (2009) 227 [arXiv:0902.1892] [INSPIRE].

[14] F. Bourliot, J. Estes, C. Kounnas and H. Partouche, *Cosmological Phases of the String Thermal Effective Potential*, *Nucl. Phys. B* **830** (2010) 330 [arXiv:0908.1881] [INSPIRE].

[15] J. Estes, C. Kounnas and H. Partouche, *Superstring Cosmology for $N_4 = 1 \to 0$ Superstring Vacua*, *Fortsch. Phys.* **59** (2011) 861 [arXiv:1003.0471] [INSPIRE].

[16] T. Coudarchet, C. Fleming and H. Partouche, *Quantum no-scale regimes in string theory*, *Nucl. Phys. B* **930** (2018) 235 [arXiv:1711.09122] [INSPIRE].

[17] T. Coudarchet and H. Partouche, *Quantum no-scale regimes and moduli dynamics*, *Nucl. Phys. B* **933** (2018) 134 [arXiv:1804.00466] [INSPIRE].

[18] H. Itoyama and T.R. Taylor, *Supersymmetry Restoration in the Compactified $\mathrm{O}(16) \times \mathrm{O}(16)'$ Heterotic String Theory*, *Phys. Lett. B* **186** (1987) 129 [INSPIRE].

[19] S. Abel, K.R. Dienes and E. Mavroudi, *Towards a nonsupersymmetric string phenomenology*, *Phys. Rev. D* **91** (2015) 126014 [arXiv:1502.03087] [INSPIRE].

[20] C. Kounnas and H. Partouche, *Super no-scale models in string theory*, *Nucl. Phys. B* **913** (2016) 593 [arXiv:1607.01767] [INSPIRE].

[21] C. Kounnas and H. Partouche, *$\mathcal{N} = 2 \to 0$ super no-scale models and moduli quantum stability*, *Nucl. Phys. B* **919** (2017) 41 [arXiv:1701.00545] [INSPIRE].

[22] I. Florakis and J. Rizos, *Chiral Heterotic Strings with Positive Cosmological Constant*, *Nucl. Phys. B* **913** (2016) 495 [arXiv:1608.04582] [INSPIRE].

[23] S. Abel and R.J. Stewart, *Exponential suppression of the cosmological constant in nonsupersymmetric string vacua at two loops and beyond*, *Phys. Rev. D* **96** (2017) 106013 [arXiv:1701.06629] [INSPIRE].

[24] S. Abel, E. Dudas, D. Lewis and H. Partouche, *Stability and vacuum energy in open string models with broken supersymmetry*, *JHEP* **10** (2019) 226 [arXiv:1812.09714] [INSPIRE].

JHEP07(2021)104

[25] S. Abel, T. Coudarchet and H. Partouche, *On the stability of open-string orbifold models with broken supersymmetry*, *Nucl. Phys. B* **957** (2020) 115100 [arXiv:2003.02545] [INSPIRE].

[26] T. Coudarchet and H. Partouche, *One-loop masses of Neumann-Dirichlet open strings and boundary-changing vertex operators*, arXiv:2011.13725 [INSPIRE].

[27] T. Coudarchet and H. Partouche, *Two-point functions of Neumann-Dirichlet open-string sector moduli*, in *9th International Conference on New Frontiers in Physics*, (2020) [arXiv:2012.14442] [INSPIRE].

[28] H. Itoyama and S. Nakajima, *Exponentially suppressed cosmological constant with enhanced gauge symmetry in heterotic interpolating models*, *PTEP* **2019** (2019) 123B01 [arXiv:1905.10745] [INSPIRE].

[29] H. Itoyama and S. Nakajima, *Stability, enhanced gauge symmetry and suppressed cosmological constant in 9D heterotic interpolating models*, *Nucl. Phys. B* **958** (2020) 115111 [arXiv:2003.11217] [INSPIRE].

[30] H. Itoyama and S. Nakajima, *Marginal deformations of heterotic interpolating models and exponential suppression of the cosmological constant*, *Phys. Lett. B* **816** (2021) 136195 [arXiv:2101.10619] [INSPIRE].

[31] S. Groot Nibbelink, O. Loukas, A. Mütter, E. Parr and P.K.S. Vaudrevange, *Tension Between a Vanishing Cosmological Constant and Non-Supersymmetric Heterotic Orbifolds*, *Fortsch. Phys.* **68** (2020) 2000044 [arXiv:1710.09237] [INSPIRE].

[32] S. Sugimoto, *Anomaly cancellations in type-I D9-$\bar{D}$9 system and the* USp(32) *string theory*, *Prog. Theor. Phys.* **102** (1999) 685 [hep-th/9905159] [INSPIRE].

[33] I. Antoniadis, E. Dudas and A. Sagnotti, *Brane supersymmetry breaking*, *Phys. Lett. B* **464** (1999) 38 [hep-th/9908023] [INSPIRE].

[34] C. Angelantonj, *Comments on open string orbifolds with a nonvanishing B_{ab}*, *Nucl. Phys. B* **566** (2000) 126 [hep-th/9908064] [INSPIRE].

[35] G. Aldazabal and A.M. Uranga, *Tachyon free nonsupersymmetric type IIB orientifolds via brane-antibrane systems*, *JHEP* **10** (1999) 024 [hep-th/9908072] [INSPIRE].

[36] C. Angelantonj, I. Antoniadis, G. D'Appollonio, E. Dudas and A. Sagnotti, *Type I vacua with brane supersymmetry breaking*, *Nucl. Phys. B* **572** (2000) 36 [hep-th/9911081] [INSPIRE].

[37] J. Mourad and A. Sagnotti, *An Update on Brane Supersymmetry Breaking*, arXiv:1711.11494 [INSPIRE].

[38] E. Dudas and J. Mourad, *Consistent gravitino couplings in nonsupersymmetric strings*, *Phys. Lett. B* **514** (2001) 173 [hep-th/0012071] [INSPIRE].

[39] G. Pradisi and F. Riccioni, *Geometric couplings and brane supersymmetry breaking*, *Nucl. Phys. B* **615** (2001) 33 [hep-th/0107090] [INSPIRE].

[40] S. Kachru, R. Kallosh, A.D. Linde and S.P. Trivedi, *de Sitter vacua in string theory*, *Phys. Rev. D* **68** (2003) 046005 [hep-th/0301240] [INSPIRE].

[41] E.A. Bergshoeff, K. Dasgupta, R. Kallosh, A. Van Proeyen and T. Wrase, $\overline{\text{D3}}$ *and dS*, *JHEP* **05** (2015) 058 [arXiv:1502.07627] [INSPIRE].

JHEP07(2021)104

[42] R. Kallosh, F. Quevedo and A.M. Uranga, *String Theory Realizations of the Nilpotent Goldstino*, *JHEP* **12** (2015) 039 [arXiv:1507.07556] [INSPIRE].

[43] I. García-Etxebarria, F. Quevedo and R. Valandro, *Global String Embeddings for the Nilpotent Goldstino*, *JHEP* **02** (2016) 148 [arXiv:1512.06926] [INSPIRE].

[44] M.P. Garcia del Moral, S. Parameswaran, N. Quiroz and I. Zavala, *Anti-D3 branes and moduli in non-linear supergravity*, *JHEP* **10** (2017) 185 [arXiv:1707.07059] [INSPIRE].

[45] I. Bena, E. Dudas, M. Graña and S. Lüst, *Uplifting Runaways*, *Fortsch. Phys.* **67** (2019) 1800100 [arXiv:1809.06861] [INSPIRE].

[46] N. Cribiori, C. Roupec, T. Wrase and Y. Yamada, *Supersymmetric anti-D3-brane action in the Kachru-Kallosh-Linde-Trivedi setup*, *Phys. Rev. D* **100** (2019) 066001 [arXiv:1906.07727] [INSPIRE].

[47] E. Dudas and S. Lüst, *An update on moduli stabilization with antibrane uplift*, *JHEP* **03** (2021) 107 [arXiv:1912.09948] [INSPIRE].

[48] I. Antoniadis, E. Dudas, S. Ferrara and A. Sagnotti, *The Volkov-Akulov-Starobinsky supergravity*, *Phys. Lett. B* **733** (2014) 32 [arXiv:1403.3269] [INSPIRE].

[49] S. Ferrara, R. Kallosh and A. Linde, *Cosmology with Nilpotent Superfields*, *JHEP* **10** (2014) 143 [arXiv:1408.4096] [INSPIRE].

[50] E. Dudas, S. Ferrara, A. Kehagias and A. Sagnotti, *Properties of Nilpotent Supergravity*, *JHEP* **09** (2015) 217 [arXiv:1507.07842] [INSPIRE].

[51] I. Antoniadis and C. Markou, *The coupling of Non-linear Supersymmetry to Supergravity*, *Eur. Phys. J. C* **75** (2015) 582 [arXiv:1508.06767] [INSPIRE].

[52] E.A. Bergshoeff, D.Z. Freedman, R. Kallosh and A. Van Proeyen, *Pure de Sitter Supergravity*, *Phys. Rev. D* **92** (2015) 085040 [*Erratum ibid.* **93** (2016) 069901] [arXiv:1507.08264] [INSPIRE].

[53] W. Fischler and L. Susskind, *Dilaton Tadpoles, String Condensates and Scale Invariance*, *Phys. Lett. B* **171** (1986) 383 [INSPIRE].

[54] W. Fischler and L. Susskind, *Dilaton Tadpoles, String Condensates and Scale Invariance. 2*, *Phys. Lett. B* **173** (1986) 262 [INSPIRE].

[55] E. Dudas, G. Pradisi, M. Nicolosi and A. Sagnotti, *On tadpoles and vacuum redefinitions in string theory*, *Nucl. Phys. B* **708** (2005) 3 [hep-th/0410101] [INSPIRE].

[56] R. Pius, A. Rudra and A. Sen, *String Perturbation Theory Around Dynamically Shifted Vacuum*, *JHEP* **10** (2014) 070 [arXiv:1404.6254] [INSPIRE].

[57] I. Basile, J. Mourad and A. Sagnotti, *On Classical Stability with Broken Supersymmetry*, *JHEP* **01** (2019) 174 [arXiv:1811.11448] [INSPIRE].

[58] R. Antonelli and I. Basile, *Brane annihilation in non-supersymmetric strings*, *JHEP* **11** (2019) 021 [arXiv:1908.04352] [INSPIRE].

[59] I. Basile and S. Lanza, *de Sitter in non-supersymmetric string theories: no-go theorems and brane-worlds*, *JHEP* **10** (2020) 108 [arXiv:2007.13757] [INSPIRE].

[60] I. Basile, *On String Vacua without Supersymmetry: brane dynamics, bubbles and holography*, Ph.D. Thesis, Scuola Normale Superiore di Pisa, Pisa (2020) [arXiv:2010.00628] [INSPIRE].

JHEP07(2021)104

[61] C. Bachas, *A Way to break supersymmetry*, hep-th/9503030 [INSPIRE].

[62] R. Blumenhagen, L. Görlich, B. Körs and D. Lüst, *Noncommutative compactifications of type-I strings on tori with magnetic background flux*, *JHEP* **10** (2000) 006 [hep-th/0007024] [INSPIRE].

[63] C. Angelantonj, I. Antoniadis, E. Dudas and A. Sagnotti, *Type I strings on magnetized orbifolds and brane transmutation*, *Phys. Lett. B* **489** (2000) 223 [hep-th/0007090] [INSPIRE].

[64] G. Aldazabal, S. Franco, L.E. Ibáñez, R. Rabadán and A.M. Uranga, $D = 4$ *chiral string compactifications from intersecting branes*, *J. Math. Phys.* **42** (2001) 3103 [hep-th/0011073] [INSPIRE].

[65] S. Kachru, J. Kumar and E. Silverstein, *Vacuum energy cancellation in a nonsupersymmetric string*, *Phys. Rev. D* **59** (1999) 106004 [hep-th/9807076] [INSPIRE].

[66] G. Shiu and S.H.H. Tye, *Bose-Fermi degeneracy and duality in nonsupersymmetric strings*, *Nucl. Phys. B* **542** (1999) 45 [hep-th/9808095] [INSPIRE].

[67] J.A. Harvey, *String duality and nonsupersymmetric strings*, *Phys. Rev. D* **59** (1999) 026002 [hep-th/9807213] [INSPIRE].

[68] R. Blumenhagen and L. Görlich, *Orientifolds of nonsupersymmetric asymmetric orbifolds*, *Nucl. Phys. B* **551** (1999) 601 [hep-th/9812158] [INSPIRE].

[69] C. Angelantonj, I. Antoniadis and K. Forger, *Nonsupersymmetric type-I strings with zero vacuum energy*, *Nucl. Phys. B* **555** (1999) 116 [hep-th/9904092] [INSPIRE].

[70] Y. Satoh, Y. Sugawara and T. Wada, *Non-supersymmetric Asymmetric Orbifolds with Vanishing Cosmological Constant*, *JHEP* **02** (2016) 184 [arXiv:1512.05155] [INSPIRE].

[71] Y. Sugawara and T. Wada, *More on Non-supersymmetric Asymmetric Orbifolds with Vanishing Cosmological Constant*, *JHEP* **08** (2016) 028 [arXiv:1605.07021] [INSPIRE].

[72] K. Aoki, E. D'Hoker and D.H. Phong, *Two loop superstrings on orbifold compactifications*, *Nucl. Phys. B* **688** (2004) 3 [hep-th/0312181] [INSPIRE].

[73] R. Iengo and C.-J. Zhu, *Evidence for nonvanishing cosmological constant in nonSUSY superstring models*, *JHEP* **04** (2000) 028 [hep-th/9912074] [INSPIRE].

[74] N. Cribiori, D. Lüst and M. Scalisi, *The gravitino and the swampland*, *JHEP* **06** (2021) 071 [arXiv:2104.08288] [INSPIRE].

[75] A. Castellano, A. Font, A. Herráez and L.E. Ibáñez, *A Gravitino Distance Conjecture*, arXiv:2104.10181 [INSPIRE].

[76] C. Angelantonj and I. Antoniadis, *Suppressing the cosmological constant in nonsupersymmetric type-I strings*, *Nucl. Phys. B* **676** (2004) 129 [hep-th/0307254] [INSPIRE].

[77] C. Angelantonj and M. Cardella, *Vanishing perturbative vacuum energy in nonsupersymmetric orientifolds*, *Phys. Lett. B* **595** (2004) 505 [hep-th/0403107] [INSPIRE].

[78] A. Sagnotti, *Open Strings and their Symmetry Groups*, in *NATO Advanced Summer Institute on Nonperturbative Quantum Field Theory (Cargese Summer Institute)*, (1987) [hep-th/0208020] [INSPIRE].

[79] G. Pradisi and A. Sagnotti, *Open String Orbifolds*, *Phys. Lett. B* **216** (1989) 59 [INSPIRE].

JHEP07(2021)104

[80] P. Hořava, *Strings on World Sheet Orbifolds*, *Nucl. Phys. B* **327** (1989) 461 [INSPIRE].

[81] P. Hořava, *Background Duality of Open String Models*, *Phys. Lett. B* **231** (1989) 251 [INSPIRE].

[82] M. Bianchi and A. Sagnotti, *On the systematics of open string theories*, *Phys. Lett. B* **247** (1990) 517 [INSPIRE].

[83] M. Bianchi and A. Sagnotti, *Twist symmetry and open string Wilson lines*, *Nucl. Phys. B* **361** (1991) 519 [INSPIRE].

[84] A. Sagnotti, *A Note on the Green-Schwarz mechanism in open string theories*, *Phys. Lett. B* **294** (1992) 196 [hep-th/9210127] [INSPIRE].

[85] C. Angelantonj and A. Sagnotti, *Open strings*, *Phys. Rept.* **371** (2002) 1 [*Erratum ibid.* **376** (2003) 407] [hep-th/0204089] [INSPIRE].

[86] E. Dudas, *Theory and phenomenology of type-I strings and M-theory*, *Class. Quant. Grav.* **17** (2000) R41 [hep-ph/0006190] [INSPIRE].

[87] J. Mourad and A. Sagnotti, *A 4D IIB Flux Vacuum and Supersymmetry Breaking*, to appear.

[88] C. Vafa, *The String landscape and the swampland*, hep-th/0509212 [INSPIRE].

[89] H. Ooguri and C. Vafa, *On the Geometry of the String Landscape and the Swampland*, *Nucl. Phys. B* **766** (2007) 21 [hep-th/0605264] [INSPIRE].

[90] E. Palti, *The Swampland: Introduction and Review*, *Fortsch. Phys.* **67** (2019) 1900037 [arXiv:1903.06239] [INSPIRE].

[91] M. Bianchi, G. Pradisi and A. Sagnotti, *Toroidal compactification and symmetry breaking in open string theories*, *Nucl. Phys. B* **376** (1992) 365 [INSPIRE].

[92] M. Bianchi, *A Note on toroidal compactifications of the type-I superstring and other superstring vacuum configurations with sixteen supercharges*, *Nucl. Phys. B* **528** (1998) 73 [hep-th/9711201] [INSPIRE].

[93] G. Pradisi, *Magnetic fluxes, NS-NS B field and shifts in four-dimensional orientifolds*, in *2nd String Phenomenology 2003*, (2003) [hep-th/0310154] [INSPIRE].

[94] S. Chaudhuri, G. Hockney and J.D. Lykken, *Maximally supersymmetric string theories in $D < 10$*, *Phys. Rev. Lett.* **75** (1995) 2264 [hep-th/9505054] [INSPIRE].

[95] E. Witten, *Toroidal compactification without vector structure*, *JHEP* **02** (1998) 006 [hep-th/9712028] [INSPIRE].

[96] R. Minasian and G.W. Moore, *K theory and Ramond-Ramond charge*, *JHEP* **11** (1997) 002 [hep-th/9710230] [INSPIRE].

[97] E. Witten, *D-branes and k-theory*, *JHEP* **12** (1998) 019 [hep-th/9810188] [INSPIRE].

[98] E. Witten, *An* SU(2) *Anomaly*, *Phys. Lett. B* **117** (1982) 324 [INSPIRE].

[99] A.M. Uranga, *D-brane probes, RR tadpole cancellation and k-theory charge*, *Nucl. Phys. B* **598** (2001) 225 [hep-th/0011048] [INSPIRE].

[100] A. Sen, *NonBPS states and Branes in string theory*, in *Advanced School on Supersymmetry in the Theories of Fields, Strings and Branes*, (1999) [hep-th/9904207] [INSPIRE].

JHEP07(2021)104

[101] E. Dudas, J. Mourad and A. Sagnotti, *Charged and uncharged D-branes in various string theories*, *Nucl. Phys. B* **620** (2002) 109 [hep-th/0107081] [INSPIRE].

[102] E. Dudas, M.A.G. Garcia, Y. Mambrini, K.A. Olive, M. Peloso and S. Verner, *Slow and Safe Gravitinos*, *Phys. Rev. D* **103** (2021) 123519 [arXiv:2104.03749] [INSPIRE].

[103] E.W. Kolb, A.J. Long and E. Mcdonough, *Catastrophic Production of Slow Gravitinos*, arXiv:2102.10113 [INSPIRE].

[104] E.W. Kolb, A.J. Long and E. Mcdonough, *The Gravitino Swampland Conjecture*, arXiv:2103.10437 [INSPIRE].

[105] Y. Ema, K. Mukaida, K. Nakayama and T. Terada, *Nonthermal Gravitino Production after Large Field Inflation*, *JHEP* **11** (2016) 184 [arXiv:1609.04716] [INSPIRE].

[106] T. Terada, *Minimal supergravity inflation without slow gravitino*, *Phys. Rev. D* **103** (2021) 125022 [arXiv:2104.05731] [INSPIRE].

[107] I. Antoniadis, K. Benakli and W. Ke, *Salvage of Too Slow Gravitinos*, arXiv:2105.03784 [INSPIRE].

JHEP07(2021)104

ECOLE DOCTORALE

Titre : Théorie des cordes : brisure de supersymétrie, stabilisation des modules et aspects cosmologiques

Mots clés : Théorie des cordes, Brisure de supersymétrie, Modules, Cosmologie

Résumé : L'objectif de cette thèse est d'explorer divers aspects de la théorie des cordes, théorie unificatrice de la matière et de toutes les interactions fondamentales incluant l'interaction gravitationnelle. Nous commençons par résumer les ingrédients clés de cette théorie et de sa construction avant d'en étudier trois facettes théoriques. Dans un premier temps, nous définissons un nouveau mécanisme de brisure de supersymétrie dans des modèles de cordes ouvertes et nous en commentons les particularités en le mettant en perspective avec des mécanismes existants. Dans un second temps, nous étudions les masses à une boucle acquises par des modules en théorie des cordes de type I avec brisure $\mathcal{N} = 2 \to \mathcal{N} = 0$ de supersymétrie implémentée par un mécanisme de Scherk–Schwarz. Différentes stratégies sont utilisées pour conclure à la stabilité ou non de la grande diversité des modules présents dans le modèle. Cela passe par exemple par le calcul de l'expansion de Taylor du potentiel effectif, par l'évaluation de fonctions de corrélation à deux points à une boucle ou encore par l'utilisation d'arguments de dualité entre les cordes hétérotiques et la théorie des cordes de type I. Enfin, dans le cadre de modèles de cordes hétérotiques, nous étudions l'effet sur la cosmologie du potentiel à une boucle générée par la brisure de supersymétrie. Nous recherchons des solutions d'espace-temps plat en éternelle expansion et nous explorons un nouveau processus pour générer une densité relique de matière noire dans des modèles avec implémentation de la température.

Title: String theory: Supersymmetry breaking, moduli stability and cosmological considerations

Keywords: String theory, Supersymmetry breaking, Moduli, Cosmology

Abstract: The purpose of this thesis is to explore various aspects of string theory, a unified theory of matter and all fundamental interactions including gravity. Some useful key ingredients of the theory and its construction are reviewed before investigating three theoretical facets of it. First, a new supersymmetry-breaking mechanism in open-string models is developed and its features are described, commented and put into perspective with other existing mechanisms. Second, one-loop masses acquired by tree-level moduli are studied in a type I string context with $\mathcal{N} = 2 \to \mathcal{N} = 0$ breaking of supersymmetry implemented by a Scherk–Schwarz mechanism. Different strategies are used to conclude on the stability or not at one loop of the wide variety of moduli present in the model, from Taylor expansion of the effective potential to the evaluation of genus-1 two-point correlation functions through arguments arising from the duality between the heterotic and type I string. Eventually, in heterotic string models, the backreaction of the one-loop potential generated by supersymmetry breaking on the cosmology is studied. Flat and ever-expanding solutions are looked for in a cold setup while a new process for generating a dark-matter relic density is developed with implementation of finite temperature.

Institut Polytechnique de Paris
91120 Palaiseau, France